



**University of
Nottingham**

UK | CHINA | MALAYSIA

**Molecular Pharming of Consensus Dengue Viral
Envelope Glycoprotein Domain III *in planta* and
Its Immunogenicity Profiles in BALB/c Mice**

Pang Ee Leen

Thesis submitted to the University of Nottingham for the degree of

Doctor of Philosophy

April 2018

Abstract

Dengue fever has emerged as one of the fastest growing health problems in recent years. Transmission of the mosquito-borne disease is widespread throughout the tropics, causing intriguing effects to the poorer populations with limited access to healthcare. At present, most vector control programmes have failed to contain the disease and no specific treatment is available yet. The existence of dengue virus as four distinct serotypes poses a significant threat as secondary infection is often manifested in a more severe form leading to hospitalisation and even death. Hence, this pushes the demand for a dengue vaccine as a long-term protective approach. Particularly for developing nations, cost is a major factor that needs to be meticulously addressed in order to provide a quick yet affordable medical relief. With that, this study aimed at producing a safe and cost-effective plant-based dengue subunit vaccine to protect against the febrile illness. A consensus sequence of the dengue envelope glycoprotein domain III (namely cEDIII) was selected as the antigenic determinant. cEDIII was expressed in two forms, i.e. as recombinant proteins with fusion to green fluorescent protein (sGFP) or cholera toxin B subunit (CTB), and as an epitope display on hepatitis B core antigen (HBcAg) virus-like particles (VLPs). All the constructs were cloned into pEAQ-*HT* vector and transient expression was achieved via agroinfiltration of *Nicotiana benthamiana* plants. Following the successful detection of heterologous proteins in *N. benthamiana*, purification procedures were carried out to harvest the recombinant proteins and chimeric HBcAg VLPs-displaying cEDIII, correspondingly. The recombinant fusion of cEDIII to CTB was shown to preserve the ability to fold into its active pentamer and bind with native gangliosides. Meanwhile, assembly of the chimeric HBcAg VLPs-displaying cEDIII was verified via transmission electron microscopy. These purified recombinant proteins and chimeric VLPs were then used for immunogenicity testing in BALB/c mice. Following vaccination with the recombinant protein, the results showed that successful production of anti-cEDIII specific response with neutralising potency

against four dengue serotypes was obtained. T cell analyses suggested that the cEDIII induced a predominant T helper (Th) 1 response while the fusion with CTB could skew the response towards a mixed Th1/Th2. Immunisation with the chimeric VLPs displaying cEDIII also achieved induction of cEDIII-specific responses, however, further evaluations are needed to warrant the successful use of these VLPs-based vaccines. Overall, the findings in this study have provided solid evidence that the development of a plant-based dengue vaccine is feasible. This is of crucial importance to battle against the upsurge of disease burden, and the production of a local vaccine could complement with Malaysian government's efforts in combating dengue disease.

Acknowledgements

First and foremost, I would like to express my deepest gratitude to my principal supervisor, Professor Sandy Loh Hwei San. Throughout these years, she has been very supportive and gives me the freedom to explore new ideas. Without her, I would not have the chance to attend international conferences and research attachments, which put myself forward in the scientific community. In fact, she is more than a supervisor to me, who always gives me emotional support when I needed the most.

To Professor George Lomonosoff, Dr. Hadrien Peyret and fellow team mates, special thanks for all the guidance, encouragement and memorable times throughout my research attachments in the John Innes Centre.

To Dr. Lai Kok Song, thank you for giving constant financial and technical support throughout my PhD study.

To Dr. Fang Chee Mun, thank you for the insightful guidance and support on the animal experiments.

To Dr. Sharifah Syed Hassan and Dr. Pong Lian Yih, thank you for sharing your time and knowledge to guide me on the virus works.

To my friends and technicians from the University of Nottingham, thank you for the companionship and motivation throughout these years.

Last but not least, to my family and Mr. Yong De Yan, thank you for the unconditional love and care throughout my entire period of study. My heartfelt thanks also go to De Yan's family for their encouragement.

Table of Contents

Abstract	i
Acknowledgments	iii
Table of Contents	iv
Abbreviations	vii
List of Figures	xvii
List of Tables	xxv
List of Published Works	xxvii
Chapter 1 General Introduction	1-1
Chapter 2 Literature Review	2-1
2.1 <i>Flaviviridae</i> family	2-3
2.2 Dengue virus (DENV)	2-4
2.3 Plants as biofactories in molecular pharming	2-30
2.4 Strategies adopted in current study to enhance vaccine presentation	2-37
2.5 Pre-clinical examples of plant-based dengue vaccine	2-45
Chapter 3 Construction of Dengue cEDIII Expression Cassettes and the Corresponding Recombinant Vectors	3-1
3.1 Introduction	3-3
3.2 Materials and methods	3-7
3.3 Results	3-28
3.4 Discussion	3-50
3.5 Conclusion	3-57

Chapter 4	Evaluation of cEDIII Protein Expression in <i>Nicotiana benthamiana</i> Receiving Recombinant Vectors Delivered via Agroinfiltration	4-1
4.1	Introduction	4-3
4.2	Materials and methods	4-6
4.3	Results	4-15
4.4	Discussion	4-36
4.5	Conclusion	4-43
Chapter 5	Protein Purification and Characterisation of Plant-made Recombinant cEDIII Fusion Proteins and Chimeric Virus-Like Particles Displaying cEDIII	5-1
5.1	Introduction	5-3
5.2	Materials and methods	5-6
5.3	Results	5-18
5.4	Discussion	5-53
5.5	Conclusion	5-62
Chapter 6	Immunological Studies of cEDIII-based Vaccine Constructs to Determine the Immunogenicity and Neutralising Activity	6-1
6.1	Introduction	6-4
6.2	Materials and methods	6-7
6.3	Results	6-22
6.4	Discussion	6-67
6.5	Conclusion	6-78

Chapter 7	General Discussion	7-1
Chapter 8	References	8-1
Chapter 9	Appendices	9-1

Abbreviations

A ₃₇₀	absorbance at 370 nm wavelength
A ₄₅₀	absorbance at 450 nm wavelength
ADE	antibody-dependent enhancement
ANOVA	analysis of variance
AP	alkaline phosphatase
APCs	antigen-presenting cells
ATCC	American Type Cell Collection
ARSM	Malaysian Remote Sensing Agency
BiP	binding immunoglobulin protein
BLAST	Basic Local Alignment Search Tool
BrdU	bromodeoxyuridine
BSA	bovine serum albumin
C	capsid
°C	degree Celsius
CAI	codon adaptation index
cEDIII	consensus sequence of envelope glycoprotein domain III
CaMV	cauliflower mosaic virus
CD	cluster of differentiation
CDC	Centers for Disease Control and Prevention
CI	cytoplasmic incompatibility

CMC	carboxymethylcellulose
CMI	cell-mediated immunity
ConA	concanavalin A
CPMV	cowpea mosaic virus
CO ₂	carbon dioxide
Co1	M-cell targeting ligand
CPE	cytopathogenic effect
Cryo-EM	cryo-electron microscopy
CS	cyclisation sequence
CT	cholera toxin
CTA	cholera toxin A subunit
CTB	cholera toxin B subunit
CYD	chimeric-yellow fever-dengue
Cys	cysteine
DCs	dendritic cells
delRNA-2	deleted RNA-2 construct
DENV	dengue virus
DENV 1-4	dengue virus serotypes 1 to 4
DF	dengue fever
DHF	dengue haemorrhagic fever
dNTPs	deoxynucleotides

dpi	day post-infiltration
DPBS	Dulbecco's phosphate-buffered saline
DSS	dengue shock syndrome
E	envelope
ECL	enhanced chemiluminescence
EDI	envelope glycoprotein domain I
EDII	envelope glycoprotein domain II
EDIII	envelope glycoprotein domain III
ELISA	enzyme-linked immunosorbent assay
ER	endoplasmic reticulum
ERAD	endoplasmic reticulum associated degradation
ERQC	endoplasmic reticulum quality control
FACS	fluorescence-activated cell sorting
FBS	fetal bovine serum
Fc γ R	Fc gamma receptor
FDA	Food and Drug Administration
FFA	focus-forming assay
FFU	focus-forming units
FMDV	foot and mouth disease virus
FRNT	focus reduction neutralisation test

FRNT40	highest serum dilution yielding 40% reduction of focus-forming units
FRNT50	highest serum dilution yielding 50% reduction of focus-forming units
FWT	fresh weight tissue
g	gram
GGs	glycine-glycine-serine
GM	genetically-modified
GM1	monosialotetrahexosylganglioside
GMP	good manufacturing practice
GPGP	glycine-proline-glycine-proline
GST	glutathione S-transferase
GUS	β -glucuronidase
HBV	hepatitis B virus
HBcAg	hepatitis B core antigen
HBsAg	hepatitis B surface glycoprotein
hCF	human cytotoxic factor
HEPA	high-efficiency particulate air
HIC	hydrophobic interaction chromatography
His	histidine
HIV	human immunodeficiency virus
HLA	human leucocyte antigen

HPV	human papillomavirus
HRP	horseradish peroxidase
<i>HT</i>	hypertranslational
IACUC	Institutional Animal Care and Use Committee
IDA	iminodiacetic acid
IEX	ion-exchange chromatography
IFA	immunofluorescence assay
IFN- γ	interferon-gamma
IgA	immunoglobulin A
IgG	immunoglobulin G
IL	interleukin
IMAC	immobilised metal affinity chromatography
INP	insoluble protein
IP	intraperitoneal
IVC	individual ventilation cage
JIC	John Innes Centre
JEV	Japanese encephalitis virus
kbp	kilo-base pairs
kDa	kilo-Dalton
KDEL	endoplasmic reticulum retention signal
l	litre

LAV	live attenuated virus
LB	Luria-Bertani (medium)
LDS-βME	lithium dodecyl sulphate sample buffer containing β-mercaptoethanol
LT	heat-labile enterotoxin
M	molar
mAb	monoclonal antibody
MBP	maltose binding protein
MCS	multiple cloning site
mEL	monomeric core particles without gene insert
MEM	minimum essential media
mHBcAg	monomeric core hepatitis B core antigen
MHC	major histocompatibility complex
MIR	major immunodominant region
MOH	Ministry of Health
MOI	multiplicity of infection
MOSTI	Ministry of Science, Technology and Innovation
Mr	molecular mass
mRNA	messenger RNA
MWCO	molecular weight cut-off
Ni ²⁺	nickel ion

Ni-NTA Agarose	agarose resin derivatized with nickel ion-nitrilotriacetic acid
NIAID	National Institute of Allergy and Infectious Diseases
NS	non-structural
NTA	nitrilotriacetic acid
OD ₆₀₀	optical density at 600 nm wavelength
ODNs	oligodeoxynucleotides
ORF	open reading frame
PBS	phosphate-buffered saline
PBST	phosphate-buffered saline supplemented with Tween-20
PCR	polymerase chain reaction
pI	isoelectric point
PIGS	polymeric immunoglobulin G scaffold
PLAPROVA	Plant Production of Vaccines
PR1a	tobacco pathogenesis-related 1a protein
Pre	pre-immune sera
prM	precursor membrane
PTGS	post-translational gene silencing
QVLP	quadrivalent virus-like particle
RE	restriction enzyme
RISC	RNA-induced silencing complex

RT	room temperature
RT-PCR	reverse transcriptase-polymerase chain reaction
rEPA	<i>Pseudomonas aeruginosa</i> exotoxin A
RIDL	Release of Insects with Dominant Lethality
S2	Schneider-2
SAv-HRP	streptavidin-horseradish peroxidase
SD	standard deviation
SDS-PAGE	sodium dodecyl sulphate-polyacrylamide gel electrophoresis
SEC	size exclusion chromatography
sGFP	green fluorescent protein
SI	stimulation index
SOC	super optimal broth with catabolite repressor
SP	soluble protein
T	triangulation number
Ta	annealing temperature
TBS	tris-buffered saline
TBST	tris-buffered saline supplemented with Tween-20
TBSV	tomato bushy stunt virus
Tc	T cytotoxic
T-DNA	transfer-DNA
TED	tris(carboxymethyl)ethylene diamine

tEL	tandem core particles without gene insert
TEM	transmission electron microscopy
TEV	tobacco etch virus
Th	T helper
tHBcAg	tandem core hepatitis B core antigen
TM	transmembrane
TMB	3, 3', 5, 5'-tetramethylbenzidine
TMV	tobacco mosaic virus
Tris-HCl	Tris-hydrochloride
UAR	upstream AUG region
UK	United Kingdom
UPR	unfolded protein response
USA	United States of America
UTR	untranslated region
UV	ultraviolet
V	voltage
v	volume
VLPs	virus-like particles
w	weight
WHO	World Health Organization
WPRO	World Health Organization Western Pacific Region

WRAIR	Walter Reed Army Institute of Research
WNV	West Nile virus
X	times
$x g$	relative centrifugal force expressed in units of gravity
YFV	yellow fever virus
ZIKV	Zika virus

List of Figures

	Page
Figure 2.1: Schematic representation of DENV genome organisation.	2-5
Figure 2.2: An illustration of the structural arrangement of E glycoproteins on a mature dengue virion.	2-5
Figure 2.3: Schematic illustration of dengue E domains.	2-7
Figure 2.4: A tertiary structure of DENV EDIII, which shows the different amino acid residues involved in virus neutralisation as indicated by different colours.	2-8
Figure 2.5: An overview on the distribution changes of DENV from year 1943 to 2013.	2-11
Figure 2.6: Statistical number of dengue cases reported from 2000 to 2017.	2-13
Figure 2.7: Overview of the infection events within a host cell, starting from (A) clathrin-mediated endocytosis, (B) pH-dependent conformational change, (C) uncoating, followed by (D) prM cleavage and virus maturation.	2-15
Figure 2.8: A cascade of cytokine events underlying the pathogenesis of DHF within an infected macrophage.	2-17
Figure 2.9: Crystallographic structure of CTB.	2-39
Figure 2.10: Structural folding of HBcAg VLPs.	2-41
Figure 2.11: The formation of HBcAg VLPs via ‘Tandem Core’ technology.	2-44
Figure 3.1: Schematic illustrations of the pEAQ- <i>HT</i> vector used in this study.	3-8

Figure 3.2:	A two-step PCR amplification process using pEAQ- <i>HT::PR1a-CTB-cEDIII-H-KDEL</i> as template to generate the new insert, PR1a-CTB-cEDIII-KDEL (xTH).	3-17
Figure 3.3:	A methodology flow chart illustrating the steps used for the construction of recombinant vectors in this study.	3-18
Figure 3.4:	C1 and C3 primers used for all PCR screening works in this study.	3-25
Figure 3.5:	PCR amplification profiles of inserts used for vector construction of cEDIII recombinant fusion proteins, namely cEDIII-sGFP-KDEL, CTB-cEDIII-KDEL, intermediate PR1a-CTB-cEDIII-KDEL (xTH) amplicon and PR1a-CTB-cEDIII-KDEL (xTH).	3-30
Figure 3.6:	PCR amplification profiles of inserts used for vector construction of chimeric mHBcAg and tHBcAg VLPs, namely cEDIII_mono, cEDIII (L)_mono and cEDIII_tandem.	3-31
Figure 3.7:	RE digestion profiles of inserts used to design the expression cassettes for cEDIII recombinant fusion proteins, namely PR1a-cEDIII-sGFP-H-KDEL and PR1a-CTB-cEDIII-H-KDEL.	3-32
Figure 3.8:	Verification of TOP10 cells transformed with pEAQ- <i>HT::cEDIII-sGFP-KDEL-H</i> .	3-33
Figure 3.9:	Verification of TOP10 cells transformed with pEAQ- <i>HT::PR1a-cEDIII-sGFP-H-KDEL</i> .	3-35
Figure 3.10:	Verification of TOP10 cells transformed with pEAQ- <i>HT::CTB-cEDIII-KDEL-H</i> .	3-37

Figure 3.11:	Verification of TOP10 cells transformed with pEAQ- <i>HT::PR1a-CTB-cEDIII-H-KDEL</i> .	3-39
Figure 3.12:	Verification of TOP10 cells transformed with pEAQ- <i>HT::PR1a-CTB-cEDIII-KDEL (xTH)</i> .	3-41
Figure 3.13:	Verification of TOP10 cells transformed with pEAQ- <i>HT::mHBcAg-cEDIII</i> .	3-43
Figure 3.14:	Verification of TOP10 cells transformed with pEAQ- <i>HT::mHBcAg-cEDIII (L)</i> .	3-45
Figure 3.15:	Verification of TOP10 cells transformed with pEAQ- <i>HT::tHBcAg-cEDIII</i> .	3-47
Figure 4.1:	A comparative UV observation of green fluorescence emitted by <i>N. benthamiana</i> leaves infiltrated with different constructs.	4-16
Figure 4.2:	Confocal microscopic observation of <i>N. benthamiana</i> leaves expressing recombinant cEDIII-sGFP fusion proteins	4-17
Figure 4.3:	Expression profiles of recombinant cEDIII-sGFP fusion proteins in <i>N. benthamiana</i> leaves.	4-19
Figure 4.4:	Kinetic expression profiles of recombinant cEDIII- sGFP fusion protein in <i>N. benthamiana</i> .	4-20
Figure 4.5:	Expression profiles of recombinant CTB-cEDIII fusion proteins in <i>N. benthamiana</i> leaves.	4-22
Figure 4.6:	Kinetic expression profiles of recombinant CTB-cEDIII fusion protein in <i>N. benthamiana</i> .	4-23
Figure 4.7:	Expression profiles of CTB-cEDIII-KDEL (xTH) fusion protein in <i>N. benthamiana</i> leaves.	4-25

Figure 4.8:	Kinetic expression profiles of CTB-cEDIII-KDEL (xTH) fusion protein in <i>N. benthamiana</i> .	4-26
Figure 4.9:	Expression profiles of mHBcAg-cEDIII protein in <i>N. benthamiana</i> host.	4-28
Figure 4.10:	Kinetic expression profiles of mHBcAg-cEDIII protein in <i>N. benthamiana</i> .	4-29
Figure 4.11:	Expression profiles of mHBcAg-cEDIII (L) protein in <i>N. benthamiana</i> host.	4-31
Figure 4.12:	Kinetic expression profiles of mHBcAg-cEDIII (L) protein in <i>N. benthamiana</i> .	4-32
Figure 4.13:	Expression profiles of tHBcAg-cEDIII protein in <i>N. benthamiana</i> host.	4-34
Figure 4.14:	Kinetic expression profiles of tHBcAg-cEDIII protein in <i>N. benthamiana</i> .	4-35
Figure 5.1:	An overview of the generic recombinant fusion protein purification procedures which were applied in this study.	5-7
Figure 5.2:	An overview of the purification procedures used to isolate the chimeric HBcAg VLPs-displaying cEDIII.	5-9
Figure 5.3:	IMAC purification_1 profiles of recombinant cEDIII fused with sGFP.	5-19
Figure 5.4:	IMAC purification_2 profiles of TEV protease-digested cEDIII-sGFP-H-KDEL protein.	5-21
Figure 5.5:	IMAC purification_1 profiles of recombinant cEDIII fused with CTB.	5-25
Figure 5.6:	IMAC purification_2 profiles of TEV protease-digested CTB-cEDIII-H-KDEL protein.	5-27

Figure 5.7:	IMAC purification_1 profiles of the variant CTB-cEDIII-KDEL (xTH) protein.	5-30
Figure 5.8:	Evaluation of the binding affinities between pentameric CTB and GM1 gangliosides (+ GM1) via ELISA.	5-31
Figure 5.9:	SEC profiling of CTB-cEDIII-KDEL (xTH) fusion protein.	5-32
Figure 5.10:	Sucrose cushion purification and detection of mHBcAg-cEDIII VLPs.	5-35
Figure 5.11:	Sucrose gradient purification and detection of mHBcAg-cEDIII VLPs.	5-36
Figure 5.12:	Sucrose cushion purification and detection of mHBcAg-cEDIII (L) VLPs.	5-38
Figure 5.13:	Sucrose gradient purification and detection of mHBcAg-cEDIII (L) VLPs.	5-39
Figure 5.14:	Electron micrographs showing the purified monomeric core VLPs.	5-41
Figure 5.15:	Electron micrographs showing the chimeric mHBcAg VLPs reacted with immunogold of DENV 1-4 monoclonal antibody.	5-44
Figure 5.16:	Sucrose cushion purification and detection of tHBcAg-cEDIII VLPs.	5-46
Figure 5.17:	Nycodenz gradient fractionation and detection profiles of tHBcAg-cEDIII VLPs.	5-47
Figure 5.18:	Electron micrograph showing the purified tandem core VLPs that were negatively stained with 2% (v/v) uranyl acetate.	5-50

Figure 5.19:	Nycodenz gradient fractionation and detection of tHBcAg-cEDIII VLPs, following deliberate handling of vacuum concentration step.	5-51
Figure 5.20:	Identification of the three His residues (in red box) responsible for the CTB-cEDIII-H-KDEL protein binding to Ni ²⁺ ion.	5-55
Figure 5.21:	Crystal structure of CTB pentamer-pentamer association, with the His13 imidazole ring coloured in red	5-57
Figure 6.1:	A schematic illustration of the animal experiment plan.	6-10
Figure 6.2:	Images of BALB/c mice held in IVC cages.	6-11
Figure 6.3:	cEDIII-specific IgG responses in mice injected with recombinant cEDIII proteins	6-23
Figure 6.4:	Examination of the mEL-specific and mHBcAg-cEDIII (L)-specific IgG titres in BALB/c mice.	6-25
Figure 6.5:	cEDIII-specific IgG antibody titres in BALB/c mice vaccinated with chimeric mHBcAg VLPs displaying cEDIII (VLPs (b) experiment).	6-27
Figure 6.6:	Immunofluorescence profiles of cross-reactivity between sera of mice immunised with recombinant cEDIII proteins and DENV 1-4 serotypes.	6-29
Figure 6.7:	Immunofluorescence profiles of interactions between mouse sera collected from VLPs (a) experiment and DENV 1-4 serotypes.	6-35
Figure 6.8:	Immunofluorescence profiles of cross-reactivity between mouse sera collected from VLPs (b) experiment and DENV 1-4 serotypes.	6-39

Figure 6.9:	Virus neutralising antibody responses of recombinant cEDIII proteins against DENV 1-4 serotypes.	6-45
Figure 6.10:	Virus neutralising antibody responses of chimeric mHBcAg VLPs-displaying cEDIII against four serotypes of DENV (VLPs (a) experiment).	6-46
Figure 6.11:	Virus neutralising antibody responses of chimeric mHBcAg VLPs-displaying cEDIII against DENV 1-4 serotypes (VLPs (b) experiment).	6-48
Figure 6.12:	Lymphoproliferative responses of the splenocytes of BALB/c mice vaccinated with recombinant cEDIII proteins.	6-50
Figure 6.13:	Lymphocyte proliferation activities of splenocytes of mice immunised with chimeric mHBcAg VLPs-displaying cEDIII (VLPs (a) experiment).	6-51
Figure 6.14:	Lymphoproliferative responses of splenocytes of mice injected with chimeric mHBcAg VLPs-displaying cEDIII (VLPs (b) experiment).	6-53
Figure 6.15:	Immunophenotyping of lymphocyte populations in splenocytes of mice vaccinated with recombinant cEDIII proteins.	6-54
Figure 6.16:	Immunophenotyping of cell populations in splenocytes of mice immunised with chimeric mHBcAg VLPs-displaying cEDIII.	6-56
Figure 6.17:	Cytokines secretion profiles of mice vaccinated with recombinant cEDIII proteins.	6-58
Figure 6.18:	Cytokines profiling of mice immunised with chimeric mHBcAg VLPs-displaying cEDIII.	6-61

Figure 6.19:	A schematic diagram of the aspects of cellular-mediated immune responses studied in this context.	6-71
Figure A3.9:	A step-wise alignment of the DNA sequencing results for PR1a-cEDIII-sGFP-H-KDEL expression cassette.	9-16
Figure A3.10:	The alignment of cEDIII sequence, which is representative of the EDIII sequence of DENV serotypes 1 to 4.	9-20
Figure A4.2:	Daily observations of the infiltrated <i>N. benthamiana</i> leaf.	9-24
Figure A4.3:	A Signal-BLAST profile that shows the predicted cleavage site of PR1a signal peptide.	9-26
Figure A5.2:	Predictive models of recombinant cEDIII fusion proteins.	9-28
Figure A5.3:	SEC chromatogram of protein standards separated under the same conditions as CTB-cEDIII-KDEL (xTH) protein.	9-30
Figure A5.4:	A comparison of different density gradient media used in VLPs purification process.	9-31
Figure A6.2:	An illustration of the barbering behaviour among female BALB/c mice used in this study	9-34
Figure A6.3:	A protein sequence alignment results of mEL and CTB-cEDIII-KDEL (xTH), as generated from protein BLAST analysis.	9-35
Figure A6.4:	A summary of the immunogenicity assessment of tHBcAg-cEDIII VLPs.	9-37

List of Tables

	Page
Table 2.1: A list of dengue vaccine candidates in clinical development.	2-23
Table 2.2: A comparison of merits offered by different expression systems.	2-32
Table 2.3: A compiled list of on-going researches on plant-based dengue vaccine development.	2-46
Table 3.1: List of synthetic sequences.	3-11
Table 3.2: List of cEDIII expression cassettes and cloning vectors used in this study.	3-13
Table 3.3: Details of PCR amplification of cEDIII inserts using Phusion [®] polymerase.	3-16
Table 3.4: Details of the REs used for digestion of cEDIII inserts and pEAQ- <i>HT</i> variant vectors.	3-21
Table 3.5: The expected size of amplicon from PCR colony screening, using C1 and C3 primers.	3-26
Table 3.6: List of primers used for sequencing of specific recombinant vector.	3-27
Table 3.7: The adjustment of codon usage for synthesised sequences.	3-28
Table 4.1: Agrobacterial suspensions used for plant infiltration in this study.	4-8
Table 4.2: Details on the extraction of heterologous proteins expressed by corresponding recombinant vectors.	4-11
Table 4.3: List of antibodies used for Western blotting in this study.	4-13

Table 5.1:	List of quantified protein yield after the final purification procedures.	5-52
Table 6.1:	A summary of the experimental design for mouse immunisation against recombinant cEDIII proteins.	6-8
Table 6.2a:	A summary of the experimental design for mouse immunisation against chimeric mHBcAg VLPs-displaying cEDIII, referred as VLPs (a) experiment.	6-8
Table 6.2b:	A summary of the experimental design for mouse immunisation against chimeric mHBcAg VLPs-displaying cEDIII, referred as VLPs (b) experiment.	6-9
Table 6.3:	The combination of antibodies used in FACS analyses.	6-19
Table 6.4:	List of reagents used for corresponding OptEIA ELISA kit.	6-20
Table 6.5:	A comparison of the immunogenicity mediated by recombinant cEDIII proteins.	6-65
Table 6.6:	A comparison of the immunogenicity mediated by chimeric mHBcAg VLPs-displaying cEDIII (VLPs (b) experiment).	6-65

List of Published Works

International peer-reviewed journals:

- Pang, E. L., and Loh, H. S. (2017). Towards development of a universal dengue vaccine – how close are we? *Asian Pacific Journal of Tropical Medicine*, 10(3), 220-228.
- Pang, E. L., and Loh, H. S. (2016). Current perspectives on dengue episode in Malaysia. *Asian Pacific Journal of Tropical Medicine*, 9(4), 395-401.

International conference abstracts:

- Pang E. L., Peyret, H., Lomonossoff, G. P., Pong, L. Y., Hassan S. S., Fang, C. M., Lai, K. S., and Loh, H. S. (2017). A plant-made consensus dengue virus envelope domain III induces antibody responses in BALB/c mice. International Conference on Molecular Biology and Biotechnology, 1 – 2 November 2017, Kuala Lumpur, Malaysia.
- Pang E. L., Peyret, H., Lomonossoff, G. P., Pong, L. Y., Hassan S. S., Fang, C. M., Lai, K. S., and Loh, H. S. (2017) Evaluation of immunogenicity of a recombinant plant-derived dengue vaccine candidate in BALB/c Mice. Plant-Based Vaccines, Antibodies & Biologics, 5 – 7 June 2017, Albufeira, Portugal.
- Pang E. L., Peyret, H., Ramirez, A., Whelan, M., Lomonossoff, G. P., Lai, K. S., and Loh, H. S. (2016). Epitope presentation of consensus dengue glycoprotein domain III on plant-derived virus-like particles. New Technologies, New Vaccines, 20 – 23 March 2016, Delaware, United States.
- Pang E.L., Peyret, H., Ramirez, A., Whelan, M., Lomonossoff, G. P., Lai, K. S., and Loh, H. S. (2015). A hepatitis B core-based production of plant virus-like particles as dengue vaccine candidate. Plant-Based Vaccines, Antibodies & Biologics, 8 – 10 June 2015, Lausanne, Switzerland.

1 General Introduction

Dengue is a mosquito-borne disease predominantly found in the tropical and subtropical regions around the globe. It is caused by dengue virus (DENV) that co-circulates in the form of four different serotypes, namely DENV 1-4. Classified as a member of the *Flaviviridae* family, DENV is an enveloped virus with 50 nm in size (Kuhn *et al.*, 2002). Severity of dengue disease can vary from undifferentiated febrile illness, dengue fever (DF) to life-threatening conditions of dengue haemorrhagic fever (DHF) and dengue shock syndrome (DSS). The progression into DHF/DSS is commonly associated with a phenomenon termed as antibody-dependent enhancement (ADE). This is where the pre-existing, non-neutralising antibodies from a heterologous DENV infection can bind with the new infecting serotype and infect Fc gamma receptor (Fc γ R)-bearing cells to gain entry into host cells (Bäck and Lundkvist, 2013).

Transmission of the disease has been reported in at least 128 countries to date, affecting over 50% of the world population (Brady *et al.*, 2012). In fact, World Health Organization (WHO) has ranked dengue as one of most important tropical diseases due to the alarming rise of disease burden. Annual incidence rate has grown dramatically high in recent decades, in which 390 million cases are predicted per annum (Bhatt *et al.*, 2013). Out of these, it was reported that 500,000 people were hospitalised with severe dengue and approximately 2.5% of them would succumb to the disease (WHO, 2017). Various factors have led to the increased epidemiology including urbanisation, mobility of populations, poor sanitary practices and global warming. Experts believe that following climate change, dengue would continue to expand in low-income and middle-income countries, whereby 4.86 billion people would be exposed to risk of dengue if socioeconomic development remains unchanged by year 2050 (Ebi and Nealon, 2016).

Generally, groups of different age, gender and ethnic are all vulnerable to dengue infection. The severity of dengue in Malaysia can be reflected from an astonishingly high percentage (91.6%) of dengue immunoglobulin G (IgG) seropositivity among

randomly-selected adults (Muhammad Azami *et al.*, 2011). The escalating trend of dengue infection is evident from approximately 7,000 cases reported every month, and it is a concern that the high seroprevalence of dengue antibodies can contribute to high fatality rate due to ADE (Pang and Loh, 2016). Moreover, the data might not represent an accurate figure due to under-reporting. Overall, these imply that the dengue episode in Malaysia is under an intense pressure of disease burden.

At present, no specific treatment nor anti-viral drug for dengue is available yet. In Malaysia, low public awareness in reducing mosquito breeding grounds is also partly responsible for the spread of disease-carrying *Aedes* mosquitoes. Thus, this has driven a major reliance on vector control programmes to suppress disease transmission. However, application of insecticides may not be a sustainable approach owing to high cost and development of chemical-resistance in *Aedes* mosquitoes (Packierisamy *et al.*, 2015). Following major investments on the plan to release genetically-modified (GM) mosquitoes, the project had been shelved in 2015 because the establishment of GM mosquitoes in the wild population was proven to be inefficient (Loh, 2015). Nevertheless, the latest strategy involves the use of *Wolbachia* as an intracellular bacterium that can help to reduce the ability of *Aedes* mosquitoes to transmit DENV. Although the field release of *Wolbachia*-infected mosquitoes has been initiated in Kuala Lumpur in March 2017 (Bernama, 2017), continuous monitoring is still needed to validate its efficacy in eradicating dengue.

Considering the limitations as mentioned above, this pushes the demand for a dengue vaccine as a long-term protective approach. To account for the existence of four antigenically-distinct DENV serotypes, production of a vaccine that is able to provide solid neutralisation against all serotypes is essential. Although the world first dengue vaccine, namely Dengvaxia[®], has been launched in December 2015, its adoption is low due to unconvincing safety and efficacy profiles (Whitehead, 2016). In fact, Philippine has recently withdrawn the use of Dengvaxia[®] following the adverse effects observed

among vaccinated children (Antiporda, 2018). Despite there are numerous vaccine candidates along the pipeline, it is still uncertain whether the demand for a reliable vaccine could be met. However, as the disease is progressing faster than it can be coped, more researches have embarked on the race to produce the first universal dengue vaccine. In this study, the production of a subunit dengue vaccine is explored. The envelope (E) glycoprotein of dengue virus has been the primary target in subunit vaccine development, and more specifically its domain III (EDIII) which harbours serotype-specific neutralising epitopes. On top of that, Leng *et al.* (2009) had aligned the EDIII sequences of DENV 1-4 to obtain a consensus sequence (cEDIII) that could inhibit the infectivity of four serotypes simultaneously. Thus, cEDIII was chosen as the antigenic determinant for this study, with the hope that tetravalent protection could be provided and hence minimises the risk of ADE.

The concept of molecular pharming has been initiated to explore plants as biofactories for pharmaceuticals production. Nowadays, plant system has drawn increasing attention to displace many existing systems based on its outstanding features of low production cost, rapid scalability, biocontainment warranty and eukaryotic processing machinery (Loh *et al.*, 2017). Comparing to the classical stable transformation, various industrial and academia laboratories have opted the use of transient expression system for the benefits of speed and convenience. The emergence of agroinfiltration has significantly transformed the transient expression platform where rapid screening or production can be achieved within a matter of days (Thuenemann *et al.*, 2013). Hence, plant-based system is opted to produce subunit dengue vaccine in this study, for which it has the potential to provide quick but affordable medical relief to developing nations.

With the intention to express cEDIII as the antigen of interest in *Nicotiana benthamiana*, several expression cassettes had been designed as laid out in Chapter 3. In specific, the cassettes were used to express cEDIII in two main forms, which are

recombinant protein and epitope displayed on virus-like particles (VLPs). This is to explore the possibility of developing a vaccine candidate with strong immunogenicity profile. The expressions as recombinant proteins include cEDIII fusion to green fluorescent protein (sGFP) and cEDIII fusion to cholera toxin B subunit (CTB). Hepatitis B core antigen (HBcAg) that has the propensity to self-assemble into VLPs, is chosen as the carrier molecule to facilitate cEDIII epitopes presentation. Besides, several strategies have been applied to improve the transgene expression including codon optimisation, use of Kozak sequence, use of RNA silencing suppressor, subcellular localisation and integration of protein linkers. All the expression cassettes were cloned into a binary vector modified from cowpea Mosaic Virus (CPMV), which is well-known as pEAQ-*HT* vector.

Following that, Chapter 4 presents the delivery of recombinant vectors into *N. benthamiana* via syringe agroinfiltration technique. Infiltrated leaves were harvested on the 6th day post-infiltration (dpi) and assessed by Western blotting analysis for the presence of heterologous proteins. Once confirmed, the expression kinetics of the recombinant cEDIII proteins and chimeric HBcAg VLPs-displaying cEDIII were evaluated in order to determine the optimal harvesting time.

Chapter 5 then describes the purification of recombinant cEDIII proteins and chimeric HBcAg VLPs-displaying cEDIII. Immobilised metal affinity chromatography (IMAC) was adopted as the main purification procedure for recombinant cEDIII proteins. Then, tobacco etch virus (TEV) protease cleavage was used to remove those extra amino acids of 6X histidine (His) tag. Meanwhile, the purification of chimeric VLPs was achieved by density gradient ultracentrifugation.

Lastly, Chapter 6 presents the immunogenicity studies of purified recombinant cEDIII proteins and chimeric HBcAg VLPs-displaying cEDIII. Immunisations of female BALB/c mice were carried out via intraperitoneal route, with a primary injection course and two booster doses. Then, the humoral immune responses were evaluated

based on the presence of cEDIII-specific antibodies and their neutralisation potencies. Cell-mediated immune responses were assessed via antigenic stimulation of immune cells and elucidating the secretion profiles of T helper (Th) 1 and/or Th2 cytokines.

Worthwhile to mention, a significant finding has been achieved in this study whereby this is the first to demonstrate that plant-based dengue vaccine candidates are able to neutralise all four DENV serotypes simultaneously. Comparing to previous studies which expressed cEDIII using bacterial system, the cEDIII protein produced in this study has attained significantly higher neutralisation titres which potentiates its value to be developed into a dengue vaccine. Furthermore, the recombinant fusion of cEDIII to CTB has boosted its overall immunogenicity whereby the fusion protein is able to fold into its active pentameric form and behaves as self-adjuvanting molecule that can stimulate a balanced Th1/Th2 cellular response. Nevertheless, the successful presentation of cEDIII epitopes on chimeric HBcAg VLPs, in immunogenic context, also represents the first example in this field.

Overall, the ultimate goal of this study aimed at developing a safe and cost-effective plant-based dengue subunit vaccine candidate via agroinfiltration strategy to protect humans against the deadly dengue fever. To achieve this, the study was organised into different scopes which embarked on the following specific objectives:

- (i) To design and construct expression cassettes containing the cEDIII antigenic determinant;
- (ii) To deliver the cEDIII recombinant vectors into *N. benthamiana* via agroinfiltration and study the protein expression profiles;
- (iii) To purify the plant-expressed recombinant cEDIII-sGFP and CTB-cEDIII fusion proteins, as well as chimeric HBcAg VLPs-expressing cEDIII; and
- (iv) To evaluate the immunogenicity of purified vaccine candidates in BALB/c mice.

2 Literature Review

Table of Contents

2.1	<i>Flaviviridae</i> family.....	2-3
2.2	Dengue virus (DENV).....	2-4
2.2.1	Prevalence and epidemiology	2-9
2.2.2	Pathogenesis and infection events.....	2-14
2.2.3	Disease treatment	2-18
2.2.4	Vector control strategies	2-19
2.2.4.1	Application of insecticides.....	2-19
2.2.4.2	Genetically-modified mosquitoes	2-20
2.2.4.3	Biocontrol agents	2-21
2.2.5	State of vaccine research.....	2-22
2.2.5.1	Live attenuated virus (LAV) chimeric vaccine	2-24
2.2.5.2	Purified inactivated whole virus vaccine	2-27
2.2.5.3	DNA vaccine.....	2-28
2.2.5.4	Subunit protein vaccine.....	2-29
2.3	Plants as biofactories in molecular pharming.....	2-30
2.3.1	Merits of plant-based expression system	2-30
2.3.2	Plant transformation strategies.....	2-33
2.3.2.1	Stable integration versus transient expression	2-33
2.3.2.2	Agroinfiltration strategy.....	2-34
2.4	Strategies adopted in current study to enhance vaccine presentation.....	2-37

2.4.1	Protein conjugation	2-37
2.4.1.1	Cholera toxin B subunit (CTB).....	2-38
2.4.2	Virus-like particles (VLPs).....	2-39
2.4.2.1	Hepatitis B core antigen (HBcAg) as antigenic carrier.	2-40
2.4.2.2	Emerging ‘Tandem Core’ technology.....	2-42
2.5	Pre-clinical examples of plant-based dengue vaccine	2-45

2.1 *Flaviviridae* family

Taxonomically, *Flaviviridae* is classified as a family of positive and single-stranded RNA viruses. This simply means that their genetic information can be utilised as messenger RNA (mRNA) and translated by host machinery. Such organisation enables RNA viruses to evolve million folds faster than the host chromosomal DNA (Holland *et al.*, 1982); thus it is not surprising that they have the abilities to bypass subsets of host surveillance system. In the evolution context, single-strand molecules are prone to high rate of non-synonymous mutation that can result in amino acid replacement. Nucleotide shuffling in myriad ways and the poor proofreading capability lead to functional changes that allow RNA viruses to strategise their adaptation in new hosts. For instance, Domingo (1997) found that the emergence of mutants with altered pathogenicity were related to stress induced by nutritional deficiencies that extend to many deprived areas.

The phylogeny of *Flaviviridae* branches into four distinctive genera, namely *Flavivirus*, *Hepacivirus*, *Pegivirus* and *Pestivirus* (Simmonds *et al.*, 2017). Among them, the genus *Flavivirus* is responsible for the widespread of diseases that cause high morbidity and mortality across the globe. This genus constitutes more than 70 enveloped viruses, many of which pose substantial health threats including dengue virus (DENV) Japanese encephalitis virus (JEV), West Nile virus (WNV) and Zika virus (ZIKV). Albeit flaviviruses have similar genomic structure and replicative strategy, they can also manifest diseases in different clinical forms such as encephalitis or haemorrhage (Fernandez-Garcia *et al.*, 2009). Besides, they are grouped into three major clusters according to the mode of transmission: mosquito-borne, tick-borne and non-vector borne (Kuno *et al.*, 1998). In particular, the movement of vector-borne pathogens into new territories is increasing, thereby exposing more than half of the world population to risk of flavivirus diseases (World Health Organization (WHO), 2014).

2.2 Dengue virus (DENV)

DENV inherently exists in the form of four distinct serotypes (DENV 1-4) that shares 65 – 70% of sequence homology (Rico-Hesse, 1990). The genome is 10.862 kilo-base pairs (kbp) long, which encodes for a single polypeptide consisting of three structural proteins: (capsid (C), envelope (E), and precursor membrane (prM)), along with seven non-structural (NS) proteins (NS1, NS2A, NS2B, NS3, NS4A, NS4B and NS5) (Henchal and Putnak, 1990). An illustration of the virus genome arrangement is shown in **Figure 2.1**. DENV presents itself as a 50 nm spherical, enveloped virus, with the E glycoproteins arranged in pairs on the mature virion (**Figure 2.2**) (Whitehead *et al.*, 2007). In fact, the three structural proteins exist in stoichiometric quantities (C, 100 amino acids; E, 495 amino acids; prM, 75 amino acids) to give rise to the icosahedral symmetry (Kuhn *et al.*, 2002). Similar to other flaviviruses, the 5' end of DENV genome contains a type 1 cap (m7GpppAmp) structure and the 3' terminus is lacking of polyadenylation signal (Gebhard *et al.*, 2011). The untranslated region (UTR) is known to modulate roles such as synthesising negative strand template for viral replication, initiating translation and packaging of plus-strand RNA into progeny virions (Markoff, 2003). In fact, there are two pairs of complementary sequences, namely 5' – 3' cyclisation sequence (CS) and 5' – 3' upstream AUG region (UAR), which are essential for long range RNA-RNA interactions (Alvarez *et al.*, 2005).

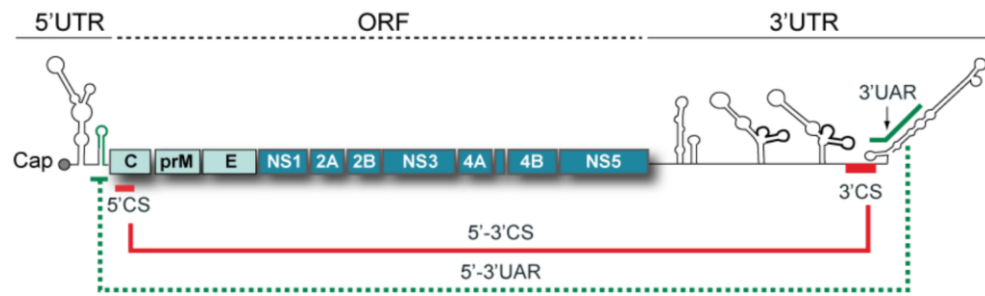


Figure 2.1: Schematic representation of DENV genome organisation. Keywords: untranslated region (UTR); open reading frame (ORF); cyclisation sequence (CS); 5' upstream AUG region (UAR); capsid (C); precursor membrane (prM); envelope (E); non-structural (NS). Image obtained from Gebhard *et al.* (2011).

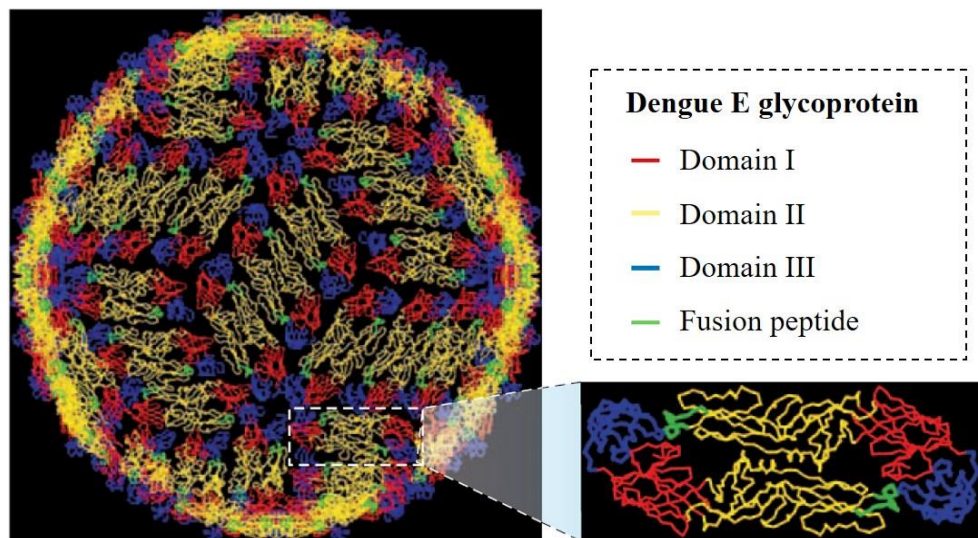


Figure 2.2: An illustration of the structural arrangement of E glycoproteins on a mature dengue virion. Distinct domains are shown in red (domain I), yellow (domain II) and blue (domain III), respectively. Image obtained from Whitehead *et al.* (2007).

During virus assembly, glycosylated prM will be specifically cleaved to yield the membrane-associated protein; whereas the arginine and lysine-rich residues on C protein have imparted it with highly-basic property to encapsidate RNA into the nucleocapsid particles (Henchal and Putnak, 1990). Besides, prM is known to prevent premature fusion of E proteins during the intracellular transport through acidic environment of trans-Golgi network (Allison *et al.*, 1995). With much interest, the 55 kilo-Dalton (kDa) E glycoprotein has been identified as the major antigenic determinant that interacts with host cellular receptors like heparin sulphate for virus entry (Faheem *et al.*, 2011). Cryo-electron microscopy (cryo-EM) shows that DENV exists as an ordered icosahedral scaffold of 90 E dimers, comprising the centrally-localised domain I (EDI), dimerisation domain II (EDII) and the immunoglobulin-like domain III (EDIII) (**Figure 2.2**) (Kuhn *et al.*, 2002).

Dengue E protein is classified as a class II fusion protein, with tightly-arranged subunits that responds to endosomal low pH to form active porin from closed β -barrel structure (Kuhn *et al.*, 2002). These proteins that arrange as dimers at neutral pH will recluster irreversibly into fusion-competent trimers upon acidification (Modis *et al.*, 2004). As shown in **Figure 2.3** (Panel A), the three soluble ectodomains (residues 1 to 392) are connected to viral membrane via a 53-residue stem segment, followed by two transmembrane (TM) domains (Nemésio *et al.*, 2011). The TM in flaviviruses is known to harbour signals for endoplasmic reticulum (ER) localisation and budding to acquire the envelope structure (Op De Beeck *et al.*, 2004). Based on Panels B and C in **Figure 2.3**, the molecular architecture shows that dengue E protein comprises predominantly β -strands and there are only two N-linked glycosylation sites on each E monomer, specifically on the asparagine residues at position 67 of EDII and position 153 of EDI (Modis *et al.*, 2003).

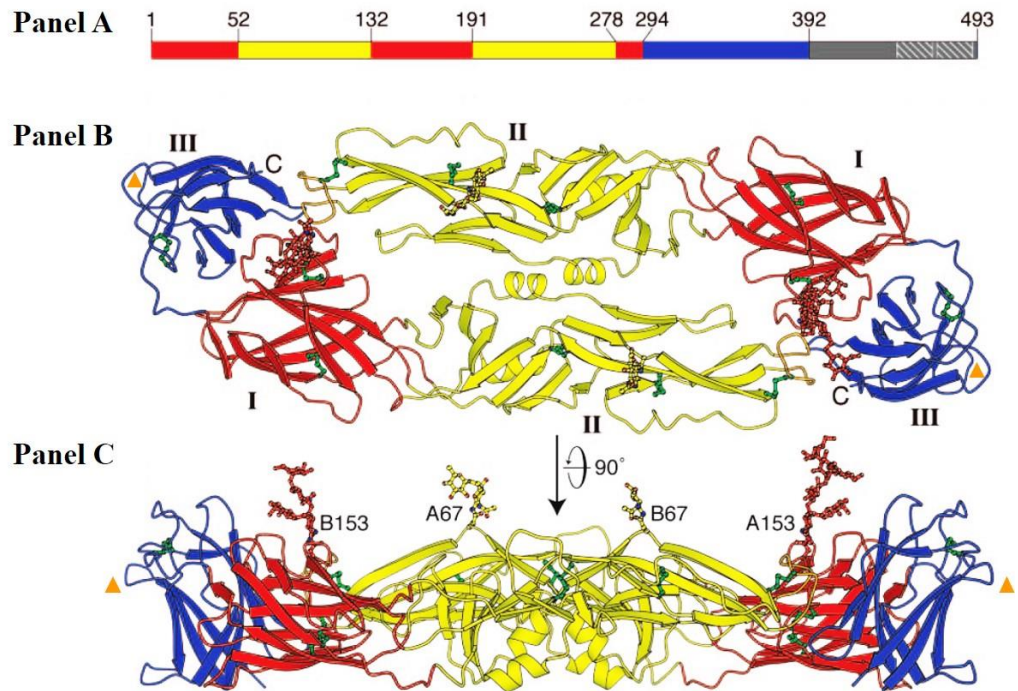


Figure 2.3: Schematic illustration of dengue E domains. Panel A: Residues arrangement of domain I (in red), domain II (in yellow), domain III (in blue) and the C-terminal transmembrane anchor is linked to folded E protein via a stem segment (in grey); Panel B: A pre-fusion conformation of dimeric E proteins along its two-fold symmetry axis; Panel C: Perpendicular view of E proteins to its two-fold axis, with the glycan on residues 67 and 153 labelled on each monomer of the dimeric E. Image reproduced with permission from Modis *et al.* (2005).

EDI is the central region with non-neutralising epitopes, acting as a hinge point for pH-induced conformational change (Roehrig *et al.*, 1998). EDII that exists as linearly discontinuous domain in E protein primary structure will make a head-to-tail contact to form dimer, but a hinge motion away from its partner is observed during the pH change to project fusion peptide at the tip (Modis *et al.*, 2003). EDII comprises epitopes that are either non-specific or reactive only after conformational change

(Roehrig *et al.*, 1998). EDIII, on the other hand, forms a highly stable structure with solvent-exposed buldge and receptor-binding motif that can elicit serotype-specific neutralisation response (Crill and Roehrig, 2001). This receptor binding loop (residues 382 to 385) is indicated with ▲ in **Figure 2.3**. A list of mammalian host cell receptors involved in binding had been explicitly described by Cruz-Oliveira *et al.* (2015). In fact, DENV EDIII is claimed to be highly antigenic (**Figure 2.4**) that can induce neutralising monoclonal antibodies and cellular immune responses (Chávez *et al.*, 2010). For these reasons, EDIII has emerged as a promising antigen for subunit vaccine production. This is also due to the notion that other structural proteins, namely EDI/II and prM, may lead to adverse antibody-dependent enhancement (ADE) event.

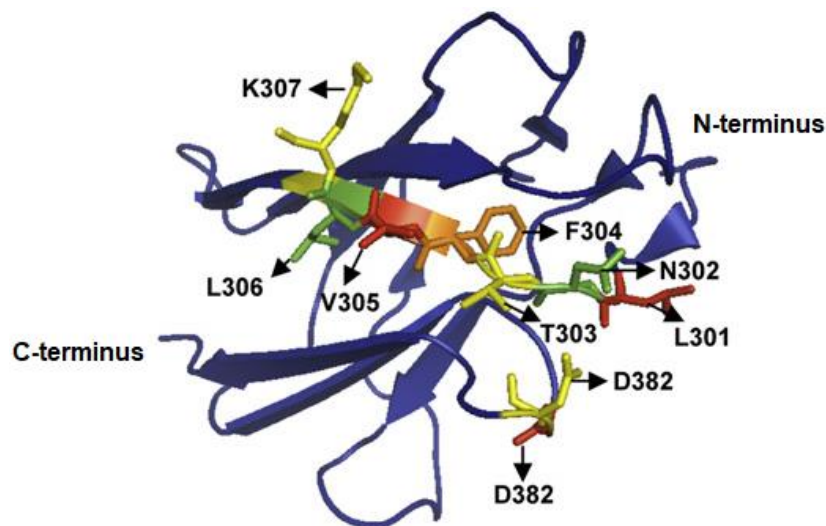


Figure 2.4: A tertiary structure of DENV EDIII, which shows the different amino acid residues involved in virus neutralisation as indicated by different colours. Image reproduced with permission from Chávez *et al.* (2010).

2.2.1 Prevalence and epidemiology

Hitherto, dengue haunts about 50% of the world population where 3.97 billion people are living in areas prone to dengue transmission (Brady *et al.*, 2012). Over the past 50 years, dengue incidence has expanded by 30 folds, spreading across the South East Asia, Americas and Western Pacific regions (WHO, 2009). In fact, the actual scenario could be worse than reported figures due to under-representation and an increasing trend of epidemiology has been predicted by many experts. Murray *et al.* (2013) had reviewed multi-factors that could drive dengue activity, including evolution of highly-virulent strain, proliferation of climate-dependent *Aedes* vectors, increased passenger travel and cargo trading, urban encroachment as well as socio-economic factors. To address the continued expansion, there is a need to devise active epidemiological surveillance systems with focused efforts on effective vector control.

The transmission of DENV has been observed from two cycles: (i) sylvatic cycle of *Aedes* mosquitoes that infect non-human primates in rain forests of Asia and Africa; and (ii) urban transmission of *A. aegypti* and *A. albopictus* that feed on human hosts (Gubler, 1998a). Interestingly, DENV isolates in most urban regions are evolved from sylvatic progenitors approximately 100 – 1500 years ago (Wang *et al.*, 2000). It is believed that the structural changes of dengue EDIII have prompted the adaptation of new peri-domestic vectors that led to resurgence of the arbovirus. According to Holmes and Twiddy (2003), the existence of DENV as four distinct serotypes could be reasoned from two hypotheses. Recent evidences were more in favour to the theory of independent lineage evolution among allopatric primate populations, instead of the sympatry evolution of antigenically-distinct serotypes to enhance transmission via ADE (Twiddy *et al.*, 2002). The present encounter of co-circulating serotypes might have by chance aggravated ADE due to antigenic dissimilarity (Holmes and Twiddy, 2003).

Dengue seems to have a longstanding history, as clinical description of a dengue-like illness known as ‘water poison’ could be found in the Chinese medical

encyclopaedia of Jin Dynasty (Gubler, 2014). The first confirmed case was coined as ‘break-bone fever’ in an epidemic that hit Philadelphia in 1780 (Rush, 1951). The term dengue which meant ‘cramp-like seizure’ in Swahili phrase only came into general use after 1827 (Rigau-Pérez, 1998). Although the earliest epidemic record could be traced back to 1780 – 1940, but it was the ecological disruptions during World War II that the intensified transmission in South East Asia and led to emergence of first dengue haemorrhagic fever (DHF) (Gubler, 1998a). Before the war, dengue outbreaks were only sporadic with one or two circulating serotypes in the tropics. It was not regarded as a major public health threat until the disease raged through Allied and Japanese forces, where movement of troops successively passed on DENV to new regions (Gubler, 2011). The first known DHF epidemic broke out in Manila within the period of 1953 – 1954, followed by Bangkok in 1975, which then expanded across South East Asia regions attributed to economic bloom and unprecedented urbanisation (WHO, 1980). In parts of Central and South American regions, the collapse of *A. aegypti* eradication campaign in early 1970s had set scene for re-infestation whereby hyperendemicity was seen following the increased circulation of new strains and serotypes (Gubler, 1998b). Ironically, the discovery of synthetic insecticides in 1940s could have led to a major breakthrough of disease eradication; however, it had failed miserably due to human negligence. Since then, disease transmission has followed the spread of its principal vector – *A. aegypti*. Continuous virus movement into new territories is mapped in **Figure 2.5**. The spread of different serotypes had accelerated in the last two decades, particularly in Asia and Latin America (Messina *et al.*, 2014). Kyle and Harris (2008) mentioned that DENV could be maintained between epidemics by overwintering in vectors, transmitted vertically in mosquitoes or could persist through silent transmission given to the high number of asymptomatic cases.

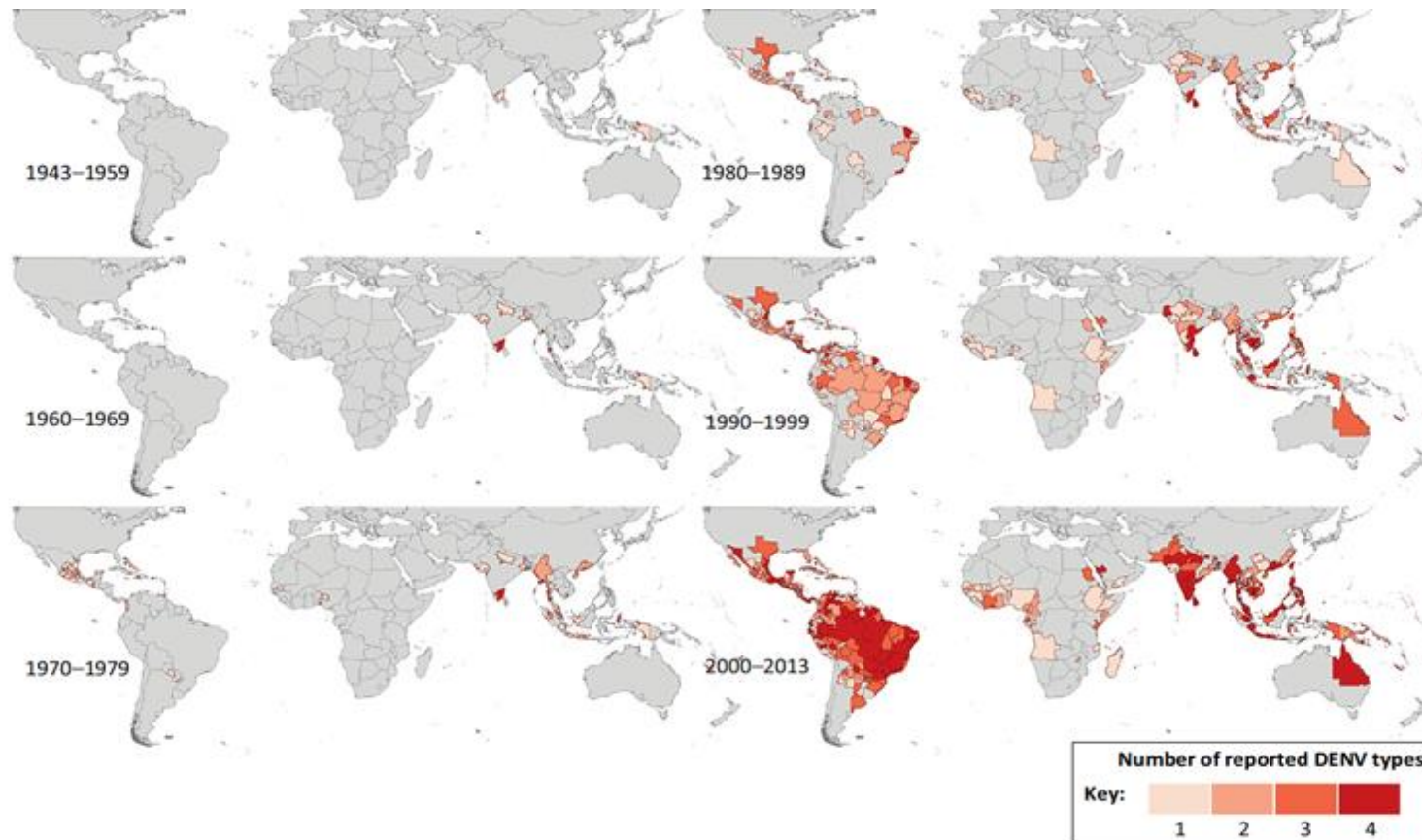


Figure 2.5: An overview on the distribution changes of DENV from year 1943 to 2013. Co-circulating serotypes 1 to 4 were denoted with different colours.

Images reproduced with permission from Messina *et al.* (2014).

The initial onset of dengue in Malaysia could be dated back to year 1901, following the transmission from Singapore to Penang (Skae, 1902). First epidemic outbreak was alarmed in 1973, recording a total of 969 dengue cases and 54 deaths (Wallace *et al.*, 1980). The condition had continued to worsen thereafter, with increasing disease infestation among urban dwellers throughout the nation (Abubakar and Shafee, 2002). All serotypes were found to be co-circulating in Malaysia, where national and states' surveillance data had noted distribution of predominant serotypes that varied over time (Mohd-Zaki *et al.*, 2014). Mudin (2015) claimed that surges of dengue cases and death tolls tend to follow 4 – 6 months after serotype shift, which may be attributed to the lack of immunity against disparate serotype. In addition, Lam (1993) suggested that the severity of disease outbreak could be predicted based on the predominant serotype at one point. Such correlation has been proven by various findings, as infection with DENV 1 or DENV 3 is more likely to occur in dengue-naïve individuals while DENV 2 appears to be associated with DHF in secondary infection (Fried *et al.*, 2010; Nisalak *et al.*, 2003; Vaughn *et al.*, 2000).

Generally, everyone is equally vulnerable to dengue infection irrespective of gender, ethnic and age groups. In Malaysia, the mostly affected community are those aged between 13 – 35 years old (Sam *et al.*, 2013). Astonishingly, 91.6% of dengue immunoglobulin G (IgG) seropositivity had been detected among randomly-selected Malaysian adults (Muhammad Azami *et al.*, 2011). Over the years 2000 – 2010, the average number of dengue cases and death tolls had seen increment of 14% and 8%, respectively per annum (Mia *et al.*, 2013). In fact, Malaysia had suffered a steep increment of 250% of number of reported cases in year 2014 alone (**Figure 2.6**). According to the latest record, a total number of 2,436 dengue cases and 2 deaths had been reported within the first two weeks of the year, as updated on 15th January 2018 (Malaysian Remote Sensing Agency (ARSM) and the Ministry of Science, Technology and Innovation (MOSTI), 2018). Considering the passive surveillance system in

Malaysia, the data may not reflect an accurate figure due to under-reporting. It is presumed that the incidence of dengue will continue to escalate if no effective intervention programmes are enforced, and situation is likely to get worse when cases peak in the spell of wet weather during monsoon season. With more than 7,000 people contracting the disease every month, it can progress into more intense scenario as seroprevalence of dengue antibodies is contributing to high fatality rate when associated with ADE during secondary infection (Pang and Loh, 2016).

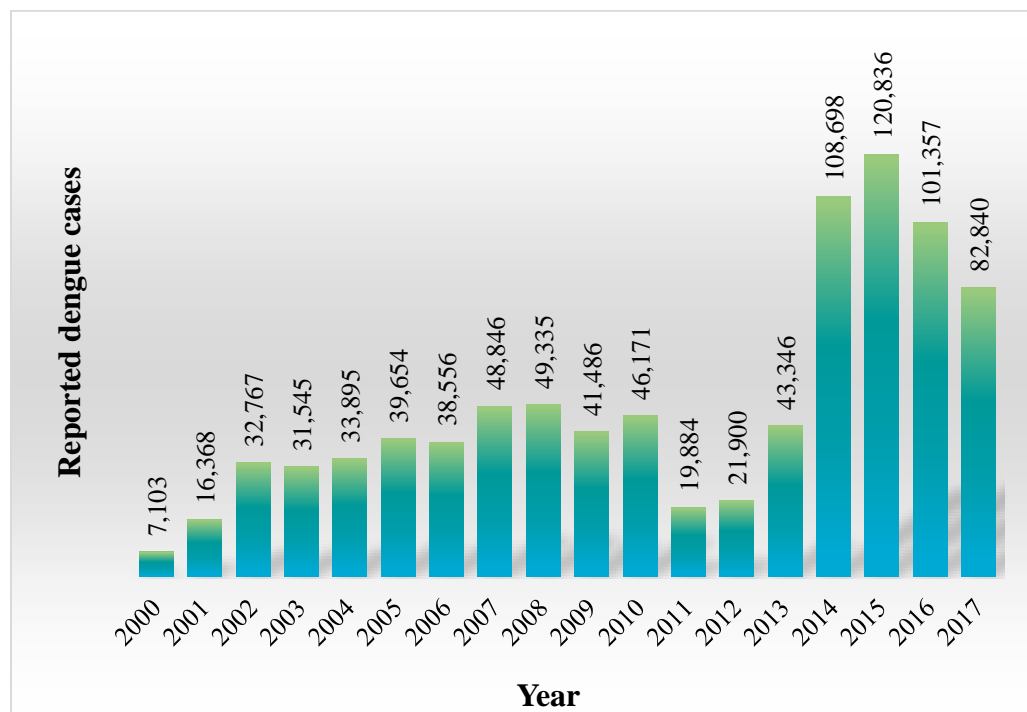


Figure 2.6: Statistical number of dengue cases reported from 2000 to 2017. Information extracted from Malaysian Remote Sensing Agency (ARSM) and the Ministry of Science, Technology and Innovation (MOSTI) (2018), and World Health Organization Western Pacific Region (WPRO) (2018).

2.2.2 Pathogenesis and infection events

Humans are infected through the bite of female *Aedes* mosquitoes that usually breed in domestic water containers. Abrupt fever accompanied by anorexia, headache, myalgia, retro-orbital pain and occasionally rashes are symptoms of classical dengue fever (DF) (Martina *et al.*, 2009). DHF however, is aggravated with haemorrhagic bleeding, thrombocytopenia and increased fluid effusion; while dengue shock syndrome (DSS) is presented by weak pulse and pressure, where profound shock may set in and lead to death within 12 – 36 hours (Martina *et al.*, 2009). Onset of DHF and DSS usually emerges during time of defervescence where physiological abnormalities of multiple organs are observed, including increased capillary permeability before hypovolemic shock (Halstead, 2015).

As infecting virus is being circulated in the peripheral blood of patients, a mosquito's bite during the febrile viraemic stage would result in disease being transmitted to another host after an extrinsic incubation period (Guzman *et al.*, 2010). Upon feeding, DENV is introduced into the bloodstream where immature skin dendritic cells (DCs), such as Langerhans cells, are targeted and local virus replication will ensue (Wu *et al.*, 2000). Then, infected DCs undergo maturation and migrate towards lymph nodes to target monocytes and macrophages (Marovich *et al.*, 2001). Infection is often amplified through dissemination of virus in the lymphatic system (Martina *et al.*, 2009).

Principally, clathrin-mediated endocytosis is deployed as the cell entry mechanism during initial infection (**Figure 2.7**). Upon binding of viral particle to cellular receptor, clathrin-coated pit will capture the complex and pinches off to the cell cytoplasm (van der Schaar *et al.*, 2008). However, during secondary infection, antigen-antibody complexes are formed between the heterotypic viruses and non-neutralising antibodies acquired from primary infection or maternal antibodies (Wang *et al.*, 2009). After internalisation, the vesicles will move through the endosomes until acidification triggers conformational change to release the uncoated single-stranded viral RNA into

cytoplasm (Green *et al.*, 2014). Translation of ORF then proceeds in rough ER to produce the polyprotein. Besides, virus-induced hypertrophy facilitates invagination of membrane to form vesicles for RNA replication, where a complementary minus-strand RNA will be synthesised to serve as template (Gebhard *et al.*, 2011). Newly-synthesised RNA then associates with the capsid, and the immature virions with prM and E proteins on surface will bud into the ER lumen (Villordo and Gamarnik, 2009). The prM is known to assist in the folding of surface-exposed E protein, and both are integrated into the lipid bilayer (Whitehead *et al.*, 2007). Following budding, the progeny virions are transported to trans-Golgi complex for prM cleavage by cellular furin protease before being released from cell (Welsch *et al.*, 2009).

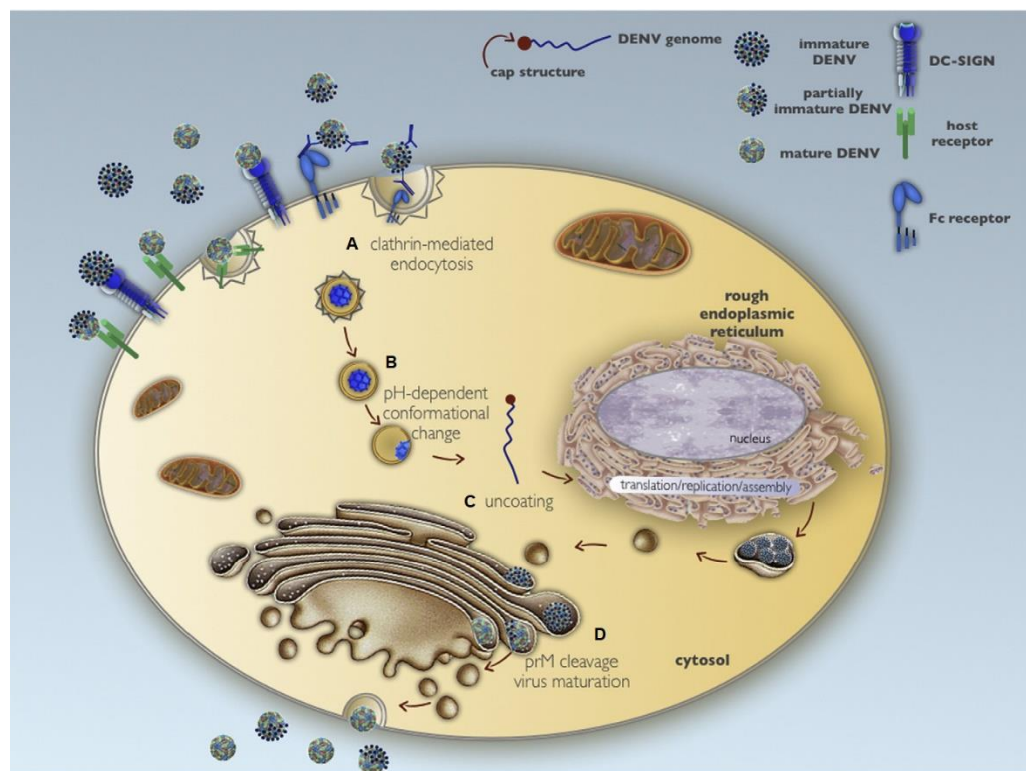


Figure 2.7: Overview of the infection events within a host cell, starting from (A) clathrin-mediated endocytosis, (B) pH-dependent conformational change, (C) uncoating, followed by (D) prM cleavage and virus maturation. Image obtained from Green *et al.* (2014).

In relation to virus pathogenesis, host immunity is often subverted by hijacking the host cellular machineries to promote infection. DENV adaption tricks are summarised as follow: (i) induction of autophagy via unfolded protein response (UPR) to trigger production of vesicles as viral replication platform; (ii) mobilisation of triglyceride by lipophagy to produce energy for replication; and (iii) sequestration of stress granules to prevent stalling of mRNA translation (Jain *et al.*, 2014). Albeit the association of disease aggravation to ADE still remains elusive, compiling evidences indicate that severe illness is resulted from increased viraemia and alteration of local milieu for viral replication (Whitehorn and Simmons, 2011). It has been proven that ADE is the strongest risk factor of DHF/DSS development (Kliks *et al.*, 1989). Jain *et al.* (2014) also emphasised that the risk of acquiring DHF in secondary infection was 40 folds higher than primary case. In specific, ADE acts by facilitating the attachment of virus-antibody complexes to Fc gamma receptor (FcγR) of a permissive cell, including monocyte and macrophage (Stephenson, 2005). Since the heterotypic serotype is not recognised for neutralisation, the pathogen is free to replicate in the macrophages and secretes vasoactive mediators that increase vascular permeability leading to hypovolemia, haemorrhage and ultimately shock (Chaudhry *et al.*, 2006). Stephenson (2005) stated that ADE could compromise disease recovery by promoting virus binding and destruction of cell-mediated immunity (CMI) components which also contain FcγR on their cell surfaces. Besides, the involvement of T cell activation in DHF/DSS has been proposed by Chaturvedi *et al.* (2000). According to **Figure 2.8**, a cascade of events is seen after the cluster of differentiation (CD)4⁺ T cells are triggered by DENV peptides presented on mononuclear cells. Then, a unique cytokine termed as human cytotoxic factor (hCF) is produced, which induces macrophages to generate free radicals and upregulate the production of proinflammatory cytokines. The balance of CMI response is also shifted from T helper (Th)1 to Th2-biased. As a result, increased plasma leakage follows with the exacerbation of disease. In addition to infection history, host genetic factors are associate with disease severity as well. For instance, the human

leucocyte antigen (HLA) allele profile is known to be unique in inducing distinct immune responses and patient with HLA-A*0207 allele is more frequently affected with DHF due to restricted antigen-binding and T cells presentation (Stephens *et al.*, 2002).

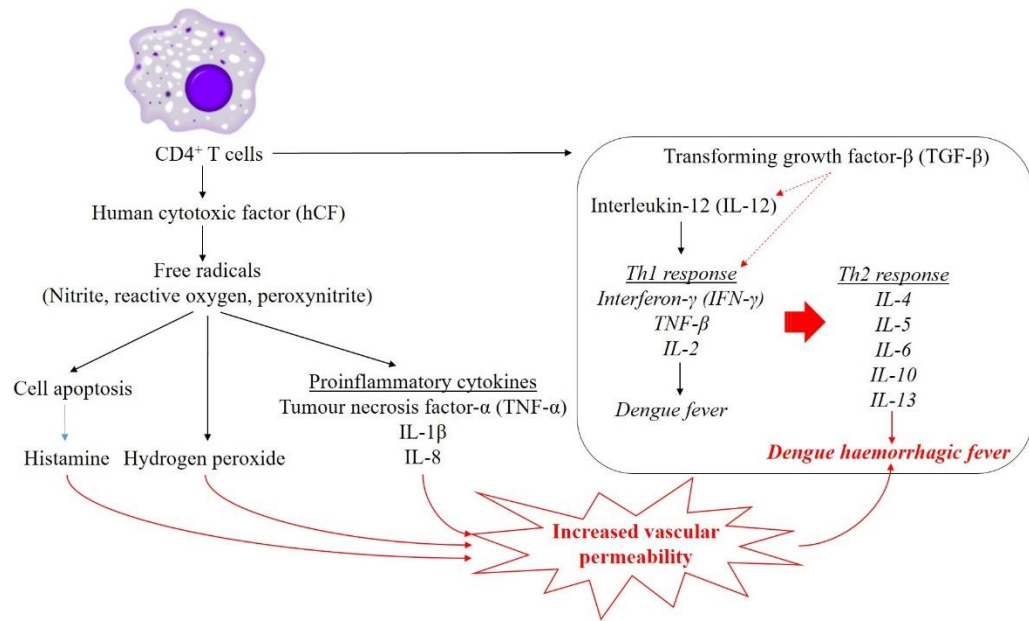


Figure 2.8: A cascade of cytokine events underlying the pathogenesis of DHF within an infected macrophage. Recruited T cells are found to release hCF and initiate a shift to Th2-type response that results in severe dengue.

Furthermore, pathogenesis of dengue disease also involves an interplay of virus virulence factor. The fitness difference between genotypes was evident as the native American DENV 2 genotype had been associated with mild disease while the introduced South East Asian genotype was afflicted with severe dengue (Rico-Hesse *et al.*, 1997). The same group then analysed the sequences of DENV 2 isolates from America and Thailand, and found that severe dengue might be related to amino acid substitutions within the polyprotein and UTRs, that led to altered antigenicity, cell attachment and viral replication (Leitmeyer *et al.*, 1999). Cologna and Rico-Hesse

(2003) also showed that the replicative ability of infectious clone was profoundly hampered when the America genotype-specific mutations was substituted into the background of South East Asia genotype. This implies that the viral determinants have evolved to increase virus output per infected cell which leads to greater disease severity.

2.2.3 Disease treatment

Current clinical practices mainly rely on administration of paracetamol and intravenous fluid, together with close monitoring of the haematocrit and platelet levels (Anfasa *et al.*, 2015). Intensive care is particularly important during the critical phase as plasma leakage could last for 24 – 48 hours and frequent fluid regime adjustments may be required throughout this period (Rajapakse *et al.*, 2012). However, fluid overload can complicate situation and lead to circulatory failure in its most severe form. Concerns are raised as fluid overload is the cause of high death tolls in Malaysia (Cheah *et al.*, 2014), which significantly reflects the incompetency in clinical management.

Up to date, there is no anti-viral drug available against dengue. This has therefore, driven public's reliance on traditional remedies that are mostly not scientifically proven. Common practices include decoction of tawa-tawa leaves and preparation of papaya leaf juice. Caution must be taken as over-dosage of certain plant extracts may be toxic. In fact, a few toxicological studies had found the genotoxic and cytotoxic properties of tawa-tawa extract (Kwan *et al.*, 2013; Rajeh *et al.*, 2012). Still, there are many on-going researches which aim to discover new drugs from the rich pool of biodiversity. For instance, a soft-gel capsule formulated with papaya leaves extract and virgin coconut oil had been introduced by the University Technology Malaysia that claimed to treat dengue (Musa, 2016). Nonetheless, it was disputed by the Ministry of Health (MOH) that the product must be clinically-tested and registered under the Drug Control Authority before releasing to the market (Mohd Shahar, 2016).

2.2.4 Vector control strategies

For decades, the only available option to curb dengue disease relies on vector control due to the lack of effective treatment and vaccine. This mainly relies on source reduction, where interventions are aimed at minimising the oviposition sites to reduce dengue transmission. Ooi *et al.* (2006) highlighted that law enforcement and public education are also crucial in driving the success of vector control. However, prevention has become increasingly problematic as these mosquitoes are circulating in close contact with humans and most major cities are populated with 15 – 20 million people (Gubler, 2011). It can be an uphill task if community engagement is not strongly advocated. Preventive measures were often hampered by public's underestimation of susceptibility to dengue infection and the lack of concerted community efforts (Wong and AbuBakar, 2013). Moreover, eradication programmes in most endemic countries have ambiguous goals with diluted commitments that are initiated only during time of epidemics (Morrison *et al.*, 2008). For instance, Malaysia adopts a passive surveillance system, which relies on health-care practitioners to notify on suspected dengue cases before dispatching officers to investigate and arrange chemical fogging (Packierisamy *et al.*, 2015). Nonetheless, WHO (2012) highlighted that successful vector control must be centred between vigilant monitoring and sustainable interventions in order to achieve significant impact. To date, disease containment comprises a number of methods ranging from chemical application, genetic control and the use of biocontrol agent. Application of these tools will be discussed in relevant to the strategies adopted in Malaysia.

2.2.4.1 Application of insecticides

Most of the regimes in practice such as insecticidal treatment and fogging have failed to produce expected disease containment due to high cost and limited effectiveness (Lacroix *et al.*, 2012). In 2010 alone, Malaysia had spent US\$73.5 million

on dengue vector control and 60% of the cost was channelled to chemical fogging and premise inspections (Packierisamy *et al.*, 2015). Furthermore, extensive applications have adversely prompted the emergence of insecticide-resistant mosquitoes. Although malathion was the first insecticide to be used for fogging; however public acceptance was low due to the pungent and oily residues (Teng and Singh, 2001). For that reason, water-based pyrethroid was used as the primary insecticide since 1996. However, the effectiveness of permethrin, deltamethrin and malathion was deteriorating as chemical resistance had been detected from the field strains across major cities in Malaysia (Ishak *et al.*, 2015; Shafie *et al.*, 2012; Wan-Norafikah *et al.*, 2010). In order to revamp vector control, a novel deltamethrin formulation was developed and used for outdoor residual spraying (Lee *et al.*, 2015a). In the long run, this would not be a cost-effective approach due to the constant need to re-formulate chemical insecticide.

2.2.4.2 Genetically-modified mosquitoes

A new vector suppression technology known as Release of Insects with Dominant Lethality (RIDL) was also adopted by the Malaysian government as part of dengue control efforts. This transgenic approach is known to outweigh the conventional irradiation of mosquitoes, which can introduce random lethal mutations and cause significant reduction in field fitness (Benedict and Robinson, 2003). Sterile male *A. aegypti* (OX513A) was engineered to harbour a dominant, repressible and late-acting lethal transgene insertion, which can be differentiated through the expression of red fluorescence (Phuc *et al.*, 2007). The study reported that, without tetracycline, high expression of the lethal factor in a positive feedback loop would limit the survival of transgenics by 95 – 97% at late-larval or early-pupal stage. Moreover, the mating competitiveness of RIDL male mosquitoes was not affected when compared to wild type strain under both laboratory and semi-field settings (Lee *et al.*, 2013; Massonnet-Bruneel *et al.*, 2013). Hence, the first open field trial was conducted in December 2010,

where genetically-modified (GM) mosquitoes were released into the uninhabited forest of Bentong. Albeit the fitness of modified strain was not affected in open field settings, the data obtained was inconclusive to demonstrate vector suppression as the release site was far beyond their natural habitats in the urbans for mating (Lacroix *et al.*, 2012). As a result, the project was shelved in 2015. Worthwhile to mention, lesson should be learnt from public backlash against the release of GM mosquitoes. This is because community engagement is indispensable to gauge support and promote sustainable implementation of a new programme.

2.2.4.3 Biocontrol agents

The use of *Wolbachia* transinfection in *A. aegypti* has gained increasing attention following the discovery of life-shortening property of *Wolbachia* in *Drosophila melanogaster* (Min and Benzer, 1997). According to Hoffmann *et al.* (2015), *Wolbachia* can suppress the ability of mosquitoes to transmit disease by altering vector reproduction via cytoplasmic incompatibility (CI) and exhibiting virus blockage activities. Although early study with *wMelPop-CLA* strain showed that it could induce complete CI, but the high fitness costs was undesirable (Yeap *et al.*, 2011). Hence, most studies have established the use of *wMel* strain for *Wolbachia* interventions (Walker *et al.*, 2011b); in which the infection could persist in the wild populations of mosquitoes for more than two years in Australia (Hoffmann *et al.*, 2014). However, it was recently found that *wMel* strain may suffer from reduced establishment when mosquitoes were exposed to heat stress, and hence the heat-tolerant *wALbB* strain was preferred given to the higher chance of persisting in natural populations (Ross *et al.*, 2017). In Malaysia, the field release of *Wolbachia*-infected mosquitoes had begun in Kuala Lumpur in March 2017. Nevertheless, the paradigm of *Wolbachia* release requires further monitoring on the direct test of efficacy. Predictions are made that dengue can mutate to acquire stronger virulence or partially escape transmission blockage; meanwhile, the evolution of

Wolbachia may be possible since life-shortening property is also limiting the bacterial establishment (Bull and Turelli, 2013).

2.2.5 State of vaccine research

The call for dengue vaccine development is an endless priority. This is not only driven by the lack of dengue-specific drugs and treatment, but also seeing that the efficacy of current vector control regimes is rather inconsistent. Waves of vaccine development have increased dramatically over the decade, with the competition to license an immunoprotective dengue vaccine has been progressing aggressively among Sanofi Pasteur, Walter Reed Army Institute of Research, Naval Medical Research Center and so on. Nonetheless, dengue vaccine development remains to be immensely challenging owing to: (i) the co-circulation of multiple serotypes with unpredictable predominance at different time points; (ii) knowledge gap in understanding DENV pathogenesis; (iii) lack of reliable animal model; and (iv) the complex interplay of host immunology (McArthur *et al.*, 2013). In general, there are two types of vaccines: the traditional one based on live attenuated or inactivated virus, and the more recent development of recombinant subunit vaccine that expresses the primary antigenic determinant. Following literatures are focused on vaccine candidates that have been assessed in clinical trials (**Table 2.1**).

Table 2.1: A list of dengue vaccine candidates in clinical development.

Product	Type	ClinicalTrials.gov identifier	Status	Company
CYD-TDV	Live attenuated virus (LAV)	NCT01373281 NCT01374516	Phase 3 (completion date revised to 2017 and 2018) *	Sanofi Pasteur
TV003/ TV005	LAV	TV003: NCT01696422 NCT02332733 NCT02406729 TV005: NCT02873260 NCT02879266 NCT02678455	TV003: Phase 2 and 3 (on-going) TV005: Phase 1 and 2 (on-going)	National Institute of Allergy and Infectious Diseases and Butantan Institute
TAK-003	LAV	NCT02747927	Phase 3 (on-going)	Takeda
TDEN	Inactivated whole virus	NCT00468858	Phase 2 (completed in 2010)	Walter Reed Army Institute of Research and GlaxoSmithKline
D1ME ¹⁰⁰	DNA	NCT00290147	Phase 1 (completed in 2009)	Naval Medical Research Institute
V180	Subunit protein	NCT01477580	Phase 1 (completed in 2014)	Hawaii Biotech

Annotation: * Denotes that clinical trials should have been completed by 2014.

2.2.5.1 Live attenuated virus (LAV) chimeric vaccine

Following 20 years of efforts, the world first dengue vaccine was licensed by Sanofi Pasteur in December 2015, branded as Dengvaxia[®]. The ChimeriVax Technology was first developed by St. Louis University to generate a molecular clone of yellow fever virus (YFV) 17D strain with JEV structural proteins (Chambers *et al.*, 1999). The C protein was excluded, or else the chimera would fail to recover due to inefficient protease processing on the JEV C/prM junction and defectiveness in viral replication and packaging. Subsequently, the chimeric virus was tested in mice and showed effective protection (Guirakhoo *et al.*, 1999). With the successful prototype, Guirakhoo *et al.* (2000) then engineered the first YFV 17D/DENV 2 chimera with heterologous prM and E proteins. Continuous efforts led to generation of a tetravalent YF/DENV 1-4 using genes from human isolates of DENV, and the chimeras obtained from RNA-transfected Vero cells were tested in non-human primates as monovalent and tetravalent formulations (Guirakhoo *et al.*, 2001). Despite tetravalency protection was displayed, the higher activity of YF/DENV 2 demanded further refinement, thus reconstruction of mutated viruses, plaque purification and dose adjustment were carried out (Guirakhoo *et al.*, 2002; Guirakhoo *et al.*, 2004). With that, the finalised tetravalent formulation consisting 5-log plaque forming units of each serotype was tested in a phase 1 trial. Referred as chimeric-yellow fever-dengue (CYD), the vaccine was shown to be well-tolerated with full seroconversion among flavivirus-naïve adults; however, the first dose induced response mainly against DENV 2 and DENV 4, thus longer immunisation schedule was proposed to limit short-term viral interference (Morrison *et al.*, 2010).

Nevertheless, several reviews have condemned that serotype interferences represent a critical issue that needs to be addressed by Sanofi. *In vivo* competition of viral replication and epitopes-linked immunodominance had been observed when the vaccine was administrated as a tetravalent formulation (Guy *et al.*, 2009). Essentially, imbalance viral replication among four monovalent serotypes can jeopardise the desired

level of immunoprotectivity (Imoto and Konishi, 2007). The phase 2b clinical trial conducted in Thailand revealed that CYD did not offer protection against DENV 2 following three doses (Halstead, 2013). The possibility of antigenic mismatch between DENV 2 and CYD 2 vaccine design was perceived as a factor that could diminish the overall efficacy (Sabchareon *et al.*, 2012). Looking at the phase 3 clinical trials, the vaccine had only conferred modest protection in Asia (56.5%) and Latin America (60.8%), and efficacy against DENV 2 still remained as the lowest (Capeding *et al.*, 2014; Villar *et al.*, 2015). In the long run, more conclusive data on its safety and efficacy profiles are still needed. This is also considering that DENV 2 is often associated with outbreaks of severe dengue. Besides, the prolonged 12-month immunisation schedule and reduced efficacy for dengue-naïve subjects present major hiccups in CYD implementation (Whitehead, 2016). Though Dengvaxia® had been approved in 19 countries, long-term safety assessment indicated that the risk of hospitalisation was higher among CYD paediatric recipients, as compared to placebo control in their third year post-vaccination (Hadinegoro *et al.*, 2015). Thus, Dengvaxia® can only be administered to individuals aged between 9 – 45 years in endemic areas (Wilder-Smith and Massad, 2016); which signifies that a universal vaccine is still not available yet. To its worst, Sanofi had recently announced that Dengvaxia® could induce severe dengue in dengue-naïve subjects following vaccination (Sanofi, 2017); and this had spurred intense backlash, particularly in the Philippines following the deaths of 8 children (Antiporda, 2018). Overall, one of the key lessons learnt is the impact of partial protection that not only fails to prevent infection but may also contribute to risk of acquiring severe dengue.

Meanwhile, another LAV vaccine candidate in the pipeline was co-developed by the National Institute of Allergy and Infectious Diseases (NIAID) and Instituto Butantan. Its preliminary work started with virus attenuation, that was achieved by nucleotide deletions in 3' UTR or chimerisation with other serotype, and the most favourable

monovalent vaccines had been selected (Durbin *et al.*, 2011). Different admixtures of the pre-selected monovalent components were then tested in a phase 1 trial, of which TV003 had been identified as the best tetravalent candidate given to the 90% seropositivity after a single dose (Durbin *et al.*, 2013). Yet, it also showed a weaker seroconversion against DENV 2 like CYD. Thus, optimisation was performed and the resulting TV005, with increased DENV 2 dose, seemed to afford higher immunogenicity as compared to TV003 (Kirkpatrick *et al.*, 2015). Nevertheless, the efficacy of TV003 was re-assessed in a DENV 2-challenge model (Kirkpatrick *et al.*, 2016), and complete protection were observed among the volunteers without signs of rash, neutropenia and thrombocytopenia. Another phase 1 trial with TV003 also showed that the candidate had performed well with 87% tetravalent response in flavivirus-experienced subjects (Whitehead *et al.*, 2017). Currently, TV003 has progressed into phase 2 and 3 clinical trials and while TV005 is being evaluated in phase 1 and 2 trials.

Takeda to which had acquired Inviragen, is also evaluating its tetravalent vaccine candidate registered as TAK-003 (also known as TDV). The vaccine virus was developed based on the genetic background of an attenuated DENV 2 strain designated as PDK-53; which was then formulated into three chimeric viruses by having the prM and E replaced from wild-type DENV 1, DENV 3 and DENV 4 correspondingly (Osorio *et al.*, 2011). Albeit phase 1 trials revealed that TDV did induce neutralising antibody response against all serotypes, but the percentage of subjects who acquired tetravalent protection varied between 44% – 80% and it was very likely attributed to lower anti-DENV 4 titres (Osorio *et al.*, 2015). Hence, the dosage of TDV-4 was increased by three-fold to boost the immunogenicity against DENV 4 (Rupp *et al.*, 2015). A recent phase 2 data showed that TAK-003 was able to sustain immune responses against four DENV serotypes in individuals aged 2 – 17 years living in dengue-endemic areas, irrespective of dosing schedule or pre-exposure to dengue infection (Sáez-Llorens *et al.*,

2017). From that, TAK-003 had presented superior safety profile that might surpass Dengvaxia® performance. A phase 3 clinical trial is currently on-going in 8 dengue-endemic countries and results are expected to be released by late 2018.

2.2.5.2 Purified inactivated whole virus vaccine

One of the earliest vaccine developments came from the attenuation of DENV through intracerebral inoculation in mice (Sabin and Schlesinger, 1945). At first, the United States Army had focused on production of mouse brain vaccines; but later on it was replaced with the safer propagation in cell cultures (Innis and Eckels, 2003). This project led by Walter Reed Army Institute of Research (WRAIR), did not yield success due to varying levels of attenuation and immunogenicity exhibited by each serotype. The adoption of serial passage in primary dog kidney cells then offered a better alternative, whereby candidates had been selected for phase 1 human trials after assessing infectivity in rhesus monkeys (Eckels *et al.*, 2003). These monovalent candidates were assessed in a series of trial runs to develop potential tetravalent formulation (Kanasa-Thanan *et al.*, 2003; Sun *et al.*, 2003). All of the studies mentioned thus far were completed in 2000 and since then, further clinical assessment was conducted in collaboration with GlaxoSmithKline (Innis and Eckels, 2003). Phase 2 trials had an expanded evaluation of selected formulations and the best candidate was identified, conferring 63% tetravalent neutralisation after administration of two dosages at 6-month apart (Sun *et al.*, 2009). Subsequent paediatric study with flavivirus-naïve children indicated that the vaccine was well-tolerated with 100% tetravalent protection acquired one month after second dose (Simasathien *et al.*, 2008). Similar testing on seronegative Thai infants recorded no adverse events, but with a lower tetravalent seroconversion of 53.5% (Watanaveeradej *et al.*, 2011). Thomas *et al.* (2013) then re-derived a new candidate known as TDEN, by subjecting the precursor strain to additional passages in fetal rhesus lung cells, formulating the monovalent components

with carbohydrate stabiliser and lyophilising the final product in tetravalent form. Clinical profile of the new candidate was shown to be safe for administration in healthy adults, despite not much differences were observed when compared to its precursor. A phase I/II trial indicated that two doses of TDEN were able to prime tetravalent protection in DENV-naïve subjects aged between 1 – 50 years old (Bauer *et al.*, 2015). Nevertheless, no information on follow-up clinical trial can be found.

2.2.5.3 DNA vaccine

On the other hand, Naval Medical Research Institute has ventured into the less-adopted DNA vaccine technology. They started off with the construction of several recombinant plasmids expressing different structural segments of DENV 1 and each construct was then injected into mice to test for optimal neutralising response (Raviprakash *et al.*, 2000). The ME100 construct that harboured the prM along with full length E sequence was chosen for further testing based on the best neutralisation activity. Partial to complete protection was observed when immunised rhesus macaques were subjected to viral challenge (Raviprakash *et al.*, 2000). Following a series of pre-clinical trials, a prototype testing of DENV 1 vaccine candidate (D1ME¹⁰⁰) was conducted among flavivirus-naïve adults in a phase 1 clinical trial (Beckett *et al.*, 2011). Unexpectedly, only those who received high dosage developed anti-dengue response but it was merely less than 50% of the subjects. A breakthrough was achieved when the tetravalent dengue DNA vaccine, consisting equal mixture of serotype-specific plasmid DNAs formulated with Vaxfectin[®], which was able to boost the anti-dengue neutralising response in primates (Porter *et al.*, 2012). A concurrent testing in New Zealand white rabbits also indicated that the DNA vaccine was well-tolerated with 100% neutralisation against all serotypes (Raviprakash *et al.*, 2012). As attractive as it may sound, though DNA vaccine is comparably stable, easy to modify and scale-up, but the ability to stimulate robust immunogenicity remains to be verified.

2.2.5.4 Subunit protein vaccine

Hawaii Biotech initially attempted to express dengue recombinant E in both yeast and mammalian cells; however, it did not yield success until the *Drosophila* Schneider-2 (S2) cell expression system was adopted (Coller *et al.*, 2011). The S2 cells were transformed to secrete full length prM sequence along with 80% N-terminal of E molecule, designated as DEN-80E (Clements *et al.*, 2010). The purified 80E subunits of each serotype were then combined and adjuvanted with ISCOMATRIX[®] for immunogenicity testing in animal models. Although neutralisation against all serotypes was obtained, but seroconversion was lower against DENV 4. Further attempts were explored by Govindarajan *et al.* (2015) to improve the immunogenicity of the tetravalent vaccine, particularly on DEN4-80E. A phase 1 clinical study of ISCOMATRIX[®]-adjuvanted V180 demonstrated that high seroconversion rates of 85.7% – 100% was obtained following administration of three doses at 1-month intervals (Lim, *et al.*, 2016). The findings thus far attested the superiority of subunit protein vaccine as immunisation of low dosage with short dosing schedule was sufficient to confer desired immune protection.

2.3 Plants as biofactories in molecular pharming

In recent years, the pressure from growing clinical demands and limitations of established systems have spurred intense interest of utilising plants as ‘green factories’ for bioproduction. With the advent of modern biotechnology, molecular techniques can now be applied to synthesise commercially valuable products using plant system, either by manipulation of biosynthetic pathway or alteration to desired-feature (Slater *et al.*, 2003). This has essentially sparked the idea of ‘Molecular Pharming’, which harnesses the power of agriculture to produce recombinant pharmaceutical proteins such as antibodies, vaccines and therapeutic enzymes. In fact, Barta *et al.* (1986) was the first to demonstrate the feasibility of using tobacco to express human-growth hormone. Since then, *in planta* production of recombinant therapeutics has gained increasing adoption until it is successfully used to produce the ZMapp monoclonal antibody cocktail as a therapeutic for Ebola treatment (Davidson *et al.*, 2015). To date, there are more than 25 plant-made pharmaceuticals that have been assessed in clinical trials (Loh *et al.*, 2017). Considering that there is only a handful of good manufacturing practice (GMP)-compliance plant manufacturing facilities around the world, the achievement attained thus far is significant and an optimistic future is foreseen from the increasing industrial engagement (Sack *et al.*, 2015).

2.3.1 Merits of plant-based expression system

Conventionally, the production of pharmaceutical proteins has mainly relied on bacteria and mammalian cells. The use of *E. coli* is essentially favoured for the simplicity and rapid growth rate which makes it possible to produce recombinant pharmaceuticals within a few hours. However, the expression of poorly-soluble or misfolded proteins has become a major drawback that limits the adoption of bacterial system (Gecchele *et al.*, 2015). The use of mammalian cell-system, on the other hand, is hindered by heavy operational costs, limited scalability and risk of contamination

with human-transmissible pathogens (Chen and Lai, 2014). Although yeast and insect cell can be used as alternative expression systems, however their propensity to mannose protein may lead to undesirable antigenicity (Demain and Vaishnav, 2009). As a result, plant system has emerged as a more convenient, economical and safer alternative that cannot be matched by many existing production systems.

As summarised in **Table 2.2**, plant generally outweighs other systems in terms of low cost, high scalability, capacity to perform protein post-translational modifications, increased safety as well as the ease of storage and distribution. Firstly, the start-up and operation costs for plant-based system are comparably lower than others since neither expensive reactor or reagent is required. In fact, the production cost of plant-made pharmaceuticals is only 2 – 10% of microbial systems and 0.1% of mammalian cell cultures (Yao *et al.*, 2015). Plants are fascinating in the sense that they are photoautotrophs that are inexpensive to grow, and production can be easily scaled-up by using established planting infrastructure. Besides, plants are able to produce complex proteins that resemble native conformation such as secretory immunoglobulin A (IgA), collagen and spider silk (Tschofen *et al.*, 2016). It is a general consensus that plants do not harbour mammalian pathogen, endotoxin or oncogene, which eliminates regulatory concerns and the cost associated with product screening and purification. Plants also offer added feature of product stability where long-term storage of protein is feasible via accumulation in cereal seeds (Ramessar *et al.*, 2008). The expression of protein in edible fruits might even exclude the need for downstream processing and cold chain shipment (Twyman, 2004).

Table 2.2: A comparison of merits offered by different expression systems. The scoring (+) was interpretatively made based on the following review papers: Demain and Vaishnav (2009); Loh *et al.* (2017); Ma *et al.* (2003).

System	Production cost	Lead time	Scalability	Post-translational processing	Purity	Storage and distribution
Bacterium	+++++	++++	++++	+	++	+++
Yeast	++++	+++	++++	++	++++	+++
Insect cell culture	+++	++	+++	+++	++	++
Plant cell culture	+++	+++	+++	++++	++++	+++
Plant	+++++	+ ^a +++ ^b	+++++	++++	++++	+++++
Mammalian cell culture	++	++	+	+++++	+	+
Animal	+	+	++	+++++	+	+

Annotation: ^a Refers to stable gene integration into plant nucleus or chloroplast; ^b Refers to transient expression of whole plant.

2.3.2 Plant transformation strategies

The history of plant transformation began in 1983, after several research groups had demonstrated the potential of introducing bacterial genes into plant genome (Bevan *et al.*, 1983; Fraley *et al.*, 1983; Herrera-Estrella *et al.*, 1983). Following that, genetic engineering of plants has been applied for fundamental study of plant physiology, genetic improvement of crop varieties and molecular pharming. To date, plant transformation is achieved via (i) stable integration of foreign gene into the plant nuclear or chloroplast genome, and (ii) transient expression of foreign gene without integration into host genetic constituent.

2.3.2.1 Stable integration versus transient expression

Stable transformation facilitates the establishment of transgenic lines with inheritable traits, which offers the reproducibility of long-term production of a biologics using master seed banks (Chen and Lai, 2014). Technically, stable gene integration can be achieved via a range of methods including *Agrobacterium*-mediated gene transfer, biolistic, polyethylene glycol treatment, microinjection and electroporation. However, the adoption of stable transformation is often held back by the long developmental time involving plant regeneration procedures, along with issues like gene silencing and potential outcrossing to food crops (Rybicki, 2009). In the 1980s, Janssen and Gardner (1989) already discovered that the frequency of gene transfer achieved by transiently-expressed β -glucuronidase (GUS) was 1,000-fold higher than stable integration. At that time, transient expression was not popular and was merely used for testing efficiency of constructs before undertaking stable transformation. Kapila *et al.* (1997) then demonstrated the feasibility of using *Agrobacterium*-mediated infiltration to achieve high level of GUS expression, and since then, transient assay has been widely adopted to produce recombinant proteins within a matter of days. Technically, it eliminates the tedious works on plant tissue culture and regeneration, and introduces biocontainment

since the transgene is not integrated into host genome. Particularly for vaccine production, transient expression enables fast screening of candidates in prompt response to emerging outbreak. Industrial processes have been deliberately optimised for scaling-up production to commercial level that can outcompete the stable transformation (D'Aoust *et al.*, 2010). Nowadays, transient expression is mostly achieved via recombinant virus infection or *Agrobacterium* infiltration system, that combines the benefits of speed and convenience as compared to transgenic expression (Thuenemann *et al.*, 2013).

2.3.2.2 Agroinfiltration strategy

To date, agroinfiltration is generally the method of choice used to deliver binary vector and plant virus-based vector into host plant. For binary vector, the transgene is inserted to the transfer-DNA (T-DNA) region and will be delivered into plant nucleus upon infiltration. Meanwhile, the initial strategy of exploiting 'full virus' as viral vector had failed due to the instability of virus genome resulting from large insertion (Gleba *et al.*, 2007). Thus, 'deconstructed' vector has been re-built to retain only elements required to drive high transgene expression and locomotion is resolved by *Agrobacterium*-mediated gene transfer. The merger of plant virus vector and *Agrobacterium* was first demonstrated by Grimsley *et al.* (1987), whereby viral infection could still be initiated upon infiltrating a construct with cauliflower mosaic virus (CaMV) genome inserted to the T-DNA. This approach does not only ensure efficient systemic spread, but also extends to the use of plant viruses that in nature are not mechanically transmissible (Peyret and Lomonosoff, 2015). At present, most viral vectors have been integrated into binary vectors such that the genetic components of viral origin are placed within the T-DNA and will be transferred into host upon infiltration (Lico *et al.*, 2008).

Agroinfiltration is mostly performed using either syringe or application of vacuum. Syringe infiltration was first described by Schöb *et al.* (1997), that involves manual injection of infiltration media using a needleless syringe. As adopted in this study, the simplicity of syringe technique has made it convenient to assess different constructs in laboratory setting, either by infiltrating the entire leaf with a specific construct or perform multiple assays as distinct spots. Adoption of vacuum infiltration however, is often primed for its automated scalability which is more suitable for industrial application (Chen *et al.*, 2013b). Recently, a new air-brush technique has been introduced to allow direct spraying of bacterial suspension onto plant (Jin *et al.*, 2015). This approach might have the potential to be mechanised into a high-throughput system since hundreds of plants could be infiltrated within 20 minutes.

Specifically, a non-replicative system is opted in this study with the use of pEAQ-*HT* binary vector. In relation to vector development, initial efforts were focused on modifying the smaller genomic RNA of cowpea mosaic virus (CPMV) to yield a replication-competent deleted RNA-2 construct (delRNA-2), which was replicated by RNA-1 (Cañizares *et al.*, 2006). Later then, it was found that high expression could be achieved with the co-inoculation of P19 silencing suppressor (Sainsbury *et al.*, 2008); whereby the transcribed mRNA was stable enough that made RNA-1 no longer required to achieve high expression. The removal of replicase had therefore led to the development of a non-replicative system. As Sainsbury and Lomonosoff (2008) continued to work on delRNA-2 design, they discovered that removal of two upstream AUG codons had boosted protein expression up to 10 folds, possibly due to enhanced translational efficiency. Since then, the new expression system based on mutated 5' UTR of delRNA-2 was termed as CPMV-hypertranslational (*HT*) system. Overall, the non-replicative nature of CPMV-*HT* makes it more attractive than replicon system, whereby it is not affected by transgene size limitation, virus exclusion nor transcript mutation issue (Peyret and Lomonosoff, 2013). Subsequent efforts give rise to the

development of pEAQ series vectors (Sainsbury *et al.*, 2009), which is now widely adopted by the Plant Production of Vaccines (PLAPROVA) consortium. In fact, various organisations have explored the use of pEAQ-*HT* system to express plant-based vaccines including Medicago's seasonal influenza plant-based quadrivalent virus-like particle (QVLP) vaccine (Pillet *et al.*, 2016), in addition to WHO-funded development of plant-based poliovirus vaccine (Marsian *et al.*, 2017).

2.4 Strategies adopted in current study to enhance vaccine presentation

Ideally, the development of vaccine products that can induce strong humoral and cell-mediated immune responses is highly desired. As purified subunit proteins may be less immunogenic than whole virus preparations, adjuvant is often formulated to boost the immunogenicity of subunit vaccines. Besides, adjuvant also improves the durability of a vaccine via reduced antigen dosage and immunisation, improves vaccine efficacy in immuno-compromised individuals and improves the quality of immune responses by guiding appropriate Th1/Th2 response (Coffman *et al.*, 2010). Aside from the conventional use of aluminium salts and oil-in-water emulsions, new strategies have focused on using alternative adjuvants such as protein conjugation partners, nanoparticles and virus-like particles (VLPs) (Gerdtts *et al.*, 2013). By doing so, this would obviate the need to mix components as in conventional vaccination. In fact, WHO also prefers the development of ‘ready-to-use’ vaccines that can enhance the efficiency, convenience and safety of immunisation programmes, and are particularly beneficial for developing nations with limited medical settings (Mansoor *et al.*, 2013).

2.4.1 Protein conjugation

To date, several types of modified bacterial toxins have been used for the design of conjugate vaccine including the non-toxic mutant of diphtheria toxin known as CRM₁₉₇ (Micoli *et al.*, 2011), *Pseudomonas aeruginosa* exotoxin A (rEPA) (Ho *et al.*, 2006), heat-labile enterotoxin (LT) from *Escherichia coli* (Martin and Nashar, 2013) and cholera toxin (CT) from *Vibrio cholerae* (Xue *et al.*, 2016). However, there was a controversy raised regarding the effectiveness of rEPA as a booster following four failed clinical trials (Pier, 2007), and the fact that it was yet to be approved for human use made it less clinically-relevant. Comparatively, LT and CT have been extensively-used and are among the strongest adjuvants for both mucosal and parental immunisations (Mattsson *et al.*, 2015). Although CT and LT share about 80% of sequence homology

(Dallas and Falkow, 1980), the use of CT is favoured for the ability to skew towards Th2 response to acquire sterilising immunity (Connell, 2010).

2.4.1.1 Cholera toxin B subunit (CTB)

The gram-negative *V. cholerae* causes cholera disease by secreting CT that binds to mucosal cells and activates the adenylate cyclase system (van Heyningen, 1976). Structurally, the toxin is made up of two subunits: the single 'heavy' 28 kDa toxic subunit A (CTA) and the 56 kDa aggregate of 'light' subunits B (CTB) (Holmgren, 1981). In specific, CTA is proteolytically split to two parts upon host entry, into the toxic-active globular CTA1 and CTA2 that protrude into the tunnel formed by CTB (Gill, 1976). As illustrated in **Figure 2.9**, five monomers of CTB will interact via 130 hydrogen bonds and 20 salt bridges to assemble as a homopentamer that embeds the CTA (Sanchez and Holmgren, 2011). The authors also highlighted that the tight packing of CTB might have contributed to its outstanding stability in intestinal milieu.

Nevertheless, the use of CT must be rendered safe as it is proven to be too toxic for clinical use. For instance, oral administration of a mere 5 µg purified CT caused diarrhoea in volunteers while those received 25 µg suffered from 20-litre cholera purge (Levine *et al.*, 1983). To avoid toxicity, CTB can be exploited as the non-toxic derivative that has the ability to induce intracellular signalling events to activate murine B cells and macrophages (Schnitzler *et al.*, 2007). This may essentially correlate to CTB affinity for monosialotetrahexosylganglioside (GM1) distributed on the surface of most nucleated cells, including leucocytes (Freytag and Clements, 2015). By conjugating antigen with CTB, enhanced antigen uptake and presentation are thus anticipated. Stratmann (2015) even stated that the total B cell repertoire can be effectively converted into antigen presenters as mediated by CTB selective binding to GM1. Nevertheless, there are a few considerations that need to be taken while designing a CTB-fusion construct. Genetic coupling to a N-terminal partner is known to hamper the pentamer

assembly (Liljeqvist *et al.*, 1997), whereas for C-terminal fusion, it is case-dependent as pentamerisation could be impaired by bulky partner that has larger molecular mass (Harakuni *et al.*, 2005). Since cEDIIII is a relatively short polypeptide with 103 amino acids, it is presumed that C-terminal fusion to CTB would not affect the conformational folding.

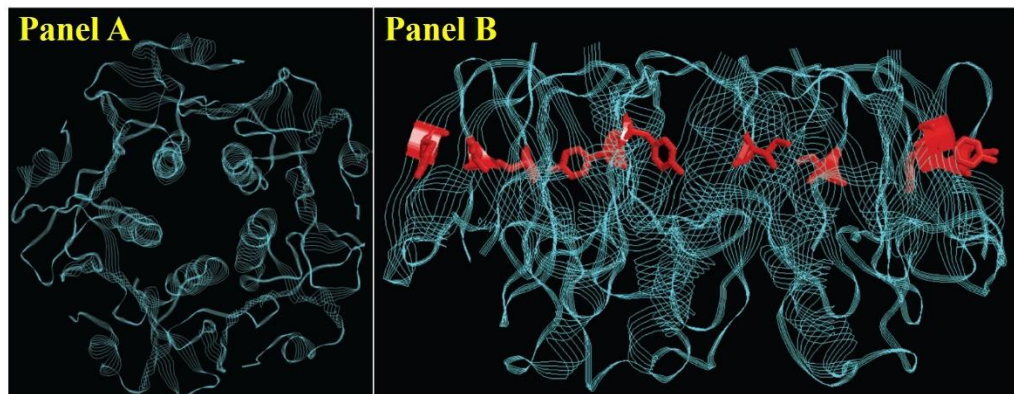


Figure 2.9: Crystallographic structure of CTB. Panel A: Conformation of CTB pentameric ring; Panel B: Conformation of CTB with embedded CTA (in red). Image obtained from Sanchez and Holmgren (2011).

2.4.2 Virus-like particles (VLPs)

In general, VLPs are made of viral capsid proteins that self-assemble into structures that strongly resemble native viral particles. The absence of genetic materials makes them inherently safer to use, without intrigued by concerns of reversion to virulence as in live attenuated or killed virus vaccine. The repetitive array of protein subunits on VLPs surface allows effective cross-linking with B cell receptors to induce activation of B cells (Zabel *et al.*, 2013). In addition, the size of VLPs is typically less than 100 nm, which allows it to passively traffic through the lymphatic system or directly internalised by antigen-presenting cells (APCs) and processed for presentation on major histocompatibility complex (MHC) to stimulate cellular immune response

(Kanekiyo and Buck, 2017). These advantages thereby promote the use of VLPs as vaccines, which are gaining wider attention following the successful use of Gardasil®/Cervarix® as human papillomavirus (HPV) vaccine, and Recombivax HB®/Energix-B® vaccine as hepatitis B virus (HBV) vaccine. For antigen presentation, VLPs can be used to display the epitopes derived from parental virus or extraneous origin (Tagliamonte *et al.*, 2017).

Nevertheless, surface display of a foreign antigen can be a significant challenge as steric constraint can interfere with particles assembly with a consequent loss of immunogenic property. Apart from the epitope size, successful antigen display also depends on the insertion site of particle carriers and the resulting geometrical architecture (Tissot *et al.*, 2010). Thus, selection of an appropriate, assembly-competent carrier is vital and utilising those that have been widely-studied could be less risky. In this context, VLPs derived from HBV are the most studied chimeric VLPs for epitope display (Pushko *et al.*, 2013). For instance, Mosquirix™ malaria vaccine is developed based on hepatitis B surface glycoprotein (HBsAg) VLPs and has progressed far to phase III trial (Kaslow and Biernaux, 2015). Alternatively, the hepatitis B core antigen (HBcAg) also has the intrinsic to form subviral capsid-like structures. The potency of HBcAg was quite evident, in which as low as 0.006 µg non-adjuvanted HBcAg could induce antibody production (Milich *et al.*, 1997b). In fact, HBcAg VLPs are claimed to be more superior than those of HBsAg. This is not only due to higher array of HBcAg protein subunits, but also based on the unique ability of HBcAg to induce co-stimulatory molecules on naïve B cells and elicit efficient APCs function (Milich *et al.*, 1997a).

2.4.2.1 Hepatitis B core antigen (HBcAg) as antigenic carrier

Depending on HBV strain, HBcAg is a 20 kDa protein made up from 183 amino acids. Two monomers of HBcAg can dimerise to form a hairpin structure bridged by the c/e1 loop of each monomer, which gives rise to the protruding spike (**Figure 2.10**,

Panel A) (Karpenko *et al.*, 2000). In certain literatures, the *c/e1* loop may be interchangeably referred as major immunodominant region (MIR). These dimers would self-assemble to form the icosahedral particles (**Figure 2.10**, Panel B), with symmetry of either triangulation number (T)=3 from 90 dimers (particle diameter: 30 nm) or forming T=4 from 120 dimers (particle diameter: 34 nm) (Crowther *et al.*, 1994). Through cryo-EM and image reconstruction, HBcAg particle is visualised as a large α -helical structure with the dimer appears as a hammer-like structure (Pumpens and Grens, 1999).

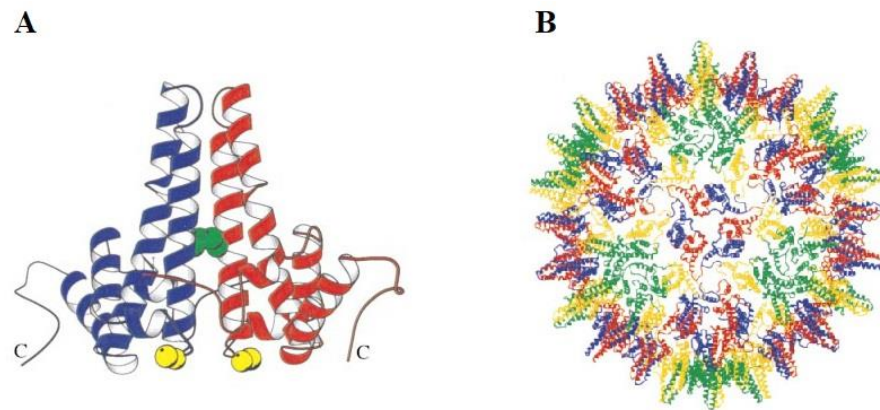


Figure 2.10: Structural folding of HBcAg VLPs. Panel A illustrates the association of two HBcAg monomers to form the dimeric interface, with Cys61-Cys61 disulphide bridge shown in green; Panel B presents the arrangement of subunits on capsid. Images reproduced with permission from Wynne *et al.* (1999).

The C-terminal end of HBcAg features a protamine-like domain at residues 150 – 183 which mediates RNA binding (Bottcher *et al.*, 1997). Though Gallina *et al.* (1989) found that deletion of the protamine-like domain would not hinder particle assembly; but it had vital role of stabilising the capsid via disulphide linkage with neighbouring dimers. Hence, this explains for the reduced stability of HBc Δ 149 truncated particles as

compared to the full-length counterpart (Thuenemann *et al.*, 2013). A full length HBcAg basically contains four cysteine (Cys) residues at positions 48, 61, 107 and 183. The connection between HBcAg dimer mainly depends on the Cys61-Cys61 intermolecular bonds, and sometimes Cys48-Cys48 (Zheng *et al.*, 1992). Wynne *et al.* (1999) reported that the Cys48 interaction however, was not found in HBc Δ 149 particles, together with Cys183 linkage which was also absence in HBc Δ 149. As a matter of fact, the instability issue would impose a product shelf-life problem if HBc Δ 149 were to be used for vaccine design. Besides, Seifer and Standring (1995) discovered that deletion of the protamine-like domain would raise the concentration threshold required for dimers to trigger capsid assembly. These findings imply that the RNA-binding domain has crucial role in mediating particle assembly and stability; and hence, this domain was also included in the HBcAg expression cassettes in this study.

Early use of HBcAg was demonstrated by Clarke *et al.* (1987), by fusing the immunogen of foot and mouth disease virus (FMDV) to the N-terminal end of HBcAg. Stahl and Murray (1989), on the other hand, successfully attempted HBcAg C-terminal fusion to HBsAg and another fusion to human immunodeficiency virus (HIV) envelope protein. Nevertheless, it was later discovered that epitope insertion into the c/e1 loop could stimulate stronger immune response by more than 10 folds (Brown *et al.*, 1991). In fact, a Schödel *et al.* (1992) proved that potent immunogenicity was most efficiently achieved by c/e1 insertion as compared to fusion to N- and C- termini. Since then, many studies have preferentially introduced foreign epitopes to c/e1 loop for the better surface exposure (Roose *et al.*, 2013).

2.4.2.2 Emerging ‘Tandem Core’ technology

Despite increasing interest has been devoted towards utilising HBcAg-based platform, it has yet to be fully developed as a vaccine vector. This is hindered by several factors that can abolish VLPs assembly. Firstly, the size of insert has a significant impact

as long peptide is prone to steric clashes since the two c/e1 loops at the dimer interface are positioned in close proximity (Pumpens and Grens, 2001). Next, the nature of insert also can affect VLPs formation, which includes hydrophobicity (Karpenko *et al.*, 2000), the propensity of inserts to homo-oligomerise (Vogel *et al.*, 2005) or form disulphide bonding with Cys residues in the inserts (Janssens *et al.*, 2010). Worthwhile to mention, insertion of the green fluorescent protein is an exceptional case where the entire 238 amino acids protein could be displayed on HBcAg particle (Kratz *et al.*, 1999). Aside from compact structure of the fluorescent protein, it seemed that flanking the insert with linkers had alleviated steric hindrance around the c/e1 loop (Nassal *et al.*, 2008). Therefore, the design of flexible linkers could be strategised to provide flexibility between the insert and carrier molecule.

Hence, several techniques have been developed over the years to address possible limitation, including: (i) *in vitro* co-expression of native HBcAg protein with modified HBcAg to generate mosaics VLPs (Vogel *et al.*, 2005); (ii) using SplitCore system to express distinct portions of HBcAg N- and C-termini that later assemble as structural dimers (Walker *et al.*, 2011a); or (iii) adopting the ‘Tandem Core’ technology that covalently joins two HBcAg monomers to give a single dimeric protein (Gehin *et al.*, 2004). Among these approaches, the latter offers the versatility of rapid genetic modification of c/e1 loop without being compromised by extensive screening or assembly procedures. According to Peyret *et al.* (2015), the tandem core approach can help to minimise steric clashes since the assembly of dimer (**Figure 2.11**, Panel A) is no longer determined by random association of individual subunit. With that, this approach offers the flexibility of incorporating a wider selection of inserts. Besides, the formation of tandem core protein allows epitope display on either of the c/e1 loop (**Figure 2.11**, Panel B). As a result, only half of the particle will be decorated with antigen of interest, and such flexibility also permits insertion of larger sequence.

Alternatively, these tandem core particles can be used to develop a multivalent vaccine where presentation of different antigens on the two c/e1 loops is feasible.

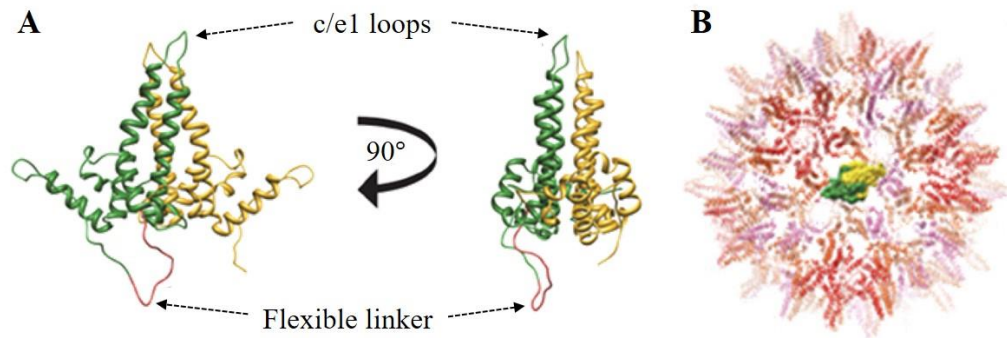


Figure 2.11: The formation of HBcAg VLPs via ‘Tandem Core’ technology. Panel A: An illustration of the tandem core protein, with two monomers (coloured in green and yellow, respectively) covalently linked by a flexible linker; Panel B: A surface representation of the tandem core protein on assembled particle. Images reproduced with permission from Peyret *et al.* (2015).

2.5 Pre-clinical examples of plant-based dengue vaccine

Since the pioneer work done on plant-based vaccine (Mason *et al.*, 1992), there is now wide adoption as proven by a number of human vaccines which are undergoing clinical trials and close to be marketed within this decade (Yusibov *et al.*, 2011). Nevertheless, research on plant-based dengue vaccine is considered relatively new in the field, with less than 20 papers reported thus far (see **Table 2.3**). The candidate antigens that have been studied are the dengue structural proteins, namely prM and E. Among all, EDIII has been the most extensively used for heterologous expression. In relative to that, this project has ventured towards production of EDIII in its consensus form, which are further elaborated in the next few chapters.

Among the studies, only four had reached until the stage of animal testing, and all of them had selected dengue EDIII as the immunogen subject (Huy and Kim, 2017; Kim *et al.*, 2016a; Kim *et al.*, 2017; Saejung *et al.*, 2007). Though virus neutralising activity had been demonstrated by Kim *et al.* (2017) and Saejung *et al.* (2007), but the two candidates were only tested against DENV 2. In the long run, only vaccine that is proven to confer momentous protection against all infecting serotypes would be harnessed for product development. Hence, more efforts are still needed to fill up the gap towards achieving an effective dengue vaccination. Based on the on-going researches listed in **Table 2.3**, it is postulated that majority of the stable transformation systems have suffered from low product yield and/or long lead time, which hauled their progression towards preclinical trial. Nonetheless, the immunogenicity of these candidates still remains to be testified; in which these would eventually pave way towards the production of a plant-based dengue vaccine with global significance. Overall, it is no doubt that molecular pharming is likely to benefit the less developed regions, in view that modern medicine and technology are scarce in most dengue-endemic areas (Ma *et al.*, 2013).

Table 2.3: A compiled list of on-going researches on plant-based dengue vaccine development.

Host plant	Transformation strategy	Expressed antigen	Tested in animal	Reference
<i>N. benthamiana</i>	Transient expression - Virus infection	DENV 2-specific EDIII	Yes	(Saejung <i>et al.</i> , 2007)
	Transient expression - Agroinfiltration	(i) DENV 2-specific truncated E (ii) DENV 2-specific truncated C/prM/E (iii) DENV 2-specific EDIII fusion to HBcAg	No	(Martinez <i>et al.</i> , 2010)
	Transient expression - Agroinfiltration	(i) cEDIII (ii) cEDIII fusion to M-cell targeting ligand (Co1)	No	(Kim <i>et al.</i> , 2015)
	Transient expression - Agroinfiltration	(i) cEDIII (ii) cEDIII fusion to CTB	Yes	(Huy and Kim, 2017)
	Transient expression - Agroinfiltration	cEDIII fusion to polymeric immunoglobulin G scaffold (PIGS)	Yes	(Kim <i>et al.</i> , 2017)
<i>N. tabacum</i>	Stable transformation - <i>Agrobacterium</i>	DENV 2-specific EDIII	No	(Kim <i>et al.</i> , 2009)

<i>N. tabacum</i>	Stable transformation <i>Agrobacterium</i>	DENV 2-specific EDIII fusion to CTB	No	(Kim <i>et al.</i> , 2010)
	Stable transformation - Biolistic	Tetravalent fusion of EDIII	No	(Gottschamel <i>et al.</i> , 2016)
<i>Oryza sativa</i>	Stable transformation - Biolistic	cEDIII	No	(Kim <i>et al.</i> , 2012)
	Stable transformation - Biolistic	cEDIII fusion to Co1	No	(Kim <i>et al.</i> , 2013b)
	Stable transformation - Biolistic	cEDIII fusion to CTB	No	(Kim <i>et al.</i> , 2013a)
	Stable transformation - Biolistic	DENV 2-specific E	No	(Kim <i>et al.</i> , 2014b)
	Stable transformation - Biolistic	(i) cEDIII (ii) cEDIII fusion to CTB	Yes	(Kim <i>et al.</i> , 2016a)
<i>Zea mays</i>	Stable transformation - <i>Agrobacterium</i>	(i) DENV 2-specific EDIII (ii) DENV 2-specific EDIII fusion to CTB	No	(Kim <i>et al.</i> , 2014a)

<i>Solanum tuberosum</i>	Stable transformation - <i>Agrobacterium</i>	DENV 2-specific EDIII fusion to CTB	No	(Kim <i>et al.</i> , 2016b)
<i>Lactuca sativa</i>	Stable transformation - Biolistic	DENV 3-specific prM/E	No	(Kanagaraj <i>et al.</i> , 2011)
<i>Cucumis melo</i>	Transient expression - Virus infection	DENV 2-specific truncated E	No	(Teoh <i>et al.</i> , 2009)
<i>Cucurbita pepo</i>	Transient expression - Virus infection	DENV 2-specific EDIII	No	(Libsittikul <i>et al.</i> , 2015)

3 Construction of Dengue cEDIII Expression Cassettes and the Corresponding Recombinant Vectors

Table of Contents

3.1	Introduction	3-3
3.2	Materials and methods.....	3-7
3.2.1	Vector.....	3-7
3.2.2	Synthetic genes	3-10
3.2.3	Overview of construction of cEDIII recombinant vectors	3-11
3.2.4	Specialised equipment.....	3-19
3.2.5	Polymerase chain reaction (PCR)	3-19
3.2.6	Plasmid DNA isolation	3-20
3.2.7	Restriction enzyme (RE) digestion	3-20
3.2.8	Agarose gel electrophoresis	3-22
3.2.9	DNA purification strategies	3-22
3.2.10	Ligation of vector and insert	3-23
3.2.11	Preparation of competent cells	3-23
3.2.12	Transformation of TOP10 competent <i>Escherichia coli</i>	3-24
3.2.13	Verification of recombinant vector	3-24
3.3	Results	3-28
3.3.1	Codon optimisation of <i>cEDIII</i> genes	3-28
3.3.2	Polymerase chain reaction (PCR) amplification of cEDIII inserts .	3-29
3.3.3	Restriction enzyme (RE) digestion of cEDIII expression cassettes	3-32

3.3.4	Screening of transformed clones.....	3-33
3.3.5	Verification by DNA sequencing.....	3-49
3.4	Discussion	3-50
3.5	Conclusion.....	3-57

3.1 Introduction

The advent of recombinant DNA technology has rapidly revolutionised vaccinology research where specific antigenic epitope can now be selectively produced. Recombinant subunit vaccine offers added advantages in terms of: (i) improved safety without concerns of viral interference, genetic recombination or reversion to virulence; (ii) easier formulation of multivalent component; and (iii) accelerated immunisation schedule is possible, which suits to military personnel and traveller's use (Coller *et al.*, 2011). Numerous expression systems have been established to date, ranging from bacterial, fungal, mammalian and plant system. Notably, a plant-based expression system has attracted increasing adoption for the benefits of low manufacturing cost, easy and scalable production and reduced risk to mammalian pathogens (Tschofen *et al.*, 2016). Therefore, if a highly immunogenic subunit vaccine can be manufactured using a high-yielding system, it does have the potential to deliver a world-changing impact to the field of vaccinology.

To explore the prospects of a plant-based vaccine, the antigenic component of dengue virus (DENV) was designed for gene delivery into *N. benthamiana*. As reviewed in **Section 2.5**, transient system has seemed to overshadow stable transformation in the efforts of deriving a dengue vaccine candidate. Agroinfiltration is generally the method of choice, as the simple and straightforward procedure has made it possible to harvest milligrams of target protein within a matter of days. For that, binary vectors and plant viral vectors are commonly used to carry the transgene to be delivered into host plants. These vectors have been developed to facilitate gene cloning works and maximise the transformation efficiency. In brief, binary vectors are engineered to harbour the transfer DNA (T-DNA) and virulence regions separately; while viral vectors are often 'deconstructed' to retain only elements required for high transgene expression. In this study, a modified binary vector based on cowpea mosaic virus (CPMV) was used accredited to its hypertranslational (*HT*) feature, known as pEAQ-*HT* vector. The non-

replicative nature of this vector has made it more attractive than viral vector since issues like virus exclusion and mutation of transcripts could be avoided (Peyret and Lomonosoff, 2013).

As DENV neutralising epitopes are identified on the envelope glycoprotein domain III (EDIII), it has now emerged as the prime candidate for vaccine development. More recently, EDIII was expressed as a consensus sequence (cEDIII) aligned between four DENV serotypes (DENV 1-4) (Huy and Kim, 2017; Kim *et al.*, 2015; Kim *et al.*, 2016a; Kim *et al.*, 2017). So far, only recombinant cEDIII produced in *E. coli* had demonstrated neutralising activities against DENV 1-4 following vaccine delivery with adjuvant (Leng *et al.*, 2009). However, *E. coli* has limited post-translational machinery function, and improper disulphide bond formation is known to affect the proper folding of antibody epitopes on EDIII structure (Roehrig *et al.*, 2004). Hence, this leads to idea of producing the cEDIII protein in plant system, which is more likely to mimic its native configuration. It is believed that cEDIII has the potential to be developed as a single component vaccine that can protect against the four co-circulating serotypes. Since cEDIII is considered as a novel molecule, the characteristics of the protein is not well-understood yet. Therefore, fusion to green fluorescent protein (sGFP) is strategised to monitor the localisation and expression level of the heterologous protein.

Concurrently with the study of cEDIII antigen, efforts are also focused on developing a vaccine candidate with strong immunogenic profile. Principally, one of the challenges in vaccine development is the need to generate and sustain strong immune responses, and subunit vaccine can be less immunogenic due to the defined amount of antigenic determinant. Hence, they require administration with adjuvant to potentiate the immune response against a specific antigen. Cholera toxin B subunit (CTB), a non-toxic derivative of *V. cholerae* toxin has been widely used as an adjuvant (**Section 2.4.1.1**). CTB has specific affinity for monosialotetrahexosylganglioside (GM1) distributed on leucocytes (Holmgren *et al.*, 1973), by which it can facilitate

optimal access to the immune system. As the CTB carrier can impart its immunostimulatory properties to bystander antigen, genetically-linked CTB-cEDIII constructs were designed here with the hope to boost the vaccine efficacy.

Besides, virus-like particles (VLPs) have gradually emerged as vaccine delivery vehicles that are spontaneously assembled from viral structural proteins (**Section 2.4.2**). These are multimeric structures that can directly stimulate immune cells by mimicking the three-dimensional conformation of native viruses. Moreover, VLPs are devoid of infectious genetic material which makes them inherently safer than attenuated or inactivated virus preparations. In this study, hepatitis B core antigen (HBcAg) was exploited for cEDIII epitope display. The resulting chimeric HBcAg VLPs are favoured for the high density of cEDIII displays on 180 – 240 copies of core protein per particle. Alternatively, ‘Tandem Core’ technology was also adopted to produce the chimeric HBcAg VLPs. Tandem core indicates a tandem fusion of two HBcAg monomers in order to produce HBcAg dimer as a single polypeptide (Peyret *et al.*, 2015). It is believed that the expression as tandem core particles can increase the chance of chimeric VLPs assembly. To enable differentiation of the variants of HBcAg VLPs, monomeric core HBcAg (mHBcAg) is used to refer a single open reading frame (ORF) of HBcAg, whereas tandem core HBcAg (tHBcAg) refers to the tandem repeat of HBcAg ORFs.

Focusing on the design and construction of cEDIII recombinant vectors, several strategies had been applied to achieve a higher expression. Firstly, codon optimisation was performed to boost translation by re-coding the rare codon in foreign gene with the synonymous codon preferred by the expression host (Angov, 2011). Kozak sequence was also added as another strategy to enhance translation efficiency. Next, subcellular targeting was used to modulate the trafficking of heterologous protein. Since proteins expressed in cytosol tend to suffer from proteolytic degradation (Benchabane *et al.*, 2008), transgene can be targeted to specific organelle such as apoplast, chloroplast, endoplasmic reticulum (ER) and mitochondria. Nonetheless, localisation also depends

on whether the protein requires specialised folding or modifications to acquire its biological function. In this study, ER retention was opted considering the benefits of protein processing and sequestration. To ensure protein retrieval to ER, a signal peptide from tobacco pathogenesis-related 1a protein (PR1a) was also added to direct the protein through the secretion pathway (Cornelissen *et al.*, 1987). Lastly, protein linker was used to improve the interactions between connecting domains in fusion proteins as well as chimeric HBcAg VLPs.

Overall, the specific objectives of this chapter are:

- (i) To design cEDIII fusion expression cassettes with sGFP;
- (ii) To design cEDIII fusion expression cassettes with CTB;
- (iii) To optimise gene sequences based on *N. benthamiana* codon usage;
- (iv) To incorporate subcellular targeting signals comprising PR1a signal peptide and/or ER retention signal (KDEL), into the cassettes of recombinant cEDIII-sGFP and CTB-cEDIII fusion proteins;
- (v) To construct chimeric mHBcAg VLPs expression cassette with *cEDIII* gene insertion at the c/e1 loop;
- (vi) To construct chimeric tHBcAg VLPs expression cassette with *cEDIII* gene inserted into the c/e1 loop of Core II region; and
- (vii) To integrate the cEDIII expression cassettes into pEAQ-*HT* vector to generate the respective recombinant vectors;

3.2 Materials and methods

3.2.1 Vector

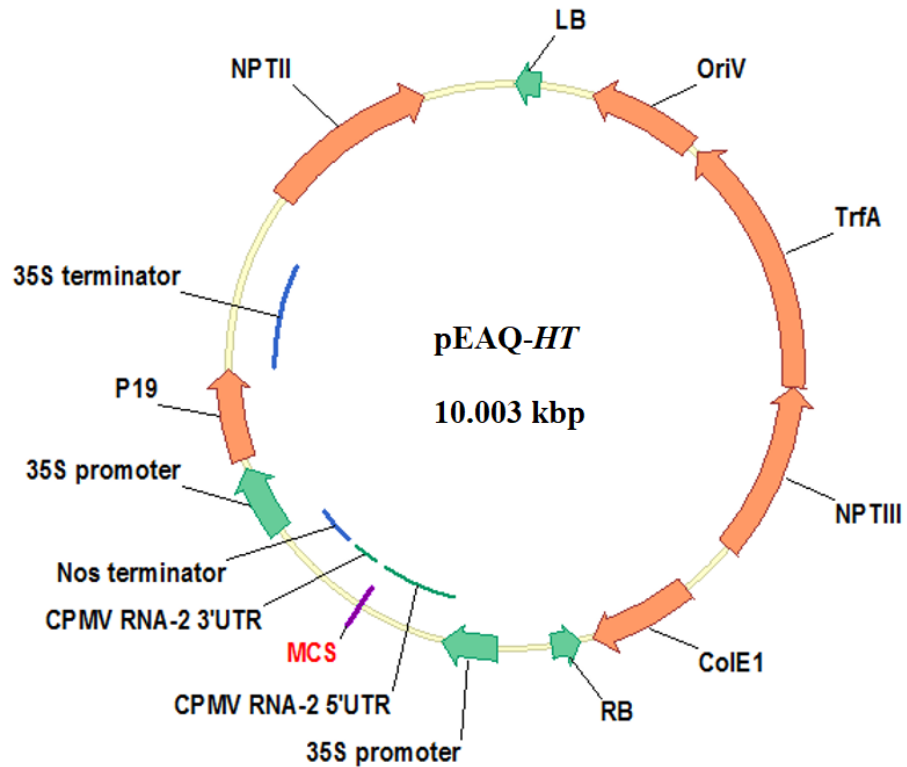
The plant-based expression vector, namely pEAQ-*HT* (Accession Number: GQ497234) was used throughout the study. A detailed illustration of the pEAQ-*HT* vector map is provided as shown in **Figure 3.1**.

For the construction of recombinant vectors of mHBcAg VLPs, a cloning vector designated as pEAQ-*HT*::mEL was used (**Appendix A3.1**). This vector was previously designed to produce monomeric core particles with empty c/e1 loop (mEL). In other words, the c/e1 region had not been modified to carry any foreign gene.

For the construction of recombinant vectors of tHBcAg VLPs, pEAQ-*HT*::tHBcAg-VHH2 was used as the cloning vector (**Appendix A3.2**). This vector was previously designed to harbour VHH2 epitopes on the c/e1 loop of the Core II region of tHBcAg VLPs.

All the vectors used in this study were kindly provided by John Innes Centre (JIC) in the United Kingdom (UK).

Panel A: Plasmid map of pEAQ-HT



Feature

LB	: Left border
OriV	: pRK2 replication origin for <i>A. tumefaciens</i>
TrfA	: Replication-essential locus
NPTIII	: Prokaryotic neomycin phosphotransferase III
ColE1	: pBR322 replication origin for <i>E. coli</i>
RB	: Right border
35S promoter	: Cauliflower mosaic virus (CaMV) 35S promoter
CPMV RNA-2 5' UTR	: 5' untranslated region from CPMV RNA-2
MCS	: Multiple cloning site
CPMV RNA-2 3' UTR	: 3' untranslated region from CPMV RNA-2
Nos terminator	: Nopaline synthase terminator
P19	: 19 kDa silencing suppressor protein
35S terminator	: CaMV 35S terminator
NPTII	: Eukaryotic neomycin phosphotransferase II

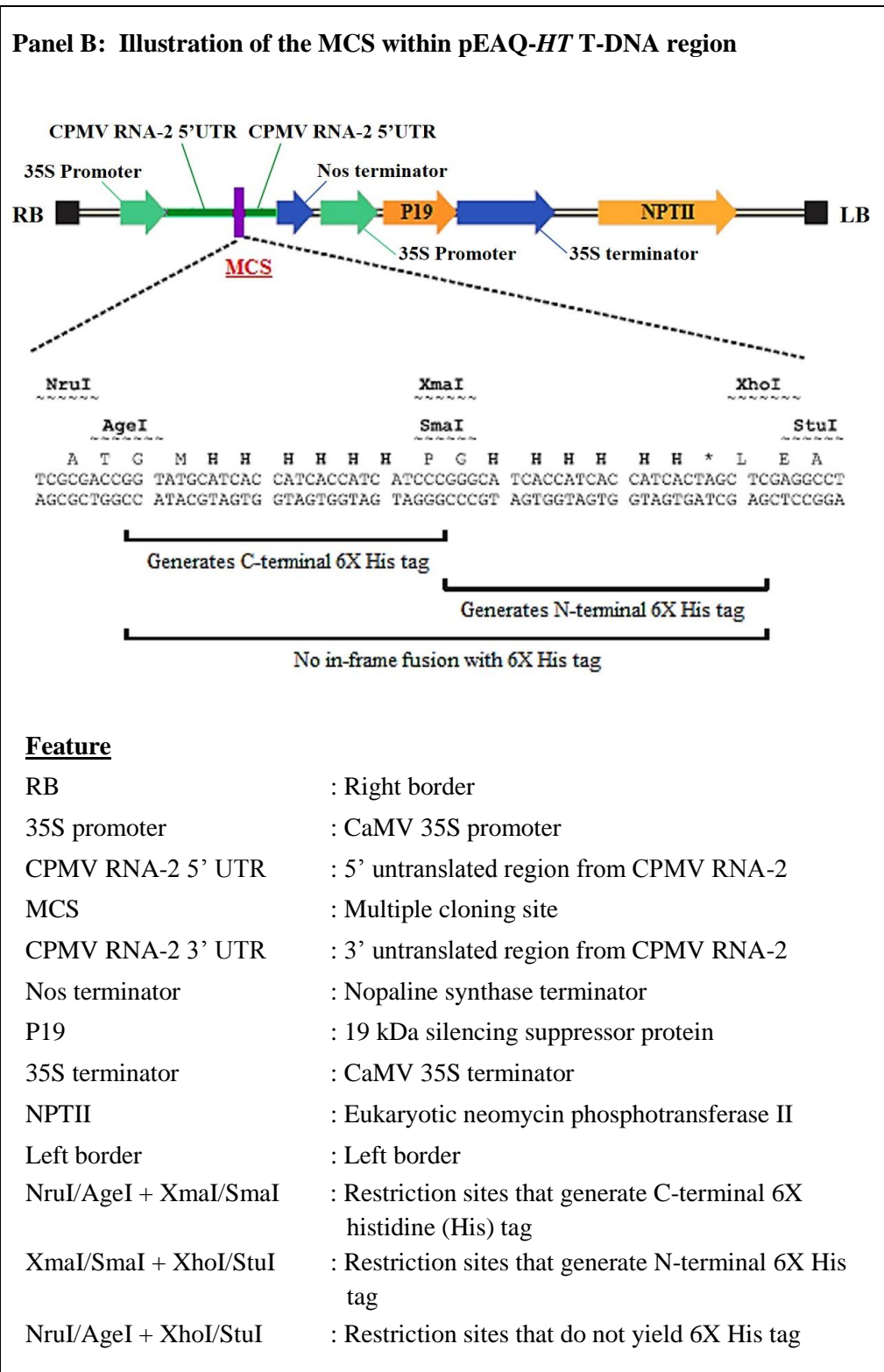


Figure 3.1: Schematic illustrations of the pEAQ-*HT* vector used in this study. Panel A: An overview of the vector; Panel B: A detailed illustration of the pEAQ-*HT* T-DNA region. Image reproduced with permission from Sainsbury *et al.* (2009).

3.2.2 Synthetic genes

All the *cEDIII* genes used for recombinant vector construction were synthesised by GeneScript (United States of America, USA) and GeneArt (USA) as stated in **Table 3.1**. In specific, these synthetic genes were codon-optimised for expression in *N. benthamiana*.

Firstly, cEDIII-sGFP-KDEL was designed as cEDIII fusion to sGFP (Accession Number: ABL09837.1), followed by ER retention signal (**Appendix A3.3**). A variant named as PR1a-cEDIII-sGFP-H-KDEL, comprising of cEDIII fusion to sGFP along with N-terminal PR1a signal peptide (Accession Number: ABV21361.1), 6X His tag and a KDEL signal (**Appendix A3.4**). These two synthetic genes were provided in pUC57 vectors.

Next, CTB-cEDIII-KDEL was synthesised as cEDIII fusion to CTB (Accession Number: U25679), followed by ER retention signal (**Appendix A3.5**). A variant labelled as PR1a-CTB-cEDIII-H-KDEL comprising of cEDIII fusion to CTB along with N-terminal PR1a signal peptide, 6X His tag and a KDEL signal (**Appendix A3.6**). These two synthetic genes were held in pUC57 vectors.

Lastly, cEDIII (L) was designed as cEDIII flanked by long glycine-glycine-serine (GGG)_n linkers (**Appendix A3.7**), which was provided in pMA-RQ vector.

Table 3.1: List of synthesised sequences.

No.	Synthesised sequence	Holding vector	Source	Appendix
1	cEDIII-sGFP-KDEL	pUC57	GeneScript, USA	A3.3
2	PR1a-cEDIII-sGFP-H-KDEL	pUC57	GeneScript, USA	A3.4
3	CTB-cEDIII-KDEL	pUC57	GeneScript, USA	A3.5
4	PR1a-CTB-cEDIII-H-KDEL	pUC57	GeneScript, USA	A3.6
5	cEDIII (L)	pMA-RQ	GeneArt, USA	A3.7

3.2.3 Overview of construction of cEDIII recombinant vectors

The cEDIII-sGFP-KDEL and CTB-cEDIII-KDEL used for gene cloning were obtained from pUC57 holding vectors. The first represents cEDIII fusion with sGFP; while the second represents cEDIII fusion with CTB (**Table 3.2**). Both gene sequences were designed with the tobacco etch virus (TEV) protease cleavage site and C-terminal KDEL signal. After the genes were isolated via polymerase chain reaction (PCR) using corresponding primers (**Table 3.3**), they were cloned into the AgeI and XmaI sites of pEAQ-*HT* vector to fuse in-frame with the C-terminal 6X His tag from the multiple cloning site (MCS) (see **Figure 3.1**, Panel B). This hence gave rise to pEAQ-*HT*::cEDIII-sGFP-KDEL-H and pEAQ-*HT*::CTB-cEDIII-KDEL-H, correspondingly.

Meanwhile, the PR1a-cEDIII-sGFP-H-KDEL and PR1a-CTB-cEDIII-H-KDEL were released from pUC57 holding vectors via restriction enzyme (RE) digestion. The former denotes cEDIII fusion with sGFP; while the latter denotes cEDIII fusion with CTB, with a glycine-proline-glycine-proline (GPGP) linker between the fusion protein to reduce potential steric constraint (**Table 3.2**). Both cassettes contain the Kozak sequence, PR1a signal peptide, TEV cleavage site, 6X His tag and KDEL signal. They

were cloned into the AgeI and XhoI sites of pEAQ-*HT* vector (see **Figure 3.1**, Panel B). The change of restriction sites allowed the KDEL signal to be placed at the very end of C-terminus upon ligation into pEAQ-*HT* vector.


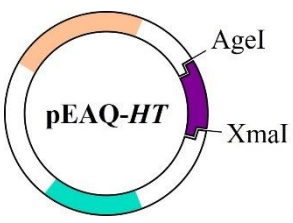
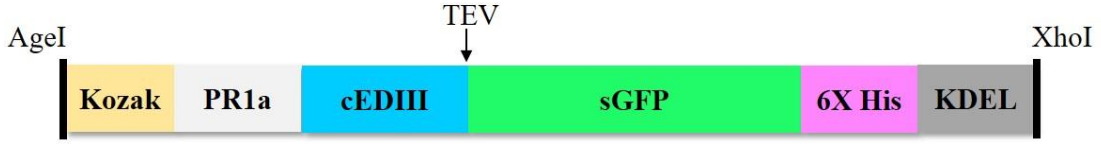
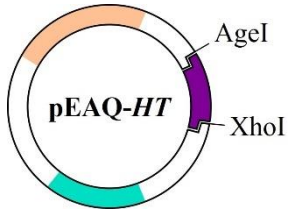
The PR1a-CTB-cEDIII-KDEL (xTH) represents a variant of PR1a-CTB-cEDIII-H-KDEL, in which the TEV protease cleavage site and 6X His tag had been removed (**Table 3.2; Figure 3.2**), and hence it was labelled as 'xTH'. The new insert, PR1a-CTB-cEDIII-KDEL (xTH) was generated via a two-step PCR amplification using the recombinant vector pEAQ-*HT*::PR1a-CTB-cEDIII-H-KDEL and specific primers (**Table 3.3**). Nonetheless, the PR1a-CTB-cEDIII-KDEL (xTH) still harbours PR1a and KDEL signals, which was then cloned into the AgeI and XhoI sites of pEAQ-*HT* vector.

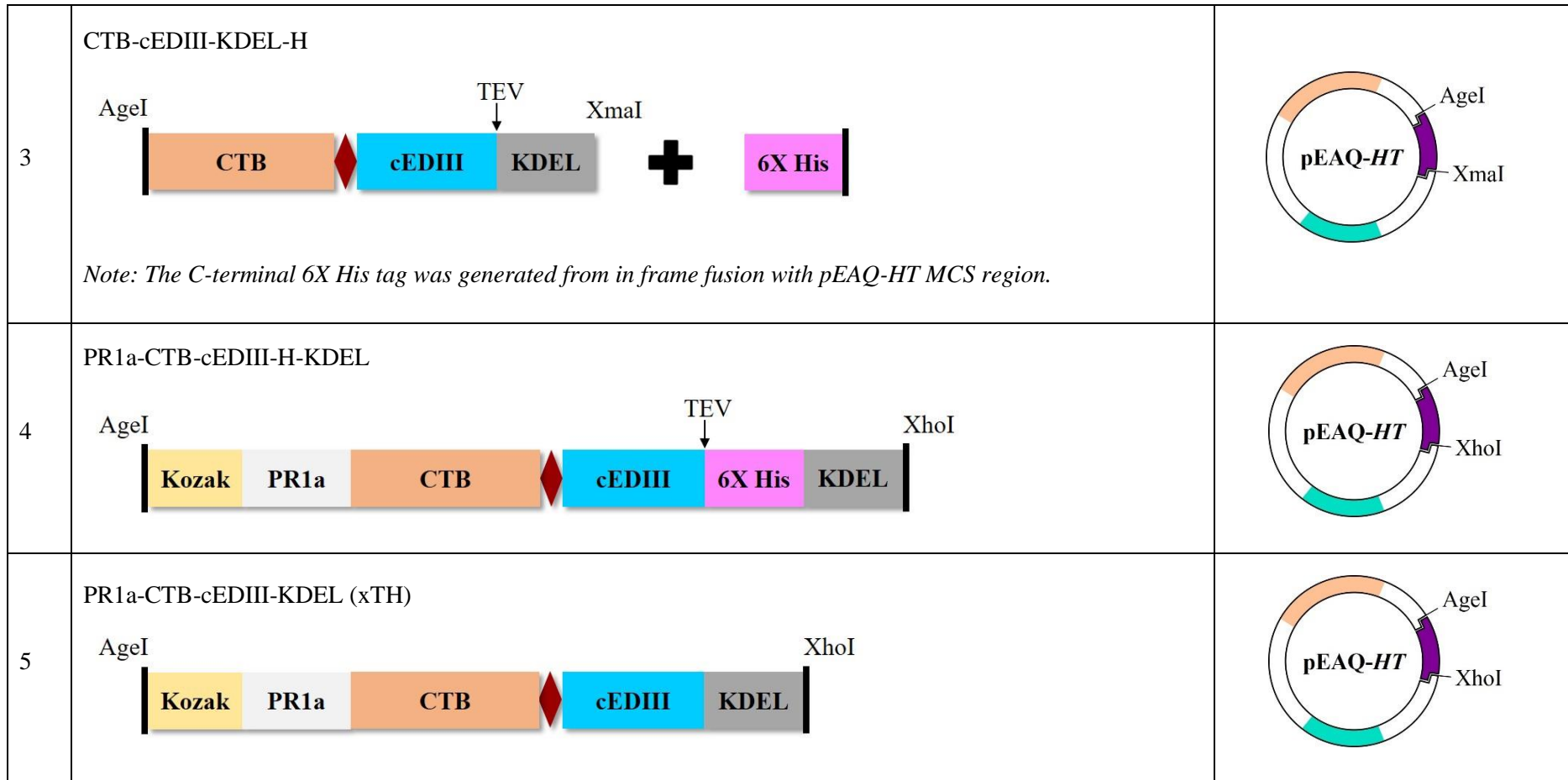
The mHBcAg-cEDIII and mHBcAg-cEDIII (L) were constructed by inserting the *cEDIII* gene into the *c/e1* loop of mHBcAg (**Table 3.2**). The cEDIII inserts, designated as cEDIII_mono and cEDIII (L)_mono, were amplified from pMA-RQ::cEDIII (L) holding vector using specific primers (**Table 3.3**). The only difference between the amplicons of cEDIII_mono and cEDIII (L)_mono is the presence of (GGG)_n linkers that flank the cEDIII; in which presence of linkers is denoted with '(L)'. Both cEDIII_mono and cEDIII (L)_mono were then inserted to pEAQ-*HT*::mEL vector through the Sall and AseI restriction sites (**Table 3.2**).

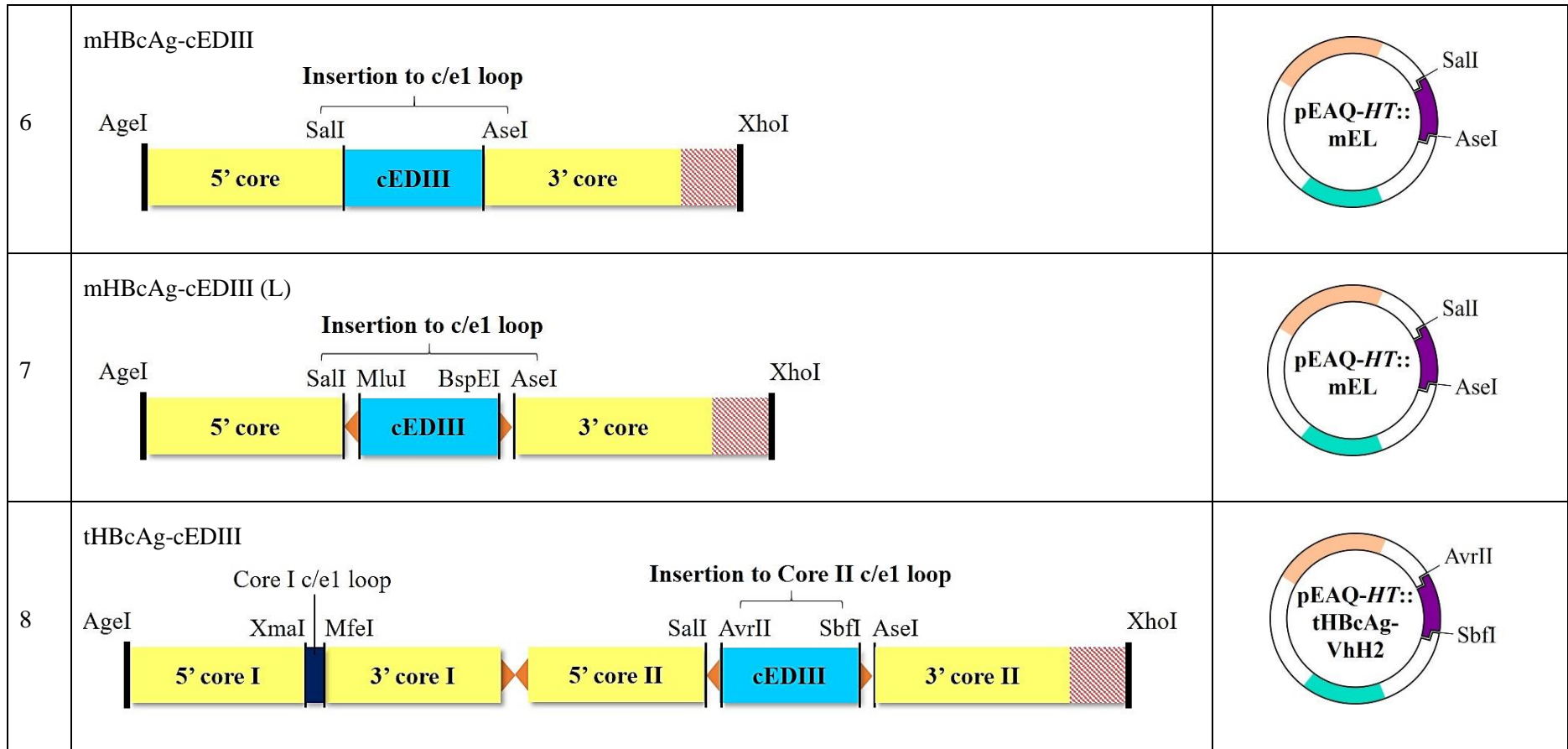
The expression cassette for tHBcAg-cEDIII was constructed by inserting *cEDIII* gene into the *c/e1* loop of tHBcAg Core II region (**Table 3.2**). In this case, the cEDIII insert was amplified from pUC57::cEDIII-sGFP-KDEL vector using specific primers (**Table 3.3**). The resulting amplicon, cEDIII_tandem was then cloned into the AvrII and SbfI restriction sites of pEAQ-*HT*::tHBcAg-VHH2 vector.

A schematic illustration of the procedures involved in the construction of all recombinant vectors is depicted in **Figure 3.3**.

Table 3.2: List of cEDIII expression cassettes and cloning vectors used in this study.

No.	Schematic representation of cEDIII expression cassette	Cloning vector
1	<p>cEDIII-sGFP-KDEL-H</p>  <p><i>Note: The C-terminal 6X His tag was generated from in frame fusion with pEAQ-HT MCS region.</i></p>	
2	<p>PR1a-cEDIII-sGFP-H-KDEL</p> 	





Annotation: TEV ↓ indicates TEV protease recognition site; ♦ Represents GPGP linker; ◀▶ Represents (GGG)_n linker; ▨ Represents nucleic acid binding domain.

Table 3.3: Details of PCR amplification of cEDIII inserts using Phusion® polymerase.

No.	Insert	Template	Primers		Ta	Expected amplicon size
			Forward	Reverse		
1	cEDIII-sGFP-KDEL	pUC57::cEDIII-sGFP-KDEL	PFGS (sGFP)	PRGS	70°C	1.089 kbp
2	CTB-cEDIII-KDEL	pUC57::CTB-cEDIII-KDEL	PFGS (CTB)	PRGS	66°C	0.753 kbp
3	Intermediate PR1a-CTB-cEDIII-KDEL (xTH) amplicon	pEAQ- <i>HT</i> ::PR1a-CTB-cEDIII-H-KDEL	CTBcED3F	CTBcED3R (1 st)	70°C	0.798 kbp
4	PR1a-CTB-cEDIII-KDEL (xTH)	Intermediate PR1a-CTB-cEDIII-KDEL (xTH) amplicon	CTBcED3F	CTBcED3R (2 nd)	70°C	0.824 kbp
5	cEDIII_mono	pMA-RQ::cEDIII (L)_mono	cED3F (mono)	cED3R (mono)	69°C	0.332 kbp
6	cEDIII (L)_mono	pMA-RQ::cEDIII (L)_mono	cED3F (monoL)	cED3R (monoL)	70°C	0.432 kbp
7	cEDIII_tandem	pUC57::cEDIII-sGFP-KDEL	cED3F	cED3R	70°C	0.333 kbp

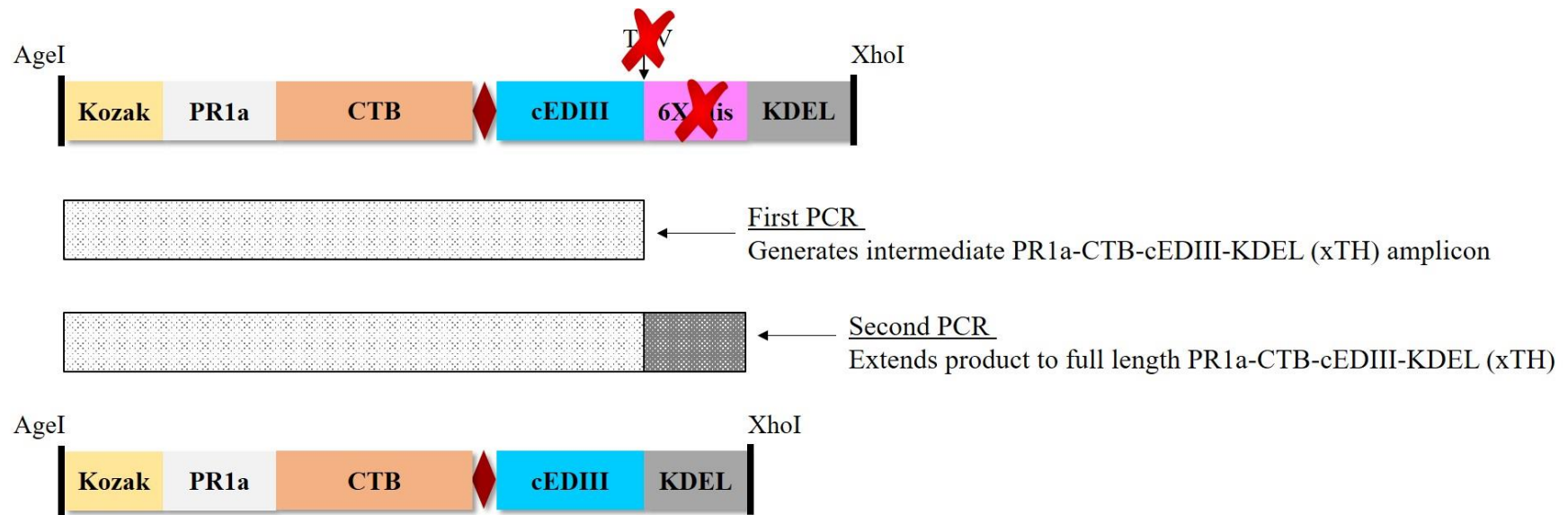


Figure 3.2: A two-step PCR amplification process using pEAQ-*HT*::PR1a-CTB-cEDIII-H-KDEL as template to generate the new insert, PR1a-CTB-cEDIII-KDEL (xTH).

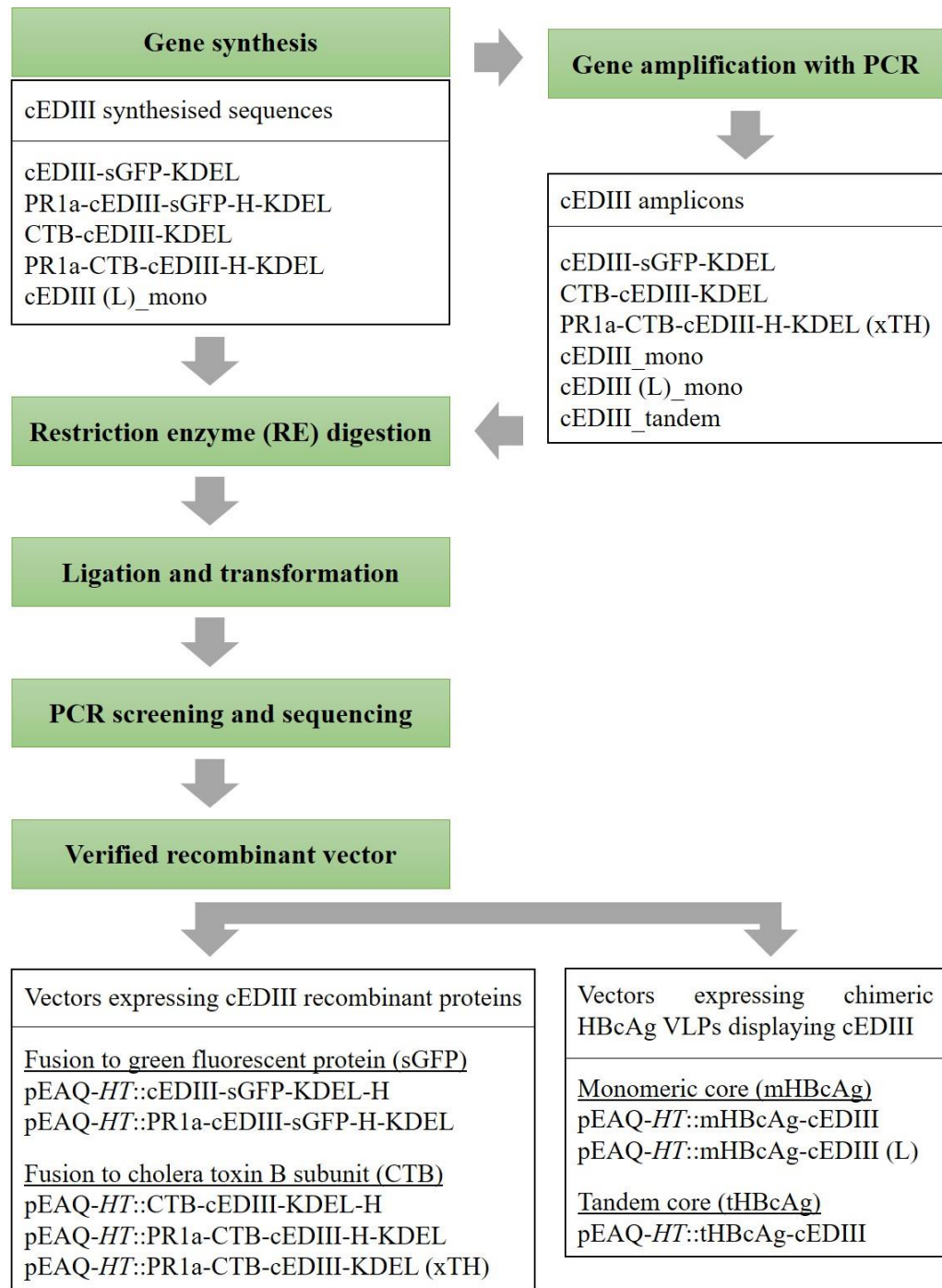


Figure 3.3: A methodology flow chart illustrating the steps used for the construction of recombinant vectors in this study.

3.2.4 Specialised equipment

Polymerase chain reaction (PCR) was performed using Mastercycler Nexus Thermal Cycler (Eppendorf, Germany). Centrifugation of 10 ml sample was carried out using 5810R Refrigerated Centrifuge (Eppendorf, Germany) while MiniSpin[®] Microcentrifuge (Eppendorf, Germany) was used for ≤ 2.0 ml sample. The purity and concentration of DNA were determined using a NanoDrop 1000 spectrophotometer (Thermo Scientific, USA). DNA gel electrophoresis was conducted using Mini-Sub[®] Cell GT System (Bio-Rad, USA), followed by imaging using GBOX F3 Gel Imaging System (Syngene, UK) or AlphaImage Gel Imaging System (Alpha Innotech, USA). Sample incubation at controlled temperature was performed using Thermomixer comfort (Eppendorf, Germany) or water bath system (Mettler, Germany). Incubation of bacterial culture was carried out using Innova 42 incubator shaker (Eppendorf, Germany) and BINDER Microbiological Incubator (Binder, Germany). Measurement of the bacterial optical density was performed using BioPhotometer Plus (Eppendorf, Germany).

3.2.5 Polymerase chain reaction (PCR)

The amplification of insert for DNA ligation was performed using Phusion[®] High-Fidelity DNA Polymerase (New England Biolabs, USA). All the PCR mixtures were prepared according to manufacturer's recommendation: 1X Phusion HF buffer containing 1.5 mM magnesium chloride, 10 mM deoxynucleotides (dNTPs), forward and reverse primers at 10 μ M each, 100 ng template DNA, 1 unit of polymerase and topped up to 50 μ l with distilled water. The PCR programme was set as follows: initial denaturation at 98°C for 30 seconds, followed by 25 cycles of denaturation at 98°C for 10 seconds, annealing at 66-70°C for 20 seconds and extension at 72°C for 30 seconds/kilo-base pair (kbp). A final elongation step was held at 72°C for 5 minutes. Lastly, collected amplicons were analysed via DNA gel electrophoresis (**Section 3.2.8**).

The annealing temperature (T_a) used for the amplification of corresponding insert is stated in **Table 3.3**. Details of the primer sequences are provided in **Appendix A3.8**.

3.2.6 Plasmid DNA isolation

Plasmid isolation was conducted according to manufacturers' instructions, using QIAprep Spin MiniPrep Kit (Qiagen, Germany) and Hybrid-Q™ Plasmid Rapidprep (GeneAll, Korea). In brief, 10 ml of overnight bacterial culture was pelleted at 4000 x g for 10 minutes at room temperature (RT). The pellet was then resuspended in 250 µl of cell suspension buffer (50 mM Tris base, pH 8.0; 10 mM ethylenediaminetetraacetic acid; 100 µg/ml ribonuclease A) and transferred to a new microcentrifuge tube. Next, 250 µl of lysis buffer (200 mM sodium hydroxide; 1% (w/v) sodium dodecyl sulphate) was added and the tube was inverted for 4 – 6 times. After 3 minutes, 250 µl of neutralisation buffer (4.2 M guanidine hydrochloride; 0.9 M potassium acetate) was added and mixed immediately by inverting 4 – 6 times. The mixture was centrifuged for 10 minutes at 15,000 x g. The supernatant was transferred to spin column and centrifuged at 15,000 x g for 30 seconds. After discarding the flow through, 750 µl of wash buffer (10 mM Tris base, pH 7.5; 80% (v/v) ethanol) was applied to the spin column and centrifuged at 15,000 x g for 30 seconds. The spin column was subjected to additional centrifugation for 1 minute to remove residual wash buffer. Lastly, the spin column was placed in a new microcentrifuge tube and 30 µl of elution buffer (10 mM Tris base; pH 8.5) was added to the centre of the column. The column was incubated at RT for 1 minute before centrifuging at 15,000 x g for 1 minute.

3.2.7 Restriction enzyme (RE) digestion

The RE double digestion (New England Biolabs, USA) was prepared as follows: 1X CutSmart buffer (20 mM Tris-acetate, pH 7.9; 10 mM magnesium acetate; 50 mM

potassium acetate; 100 µg/ml BSA) or 1X NEBuffer 3.1 (50 mM Tris-hydrochloride (Tris-HCl), pH 7.9; 10 mM magnesium chloride; 100 mM sodium chloride; 100 µg/ml BSA), 500 ng of DNA, 5 units of enzymes and topped up to 25 µl with distilled water. All the reactions were incubated at 37°C using water bath. Specific details of the double digestion set up for each insert and vector are stated in **Table 3.4**.

Table 3.4: Details of the REs used for digestion of cEDIII inserts and pEAQ-*HT* variant vectors.

No.	Template	RE		Incubation time
		1	2	
1	<u>Insert</u> cEDIII-sGFP-KDEL CTB-cEDIII-KDEL <u>Vector</u> pEAQ- <i>HT</i>	AgeI	XmaI	4 hours
2	<u>Insert</u> PR1a-cEDIII-sGFP-H-KDEL PR1a-CTB-cEDIII-H-KDEL PR1a-CTB-cEDIII-KDEL (xTH) <u>Vector</u> pEAQ- <i>HT</i>	AgeI	XhoI	4 hours
3	<u>Insert</u> mHBcAg-cEDIII mHBcAg-cEDIII (L) <u>Vector</u> pEAQ- <i>HT</i> ::mEL	SalI	AseI	4 hours
4	<u>Insert</u> tHBcAg-cEDIII <u>Vector</u> pEAQ- <i>HT</i> ::tHBcAg-VHH2	AvrII	SbfI	4 hours

3.2.8 Agarose gel electrophoresis

Agarose gel electrophoresis was used to analyse DNA fragments of PCR amplicons, RE-digested products and integrity of plasmids. Gel containing 1% (w/v) agarose was pre-stained with 0.5 mg/ml ethidium bromide (Thermo Scientific, USA) or SYBR Safe (Thermo Scientific, USA) at 1:10,000 dilution in TBE buffer (89 mM Tris; 89 mM boric acid; 2 mM ethylenediaminetetraacetic acid). DNA separation was conducted at 90 V for 45 – 60 minutes, using either Hyperladder™ 1 kbp DNA Ladder (Bioline, UK) or GeneRuler™ 1 kbp DNA Ladder (Thermo Scientific, USA) as reference marker.

3.2.9 DNA purification strategies

Purification of PCR amplicons was performed using QIAquick PCR purification kit (Qiagen, Germany) and Expin™ Combo GP (GeneAll, Korea). In brief, 5 volumes (µl) of DNA binding buffer (5 M guanidine hydrochloride; 30% (v/v) isopropanol) were mixed with 1 volume (µl) of DNA sample and mixed by vortexing. The mixture was transferred to a spin column with collection tube, and centrifuged at 15,000 x g for 30 seconds. The flow through was discarded before adding 750 µl of wash buffer (10 mM Tris base, pH 7.5; 80% (v/v) ethanol) and centrifuged at 15,000 x g for 30 seconds. Centrifugation was repeated for another 1 minute to remove residual liquid. Lastly, the column was placed in a clean microcentrifuge tube and 30 µl of elution buffer (10 mM Tris base; pH 8.5) was applied. The column was incubated at RT for 5 minutes before centrifuging at 15,000 x g for 1 minute.

RE-digested products were purified from agarose gel using QIAquick PCR purification kit (Qiagen, Germany) and Expin™ Combo GP (GeneAll, Korea). Firstly, the DNA band of interest was excised using a razor blade. Following that, 3 volumes (µl) of neutralisation and binding buffer (20 mM Tris base, pH 6.6; 5.5 M guanidine thiocyanate) was added to each volume (mg) of excised gel. The mixture was incubated

at 50°C for 10 minutes until the gel had completely dissolved. Then, 1 gel volume of 100% (v/v) isopropanol was added and vortexed to mix. The mixture was transferred to a spin column with collection tube and centrifuged at 15,000 x g for 1 minute. The flow through was discarded and 700 µl of wash buffer (10 mM Tris base, pH 7.5; 80% (v/v) ethanol) was added, followed by centrifugation at 15,000 x g for 1 minute. Residual buffer was removed by an additional 1-minute centrifugation. Lastly, 30 µl of elution buffer (10 mM Tris base; pH 8.5) was applied to the column for 5 minutes, followed by centrifugation at 15,000 x g for 1 minute.

The purity and concentration of purified DNA products were determined using a NanoDrop 1000 spectrophotometer before further use.

3.2.10 Ligation of vector and insert

All the RE-digested inserts were ligated into pEAQ-*HT* vector at the molar ratio of 3:1 using T4 DNA ligase (New England Biolabs, USA). The reaction mixture was prepared as follows: 1X T4 DNA ligase buffer (50 mM Tris-HCl, pH 7.5; 10 mM magnesium chloride; 10 mM dithiothreitol; 1 mM adenosine triphosphate), 50 ng of vector, 150 ng of insert, 200 units of T4 ligase and topped up to 10 µl with distilled water. Then, ligation was performed overnight at 4°C.

3.2.11 Preparation of competent cells

TOP10 competent *Escherichia coli* was prepared according to the method described by Nishimura *et al.* (1990). Firstly, glycerol stock of TOP10 cells was revived by streaking on Luria-Bertani (LB) agar plate (10 g/l tryptone; 5 g/l yeast extract; 10 g/l sodium chloride; 15 g/l agar). A single colony was picked on the next day and inoculated in LB broth culture (10 g/l tryptone; 5 g/l yeast extract; 10 g/l sodium chloride). After overnight incubation, the bacterial cells were sub-cultured into a conical flask

containing 50 ml of super optimal broth with catabolite repressor (SOC) media (20 g/l tryptone; 5 g/l yeast extract; 0.5 g/l sodium chloride; 5 g/l magnesium sulphate heptahydrate; 20 mM glucose) and transferred to an incubator shaker set at 37°C. The optical density at 600 nm wavelength (OD₆₀₀) was checked at every 15-minute intervals. Once OD₆₀₀ = 0.5 was reached, the cells were stored on ice for 10 minutes and then centrifuged at 1,500 x g at 4°C for 10 minutes. Lastly, pellet was recovered in 0.5 ml of SOC and 2.5 ml of storage medium containing 36% (v/v) glycerin, 12% (w/v) polyethylene glycol and 12 mM magnesium sulphate heptahydrate dissolved in LB broth. The competent cells were then stored at -80°C.

3.2.12 Transformation of TOP10 competent *Escherichia coli*

All the ligated mixtures were introduced into TOP10 competent cells using heat-shock method. Briefly, the cells were thawed on ice before mixing with 100 ng of DNA. After the 30-minute incubation on ice, the cells were heat-shocked in 42°C water bath for 45 seconds and then chilled immediately on ice for 2 minutes. SOC media was aseptically added and the cells were left to recover with shaking at 37°C for 1 hour. Lastly, transformed cells were spread on LB agar plate supplemented with 50 µg/ml of kanamycin. The plate was incubated at 37°C for 16 hours and the colonies were subjected to PCR screening.

3.2.13 Verification of recombinant vector

For PCR screening of bacterial colony, GoTaq[®] Green Master Mix (Promega, USA) and Recombinant Taq DNA polymerase (Thermo Scientific, USA) were used. PCR reaction mixtures were prepared as described in **Section 3.2.5**; except for the template that was substituted with transformed clone picked from selective agar plate. For colony screening use, C1 and C3 primers had been specifically designed to span

from CPMV RNA-2 5'UTR to CPMV RNA-2 3' UTR of the pEAQ-*HT* vector (**Figure 3.4**, as highlighted in yellow). All the thermocycling conditions were set as follows: initial denaturation at 95°C for 5 minutes, followed by 30 cycles of denaturation at 95°C for 1 minute, annealing at 58°C for 45 seconds and extension at 72°C for 1 minute/kbp. A final elongation step was held at 72°C for 5 minutes. The expected size of PCR product amplified from transformed clone is summarised in **Table 3.5**.

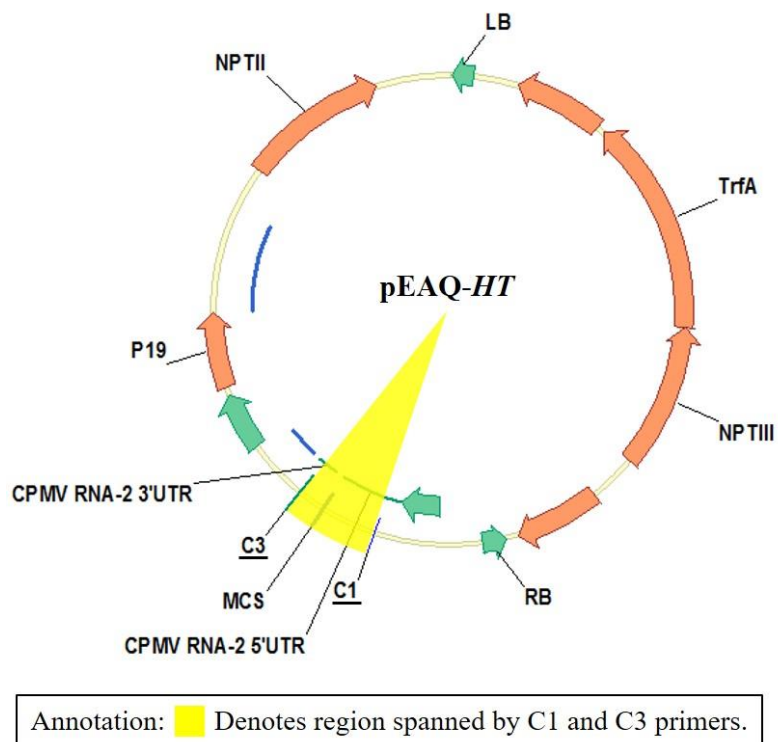


Figure 3.4: C1 and C3 primers used for all PCR screening works in this study.

Table 3.5: The expected size of amplicon from PCR colony screening, using C1 and C3 primers.

No.	Transformed clone	Expected amplicon size
1	pEAQ- <i>HT</i> :: cEDIII-sGFP-KDEL-H	1.644 kbp
2	pEAQ- <i>HT</i> :: PR1a-cEDIII-sGFP-H-KDEL	1.729 kbp
3	pEAQ- <i>HT</i> :: CTB-cEDIII-KDEL-H	1.308 kbp
4	pEAQ- <i>HT</i> :: PR1a-CTB-cEDIII-H-KDEL	1.396 kbp
5	pEAQ- <i>HT</i> :: PR1a-CTB-cEDIII-KDEL (xTH)	1.357 kbp
6	pEAQ- <i>HT</i> :: mHBcAg-cEDIII	1.435 kbp
7	pEAQ- <i>HT</i> :: mHBcAg-cEDIII (L)	1.534 kbp
8	pEAQ- <i>HT</i> :: tHBcAg-cEDIII	2.087 kbp
9	pEAQ- <i>HT</i>	0.603 kbp
10	pEAQ- <i>HT</i> ::mEL	1.156 kbp
11	pEAQ- <i>HT</i> ::tHBcAg-VHH2	2.162 kbp

Upon PCR confirmation of putative clones, the recombinant vectors were extracted (described in **Section 3.2.6**) and subsequently sent for sequencing. At least four primers were used to map each cassette (**Table 3.6**), so that these sequenced fragments could cover greater read length of the pEAQ-*HT* MCS region (**Figure 3.1**, Panel B). The Sanger sequencing results obtained from Eurofins Genomics (Germany) and First Base Laboratories (Singapore) were assembled using Sequence Scanner Software 2, followed by analyses with nucleotide Basic Local Alignment Search Tool (BLAST) and Vector NTI Software (Thermo Scientific, USA) for further verification.

Table 3.6: List of primers used for the sequencing of specific recombinant vector.

No.	Recombinant vector	Sequencing primer
1	pEAQ- <i>HT</i> :: cEDIII-sGFP-KDEL-H	<ul style="list-style-type: none"> ▪ C1 ▪ C3 ▪ cED3F ▪ cED3R
2	pEAQ- <i>HT</i> :: PR1a-cEDIII-sGFP-H-KDEL	<ul style="list-style-type: none"> ▪ C1 ▪ C3 ▪ cED3F ▪ cED3R
3	pEAQ- <i>HT</i> :: CTB-cEDIII-KDEL-H	<ul style="list-style-type: none"> ▪ C1 ▪ C3 ▪ cED3F ▪ cED3R
4	pEAQ- <i>HT</i> :: PR1a-CTB-cEDIII-H-KDEL	<ul style="list-style-type: none"> ▪ C1 ▪ C3 ▪ cED3F ▪ cED3R
5	pEAQ- <i>HT</i> :: PR1a-CTB-cEDIII-KDEL (xTH)	<ul style="list-style-type: none"> ▪ C1 ▪ C3 ▪ cED3F ▪ CTBcED3F ▪ CTBcED3R (2nd)
6	pEAQ- <i>HT</i> :: mHBcAg-cEDIII	<ul style="list-style-type: none"> ▪ C1 ▪ C3 ▪ 5' MCS ▪ 3' MCS ▪ 5' core c/e1 ▪ 3' core c/e1
7	pEAQ- <i>HT</i> :: mHBcAg-cEDIII (L)	<ul style="list-style-type: none"> ▪ C1 ▪ C3 ▪ 5' MCS ▪ 3' MCS ▪ 5' core c/e1 ▪ 3' core c/e1
8	pEAQ- <i>HT</i> :: tHBcAg-cEDIII	<ul style="list-style-type: none"> ▪ C1 ▪ C3 ▪ 5' MCS ▪ 3' MCS ▪ 5' core c/e1 ▪ 3' core c/e1

3.3 Results

3.3.1 Codon optimisation of *cEDIII* genes

The codon preference of *cEDIII* genes had been adjusted according to *N. benthamiana* codon usage in order to enhance heterologous gene expression. As shown in **Table 3.7**, successful codon optimisation was reflected from the higher codon adaptation index (CAI) obtained for all synthesised sequences. The index is used to assess how well the codon usage of a gene matches to the reference set in the expression host, and an ideal CAI of 1.0 would indicate that the frequency of synonymous codon used is the same. In this case, the optimised indexes were considered as satisfactory with values ≥ 0.85 .

Table 3.7: The adjustment of codon usage for synthesised sequences.

No.	Synthesised sequences	Codon adaptation index (CAI)	
		Before optimisation	After optimisation
1	cEDIII-sGFP-KDEL	0.64	0.86
2	PR1a-cEDIII-sGFP-H-KDEL	0.65	0.87
3	CTB-cEDIII-KDEL	0.78	0.86
4	PR1a-CTB-cEDIII-H-KDEL	0.77	0.85

3.3.2 Polymerase chain reaction (PCR) amplification of cEDIII inserts

Specific cEDIII inserts were amplified using high fidelity Phusion[®] Taq to isolate inserts for cloning into expression vectors, pEAQ-*HT*, pEAQ-*HT*::mEL and pEAQ-*HT*::tHBcAg-VHH2.

Expression cassettes that were designed to express cEDIII recombinant fusion proteins, namely cEDIII-sGFP-KDEL, CTB-cEDIII-KDEL and PR1a-CTB-cEDIII-KDEL (xTH), were successfully isolated by PCR as shown in **Figure 3.5**.

For cEDIII inserts that were designed for presentation on the c/e1 loop of mHBcAg and tHBcAg VLPs, namely cEDIII_mono, cEDIII (L)_mono and cEDIII_tandem, successful amplification was achieved as presented in **Figure 3.6**.

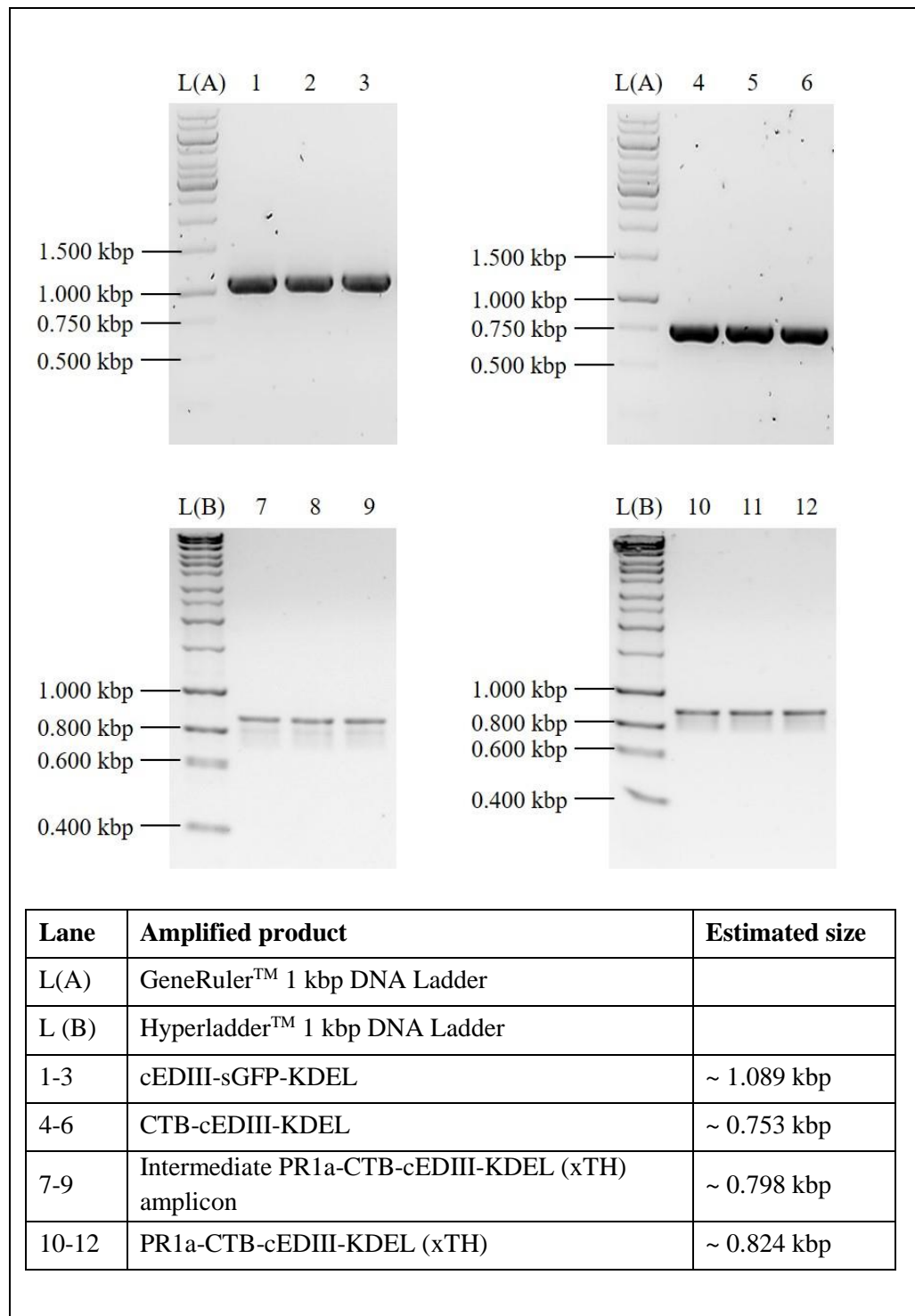


Figure 3.5: PCR amplification profiles of inserts used for vector construction of cEDIII recombinant fusion proteins, namely cEDIII-sGFP-KDEL, CTB-cEDIII-KDEL, intermediate PR1a-CTB-cEDIII-KDEL (xTH) amplicon and PR1a-CTB-cEDIII-KDEL (xTH).

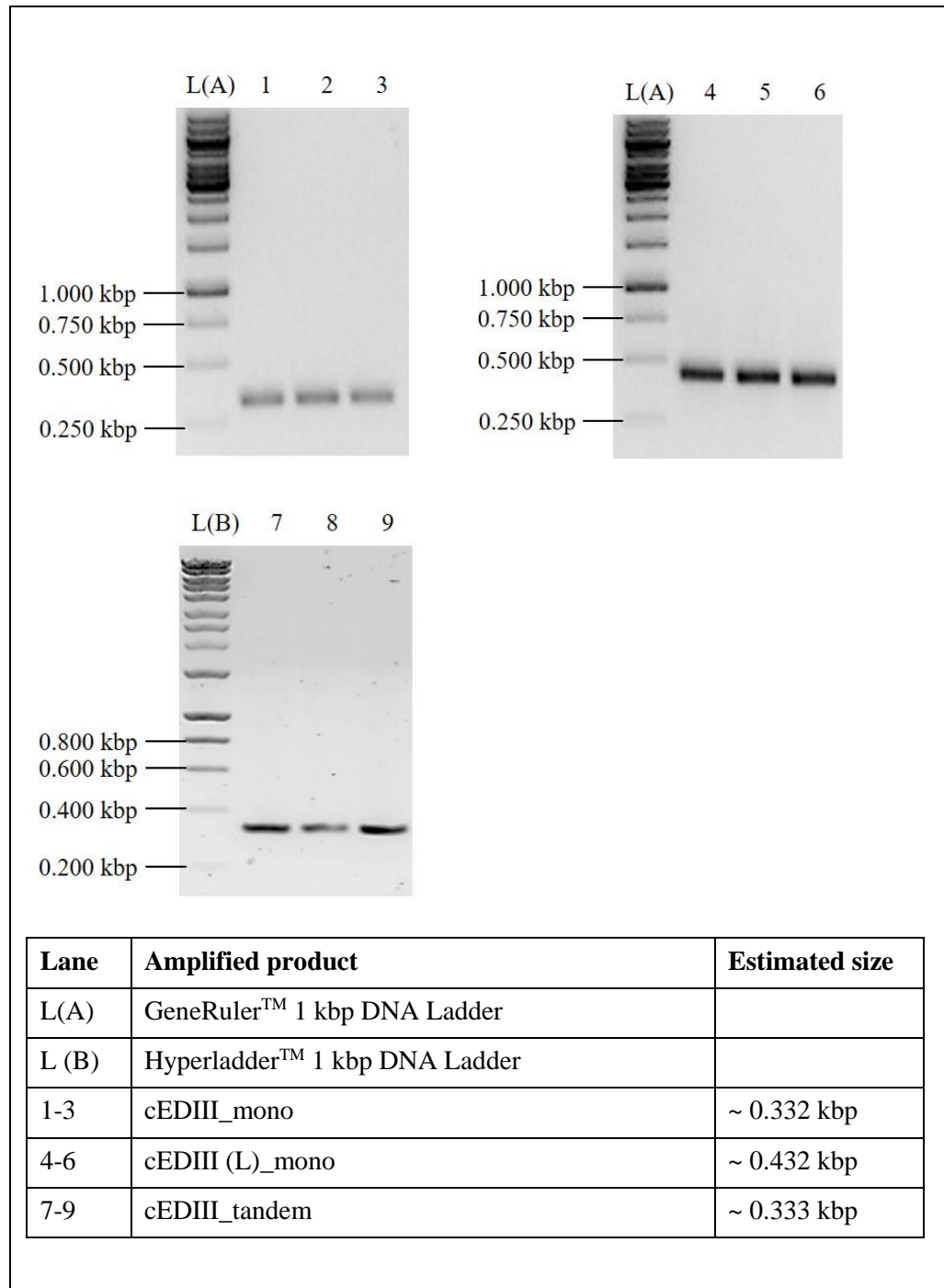


Figure 3.6: PCR amplification profiles of inserts used for vector construction of chimeric mHBcAg and tHBcAg VLPs, namely cEDIII_mono, cEDIII (L)_mono and cEDIII_tandem.

3.3.3 Restriction enzyme (RE) digestion of cEDIII expression cassettes

Two cEDIII expression cassettes that were designed to produce cEDIII recombinant fusion proteins, namely PR1a-cEDIII-sGFP-H-KDEL and PR1a-CTB-cEDIII-H-KDEL, were directly isolated from the pUC57 holding vectors as illustrated in **Figure 3.7**. Digested fragments were then purified from DNA gel and cloned into pEAQ-*HT* vector.

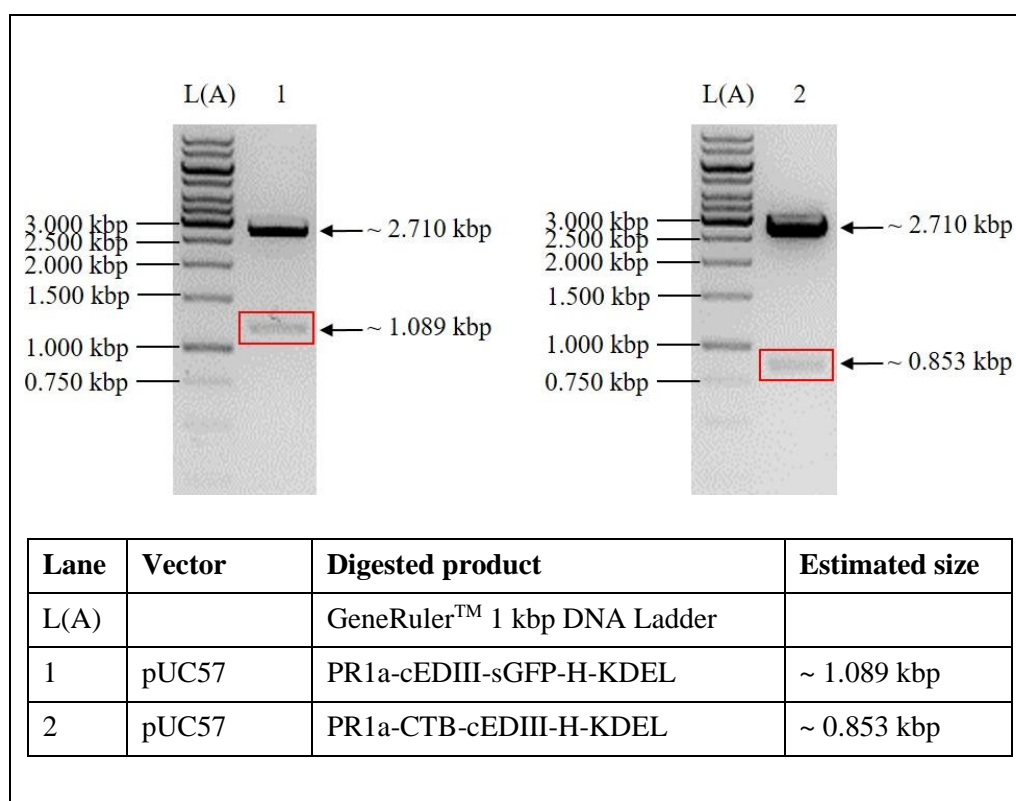
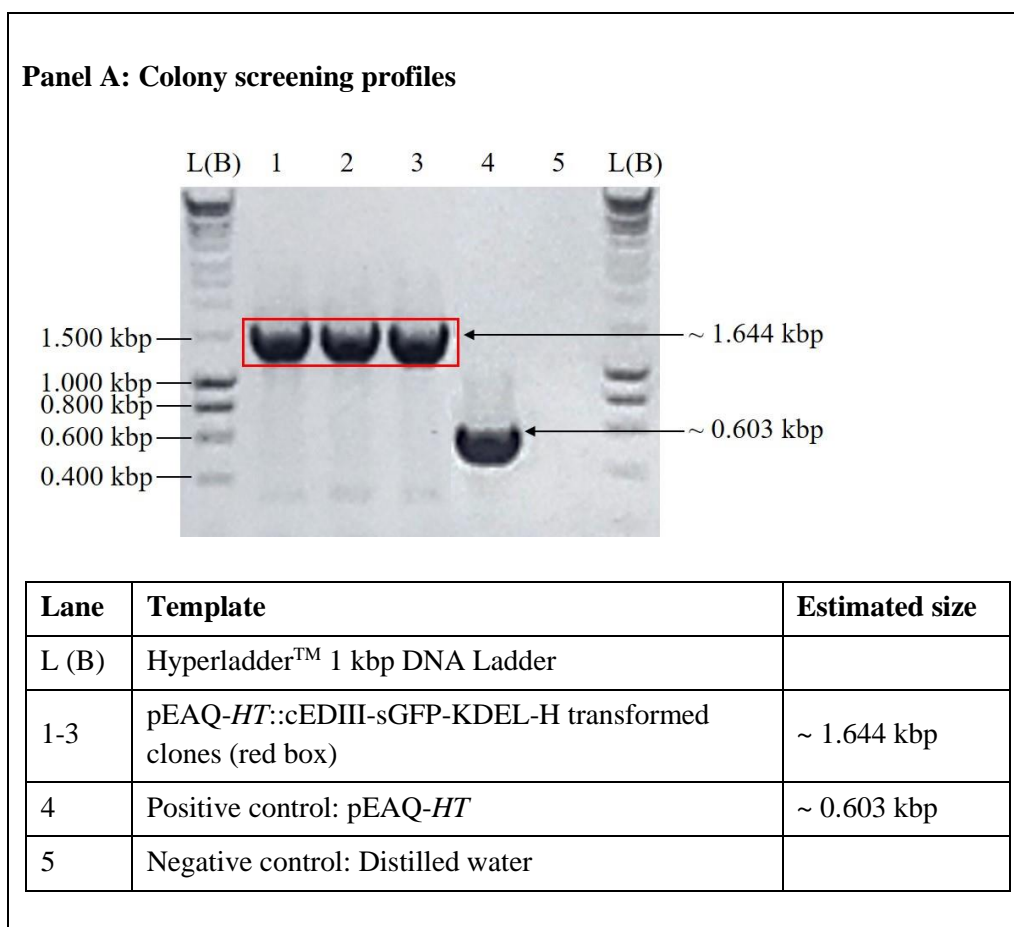


Figure 3.7: RE digestion profiles of inserts used to design the expression cassettes for cEDIII recombinant fusion proteins, namely PR1a-cEDIII-sGFP-H-KDEL and PR1a-CTB-cEDIII-H-KDEL. Successful isolation of desired products was indicated by red box.

3.3.4 Screening of transformed clones

All the transformed clones were analysed by PCR screening to confirm the presence of transgene. Colony screening profiles for the following recombinant vectors were obtained after amplification with C1 and C3 primers: pEAQ-*HT*::cEDIII-sGFP-KDEL-H (**Figure 3.8**); pEAQ-*HT*::PR1a-cEDIII-sGFP-H-KDEL (**Figure 3.9**); pEAQ-*HT*::CTB-cEDIII-KDEL-H (**Figure 3.10**); pEAQ-*HT*::PR1a-CTB-cEDIII-H-KDEL (**Figure 3.11**); pEAQ-*HT*::PR1a-CTB-cEDIII-KDEL (xTH) (**Figure 3.12**); pEAQ-*HT*::mHBcAg-cEDIII (**Figure 3.13**); pEAQ-*HT*::mHBcAg-cEDIII (L) (**Figure 3.14**) and pEAQ-*HT*::tHBcAg-cEDIII (**Figure 3.15**). Verified clones harbouring the expected amplicon size (as highlighted in red box) were selected for sequencing confirmation.



Panel B: Schematic diagram of recombinant vector

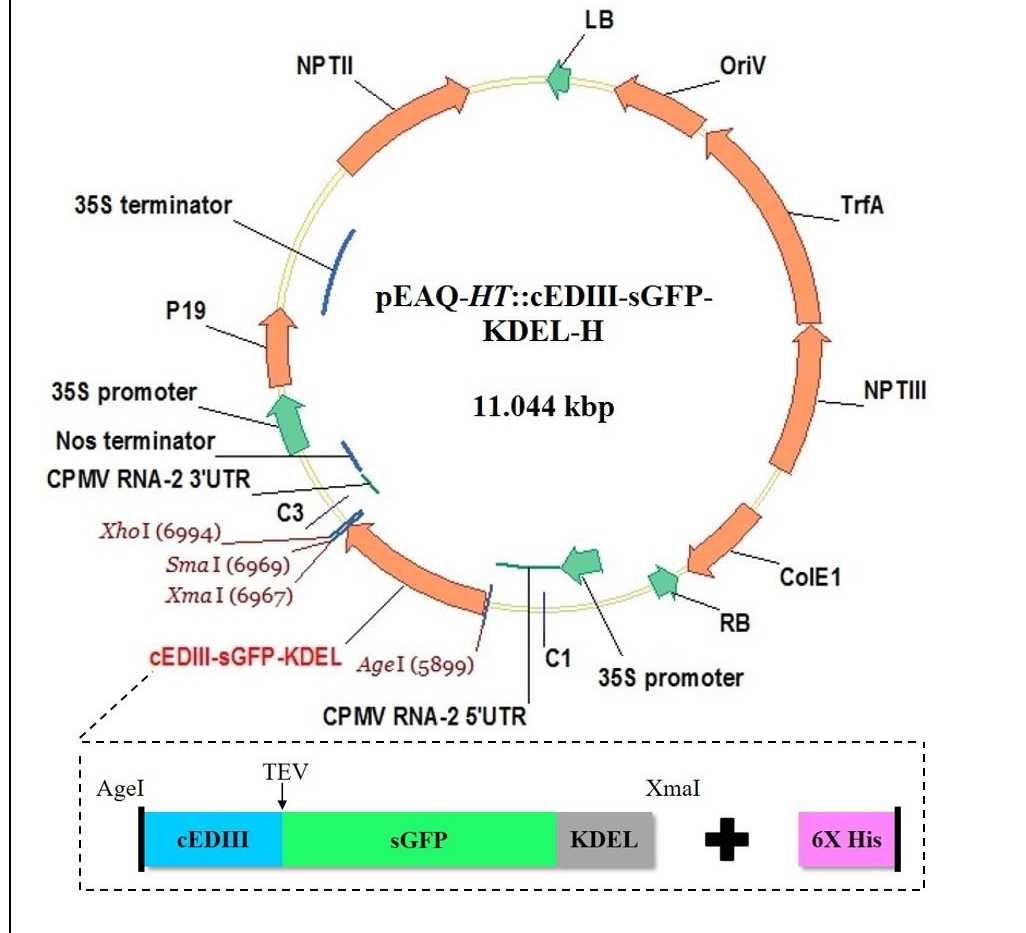
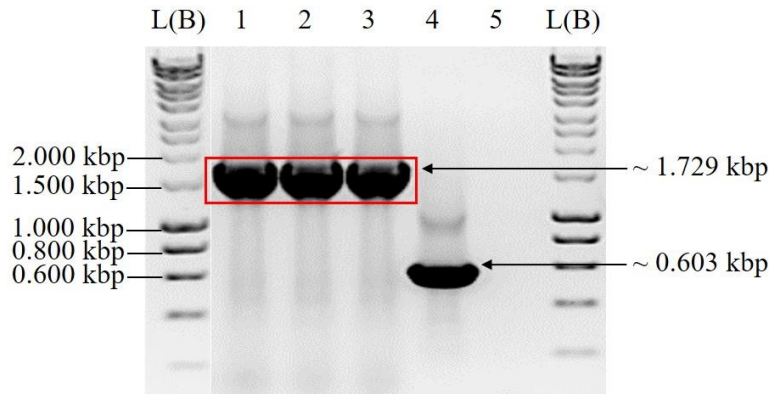


Figure 3.8: Verification of TOP10 cells transformed with pEAQ-HT::cEDIII-sGFP-KDEL-H. Panel A: PCR colony screening profiles using C1 and C3 primers, by which the pEAQ-HT::cEDIII-sGFP-KDEL-H vector was successfully detected in putative clones (red box). The pEAQ-HT vector served as a positive control for the PCR. Panel B: Schematic illustration of the recombinant vector with cEDIII-sGFP-KDEL-H expression cassette.

Panel A: Colony screening profiles



Lane	Template	Estimated size
L (B)	Hyperladder™ 1 kbp DNA Ladder	
1-3	pEAQ- <i>HT</i> ::PR1a-cEDIII-sGFP-H-KDEL transformed clones (red box)	~ 1.729 kbp
4	Positive control: pEAQ- <i>HT</i>	~ 0.603 kbp
5	Negative control: Distilled water	

Panel B: Schematic diagram of recombinant vector

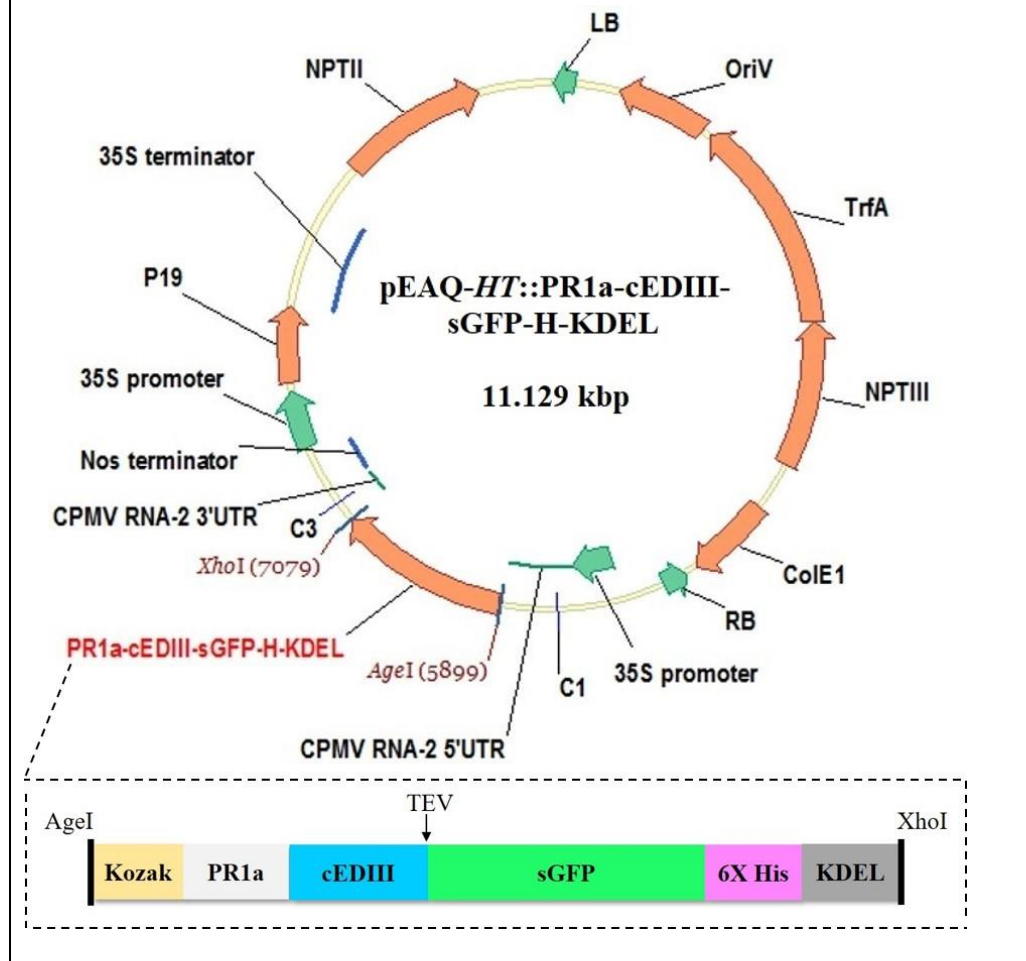
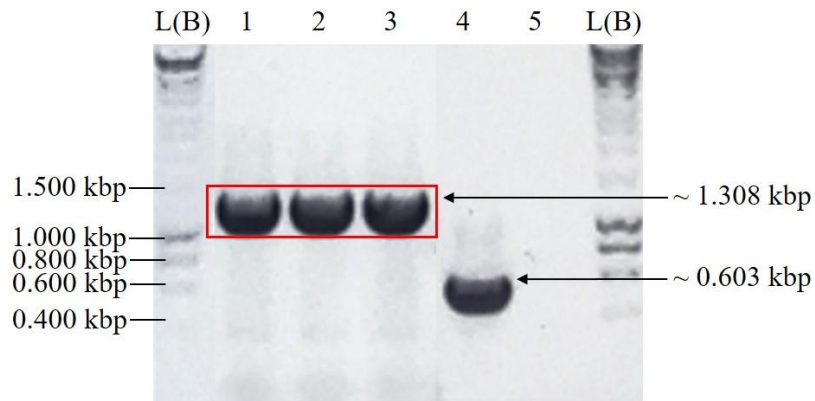


Figure 3.9: Verification of TOP10 cells transformed with pEAQ-*HT*::PR1a-cEDIII-sGFP-H-KDEL. Panel A: PCR screening profiles using C1 and C3 primers, by which the pEAQ-*HT*::PR1a-cEDIII-sGFP-H-KDEL vector was successfully detected in putative clones (red box). The pEAQ-*HT* vector served as a positive control for the PCR. Panel B: Schematic illustration of the recombinant vector with PR1a-cEDIII-sGFP-H-KDEL expression cassette.

Panel A: Colony screening profiles



Lane	Template	Estimated size
L (B)	Hyperladder™ 1 kbp DNA Ladder	
1-3	pEAQ- <i>HT</i> ::CTB-cEDIII-KDEL-H transformed clones (red box)	~ 1.308 kbp
4	Positive control: pEAQ- <i>HT</i>	~ 0.603 kbp
5	Negative control: Distilled water	

Panel B: Schematic diagram of recombinant vector

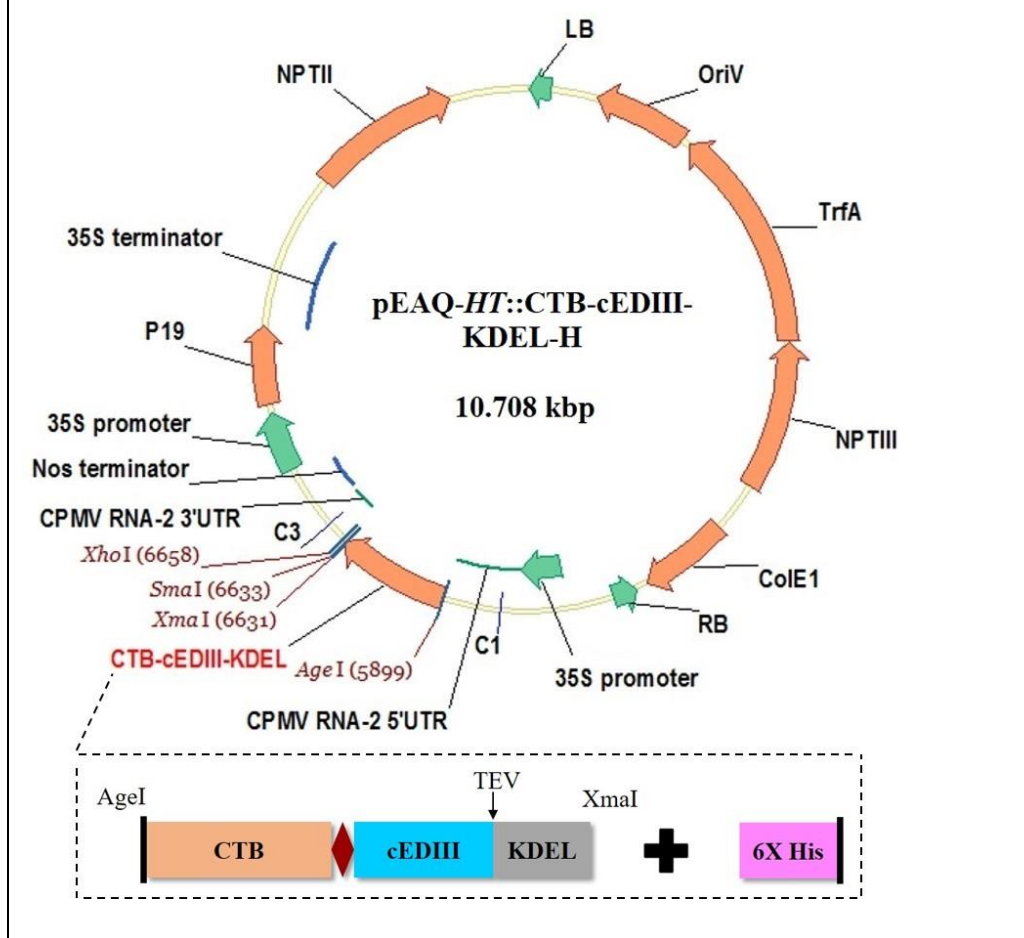
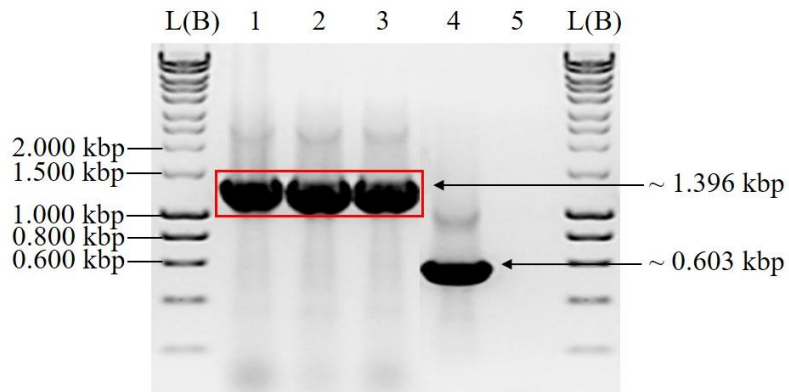


Figure 3.10: Verification of TOP10 cells transformed with pEAQ-HT::CTB-cEDIII-KDEL-H. Panel A: PCR screening profiles using C1 and C3 primers, by which the pEAQ-HT::CTB-cEDIII-KDEL-H vector was successfully detected in putative clones (red box). The pEAQ-HT vector served as a positive control for the PCR. Panel B: Schematic illustration of the recombinant vector with CTB-cEDIII-KDEL-H expression cassette.

Panel A: Colony screening profiles



Lane	Template	Estimated size
L (B)	Hyperladder™ 1 kbp DNA Ladder	
1-3	pEAQ- <i>HT</i> ::PR1a-CTB-cEDIII-H-KDEL transformed clones (red box)	~ 1.396 kbp
4	Positive control: pEAQ- <i>HT</i>	~ 0.603 kbp
5	Negative control: Distilled water	

Panel B: Schematic diagram of recombinant vector

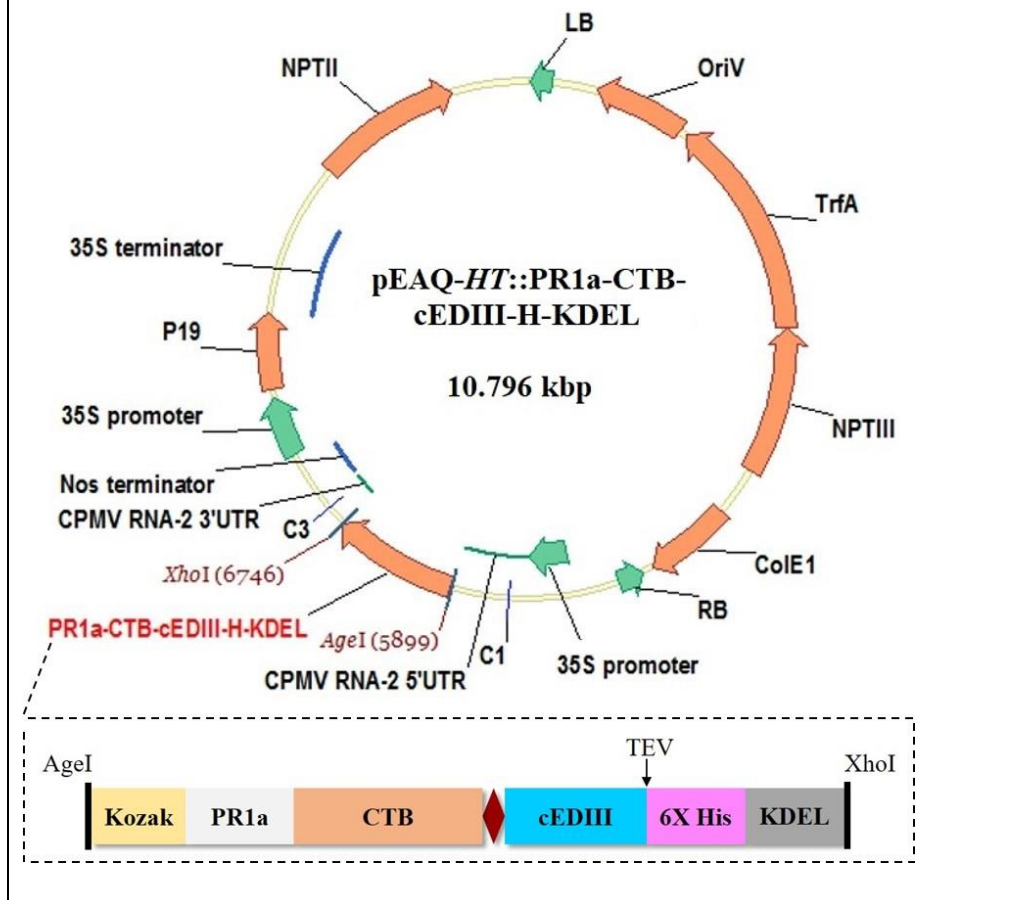
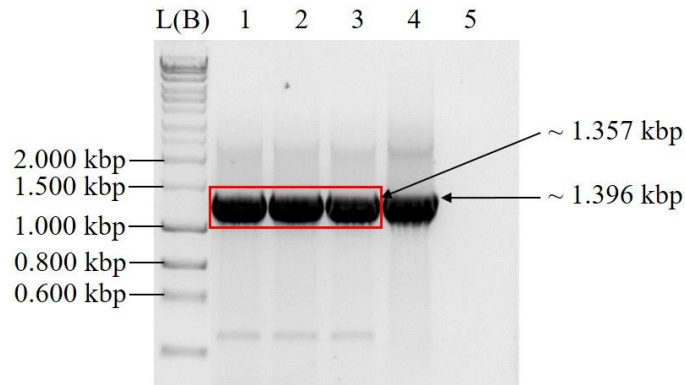


Figure 3.11: Verification of TOP10 cells transformed with pEAQ-*HT*::PR1a-CTB-cEDIII-H-KDEL. Panel A: PCR screening profiles using C1 and C3 primers, by which the pEAQ-*HT*::PR1a-CTB-cEDIII-H-KDEL vector was successfully detected in putative clones (red box). The pEAQ-*HT* vector served as a positive control for the PCR. Panel B: Schematic illustration of the recombinant vector with PR1a-CTB-cEDIII-H-KDEL expression cassette.

Panel A: Colony screening profiles



Lane	Template	Estimated size
L (B)	Hyperladder™ 1 kbp DNA Ladder	
1-3	pEAQ- <i>HT</i> ::PR1a-CTB-cEDIII-H-KDEL (xTH) transformed clones (red box)	~ 1.357 kbp
4	Positive control: pEAQ- <i>HT</i> ::PR1a-CTB-cEDIII-H-KDEL	~ 1.396 kbp
5	Negative control: Distilled water	

Panel B: Schematic diagram of recombinant vector

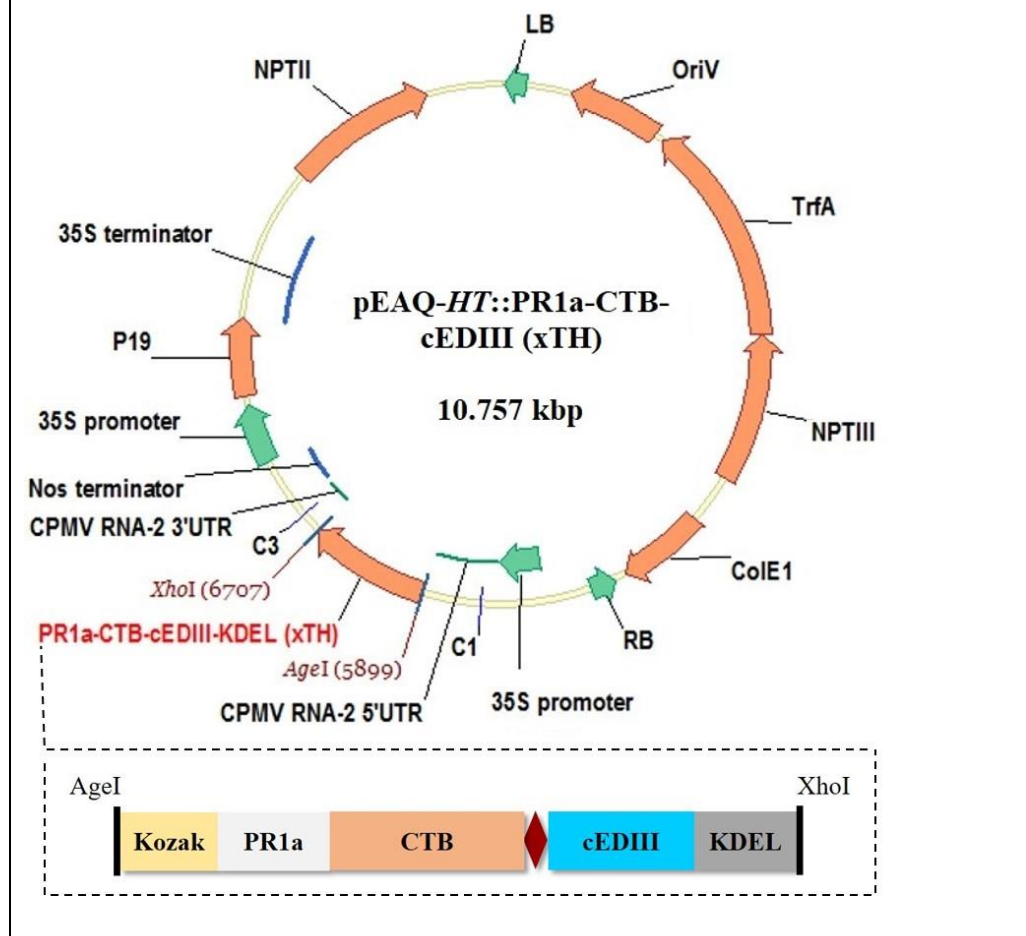
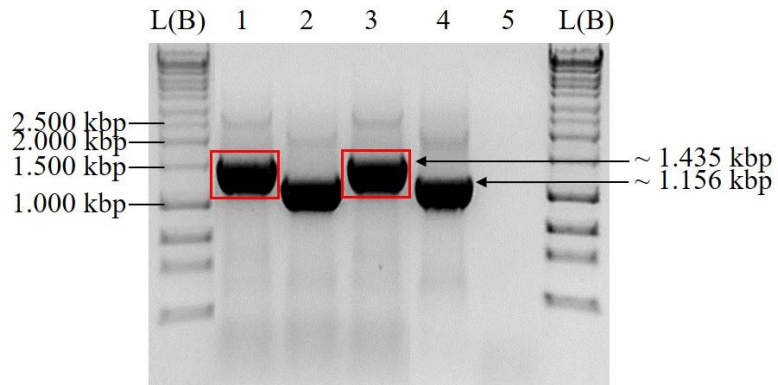


Figure 3.12: Verification of TOP10 cells transformed with pEAQ-*HT*::PR1a-CTB-cEDIII-KDEL (xTH). Panel A: PCR screening profiles using C1 and C3 primers, by which the pEAQ-*HT*::PR1a-CTB-cEDIII-KDEL (xTH) vector was successfully detected in putative clones (red box). The pEAQ-*HT*::PR1a-CTB-cEDIII-H-KDEL vector served as a positive control for the PCR. Panel B: Schematic illustration of the recombinant vector with PR1a-CTB-cEDIII-KDEL (xTH) cassette.

Panel A: Colony screening profiles



Lane	Template	Estimated size
L (B)	Hyperladder™ 1 kbp DNA Ladder	
1-3	pEAQ- <i>HT</i> ::mHBcAg-cEDIIII transformed clones (red box)	~ 1.435 kbp
4	Positive control: pEAQ- <i>HT</i> ::mEL	~ 1.156 kbp
5	Negative control: Distilled water	

Panel B: Schematic diagram of recombinant vector

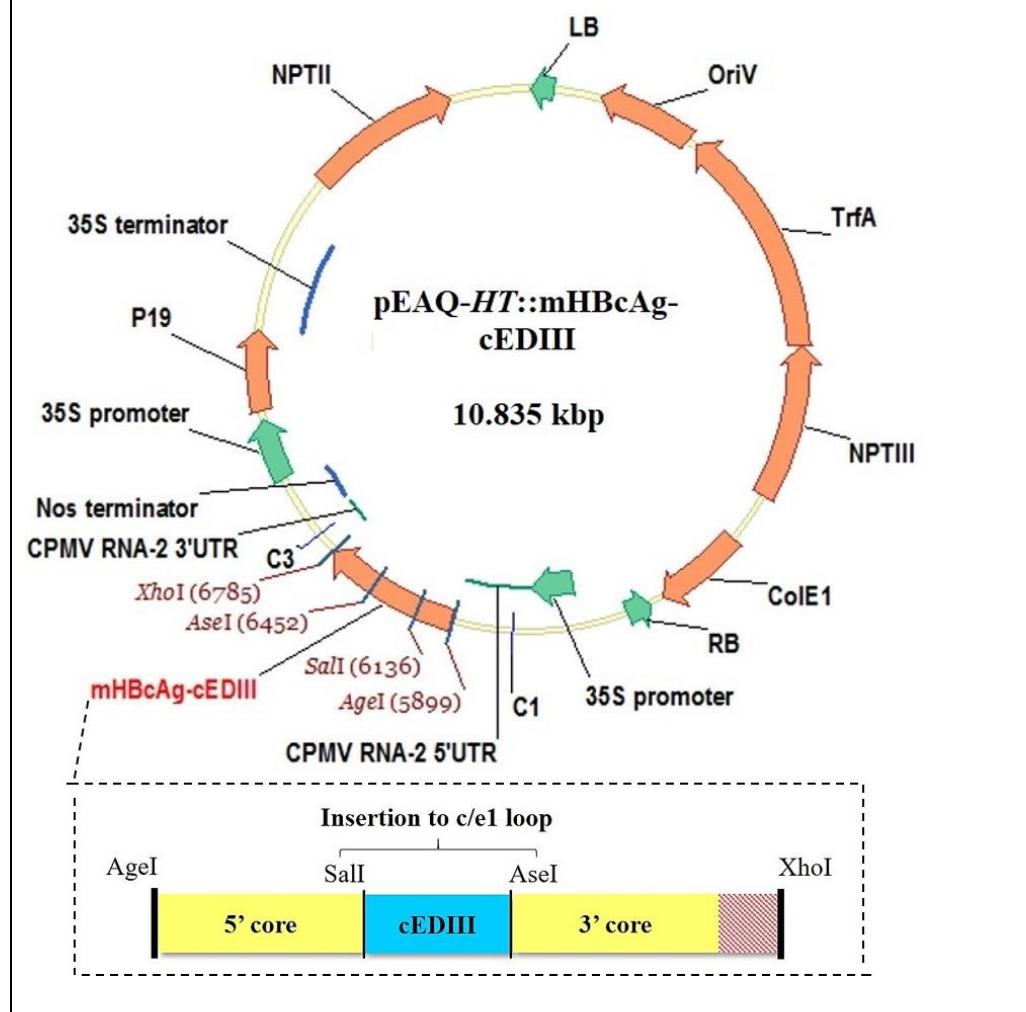
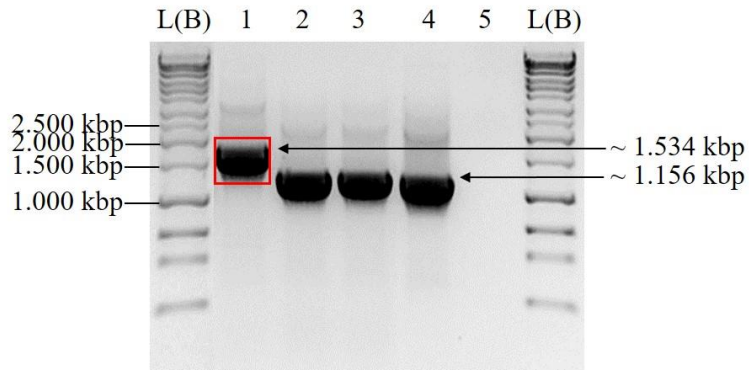


Figure 3.13: Verification of TOP10 cells transformed with pEAQ-*HT*::mHBcAg-cEDIII. Panel A: PCR colony screening profiles using C1 and C3 primers, by which the pEAQ-*HT*::mHBcAg-cEDIII vector was successfully detected in putative clones (red box). The pEAQ-*HT*::mEL vector served as a positive control for the PCR. Panel B: Schematic illustration of the recombinant vector with mHBcAg-cEDIII expression cassette.

Panel A: Colony screening profiles



Lane	Template	Estimated size
L (B)	Hyperladder™ 1 kbp DNA Ladder	
1-3	pEAQ- <i>HT</i> ::mHBcAg-cEDIII (L) transformed clones (red box)	~ 1.534 kbp
4	Positive control: pEAQ- <i>HT</i> ::mEL	~ 1.156 kbp
5	Negative control: Distilled water	

Panel B: Schematic diagram of recombinant vector

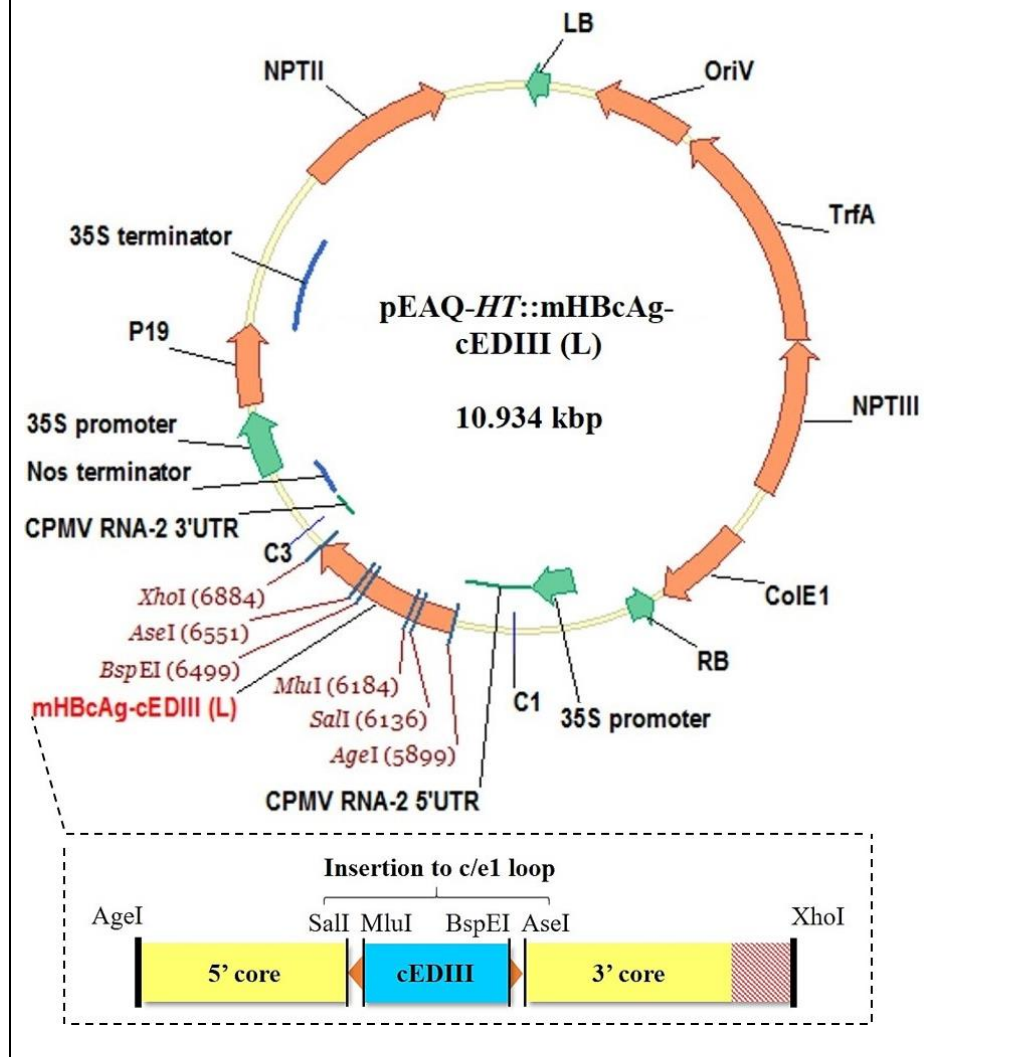
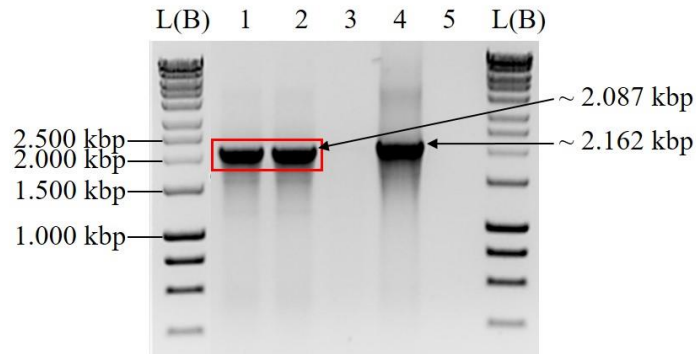


Figure 3.14: Verification of TOP10 cells transformed with pEAQ-*HT*::mHBcAg-cEDIII (L). Panel A: PCR colony screening profiles using C1 and C3 primers, by which the pEAQ-*HT*::mHBcAg-cEDIII (L) vector was successfully detected in putative clone (red box). The pEAQ-*HT*::mEL vector served as a positive control for the PCR. Panel B: Schematic illustration of the recombinant vector with mHBcAg-cEDIII (L) expression cassette.

Panel A: Colony screening profiles



Lane	Template	Estimated size
L (B)	Hyperladder™ 1 kbp DNA Ladder	
1-3	pEAQ- <i>HT</i> ::tHBcAg-cEDIII transformed clones (red box)	~ 2.087 kbp
4	Positive control: pEAQ- <i>HT</i> ::tHBcAg-VHH2	~ 2.162 kbp
5	Negative control: Distilled water	

Panel B: Schematic diagram of recombinant vector

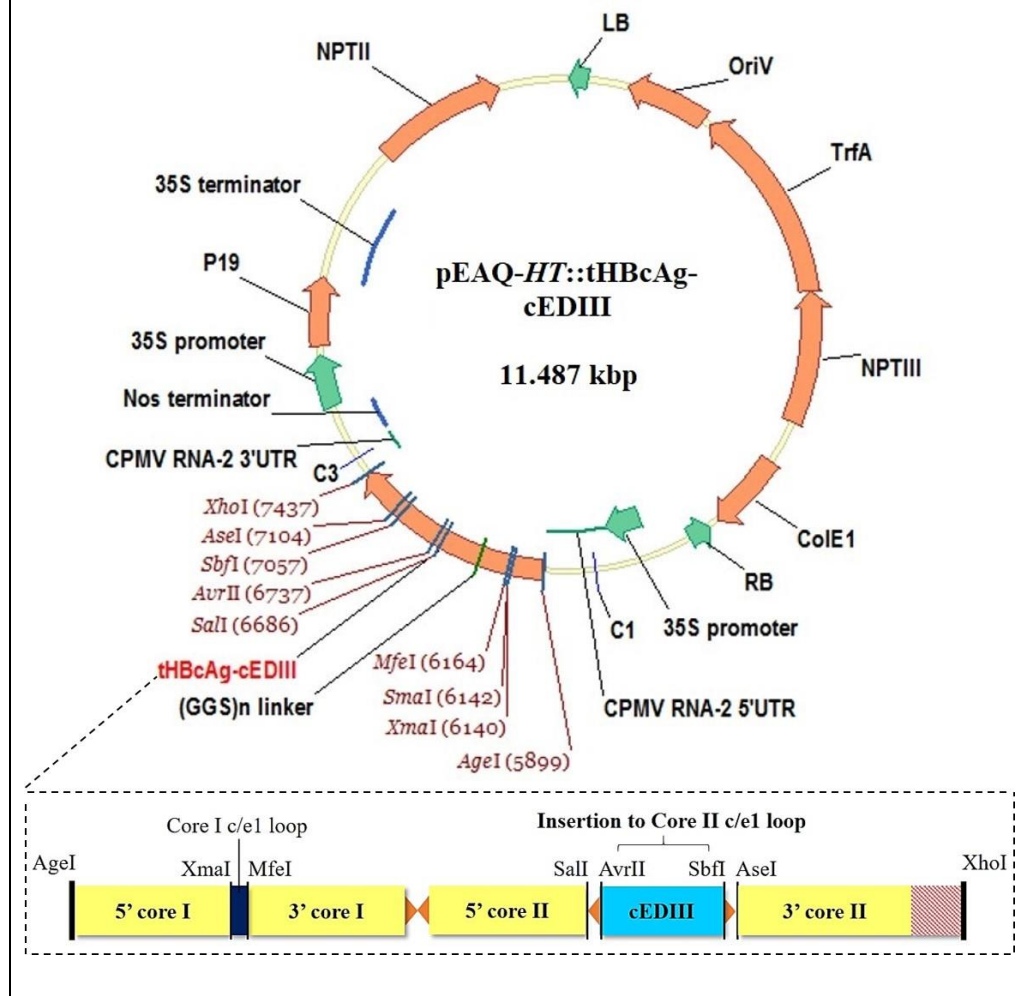


Figure 3.15: Verification of TOP10 cells transformed with pEAQ-*HT*::tHBcAg-cEDIII. Panel A: PCR colony screening profiles using C1 and C3 primers, by which the pEAQ-*HT*::tHBcAg-cEDIII vector was successfully detected in putative clones (red box). The pEAQ-*HT*::tHBcAg-VHH2 vector served as a positive control for the PCR. Panel B: Schematic illustration of the recombinant vector with tHBcAg-cEDIII expression cassette.

3.3.5 Verification by DNA sequencing

Following analyses of the sequencing results, all the recombinant vectors were confirmed to harbour expected expression cassettes without mismatched or frame shift mutation. An example of the stepwise alignment of sequencing results with the expected DNA sequence is shown in **Appendix A3.9**. These verified recombinant vectors were then delivered into *N. benthamiana* plants through agroinfiltration, which is discussed in **Chapter 4**.

3.4 Discussion

This chapter essentially describes the construction process of recombinant vectors used to achieve plant-based cEDIII production in *N. benthamiana*. As mentioned, cEDIII represents a novel vaccine candidate that is generated from the alignment of EDIII sequence from different strains of the four DENV serotypes. As illustrated in **Appendix A3.10**, a consensus sequence of serotype-specific EDIII was individually obtained before these four sequences were re-aligned to generate the cEDIII that is representative of DENV serotypes 1 to 4. The use of cEDIII for vaccine development is justified by the need to confer a simultaneous protection against all DENV serotypes to avoid immune interference. Moreover, considering that virus mutation is likely to happen, a vaccine that can provide consistent protection in the long run will be more highly valued. In fact, DENV clade replacements had been detected in recent years which was correlated to recurrences of disease outbreaks (Teoh *et al.*, 2013). Although some researchers might argue that a tetravalent vaccine also can be derived by combining the monovalent component of each serotype (Block *et al.*, 2010), however this demands for a series of empirical trials in order to determine the best formulation. Therefore, from a production standpoint, generating a single cEDIII protein as the principal component should be able to reduce the underlying costs.

With the aim to achieve high transgene expression, codon optimisation of the *cEDIII* gene, along with its fusion partner including *sGFP* gene and *CTB* gene was performed based on *N. benthamiana* codon usage bias. Codon bias is inherently unique to each species, as it defines specific preference over synonymous codon due to degeneracy of the genetic code. In most cases, the transgene donor and host species are likely to show divergence in their codon usage due to the difference in cognate transfer-RNA (Ikemura, 1985). As a result, this would have a profound impact on the protein expression level as rare codons can reduce the efficiency of translation by tuning the elongation rates (Quax *et al.*, 2015). Besides, re-coding the codons of foreign insert had

been shown to favour soluble protein production on top of boosting gene expression by 4–1000 folds (Angov *et al.*, 2008). This suggests that formation of insoluble aggregates can be minimised, thereby yielding a soluble functional protein that is more likely to assume native conformation. Codon optimisation is usually achieved by maximising the CAI to match the synonymous codon used by the expression host. Ranging from 0 to 1, all the synthesised sequences had been optimised to a high CAI of ≥ 0.85 , as compared to the native sequences with values between 0.6–0.7 (**Table 3.7**). Since CAI also serves as a predictive tool to characterise gene expression (Sharp and Li, 1987), it is foreseen that relatively high *cEDIII* gene expression can be achieved in *N. benthamiana* host plants.

The pEAQ-*HT* expression vector has been designed to allow direct gene insertion by restriction enzyme-based cloning, and inclusion of 6X His tag also can be tailored as desired (**Figure 3.1**, Panel B). In this study, the insertion of *cEDIII* fusion construct at (i) AgeI + XmaI sites and (ii) AgeI + XhoI sites, has facilitated the production of (i) C-terminal His-tagged protein and (ii) the unfused variant to study the optimal positioning of ER retention signal (**Table 3.2**). In fact, it is presumed that shuffling of KDEL signal would influence the protein accumulation level. Besides, the use of non-replicative pEAQ-*HT* system can omit concerns of biocontainment and potential genetic drift that have been described in **Section 2.3.2.2**. Another outstanding feature of pEAQ-*HT* is that, the vector has been designed to harbour P19 cassette on the same T-DNA region. Hence, this obviates the need to co-infiltrate another bacterial suspension to deliver the P19 construct, which is routinely done for most transient expression vectors such as MagnICON, pBY030 and pPZP. Post-translational gene silencing (PTGS) is often manifested by plant to defend against foreign materials including viruses and transgenes (Ratcliff *et al.*, 1997). To counter against PTGS, P19 helps to sequester the small double stranded RNAs generated by Dicer-Like enzyme from being incorporated into the RNA-induced silencing complex (RISC) (Silhavy *et al.*, 2002). This is because RISC can use

these effector molecules to initiate sequence-specific knockdown via mRNA degradation and inhibition of translation (Burgyán and Havelda, 2011). The P19 protein from tomato bushy stunt virus (TBSV) is preferred over other silencing suppressors such as cucumber mosaic virus 2b protein and potato virus Y P1-HC-protease, as the tombusvirus-encoded P19 is also able to boost the amount of co-expressed protein by 50 folds (Voinnet *et al.*, 2003). Therefore, it is useful to have the P19 concurrently expressed by pEAQ-*HT* to inhibit PTGS from stalling desired gene expression.

Hitherto, pEAQ-*HT* vector has been used to express a variety of products in plants ranging from recombinant proteins, active enzymes to VLPs. The versatility of pEAQ-*HT* vector has made it an excellent choice for *in planta* production of cEDIII as recombinant proteins and VLPs, in which their immunogenic potential can be relatively compared. Recombinant protein subunit vaccines are favoured for the defined production of specific antigen that is sufficient to evoke a protective immune response. In this case, cEDIII proved to be suitable as it can induce anamnestic antibody response following a challenge study with DENV (Leng *et al.*, 2009). On the other hand, VLPs-based vaccines can be regarded as a more highly-organised form of subunit vaccines. The repetitive array of protein subunits seems to offer VLPs the superiority as stand-alone vaccine, as compared to recombinant proteins that may be poorly presented to the immune system (Noad and Roy, 2003). Thus, the potential of VLPs development with enhanced cEDIII presentation is explored.

Since clear knowledge on the expression profile of cEDIII is imperative for downstream application, it is tagged with a sGFP partner to enable detection of the fluorescent fusion protein during expression and purification. sGFP is a non-destructive reporter that also allows *in situ* monitoring of the protein localisation under ultraviolet (UV) light. As protein translation starts from the 5' end, sGFP is preferentially fused to the C-terminus of cEDIII so that the expression of an intact cEDIII can be ascertained. A TEV protease recognition site was engineered between the cEDIII and sGFP (**Table**

3.2), in order to facilitate separation of cEDIII from the downstream sGFP and 6X His tag during purification. The cleavage using TEV protease was selected based on ExPASy Peptide Cutter software analysis.

Albeit the cholera toxin (CT) produced by *V. cholerae* has been described as one of strongest adjuvants (**Section 2.4.1.1**), the use of whole CT has been proven to be too toxic (Levine *et al.*, 1983). Therefore, with the aim of exploiting CT adjuvanticity, cEDIII fusion with the non-toxic component CTB is opted. The tight packing of CTB monomers into its pentasaccharide structure would make an excellent carrier for cEDIII antigen presentation to the immune system. Moreover, it is foreseen that formation of pentamer can help to stabilise the fusion protein in place. In this study, cEDIII was designed to fuse at the C-terminus of CTB partner. Liljeqvist *et al.* (1997) reported that this way of CTB C-terminal fusion had the most efficient binding to GM1 due to reduced steric hindrance, as the GM1 binding pocket was found near to the N-terminus of CTB. Following the successful vector construction, the adjuvanticity of CTB-cEDIII fusion protein can be explored later in this study. The efficacy of CTB had been proven to be so robust that it could boost the survival rate of immunised mice to 100% when the administration of antigen alone could not rescue the animals at all (Lee *et al.*, 2015b).

In this study, recombinant fusion proteins were targeted to ER to regulate protein glycosylation and accumulation. KDEL signal primarily helps to direct the retrograde transport of protein back to ER lumen upon recognition by KDEL receptor in *cis*-Golgi (Pelham, 1996). Due to the fact that plant and mammalian have different N-glycan processing in late Golgi apparatus, ER localisation is integrated with the hope to avoid improper glycosylation of cEDIII protein which may lead to inactivation of epitope reactivity or even elicit adverse immunogenicity (Lisowska, 2002). Plants generally produce $\beta(1, 2)$ -xylose and $\alpha(1, 3)$ -fucose residues instead of mammalian core $\alpha(1,6)$ -linked fucose and terminal sialic acids (Faye *et al.*, 2005). Besides, localisation to ER is expected to improve the yield of heterologous protein. This was supported by He *et al.*

(2014) findings, where ER retention had led to high accumulation of West Nile virus recombinant EDIII at 73 µg/g fresh weight tissue (FWT), while no yields were detected from cytosol- and chloroplast-targeted constructs. Given that the redox environment is highly regulated in ER (Ellgaard, 2004), optimal oxidoreductase activity can be achieved to form the disulphide bonds in cEDIII. This issue is highlighted because the correct folding of antibody recognition epitope on DENV EDIII lies upon the disulphide linkage between cysteine (Cys)28 and Cys59 (Suzarte *et al.*, 2014). For the 103 amino acids long cEDIII, these Cys residues are identified at positions 8 and 39 instead. The difference in Cys positions can be explained by the consensus sequence alignment of cEDIII (**Appendix A3.10**). For the reasons above, ER retention seems to be indispensable for the sequestration of correctly folded cEDIII protein in a stable cellular compartment. Since KDEL is the crucial mediator in regulating protein retrieval, several improvements were initiated such as (i) combinatory design with PR1a signal to improve protein trafficking across the secretory pathway and (ii) shuffling KDEL signal to the C-terminal end of expression cassette to avoid hindrance for receptor recognition.

In terms of VLPs-based vaccine development, albeit production of dengue VLPs had been explored by several studies (Liu *et al.*, 2010; Mani *et al.*, 2013; Sugrue *et al.*, 1997; Zhang *et al.*, 2011), these previous initiatives do not sound practical due to the following reasons: (i) the neutralising antibody responses acquired by mice were generally weak; (ii) co-expressing the DENV precursor membrane (prM) and envelope domain I/II (EDI/EDII) can trigger adverse antibody-dependent enhancement (ADE); and (iii) the need to express four monovalent VLPs and adjust the tetravalent formulation. Hence, it would be more sensible to produce chimeric VLPs, whereby these VLPs are able to self-assemble while presenting the foreign DENV antigens on their viral surfaces. In this study, the VLPs derived from hepatitis B core antigen (HBcAg) have been utilised for cEDIII epitope display. As the stand-alone stability of DENV domain III has made it intrinsically different from other parts of the E protein

(Soares and Caliri, 2013), it is believed that cEDIII can behave as an independent entity and would not interrupt the assembly of viral particles.

Technically, *cEDIII* gene was incorporated into the *c/e1* loop to maximise exposure on the protruding spikes of assembled VLPs. There are supporting evidences whereby *c/e1* insertion can induce stronger immunogenicity than N- and C-terminal fusions as reviewed in **Section 2.4.2.1**. Besides, a full length mHBcAg sequence was used for gene construction including the nucleic acid binding domain (**Table 3.2**). This is because the RNA-binding domain can help to stabilise the particle via disulphide linkage with neighbouring dimers and modulate cell-mediated immune response (**Section 2.4.2.1**). One of the issues encountered during the construction of mHBcAg-based recombinant vectors was the high frequency of self-ligation events (**Figures 3.13 and 3.14**). This can be prevented in future by dephosphorylating the linearised vector using alkaline phosphatase prior ligation. As a result, vector DNA without the 5' phosphate group would not be able to self-ligate but still contains the 3'-hydroxyl group to form phosphodiester bond with the insert.

The tandem core HBcAg design had been adopted due to the concern that the two copies of cEDIII inserts at HBcAg dimer interface might suffer from steric clashes which could abrogate particle assembly (**Section 2.4.2.2**). Thus, tandem core strategy is used to alleviate the steric constraints as VLPs are now assembled from the dimers of HBcAg protein, expressed from the two ORFs of HBcAg that have been covalently linked (Peyret *et al.*, 2015). The *cEDIII* gene was inserted into the *c/e1* loop of Core II, so that this would minimise disruption to VLPs assembly as the translation moved in 5' → 3' direction from the unmodified Core I (**Table 3.2**). With this, the tandem core would have greater flexibility as only half of each particle was decorated with cEDIII antigens. Worthwhile to mention, this work signifies the first report on developing a HBcAg-based dengue vaccine using plant system.

Besides, Kozak sequence was included in most of the cEDIII expression cassettes (**Table 3.2**) as an additional strategy to achieve optimal gene expression. Basically, Kozak sequence refers to nucleotide sequences that surround the ATG initiation codon. Kozak plays a key role in initiating protein translation as it serves as the binding site for small (40S) ribosomal subunit that moves from the 5' 7-methyl-guanylate cap of eukaryotes mRNA (Kozak, 1999). In specific, AACA had been identified as the general Kozak sequence for plant (Lütcke *et al.*, 1987); therefore, this sequence was inserted preceding the start codon of cEDIII expression cassettes.

With the interest of facilitating interactions between protein domains, two different types of linkers have been used in this study. First of all, a rigid linker is used for the spatial separation of CTB and cEDIII proteins so that their independent functionality can be maintained (Zhao *et al.*, 2008). For that, proline is the most preferred amino acid as it does not have amide hydrogen to donate and the stiffness makes it a good 'breaker' of secondary structure (George and Heringa, 2003). Meanwhile, a flexible linker of (GGS)_n has been designed to facilitate interaction between the cEDIII inserts and core protein subdomains (expression cassettes: mHBcAg-cEDIII (L) and tHBcAg-cEDIII, **Table 3.2**). As this approach has been proven useful in Kratz *et al.* (1999) findings, it is hoped that the (GGS)_n linkers can help to minimise the steric constraints and stabilise the chimeric HBcAg VLPs-expressing cEDIII epitopes.

3.5 Conclusion

In summary, all the cEDIII expression cassettes that were designed had been successfully cloned into pEAQ-*HT* binary vector. Recombinant vectors that were constructed for expression of recombinant proteins include: (i) cEDIII fusion to sGFP protein, namely pEAQ-*HT*::cEDIII-sGFP-KDEL-H and pEAQ-*HT*::PR1a-cEDIII-sGFP-H-KDEL; as well as (ii) cEDIII fusion to CTB partner, namely pEAQ-*HT*::CTB-cEDIII-KDEL-H, pEAQ-*HT*::PR1a-CTB-cEDIII-H-KDEL and pEAQ-*HT*::PR1a-CTB-cEDIII-KDEL (xTH). Meanwhile, recombinant vectors that were constructed to express chimeric HBcAg VLPs based on (i) monomeric core were pEAQ-*HT*::mHBcAg-cEDIII and pEAQ-*HT*::mHBcAg-cEDIII (L), whereas the construct developed based on tandem core was pEAQ-*HT*::tHBcAg-cEDIII. Furthermore, improvement strategies such as codon optimisation, incorporation of ER trafficking signal along with design of protein linkers had been integrated to aim for high transgene expression. These recombinant vectors are now ready for expression studies in *N. benthamiana* by which details are presented in the **Chapter 4**.

4 Evaluation of cEDIII Protein Expression in *Nicotiana benthamiana* Receiving Recombinant Vectors Delivered via Agroinfiltration

Table of Contents

4.1	Introduction	4-3
4.2	Materials and methods.....	4-6
4.2.1	Plant growth	4-6
4.2.2	Specialised equipment.....	4-6
4.2.3	Preparation and transformation of LBA4404 competent <i>Agrobacterium tumefaciens</i>	4-7
4.2.4	Inoculation of agrobacterial suspension.....	4-8
4.2.5	Ultraviolet (UV) observation and photography	4-9
4.2.6	Confocal microscopy	4-9
4.2.7	Protein extraction	4-9
4.2.8	Sodium dodecyl sulphate-polyacrylamide gel electrophoresis (SDS-PAGE).....	4-12
4.2.9	Coomassie blue gel staining.....	4-12
4.2.10	Western blotting.....	4-12
4.3	Results	4-15
4.3.1	Ultraviolet (UV) detection of recombinant cEDIII fused to green fluorescent protein (sGFP).....	4-15
4.3.2	Expression of recombinant cEDIII in fusion to green fluorescent protein (sGFP).....	4-18

4.3.3	Expression of recombinant cEDIII in fusion to cholera toxin B subunit (CTB)	4-21
4.3.4	Expression of monomeric core virus-like particles (VLPs) with cEDIII epitopes display	4-27
4.3.5	Expression of tandem core virus-like particles (VLPs) displaying cEDIII epitopes	4-33
4.4	Discussion	4-36
4.5	Conclusion.....	4-43

4.1 Introduction

The era of molecular pharming has driven the production of various plant-based biologics by which many are now being assessed in clinical trials. The delivery of transgene into host plant can be achieved via several strategies that either involve stable transformation or transient expression. In the early days, transient expression is mainly used to assess the activity of gene constructs prior stable integration. However, the establishment of stable production system can be cumbersome due to the time-consuming process of selection and regeneration of stable lines, potential genetic drift and vulnerability to epigenetic factors (Menassa *et al.*, 2012). Therefore, various academic and industrial laboratories have switched to transient expression technology as it enables efficient delivery of products within a timescale of days. In fact, there is a notion that the ‘classical’ stable transformation might soon be displaced by the transient expression system that shows promise of high competitiveness (Rybicki, 2010).

The introduction of agroinfiltration has rapidly revolutionised the manner where transient expression is achieved to date. This *Agrobacterium*-mediated transformation for transient gene expression is favoured for the speed and simplicity of procedures, by which leaves of potted plant can be easily infiltrated using a needless syringe, via vacuum application or air-brushing. Upon infiltration, the intercellular spaces within the leaf of host plant will be replaced by agrobacterial suspension harbouring the desired transgene. As discussed, both binary and viral vectors can be used for gene delivery via agroinfiltration (**Section 2.3.2.2**). In relation to this study, the pEAQ-*HT* vector developed from cowpea mosaic virus (CPMV) is used. It is a binary vector that relies on the integration of transfer DNA (T-DNA) into plant nucleus for the transgene to be transcribed and expressed. Essentially, the best of three biological systems is combined here: the plant eukaryotic expression system, the hypertranslational (*HT*) features of CPMV and the high transfection efficiency of *Agrobacterium*.

In this study, cEDIII recombinant vectors were designed to exploit the expression system of *N. benthamiana*. These vectors were differentiated into two main types, to express as (i) recombinant fusion proteins with either green fluorescent protein (sGFP) or cholera toxin B subunit (CTB); and (ii) chimeric hepatitis B core antigen (HBcAg) virus-like particles (VLPs) displaying cEDIII epitopes. As mentioned, these represent different variants of cEDIII vaccine candidates that would be assessed for their corresponding immunogenic potential. So, with the aim of recovering a satisfactory amount of heterologous proteins, several strategies had been applied during the construction of cEDIII recombinant vectors (**Chapter 3**). These include synthesising *cEDIII* genes with optimised *N. benthamiana* codons and adding the Kozak sequence to improve efficiency of translation. The use of pEAQ-*HT* vector offers the co-expression of P19 gene silencing suppressor to prevent adverse turnover of transgene products. Besides, signal peptides were used to target the cEDIII recombinant fusion proteins to endoplasmic reticulum (ER) for high protein accumulation, which comprised of tobacco pathogenesis related protein 1a (PR1a) signal peptide and ER retention signal (KDEL). Protein linkers were also used to alleviate potential steric hindrance between the neighbouring domains in cEDIII fusion proteins and chimeric HBcAg VLPs.

Following the successful construction of cEDIII recombinant vectors, this chapter presents the delivery of desired transgene into *N. benthamiana*. Upon transformation into *Agrobacterium tumefaciens*, syringe infiltration was used to inoculate the bacterial suspension harbouring recombinant vectors into the host plants. Firstly, the infiltrated leaves were harvested on 6th day post-infiltration (dpi) to verify the expression of delivered cEDIII transgenes. The localisation of recombinant cEDIII-sGFP fusion protein was determined via confocal microscopy. Then, time-course analyses were used to evaluate the expression kinetics of different cEDIII constructs. Owing to the poorly-soluble monomeric core HBcAg (mHBcAg) and tandem core HBcAg (tHBcAg) VLPs, buffer optimisation was used to enhance the recovery of sample.

Overall, the specific objectives for this chapter are set as follows:

- (i) To deliver all the constructed recombinant vectors into *N. benthamiana* via syringe infiltration;
- (ii) To verify the ability of the recombinant vectors to express cEDIII fusion proteins and chimeric HBcAg VLPs with cEDIII epitopes;
- (iii) To examine the effect of subcellular localisation on the expression of recombinant cEDIII fusion proteins; and
- (iv) To study the expression kinetics of cEDIII fusion proteins and chimeric HBcAg VLPs with cEDIII epitopes in *N. benthamiana*.

4.2 Materials and methods

4.2.1 Plant growth

In this study, 5 – 6 weeks old *N. benthamiana* plants grown in glasshouse and plant growth chamber were used for agroinfiltration. To grow the plants, a controlled environment was set at 25°C, 70% humidity, with 16 hours of daylight period. These plants were watered on alternate days and fertiliser was applied on a weekly basis.

4.2.2 Specialised equipment

Conviron plant growth chamber was used to grow the *N. benthamiana* plants (Conviron, Canada) under regulated conditions. Transformation of *Agrobacterium* was performed using either a water bath system (Mettler, Germany) or Electroporator 2510 (Eppendorf, Germany). Innova 42 incubator shaker (Eppendorf, Germany) was used to incubate bacterial broth culture while BINDER Microbiological Incubator (Binder, Germany) was used for bacterial plate incubation. Measurement of the bacterial optical density was performed using BioPhotometer Plus (Eppendorf, Germany). Most centrifugation works were performed using 5810R Refrigerated Centrifuge (Eppendorf, Germany). The ultraviolet (UV) observation of infiltrated *N. benthamiana* leaves was illuminated using Blak-Ray lamps (Ultra-Violet Product Ltd, USA). Besides, LSM 780 confocal microscope (Zeiss, Germany) was also used to detect fluorescence emission. The homogenisation of plant extract could be performed using Omni Bead Ruptor 24 homogenizer (Camlab, USA). Thermomixer (Eppendorf, Germany) was used to heat up loading sample for protein gel. Protein gel electrophoresis was performed using either NuPAGE® system (Invitrogen, USA) or Mini-PROTEAN® Tetra Cell system (Bio-Rad, USA). Subsequent electroblotting was conducted using either Mini Trans-Blot® Cell (Bio-Rad, USA) or XCell II™ Blot Module (Invitrogen, USA). Images of coomassie blue-stained protein gel and colorimetric development on Western blot membrane were recorded using GS-800™ calibrated densitometer (Bio-Rad, USA). Meanwhile,

ImageQuant LAS 500 (GE Healthcare, USA) was used as a chemiluminescence imaging system.

4.2.3 Preparation and transformation of LBA4404 competent *Agrobacterium tumefaciens*

The *A. tumefaciens* strain LBA4404 was used to deliver the recombinant vectors into *N. benthamiana* plant throughout the study. Competent cells of LBA4404 were prepared according to the method described in **Section 3.2.11**.

The transformation of LBA4404 competent cells was performed via freeze-thaw method described by Hofgen and Willmitzer (1988). In brief, the competent cells were thawed on ice for 5 minutes before adding 100 ng of recombinant vector. After 30 minutes, the bacterial cells were immersed in liquid nitrogen for 10 seconds, followed by 4-minute incubation in 37°C water bath and another 2-minute incubation on ice. Then, super optimal broth with catabolite repressor (SOC) media was aseptically added and the cells were left to recover in 28°C incubator shaker for 1 hour. Lastly, transformed cells were spread on Luria-Bertani (LB) agar plate containing 50 µg/ml of kanamycin and 50 µg/ml rifampicin, followed by incubation at 28°C for 48 hours.

Alternatively, the LBA4404 competent cells were also transformed via electroporation protocol stated by Main *et al.* (1995). Likewise, 100 ng of recombinant vector was added to the competent cells thawed on ice beforehand. Then, the mixture of LBA4404 cells and DNA was transferred to a pre-chilled cuvette (Eppendorf, Germany) and electroporated at 2500 V. SOC media was immediately added and the cells incubated in 28°C incubator shaker for 1 hour. Transformed cells were then spread on LB agar plate containing 50 µg/ml of kanamycin and 50 µg/ml rifampicin, followed by incubation at 28°C for 48 hours. Following the incubation, transformed colonies were picked from the selective plate for PCR screening (**Section 3.2.13**).

4.2.4 Inoculation of agrobacterial suspension

Agroinfiltration of *N. benthamiana* was performed based on Sainsbury *et al.* (2012). Overnight *A. tumefaciens* culture was harvested and diluted to optical density at 600 nm wavelength (OD₆₀₀) of 0.4 with infiltration buffer containing 10 mM MES (pH 5.6), 10 mM magnesium chloride and 100 µM acetosyringone. After that, the diluted agrobacterial suspension harbouring the recombinant vectors (**Table 4.1**) was infiltrated into 5 – 6 weeks old *N. benthamiana* plants.

To perform the syringe infiltration, a 1 ml needless syringe (Terumo, Japan) was filled with agrobacterial suspension and pressed against the lower epidermis of a *N. benthamiana* leaf. By applying a counter-pressure to the other side of the leaf, the suspension was then injected into the airspaces of the leaf. Lastly, the infiltrated plants were placed back to their usual growth conditions.

Table 4.1: Agrobacterial suspensions used for plant infiltration in this study.

No.	LBA4404 cells harbouring expression vector	OD ₆₀₀ dilution
1	pEAQ- <i>HT</i> ::cEDIII-sGFP-KDEL-H	0.4
2	pEAQ- <i>HT</i> ::PR1a-cEDIII-sGFP-H-KDEL	0.4
3	pEAQ- <i>HT</i> ::CTB-cEDIII-KDEL-H	0.4
4	pEAQ- <i>HT</i> ::PR1a-CTB-cEDIII-H-KDEL	0.4
5	pEAQ- <i>HT</i> ::PR1a-CTB-cEDIII-KDEL (xTH)	0.4
6	pEAQ- <i>HT</i> ::mHBcAg-cEDIII	0.4
7	pEAQ- <i>HT</i> ::mHBcAg-cEDIII (L)	0.4
8	pEAQ- <i>HT</i> ::tHBcAg-cEDIII	0.4
9	pEAQ- <i>HT</i>	0.4
10	pEAQ- <i>HT</i> ::GFP	0.4
11	pEAQ- <i>HT</i> ::mEL	0.4
12	pEAQ- <i>HT</i> ::tEL	0.4

4.2.5 Ultraviolet (UV) observation and photography

N. benthamiana plants that were infiltrated with recombinant cEDIII-sGFP vectors, namely pEAQ-*HT*::cEDIII-sGFP-KDEL-H and pEAQ-*HT*::PR1a-cEDIII-sGFP-H-KDEL, were viewed using handheld Blak-Ray UV lamps. In addition, plants infiltrated with pEAQ-*HT* and pEAQ-*HT*::GFP vectors were used as negative and positive controls, correspondingly. Upon UV excitation in the dark room, photographs of green fluorescence emitted by cEDIII-sGFP-expressing leaves were taken by Mr. Andrew Davis (JIC, UK).

4.2.6 Confocal microscopy

LSM 780 confocal microscope was used to visualise the expression of recombinant cEDIII-sGFP in *N. benthamiana* leaves. Roughly 1 cm² segment of infiltrated leaf was excised and mounted onto a coverslip, with the abaxial side facing upwards. Then, 40X/1.3 water lens was used and visualisation was conducted using GFP filter at 488 nm wavelength.

4.2.7 Protein extraction

A small-scale protein extraction was used to screen for the expression of cEDIII recombinant vector. Unless otherwise specified, the infiltrated leaves were harvested on 6th dpi. Leaf discs corresponding to 100 mg of fresh weight tissue (FWT) were sampled. After adding 3X volume (w/v) of extraction buffer, leaf tissues were homogenised with a ¼-inch ceramic beads (MP Biomedicals, USA) using the Omni Bead Ruptor 24 homogenizer. Or alternatively, infiltrated leaves were ground using liquid nitrogen in a pre-chilled mortar. The lysate was then centrifuged at 15,000 x g, 4°C for 10 minutes and the supernatant was kept as soluble protein (SP). The SP extract was heated with lithium dodecyl sulphate sample buffer (141 mM Tris base; 106 mM Tris-hydrochloride;

2% (w/v) lithium dodecyl sulphate; 10% (v/v) glycerol; 0.51 mM EDTA; 0.22 mM SERVA Blue G; 0.175 mM phenol red) containing β -mercaptoethanol (LDS- β ME) at 99°C for 10 – 20 minutes before used for analysis. Meanwhile, insoluble protein (INP) could be harvested from the pellet by heating with LDS- β ME and subjected to another round of centrifugation. In specific, optimisation of buffer pH and compositions was done for the extraction of monomeric core and tandem core VLPs in order to increase recovery of SP. Details of the extraction buffer used and the estimated size of corresponding protein, in kilo-Dalton (kDa), are stated in **Table 4.2**. The specific composition for each extraction buffer can be found at **Appendix A4.1**.

Table 4.2: Details on the extraction of heterologous proteins expressed by corresponding recombinant vectors.

No.	Expressed protein	Delivered recombinant vector	Protein extraction buffer	Estimated protein size
1	cEDIII-sGFP-KDEL-H	pEAQ- <i>HT</i> ::cEDIII-sGFP-KDEL-H	Tris extraction buffer	~ 40 kDa
2	cEDIII-sGFP-H-KDEL	pEAQ- <i>HT</i> ::PR1a-cEDIII-sGFP-H-KDEL	Tris extraction buffer	~ 40 kDa
3	CTB-cEDIII-KDEL-H	pEAQ- <i>HT</i> ::CTB-cEDIII-KDEL-H	Tris extraction buffer	~ 28 kDa
4	CTB-cEDIII-H-KDEL	pEAQ- <i>HT</i> ::PR1a-CTB-cEDIII-H-KDEL	Tris extraction buffer	~ 28 kDa
5	CTB-cEDIII-KDEL (xTH)	pEAQ- <i>HT</i> ::PR1a-CTB-cEDIII-KDEL (xTH)	Tris extraction buffer	~ 26 kDa
6	mHBcAg-cEDIII	pEAQ- <i>HT</i> ::mHBcAg-cEDIII	<ul style="list-style-type: none"> ▪ VLPs extraction buffer A ▪ VLPs extraction buffer B 	~ 34 kDa
7	mHBcAg-cEDIII (L)	pEAQ- <i>HT</i> ::mHBcAg-cEDIII (L)	<ul style="list-style-type: none"> ▪ VLPs extraction buffer A ▪ VLPs extraction buffer B 	~ 36 kDa
8	tHBcAg-cEDIII	pEAQ- <i>HT</i> ::tHBcAg-cEDIII	<ul style="list-style-type: none"> ▪ Sodium phosphate extraction buffer ▪ VLPs extraction buffer A 	~ 55 kDa

4.2.8 Sodium dodecyl sulphate-polyacrylamide gel electrophoresis (SDS-PAGE)

Same volume of sample was loaded into each protein well, and SeeBlue Plus2 Pre-Stained Standard (Invitrogen, USA) was used as the protein marker throughout the study (**Appendix A4.1**). In specific, the two different SDS-PAGE systems used were described below.

NuPAGE® Bis-Tris pre-cast gels (Invitrogen, USA), containing 12% (w/v) and 4% – 12% (w/v) gradient acrylamide, were electrophoresed at 200 V for 50 minutes. Based on the desired molecular weight separation, NuPAGE® MOPS SDS Running Buffer (50 mM Tris base, pH 7.7; 50 mM MOPS; 0.1% (w/v) sodium dodecyl sulphate; 1 mM ethylenediaminetetraacetic acid) or MES SDS Running Buffer (50 mM Tris base, pH 7.3; 50 mM MES; 0.1% (w/v) sodium dodecyl sulphate; 1 mM ethylenediaminetetraacetic acid) was selected accordingly.

Alternatively, 12% (w/v) polyacrylamide gel was prepared using Mini-PROTEAN® Tetra Cell system and electrophoresis was carried out at 150 V for 60 minutes using Laemmli running buffer (**Appendix A4.1**).

4.2.9 Coomassie blue gel staining

Following electrophoresis, the protein gel was stained with InstantBlue (Expedeon, UK) for at least 1 hour. Then, the protein gel was destained with deionised water overnight before imaging.

4.2.10 Western blotting

For immunoblotting analysis, electrophoresed proteins were transferred onto a nitrocellulose membrane (Millipore, USA). The assembled blotting sandwich was

immersed in a transfer apparatus filled with Transfer Buffer, and wet-transfer was conducted using either system described as follows:

Mini Trans-Blot® Cell set at 100 V for 60 minutes, with constant cooling by ice bath. Or alternatively, the XCell II™ Blot Module was used and voltage was set at 25 V for 80 minutes.

Blotted membrane was blocked with 5% milk (w/v) in phosphate-buffered saline (PBS) containing 0.05% (v/v) Tween-20 (PBST) for at least 1 hour. Membrane was subsequently incubated with either DENV 1-4, HBcAg, Tetra-His or cholera toxin (CT) primary antibody for 1 hour. Then, the membrane was washed three times with PBST at 5-minute intervals before incubation with mouse or rabbit immunoglobulin G (IgG) horseradish peroxidase (HRP)-conjugated secondary antibody for another hour. Washing steps were repeated for at least three times before detection. Details of the antibodies used are provided in **Table 4.3**.

Table 4.3: List of antibodies used for Western blotting in this study.

Antibody name	Species	Dilution	Source
DENV 1-4 monoclonal antibody	Mouse	1:2,000	Thermo Scientific, USA
HBcAg monoclonal antibody	Mouse	1:4,000	Abcam, UK
Tetra-histidine (His) monoclonal antibody	Mouse	1:2,000	Qiagen, Germany
CT polyclonal antibody	Rabbit	1:8,000	Sigma, USA
Mouse IgG (H+L) HRP-conjugated polyclonal antibody	Goat	1:10,000	Invitrogen, USA
Rabbit IgG (H+L) HRP-conjugated polyclonal antibody	Goat	1:20,000	Agrisera, Sweden

To perform chemiluminescent detection, enhanced chemiluminescence (ECL) solution was added (**Appendix A4.1**) and developed signal was digitally captured using ImageQuant LAS 500. Meanwhile, colorimetric-based detection was done by adding 1 ml of 3, 3', 5, 5'-tetramethylbenzidine (TMB) substrate (KPL, USA) until a distinct purple colour was observed. The membrane was briefly rinsed with deionised water before images were captured by using GS-800™ calibrated densitometer.

4.3 Results

4.3.1 Ultraviolet (UV) detection of recombinant cEDIII fused to green fluorescent protein (sGFP)

Under UV light illumination, the green fluorescence emitted by cEDIII-sGFP recombinant proteins (expression vectors: pEAQ-*HT*::cEDIII-sGFP-KDEL-H and pEAQ-*HT*::PR1a-cEDIII-sGFP-H-KDEL) was observed (**Figure 4.1**). Notably, stronger signal was detected from the leaf infiltrated with the improved construct (expression vector: pEAQ-*HT*::PR1a-cEDIII-sGFP-H-KDEL) as compared to the leaf infiltrated with the initial construct (expression vector: pEAQ-*HT*::cEDIII-sGFP-KDEL-H). Both healthy and pEAQ-*HT*-infiltrated leaves were included as negative controls, for which no green fluorescence was observed from these leaves. In fact, only autofluorescence of damaged tissue was detected from the leaf infiltrated with pEAQ-*HT* (mock). Leaf infiltrated with pEAQ-*HT*::GFP vector was used as positive control, and it exhibited the strongest fluorescence as expected.

Confocal microscopic observation of the localisation of recombinant cEDIII-sGFP is shown in **Figure 4.2**. Panel A shows the trafficking of the recombinant cEDIII-sGFP expressed by the initial construct (expression vector: pEAQ-*HT*::cEDIII-sGFP-KDEL-H) to the cytosol region. Meanwhile, Panel B presents localisation of the recombinant cEDIII-sGFP to the intricate networks of ER, as mediated by the improved construct (expression vector: pEAQ-*HT*::PR1a-cEDIII-sGFP-H-KDEL). Such observation suggests that the improved construct had facilitated efficient protein trafficking to the ER. Panel C however, shows image of pEAQ-*HT*-infiltrated leaf to discriminate against background autofluorescence. Future improvement may consider the use of organelle marker antibody to confirm protein localisation to the ER.



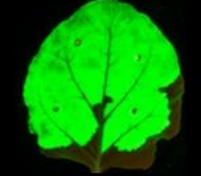


Construct used for agroinfiltration	Image of infiltrated leaf observed under UV light	Detection of green fluorescence
<u>Before improvement</u> pEAQ- <i>HT</i> ::cEDIII-sGFP-KDEL-H		Fluorescence detected (scoring: +)
<u>After improvement</u> pEAQ- <i>HT</i> ::PR1a-cEDIII-sGFP-H-KDEL		Fluorescence detected (scoring: +++)
<u>Positive control</u> pEAQ- <i>HT</i> ::GFP		Fluorescence detected (scoring: +++++)
<u>Mock</u> pEAQ- <i>HT</i>		Autofluorescence
<u>Healthy plant</u> No infiltration		No fluorescence

Figure 4.1: A comparative UV observation of green fluorescence emitted by *N. benthamiana* leaves infiltrated with different constructs. A scoring was made based on the intensity of fluorescence.

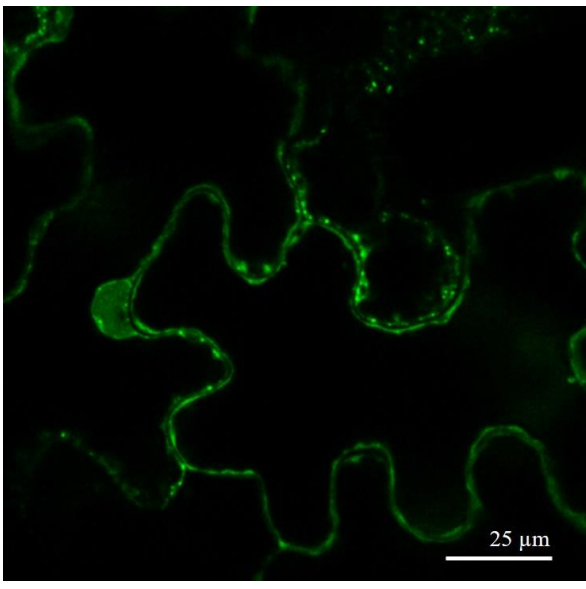
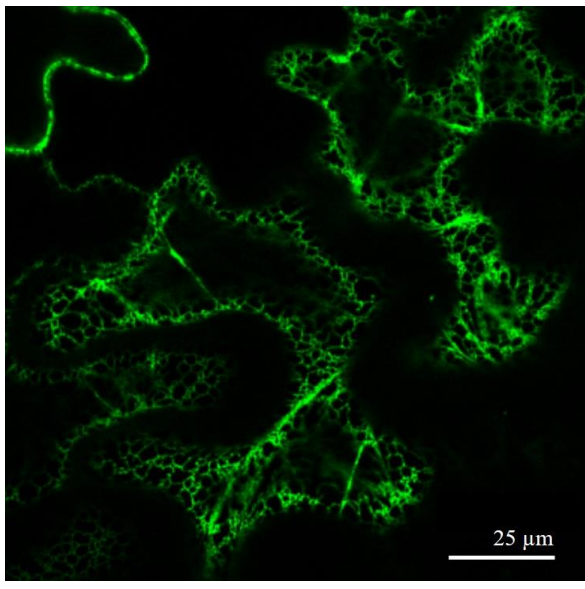
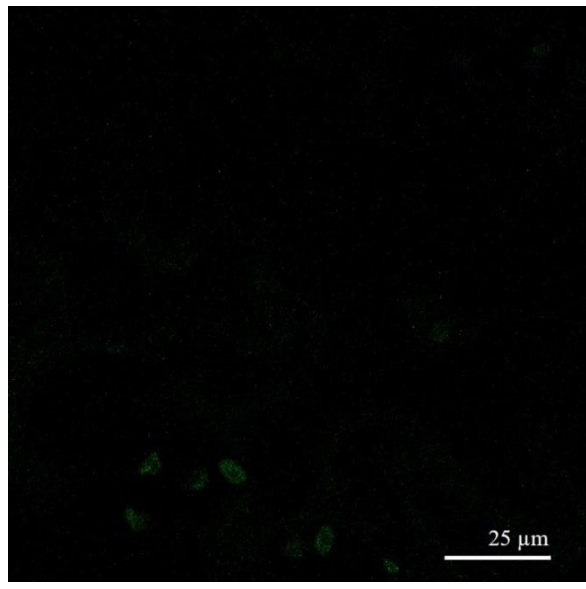
Panel A Infiltrated with pEAQ- <i>HT</i> ::cEDIII-sGFP-KDEL-H (initial construct)	Panel B Infiltrated with pEAQ- <i>HT</i> ::PR1a-cEDIII-sGFP-H-KDEL (improved construct)	Panel C Infiltrated with pEAQ- <i>HT</i> (mock)
		
Green fluorescence detected in cytoplasm	Green fluorescence detected in ER	Only background autofluorescence detected

Figure 4.2: Confocal microscopic observation of *N. benthamiana* leaves expressing recombinant cEDIII-sGFP fusion proteins. Infiltration was conducted using the initial construct pEAQ-*HT*::cEDIII-sGFP-KDEL-H (Panel A), the improved construct pEAQ-*HT*::PR1a-cEDIII-sGFP-H-KDEL (Panel B) and the mock pEAQ-*HT* without gene insertion (Panel C).

4.3.2 Expression of recombinant cEDIII in fusion to green fluorescent protein (sGFP)

Successful expression of recombinant cEDIII-sGFP in *N. benthamiana* was achieved as shown in **Figure 4.3**. Immunoblot analysis was able to detect the soluble protein (SP) expressed by the two cEDIII-sGFP recombinant vectors, namely pEAQ-*HT*::cEDIII-sGFP-KDEL-H and pEAQ-*HT*::PR1a-cEDIII-sGFP-H-KDEL. Denser bands were detected from the leaves infiltrated with improved construct (expression vector: pEAQ-*HT*::PR1a-cEDIII-sGFP-H-KDEL) as compared to the initial construct (expression vector: pEAQ-*HT*::cEDIII-sGFP-KDEL-H). This conformed to the speculation that inclusion of PR1a helped to mediate more efficient protein retention in the ER. Besides, degraded products were found in the SP extracts of pEAQ-*HT*::cEDIII-sGFP-KDEL-H infiltrated leaves. Since no signal was obtained from the extract of pEAQ-*HT*-infiltrated leaf, this confirmed that the mock sample was free of gene insert and the expression of recombinant vectors in infiltrated plant is authentic. The pEAQ-*HT*::PR1a-cEDIII-sGFP-H-KDEL vector was selected for further study based on the higher expression level.

Following that, a time-course analysis was used to determine the peak accumulation of recombinant cEDIII-sGFP fusion protein (**Figure 4.4**). Panel A shows that chlorosis of pEAQ-*HT*::PR1a-cEDIII-sGFP-H-KDEL-infiltrated leaf was visible starting from 6th dpi, and necrosis was seen on 9th dpi. The Western blot profiles in Panel B indicate that the SP of recombinant cEDIII-sGFP had accumulated at persistently high level until 9th dpi. As different cells in host plant might exhibit unsynchronised state of protein expression, 6th dpi was selected as the optimal harvesting time to compromise for late responders while avoiding severe leaf distortions.

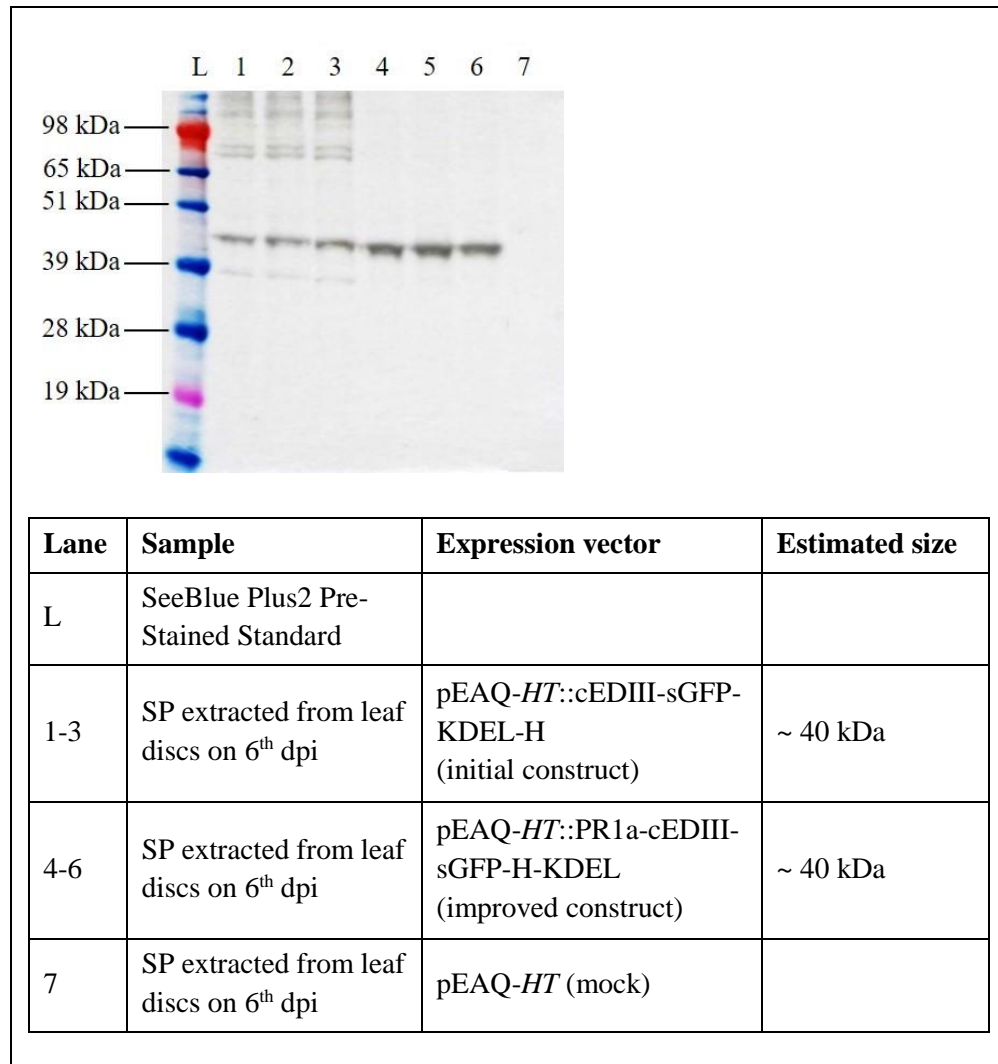
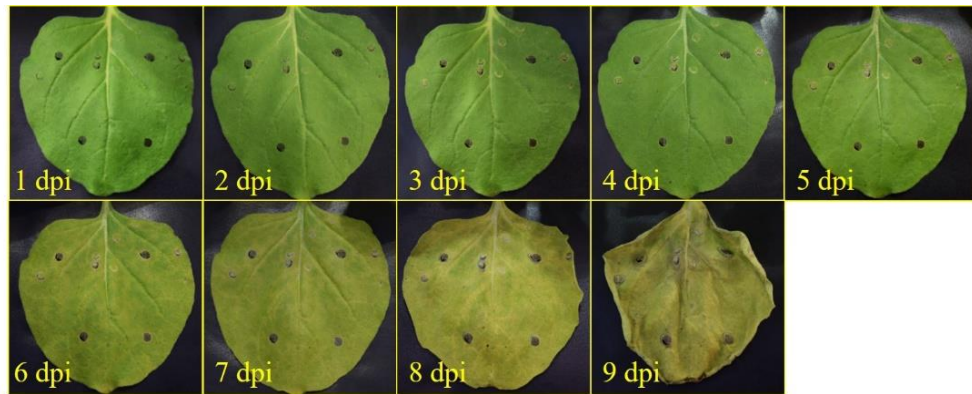
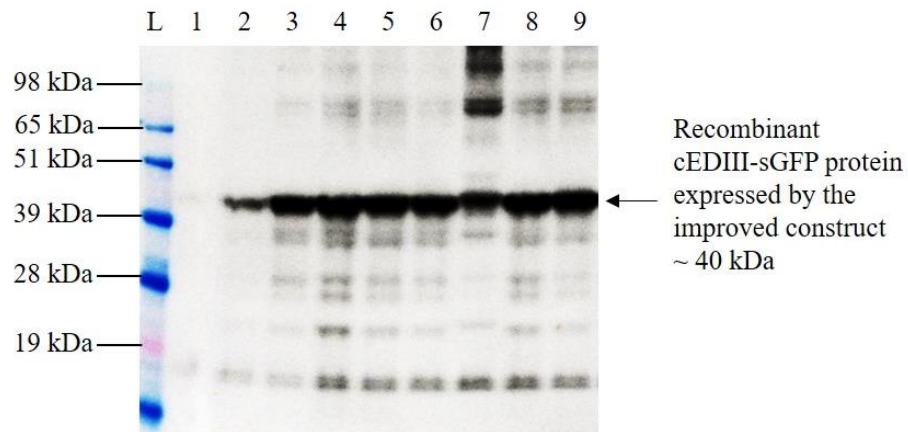


Figure 4.3: Expression profiles of recombinant cEDIII-sGFP fusion proteins in *N. benthamiana* leaves. Immunoblot detection was performed using Tetra-His monoclonal antibody, to verify and compare the expressions mediated by pEAQ-*HT*::cEDIII-sGFP-KDEL-H and pEAQ-*HT*::PR1a-cEDIII-sGFP-H-KDEL vectors. Both vectors were able to express the recombinant cEDIII-sGFP fusion proteins by which pEAQ-*HT*::PR1a-cEDIII-sGFP-H-KDEL presented a higher level.

Panel A: Physical appearance of *N. benthamiana* infiltrated leaf



Panel B: Western blot probed with Tetra-His monoclonal antibody



Lane	Sample	Expression vector	Estimated size
L	SeeBlue Plus2 Pre-Stained Standard		
1-9	SP extracted from leaf discs from 1 st – 9 th dpi	pEAQ- <i>HT</i> ::PR1a-cEDIII-sGFP-H-KDEL (improved construct)	~ 40 kDa

Figure 4.4: Kinetic expression profiles of recombinant cEDIII-sGFP fusion protein in *N. benthamiana*. Panel A: Daily observations of infiltrated leaf; Panel B: Immunoblotting of cEDIII-sGFP fusion protein extracted from 1st – 9th dpi, as detected using Tetra-His monoclonal antibody. The harvest time for cEDIII-sGFP-H-KDEL protein was determined as 6th dpi.

4.3.3 Expression of recombinant cEDIII in fusion to cholera toxin B subunit (CTB)

The expressions of recombinant CTB-cEDIII fusion proteins were successfully achieved, as mediated by the pEAQ-*HT*::CTB-cEDIII-KDEL-H and pEAQ-*HT*::PR1a-CTB-cEDIII-H-KDEL expression vectors (**Figure 4.5**). Based on the immunoblot profiles, greater signal strength was detected from the SP extract of leaves infiltrated with the improved construct (expression vector: pEAQ-*HT*::PR1a-CTB-cEDIII-H-KDEL) in comparison to the initial construct (expression vector: pEAQ-*HT*::CTB-cEDIII-KDEL-H). Once again, the higher protein accumulation has probably corresponded to the improved trafficking mediated by PR1a signal. No band was detected from the SP of leaves infiltrated with pEAQ-*HT* vector, as expected. The pEAQ-*HT*::PR1a-CTB-cEDIII-H-KDEL expression vector was selected for further study.

Time-course analysis of the expression of CTB-cEDIII fusion protein is shown in **Figure 4.6**. Panel A reveals that leaf chlorosis of *N. benthamiana* plant infiltrated with pEAQ-*HT*::PR1a-CTB-cEDIII-H-KDEL could be spotted on 7th dpi as necrosis became progressively visible on 9th dpi. Besides, the Western blot profiles in Panel B suggests that satisfactory expression of recombinant CTB-cEDIII was detected between 4th dpi to 7th dpi. Therefore, harvesting on 6th dpi would be ideal given to the milder leaf yellowing.

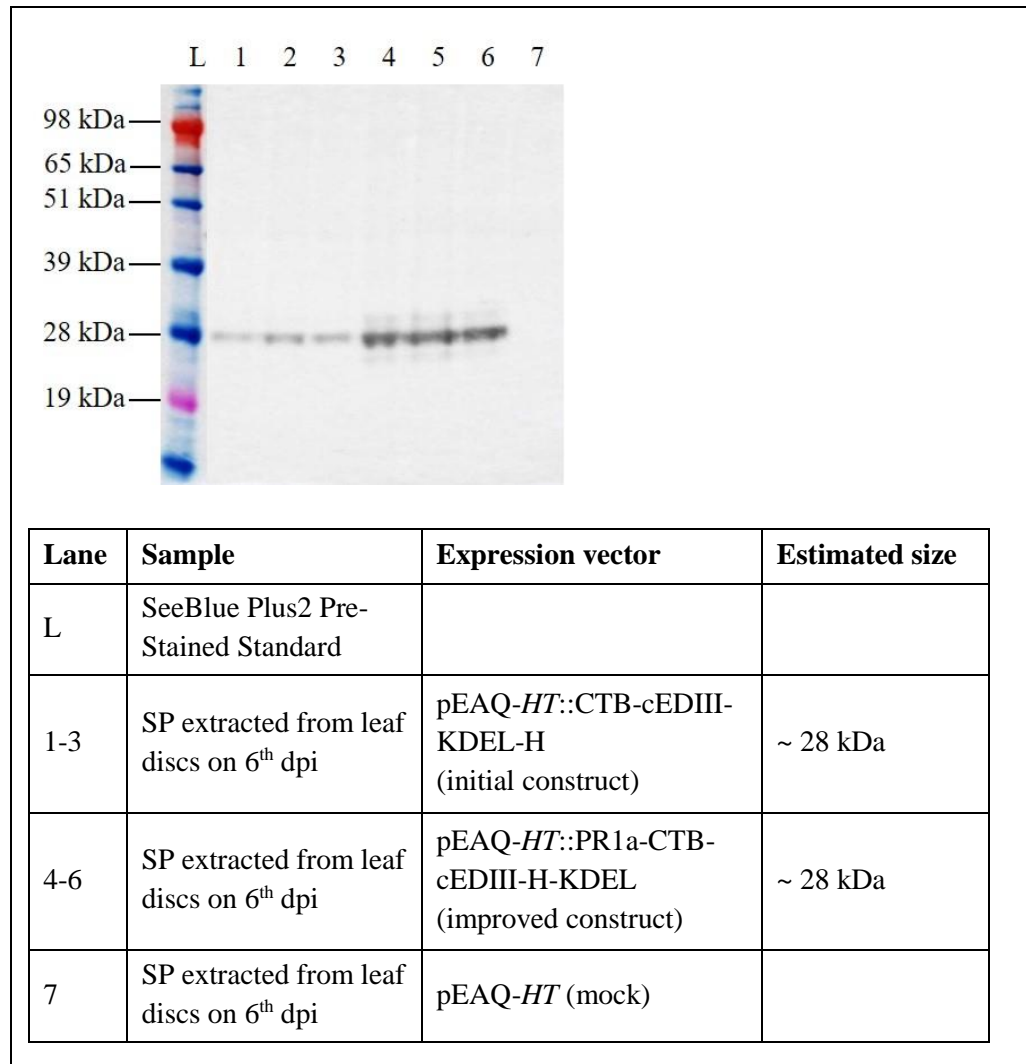
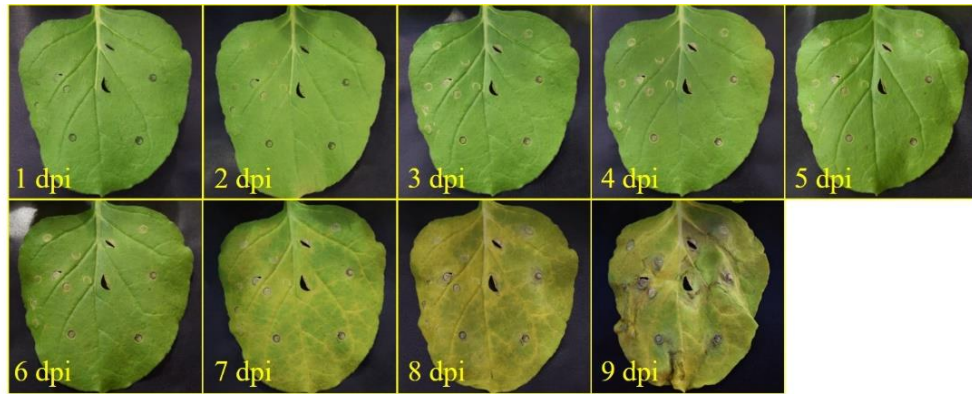
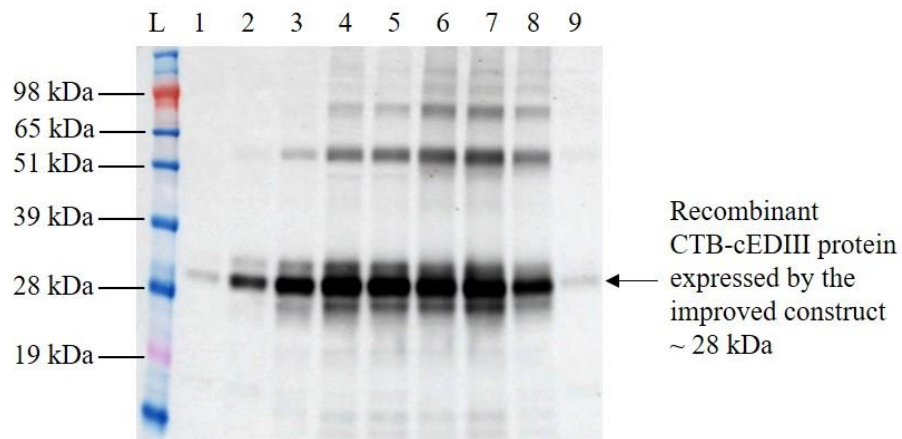


Figure 4.5: Expression profiles of recombinant CTB-cEDIII fusion proteins in *N. benthamiana* leaves. Immunoblot detection was performed using Tetra-His monoclonal antibody, to verify and compare the expressions mediated by pEAQ-*HT*::CTB-cEDIII-KDEL-H and pEAQ-*HT*::PR1a-CTB-cEDIII-H-KDEL vectors. Both vectors were able to express the recombinant CTB-cEDIII fusion proteins by which pEAQ-*HT*::PR1a-CTB-cEDIII-H-KDEL presented a higher level.

Panel A: Physical appearance of *N. benthamiana* infiltrated leaf



Panel B: Western blot probed with Tetra-His monoclonal antibody



Lane	Sample	Expression vector	Estimated size
L	SeeBlue Plus2 Pre-Stained Standard		
1-9	SP extracted from leaf discs from 1 st – 9 th dpi	pEAQ- <i>HT</i> ::PR1a-CTB-cEDIII-H-KDEL (improved construct)	~ 28 kDa

Figure 4.6: Kinetic expression profiles of recombinant CTB-cEDIII fusion protein in *N. benthamiana*. Panel A: Daily observations of infiltrated leaf; Panel B: Immunoblotting of CTB-cEDIII fusion protein extracted from 1st – 9th dpi, as detected using Tetra-His monoclonal antibody. The harvest time for CTB-cEDIII-H-KDEL protein was determined as 6th dpi.

Successful expression of the xTH version of recombinant CTB-cEDIII (expression vector: pEAQ-*HT*::PR1a-CTB-cEDIII-KDEL (xTH)) was verified from the detection of expected bands (**Figure 4.7**). In this case, the Western blot membrane was probed with DENV 1-4 monoclonal antibody (Panel A) due to the absence of 6X His tag in the expression cassette (see **Table 3.2**). Tetra-His monoclonal antibody was used for the detection of same set of protein samples. As expected, no signals were obtained from the CTB-cEDIII-KDEL (xTH) samples (expression vector: pEAQ-*HT*::PR1a-CTB-cEDIII-KDEL (xTH)) when the blot was probed with Tetra-His antibody (Panel B). Meanwhile, the positive control CTB-cEDIII-H-KDEL fusion protein (expression vector: pEAQ-*HT*::PR1a-CTB-cEDIII-H-KDEL) was detected in Panels A and B as it contained both cEDIII protein and 6X His tag. No signals were obtained from the SP of pEAQ-*HT*-infiltrated leaves.

The kinetic expression profiles of CTB-cEDIII-KDEL (xTH) fusion protein are presented in **Figure 4.8**. Panel A shows that the leaf infiltrated with pEAQ-*HT*::PR1a-CTB-cEDIII-KDEL (xTH) exhibited chlorosis starting from 5th dpi. Remarkably, no sign of leaf necrosis was recorded throughout the time-course study. Satisfactory accumulation of CTB-cEDIII-KDEL (xTH) fusion protein was detected between 3rd dpi – 7th dpi. After consideration, 6th dpi was chosen as the harvesting day for the reasons of milder leaf distortion and to accommodate for late responders of protein expression.

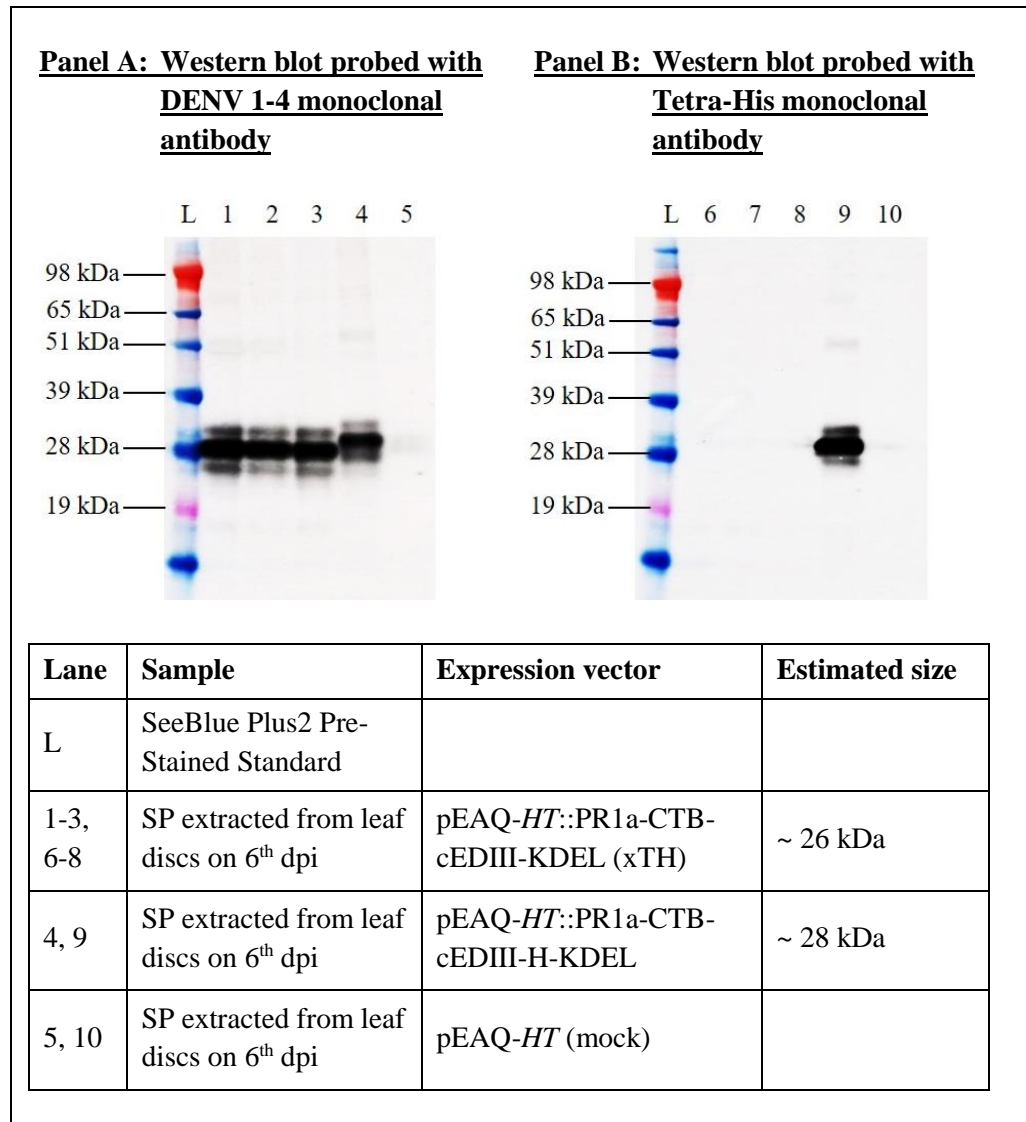
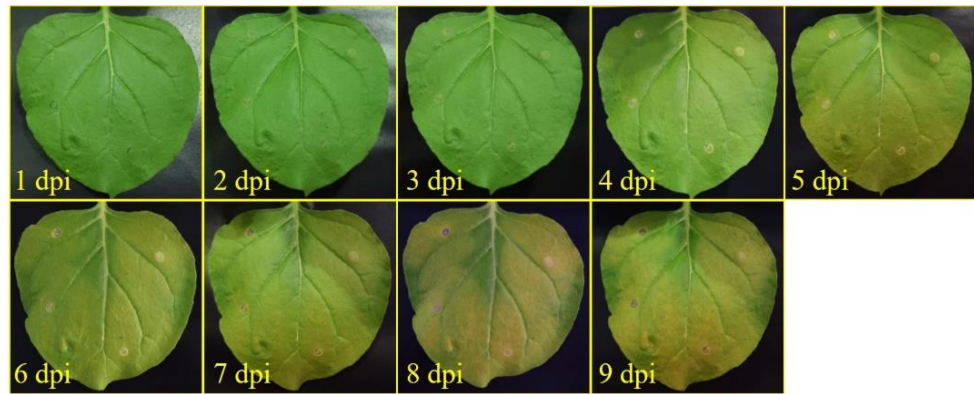
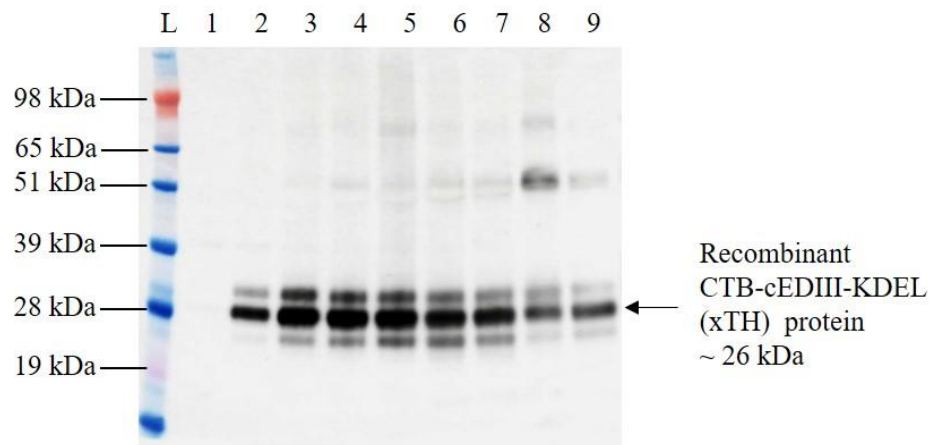


Figure 4.7: Expression profiles of CTB-cEDIII-KDEL (xTH) fusion protein in *N. benthamiana* leaves. Immunoblot detection was performed using two different primary antibodies (Panel A: DENV 1-4 monoclonal antibody; Panel B: Tetra-His monoclonal antibody) by which the expression of recombinant CTB-cEDIII-KDEL (xTH) protein mediated by pEAQ-*HT*::PR1a-CTB-cEDIII-KDEL (xTH) vector had been verified.

Panel A: Physical appearance of *N. benthamiana* infiltrated leaf



Panel B: Western blot probed with DENV 1-4 monoclonal antibody



Lane	Sample	Expression vector	Estimated size
L	SeeBlue Plus2 Pre-Stained Standard		
1-9	SP extracted from leaf discs from 1 st – 9 th dpi	pEAQ- <i>HT</i> ::PR1a-CTB-cEDIII-KDEL (xTH)	~ 26 kDa

Figure 4.8: Kinetic expression profiles of CTB-cEDIII-KDEL (xTH) fusion protein in *N. benthamiana*. Panel A: Daily observations of infiltrated leaf; Panel B: Immunoblotting of CTB-cEDIII-KDEL (xTH) protein extracted on 1st – 9th dpi, detected with anti-DENV 1-4 antibody. The harvest time for CTB-cEDIII-KDEL (xTH) protein was determined as 6th dpi.

4.3.4 Expression of monomeric core virus-like particles (VLPs) with cEDIII epitopes display

Based on **Figure 4.9**, the monomeric core HBcAg that was modified for cEDIII epitopes display had been produced in *N. benthamiana* (expression vector: pEAQ-*HT*::mHBcAg-cEDIII). Panel A presents successful detection of mHBcAg-cEDIII SP using HBcAg monoclonal antibody with the estimated size around ~ 34 kDa. No signal was seen from the sample extracted from pEAQ-*HT*-infiltrated leaf. But given to the faint bands, the extraction buffer was re-formulated in order to increase the protein yield. Panel B indicates that the buffer optimisation was useful as a denser band of mHBcAg-cEDIII SP was obtained following the change of buffer to VLPs extraction buffer B.

The time-course analysis on mHBcAg-cEDIII protein was performed as shown in **Figure 4.10**. Based on Panel A observations, signs of leaf yellowing could be observed from pEAQ-*HT*::mHBcAg-cEDIII-infiltrated leaf from 6th dpi onwards. Immunoblotting assay showed the accumulation of mHBcAg-cEDIII SP (Panel B) at high expression level from 3rd to 6th dpi. Hence, the optimal harvest time was set as 4th dpi.

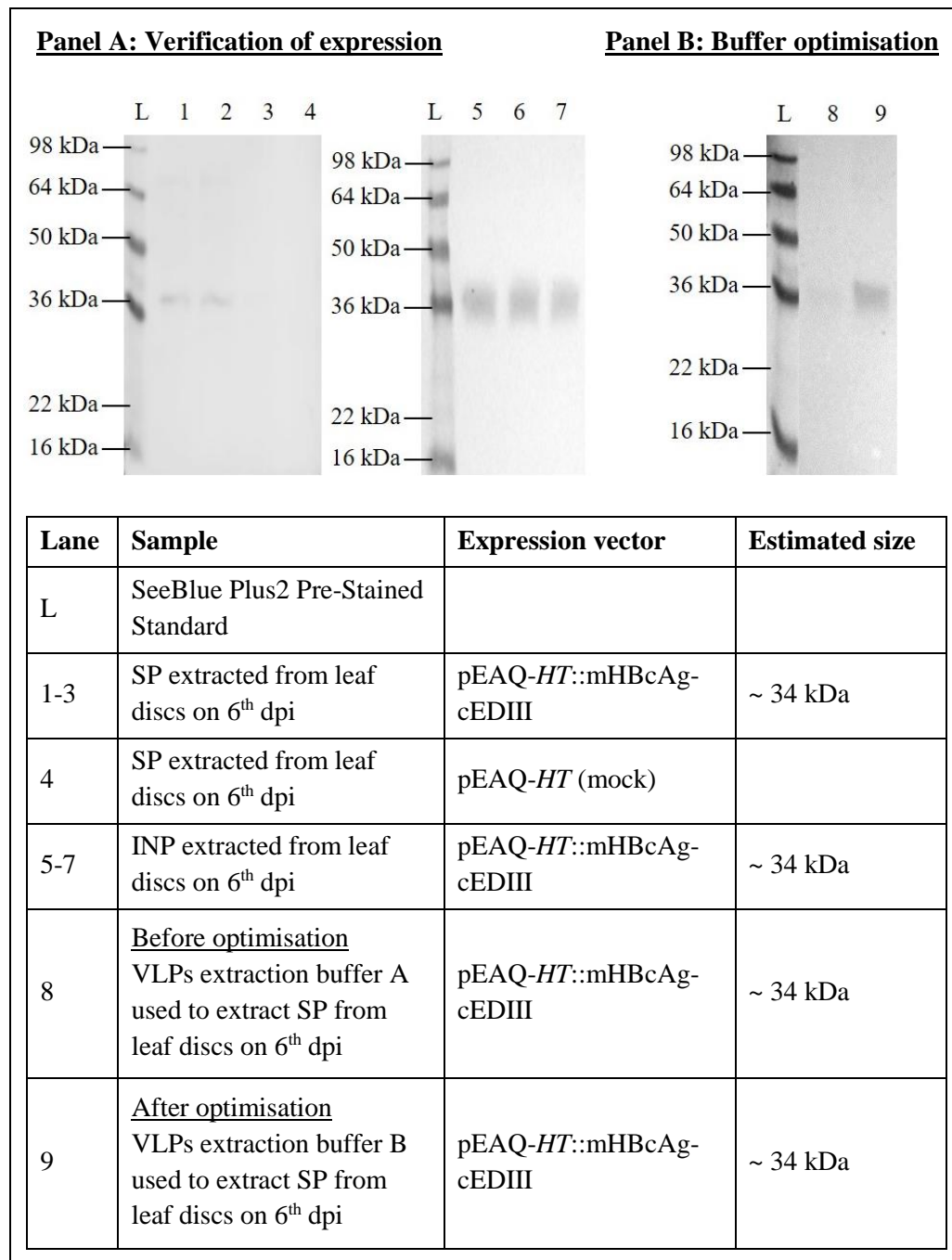
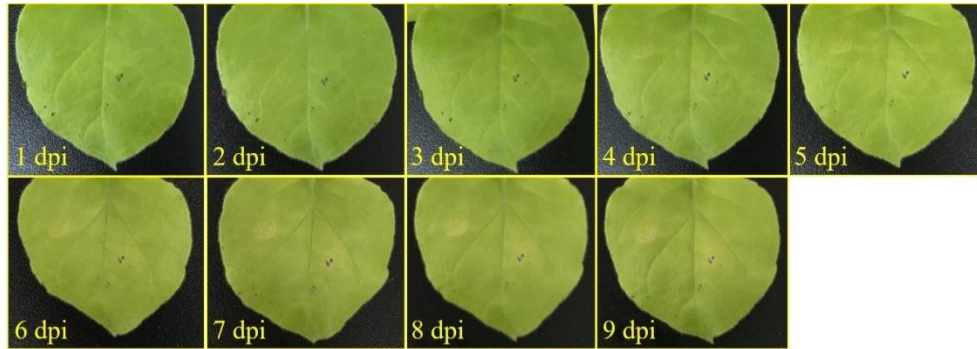
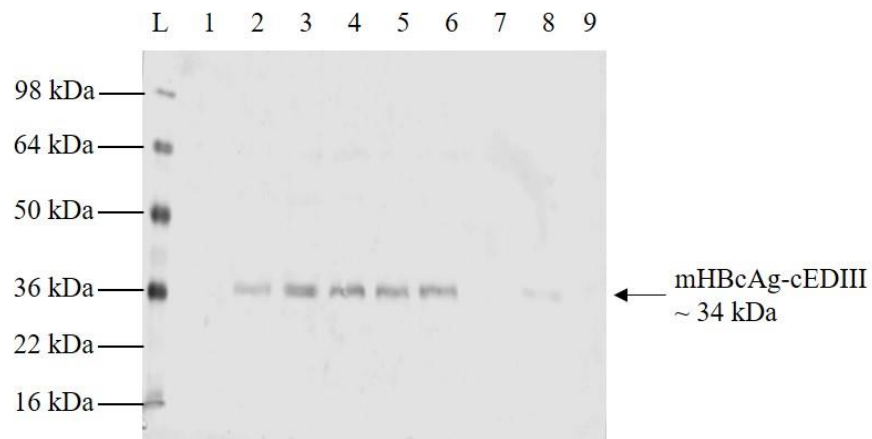


Figure 4.9: Expression profiles of mHBcAg-cEDIII protein in *N. benthamiana* host. Immunoblot detection was performed using HBcAg monoclonal antibody, to detect the expression mediated by pEAQ-*HT*::mHBcAg-cEDIII vector (Panel A: Verification of mHBcAg-cEDIII expression; Panel B: Buffer optimisation). The recombinant vector was successfully shown to express mHBcAg-cEDIII protein.

Panel A: Physical appearance of *N. benthamiana* infiltrated leaf



Panel B: Western blot probed with HBcAg monoclonal antibody



Lane	Sample	Expression vector	Estimated size
L	SeeBlue Plus2 Pre-Stained Standard		
1-9	SP extracted from leaf discs from 1 st – 9 th dpi	pEAQ- <i>HT</i> ::mHBcAg-cEDIII	~ 34 kDa

Figure 4.10: Kinetic expression profiles of mHBcAg-cEDIII protein in *N. benthamiana*. Panel A: Daily observations of infiltrated leaf; Panel B: Immunoblotting of mHBcAg-cEDIII proteins extracted on 1st – 9th dpi, as detected using HBcAg monoclonal antibody. The harvest time for mHBcAg-cEDIII protein was determined as 4th dpi.

The production of a variant monomeric core HBcAg with cEDIII display, known as mHBcAg-cEDIII (L) (expression vector: pEAQ-*HT*::mHBcAg-cEDIII (L)) had been successfully achieved in *N. benthamiana* as well (**Figure 4.11**). Buffer optimisation was conducted to improve the extraction of mHBcAg-cEDIII (L) protein, by which higher yield was obtained using the optimised VLPs extraction buffer B. As a reminder, the only difference between the expression cassettes of mHBcAg-cEDIII and mHBcAg-cEDIII (L) is the presence of (GGS)_n linkers that flanked the cEDIII insert (described in **Section 3.2.3**).

The kinetic expression profiles of mHBcAg-cEDIII (L) protein are presented in **Figure 4.12**. In this case, the pEAQ-*HT*::mHBcAg-cEDIII (L)-infiltrated leaf appeared to suffer from leaf crinkle and yellowing since 5th dpi (Panel A). The immunoblot profiles in Panel B imply that high mHBcAg-cEDIII (L) expression was achieved between 2nd to 4th dpi. With that, 4th dpi was chosen as the optimal time for large-scale harvest.

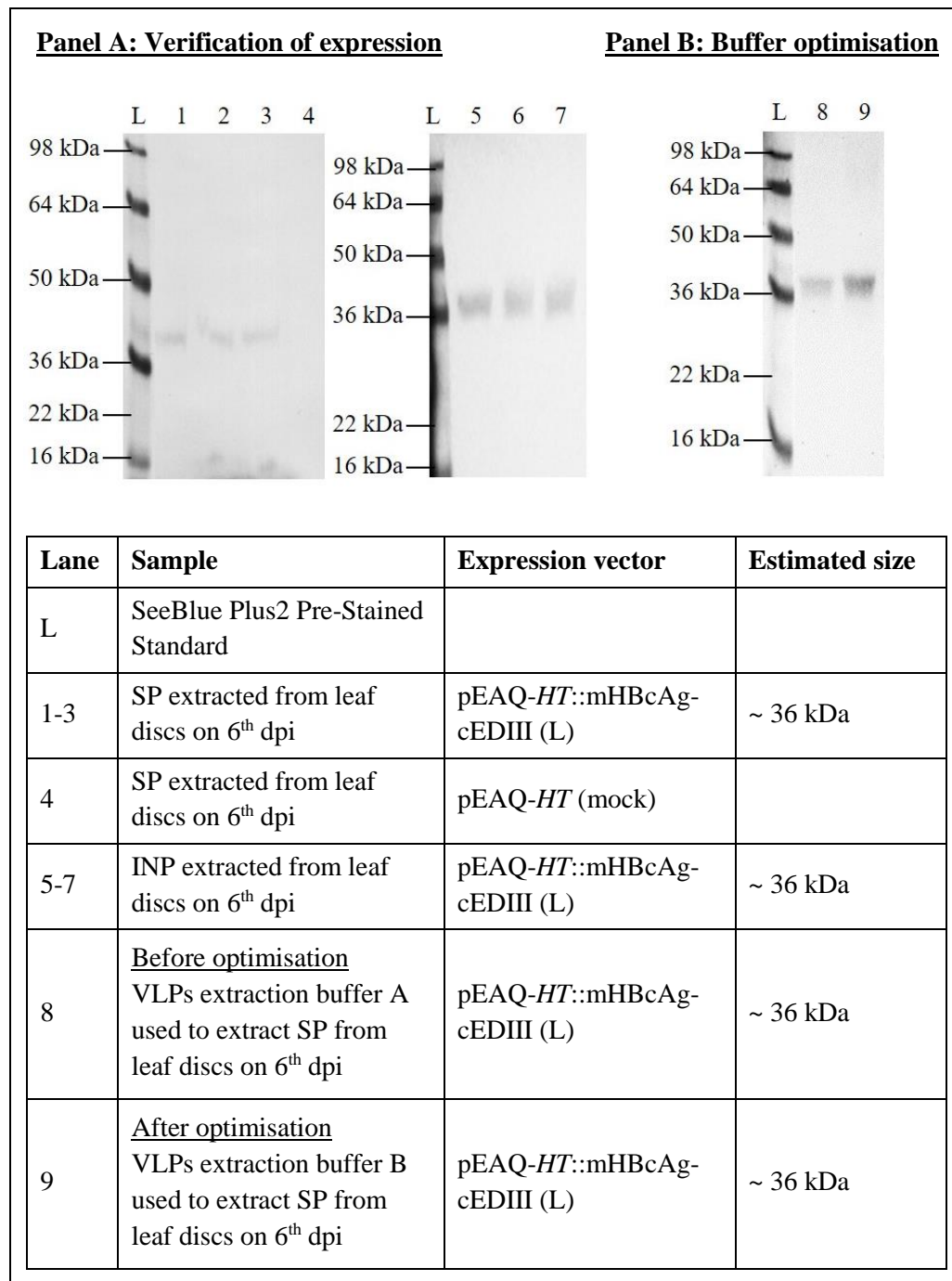
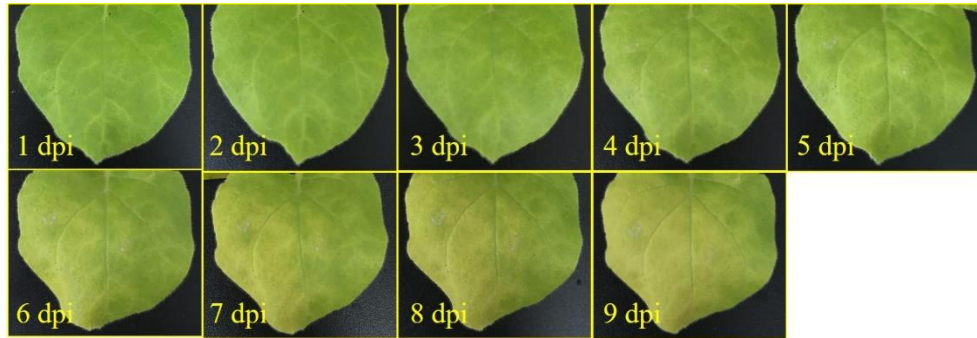
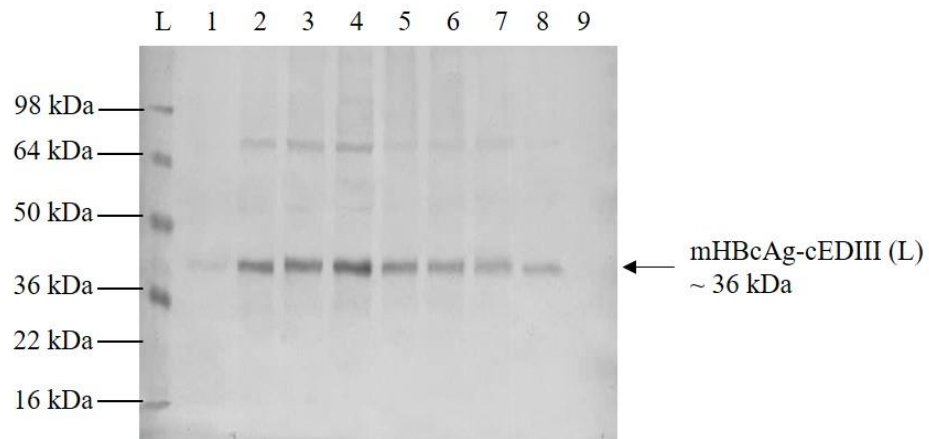


Figure 4.11: Expression profiles of mHBcAg-cEDIII (L) protein in *N. benthamiana* host. Immunoblot detection was performed using HBcAg monoclonal antibody, to verify the expression mediated by pEAQ-*HT*::mHBcAg-cEDIII (L) vector. It is found that the vector was able to express mHBcAg-cEDIII (L) protein.

Panel A: Physical appearance of *N. benthamiana* infiltrated leaf



Panel B: Western blot probed with HBcAg monoclonal antibody



Lane	Sample	Expression vector	Estimated size
L	SeeBlue Plus2 Pre-Stained Standard		
1-9	SP extracted from leaf discs from 1 st – 9 th dpi	pEAQ- <i>HT</i> ::mHBcAg-cEDIII (L)	~ 36 kDa

Figure 4.12: Kinetic expression profiles of mHBcAg-cEDIII (L) protein in *N. benthamiana*. Panel A: Daily observations of infiltrated leaf; Panel B: Immunoblotting of mHBcAg-cEDIII (L) proteins extracted on 1st – 9th dpi, as detected using HBcAg monoclonal antibody. The harvest time for mHBcAg-cEDIII (L) protein was determined as 4th dpi.

4.3.5 Expression of tandem core virus-like particles (VLPs) displaying cEDIII epitopes

Successful expression of the tandem core construct with cEDIII displays had been achieved using *N. benthamiana* (**Figure 4.13**). The yield of tHBcAg-cEDIII SP (expression vector: pEAQ-*HT*::tHBcAg-cEDIII) was enormously low that it was barely detectable (Panel A). In this case, the insoluble protein (INP) of pEAQ-*HT*::tHBcAg-cEDIII-infiltrated leaf was also recovered for validation purpose. As anticipated, bands that corresponded to tHBcAg-cEDIII proteins were detected. Subsequently, buffer optimisation was done to increase the yield of tHBcAg-cEDIII protein (Panel B). With the use of new buffer labelled as VLPs extraction buffer A, a higher amount of SP for tHBcAg-cEDIII sample could be harvested.

The kinetic expression profiles of tHBcAg-cEDIII protein (expression vector: pEAQ-*HT*::tHBcAg-cEDIII) can be found at **Figure 4.14**. Panel A shows that symptom of leaf chlorosis was observed from 7th dpi onwards, which led to visible necrosis on 9th dpi. Meanwhile, the immunoblot profiles in Panel B suggest that increasing accumulation of tHBcAg-cEDIII SP could be seen from 6th dpi onwards. As modest necrosis was observed on 9th dpi, it was more sensible to set 8th dpi as the optimal harvest time.

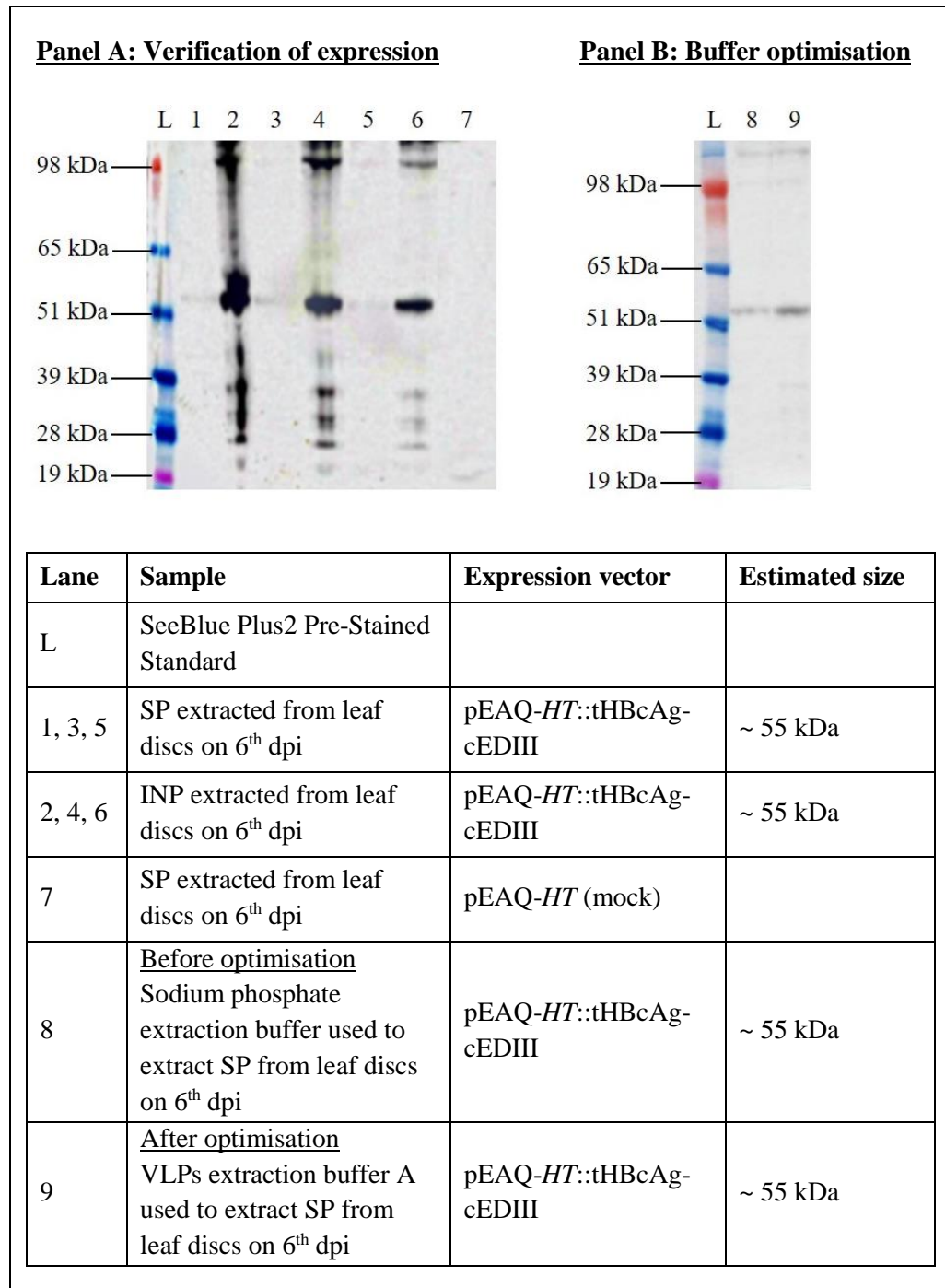
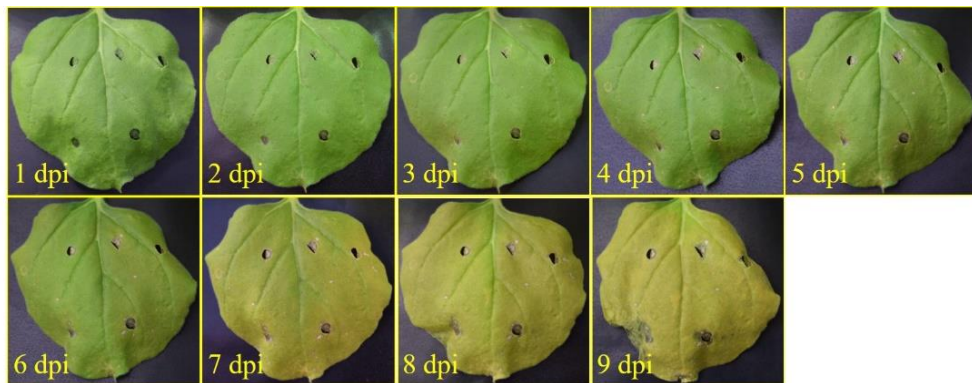


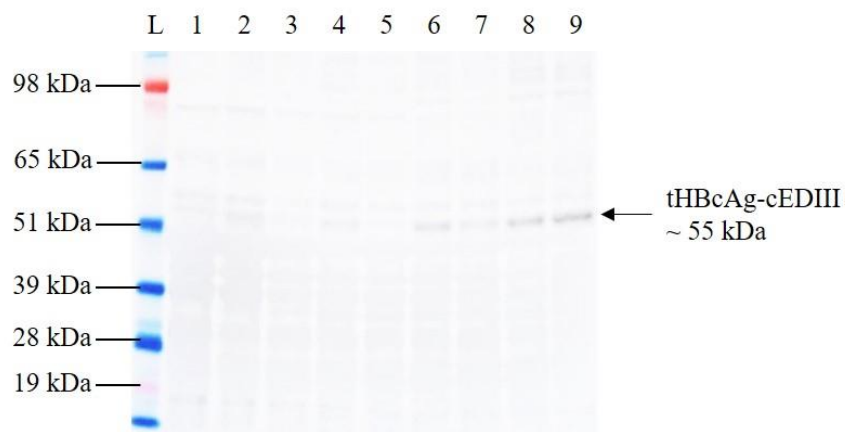
Figure 4.13: Expression profiles of tHBcAg-cEDIII protein in *N. benthamiana* host.

Immunoblot detection was performed using HBcAg monoclonal antibody, to verify the expression mediated by pEAQ-*HT*::tHBcAg-cEDIII vector. The tHBcAg-cEDIII protein was successfully expressed, but was mostly in insoluble form.

Panel A: Physical appearance of *N. benthamiana* infiltrated leaf



Panel B: Western blot probed with HBcAg monoclonal antibody



Lane	Sample	Expression vector	Estimated size
L	SeeBlue Plus2 Pre-Stained Standard		
1-9	SP extracted from leaf discs from 1 st – 9 th dpi	pEAQ- <i>HT</i> ::tHBcAg-cEDIII	~ 55 kDa

Figure 4.14: Kinetic expression profiles of tHBcAg-cEDIII protein in *N. benthamiana*.

Panel A: Daily observations of infiltrated leaf; Panel B: Immunoblotting of tHBcAg-cEDIII proteins extracted on 1st – 9th dpi, as detected using HBcAg monoclonal antibody. The harvest time for tHBcAg-cEDIII protein was determined as 8th dpi.

4.4 Discussion

This chapter focuses on the delivery of cEDIII recombinant vectors into *N. benthamiana* via agroinfiltration. Subsequent expression profiling has allowed assessment of the stability of expressed proteins in order to select the most ideal candidates to proceed with downstream purification study. In this study, *N. benthamiana* is host species of choice given to its short life cycle and succulent vegetative growth. *N. benthamiana* plants are ready for infiltration in 5 – 6 weeks, and the succulent leaves make them easier to be infiltrated. Besides, its high biomass production is favoured for the potential to harvest high product yield. *N. benthamiana* plant is highly susceptible to *Agrobacterium* infection, which is useful to mediate the initial entry and delivery of expression vectors in achieving successful transformation (Klimyuk *et al.*, 2014). As *N. benthamiana* is a non-food and non-feed crop, thereby eliminating the risk of contaminating the food chain. For these reasons, *N. benthamiana* is also preferably used by various biopharmaceutical companies such as Icon Genetics, Medicago Inc. and Kentucky Processing. Only *N. benthamiana* plants aged between 5 – 6 weeks were used for agroinfiltration because flowering was observed 6 weeks after germination. According to Leuzinger *et al.* (2013), flower development is not desirable as the diversion of nutrients away from leaves could affect the accumulation of heterologous proteins.

Syringe infiltration has been fully adopted as the transformation approach in this study. The syringe technique is exceptionally straightforward where it does not need dedicated equipment or special set-up. It is cost-effective and productive in the sense that different transgenes or expression strategies can be easily tested in parallel. For vaccine development, it is the method of choice for rapid screening of candidates in response to emerging pandemics such as dengue in this context. Arguably, manual inoculation may not be technically consistent, but variation can be compensated by harvesting leaf replica from same and different plants. Chen *et al.* (2013b) also agreed

that syringe infiltration is ideal for laboratory-scale expression, purification and pre-clinical testing of plant-derived protein. The alternative vacuum infiltration however, is more suitable for industrial application by which the efficacy of a specific vaccine has been proven and is set for large-scale production. Moreover, application of vacuum demands for more stringent optimisation of parameters such as the pressure setting and treatment duration (Loh and Baranzan, 2014). This is crucial so that the mechanical injuries experienced by the plant can be reduced to minimal while still able to acquire satisfactory protein expression.

Apart from the design of expression cassettes (**Chapter 3**), the strain of *Agrobacterium* and the bacterial concentration used for infiltration can affect the protein expression as well. Various laboratory strains of *Agrobacterium* have been tested for transient expression including LBA4404, GV3101, EHA105 and C58C1. In this study, LBA4404 was chosen as it is the preferred strain used for transfer of pEAQ vector (Sainsbury *et al.*, 2009), although strains like AGL1 and GV3101 have also been used with success (Dennis *et al.*, 2018; Mardanova *et al.*, 2015). In regard to the agrobacterial concentration, a constant OD₆₀₀ of 0.4 was used throughout this study, which was in line with the recommended range of OD₆₀₀ at 0.3 – 0.4 (Li, 2011; Shamloul *et al.*, 2014; Wroblewski *et al.*, 2005). This is because high bacterial density tends to trigger hypersensitive response that can lead to tissue necrosis, whereas low amount of *Agrobacterium* may result in insufficient gene delivery (Leuzinger *et al.*, 2013). As presented in this study, reliable and high level of transient gene expression was achieved at the chosen OD₄₀₀ of 0.4, without severely affected by hypersensitivity responses.

In this study, all the cEDIII recombinant proteins were targeted to ER as the final cellular destination. To achieve this, two variants of expression cassettes were designed for recombinant cEDIII-sGFP, namely pEAQ-*HT*::cEDIII-sGFP-KDEL-H (initial construct) and pEAQ-*HT*::PR1a-cEDIII-H-KDEL (improved construct). Likewise, two variants were also designed for recombinant CTB-cEDIII, namely pEAQ-*HT*::CTB-

cEDIII-KDEL-H (initial construct) and pEAQ-*HT*::PR1a-CTB-cEDIII-H-KDEL (improved construct). A functional KDEL motif plays a key role in retaining the recombinant proteins in ER. However, the lack of PR1a signal from initial construct of cEDIII-sGFP seemed to have driven protein localisation to cytoplasm (**Figure 4.2**), whereas the improved construct with PR1a signal had directed the cEDIII-sGFP proteins to the ER compartment. Coherent to the expression profiles of cEDIII-sGFP (**Figure 4.3**) and CTB-cEDIII (**Figure 4.5**) proteins, the absence of PR1a in their initial constructs were indeed marked with poorer expressions. These show that the combinatory use of PR1a and KDEL signals is more effective in regulating protein localisation to ER, which mediates protein folding and accumulation in a more stable environment (Xu *et al.*, 2002). Besides, previous studies claimed that KDEL signal must be positioned at the extreme C-terminus to render proper retention (Miesenbock and Rothman, 1995; Munro and Pelham, 1987). Consistent to that, efficient ER retention was achieved after shuffling the KDEL position, as shown in pEAQ-*HT*::PR1a-cEDIII-sGFP-H-KDEL and pEAQ-*HT*::PR1a-CTB-cEDIII-H-KDEL (**Table 3.2**). Overall, these efforts have fulfilled the objectives to increase the yield of cEDIII recombinant protein via gene cassettes improvement. Worthwhile to mention, the improved constructs of cEDIII-sGFP (expression vector: pEAQ-*HT*::PR1a-cEDIII-sGFP-H-KDEL) and CTB-cEDIII (expression vector: pEAQ-*HT*::PR1a-CTB-cEDIII-H-KDEL) had a Kozak sequence at their N-termini. The beneficial use of Kozak sequence is long known since Jones *et al.* (1988) reported that it could boost the expression of bacterial chitinase gene (*chiA*) by 8 folds in transgenic tobacco. To date, Kozak sequence is commonly used in several pEAQ-based expression vectors as demonstrated by Kanagarajan *et al.* (2012) and Peyret *et al.* (2015). Though the insertion of Kozak sequence may have contributed to the enhanced expression, but it should be noted that Kozak sequence does not regulate protein trafficking.

Reinstating the subcellular localisation effects, it was discovered that the *N. benthamiana* leaf infiltrated with initial constructs of recombinant cEDIII-sGFP (expression vector: pEAQ-*HT*::cEDIII-sGFP-KDEL-H) and CTB-cEDIII (expression vector: pEAQ-*HT*::CTB-cEDIII-KDEL-H) had suffered from much earlier necrosis on 7th dpi (**Appendix A4.2**). It is believed that the cell death is correlated to the transient over-expression of recombinant proteins. This happens when the capacity of protein processing system is no longer able to cope with the translation event, thereby generating an abundance of unfolded or misfolded proteins (Fanata *et al.*, 2013). To this end, the accumulation of unfolded proteins can impose ER stress which activates the unfolded protein response (UPR) to initiate protein repair. ER quality control (ERQC) system will monitor these processes and identifies misfolded conformations for ER associated degradation (ERAD) via ubiquitination (Schröder and Kaufman, 2005). Principally, ER houses molecular chaperones and enzymes that assist in protein folding and post-translational modifications. Subcellular localisation to ER can help to prolong the time in ER lumen to increase chance of proper protein folding and assembly. Yet, this was not mitigated for cytoplasm-localised constructs, namely pEAQ-*HT*::cEDIII-sGFP-KDEL-H and pEAQ-*HT*::CTB-cEDIII-KDEL-H. Similar findings were reported by Hamorsky *et al.* (2015), suggesting that the massive tissue damage suffered by non-ER-retained construct is associated with the overloaded ERQC and ERAD systems. The prolonged ER stress can cause severe damage to plant organelles that eventually leads to cell death.

Upon translocation, a signal peptide is generally removed from the mature protein in the ER lumen, and this should apply to PR1a as well. The Signal-BLAST software was used to analyse the PR1a amino acid sequence and a cleavage site was predicted after the last residue of PR1a signal peptide (**Appendix A4.3**), which hereafter labelled as position -1. An early study done by von Heijne (1983) proposed that the small, neutral residues at positions -1 and -3 would fit into the pocket of signal peptidase before

cleavage takes place between positions -1 and +1 of the mature protein. Such patterns of amino acids conform to the PR1a sequence used in this study, where small alanine and cysteine residues are found at positions -1 and -3, respectively. In accordance with von Heijne (1983), it is speculated that the PR1a signal peptide would be post-translationally removed, and hence PR1a is not included in the estimation of protein molecular weight (**Table 4.2**)

While satisfactory amount of cEDIII-sGFP and CTB-cEDIII recombinant proteins could be harvested, problems were encountered with low recovery of chimeric HBcAg VLPs displaying cEDIII. The expression of HBcAg proteins in cytosol could in part explain for the low abundance. PR1a and KDEL signals were not incorporated into the expression cassettes of monomeric core and tandem core VLPs (**Table 3.2**) due to the concern that protein trafficking might disrupt VLPs assembly. Since the objective here was to develop chimeric VLPs that can display cEDIII epitopes, the localisation strategy was omitted with the primary hope that correctly assembled VLPs could be obtained. Apart from the low expression, most of these HBcAg-based proteins were detected in the insoluble pellet, possibly due to the macromolecular structures of VLPs which are hard to be solubilised. As protein solubility is dependent on the interactions of its surface residues with surrounding solution, new extraction buffers were formulated by considering the following aspects: (i) adding Triton X-100 detergent to assist the dissolution and release of VLPs from insoluble cell components, as stated by Gaik *et al.* (2008); (ii) use a low-salt condition (100 mM sodium chloride) to provide ionic strength that reduces formation of aggregates, of which was shown to be effective by Zahin *et al.* (2016); and (iii) adjusting the pH of extraction buffer away from the predicted isoelectric point (pI) to increase protein solubility (Abdalla *et al.*, 2016). The pI of mHBcAg-cEDIII, mHBcAg-cEDIII (L) and tHBcAg-cEDIII proteins was predicted using the ExPASy ProtParam tool. Consequently, buffer optimisation proved to be useful as greater amount of SP extracts of mHBcAg-cEDIII (**Figure 4.9**),

mHBcAg-cEDIII (L) (**Figure 4.11**) and tHBcAg-cEDIII (**Figure 4.13**) proteins could be recovered. Though VLPs extraction buffer A can mediate satisfactory recovery of soluble mHBcAg-cEDIII and mHBcAg-cEDIII (L) proteins; yet, a further pH adjustment which gave rise to VLPs extraction buffer B produced more soluble monomeric core proteins. Given that each protein has its own unique properties, it could be better to determine the extraction conditions on case-to-case basis. This was rationalised from the observation that even the slightest change of the HBcAg sequence in monomeric core and tandem core can affect its overall solubility. Nonetheless, protease inhibitor cocktail was added in all the protein extraction buffers (**Appendix A4.1**) to reduce proteolytic degradation during extraction and purification procedures.

In general, maximum protein expression is usually observed between 4th – 6th dpi (Joensuu *et al.*, 2010; Kanagarajan *et al.*, 2012; Nausch *et al.*, 2012). Thus, the expression kinetics within this timeline were studied along with an allowance of ± 3 days to buffer for ‘exceptional’ case. The profiles were used to gauge the ideal harvest time which is assessed based on two aspects: (i) the peak accumulation of target protein; and (ii) the post-infiltration morphological distortions. Necrotic tissues should be avoided as they are flaccid and usually contain higher amount of phenolic and alkaloids that could be introduced into downstream purification. In fact, the antimicrobial exudate produced by necrotic tissues can inhibit efficient colonisation and gene delivery by the *Agrobacterium* (Pitzschke, 2013). Hence, it is projected that the protein yield in these leaf tissues could be drastically low. To minimise bias effects, the expression kinetics of each construct were analysed from at least 5 replicates of infiltrated *N. benthamiana* that were grown from the same batch. In summary, the optimal harvest time for each construct was determined as follows: (i) 6th dpi for pEAQ-*HT*::PR1a-cEDIII-sGFP-H-KDEL, pEAQ-*HT*::PR1a-CTB-cEDIII-H-KDEL and pEAQ-*HT*::PR1a-CTB-cEDIII-KDEL (xTH); (ii) 4th dpi for pEAQ-*HT*::mHBcAg-cEDIII and pEAQ-*HT*::mHBcAg-cEDIII (L); and lastly (iii) 8th dpi for pEAQ-*HT*::tHBcAg-cEDIII. Except for pEAQ-

HT::tHBcAg-cEDIII, the expression of other constructs did fall within the recommended harvesting time of 4th – 6th dpi. The kinetic profiling was only conducted once since it was used for qualitative analyses. Nevertheless, yield quantification was performed after obtaining the purified products (**Chapter 5**).

4.5 Conclusion

This chapter concludes with the successful *in planta* expression of cEDIII recombinant proteins and chimeric HBcAg VLPs displaying cEDIII, following gene delivery via syringe infiltration.

The expression mediated by corresponding cEDIII-sGFP and CTB-cEDIII expression vectors had been evaluated in this study, in which the expression vectors named as pEAQ-*HT*::PR1a-cEDIII-sGFP-H-KDEL, pEAQ-*HT*::PR1a-CTB-cEDIII-H-KDEL and pEAQ-*HT*::PR1a-CTB-cEDIII-KDEL (xTH) had been selected to proceed with large-scale purification (**Chapter 5**). On top of that, the improved ER localisation mediated by both PR1a and KDEL signals has been clearly addressed in this chapter.

Meanwhile, successful expression of the monomeric core constructs (expressed by: pEAQ-*HT*::mHBcAg-cEDIII and pEAQ-*HT*::mHBcAg-cEDIII (L)) and tandem core construct (expressed by: pEAQ-*HT*::tHBcAg-cEDIII) was presented, even though most of these proteins were harvested in insoluble form. Hence, new extraction buffers were formulated to facilitate greater recovery of the SP. The proteins expressed by these constructs were then purified to assess their abilities to assemble into VLPs, by which are described in **Chapter 5**.

Lastly, kinetic analyses had provided information on the accumulation of heterologous proteins and the post-infiltration symptoms. These findings were useful in order to determine the optimal harvest time to proceed with subsequent purification and quantification studies (**Chapter 5**).

5 Protein Purification and Characterisation of Plant-made Recombinant cEDIII Fusion Proteins and Chimeric Virus-Like Particles Displaying cEDIII

Table of Contents

5.1	Introduction	5-3
5.2	Materials and methods.....	5-6
5.2.1	Overview of the protein purification procedures	5-6
5.2.2	Specialised equipment	5-10
5.2.3	Large-scale sample harvest.....	5-10
5.2.4	Purification of recombinant cEDIII fusion proteins	5-11
5.2.4.1	Immobilised metal affinity chromatography (IMAC) under native condition.....	5-11
5.2.4.2	Tobacco etch virus (TEV) protease digestion	5-12
5.2.5	Characterisation of CTB-cEDIII-KDEL (xTH) protein.....	5-12
5.2.5.1	GM1 ganglioside enzyme-linked immunosorbent assay (GM1-ELISA).....	5-12
5.2.5.2	Size exclusion chromatography (SEC)	5-13
5.2.6	Purification of chimeric virus-like particles (VLPs)-displaying cEDIII	5-14
5.2.6.1	Sucrose cushion.....	5-14
5.2.6.2	Sucrose/nycodenz gradient	5-14
5.2.7	Characterisation of chimeric virus-like particles (VLPs)-displaying cEDIII	5-15
5.2.7.1	Transmission electron microscopy (TEM).....	5-15

5.2.7.2	Immunogold labelling	5-15
5.2.8	Dialysing protein	5-16
5.2.9	Concentrating protein	5-16
5.2.10	Yield quantification	5-16
5.3	Results	5-18
5.3.1	Step-by-step isolation of cEDIII protein.....	5-18
5.3.2	Purification of CTB-cEDIII fusion protein.....	5-24
5.3.3	Purification of monomeric core virus-like particles (VLPs) displaying cEDIII	5-35
5.3.4	Purification of tandem core virus-like particles (VLPs) displaying cEDIII	5-45
5.3.5	Quantification of purified protein sample.....	5-52
5.4	Discussion	5-53
5.5	Conclusion.....	5-62

5.1 Introduction

Following expression studies in plant, protein purification is used to isolate pure product from a complex mixture of crude proteins in host cell. It engages a series of processes starting from cell lysis, clarification of soluble components to fractionation of desired proteins from host impurities. Besides, purification also facilitates the enrichment of a protein sample so that its structure and function can be characterised. The most challenging part however, is to recover heterologous protein with preserved functionality for downstream application. Hitherto, various methods have been developed for the purification of biological samples and a couple of them are discussed in relevant to the techniques applied in this study.

Protein extraction from *N. benthamiana* leaves begins with physical cell lysis, as the rigid cellulose walls need to be sheared via homogeniser or manual grinding to release the cell contents. Unavoidably, some contaminants are also released during cell disruption including proteases, phenolics, photosynthetic pigments and *Agrobacterium*. Therefore, formulation of extraction buffer with appropriate pH, ionic strength and additives is crucial to maximise recovery of heterologous proteins (Laing and Christeller, 2004), which has been discussed in **Chapter 4**. Other particulate materials or unbroken cells could be removed via clarification at high-speed centrifugation or syringe filters before proceeding to purification procedures.

Principally, chromatography refers to an analytical technique where molecules in the applied mixture is separated from each other at the stationary phase as they move in a definite direction with the aid of mobile phase. Protein separation mainly relies on several principles such as affinity, charge, hydrophobicity and size difference. Among these, affinity chromatography is often chosen based on its high-throughput and specific binding properties. Technically, high affinity ligands are attached to the resin surface to capture target proteins prior eluted by changes in molecular interactions. Commonly used affinity tags to date include 6X histidine (His) tag, FLAG tag (with the sequence

motif, DYKDDDDK), glutathione S-transferase (GST) and maltose-binding protein (MBP) (Zhao *et al.*, 2013). The immobilised metal affinity chromatography (IMAC) introduced by Porath *et al.* (1975), is one of the most popular affinity-based methods used to date. Hence, it was adopted as the main purification strategy to recover recombinant cEDIII fusion proteins in this study.

Other chromatographic methods may be applied as further polishing step when the characteristics of a heterologous protein is more well-studied. For instance, size exclusion chromatography (SEC) is often used to fractionate protein according to molecular weight difference. As molecules pass through the sieving medium, those smaller than the pores inside the gels will penetrate through and take a longer path to be eluted as compared to larger molecules (Duong-Ly and Gabelli, 2014a). In ion-exchange chromatography (IEX), proteins are separated based on the electrostatic interactions between charged protein groups and the oppositely charged stationary phase matrix (Duong-Ly and Gabelli, 2014b). In contrast, purification via hydrophobic interaction chromatography (HIC) relies on the hydrophobic properties of protein molecules and adsorbents, as well as the salt concentration in mobile phase, which is particularly useful to separate aggregated species from monomeric form (McCue, 2014).

Meanwhile, density gradient ultracentrifugation is a simpler procedure used to separate the virus-like particles (VLPs) in a suspension according to density. High centrifugal force is applied to pull the particles and plant constituents down through the density medium, which will eventually sediment at different rates. This type of ultracentrifugation is sub-divided into two types known as rate zonal and isopycnic. The main difference comes from the type of gradient medium, where rate zonal uses a lower density solution such as sucrose to separate particles based on their size and shape; while isopycnic relies on high-density solution like caesium chloride and nycodenz to separate particles until they reaches the equilibrium density (Dijkstra and de Jager, 1998). In rate zonal separation, sample is overlaid on a pre-formed, continuous gradient of sucrose

and centrifuged for 2 – 3 hours to avoid pelleting. For isopycnic separation, particles are also overlaid on pre-formed gradient, but they will never sediment regardless of centrifugation time as the gradient solution is much denser. The so-called sucrose cushion, is used as an initial step to concentrate VLPs from clarified lysate (Peyret, 2015). This method is slightly different as it only uses a small volume of discontinuous density gradient for sample enrichment.

In this chapter, large-scale harvest was carried out to recover high amount of recombinant cEDIII fused to green fluorescent protein (sGFP) and recombinant cEDIII fused to cholera toxin B subunit (CTB). On top of that, the chimeric hepatitis B core antigen (HBcAg) VLPs were also recovered, which comprised of monomeric core HBcAg (mHBcAg) VLPs-displaying cEDIII and tandem core HBcAg (tHBcAg) VLPs-expressing cEDIII. These purified samples would then be used for immunogenicity testing in **Chapter 6**.

With that, the specific objectives for this chapter are:

- (i) To purify recombinant cEDIII fusion proteins, namely cEDIII-sGFP-H-KDEL, CTB-cEDIII-H-KDEL and CTB-cEDIII-KDEL (xTH) with IMAC under native conditions;
- (ii) To perform subsequent removal of affinity tag via TEV protease cleavage;
- (iii) To prepare the recombinant cEDIII fusion protein that would be used for immunogenicity test;
- (iv) To study the pentameric folding of CTB-cEDIII-KDEL (xTH) protein;
- (v) To purify the mHBcAg-cEDIII, mHBcAg-cEDIII (L) and tHBcAg-cEDIII proteins via density gradient ultracentrifugation;
- (vi) To assess the ability of purified mHBcAg-cEDIII, mHBcAg-cEDIII (L) and tHBcAg-cEDIII proteins to assemble into VLPs; and
- (vii) To prepare the chimeric HBcAg VLPs samples that would be used for immunogenicity test.

5.2 Materials and methods

5.2.1 Overview of the protein purification procedures

Two distinct protein purification strategies were used to isolate the recombinant cEDIII fusion proteins and chimeric HBcAg VLPs-displaying cEDIII.

An overview of the procedures involved in the purification of recombinant cEDIII fusion proteins is shown in **Figure 5.1**. Recombinant cEDIII fusion proteins that were purified in this study comprised of cEDIII-sGFP-H-KDEL fusion protein (expressed by pEAQ-*HT*::PR1a-cEDIII-sGFP-H-KDEL), CTB-cEDIII-H-KDEL fusion protein (expressed by pEAQ::*HT*::PR1a-CTB-cEDIII-H-KDEL) and CTB-cEDIII-KDEL (xTH) fusion protein (expressed by pEAQ-*HT*::PR1a-CTB-cEDIII-KDEL (xTH)). Procedure that was carried out for each cEDIII fusion protein is listed according to the numbered steps in **Figure 5.1**. Following sample lysis and clarification, first round IMAC was used to isolate His-tagged recombinant proteins in the eluted fraction, by which it was referred as IMAC purification_1. Next, TEV protease was used to digest the cEDIII-sGFP-H-KDEL and CTB-cEDIII-H-KDEL fusion proteins at the designed cleavage site (refer to **Table 3.2**). A second round IMAC, referred as IMAC purification_2, was then conducted to isolate TEV protease-digested protein in the flow-through fraction. In fact, the AcTEVTM protease used in this study contained 6X His tag that would bind to Ni²⁺-charged resin and hence, could be effectively separated from the target protein at the flow-through step. Lastly, the purified proteins were dialysed against phosphate-buffered saline (PBS) and concentrated.

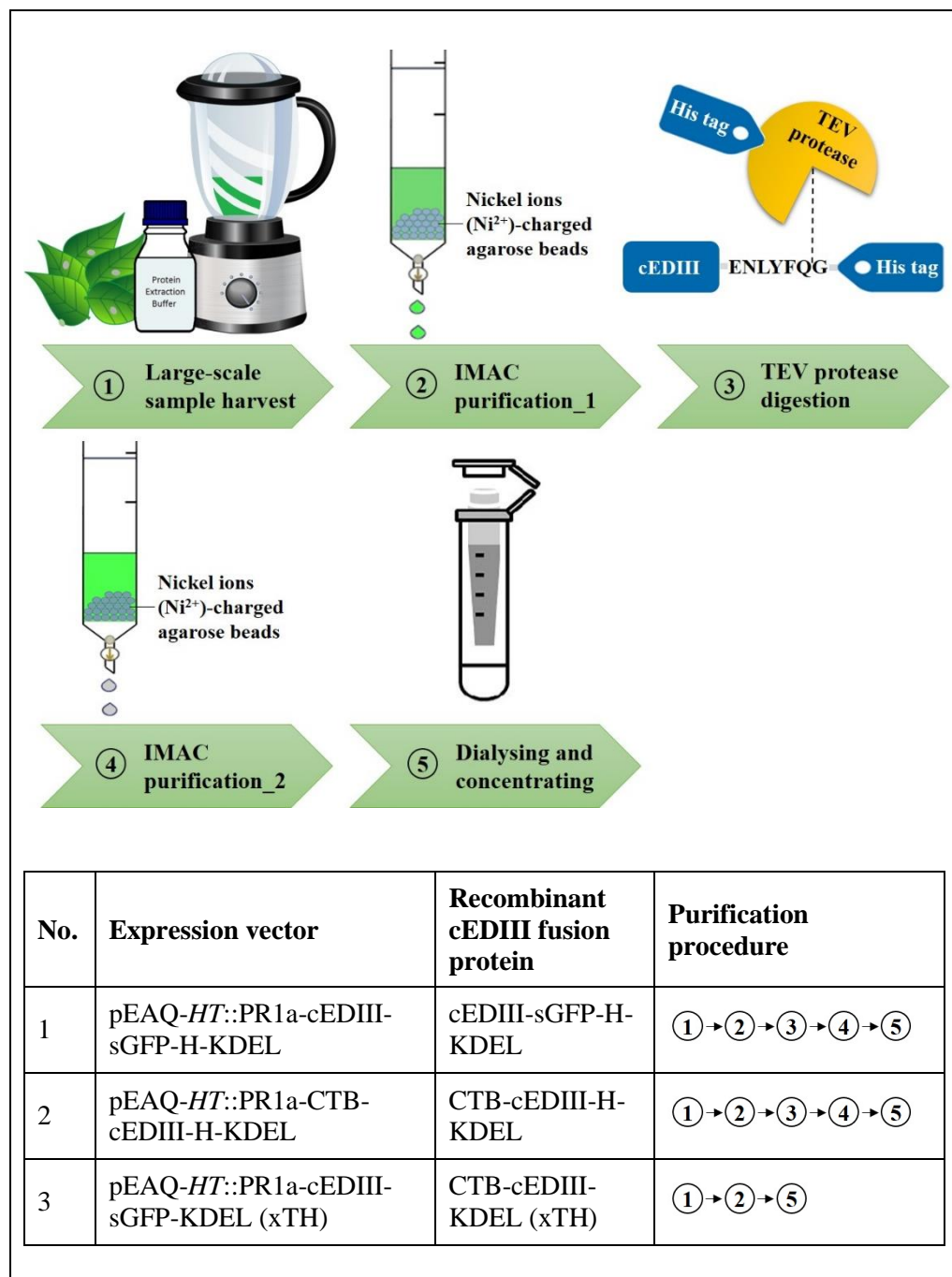


Figure 5.1: An overview of the generic recombinant fusion protein purification procedures which were applied in this study. Note that IMAC purification_1 and IMAC purification_2 are used to differentiate first and second round IMAC, correspondingly.

Meanwhile, an overview of the steps involved in the purification of chimeric HBcAg VLPs-displaying cEDIII is illustrated in **Figure 5.2**. Chimeric VLPs that were purified in this chapter including mHBcAg-cEDIII (expressed by pEAQ-*HT*::mHBcAg-cEDIII), mHBcAg-cEDIII (L) (expressed by pEAQ-*HT*::mHBcAg-cEDIII (L)) and tHBcAg-cEDIII (expressed by pEAQ-*HT*::tHBcAg-cEDIII). These chimeric VLPs were purified in the order of numbered steps in **Figure 5.2**. Following sample lysis and clarification, the plant lysate was subjected to sucrose cushion to isolate the chimeric VLPs. Next, sucrose fractions containing the desired VLPs were concentrated using vacuum concentrator and further purified via sucrose/nycodenz gradient. Lastly, the purified VLPs samples were dialysed against PBS and concentrated.

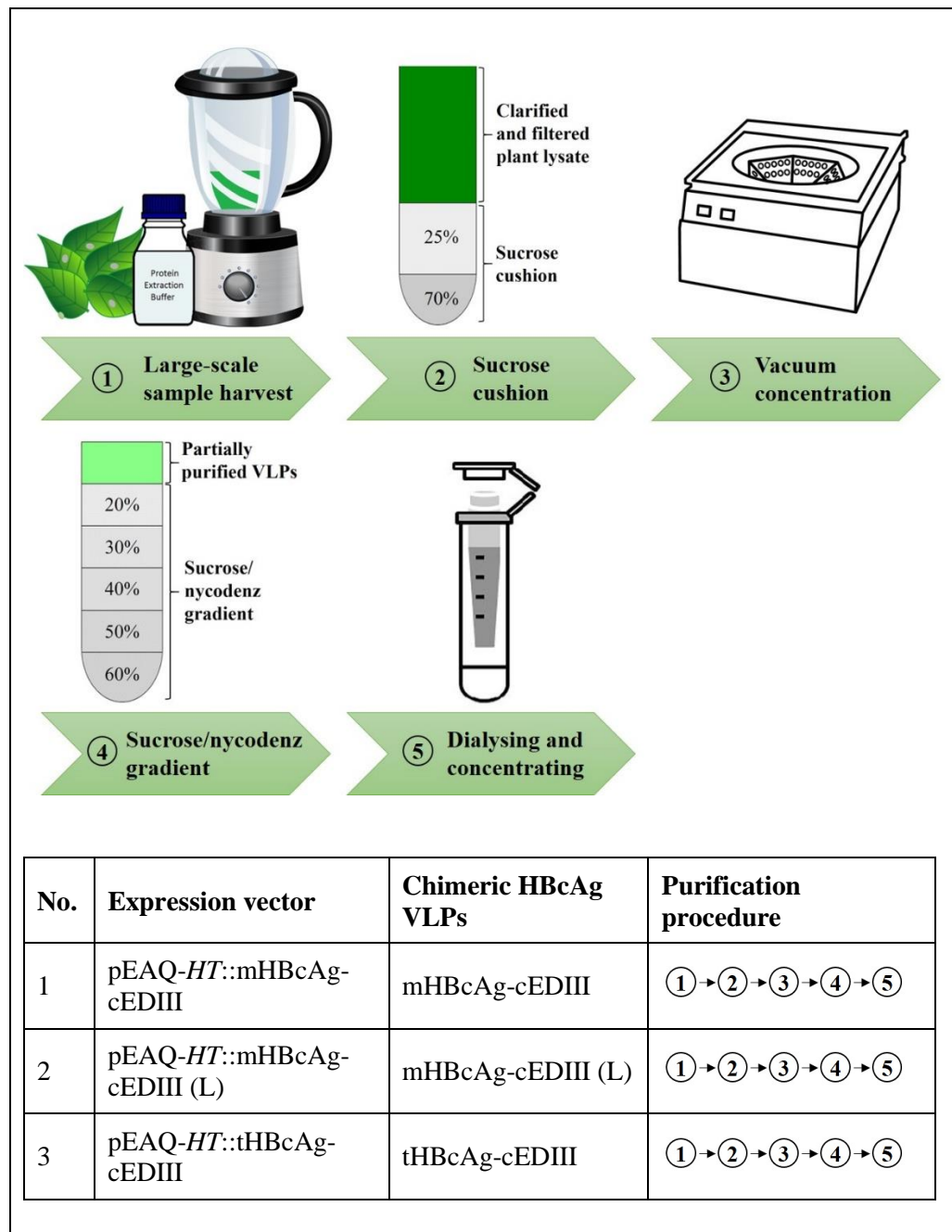


Figure 5.2: An overview of the purification procedures used to isolate the chimeric HBcAg VLPs-displaying cEDIII. Note that sucrose cushion is used to obtain enriched sample before further purification by sucrose/nycodenz gradient.

5.2.2 Specialised equipment

Clarification spin of homogenised leaf extract was performed using either 5810R Refrigerated Centrifuge (Eppendorf, Germany) or Sorvall Evolution RC Superspeed Centrifuge (Thermo Scientific, USA). Thermomixer comfort (Eppendorf, Germany) was used to incubate the TEV protease reaction at 30°C. BINDER Microbiological Incubator (Binder, Germany) was used to incubate the GM1-ELISA plate at 37°C. SEC analysis was carried out using ÄKTA Avant (GE Healthcare, USA). High-speed ultracentrifugation was performed using either Optima XE Ultracentrifuge (Beckman Coulter, USA) or WX Ultra Ultracentrifuge (Thermo Scientific, USA). Transmission electron microscopy (TEM) was carried out using FEI Tecnai 20 transmission electron microscope (FEI, USA) and HT7700 Electron Microscope (Hitachi, Japan). Vacuum concentration was conducted using SpeedVac concentrator (Thermo Scientific, USA) and Concentrator Plus (Eppendorf, Germany).

5.2.3 Large-scale sample harvest

Large-scale extraction was conducted based on the optimal harvest time that had been determined for each construct (**Chapter 4**). Fresh *N. benthamiana* leaves were harvested in bulk, having the large veins and non-infiltrated areas removed. After weighing, the leaf tissues (~ 40 – 80 g) were homogenised with 3X (w/v) volume of extraction buffer (**Table 4.2**) using a blender. Crude lysate was filtered through one layer of Miracloth (Calbiochem, USA) before centrifugation at 15,000-20,000 x g for 20 – 30 minutes at 4°C. To ensure complete removal of cell debris, the clarified extract was filtered with 0.45 µm and 0.2 µm syringe filters (Sartorius, Germany) prior to purification process.

5.2.4 Purification of recombinant cEDIII fusion proteins

5.2.4.1 Immobilised metal affinity chromatography (IMAC) under native condition

Agarose resin derivatized with nickel ion (Ni^{2+})-nitrilotriacetic acid, in short known as Ni-NTA Agarose (Qiagen, Germany) was used to purify His-tagged cEDIII fusion proteins: cEDIII-sGFP-H-KDEL (expressed by pEAQ-*HT*::PR1a-cEDIII-sGFP-H-KDEL), CTB-cEDIII-H-KDEL (expressed by pEAQ-*HT*::PR1a-CTB-cEDIII-H-KDEL) and CTB-cEDIII-KDEL (xTH) (expressed by pEAQ-*HT*::PR1a-CTB-cEDIII-KDEL (xTH)). Firstly, 5 ml of Ni-NTA slurry was transferred to a 50-ml tube and briefly centrifuged at 1,000 x g, 4°C for 5 minutes. The supernatant was removed and the Ni-NTA slurry was equilibrated with tris extraction buffer (**Appendix A5.1**) before another round of centrifugation. The equilibration step was repeated for 3 times before adding 20 ml of clarified plant lysate. For IMAC purification_2 (see **Figure 5.1**), the input sample was changed to TEV-digested protein (**Section 5.2.4.2**).

After that, the mixture was gently mixed at 4°C for 1 hour before loaded into gravity flow column (Thermo Scientific, USA). Upon loading, the flow-through fraction was immediately collected. The column was washed with 5-column volumes of tris extraction buffer, followed by three washes with 5-column volumes of IMAC washing buffers containing 5 – 20 mM of imidazole. These wash fractions were kept for analyses. Lastly, the His-tagged protein was eluted using 2-column volumes of IMAC elution buffer and subjected to SDS-PAGE (**Section 4.2.8**) and Western blotting analyses (**Section 4.2.10**) as previously described. Details of the buffer used can be found at **Appendix A5.1**.

5.2.4.2 Tobacco etch virus (TEV) protease digestion

AcTEV™ (Thermo Fischer, USA) protease was used for the removal of 6X His tag from IMAC-purified cEDIII-sGFP-H-KDEL and CTB-cEDIII-H-KDEL fusion proteins. The cleavage reaction was modified from manufacturer's protocol and set up as follows: 1X TEV Buffer (50 mM Tris-hydrochloride, pH 8.0; 0.5 mM ethylenediaminetetraacetic acid), 1 mM dithiothreitol, 100 units of TEV protease, 100 mg of fusion protein and topped up to 500 µl of distilled water. The reaction tube was then incubated at 30°C for 24 hours.

5.2.5 Characterisation of CTB-cEDIII-KDEL (xTH) protein

5.2.5.1 GM1 ganglioside enzyme-linked immunosorbent assay (GM1-ELISA)

GM1 refers to monosialotetrahexosylganglioside, which are gangliosides present on antigen presenting cells (see **Section 2.4.1.1**). As the pentamers of CTB have high binding affinities for GM1 gangliosides, GM1-ELISA was used to characterise the pentameric folding of CTB-cEDIII-KDEL (xTH) fusion protein (Centers for Disease Control and Prevention (CDC), 2013). In brief, a 96-well microtitre plate (SPL, Korea) was coated with 2 µg/ml of GM1 (Sigma, USA) in sodium bicarbonate buffer (**Appendix A5.1**) overnight at 4°C. Another plate was coated with 2 µg/ml of bovine serum albumin (BSA) (Sigma, USA) to serve as assay control.

On the next day, the wells were washed with PBS containing 0.05% (v/v) Tween-20 (PBST) for three times before blocking with 1% (w/v) BSA in PBST for 1 hour at room temperature (RT). Then, CTB-cEDIII-KDEL (xTH) protein was added in duplicates, along with purified cEDIII and mHBcAg-cEDIII proteins to serve as sample controls. All the proteins were serially-diluted in two-fold starting from the concentration of 100 ng/ml. After 1 hour-incubation at 37°C, the wells were washed with PBST for five times. Next, cholera toxin (CT) polyclonal antibody produced in

rabbit (Sigma, USA) was added at 1:8,000 dilution and incubated at 37°C for 1 hour. Washing steps were repeated before adding goat anti-rabbit immunoglobulin G (IgG), horseradish peroxidase (HRP)-conjugate (Agrisera, Sweden) at 1:20,000 dilution for another hour of incubation at 37°C. After final washes, 3, 3', 5, 5'-tetramethylbenzidine (TMB) substrate (BD, USA) was added. The absorbance at 450 nm wavelength (A_{450}) was measured using Epoch microplate reader (Biotek, USA), with the correction wavelength at 570 nm. The results were presented as means \pm standard deviation (SD) of the A_{450} readings obtained from three independent experiments.

5.2.5.2 Size exclusion chromatography (SEC)

For further characterisation of the pentameric folding of CTB-cEDIII-KDEL (xTH) fusion protein, the IMAC-purified sample was sent to Malaysia Genome Institute (Bangi, Malaysia) for SEC analysis. Approximately 500 μ l of the protein sample was loaded onto Superdex 200 10/300 GL column (GE Healthcare, USA) and separated by ÄKTA Avant at flow rate of 0.5 ml min⁻¹. Besides, the following protein standards (GE Healthcare, USA) with different molecular mass (M_r) were analysed under the same conditions: ribonuclease A (13.7 kDa), ovalbumin (43 kDa) and conalbumin (75 kDa). The chromatogram of protein standards was then used to estimate the molecular weight of fractionated CTB-cEDIII-KDEL (xTH) sample. Eluted fractions were analysed by Western blotting as described in **Section 4.2.10**.

5.2.6 Purification of chimeric virus-like particles (VLPs)-displaying cEDIII

5.2.6.1 Sucrose cushion

Sucrose cushion was used to remove cell debris and organelles from the clarified lysates of mHBcAg-cEDIII (expressed by pEAQ-*HT*::mHBcAg-cEDIII), mHBcAg-cEDIII (L) (expressed by pEAQ-*HT*::mHBcAg-cEDIII (L)) and tHBcAg-cEDIII (expressed by pEAQ-*HT*::tHBcAg-cEDIII). Firstly, the lysate was overlaid onto 25% and 70% (w/v) sucrose solutions in an Ultra-Clear[®] tube (Beckman Coulter, USA). The sample was centrifuged at 30,000 rpm (167,000 x g), 4°C for 2.5 hours using either SW 32 Ti rotor (Beckman Coulter, USA) or SureSpin 630/36 (Thermo Scientific, USA) rotor. Upon completion, the sample was fractionated by piercing through the bottom of the Ultra-Clear[®] tube using 25 G needle (Terumo, USA). Subsequently, collected fractions were analysed via SDS-PAGE (**Section 4.2.8**) and Western blotting (**Section 4.2.10**). At this point, the presence of partially-purified VLPs could be verified via TEM (**Section 5.2.7.1**).

5.2.6.2 Sucrose/nycodenz gradient

After identifying the sucrose cushion fractions that contained assembled VLPs, these fractions could be further purified using gradient made from 20% – 60% (w/v) of sucrose/nycodenz solutions. Ultracentrifugation was then carried out at 40,000 rpm (274,000 x g), 4°C using either SW 41 Ti rotor (Beckman Coulter, USA) or TH-641 rotor (Thermo Scientific, USA). The rate-zonal separation in sucrose solution was performed for 2.5 hours, while isopycnic separation in nycodenz solution could be extended up to 24 hours. Likewise, fractionated samples were analysed via SDS-PAGE (**Section 4.2.8**) and Western blotting (**Section 4.2.10**). VLPs-containing fractions were then pooled and visualised using TEM (**Section 5.2.7.1**).

5.2.7 Characterisation of chimeric virus-like particles (VLPs)-displaying cEDIII

5.2.7.1 Transmission electron microscopy (TEM)

Approximately 10 µl of the purified VLPs sample was adsorbed onto a copper-palladium grid, and washed with sterile distilled water before negatively stained with 2% (w/v) of uranyl acetate. Particles were viewed using FEI Tecnai 20 TEM at 50,000X magnification unless otherwise stated. Most of the TEM imaging procedures were carried out with assistance from Dr. Hadrien Peyret (JIC, UK).

5.2.7.2 Immunogold labelling

Based on the protocol described by Chua *et al.* (2013), immunogold labelling was performed for chimeric mHBcAg VLPs samples, namely mHBcAg-cEDIII and mHBcAg-cEDIII (L). In brief, purified sample was diluted in tris-buffered saline (TBS) (**Appendix A5.1**) and adsorbed onto formvar-carbon coated nickel grid (Electron Microscopy Sciences, USA). The grid was briefly rinsed with a few drops of distilled water before incubating with 100 µl of solution containing: 1% (w/v) BSA for 30 minutes at RT, followed by DENV 1-4 monoclonal antibody (see **Table 4.3**) at 1:100 dilution for 1 hour at RT. The grid was then washed with TBS for three times at every 5-minute intervals. Next, 10-nm colloidal gold-tagged goat anti-mouse IgG polyclonal antibody (Sigma, USA) was added at 1:100 dilution and incubated at RT for 1 hour. Five washing steps were repeated as above before rinsing with distilled water. Lastly, the grid was negatively-stained with 2% (w/v) of uranyl acetate, air-dried and examined under HT7700 Electron Microscope.

5.2.8 Dialysing protein

In general, Float-A-Lyzer device (Sigma, USA) was used for the dialysis of small volume sample. Dialysis device with molecular weight cut-off (MWCO) of 3.5-5 kDa was used for dialysis of recombinant cEDIII fusion proteins; whereas device with 100 kDa MWCO was used to dialyse chimeric HBcAg VLPs-displaying cEDIII samples. For larger volume sample, SnakeSkin™ 7.5 kDa MWCO dialysis tubing (Thermo Scientific, USA) was generally used. The dialysis was carried out in 5 litres beaker containing desired buffer, with a total of three buffer changes over 24 hours.

5.2.9 Concentrating protein

To perform vacuum concentration, VLPs fractions were buffer-exchanged into 20 mM ammonium bicarbonate buffer (**Section 5.2.8**) and then centrifuged in the vacuum concentrator.

To prepare samples for immunogenicity test, Macrosep Advance 3K Omega Centrifugal Device (Pall, USA) was used to concentrate the following vaccine candidates: cEDIII protein, CTB-cEDIII-KDEL (xTH) fusion protein, mHBcAg-cEDIII VLPs, mHBcAg-cEDIII (L) VLPs and tHBcAg-cEDIII VLPs. Based on manufacturer's recommendation, the purified protein was concentrated to at least 10 folds before reconstituting with PBS to desired volume.

5.2.10 Yield quantification

Quick quantification of a protein concentration could be determined using a Nanodrop spectrophotometer (Thermo Scientific, USA). To obtain a more precise quantification, either Modified Lowry Protein Assay Reagent Kit (Thermo Scientific, USA) or Pierce BCA Protein Assay Kit (Thermo Scientific, USA) was used.

The protocol for Modified Lowry kit was performed as follows: (i) Protein sample and BSA standards were transferred in triplicates to a microplate; (ii) Modified Lowry Reagent was added and the plate was incubated at RT for 10 minutes; (iii) 1X Folin-Ciocalteu Reagent was added and incubated at RT for another 30 minutes; and lastly (iv) the absorbance at 750 nm was measured using CLARIOstar microplate reader (BMG LABTECH, Germany). The average 750 nm absorbance values were subtracted from average blank values, and the protein concentration was determined based on the BSA standard curve.

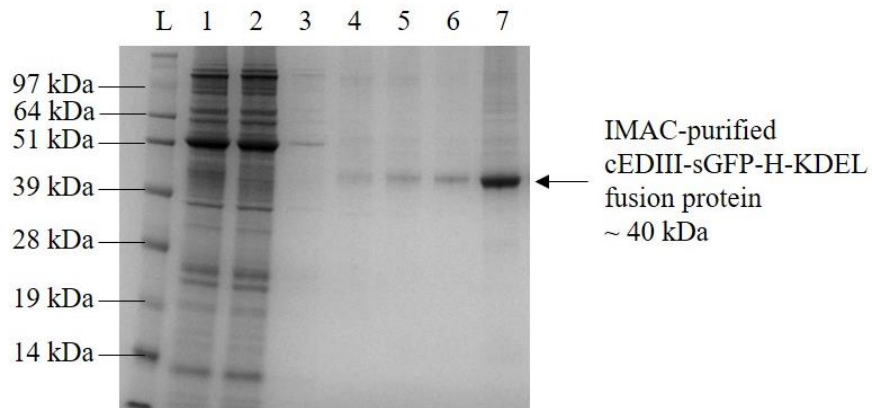
Meanwhile, the protocol for Pierce BSA kit was performed in the following order: (i) Protein sample and BSA standards were transferred in triplicates to a microplate; (ii) BCA Working Reagent was added and the plate incubated at 37°C for 30 minutes; and lastly (iii) the absorbance at 562 nm was measured using VersaMax microplate reader (Molecular Devices, USA). The average 562 nm absorbance values were subtracted from average blank values, and protein concentration was determined based on the BSA standard curve.

5.3 Results

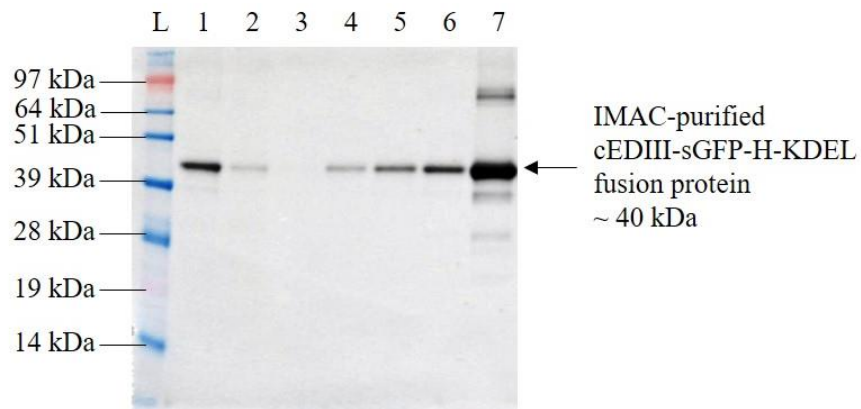
5.3.1 Step-by-step isolation of cEDIII protein

Following the large-scale extraction on 6th dpi, IMAC purification_1 (**Figure 5.1**) was used to harvest the recombinant cEDIII fused with sGFP (expressed by pEAQ-*HT::PR1a-cEDIII-sGFP-H-KDEL* vector) from clarified plant lysate (**Figure 5.3**). As shown in Panels A and B, the washing steps with low concentrations of imidazole had removed some of the weakly bound proteins and non-specific binding of endogenous proteins. The eluted fraction harbouring the desired products at ~ 40 kDa was collected and is referred as IMAC-purified cEDIII-sGFP-H-KDEL fusion protein thereafter.

Panel A: Coomassie blue-stained gel



Panel B: Western blot probed with Tetra-His monoclonal antibody



Lane	Sample	Estimated protein size
L	SeeBlue Plus2 Pre-Stained Standard	
1	Clarified plant lysate	cEDIII-sGFP-H-KDEL: ~ 40 kDa
2	Flow-through fraction	
3-6	Washing steps with 0 mM, 5 mM, 10 mM and 20 mM imidazole	
7	Eluted fraction	

Figure 5.3: IMAC purification_1 profiles of recombinant cEDIII fused with sGFP.

Panel A: SDS-PAGE profiles of coomassie blue-stained IMAC fractions;
 Panel B: Western blot profiles of sample fractions detected with Tetra-His monoclonal antibody. The cEDIII-sGFP-H-KDEL fusion protein was harvested from the eluted fraction.

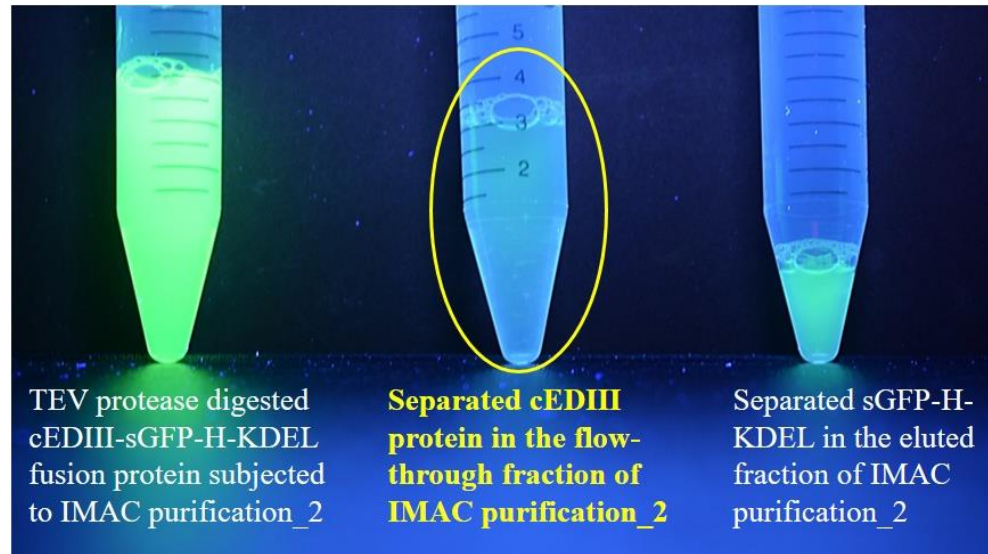
IMAC-purified cEDIII-sGFP fusion protein was then subjected to TEV protease cleavage in order to isolate cEDIII protein. SWISS modelling was used to check the accessibility of the cleavage site as depicted in **Appendix A5.2**. Following cleavage, the cEDIII protein that was detached from its sGFP partner and 6X His tag, was harvested from the flow-through fraction of IMAC purification_2, by which the results are depicted in **Figure 5.4**. With ultraviolet (UV) illumination, green fluorescence was not seen in the flow-through fraction that harboured purified cEDIII only (Panels A and B). In contrast, fluorescence was detected from the eluted fraction containing the sGFP protein. Both coomassie blue-stained gel (Panel C) and Western blot profiles (Panel D) confirmed the presence of cEDIII protein with Mr of ~11 kDa. The TEV protease that could bind to Ni²⁺-charged resin column would remain in the eluted fraction as well. Future study may consider the use of antibody against sGFP to differentiate the sGFP-H-KDEL fragment and TEV protease in eluted fraction since both have similar band size of ~ 28 kDa.

Panel A: Schematic illustration of TEV protease reaction

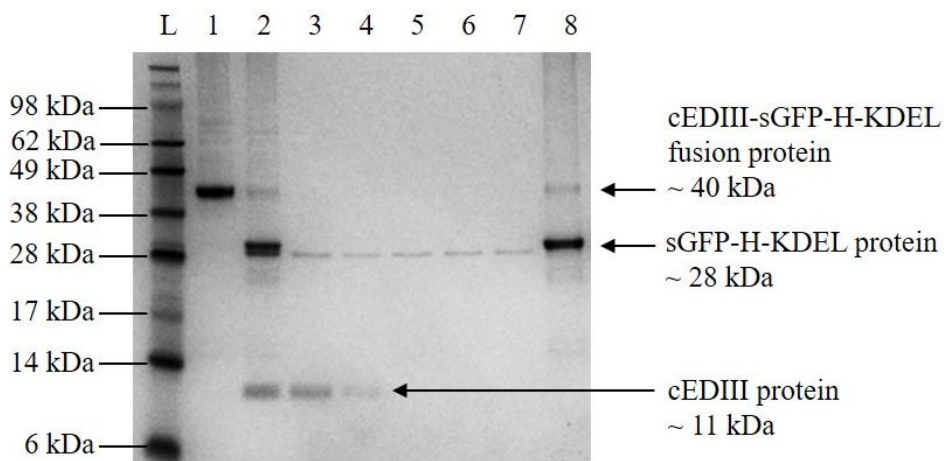
TEV protease cleavage site



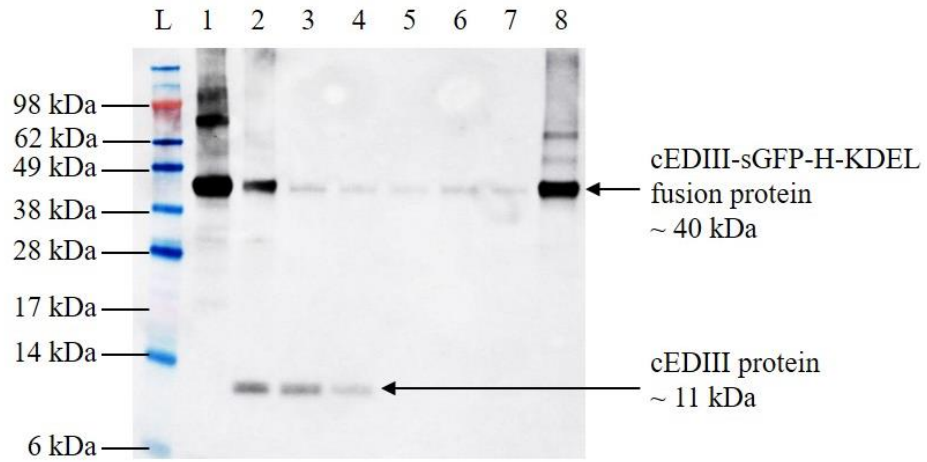
Panel B: Ultraviolet (UV) detection of green fluorescence



Panel C: Coomassie-blue stained gel



Panel D: Western blot probed with DENV 1-4 monoclonal antibody



Lane	Sample	Estimated protein size	Panel C	Panel D
L	SeeBlue Plus2 Pre-Stained Standard			
1	IMAC-purified cEDIII-sGFP-H-KDEL protein	cEDIII-sGFP-H-KDEL: ~ 40 kDa	+	+
2	TEV protease-digested cEDIII-sGFP-H-KDEL protein	cEDIII: ~ 11 kDa	+	+
		sGFP-H-KDEL: ~ 28 kDa	+	-
		cEDIII-sGFP-H-KDEL: ~ 40 kDa	+	+
		TEV protease: ~ 28 kDa	+	-
3	Flow through fraction	cEDIII: ~ 11 kDa	+	+
		sGFP-H-KDEL: ~ 28 kDa	-	-
		cEDIII-sGFP-H-KDEL: ~ 40 kDa	-	+
4	Washing steps with 0 mM imidazole	cEDIII: ~ 11 kDa	+	+
		sGFP-H-KDEL: ~ 28 kDa	-	-
		cEDIII-sGFP-H-KDEL: ~ 40 kDa	-	+

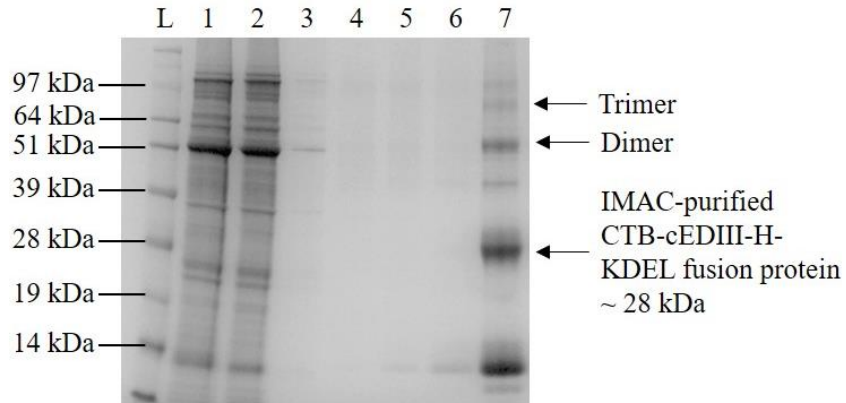
5-7	Washing steps with 5 mM, 10 mM and 20 mM imidazole	cEDIII: ~ 11 kDa	-	-
		sGFP-H-KDEL: ~ 28 kDa	-	-
		cEDIII-sGFP-H-KDEL: ~ 40 kDa	-	+
8	Eluted fraction	cEDIII: ~ 11 kDa	-	-
		sGFP-H-KDEL: ~ 28 kDa	+	-
		cEDIII-sGFP-H-KDEL: ~ 40 kDa	+	+
		TEV protease: ~ 28 kDa	+	-

Figure 5.4: IMAC purification₂ profiles of TEV protease-digested cEDIII-sGFP-H-KDEL protein. Panel A: Schematic illustration of the digestion reaction; Panel B: Detection of green fluorescence under UV light; Panel C: Coomassie blue-stained gel profiles of IMAC fractions; Panel D: Western blot profiles of sample fractions detected with DENV 1-4 monoclonal antibody. The cEDIII protein had been successfully obtained as evident from the loss of green fluorescence (yellow circle in Panel B) and presence of ~11 kDa bands in Panels C and D.

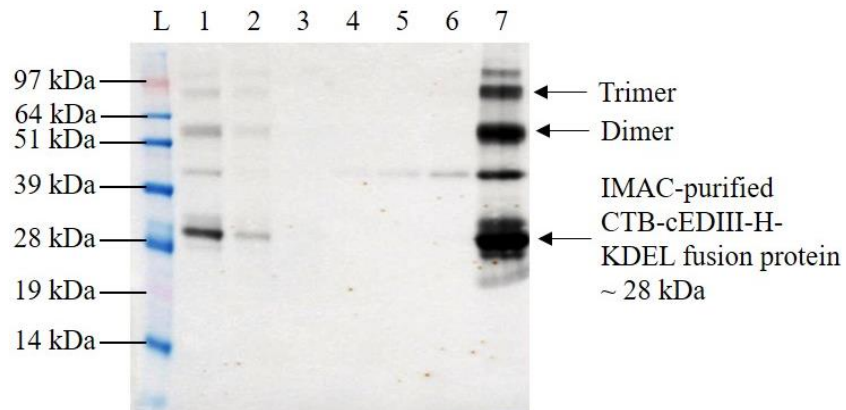
5.3.2 Purification of CTB-cEDIII fusion protein

After large-scale harvesting on 6th dpi, the IMAC purification_1 profiles of CTB-cEDIII-H-KDEL protein (expressed by pEAQ-*HT*::PR1a-CTB-cEDIII-H-KDEL vector) are shown in **Figure 5.5**. Panels A and B indicate that the protein of interest of ~ 28 kDa was successfully captured in the eluted fraction, which was designated as IMAC-purified CTB-cEDIII-H-KDEL protein thereafter. On top of that, multimerisation patterns of dimer and trimer could be seen around ~ 56 kDa and ~ 84 kDa, respectively. The bands resolved between 30 kDa – 40 kDa could be deciphered as interactions between the multimeric proteins.

Panel A: Coomassie blue-stained gel



Panel B: Western blot probed with Tetra-His monoclonal antibody



Lane	Sample	Estimated protein size
L	SeeBlue Plus2 Pre-Stained Standard	
1	Clarified plant lysate	CTB-cEDIII-H-KDEL: ~ 28 kDa
2	Flow-through fraction	
3-6	Washing steps with 0 mM, 5 mM, 10 mM and 20 mM imidazole	
7	Eluted fraction	

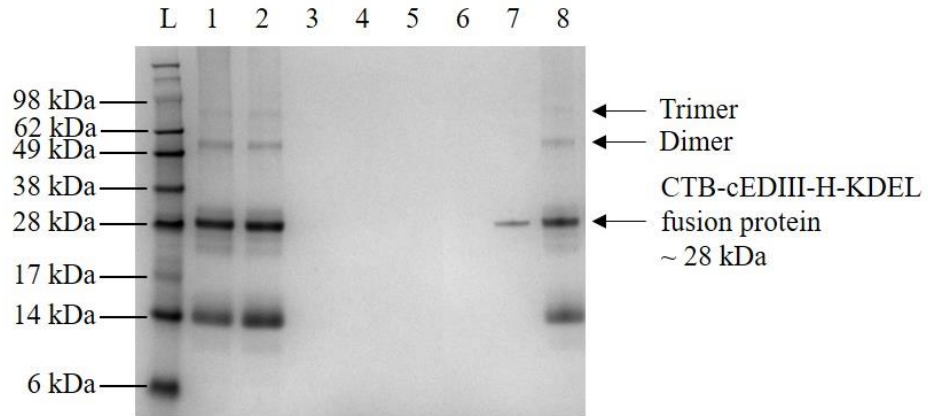
Figure 5.5: IMAC purification_1 profiles of recombinant cEDIII fused with CTB. Panel A: SDS-PAGE profiles of coomassie blue-stained IMAC fractions; Panel B: Western blot profiles of sample fractions detected with Tetra-His monoclonal antibody. The CTB-cEDIII-H-KDEL fusion protein was successfully isolated from the eluted fraction.

Likewise, TEV protease digestion was set up to remove the C-terminal 6X His tag from IMAC-purified CTB-cEDIII-H-KDEL protein (**Figure 5.6**, Panel A). SWISS modelling predicted that the TEV cleavage site was not structurally buried (**Appendix A5.2**). However, the IMAC purification_2 profiles of digested-CTB-cEDIII-H-KDEL indicate that protease cleavage might not be successful. This is because the expected CTB-cEDIII protein could not be detected in the flow-through fraction of both Panels B and C. Thus, it was speculated that the digested protein had retained similar binding efficiency to the Ni²⁺-charged resin, and the CTB-cEDIII protein was recovered along with the CTB-cEDIII-H-KDEL protein during elution step. Meanwhile, the digested fragment of H-KDEL may have run off the gel due to the small molecular size.

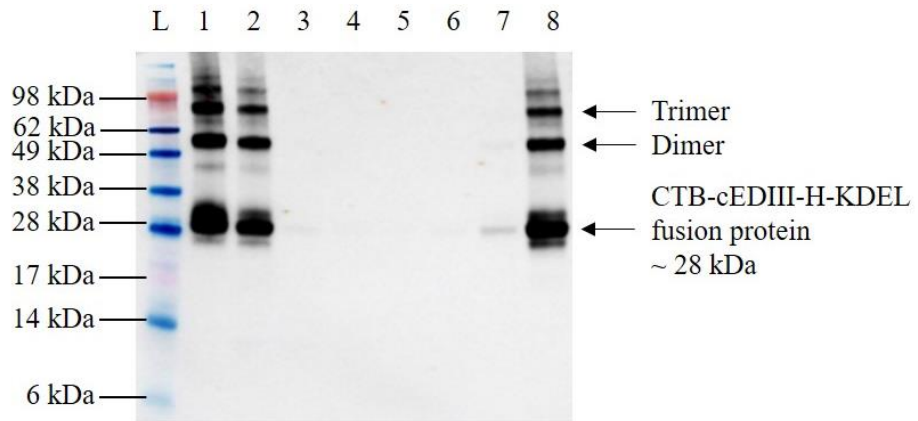
Panel A: Schematic illustration of TEV protease reaction



Panel B: Coomassie blue-stained gel



Panel C: Western blot probed with DENV 1-4 monoclonal antibody



Lane	Sample	Estimated protein size	Panel C	Panel D
L	SeeBlue Plus2 Pre-Stained Standard			
1	IMAC-purified CTB-cEDIII-H-KDEL protein	CTB-cEDIII-H-KDEL: ~ 28 kDa	+	+

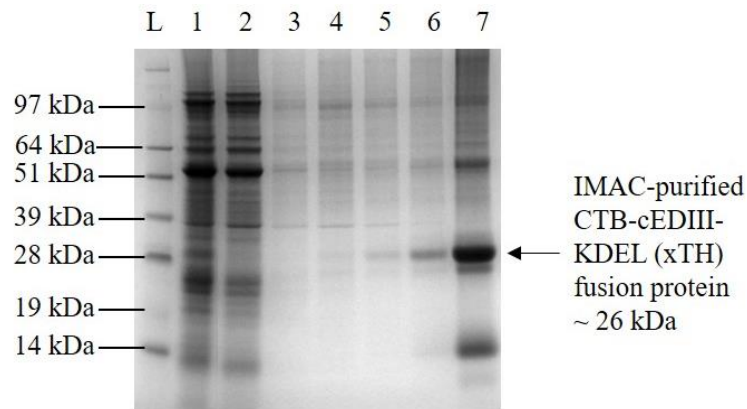
2	TEV protease-digested CTB-cEDIII-H-KDEL protein	CTB-cEDIII: ~ 27 kDa	+	+
		H-KDEL: ~ 1 kDa	-	-
		CTB-cEDIII-H-KDEL: ~ 28 kDa	+	+
		TEV protease: ~ 28 kDa	+	-
3	Flow through fraction	CTB-cEDIII: ~ 27 kDa	-	-
		H-KDEL: ~ 1 kDa	-	-
		CTB-cEDIII-H-KDEL: ~ 28 kDa	-	-
4-6	Washing steps with 0 mM, 5 mM and 10 mM imidazole	CTB-cEDIII: ~ 27 kDa	-	-
		H-KDEL: ~ 1 kDa	-	-
		CTB-cEDIII-H-KDEL: ~ 28 kDa	-	-
7	Washing steps with 20 mM imidazole	CTB-cEDIII: ~ 27 kDa	+	+
		H-KDEL: ~ 1 kDa	-	-
		CTB-cEDIII-H-KDEL: ~ 28 kDa	+	+
8	Eluted fraction	CTB-cEDIII: ~ 27 kDa	+	+
		H-KDEL: ~ 1 kDa	-	-
		CTB-cEDIII-H-KDEL: ~ 28 kDa	+	+
		TEV protease: ~ 28 kDa	+	-

Figure 5.6: IMAC purification₂ profiles of TEV protease-digested CTB-cEDIII-H-KDEL protein. Panel A: Schematic illustration of the digestion reaction; Panel B: Coomassie blue-stained gel profiles of IMAC fractions; Panel

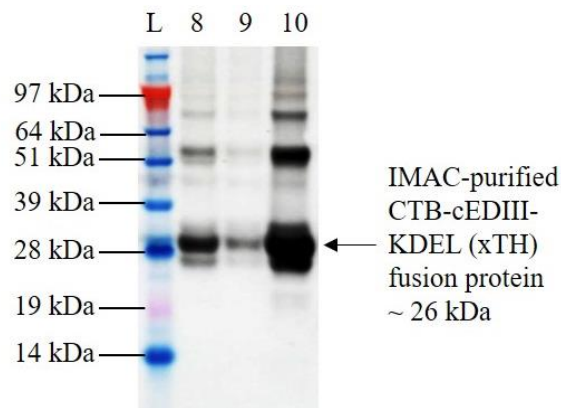
C: Western blot profiles of sample fractions detected with DENV 1-4 monoclonal antibody. The CTB-cEDIII protein could still bind to Ni²⁺-charged resin despite after TEV cleavage, and hence was detected in the eluted fraction of Panels B and C.

Following that, an alternative purification approach was attempted using the expression vector pEAQ-*HT*::PR1a-CTB-cEDIII-KDEL (xTH). The expressed protein, named as CTB-cEDIII-KDEL (xTH), represents a variant of CTB-cEDIII-H-KDEL protein but without the TEV protease cleavage site and 6X His tag. Based on **Figure 5.7**, the IMAC purification_1 results indicate that omitting the 6X His tag in cassette design did not alter the binding of CTB-cEDIII-KDEL (xTH) protein to Ni²⁺-charged resin. Hence, the desired protein could be harvested from the eluted fraction as verified by SDS-PAGE (Panel A) and Western blotting (Panel B). It was postulated that the increase of protein size of Mr ~ 2 kDa may be attributed to protein glycosylation.

Panel A: Coomassie blue-stained gel



Panel B: Western blot probed with DENV 1-4 monoclonal antibody



Lane	Sample	Estimated protein size
L	SeeBlue Plus2 Pre-Stained Standard	
1, 8	Clarified plant lysate	CTB-cEDIII-KDEL (xTH): ~ 26 kDa
2, 9	Flow-through fraction	
3-6	Washing steps with 0 mM, 5 mM, 10 mM and 20 mM imidazole	
7, 10	Eluted fraction	

Figure 5.7: IMAC purification_1 profiles of the variant CTB-cEDIII-KDEL (xTH) protein. Panel A: SDS-PAGE profiles of coomassie blue-stained IMAC fractions; Panel B: Western blot profiles of sample fractions detected with Tetra-His monoclonal antibody. The CTB-cEDIII-KDEL (xTH) fusion protein was successfully harvested from the eluted fraction.

With the successful isolation of CTB-cEDIII-KDEL (xTH) fusion protein that does not have the 6X His tag, this protein was used for characterisation study in order to determine its functional binding to GM1 gangliosides. Based on the GM1-ELISA analysis (**Figure 5.8**), it was revealed that the purified CTB-cEDIII-KDEL (xTH) protein interacted with the coated GM1. This result was consolidated by negative controls, whereby the cEDIII and mHBcAg-cEDIII did not demonstrate binding to GM1 gangliosides. Furthermore, none of these protein samples gave signals when BSA was used as the coating agent.

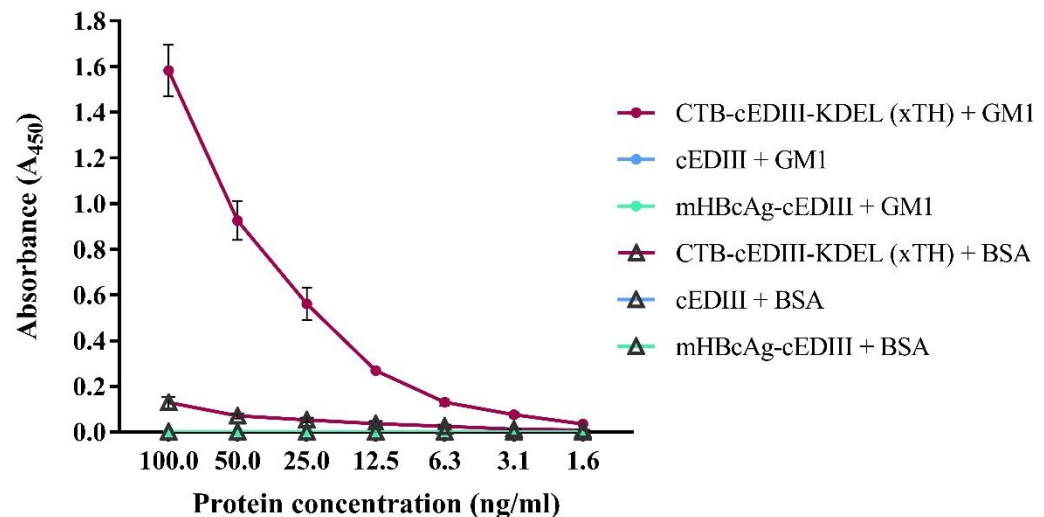
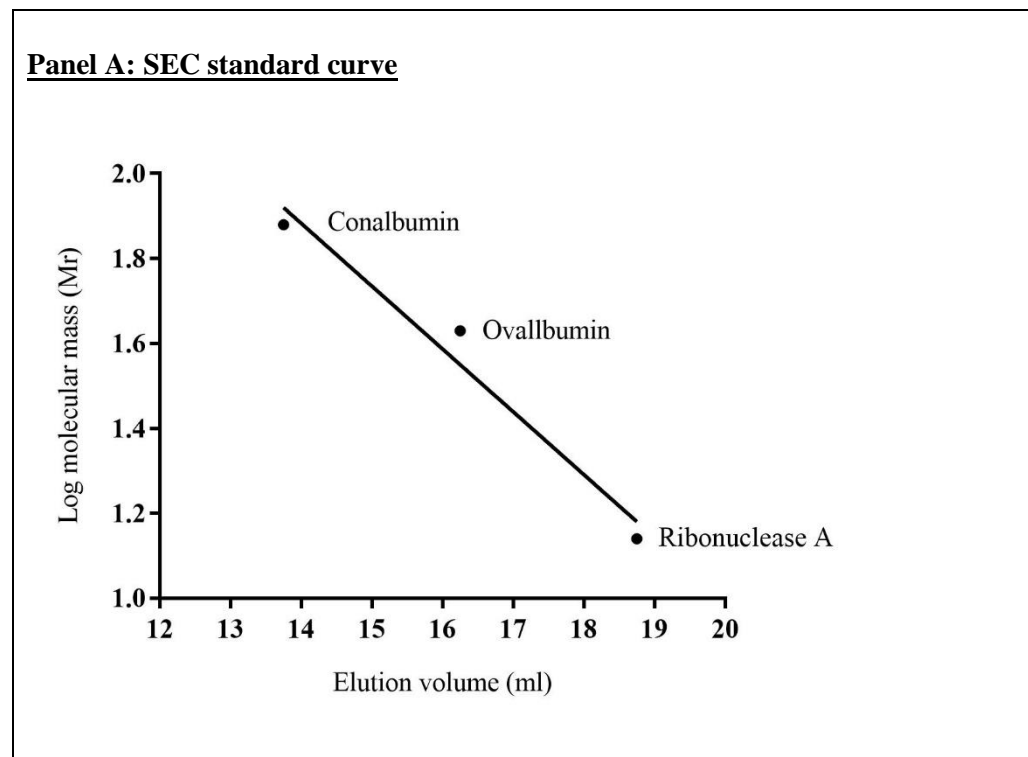
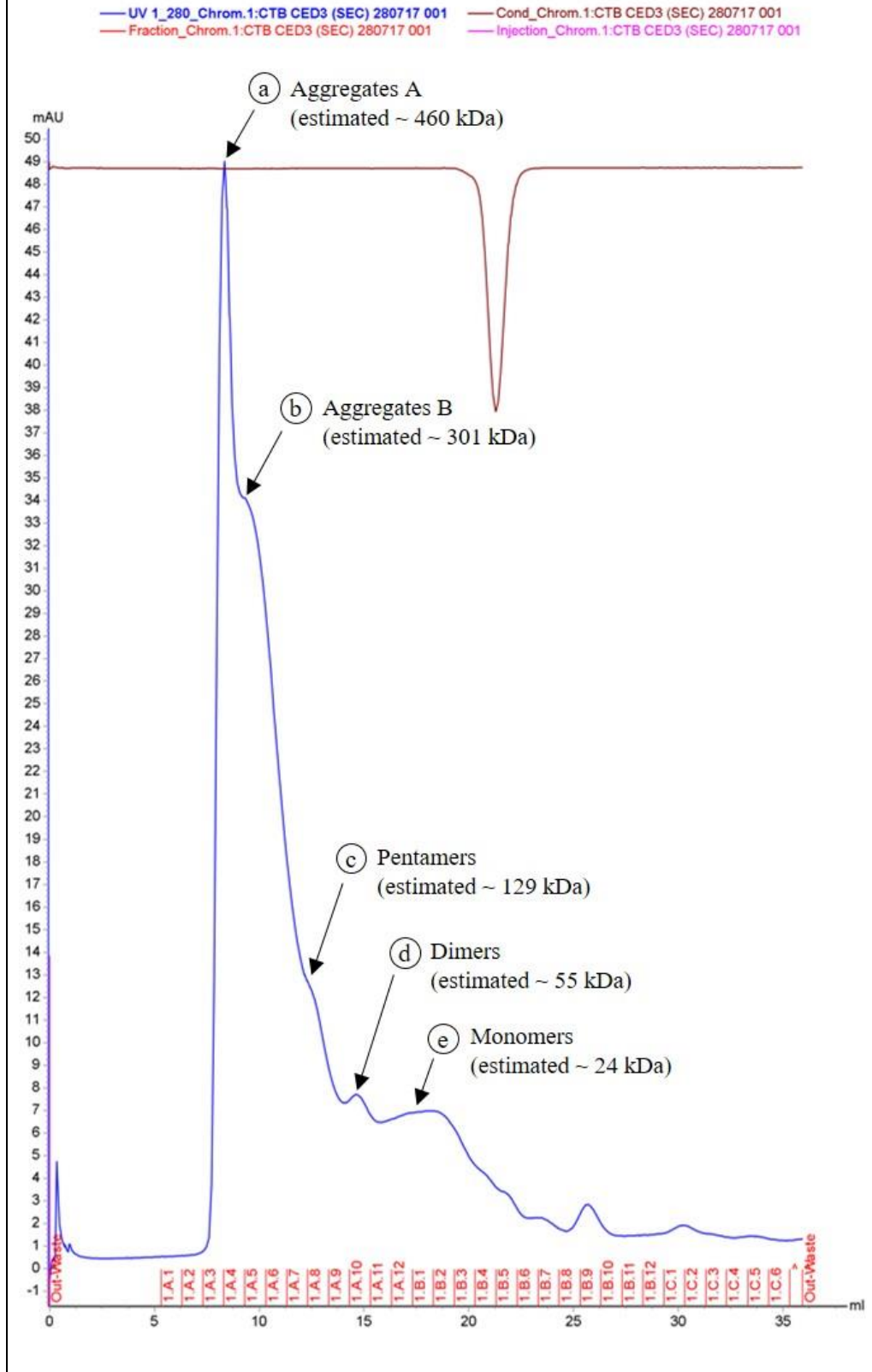


Figure 5.8: Evaluation of the binding affinities between pentameric CTB and GM1 gangliosides (+ GM1) via ELISA. Alternative plate was coated with BSA (+ BSA) to serve as negative control. The proteins used for testing were serially-diluted in two-fold starting from 100 ng/ml. The data are expressed as mean \pm SD of the A_{450} readings of three independent experiments. Overall, CTB-cEDIII-KDEL (xTH) fusion protein showed high binding affinity to GM1 ganglioside, but not the cEDIII and mHBcAg-cEDIII proteins.

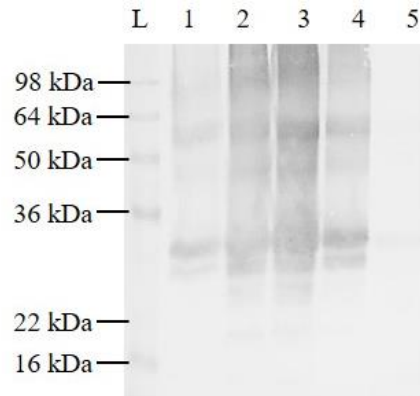
Besides, SEC was also conducted to examine the pentameric folding of CTB-cEDIII-KDEL (xTH) protein. Protein standards that were separated under the same conditions (**Appendix A5.3**) were used to determine the molecular mass (Mr) of peaks resolved from CTB-cEDIII-KDEL (xTH) sample. Based on the analysed SEC chromatogram (**Figure 5.8**, Panel A), several peaks which probably represent the pentamers (fractions A8 and A9), dimers (fractions A10 and A11) and monomers (fractions A12 to B3) had been annotated. These fractions containing the monomers, dimers and pentamers were individually pooled and analysed via Western blotting; and as expected, the predicted monomer in Lane 5 detected only a single band at ~ 26 kDa. On top of that, aggregates of CTB-cEDIII-KDEL (xTH) were identified in fractions A4 to A7, with the Mr estimated at ~ 301 kDa and ~ 460 kDa. Nonetheless, multiple bands of oligomers were seen from the Western blot profiles due to partial denaturation of protein samples. To prevent this, future improvement may omit the use of reducing agent for better differentiation of proteins that migrate on the basis of Mr.



Panel B: SEC chromatogram of CTB-cEDIIL-KDEL (xTH) protein



Panel C: Western blot probed with cholera toxin (CT) polyclonal antibody



Lane	Sample	Estimated band size
L	SeeBlue Plus2 Pre-Stained Standard	
1	Purified CTB-cEDIII-KDEL (xTH) protein	Monomer: ~ 26 kDa Dimer: ~ 52 kDa Pentamer: ~ 130 kDa Aggregates: > 130 kDa
2	Pooled fractions A4 – A7 (Ⓐ and Ⓑ)	
3	Pooled fractions A8 – A9 (Ⓒ)	
4	Pooled fractions A10 – A11 (Ⓓ)	
5	Pooled fractions A12 – B3 (Ⓔ)	

Figure 5.9: SEC profiling of CTB-cEDIII-KDEL (xTH) fusion protein. Panel A: The standard curve used to define Mr; Panel B: SEC chromatogram results; Panel C: Western blot profiles of the different pooled fractions, as detected with CT polyclonal antibody. SEC yielded several fractions that might correspond to different oligomeric states of this CTB fusion protein.

5.3.3 Purification of monomeric core virus-like particles (VLPs) displaying cEDIII

N. benthamiana leaves infiltrated with the recombinant vector pEAQ-*HT::mHBcAg-cEDIII* were harvested on 4th dpi, clarified and partially-purified via sucrose cushion. The profiles of fractionated samples are shown in **Figure 5.10**, in which the 70% sucrose fraction appeared to be ‘cleaner’ than the interface fraction (Panel A). The presence of mHBcAg-cEDIII VLPs in both 70% sucrose and interface fractions were confirmed via Western blotting (Panel B). These VLPs-containing fractions were pooled and subjected to sucrose gradient for further purification.

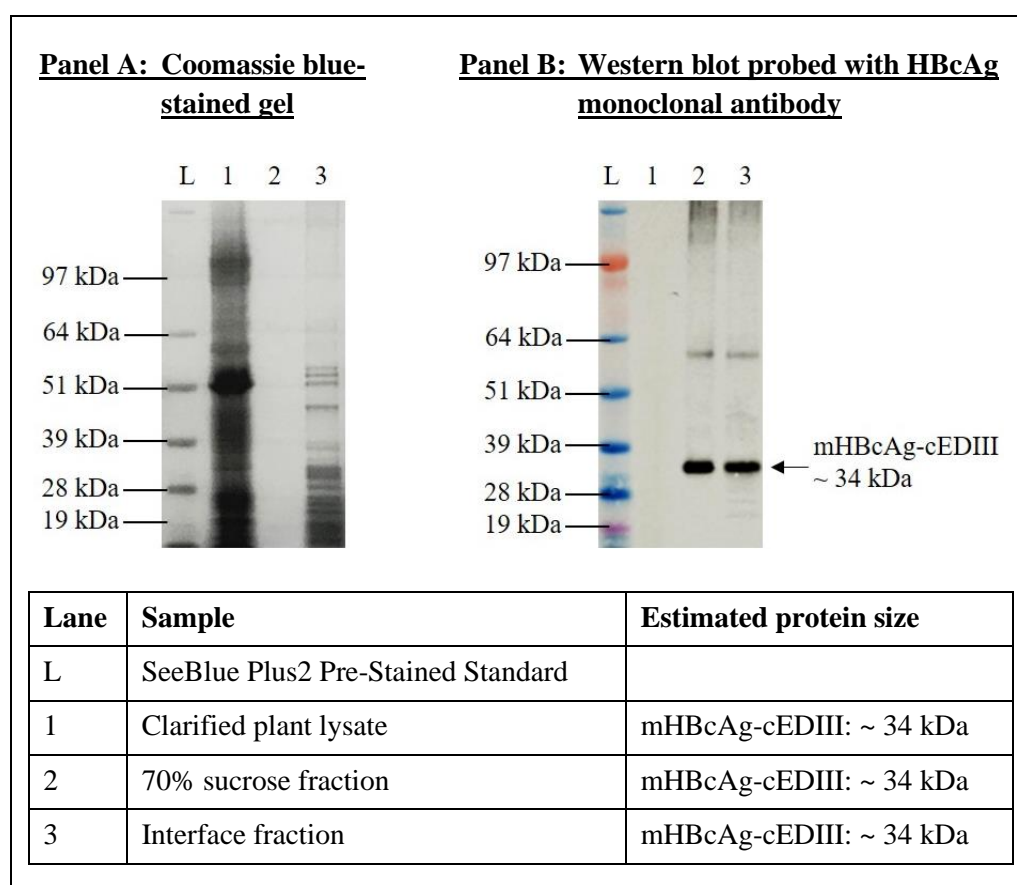
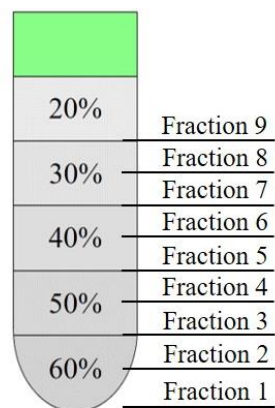


Figure 5.10: Sucrose cushion purification and detection of mHBcAg-cEDIII VLPs.

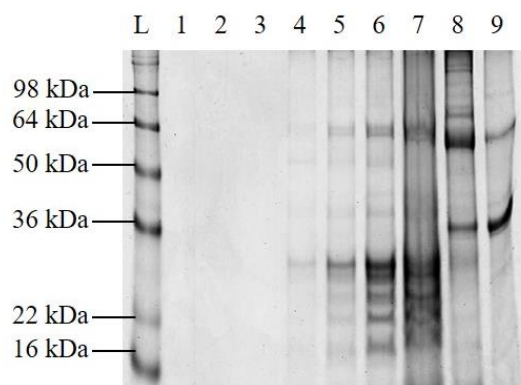
Panel A: SDS-PAGE analysis of fractionated samples; Panel B: Western blot profiles showing that the VLPs were successfully detected in the 70% sucrose and interface fractions using HBcAg monoclonal antibody.

Following sucrose gradient ultracentrifugation, the mHBcAg-cEDIII VLPs sample was fractionated (**Figure 5.11**, Panel A) before examination via SDS-PAGE (Panel B) and Western blotting (Panel C) techniques. The coomassie blue-stained gel revealed that a significant amount of plant endogenous proteins was present in fractions 4 – 9. The desired VLPs, however were detected in fractions 4 – 6, corresponding to sedimentation between 40% – 50% concentration of sucrose. With that, the mHBcAg-cEDIII VLPs in fraction 4 were harvested and subjected to protein dialysis. Similar procedure was employed to purify the monomeric core without gene insert (mEL) as control.

Panel A: Sample fractionation



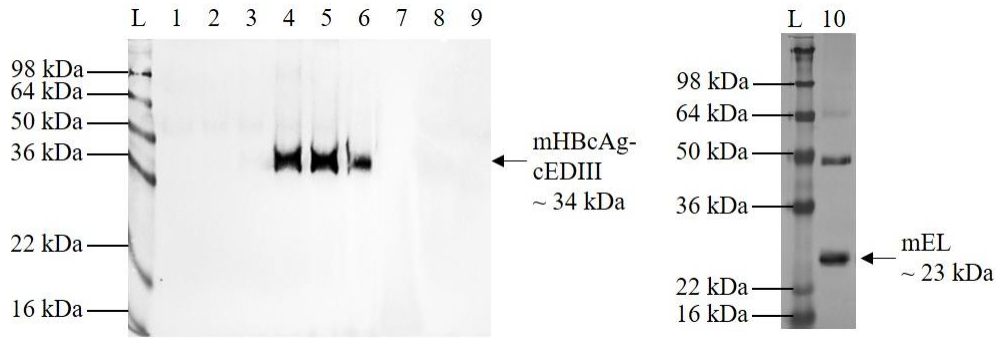
Panel B: Coomassie-blue stained gel



Panel C: Western blotting

(i) DENV 1-4 monoclonal antibody used to detect mHBcAg-cEDIII VLPs

(ii) HBcAg monoclonal antibody used to detect mEL VLPs



Lane	Sample	Estimated protein size
L	SeeBlue Plus2 Pre-Stained Standard	
1-2	Fractions 1-2	mHBcAg-cEDIII: ~ 34 kDa
3-4	Fractions 3-4	mHBcAg-cEDIII: ~ 34 kDa
5-6	Fractions 5-6	mHBcAg-cEDIII: ~ 34 kDa
7-8	Fractions 7-8	mHBcAg-cEDIII: ~ 34 kDa
9	Fraction 9	mHBcAg-cEDIII: ~ 34 kDa
10	Purified mEL VLPs control	mEL: ~23 kDa

Figure 5.11: Sucrose gradient purification and detection of mHBcAg-cEDIII VLPs.

Panel A: A schematic illustration of the fractionation of VLPs sample after ultracentrifugation; Panel B: SDS-PAGE profiles of the recovered fractions; Panel C: Western blot profiles of fractionated mHBcAg-cEDIII VLPs as detected using DENV 1-4 monoclonal antibody. Fraction 4 was harvested and used for downstream application.

Purification of mHBcAg-cEDIII (L) VLPs expressed by recombinant vector pEAQ-*HT::mHBcAg-cEDIII (L)* was conducted on 4th dpi following large extraction and clarification. The separation on a sucrose cushion yielded several fractions as shown in **Figure 5.12**. Similarly, the 70% sucrose fraction resolved a cleaner fraction on SDS-PAGE gel (Panel A) with lesser background proteins as compared to the interface fraction. Western blotting (Panel B) confirmed the presence of mHBcAg-cEDIII (L) VLPs in 70% and interface fractions, which were harvested for further purification step by using sucrose gradient.

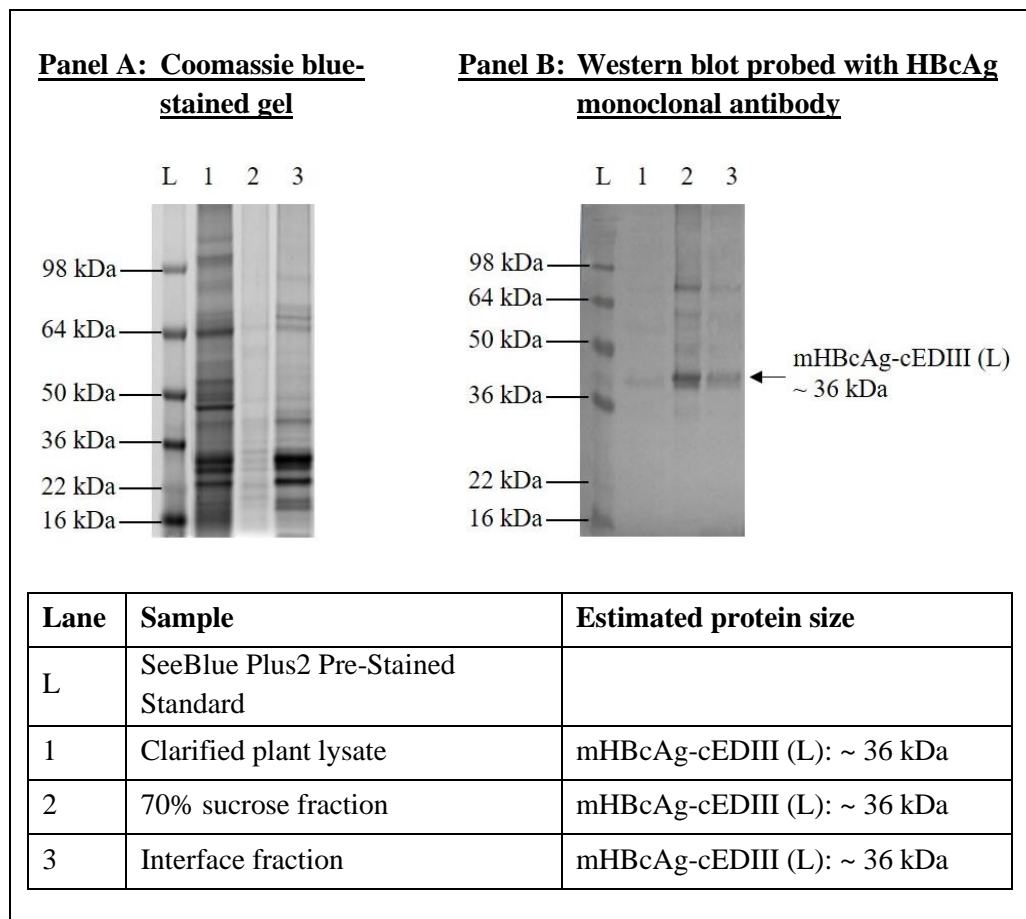
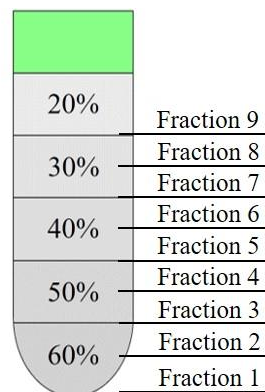


Figure 5.12: Sucrose cushion purification and detection of mHBcAg-cEDIII (L) VLPs.

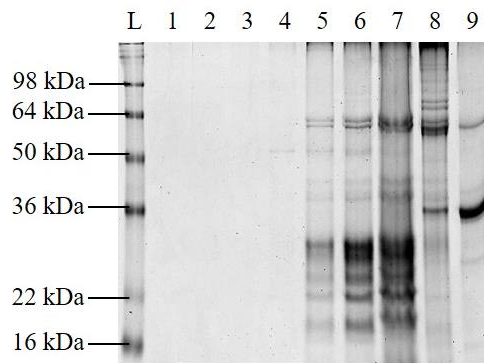
Panel A: SDS-PAGE profiles of fractionated samples; Panel B: Western blot profiles showing that the VLPs were successfully detected in the 70% sucrose and interface fractions using HBcAg monoclonal antibody.

Sucrose gradient analysis of partially-purified mHBcAg-cEDIII (L) is presented in **Figure 5.13**. After ultracentrifugation, the sample was fractionated from bottom of the tube (Panel A). The SDS-PAGE profiles (Panel B) indicate that increasing amount of background proteins could be detected from fraction 5 onwards, and the presence of mHBcAg-cEDIII (L) VLPs could not be clearly differentiated. Only upon Western blotting (Panel C), the presence of mHBcAg-cEDIII (L) VLPs was found in fractions 4 – 6 which implies their sedimentations around 40% – 50% of sucrose concentrations. Following that, fraction 4 was collected for protein dialysis before downstream testing. The mEL VLPs were purified in similar manner as assay control.

Panel A: Sample fractionation



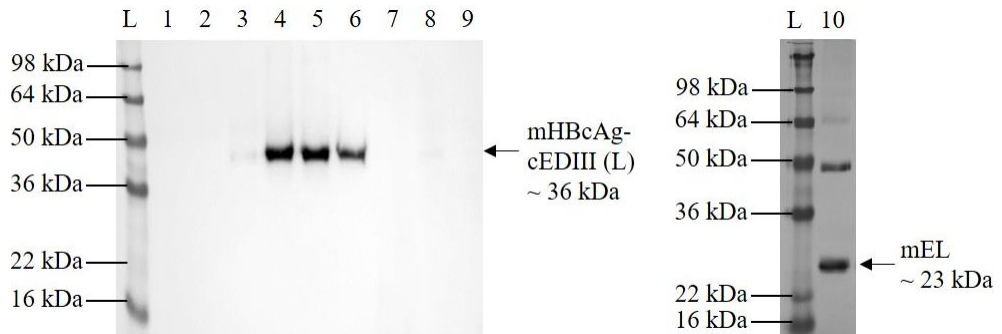
Panel B: Coomassie-blue stained gel



Panel C: Western blotting

(i) DENV 1-4 monoclonal antibody used to detect mHBcAg-cEDIII (L) VLPs

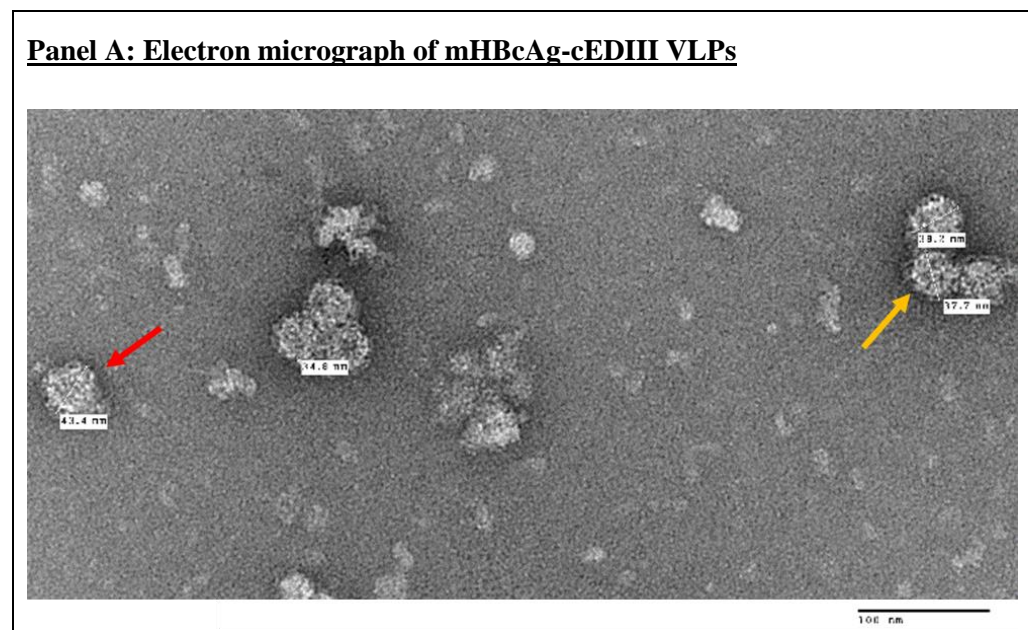
(ii) HBcAg monoclonal antibody used to detect mEL VLPs



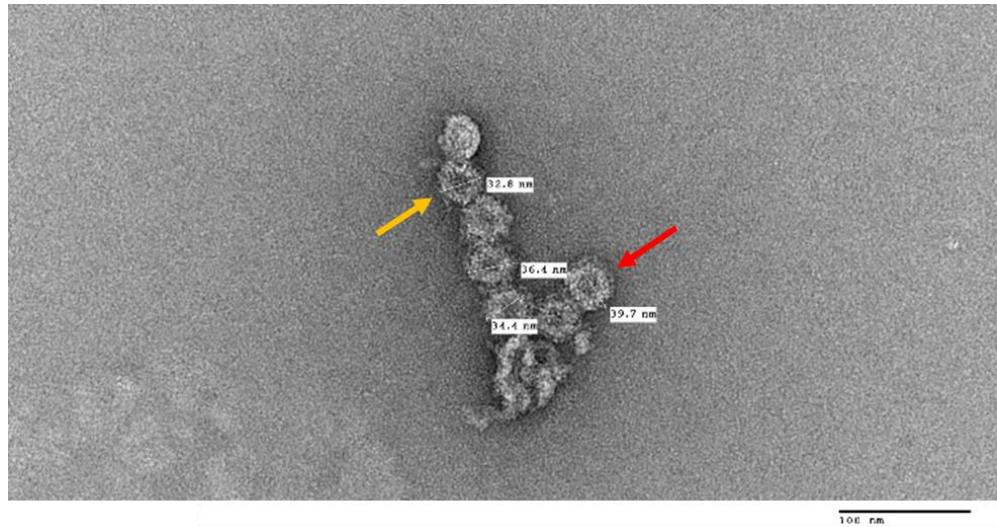
Lane	Sample	Estimated protein size
L	SeeBlue Plus2 Pre-Stained Standard	
1-2	Fractions 1-2	mHBcAg-cEDIII (L): ~ 36 kDa
3-4	Fractions 3-4	mHBcAg-cEDIII (L): ~ 36 kDa
5-6	Fractions 5-6	mHBcAg-cEDIII (L): ~ 36 kDa
7-8	Fractions 7-8	mHBcAg-cEDIII (L): ~ 36 kDa
9	Fraction 9	mHBcAg-cEDIII (L): ~ 36 kDa
10	Purified mEL VLPs control	mEL: ~ 23 kDa

Figure 5.13: Sucrose gradient purification and detection of mHBcAg-cEDIII (L) VLPs. Panel A: A schematic illustration of the fractionation of VLPs sample after ultracentrifugation; Panel B: SDS-PAGE profiles of the recovered fractions; Panel C: Western blot profiles of fractionated mHBcAg-cEDIII (L) VLPs sample as detected using DENV 1-4 monoclonal antibody. Fraction 4 was harvested and used for downstream application.

In order to conclusively characterise the assembly of purified VLPs, TEM was used to check the particles conformation. As illustrated in **Figure 5.14**, both mHBcAg-cEDIII VLPs (Panel A) and mHBcAg-cEDIII (L) VLPs (Panel B) did assemble into particles with the characteristics spikes on surface. A majority of these VLPs appeared with large symmetry, though the smaller symmetry could be spotted as well. The mean particle size for mHBcAg-cEDIII VLPs measured is approximately 38 nm whereas mHBcAg-cEDIII (L) VLPs have a mean diameter of 36 nm. These measurements with TEM are used as rough approximations. Besides, aggregation of particles was noted and this could affect the precision in measurement. As compared to the uniformly-shaped mEL VLPs (Panel C), the chimeric mHBcAg VLPs with cEDIII epitopes seemed to exhibit an uneven surface layer which is hereafter termed as ‘knobbly’ appearance. Meanwhile, the spiky appearance was more prominent in mEL VLPs. Insertion of cEDIII has contributed to an increase of 9 – 11 nm in particle’s size.



Panel B: Electron micrograph of mHBcAg-cEDIII (L) VLPs



Panel C: Electron micrographs of mEL VLPs

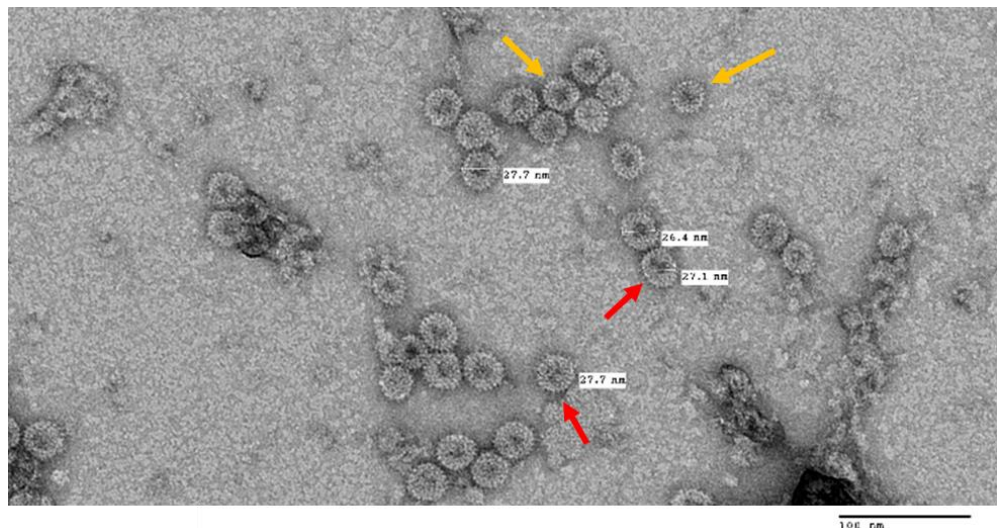
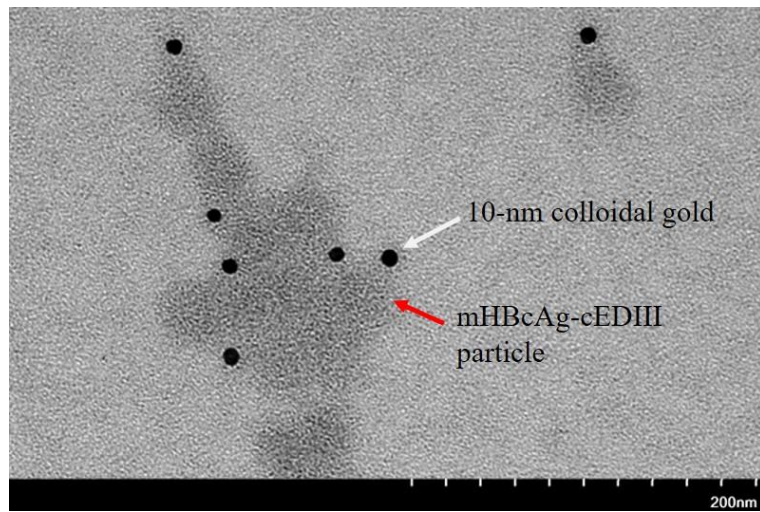


Figure 5.14: Electron micrographs showing the purified monomeric core VLPs. The VLPs were negatively stained with 2% (v/v) uranyl acetate and visualised at 50,000X magnification. Panel A: mHBcAg-cEDIII VLPs; Panel B: mHBcAg-cEDIII (L) VLPs; Panel C: mEL VLPs control. Scale bar = 100 nm. Red arrow is used to indicate VLPs with large symmetry and orange arrow refers to those with smaller symmetry. Successful assembly of the chimeric mHBcAg VLPs with cEDIII epitopes were shown.

In addition, immunogold labelling was specifically used to locate the cEDIII antigens displayed on assembled VLPs. Based on **Figure 5.15**, both mHBcAg-cEDIII VLPs (Panel A) and mHBcAg-cEDIII (L) VLPs (Panel B) were successfully labelled with the 10-nm colloidal gold as indicated by white arrows. To a certain extent, the aggregation of particles might have hindered optimal labelling as not every particle was tagged with the gold antibody. Nonetheless, it was significant that the mHBcAg-cEDIII VLPs and mHBcAg-cEDIII (L) VLPs still preserved the expected antigenicity to react with DENV 1-4 monoclonal antibody.

Panel A: Electron micrograph of mHBcAg-cEDIII VLPs



Panel B: Electron micrograph of mHBcAg-cEDIII (L) VLPs

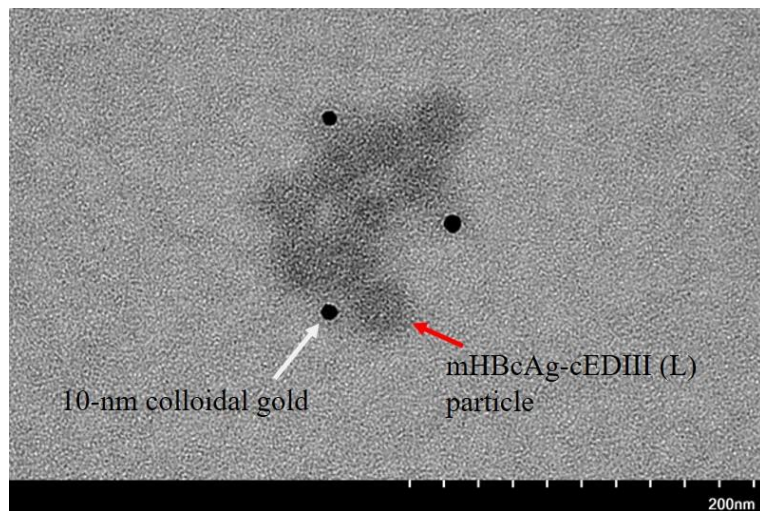


Figure 5.15: Electron micrographs showing the chimeric mHBcAg VLPs reacted with immunogold of DENV 1-4 monoclonal antibody. Purified VLPs were subjected to immunogold labelling and imaged at 100,000X magnification. Scale bar = 200 nm. Panel A: mHBcAg-cEDIII VLPs; Panel B: mHBcAg-cEDIII (L) VLPs.

5.3.4 Purification of tandem core virus-like particles (VLPs) displaying cEDIII

Leaves infiltrated with the recombinant vector pEAQ-*HT*::tHBcAg-cEDIII were harvested on 8th dpi for large-scale purification. The first-step isolation of tHBcAg-cEDIII VLPs from plant contaminants was achieved by sucrose cushion (**Figure 5.16**). As seen from the SDS-PAGE profiles (Panel A), the 70% sucrose fraction gave a cleaner separation as compared to the interface fraction. However, the signal strength of this 70% sucrose fraction appeared to be very weak on the immunoblot membrane (Panel B). The tHBcAg-cEDIII VLPs were mostly detected in the interface fraction, around the expected size of ~ 55 kDa. Nonetheless, the 70% sucrose and interface fractions were collected to include all the VLPs present in the sample and further purified by nycodenz gradient.

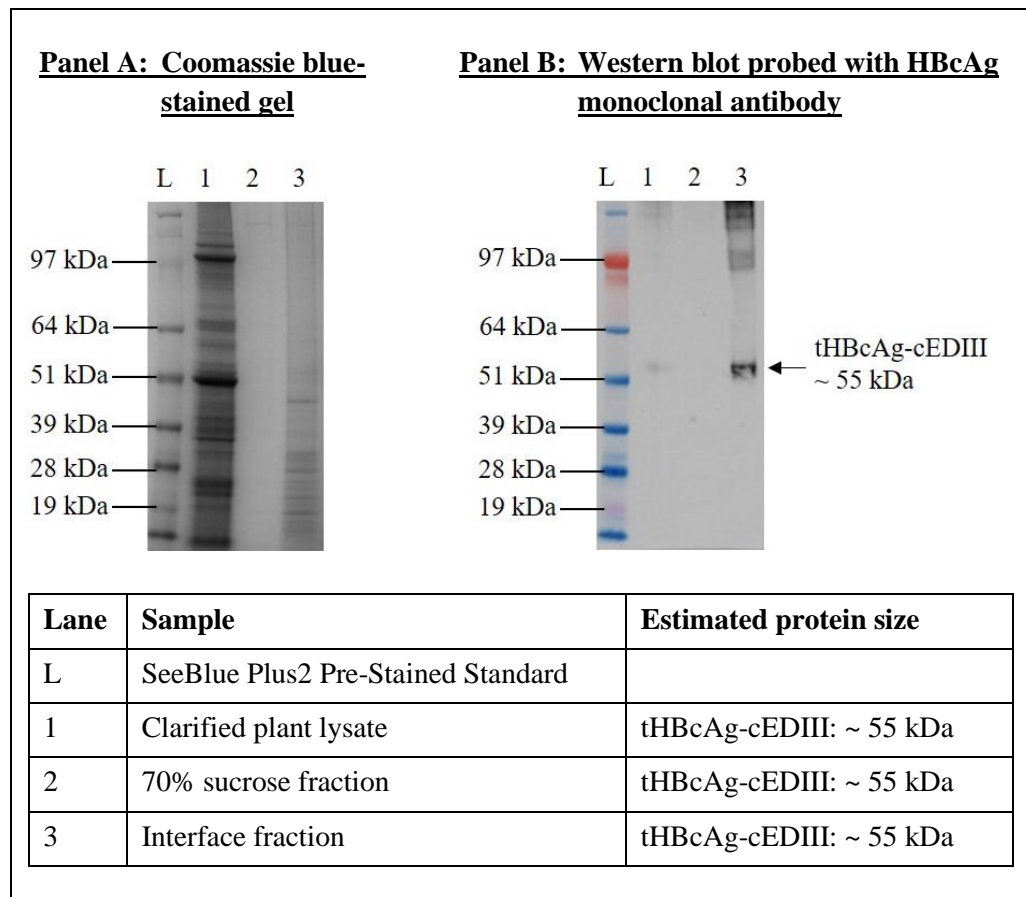


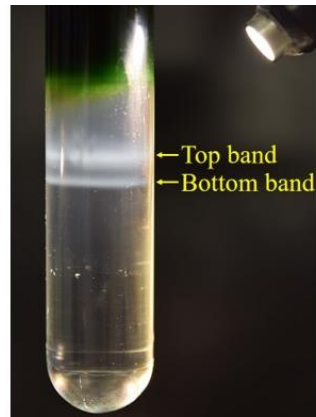
Figure 5.16: Sucrose cushion purification and detection of tHBcAg-cEDIII VLPs.

Panel A: SDS-PAGE profiles of fractionated samples; Panel B: Western blot profiles showing that the VLPs were successfully detected in the 70% sucrose and interface fractions using HBcAg monoclonal antibody.

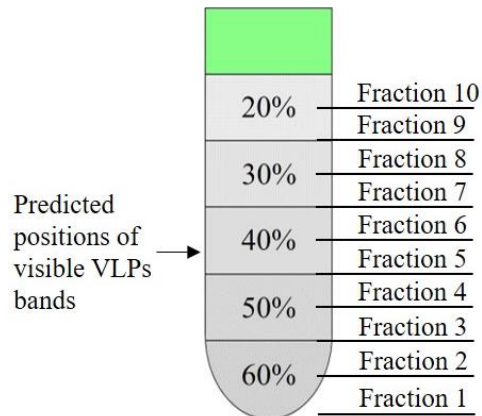
With the use of nycodenz gradient, the presence of VLPs can be visualised due to their light-scattering properties (**Figure 5.17**). As revealed in Panel A, two greyish bands were observed upon illumination, with the sedimentation of green contaminants towards the top of the gradient. These grey bands were collected from the side of tube, followed by fractionation of the remaining gradient from the bottom of the tube (Panel B). The collected fractions were then analysed with SDS-PAGE (Panel C) and Western blotting (Panel D) techniques. Following immunoblotting, those grey bands were confirmed to be tHBcAg-cEDIII VLPs, and the sedimentation point of tHBcAg-cEDIII

VLPs was estimated at 40% nycodenz concentration. Similar purification procedures were used to isolate the tandem core particles without gene insert (tEL) as control.

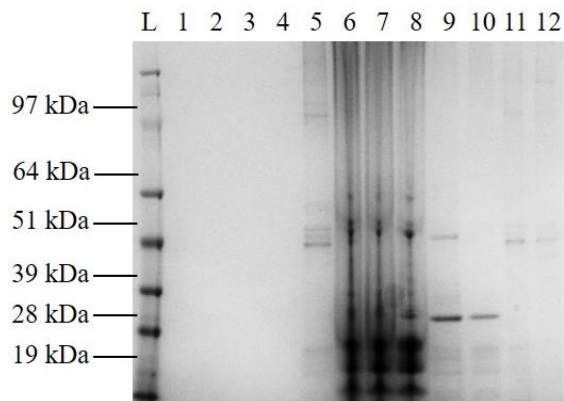
Panel A: Visible bands of VLPs



Panel B: Sample fractionation



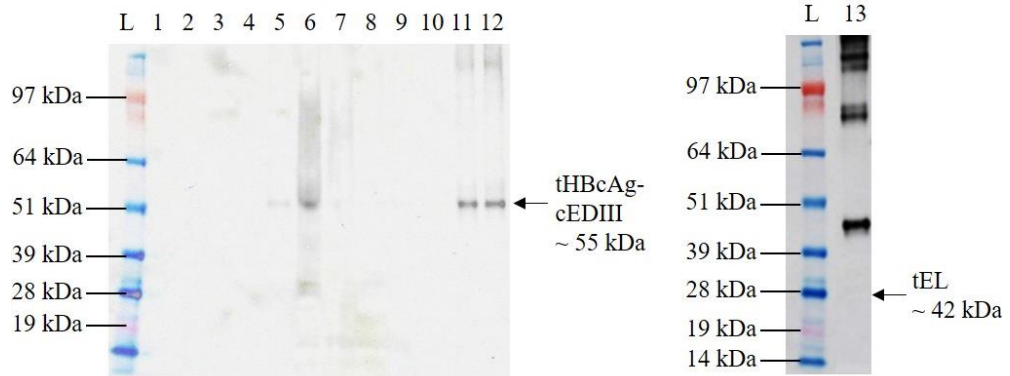
Panel C: Coomassie blue-stained gel



Panel D: Western blotting

(i) DENV 1-4 monoclonal antibody used to detect tHBcAg-cEDIII VLPs

(ii) HBcAg monoclonal antibody used to detect tEL VLPs

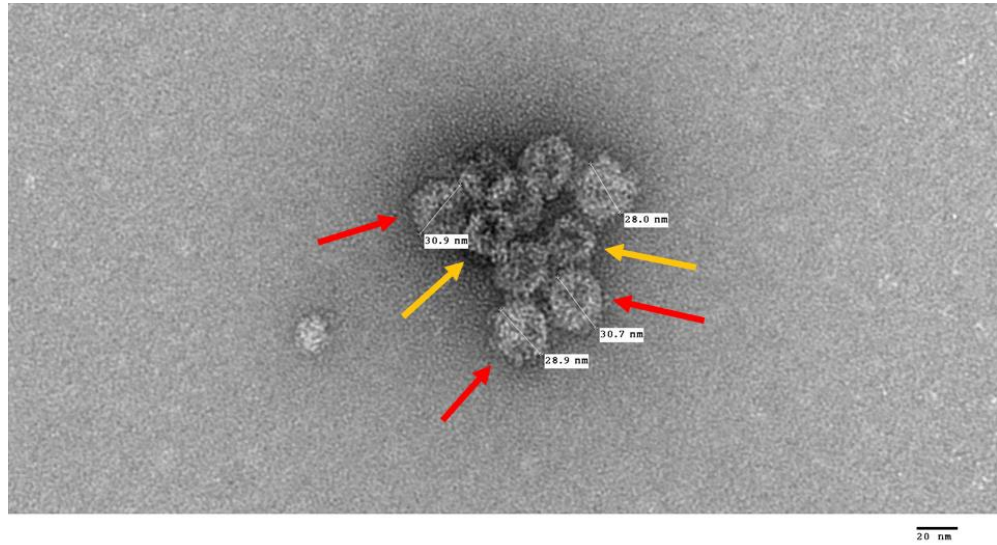


Lane	Sample	Estimated protein size
L	SeeBlue Plus2 Pre-Stained Standard	
1-2	Fractions 1-2	tHBcAg-cEDIII: ~ 55 kDa
3-4	Fractions 3-4	tHBcAg-cEDIII: ~ 55 kDa
5-6	Fractions 5-6	tHBcAg-cEDIII: ~ 55 kDa
7-8	Fractions 7-8	tHBcAg-cEDIII: ~ 55 kDa
9-10	Fraction 9-10	tHBcAg-cEDIII: ~ 55 kDa
11	Top band	tHBcAg-cEDIII: ~ 55 kDa
12	Bottom band	tHBcAg-cEDIII: ~ 55 kDa
13	Purified tEL VLPs control	tEL: ~ 42 kDa

Figure 5.17: Nycodenz gradient fractionation and detection profiles of tHBcAg-cEDIII VLPs. Panel A: Visualisation of VLPs band in nycodenz gradient; Panel B: Fractionation of VLPs sample after ultracentrifugation; Panel C: SDS-PAGE profiles of the recovered fractions; Panel D: Western blot detection of fractionated VLPs using DENV 1-4 monoclonal antibody. The tHBcAg-cEDIII VLPs could be harvested from the visible grey bands.

Following sample purification, TEM imaging revealed that plant-produced tHBcAg-cEDIII did assemble into VLPs (**Figure 5.18**, Panel A), which were visualised as a mixture of large and small aggregated particles. These particles exhibit the ‘knobbly’ morphology and constitute an average particle size of 30 nm in diameter. In contrast, the tEL appeared to be smaller and more regular in shape with prominent spikes on their surface (Panel B). Purified tEL sample constituted mostly T=4 particles, with an average size of 27 nm in diameter. The tHBcAg-cEDIII particles had an increase of 3 nm in diameter when compared to tEL control.

Panel A: Electron micrographs of tHBcAg-cEDIII VLPs



Panel B: Electron micrographs of tEL VLPs control

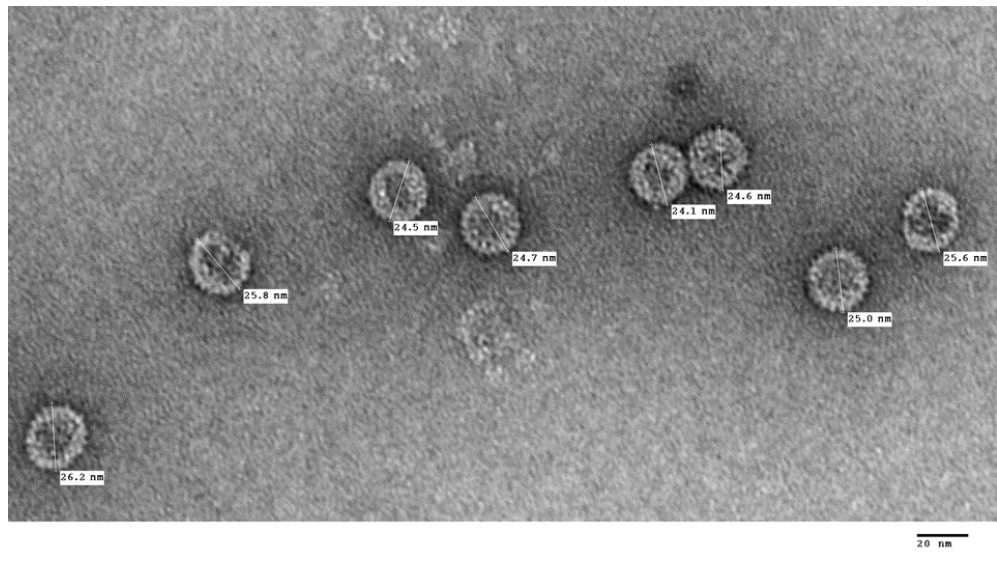


Figure 5.18: Electron micrograph showing the purified tandem core VLPs that were negatively stained with 2% (v/v) uranyl acetate. Panel A: tHBcAg-cEDIII VLPs visualised at 80,000X magnification; Panel B: tEL VLPs control visualised at 100,000X magnification. Scale bar = 20 nm. Red arrow is used to specify particle with large symmetry, while orange arrow denotes those with smaller symmetry. The chimeric tHBcAg VLPs with cEDIII epitopes had successfully assembled into viral particles.

Nonetheless, efforts were made in resolving particles aggregation and significant success was obtained for the purification of tHBcAg-cEDIII sample (**Figure 5.19**). Stringent handling during the vacuum concentration step yielded only a single iridescent band on the nycodenz gradient after ultracentrifugation (Panel A). Subsequent TEM imaging also confirmed that the grey band harboured less aggregated VLPs (Panel B), with a mixture of large and small particles.

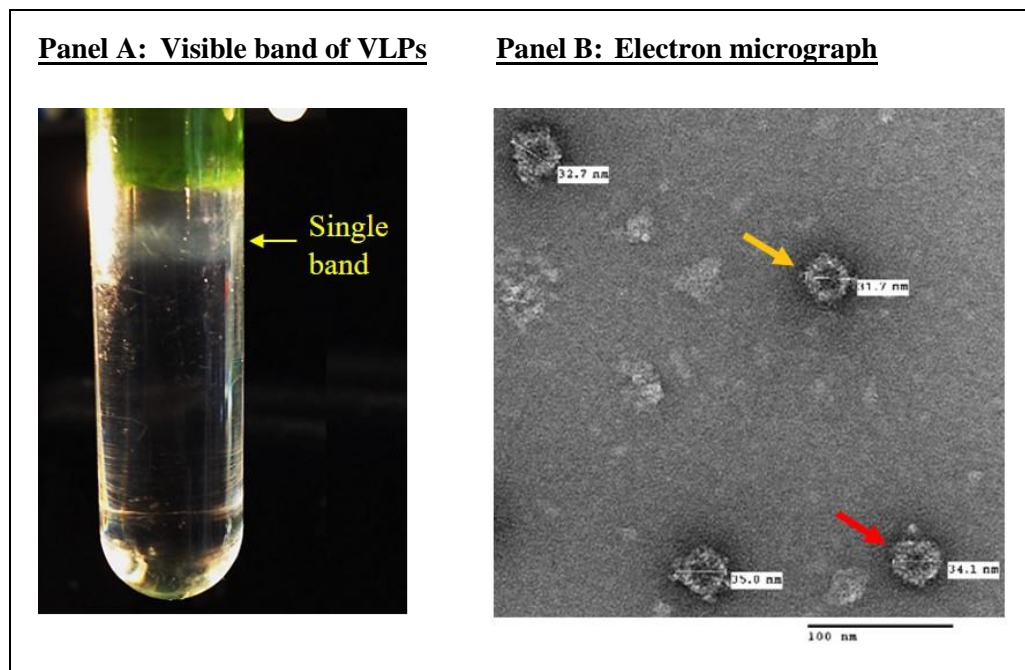


Figure 5.19: Nycodenz gradient fractionation and detection of tHBcAg-cEDIII VLPs, following deliberate handling of vacuum concentration step. Panel A: Single band of VLPs observed from nycodenz gradient; Panel B: TEM imaging of the collected single band. Scale bar = 100 nm. Red and orange arrows are used to indicate large and small particles, correspondingly. Stringent sample processing led to less aggregated tHBcAg-cEDIII particles.

5.3.5 Quantification of purified protein sample

After purification procedures, recovered protein samples were dialysed against PBS buffer and subjected to quantification (**Table 5.1**). The yield was expressed as protein content per unit of fresh weight tissue (FWT). Overall, it was noted that recombinant fusion proteins could be harvested at higher level than the chimeric VLPs in *N. benthamiana*. Among the fusion proteins, the yield of CTB-cEDIII-KDEL (xTH) protein were doubled of cEDIII-sGFP-H-KDEL protein. Meanwhile, almost equivalent yield levels were obtained for all the chimeric HBcAg VLPs (monomeric core: mHBcAg-cEDIII and mHBcAg-cEDIII (L); tandem core: tHBcAg-cEDIII).

Table 5.1: List of quantified protein yield after the final purification procedures.

No.	Purified protein sample	Yield
1	Fusion protein: cEDIII-sGFP-H-KDEL	130 – 170 mg/kg
2	Protein: cEDIII	13 – 14 mg/kg
3	Fusion protein: CTB-cEDIII-KDEL (xTH)	310 – 340 mg/kg
4	Monomeric core VLPs: mHBcAg-cEDIII	13 – 15 mg/kg
5	Monomeric core VLPs: mHBcAg-cEDIII (L)	16 – 17 mg/kg
6	Tandem core VLPs: tHBcAg-cEDIII	12 – 16 mg/kg

5.4 Discussion

In this study, cEDIII as the antigen of interest has been designed to express either as recombinant fusion protein or as epitope display on chimeric HBcAg VLPs. Therefore, two different purification approaches had been used to recover proteins for downstream immunogenicity testing.

During vector construction, 6X His tag was added to the C-terminal ends of recombinant cEDIII fusion protein to enable purification via IMAC. In this technique, His-tagged protein is chelated based on the high affinity for transition metal ions such as Ni^{2+} , Co^{2+} , Cu^{2+} and Zn^{2+} . His residue exhibits the strongest interaction with metal ions because it has electron donor groups on the imidazole ring that can readily form coordination bond (Bornhorst and Falke, 2000). To date, NTA is the preferred chelating agent used to fix metal ions on agarose, as other ligands like iminodiacetic acid (IDA) and tris(carboxymethyl)ethylene diamine (TED), suffer from low purity and/or high metal leaching issue (Block *et al.*, 2009). This is associated with the coordination sites available on Ni^{2+} ; and NTA turns out to have the most effective ratio for interaction with the ligand and protein imidazole ring. With that, effective isolation of His-tagged recombinant cEDIII protein had been achieved with Ni-NTA in this chapter. Stringent washes with 5 mM to 20 mM imidazole had been employed to prevent high background binding to the metal ions.

To isolate cEDIII protein, TEV protease was used to cleave its translationally-fused sGFP and C-terminal 6X His tag. Removal of the affinity tag was justified by reports that His tag can negatively affect the folding or activity of certain proteins (Amor-Mahjoub *et al.*, 2006; Chant *et al.*, 2005; Horchani *et al.*, 2009). **Figure 5.4** shows that the IMAC-purified cEDIII-sGFP-H-KDEL fusion protein was successfully cleaved into two parts, comprising ~ 28 kDa sGFP-H-KDEL and ~ 11 kDa cEDIII. Though the protease digestion was successful, but cleavage efficiency was considerably low. For every 100 μg of digested cEDIII-sGFP-H-KDEL protein, only 13 – 14 μg of

cEDIII protein could be recovered. Assuming that the protease cleavage is 100% efficient, the digestion should yield ~ 28 µg of cEDIII protein and ~ 72 µg of separated sGFP-H-KDEL. However, this assumption was arbitrarily made based on the ratio of the size difference of cEDIII and sGFP-H-KDEL proteins, at 11 kDa and 28 kDa, respectively. The two-fold loss of cEDIII protein could explain for the low yield, even though IMAC-purified cEDIII-sGFP-H-KDEL could be harvested at 130 – 170 mg/kg FWT (**Table 5.1**). The protein modelling of cEDIII-sGFP-H-KDEL suggests that the TEV recognition site is not sterically hindered (**Appendix A5.2**). Thus, optimisation of the TEV digestion reaction was performed. The best condition was hence set at long incubation time of 24 hours, along with doubled TEV enzyme concentration as compared to manufacturer's recommendation.

Since cEDIII is generated from multiple sequence alignment, little is known regarding the novel protein. Other than His tag isolation, the use of other chromatographic methods could be fairly challenging since cEDIII has not been well-characterised. It is presumed that cEDIII also folds into a β barrel configuration, with the nine β strands typically found on dengue EDIII (Huang *et al.*, 2007; Volk *et al.*, 2007). However, a thermodynamic study revealed that cEDIII exhibited greater stability than the serotype-specific EDIII when exposed to heat or chemical denaturants (Zidane *et al.*, 2013). As current strategy involved multi-step processing that can cause gradual protein losses, there is a need to devise an alternative approach to isolate cEDIII in future. Immuno-affinity chromatography may be opted to achieve high yield and purity, but it requires greater investment on antibodies to set up the stationary phase.

Similar strategy was adopted for the purification of CTB-cEDIII-H-KDEL protein. Despite initial protein isolation via IMAC purification_1 was successful, but the subsequent TEV protease cleavage did not yield expected results. **Figure 5.6** reveals that the digested protein was still firmly bound to the Ni²⁺-charged resin despite expected removal of 6X His tag. Protein modelling did indicate that the TEV cleavage

site was not structurally hidden (**Appendix A5.2**), and increased amount of TEV enzyme was not able to rectify the problem as well. Soon after, the root cause was identified as the inherent binding affinity of CTB to Ni²⁺ ions. In specific, the binding was mediated by three His residues at positions 13, 57 and 94, as discovered by Dertzbaugh and Cox (1998). Analysis of the CTB-cEDIII-H-KDEL protein sequence conforms to the findings, whereby the three His residues could be identified (**Figure 5.20**). Therefore, the new CTB-cEDIII-KDEL (xTH) variant was designed to obviate the protease cleavage step for affinity tag removal. A significant finding was achieved when the CTB-cEDIII-KDEL (xTH) fusion protein could be retrieved via IMAC purification_1 (**Figure 5.7**). This also reduces the need for tedious purification process and associated costs. Novelty stands out here as the first report on single step isolation of recombinant cEDIII protein fused to CTB.

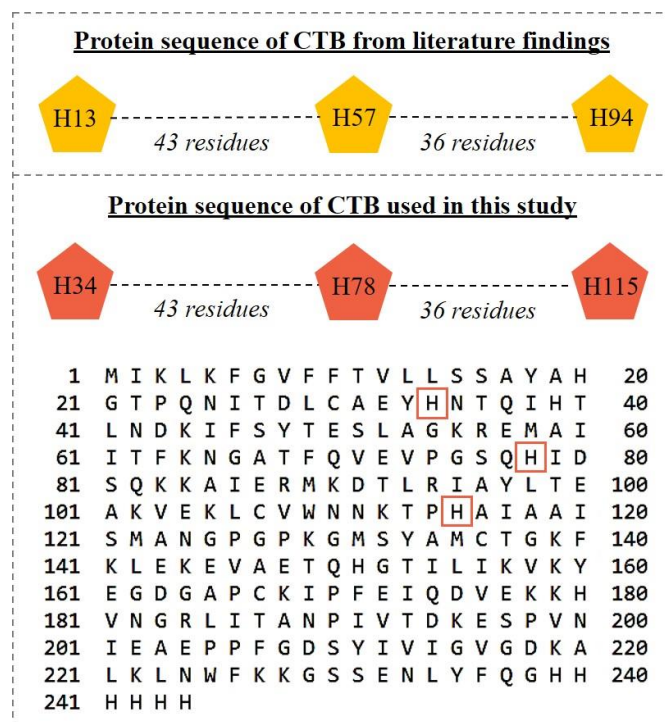


Figure 5.20: Identification of the three His residues (in red box) responsible for the CTB-cEDIII-H-KDEL protein binding to Ni²⁺ ion, as reported by Dertzbaugh and Cox (1998).

In the event of cholera infection, CTB-GM1 binding occurs at the apical membrane of polarised cell before the toxin is internalised into vesicles and dissociates into A and B subunits in the ER (Lencer *et al.*, 1999). Structural configuration of CTB is crucial as its adjuvant effect depends on the binding of pentameric form to GM1 gangliosides on cellular surfaces (Merritt *et al.*, 1994). Hence, GM1-ELISA was performed to characterise the resemblance of plant-derived protein to its native conformation. Commercial CTB is often added as a positive control, so that it can gauge the expression level of recombinant protein as well. However, Malaysia government has classified it under the Dangerous Drugs and Psychotropic Substances; and hence could not be obtained due to permit restriction. With no option, cEDIII and mHBcAg-cEDIII purified proteins were included as negative controls to differentiate any false-positive binding. Based on **Figure 5.8**, molecular recognition of the CTB-cEDIII-KDEL (xTH) protein to GM1 receptor could be detected at concentration as low as 10 ng/ml. So, it is presumed that the fusion protein can bind to GM1 to the same extent as native CTB. Nonetheless, this speculation still needs to be validated with inclusion of commercial CTB in future. For cEDIII and mHBcAg-cEDIII proteins, despite being expressed from the same expression vector and/or purified using similar strategy, both proteins could not interact with GM1 at all. This proved that plant-produced CTB-cEDIII-KDEL (xTH) protein did fold into biologically active pentamers via specific recognition to the GM1 gangliosides.

In addition to GM1-ELISA, SEC was used to study the pentamerisation of CTB-cEDIII-KDEL (xTH) protein and several peaks that corresponded to various oligomeric states were obtained (**Figure 5.9**). According to Lesieur *et al.* (2002), hydrogen network is responsible for the assembly of CTB pentameric complexes, that can occur either via (i) interaction of dimer with trimer or (ii) coupling of monomer with tetramer. The presence of high molecular mass (Mr) molecules, designated as Aggregates A and B, could be deciphered as pentamer-pentamer interaction. According to Merritt *et al.*

(1995), CTB pentamers tend to interact with each other via reciprocal insertion of the His13 imidazole ring from one subunit of each pentamer into another pentamer, when they are not bound to GM1 receptor (**Figure 5.21**). Successive pairs of interacting pentamers thus, can give rise to an infinite chains of linked pentamers. The Aggregate B may represent shorter intermediates of Aggregate A. Collectively, it seems that the CTB-cEDIII-KDEL (xTH) fusion protein has not only preserved the ability to assemble into pentamer, but also demonstrates an inclined propensity to associate into high Mr molecules. The formation of pentamer and aggregates has most likely protected the fusion protein from proteolytic degradation (Kwon *et al.*, 2013), where no significant yield loss was noted after 1.5 years of storage. Nonetheless, the aggregates have not hindered binding to GM1 gangliosides as validated from GM1-ELISA. With the knowledge of protein oligomerisation, it is possible to integrate SEC as a polishing step to achieve enhanced purity. Technically, the flow rate can be reduced to acquire better-resolved peaks. As Lee *et al.* (2014) observed that the different linker designs between CTB and the fused antigen could affect the oligomeric states of fusion protein, this may be an interesting subject for future follow-up.

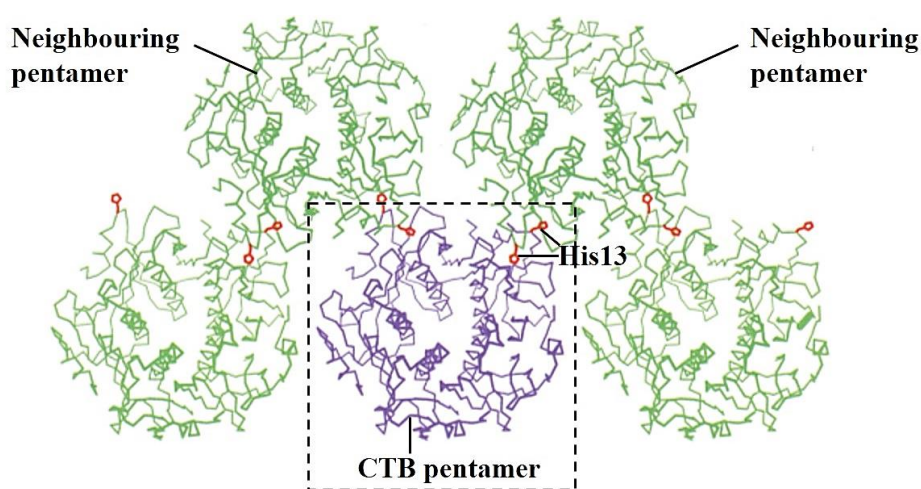


Figure 5.21: Crystal structure of CTB pentamer-pentamer association, with the His13 imidazole ring coloured in red. Image obtained from Merritt *et al.* (1995).

In terms of VLPs purification, the procedures begin with sucrose cushion to isolate and concentrate VLPs from plant lysate, which then leaves density gradient to further purify the particles. A gentle purification procedure was preferred as Fuscaldo *et al.* (1971) claimed that pelleting was liable to cause particles damage. In fact, the use of sucrose gradient has been reported in various purification works (Mathew *et al.*, 2014; Shoji *et al.*, 2015; Yang *et al.*, 2017; Zahmanova *et al.*, 2014). Despite being the most economical material, sucrose forms very viscous solution that can exert high osmotic effects at concentration as low as 10% (w/v) (Griffiths, 2000). Furthermore, soluble proteins which have similar sizes but disparate densities could not be effectively separated using rate zonal centrifugation. Hence, nycodenz gradient was adopted as an alternative measure for purification of tandem core VLPs. Nycodenz is an inert aromatic compound that can form isopycnic gradient, which is particularly useful for VLPs that can react with caesium chloride (Gugerli, 1984). Isopycnic generally means ‘of the same density’, where VLPs will migrate until the equilibrium sedimentation is reached despite of running hours (Luttmann *et al.*, 2006). Swing-bucket rotors were used in all ultracentrifugation works to prevent mixing of layers.

With sucrose cushion, the VLPs within plant lysate would travel through the 25% sucrose layer and eventually rested at the interface with 70% sucrose solution. However, a thick green band was visible at the interface region as well. According to Peyret (2015), this band is likely to overlap with migrating VLPs that co-sediment slightly below. Coherent to that, tandem core VLPs-displaying GFP were found to accumulate predominantly in the 40% fraction (Peyret *et al.*, 2015). Ideally, harvesting only the 70% fraction will yield a clean isolated sample. But, due to the low expression of all chimeric HBcAg VLPs constructs in this study, the interface fraction was collected along with the 70% fraction to recover all the VLPs present in the sample. Some of the green impurities were removed by clarification after vacuum concentration. Further purification via density gradient serves to facilitate cleaner separation with more

consistent fractions. Based on **Appendix A5.4**, an inference is drawn whereby nycodenz can offer better separation of plant impurities than sucrose. In fact, the visible light-scattering bands in nycodenz gradient can facilitate rapid identification of particles aggregation (Sathananthan *et al.*, 1997); which was seen from the denser band of the two VLPs sub-populations shown in **Figure 5.17**.

Next, TEM was used to validate the presence of correctly assembled VLPs. Looking at the monomeric core VLPs, both mHBcAg-cEDIII and mHBcAg-cEDIII (L) VLPs (**Figure 5.14**) were imaged as larger and ‘knobbly’ particles as compared to the empty VLPs without cEDIII, namely mEL. The increase in particle diameter strongly indicates epitope projections on the VLPs surface. However, subsequent immunogold labelling (**Figure 5.15**) showed that not every particle was tagged with the 10-nm colloidal gold. There are two possibilities that can lead to this: (i) too high concentration of primary antibody causes steric hindrance that hinders gold probe attachment (Dopping-Hepenstal and Beesley, 1993); or (ii) some of the cEDIII epitopes might have been masked from antibody recognition due to VLPs aggregation.

Meanwhile, tHBcAg-cEDIII particle also had the ‘knobbly’ morphology (**Figure 5.18**) and were relatively larger than its empty counterpart, namely tEL. Such observation also proves that cEDIII epitopes were presented on the particle surface. Besides, measurement of particle diameter reveals that tHBcAg-cEDIII particles were roughly 6 – 8 nm smaller than the monomeric core VLPs with similar cEDIII displays. The size difference was expected because cEDIII was inserted to the Core II of tandem core HBcAg cassette (see **Table 3.2**), and hence only half of the chimeric VLPs were decorated with cEDIII epitopes.

Several factors might have caused VLPs aggregation, and the first aspect is speculated from accidental heat-shock of sample during vacuum concentration. Peyret (2015) also found that a sample could rapidly heat up if it was not kept on ice immediately after vacuum evaporation, leading to aggregation or sample loss. In fact,

some heat-labile particles can aggregate following tube transfer from 4°C to RT (Shi *et al.*, 2005). Secondly, the choice of density gradient material might not be ideal. Gias *et al.* (2008) believed that sucrose can cause severe hyperosmotic damage and hamper recovery of VLPs. Thirdly, the properties of antigenic epitope might have contributed to particles aggregation. It was found that the chimeric VLPs-displaying cEDIII (monomeric core: mHBcAg-cEDIII and mHBcAg-cEDIII (L); tandem core: tHBcAg-cEDIII) tend to exhibit more prominent aggregation as compared to their empty counterparts, namely mEL and tEL correspondingly. The insertion of cEDIII could have altered the particles surface hydrophobicity; which was in line with Shi *et al.* (2005) finding that the hydrophobic surface exposed on human papillomavirus (HPV) VLPs was partially responsible for aggregation.

A major concern with particles aggregation is the possible obstruction of immunogenic display which can affect vaccine potency. Hence, rectification was focused on stringent handling of sample particularly during vacuum evaporation. A centrifugal concentrator was not opted in early concentration step as the plant debris in interface fraction could clog the filter unit. With the deliberate efforts, aggregation of tHBcAg-cEDIII particles were no longer detected after ultracentrifugation on a nycodenz gradient (**Figure 5.19**). These results have indirectly provided an insight to the VLPs properties, deciphering them as heat-sensitive molecules. However, similar efforts did not yield positive results for the purification of monomeric core VLPs via sucrose gradient. So following the discussions above, it seems likely that the use of sucrose has caused osmolarity damage to the particles (Zeddami *et al.*, 2008). Due to limitations, this issue has not been addressed and remained to be verified in future study. Paradoxically, a research team had focused on producing VLPs in highly aggregated forms as they claimed that aggregates could induce stronger cell-mediated immunity (Suzarte *et al.*, 2014; Valdés *et al.*, 2009). Despite so, induction of aggregates may not be ideal as the immunogenic properties can vary from batch-to-batch.

In general, protein quantification showed that the yields obtained for fusion proteins were at least 10 folds higher than the chimeric HBcAg VLPs (**Table 5.1**). Two aspects may have attributed to the yield difference. The first aspect was due to expression efficiency: the entire gene sequence of cEDIII fusion proteins were codon-optimised according to *N. benthamiana* usage and they were sequestered in the endoplasmic reticulum (ER); meanwhile, only the *cEDIII* gene in chimeric HBcAg VLPs constructs was codon-optimised for *N. benthamiana* expression and no subcellular targeting was involved (as discussed in **Chapter 4**). The second aspect may be attributed to purification efficiency: enrichment of His-tagged fusion proteins were easily achieved via chelating metal ions; while harvesting of chimeric HBcAg VLPs was achieved via step-wise fractionation of density gradient. Comparing between the cEDIII fusion to sGFP and CTB, it seems that fusion with CTB has led to higher yield possibly due to its ability to enhance solubility and stability of fusion protein (Harakuni, *et al.*, 2005). Between the mHBcAg and tHBcAg chimeric VLPs, it was deduced that tHBcAg-cEDIII VLPs were expressed at higher level. This was because tHBcAg-cEDIII VLPs were recovered with higher purity using nycodenz gradient, even though protein quantification (**Table 5.1**) showed that both mHBcAg and tHBcAg chimeric VLPs samples were purified at almost equivalent yields. This speculation is also made based on the rationale of tandem core development, which aims to reduce steric clashes and boost accumulation of assembled VLPs (Peyret *et al.*, 2015).

5.5 Conclusion

Following successful protein expression, purification procedures were performed to isolate and characterise the target proteins that would be used for immunogenicity testing. Two different approaches had been strategized here for the purification of recombinant fusion proteins, namely cEDIII and CTB-cEDIII-KDEL (xTH) as well as the chimeric HBcAg VLPs, namely mHBcAg-cEDIII, mHBcAg-cEDIII (L) and tHBcAg-cEDIII.

Despite the purification efficiency of cEDIII protein was rather low, yet a satisfactory amount of sample could still be obtained. Purification of CTB-cEDIII-KDEL (xTH) protein however, could be easily achieved via a single IMAC procedure due to its inherent affinity for Ni²⁺ ions. Besides, oligomerisation of CTB-cEDIII-KDEL (xTH) fusion protein had been characterised via SEC which was valuable for better understanding of the protein organisation.

On the other hand, ultracentrifugal separation of VLPs was successful and the assembly of chimeric VLPs also had been identified via TEM imaging. It was proposed that isopycnic density gradient would serve as a better choice for future recovery of VLPs with higher purity.

6 Immunological Studies of cEDIII-based Vaccine Constructs to Determine the Immunogenicity and Neutralising Activity

Table of Contents

6.1	Introduction	6-4
6.2	Materials and methods.....	6-7
6.2.1	Overview of vaccination schedule	6-7
6.2.2	Housing of mice	6-11
6.2.3	Intraperitoneal (IP) injection.....	6-11
6.2.4	Serum collection	6-12
6.2.4.1	Through saphenous vein	6-12
6.2.4.2	Through cardiac puncture	6-12
6.2.5	Specialised equipment.....	6-13
6.2.6	Propagation Vero cell line.....	6-13
6.2.7	Dengue virus stock preparation.....	6-14
6.2.8	Serological analyses.....	6-15
6.2.8.1	Immunoglobulin G (IgG) enzyme-linked immunosorbent assay (ELISA).....	6-15
6.2.8.2	Immunofluorescence assay (IFA)	6-16
6.2.8.3	Focus reduction neutralisation test (FRNT).....	6-16
6.2.9	Spleen collection.....	6-17
6.2.10	Lymphocytes screening assays	6-17
6.2.10.1	Splenocytes culture and stimulation.....	6-17
6.2.10.2	Lymphocytes proliferation test	6-18

6.2.10.3	Fluorescence-activated cell sorting (FACS)	6-18
6.2.10.4	Secretory cytokines profiling	6-19
6.2.11	Statistical analyses	6-21
6.3	Results	6-22
6.3.1	Measurement of anti-dengue immunoglobulin G (IgG)	6-22
6.3.1.1	Recombinant cEDIII proteins	6-22
6.3.1.2	Chimeric mHBcAg VLPs-displaying cEDIII	6-24
6.3.2	Immunofluorescence detection of serum antibodies binding to native dengue virus	6-28
6.3.2.1	Recombinant cEDIII proteins	6-28
6.3.2.2	Chimeric mHBcAg VLPs-displaying cEDIII	6-34
6.3.3	Evaluation of virus neutralising antibody production	6-44
6.3.3.1	Recombinant cEDIII proteins	6-44
6.3.3.2	Chimeric mHBcAg VLPs-displaying cEDIII	6-46
6.3.4	Assessing lymphocytes proliferation following antigen stimulation	6-49
6.3.4.1	Recombinant cEDIII proteins	6-49
6.3.4.2	Chimeric mHBcAg VLPs-displaying cEDIII	6-51
6.3.5	Flow cytometric immunophenotyping	6-54
6.3.5.1	Recombinant cEDIII proteins	6-54
6.3.5.2	Chimeric mHBcAg VLPs-displaying cEDIII	6-56
6.3.6	Measurement of secretory cytokines levels	6-58
6.3.6.1	Recombinant cEDIII proteins	6-58
6.3.6.2	Chimeric mHBcAg VLPs-displaying cEDIII	6-61

6.3.7	Comparative evaluation of the immunogenicity of different vaccine constructs	6-63
6.4	Discussion	6-66
6.5	Conclusion.....	6-77

6.1 Introduction

The development of a protective and durable dengue vaccine has been longed for prevention against the deadly disease. After decades of research, it is now understood that pre-existing antibodies can lead to severe dengue due to antibody-dependent enhancement (ADE). Such complication imposes a major hiccup for vaccine development as secondary encounter of a different serotype can jeopardise the efficacy of a vaccine if tetravalent protection is not observed at the first place. Hence, one of the key requirements for a dengue vaccine is the ability to neutralise all four dengue serotypes (DENV 1-4) simultaneously. Up to date, no such vaccine is available yet including the pioneer Dengvaxia[®]. Despite there are several vaccine candidates in the pipeline (reviewed in **Section 2.2.5**), the call for a reliable vaccine has continued to intensify as the disease is progressing at a pace faster than it can be coped.

Following the purification of vaccine candidates, immunogenicity testing is needed to assess the product safety and efficacy. This is to comply with the Food and Drug Administration (FDA) regulation, where pharmaceuticals intended for human use should observe a proof of protective response in animal subjects. Thereby, the immunogenicity data are crucial in determining whether the product will progress to human clinical trials. Animal models that are routinely used for testing include rodents and non-human primates. Although wild-type mice are known to be inherently resistant to dengue infection, but BALB/c mice are immuno-competent and are commonly used for the evaluation of immunogenicity of vaccine candidate. Besides, Leng *et al.* (2009) had successfully tested the *E. coli*-produced cEDIII in 6 – 8 weeks old BALB/c mice.

After vaccine administration, several responses can be assessed including the antigen-specific antibody titre, differentiation of antibody isotypes, type of immunity and duration of responses. A long-term immunity is anticipated as it defines the ability to rapidly reactivate memory cells into immune effectors upon exposure to the same antigen. Principally, humoral immunity and cell-mediated immunity (CMI) are the two

arms of the immune system. Humoral immune response is mediated by antibody molecules produced by B cells to prevent the spread of pathogens in body fluid. In this study, the neutralisation potency of antibodies is vital to inhibit DENV infection, either by blocking the attachment of virus to host cell or by blocking the post-attachment steps (Dowd and Pierson, 2011).

Meanwhile, the CMI relies on T cells to respond to aberrant markers that are displayed by the major histocompatibility complex (MHC) on antigen-presenting cells (APCs). Two distinct T cells can be activated, namely: (i) T helper (Th) cells, of Th1 and Th2 subtypes that express cluster of differentiation (CD)4 and (ii) T cytotoxic (Tc) cells that express CD8. Upon antigen presentation to naïve T cells, differentiation into immune effectors of Th1/Th2 subtype will ensue. Th1 response mainly activates the Tc and natural killer cells to help in removing virus-infected cells that are shielded from circulating antibodies; while Th2 cells assist in the growth and differentiation of antibody-secreting B cells (Lydyard *et al.* 2011). Hence, the development of both Th1 and Th2 immune responses are crucial to help in combating the deadly viral disease. As cytokines are the signalling molecules that mediate intercellular communication, profiling studies could help to identify the type of immune effectors that are predominantly elicited.

In this chapter, the humoral response in BALB/c mice was analysed based on cEDIII-specific antibodies production and most importantly, the neutralisation potency of these antibodies to inhibit DENV infection. Since the consensus sequence is used, a state of protective immunisation against DENV 1-4 is anticipated. Meanwhile, the T cell responses were assessed in several aspects including the lymphoproliferative responses of splenocytes to cEDIII stimulation, immunophenotyping of cells according to CD markers and secretory cytokines production. Since the cEDIII antigen was expressed in two different forms, as recombinant proteins and epitope display on chimeric hepatitis B core antigen (HBcAg) virus-like particles (VLPs), their

immunogenic potential could be evaluated based on the corresponding humoral and cell-mediated immune responses. In addition, the presentation of the immunogenicity results of chimeric tHBcAg displaying cEDIII (vaccine candidate: tHBcAg-cEDIII VLPs) was made in this chapter as well, as previously tested by iQur Ltd. (UK).

Overall, the specific objectives for this chapter are set as follows:

- (i) To immunise female BALB/c mice with the purified recombinant proteins (vaccine candidates: recombinant cEDIII and recombinant CTB-cEDIII-KDEL (xTH) fusion protein) and chimeric mHBcAg VLPs-displaying cEDIII (vaccine candidates: mHBcAg-cEDIII VLPs and mHBcAg-cEDIII (L) VLPs);
- (ii) To collect mouse serum and check for cEDIII-specific immunoglobulin G (IgG) production;
- (iii) To examine the ability of raised antibodies to recognise native DENV 1-4;
- (iv) To determine the neutralising potential of vaccine candidates;
- (v) To assess the lymphoproliferative response of cultured splenocytes to cEDIII stimulation;
- (vi) To perform immunophenotyping via fluorescence-activated cell sorting (FACS) analysis;
- (vii) To evaluate the cytokine secretion profiles; and
- (viii) To compare the efficacy of the afore-mentioned vaccine candidates.

6.2 Materials and methods

6.2.1 Overview of vaccination schedule

The animal experiment was conducted in the animal facility located at Monash University Malaysia, with a total of 122 female BALB/c mice permitted for testing. Protocols were approved by the Animal Ethics Committee of Monash University (reference number: MARP/2016/018) as well as the Animal Welfare and Ethical Review Body of Nottingham University (reference number: UNMC10).

In general, a dosage of 20 µg (unless otherwise stated) of purified vaccine construct was prepared in a volume of 200 µl phosphate-buffered saline (PBS) for each individual mouse, either with or without 1 mg of alum adjuvant (Sigma, Germany). In this study, two independent mouse experiments were designed for immunisation against recombinant cEDIII proteins (**Table 6.1**). Likewise, two mouse experiments also had been conducted for immunisation against chimeric mHBcAg VLPs-displaying cEDIII. In this case, two different experimental designs had been strategised, referred as VLPs (a) (**Table 6.2a**) and VLPs (b) (**Table 6.2b**). In specific, VLPs (b) represents an improvement of VLPs (a), whereby two amendments had been made, including: (i) adding two new vaccine constructs namely G7-V and G8-V; and (ii) changing the antigen dosage of G5-V to G8-V to 30 µg.

Each immunisation test was scheduled for 6 weeks starting from the day when the 7 – 8 weeks old mice were obtained until the end of vaccination. A step-by-step methodology is illustrated in **Figure 6.1**.

Table 6.1: A summary of the experimental design for mouse immunisation against recombinant cEDIII proteins.

Grouping	Purified vaccine construct
Group 1 (G1-R)	PBS control
Group 2 (G2-R)	Alum (1 mg) control
Group 3 (G3-R)	cEDIII (20 µg)
Group 4 (G4-R)	cEDIII (20 µg) + Alum (1 mg)
Group 5 (G5-R)	CTB-cEDIII-KDEL (xTH) (20 µg)
Group 6 (G6-R)	CTB-cEDIII-KDEL (xTH) (20 µg) + Alum (1 mg)

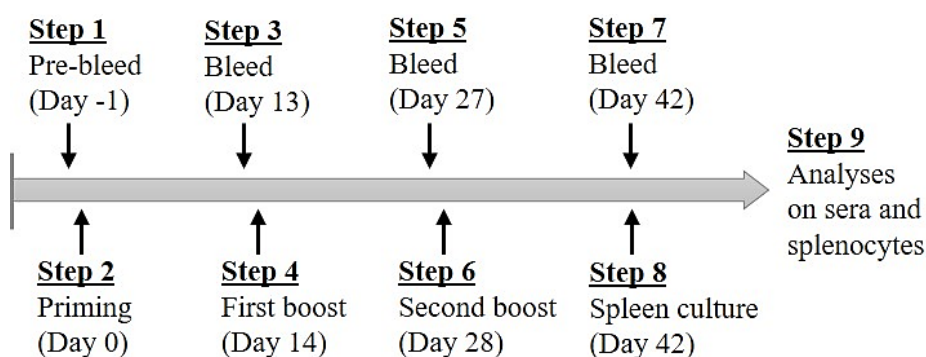
Table 6.2a: A summary of the experimental design for mouse immunisation against chimeric mHBcAg VLPs-displaying cEDIII, referred as VLPs (a) experiment.

Grouping	Purified vaccine construct
Group 1 (G1-V)	PBS control
Group 2 (G2-V)	Alum (1 mg) control
Group 3 (G3-V)	mEL (20 µg)
Group 4 (G4-V)	mEL (20 µg) + Alum (1 mg)
Group 5 (G5-V)	mHBcAg-cEDIII (L) (20 µg)
Group 6 (G6-V)	mHBcAg-cEDIII (L) (20 µg) + Alum (1 mg)

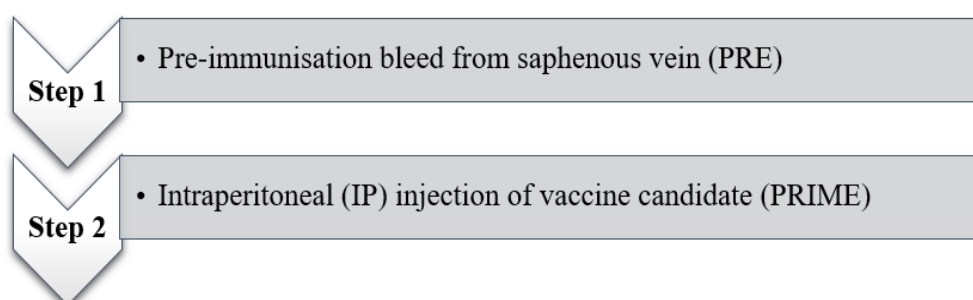
Table 6.2b: A summary of the experimental design for mouse immunisation against chimeric mHBcAg VLPs-displaying cEDIII, referred as VLPs (b) experiment.

Grouping	Purified vaccine construct
Group 1 (G1-V)	PBS control
Group 2 (G2-V)	Alum (1 mg) control
Group 3 (G3-V)	mEL (20 µg)
Group 4 (G4-V)	mEL (20 µg) + Alum (1 mg)
Group 5 (G5-V)	mHBcAg-cEDIII (L) (30 µg)
Group 6 (G6-V)	mHBcAg-cEDIII (L) (30 µg) + Alum (1 mg)
Group 7 (G7-V)	mHBcAg-cEDIII (30 µg)
Group 8 (G8-V)	mHBcAg-cEDIII (30 µg) + Alum (1 mg)

Panel A: An overview of immunisation schedule



Panel B: Stepwise methodology



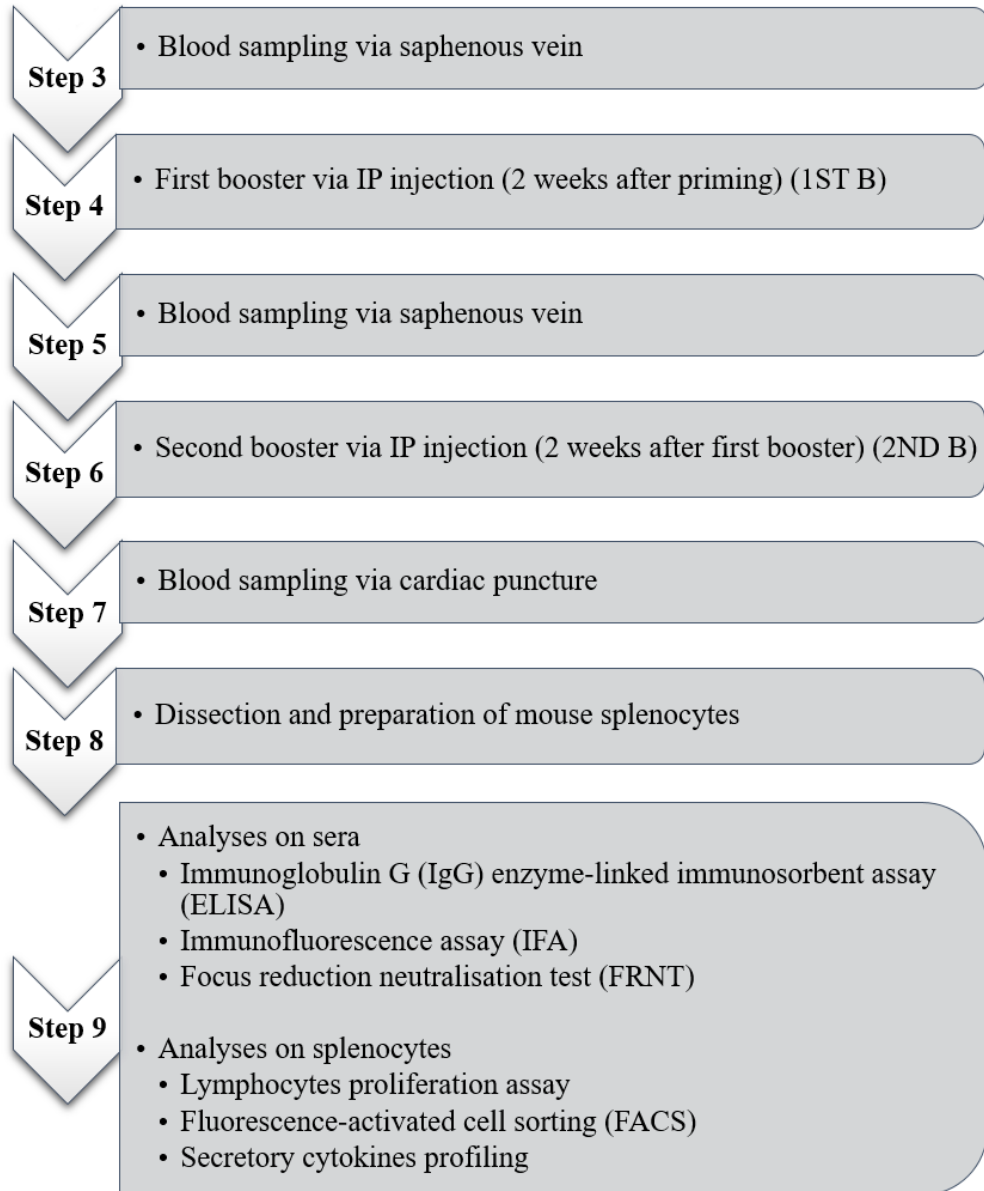


Figure 6.1: A schematic illustration of the animal experiment plan. Panel A: Immunisation schedule. Mice were primed on day 0 and received boosters on day 14 and day 21. Blood samples were collected on day -1, day 13, day 27 and day 42. Splenocytes were cultured after cardiac puncture. Panel B: A step-by-step description of the methodology involved.

6.2.2 Housing of mice

BALB/c mice were held in individual ventilation cage (IVC) to provide clean air circulation through high-efficiency particulate air (HEPA) filter. Housing temperature was set at 22°C with relative humidity of 55%. For hygienic purpose, the corncob bedding and absorbent papers were changed weekly. Each individual mouse was identified based on indelible mark on tail.

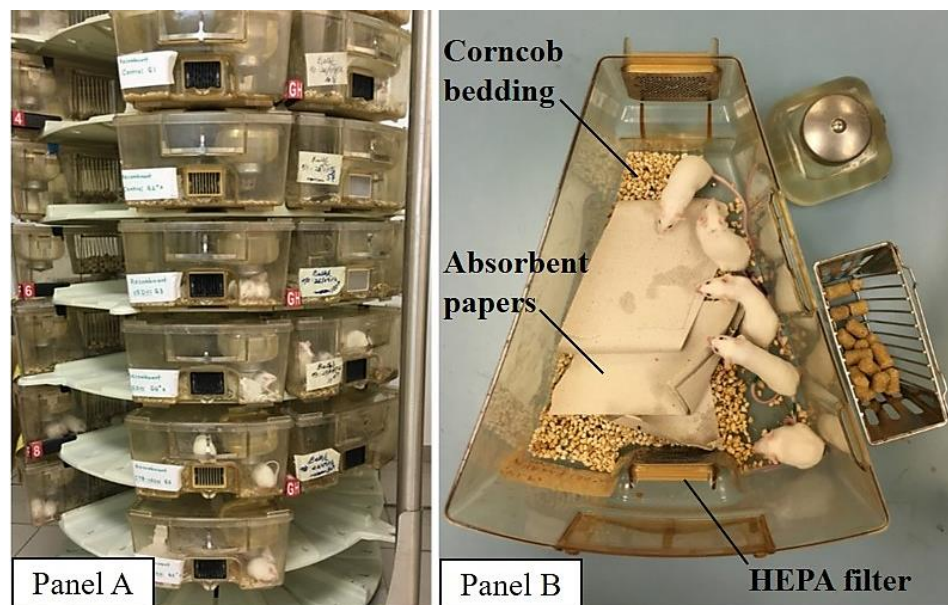


Figure 6.2: Images of BALB/c mice held in IVC cages. Panel A: Housing of mice within the animal facility; Panel B: An example of 4 – 5 BALB/c mice grouped in one cage.

6.2.3 Intraperitoneal (IP) injection

To perform IP injection, the mouse was first manually restrained using one hand and held in supine position with its posterior end slightly elevated. Prepared antigen was then injected into the mouse's peritoneal cavities using a 25 G needle (BD, USA). These mice were monitored daily for abnormal behaviours such as ruffling of fur, slowing of activity, soft stool and weight loss.

6.2.4 Serum collection

6.2.4.1 Through saphenous vein

The mouse was manually restrained and the fur on the back of hind leg was removed using hair-removal cream (Veet, UK). Once the saphenous vein was visible, it was punctured with a 27 G needle (BD, USA) and roughly 50 µl of blood was collected. Lastly, the punctured site was compressed with sterile cotton wool to stop bleeding. After centrifugation at 1,000 x g, 4°C for 10 minutes, the serum was harvested from the supernatant and kept at -80 °C.

6.2.4.2 Through cardiac puncture

Two weeks after the final immunisation, the mouse was deeply anesthetized with 10 mg/kg of xylazine (Ilium, Australia) and 100 mg/kg ketamine (Ilium, Australia) to perform cardiac puncture. The IP injection volume of the drug was prepared according to individual body weight, with the formula obtained from (Pennsylvania Institutional Animal Care and Use Committee (IACUC), 2016). Once the heart was located, a 27 G needle (BD, USA) was inserted and slight negative pressure was applied to the syringe plunger. About 700 µl of blood was collected from each mouse. Confirmation of euthanasia was performed by placing the mice in carbon dioxide chamber.

$$\text{Injection volume} = \text{Body weight (kg)} \times \frac{\text{Dosage (mg/kg)}}{\text{Concentration (mg/ml)}}$$

6.2.5 Specialised equipment

Incubation of Vero cell line and splenocytes culture was carried out using Forma 380 Steri Cycle CO₂ Incubator (Thermo Scientific, USA) and BINDER CB 150 CO₂ Incubator (Binder, Germany). Centrifugation of samples was conducted using Microfuge 22R Refrigerated Microcentrifuge (Beckman Coulter, USA) and Eppendorf 5810R Refrigerated Centrifuge (Eppendorf, Germany). Olympus IX-81 inverted fluorescence microscope (Olympus, Japan) was used for microscopic imaging of immunofluorescence samples. Accuri C6 Cytometer (BD, USA) was used for fluorescence-activated cell sorting (FACS) analyses. Absorbance measurement for enzyme-linked immunosorbent assay (ELISA) was performed using either Benchmark Plus Microplate Reader (Bio-Rad, USA) or Epoch Microplate Reader (Biotek, USA), as stated.

6.2.6 Propagation Vero cell line

Vero cell line (ATCC[®] CCL-81[™]) (American Type Cell Collection (ATCC), USA) was used throughout the study as this cell line had been widely used to study dengue infection. Vero cells were maintained in minimum essential media (MEM)-10 medium (**Appendix A6.1**) and grown at 37°C incubator with 5% carbon dioxide (CO₂) until 80% cell confluency was reached. To passage confluent cells, MEM-10 medium was removed and the cells were washed with 1X Dulbecco's phosphate-buffered saline (DPBS) (Nacalai Tesque, Japan). TrypLE Express (Thermo Scientific, USA) was then added and the flask was incubated at 37°C for 10 minutes. Subsequently, an equal volume of MEM-10 medium was added to inactivate the trypsin. Desired cell dilution was prepared and the culture flask was placed back to 37°C/5% CO₂ incubator.

6.2.7 Dengue virus stock preparation

All the virus samples used in this study were obtained from Dr. Sharifah Syed Hassan (Monash University Malaysia), which were isolated from DENV-infected patient sera and the specific serotypes DENV 1-4 had been confirmed by multiplex reverse transcriptase-polymerase chain reaction (RT-PCR) (Yong *et al.*, 2007) or whole genome sequencing.

To propagate DENV, 70 – 80% confluent Vero cells were washed and re-fed with MEM-2 medium (**Appendix A6.1**) before adding the virus sample at multiplicity of infection (MOI) of 0.1. Then, infected cells were incubated for 5 – 6 days and were monitored daily for cytopathogenic effect (CPE) using an inverted microscope. To harvest the virus, the flask was freeze-thawed for three times before centrifuged at 200 x g, 4°C for 10 minutes.

Virus titre was then determined via focus-forming assay (FFA). In brief, Vero cells were seeded at 1×10^5 cells/well in a 24-well culture plate and grown overnight. After removing the MEM-10 medium, 10-fold serially diluted virus samples were added to the wells in duplicate. Then, the plate was incubated at 37°C for 1 hour, with gentle swirling at every 15-minute intervals. Lastly, the virus inoculum was removed and 4% (v/v) carboxymethylcellulose (CMC) in 2X plaque medium (**Appendix A6.1**) was added to each well. The plate was then incubated in 37°C/5% CO₂ incubator for 4 days.

On the 4th day, the formed virus foci were detected via immunostaining technique. In brief, the MEM-2 medium was removed and cells were washed with tris-buffered saline (TBS) (**Appendix A6.1**). Fixation was done by adding 80% (v/v) ice-cold acetone for 10 minutes. The monolayer was washed twice prior blocking with 1% (w/v) BSA/TBS containing 0.5% (v/v) Triton X-100. After 1-hour incubation at 37°C, blocking buffer was aspirated and DENV 1-4 monoclonal antibody (Thermo Scientific, USA) was added at 1:2,000 dilution. The plate was incubated at 37°C for 1 hour, followed by three washes with TBS supplemented with 0.1 % (v/v) Tween-20 (TBST)

at 5-minute intervals. Next, goat anti-mouse IgG alkaline phosphatase (AP)-labelled antibody (Santa Cruz Biotechnology, USA) was added at 1:2,000 dilution and incubated at 37°C for another hour. Washing steps were repeated and residual liquid was removed by tapping on paper towel. Lastly, AP-based substrate (**Appendix A6.1**) was added until optimal development was acquired. The focus-forming units (FFU) were manually counted and virus titre was calculated based on the average number of FFU in duplicate wells.

6.2.8 Serological analyses

6.2.8.1 Immunoglobulin G (IgG) enzyme-linked immunosorbent assay (ELISA)

A 96-well immuno-plate (SPL, Korea) was coated with 2 µg/ml of purified CTB-cEDIII-KDEL (xTH) protein in sodium bicarbonate buffer (**Appendix A6.1**) at 4°C. On the next day, the wells were washed with PBS supplemented with 0.05% (v/v) Tween-20 (PBST) for five times before blocking with 5% (w/v) low-fat milk/PBS at room temperature (RT). After 1 hour, the washing steps were repeated. To determine the IgG titre of individual mouse, 100 µl of serum sample was applied to the wells in duplicate along with PBS diluent as negative control. The pooled sera of G4-R (**Table 6.1**) was used as the reference standard for all ELISA. The plate was incubated at 37°C for 1 hour, followed by five washes with PBST. Next, goat anti-mouse IgG horseradish peroxidase (HRP)-conjugated secondary antibody (Invitrogen, USA) was added at 1:5,000 dilution and incubation was set at 37°C for another hour. Washing steps were repeated prior adding 3, 3', 5, 5'-tetramethylbenzidine (TMB) substrate (BD, USA). After 15 minutes, the colorimetric reaction was terminated with 0.1 M phosphoric acid and the absorbance at 450 nm wavelength (A_{450}) was measured using Benchmark Plus Microplate Reader, at a correction wavelength at 570 nm. Data were plotted as the mean of ELISA unit (E.U.) ± standard deviation (SD) against different time points of serum collection.

6.2.8.2 Immunofluorescence assay (IFA)

Vero cells were seeded at 1×10^5 cells/ml into each well of a 24-well culture plate. After overnight plating, monolayer was washed with 1X DPBS, re-fed with MEM-2 medium and the virus inoculum was added at MOI = 0.1. After further incubation for 4 days, the infection medium was removed and monolayer was washed with 1X DPBS. Cells were fixed with 80% (v/v) ice-cold acetone for 10 minutes. Blocking was done with 1% (w/v) BSA/PBS supplemented with 0.5% Triton X-100 for 1 hour at 37°C. Next, heat-inactivated mouse sera were pooled in group and added at 1:25 dilution. DENV 1-4 antibody (Thermo Scientific, USA) at 1:100 dilution was included as positive control. Meanwhile, wells with pre-immune sera and Vero cells only were used as negative controls. Plate incubation was set at 37°C for 1 hour, followed by three washes with PBST at 5-minute intervals. Next, AlexaFluor®488-conjugated goat anti-mouse IgG secondary antibody (Thermo Scientific, USA) was added at 1:2,500 dilution and incubated for another hour at 37°C. Washing steps were repeated and Hoechst 33342 Solution (Thermo Scientific, USA) was added into each well at 1:2,000 dilution. After 10-minute incubation at RT, wells were washed with PBS before examination under Olympus IX-81 inverted fluorescence microscope.

6.2.8.3 Focus reduction neutralisation test (FRNT)

Approximately 1×10^5 cells/ml of Vero cells were seeded into each well of the 24-well plate and incubated at 37°C/5% CO₂ for 24 hours. Heat-inactivated mouse sera used for IFA were serially diluted in three-fold in MEM-2 medium starting from 1:25 dilution. Serum was then mixed with virus inoculum at 1:1 ratio, and allowed to incubate at 37°C/5% CO₂ for 1 hour. Next, the serum-virus mixture was transferred to the culture plate containing pre-formed Vero cell monolayer. Virus adsorption was performed at 37°C/5% CO₂ for 1 hour. Each serum-virus mixture was tested in duplicate with three experimental controls: Vero-cell control, virus-only control and a positive control of

DENV-infected patient serum. Lastly, mixtures were removed before overlaying each well with 4% (v/v) CMC in 2X plaque medium, and the plate was incubated for another 4 days. All the subsequent steps involved in foci development were performed as described in **Section 6.2.7**. Developed virus foci were manually counted and the neutralizing antibody titre was determined based on the highest dilution yielding 50% reduction of FFU (FRNT50) as compared to the virus-only control. Each FRNT experiment was repeated at least two times. Data were expressed as the mean FRNT50 obtained from different immunisation groups.

6.2.9 Spleen collection

After euthanasia (**Section 6.2.4.2**), the mouse was dissected to harvest the spleen organ. In brief, the body was wiped with 70% (v/v) ethanol and incised with a sterile scissor. Once the spleen was located, sterile forceps was used to remove the organ and immediately transferred to cold RPMI-10 medium (**Appendix A6.1**).

6.2.10 Lymphocytes screening assays

6.2.10.1 Splenocytes culture and stimulation

The mouse spleens were pooled in group and single cell suspensions were prepared by gently mashing them between two sterile frosted microscope slides. The cell suspension was then spun at 200 x g for 5 minutes at 4°C, followed by incubation with ACK lysing buffer (**Appendix A6.1**) to remove the erythrocytes. The supernatant was filtered through 30 µm nylon cell strainer (SPL, Korea) prior cell counting. Splenocytes from each group were seeded at 8 x 10⁶ cells/well in a 6-well plate and stimulated with 5 µg/ml of CTB-cEDIII-KDEL (xTH) protein for 72 hours at 37°C/5% CO₂ incubator. Wells with RPMI-10 medium and 5 µg/ml concanavalin A (ConA) (Sigma, Germany) were included as negative and positive controls, respectively.

6.2.10.2 Lymphocytes proliferation test

After 72 hours, 100 µl of the splenocytes from **Section 6.2.10.1** were transferred in triplicate into a 96-well plate, and subsequent steps were conducted based on bromodeoxyuridine (BrdU) cell proliferation assay protocol (Roche, Switzerland). In brief, BrdU labelling reagent was added at 1:100 dilution into each well and incubated for another 24 hours. Then, the labelling solution was removed and the cells were dried in 60°C oven for 1 hour. FixDenat solution was added into each well for 30 minutes, followed by anti-BrdU-POD working solution at 1:100 dilution for 90 minutes. The wells were rinsed three times with 1X Washing Solution before adding the Substrate Solution. After 30 minutes, absorbance at 370 nm wavelength (A_{370}) was measured using Epoch Microplate Reader, with a correction wavelength of 492 nm. With reference to Heo *et al.* (2015), the stimulation index (SI) was then calculated as:

$$SI = \frac{\text{Mean } A_{370} \text{ readings of stimulated splenocytes}}{\text{Mean } A_{370} \text{ readings of unstimulated splenocytes}}$$

6.2.10.3 Fluorescence-activated cell sorting (FACS)

The splenocytes from **Section 6.2.10.1** were collected after 72 hours and centrifuged at 200 x g for 10 minutes at 4°C to harvest the pellet for FACS analyses. Pellet was re-suspended with staining buffer (**Appendix A6.1**) and cell counting was done using haemocytometer. About 2.5×10^6 of cells were aliquoted from corresponding splenocytes group and re-suspended in staining buffer containing 10% (v/v) normal rat serum (Invitrogen, USA). These cells were blocked with 1 µg of purified rat anti-mouse CD16/CD32 antibody (BD, USA) on ice for 30 minutes in dark. Then, 1×10^6 cells were aliquoted into microcentrifuge tube for antibodies staining (**Table 6.3**). A single tube was prepared for each splenocytes group for each marker combination. After the antibodies were added, tubes were incubated on ice for 30

minutes. Cells were washed with staining buffer and spun down at 200 x g, at 4°C for 5 minutes. Next, 2% (v/v) paraformaldehyde/PBS was added and allowed to incubate at RT for 10 minutes. Stained cells were centrifuged at 200 x g for 5 minutes, re-suspended in 1X PBS and stored at 4°C away from light. On the day of analysis, 50,000 of events were collected using the fast fluidics setting of Accuri C6 cytometer. Data were then analysed using Accuri C6 software, where gating and fluorescence compensation could be done. With this, immunophenotyping allowed a qualitative assessment of the different lymphocyte populations present in the splenocytes.

Table 6.3: The combination of antibodies used in FACS analyses.

No.	Marker combination
1	CD19 ^{PE} (Thermo Scientific, USA) at 1:400 dilution CD3 ^{APC} (Thermo Scientific, USA) at 1:200 dilution Remarks: To differentiate B and T lymphocytes
2	CD3 ^{APC} (Thermo Scientific, USA) at 1:200 dilution CD4 ^{PE} (Thermo Scientific, USA) at 1:400 dilution CD8 ^{FITC} (Thermo Scientific, USA) at 1:400 dilution Remarks: To differentiate T cells into Th and Tc

6.2.10.4 Secretory cytokines profiling

The supernatants of mouse splenocytes obtained from the centrifugation in **Section 6.2.10.3** were kept for secretory cytokines analyses. In specific, OptEIA ELISA kits (BD, USA) were used to determine the levels of following cytokines: interferon-gamma (IFN- γ), interleukin-2 (IL-2), IL-4, IL-10 and IL-12. In brief, a 96-well immunoplate (SPL, Korea) was coated with corresponding capture antibody (**Table 6.4**) overnight. The wells were washed three times with PBST before blocking with assay diluent (**Appendix A6.1**) at RT for 1 hour. The washing steps were repeated, followed

by adding 100 µl of the sample and ELISA standard to duplicate wells. The plate was sealed and incubated at RT for 2 hours. After five washes with PBST, corresponding working detector solution (**Table 6.4**) was added and incubated for another hour at RT. TMB substrate solution (BD, USA) was added after final washes and incubated in dark for 30 minutes. Lastly, 0.1 M phosphoric acid was added to stop the reaction and the A₄₅₀ reading was measured using Epoch Microplate Reader, at a correction wavelength at 570 nm. The results were then expressed as the mean cytokine concentration (pg/ml) ± SD of different vaccine groups.

Table 6.4: List of reagents used for corresponding OptEIA ELISA kit.

No.	OptEIA ELISA kit	Capture antibody	Working detector
1	IFN- γ (BD, USA)	Anti-mouse IFN- γ at 1:250 dilution in sodium bicarbonate buffer	Biotinylated anti-mouse IFN- γ at 1:500 dilution + Streptavidin-horseradish peroxidase (SAv-HRP) conjugate at 1:250 dilution
2	IL-2 (BD, USA)	Anti-mouse IL-2 at 1:250 dilution in sodium bicarbonate buffer	Biotinylated anti-mouse IL-2 at 1:500 dilution + SAv-HRP at 1:250 dilution
3	IL-4 (BD, USA)	Anti-mouse IL-4 at 1:250 dilution in sodium bicarbonate buffer	Biotinylated anti-mouse IL-4 at 1:1,000 dilution + SAv-HRP at 1:250 dilution
4	IL-10 (BD, USA)	Anti-mouse IL-10 at 1:250 dilution in sodium phosphate buffer	Biotinylated anti-mouse IL-10 at 1:250 dilution + SAv-HRP at 1:250 dilution
5	IL-12 (BD, USA)	Anti-mouse IL-12 at 1:250 dilution in sodium phosphate buffer	Biotinylated anti-mouse IL-12 at 1:250 dilution + SAv-HRP at 1:250 dilution

6.2.11 Statistical analyses

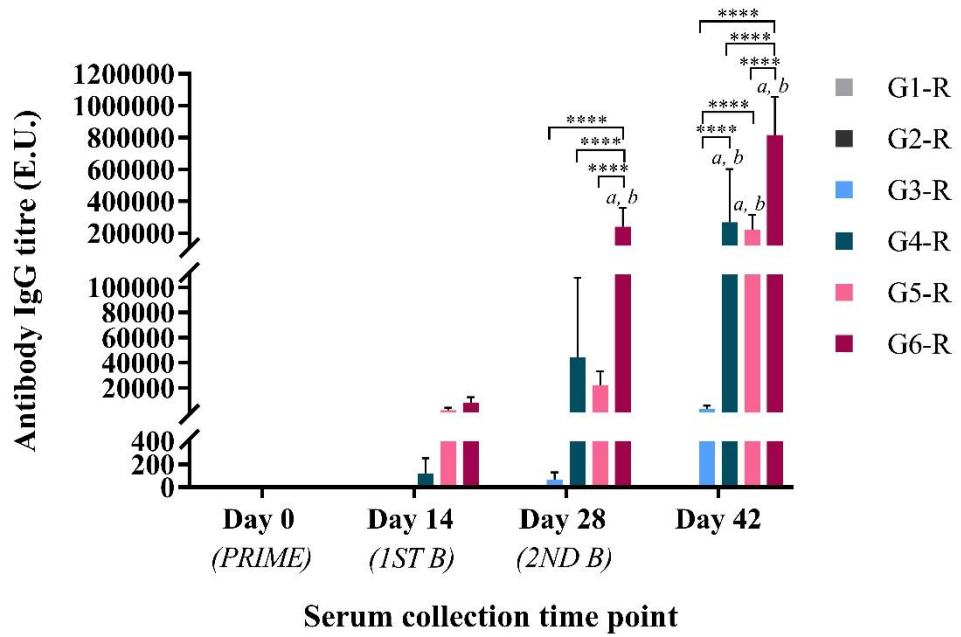
GraphPad Prism 7 was used for all statistical analyses in this study. In **Section 6.2.8.1**, two-way analysis of variance (ANOVA) was performed followed by a Tukey multiple comparisons test to calculate the degree of significance of IgG titre produced by different immunisation groups. In **Section 6.2.8.3**, two-way ANOVA was done followed by a Tukey multiple comparisons test to determine the degree of significance of FRNT50 induced by different immunisation groups. In **Section 6.2.10.2**, two-way ANOVA was used to assess the lymphoproliferative responses of splenocytes stimulated with CTB-cEDIII-KDEL (xTH) antigen and ConA mitogen, followed by a Tukey multiple comparisons test to compare the responses between different vaccine groups. In **Section 6.2.10.4**, two-way ANOVA was performed followed by a Sidak multiple comparisons test to calculate the degree of significance of secretory cytokines production among different vaccine groups. Ultimately, the significance levels were denoted at $P \leq 0.05$ with *, $P \leq 0.01$ with **, $P \leq 0.001$ with ***, and $P \leq 0.0001$ with **** in the charts.

6.3 Results

6.3.1 Measurement of anti-dengue immunoglobulin G (IgG)

6.3.1.1 Recombinant cEDIII proteins

To study the immunogenicity of vaccinated proteins, mouse sera were collected at four different time points to analyse for anti-cEDIII IgG antibody responses. **Figure 6.3** presents the IgG production of BALB/ mice immunised with recombinant cEDIII proteins (**Table 6.1**). Overall, high levels of antibodies were obtained when the mice were vaccinated with proteins formulated with alum. The production of antibodies could be ranked in a descending order of G6-R > G4-R > G5-R > G3-R. The highest anti-cEDIII production was observed from mice immunised with alum-adjuvanted CTB-cEDIII-KDEL (xTH) while cEDIII protein alone gave the weakest response. Comparing the adjuvant efficacy, CTB fusion to cEDIII had significantly boosted the immunogenicity by 63.3 folds while alum-adjuvanted cEDIII had contributed to 77.4-fold increase in anti-cEDIII production by the end of immunisation. A further 3.7-fold boost was obtained when the CTB-cEDIII-KDEL (xTH) protein was formulated with alum. Nonetheless, discernible antibodies production could be observed 2 weeks after priming, particularly for mice immunised with G4-R, G5-R and G6-R. No ELISA signals were seen from day 0 pre-immune samples, as well as the control groups G1-R and G2-R; which thereby validated the specificity of anti-cEDIII IgG response. Similar trend was generally obtained from the two independent experiments.



Annotation	
G1-R: PBS control	G2-R: Alum control
G3-R: cEDIII	G4-R: cEDIII + Alum
G5-R: CTB-cEDIII-KDEL (xTH)	G6-R: CTB-cEDIII-KDEL (xTH) + Alum

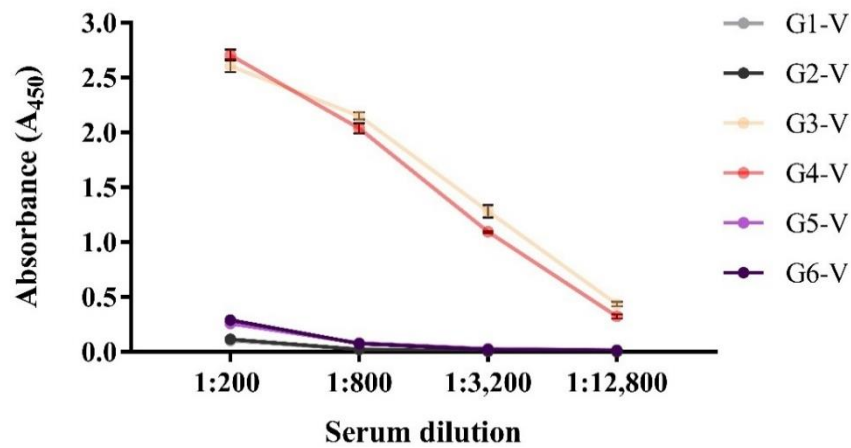
Figure 6.3: cEDIII-specific IgG responses in mice injected with recombinant cEDIII proteins (Table 6.1). The BALB/c mice were immunised intraperitoneally with 20 µg of recombinant proteins at every 14-day intervals over a period of 42 days. The results were shown as mean of E.U. ± SD of two independent experiments (n = 10) against different serum collection time points. Tukey multiple comparisons test was used to calculate the degree of significance between the vaccine groups, by which **** represented $P \leq 0.0001$. Note that *a* indicates a degree of significance of $P \leq 0.0001$ as compared to G1-R control group, while *b* denotes a degree of significance of $P \leq 0.0001$ as compared to G2-R control group. Successful anti-cEDIII antibodies production was observed from all vaccinated groups.

6.3.1.2 Chimeric mHBcAg VLPs-displaying cEDIII

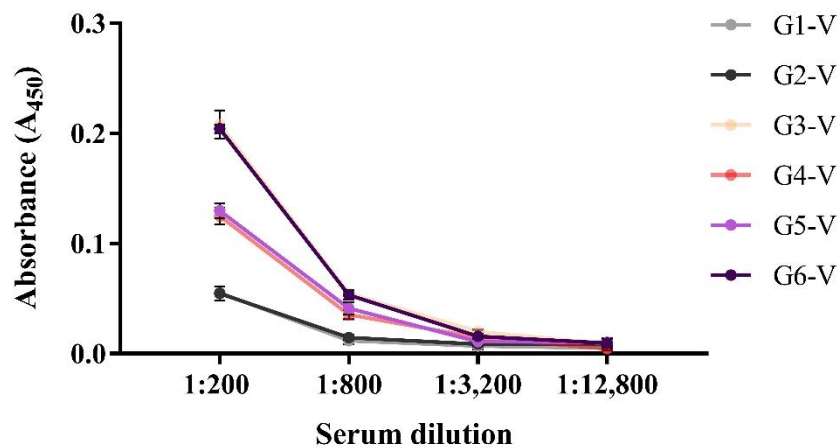
(i) VLPs (a) experiment

During the first immunisation with chimeric mHBcAg VLPs-displaying cEDIII, the presence of cEDIII-specific antibodies could not be detected. Thus, this led to an investigation study to examine whether the administered VLPs were recognised by the mouse immune system (**Figure 6.4**). For that purpose, two purified proteins were used to coat the immuno-plates, namely mEL (Panel A) and mHBcAg-cEDIII (L) (Panel B), by which they were used for injection in VLPs (a) experiment (see **Table 6.2a**). As anticipated, successful antiserum binding was demonstrated as shown in both Panels A and B. This thereby signified that antibodies were successfully generated against the particle. As the responses for G5-V and G6-V were noticeably lower in Panel A, this led to the speculation that the administered dosage of G5-V and G6-V may be insufficient. G3-V and G4-V refers to mEL VLPs, which also harbour the same mHBcAg backbone except that they are smaller in size due to the absence of cEDIII insert in the c/e1 loop. Because of the molecular size difference, a concentration of 20 µg may not reflect an equivalent number of particles in the injection dose.

Panel A Mouse Sera Anti-mEL Humoral Response



Panel B Mouse Sera Anti-mHBcAg-cEDIII (L) Humoral Response

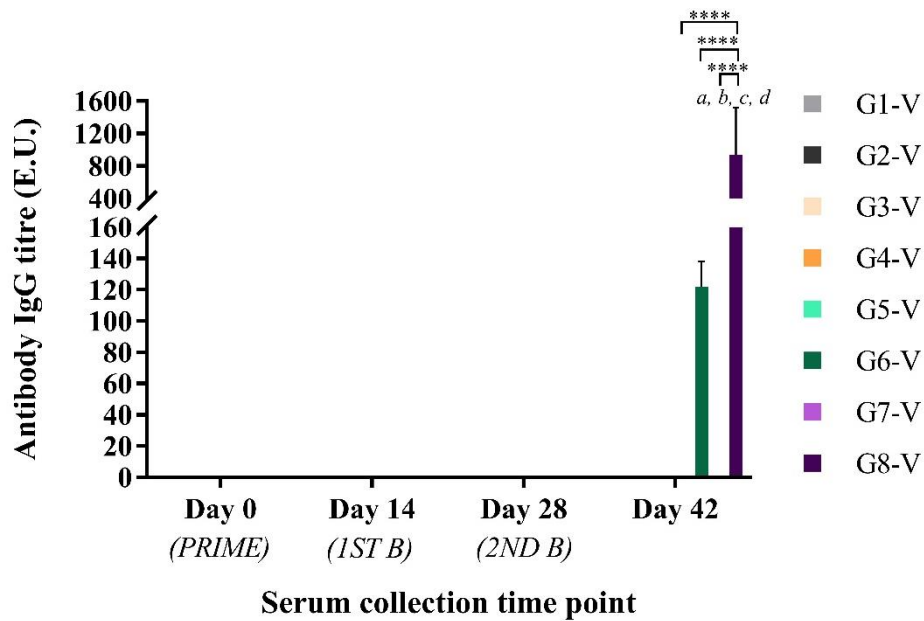


Annotation	
G1-V: PBS control	G2-V: Alum control
G3-V: mEL	G4-V: mEL + Alum
G5-V: mHBcAg-cEDIII (L)	G6-V: mHBcAg-cEDIII (L) + Alum

Figure 6.4: Examination of the mEL-specific (Panel A) and mHBcAg-cEDIII (L)-specific (Panel B) IgG titres in BALB/c mice. The serum samples (n = 5) were pooled in group and assayed in duplicate wells. Results were expressed as the average of A₄₅₀ readings of corresponding groups. Antiserum binding of G5-V and G6-V was demonstrated in both panels.

(ii) VLPs (b) experiment

The anti-cEDIII IgG response induced by chimeric mHBcAg VLPs-displaying cEDIII from VLPs (b) experiment (**Table 6.2b**) was presented in **Figure 6.5**. In fact, this result presents a successful modification to the first experiment, referred as VLPs (a), which did not produce cEDIII-specific antibodies but showed response against mEL and mHBcAg-cEDIII (L). To this end, the BALB/c mice were injected with an increase dosage of 30 µg for G5-V, G6-V, G7-V and G8-V. ELISA results revealed that anti-cEDIII IgG could be found from G6-V and G8-V. Apparently, formulation with alum had boosted the immunogenicity of chimeric mHBcAg VLPs-displaying cEDIII. Slightly higher anti-cEDIII response was provided by mHBcAg-cEDIII VLPs as compared to mHBcAg-cEDIII (L) VLPs. No signals were seen from the control groups G1-V to G4-V, as well as the day 0 pre-immune samples (**Figure 6.5**).



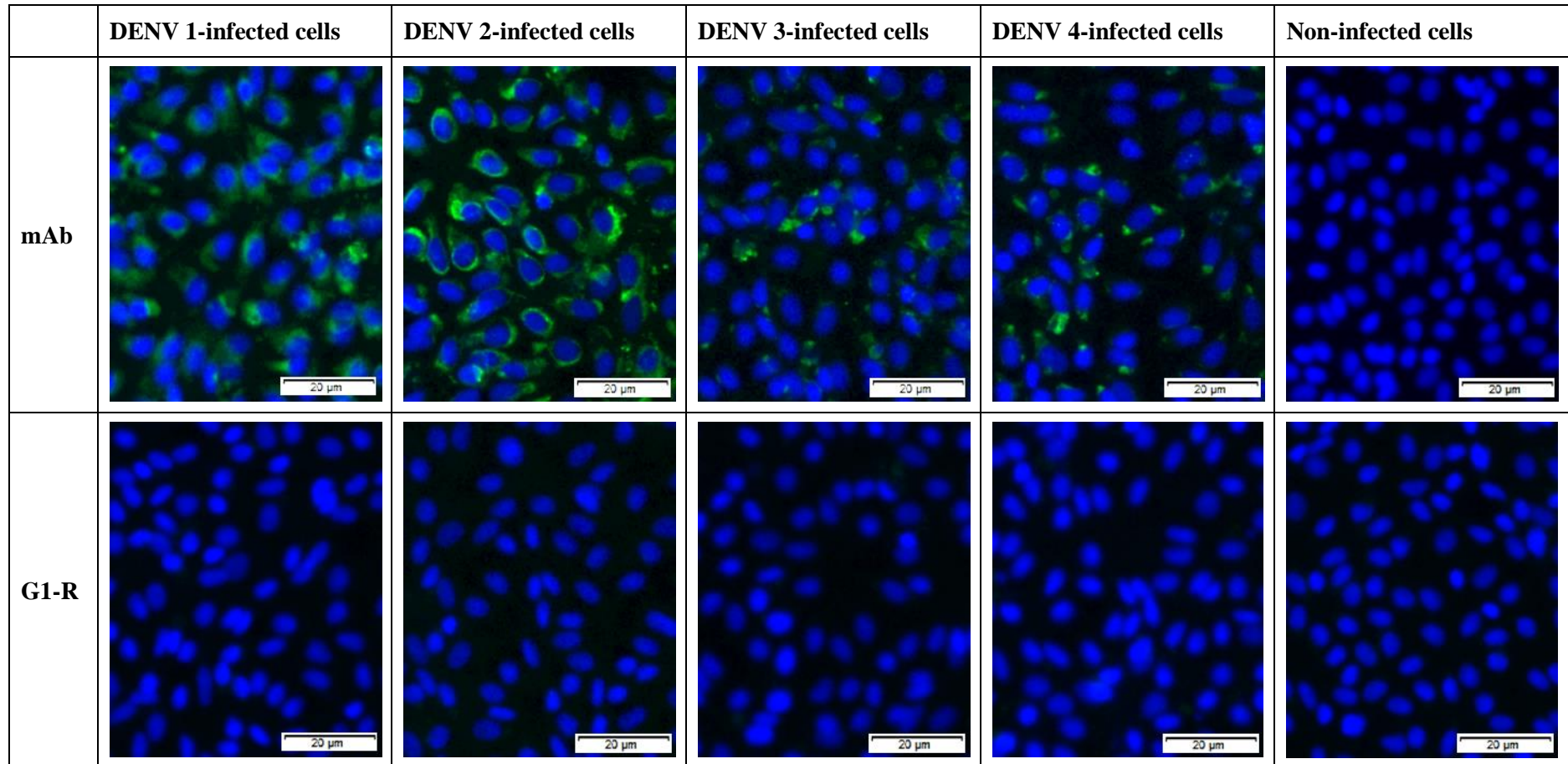
Annotation	
G1-V: PBS control	G2-V: Alum control
G3-V: mEL	G4-V: mEL + Alum
G5-V: mHBcAg-cEDIII (L)	G6-V: mHBcAg-cEDIII (L) + Alum
G7-V: mHBcAg-cEDIII	G8-V: mHBcAg-cEDIII + Alum

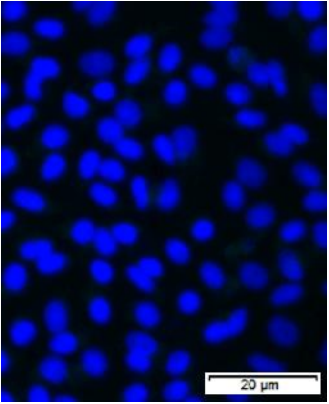
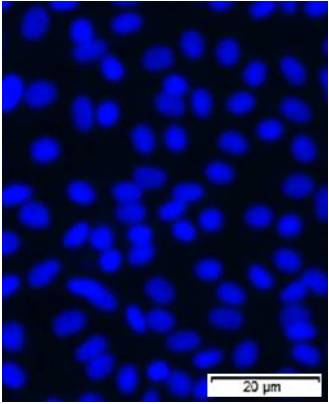
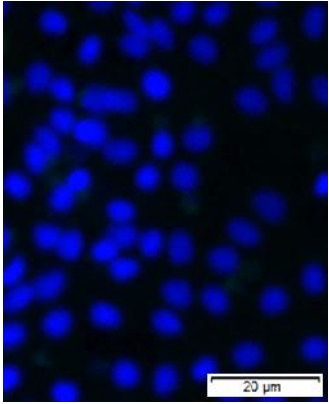
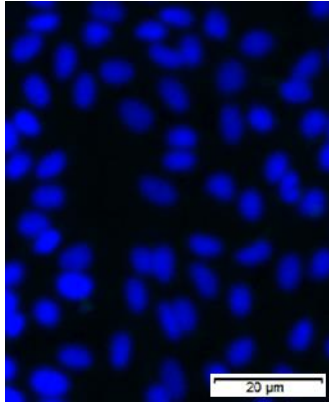
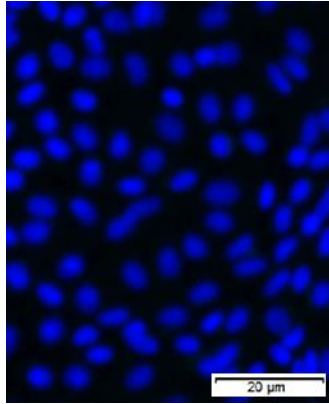
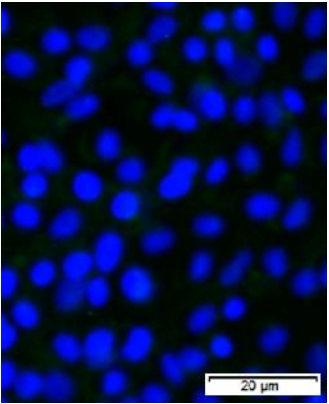
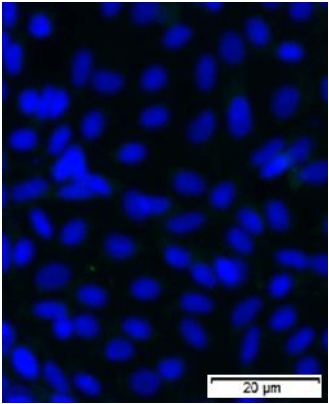
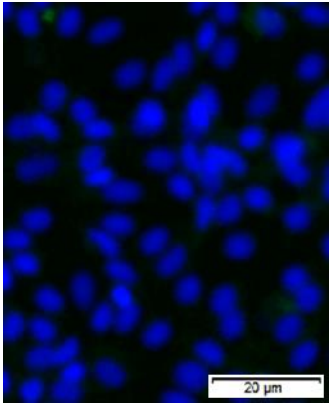
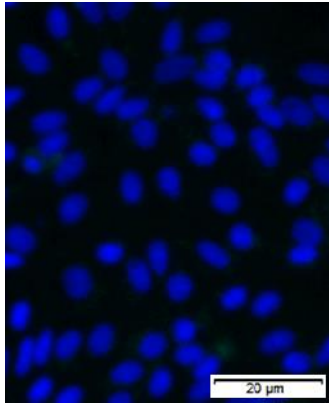
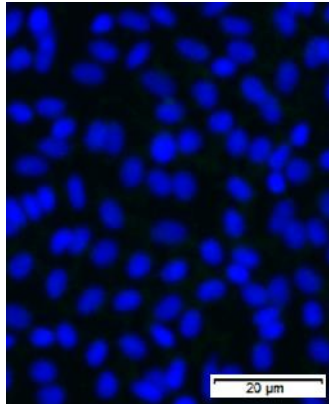
Figure 6.5: cEDIII-specific IgG antibody titres in BALB/c mice vaccinated with chimeric mHBcAg VLPs displaying cEDIII (VLPs (b) experiment; **Table 6.2b**). The mice (n = 4) were injected intraperitoneally with 30 µg of chimeric VLPs at every 14-day intervals over a period of 42 days. The results were presented as mean of E.U. ± SD against different time points of serum collection. Tukey multiple comparisons test was used to calculate the degree of significance between the vaccine groups, whereby **** signified $P \leq 0.0001$. Note that the symbols *a, b, c, d* indicate the degree of significance of $P \leq 0.0001$ as compared to G1-V, G2-V, G3-V and G4-V, correspondingly. Production of anti-cEDIII antibodies could be detected from G6-V and G8-V.

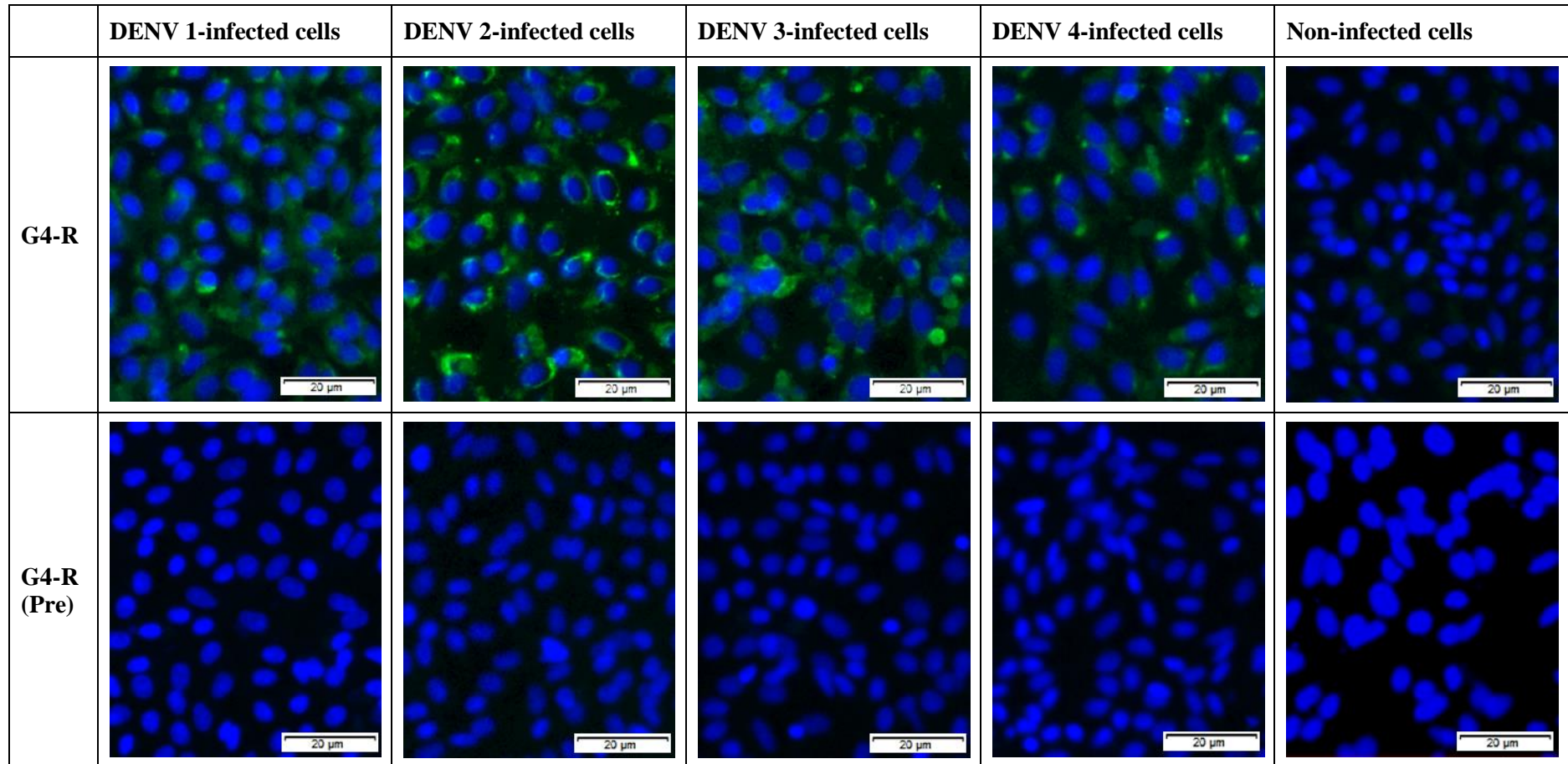
6.3.2 Immunofluorescence detection of serum antibodies binding to native dengue virus

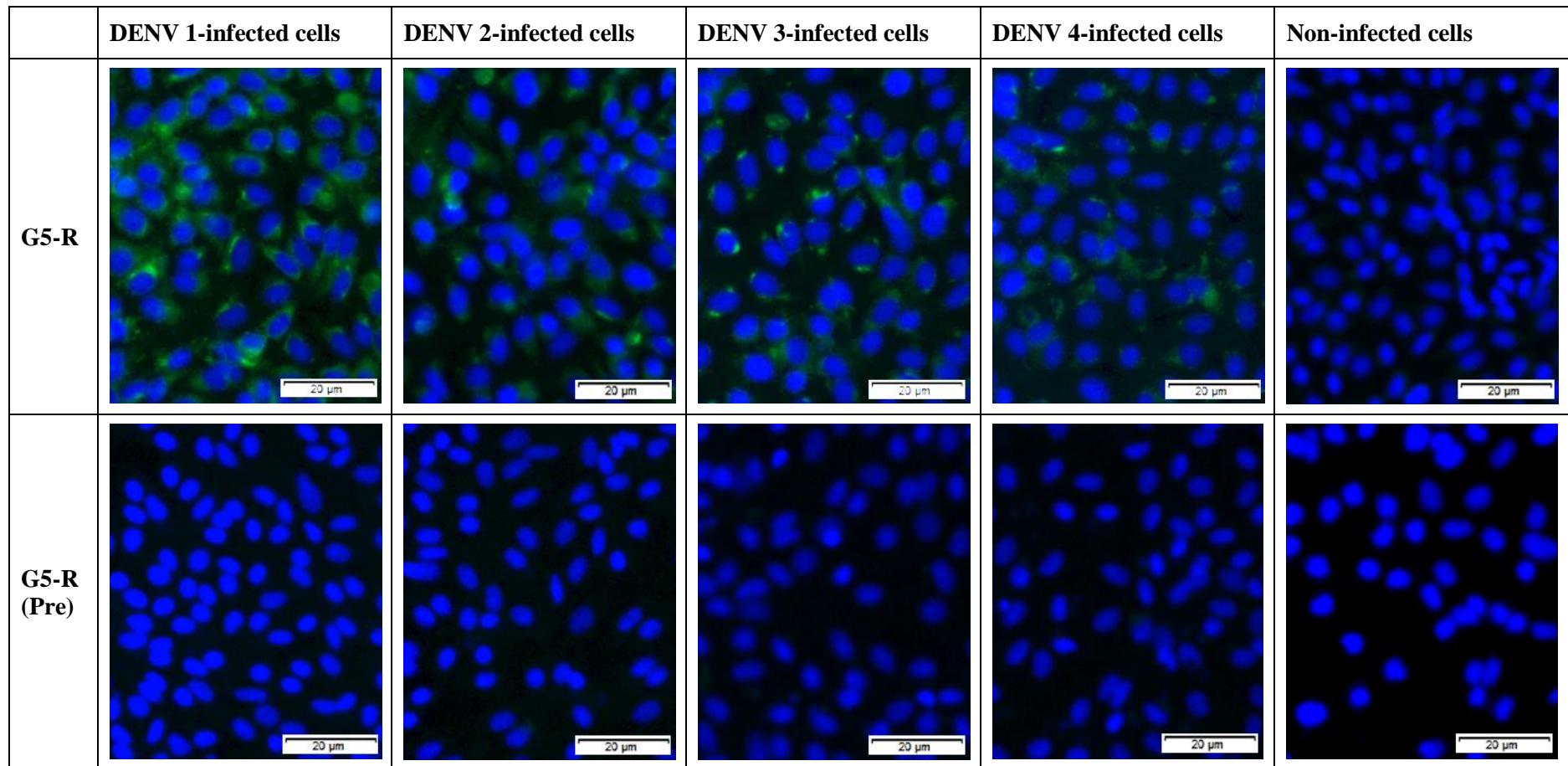
6.3.2.1 Recombinant cEDIII proteins

Following the successful detection of anti-cEDIII IgG, mouse sera were pooled in each group to test for recognition of native DENV 1-4 serotypes via IFA. **Figure 6.6** presents the immunofluorescence results for antibodies raised against recombinant cEDIII protein. After applying the heat-inactivated sera on DENV-infected and non-infected Vero cells, green fluorescence was detected from all the infected cells treated with G4-R, G5-R and G6-R serum samples. Correspondingly, their pre-immune sera (Pre) did not bind to any of the native dengue viruses. Meanwhile, green fluorescence was not seen from the Vero cells incubated with G3-R sera, despite of the modest IgG production. Control groups, G1-R and G2-R, did not recognise the native viruses as expected. For validation purpose, DENV 1-4 monoclonal antibody (mAb) was incorporated as a positive control which showed intense green fluorescence. Hoechst dye was used to stain the nuclei of Vero cells with blue fluorescence. Similar observations were recorded from the two independent experiments.



	DENV 1-infected cells	DENV 2-infected cells	DENV 3-infected cells	DENV 4-infected cells	Non-infected cells
G2-R					
G3-R					





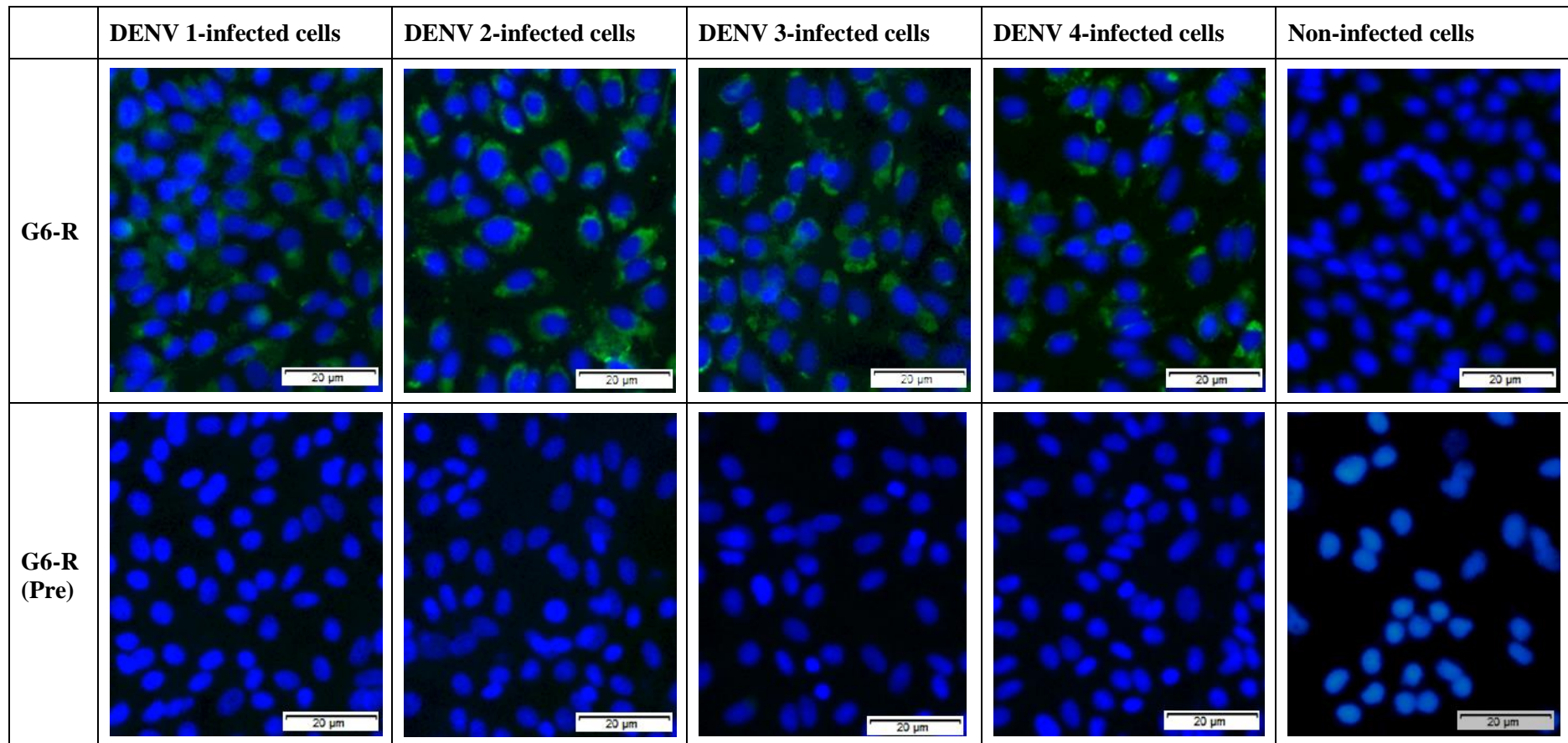
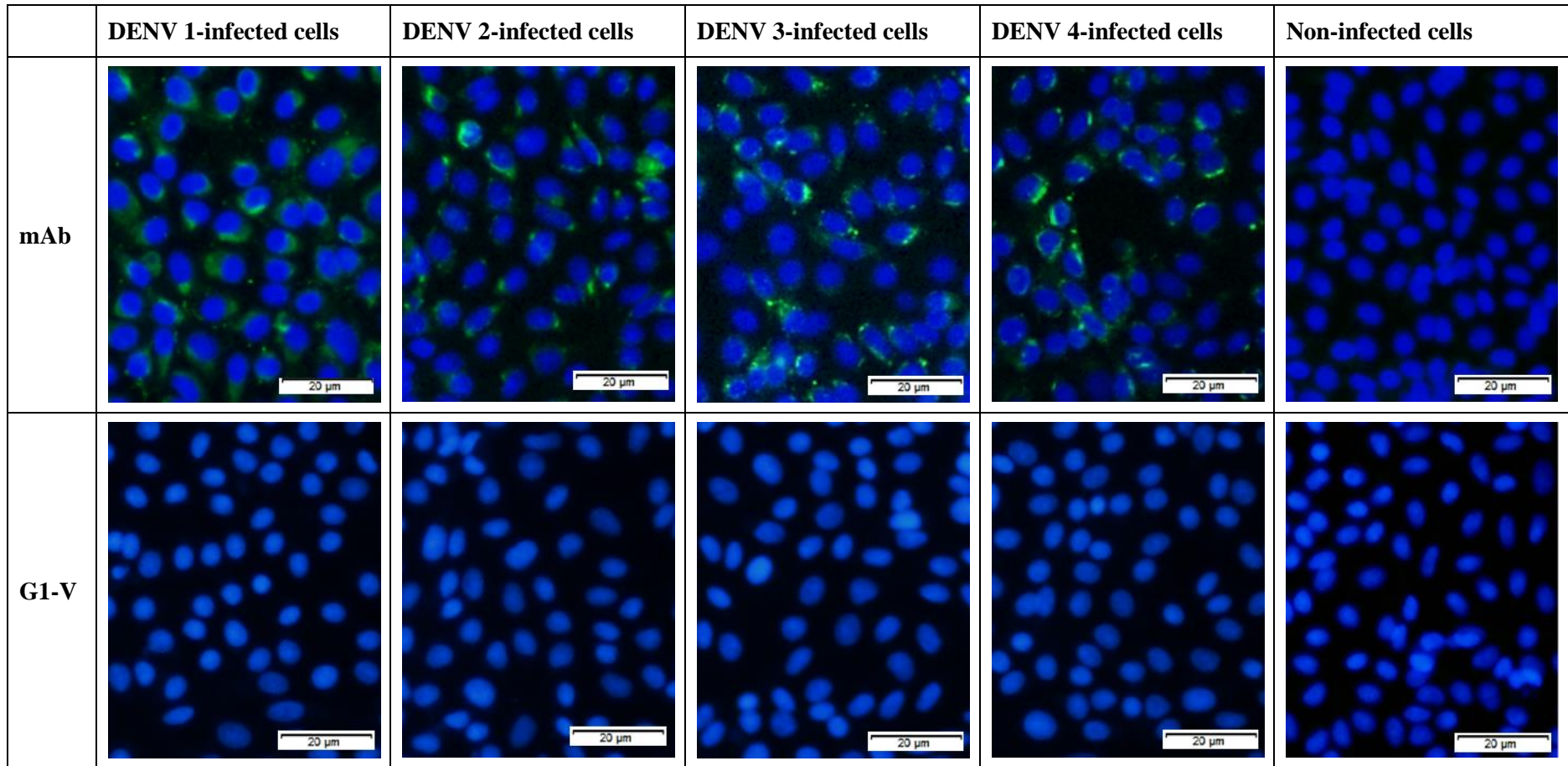


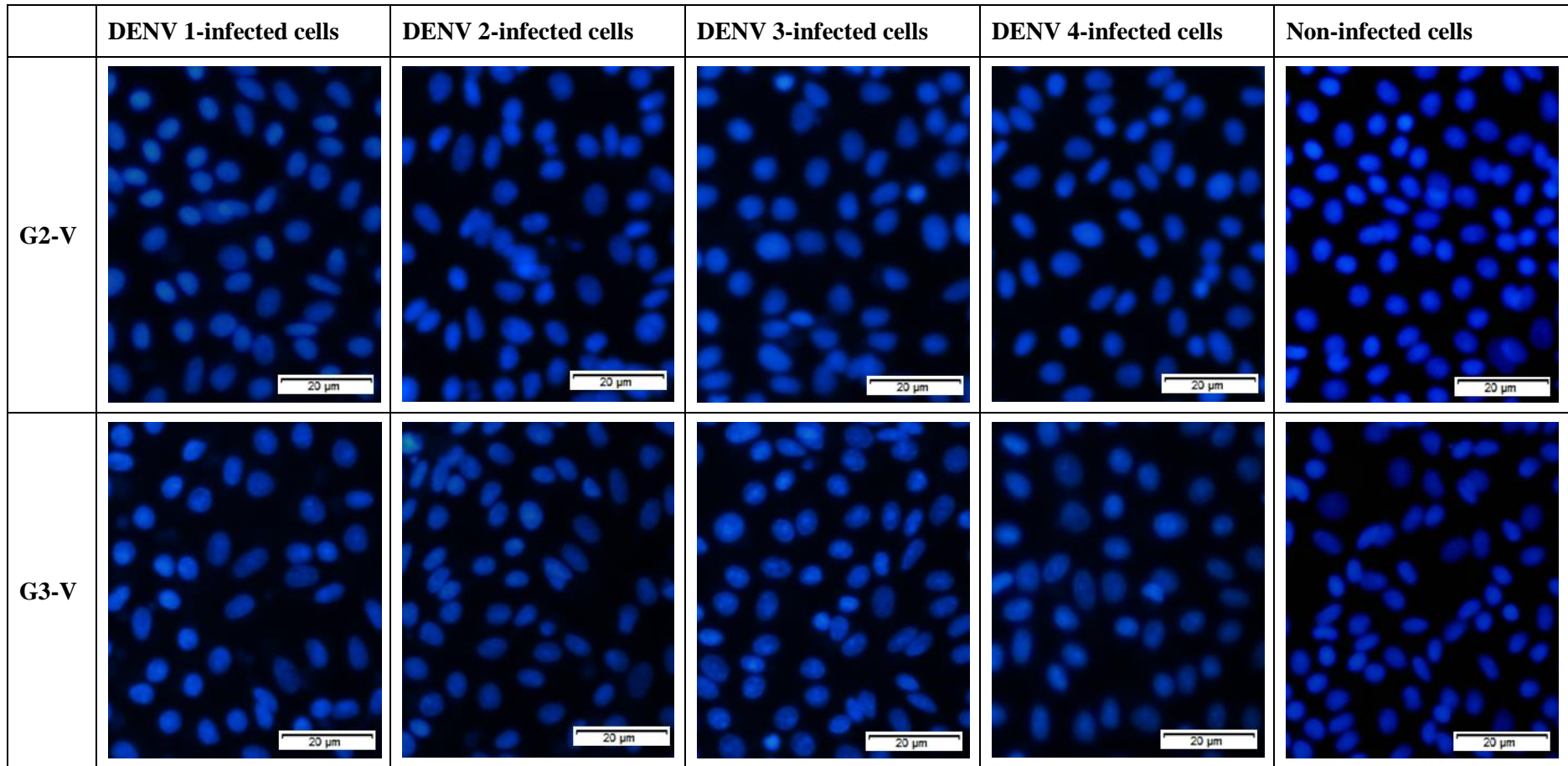
Figure 6.6: Immunofluorescence profiles of cross-reactivity between sera of mice immunised with recombinant cEDIII proteins and DENV 1-4 serotypes.

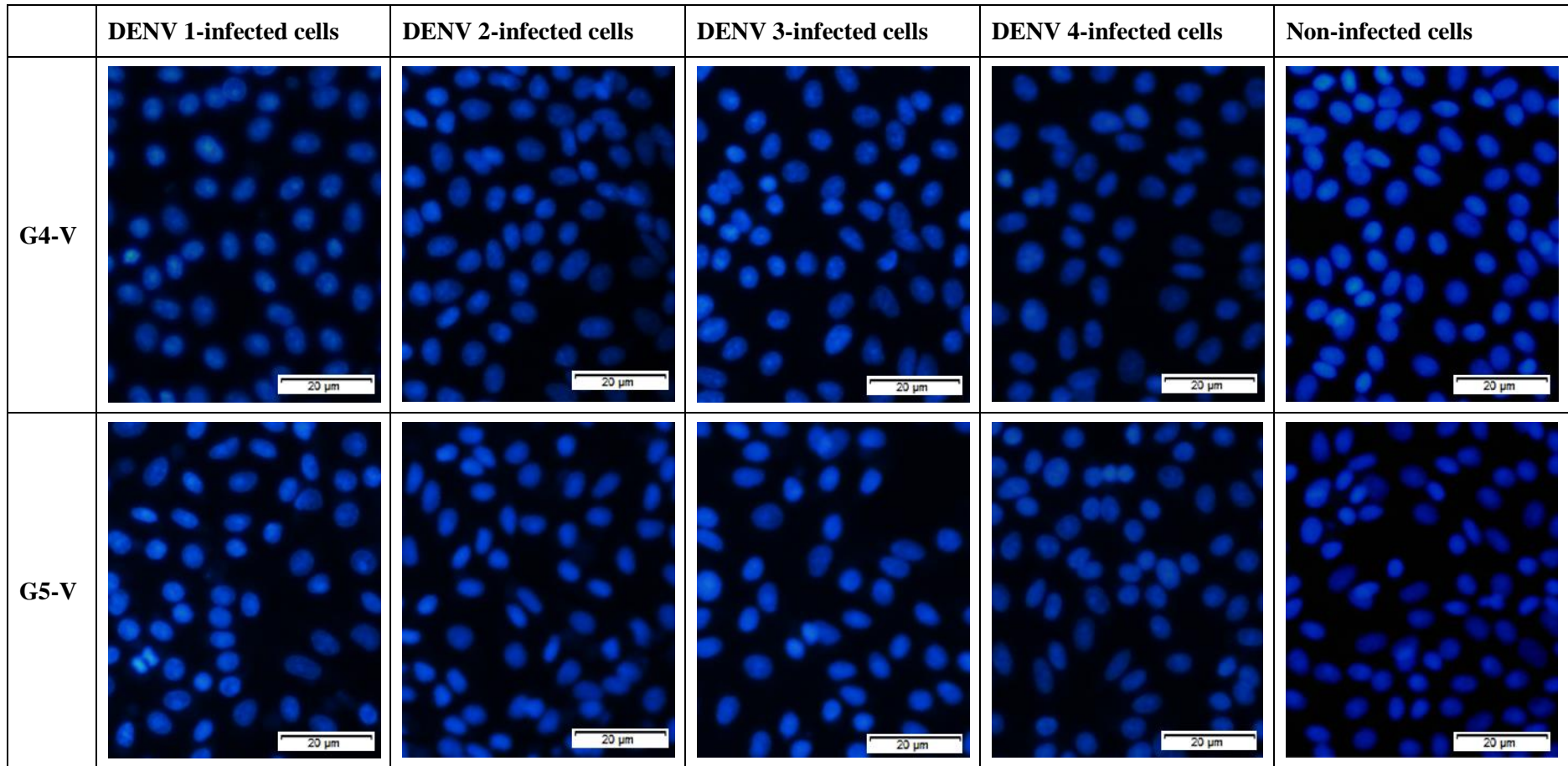
Visualisation was made at 200X magnification, with successful recognition of viruses portrayed by green dye emission.

6.3.2.2 Chimeric mHBcAg VLPs-displaying cEDIII

After assessing the cEDIII-specific response in mice, IFA was used to test the ability of antibodies raised against mHBcAg VLPs-displaying cEDIII to recognise native DENV 1-4 serotypes. The immunofluorescence results for mouse sera collected from VLPs (a) experiment and VLPs (b) experiment are presented in **Figure 6.7** and **Figure 6.8**, respectively. For both VLPs (a) and VLPs (b), none of the groups had reacted with the native DENV 1-4 except for mAb that served as the positive control. No green fluorescence was detected from the samples G5-V and G6-V as shown in **Figure 6.7**, as well as samples G5-V, G6-V, G7-V and G8-V as shown in **Figure 6.8**, which made them indistinguishable to the G1-V and G2-V control groups. In fact, only Hoechst-stained cell nuclei were visible in all samples.







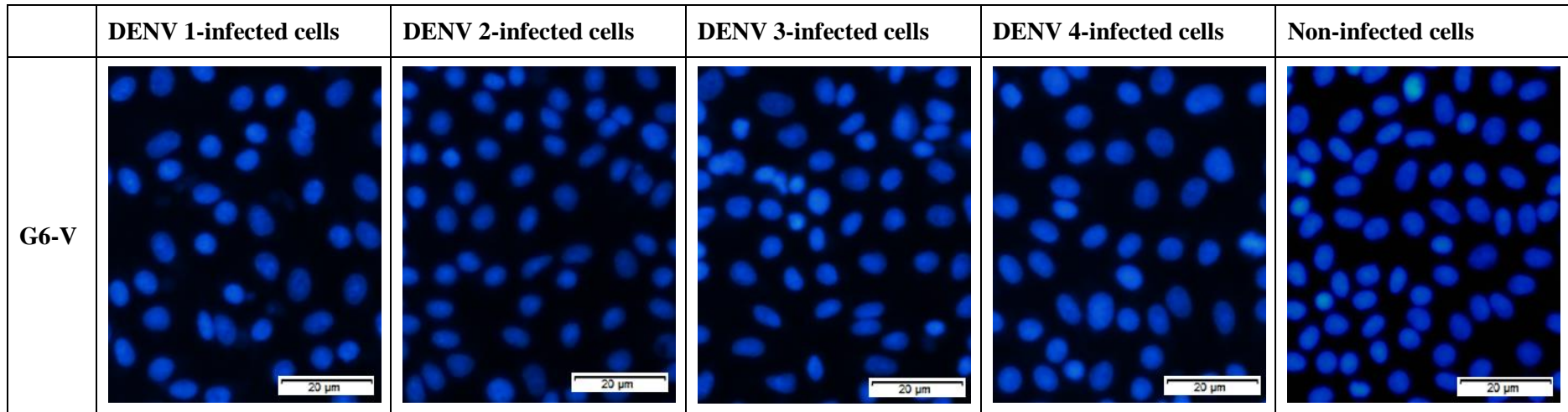
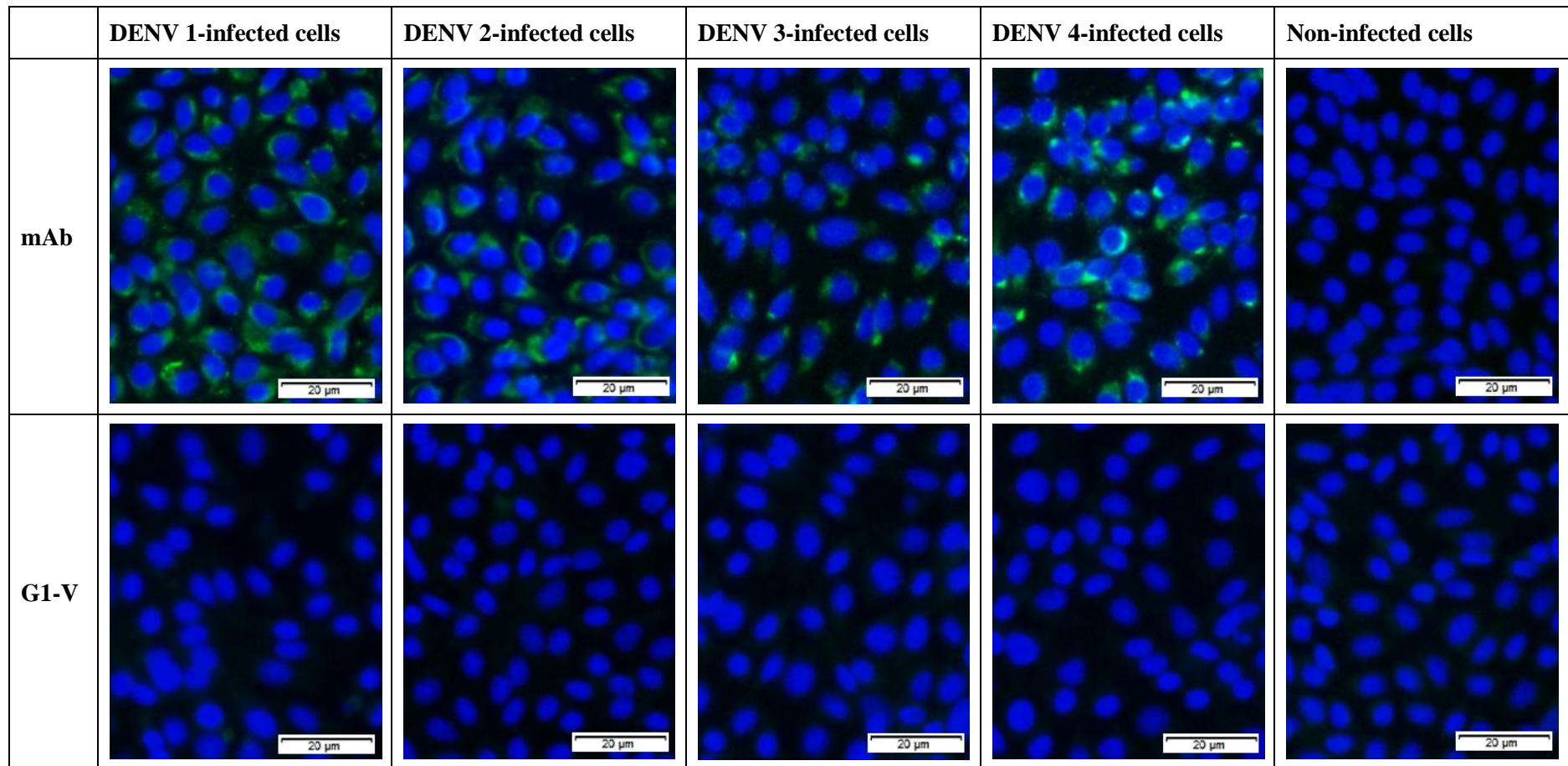
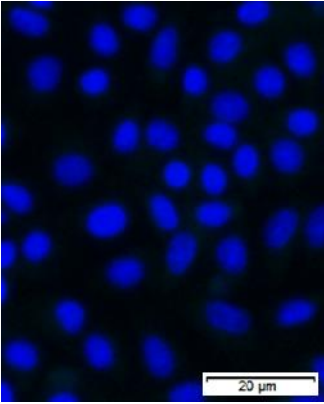
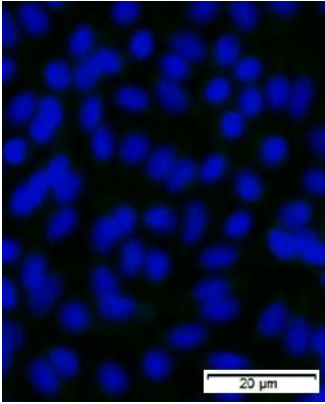
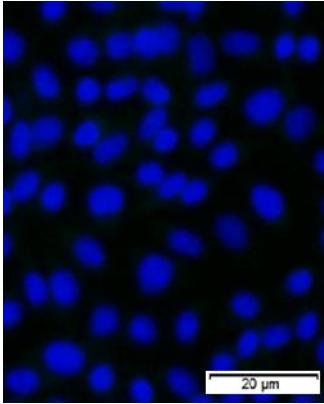
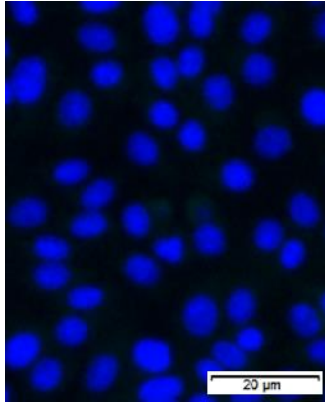
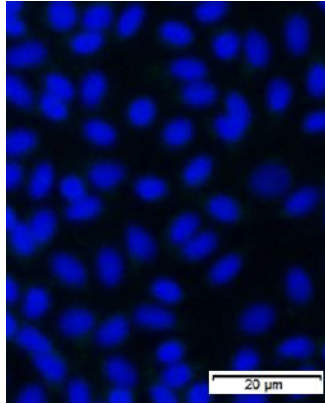
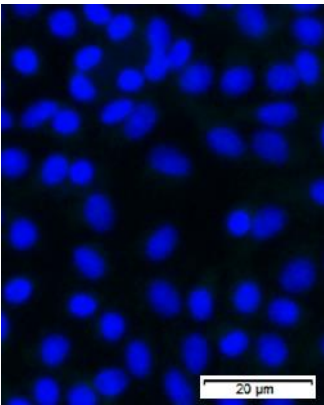
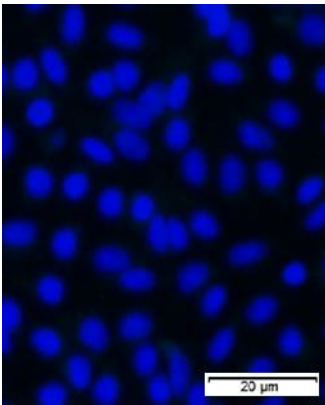
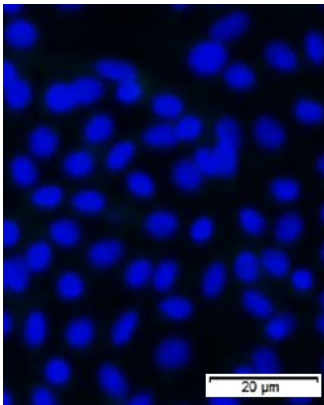
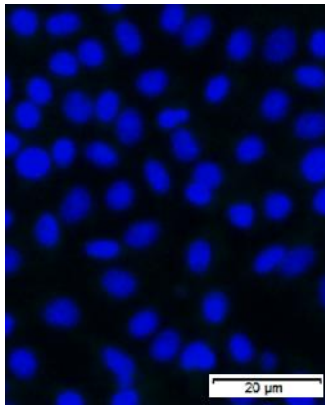
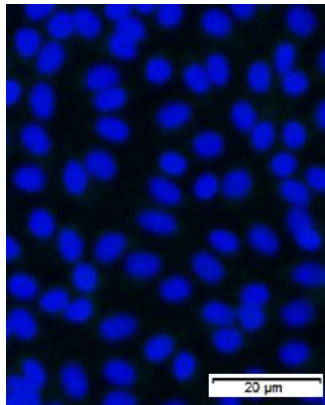
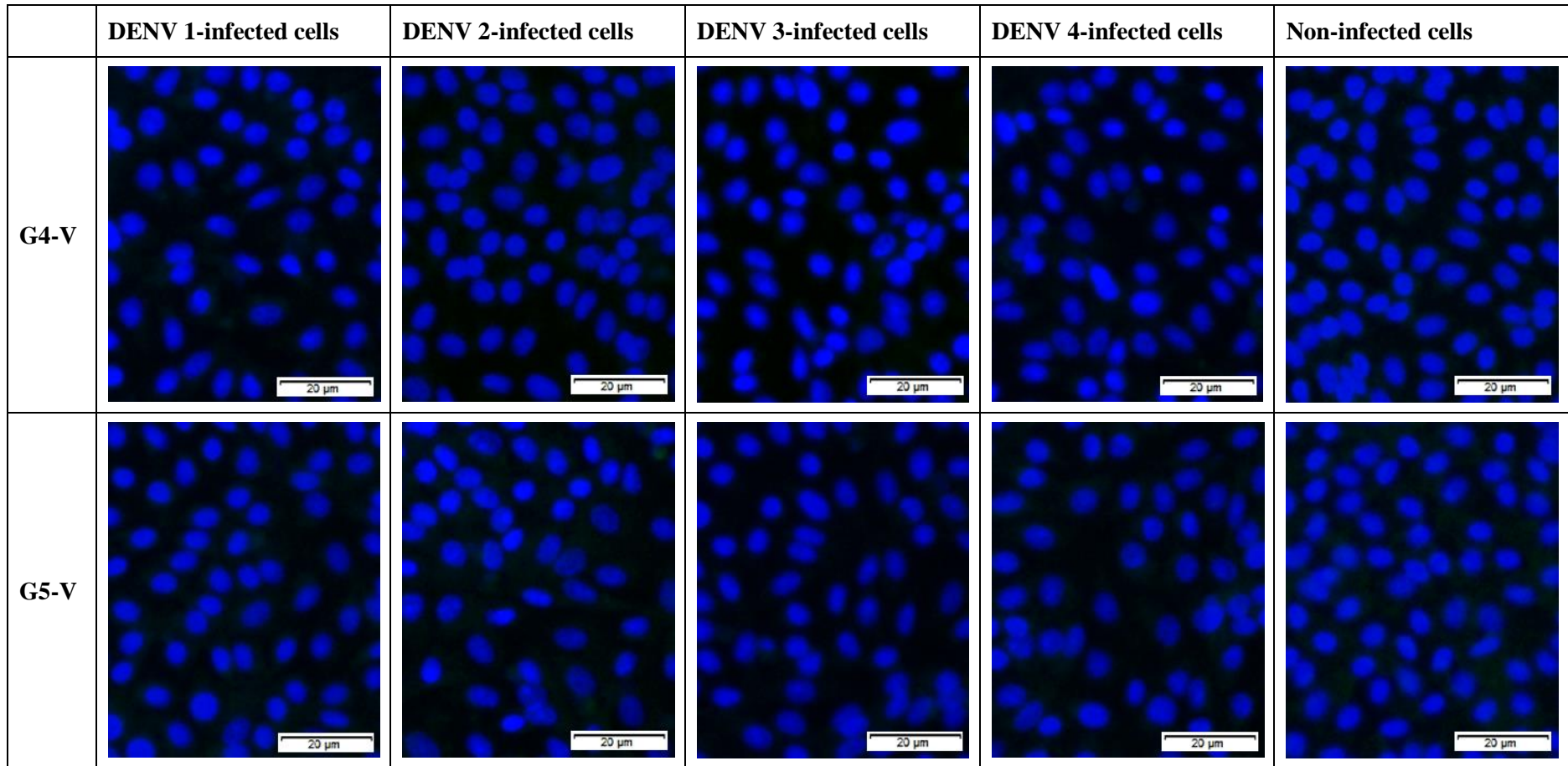
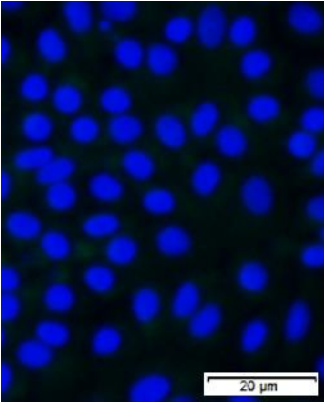
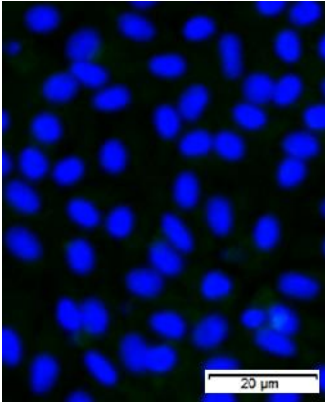
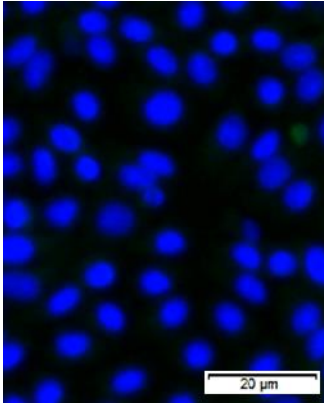
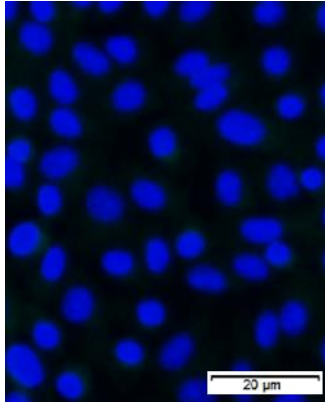
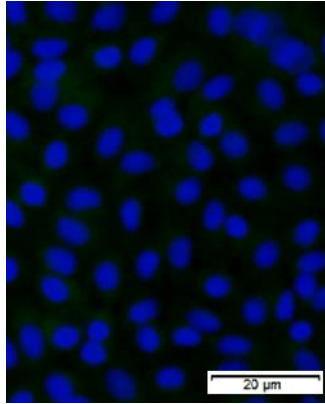
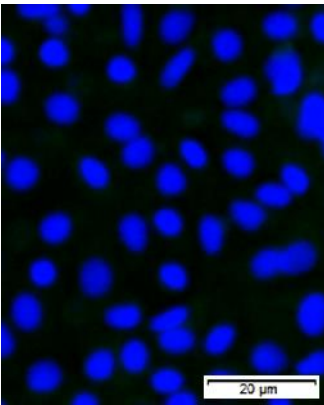
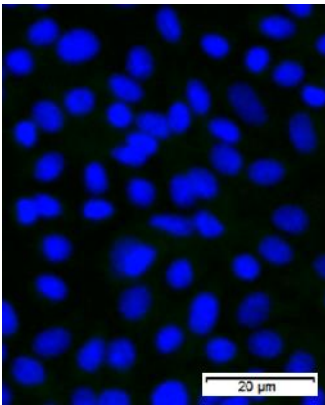
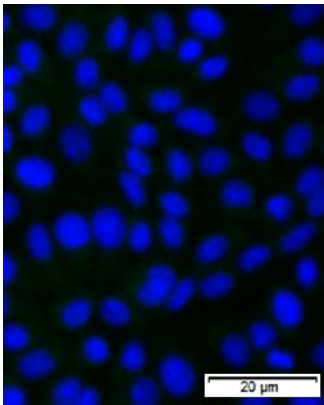
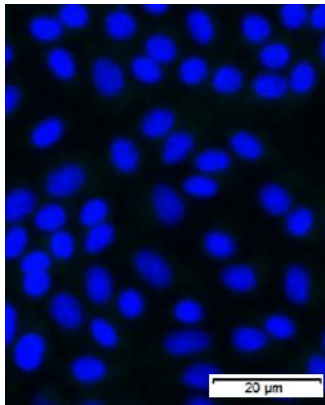
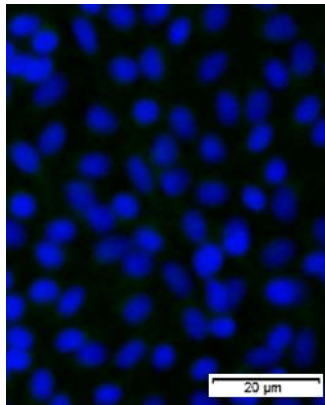


Figure 6.7: Immunofluorescence profiles of interactions between mouse sera collected from VLPs (a) experiment and DENV 1-4 serotypes. Images were captured at the magnification of 200X. All the mouse sera failed to react with the native viruses.



	DENV 1-infected cells	DENV 2-infected cells	DENV 3-infected cells	DENV 4-infected cells	Non-infected cells
G2-V					
G3-V					



	DENV 1-infected cells	DENV 2-infected cells	DENV 3-infected cells	DENV 4-infected cells	Non-infected cells
G6-V					
G7-V					

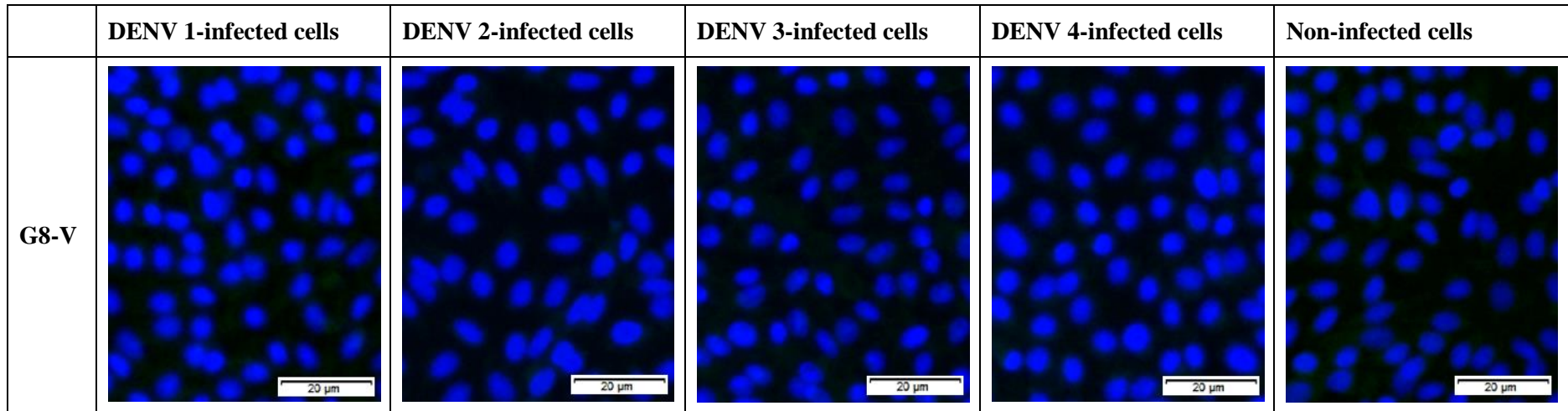


Figure 6.8: Immunofluorescence profiles of cross-reactivity between mouse sera collected from VLPs (b) experiment and DENV 1-4 serotypes. Observation was made at 200X magnification, with which all the serum samples failed to bind with the native viruses.

6.3.3 Evaluation of virus neutralising antibody production

6.3.3.1 Recombinant cEDIII proteins

Following the immunofluorescence recognition of native dengue viruses, the neutralisation potential of raised antibodies was further evaluated via FRNT. **Figure 6.9** illustrates the neutralisation activities of the sera collected from mice immunised with recombinant cEDIII proteins. Notably, the mouse sera of G4-R, G5-R and G6-R demonstrated high reduction of virus FFU as compared to G1-R and G2-R control groups. In specific, G4-R and G6-R showed significant neutralising activities against DENV serotypes 2, 3 and 4. Albeit their responses against DENV 1 was not statistically significant, but their neutralising ability was evidenced. Meanwhile, G5-R exhibited an equivalent inhibition of all four serotypes. A sample of DENV-infected patient serum was included as positive control, by which could neutralise all the four DENV serotypes at the highest dilution (1:675) tested. Overall, the results imply that both recombinant cEDIII and CTB-cEDIII-KDEL (xTH) proteins could simultaneously neutralise DENV serotypes 1-4, and stronger response is acquired with the use of alum adjuvant.

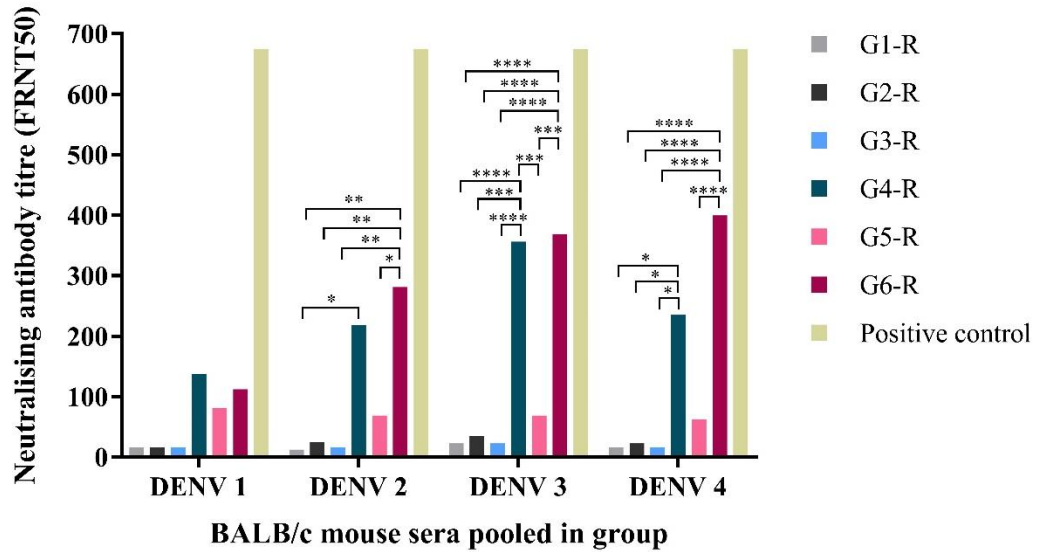


Figure 6.9: Virus neutralising antibody responses of recombinant cEDIII proteins against DENV 1-4 serotypes. Mouse sera from day 42 were pooled in each group and serially-diluted in three-fold magnitude starting from 1:25 dilution. The neutralising antibody titre was determined based on the reciprocal of the highest serum dilution that neutralised $\geq 50\%$ of the DENV (FRNT50), as compared to virus-only control. Results ($n = 8$) were expressed as the mean FRNT50 of two independent mouse experiments. Tukey multiple comparisons test was used to calculate the degree of significance between the vaccine groups where; $*P \leq 0.05$, $**P \leq 0.01$, $***P \leq 0.001$ and $****P \leq 0.0001$. Significant neutralisation activities were observed from G4-R and G6-R. A DENV-infected patient serum was used as a positive control, which could neutralise DENV 1-4 serotypes at the highest dilution tested.

6.3.3.2 Chimeric mHBcAg VLPs-displaying cEDIII

(i) VLPs (a) experiment

The FRNT results for antibodies raised against mHBcAg VLPs-displaying cEDIII from VLPs (a) experiment are shown in **Figure 6.10**. However, no neutralising response was obtained in mice vaccinated with G5-V and G6-V, by which correspond to the mHBcAg-cEDIII (L) VLPs. The assay was shown to be valid as the positive control could neutralise the DENV at the highest dilution of 1:675. In line with the IFA results (**Figure 6.7**), the antiserum was not able to bind with the native dengue viruses, and therefore did not show an inhibition of virus infectivity.

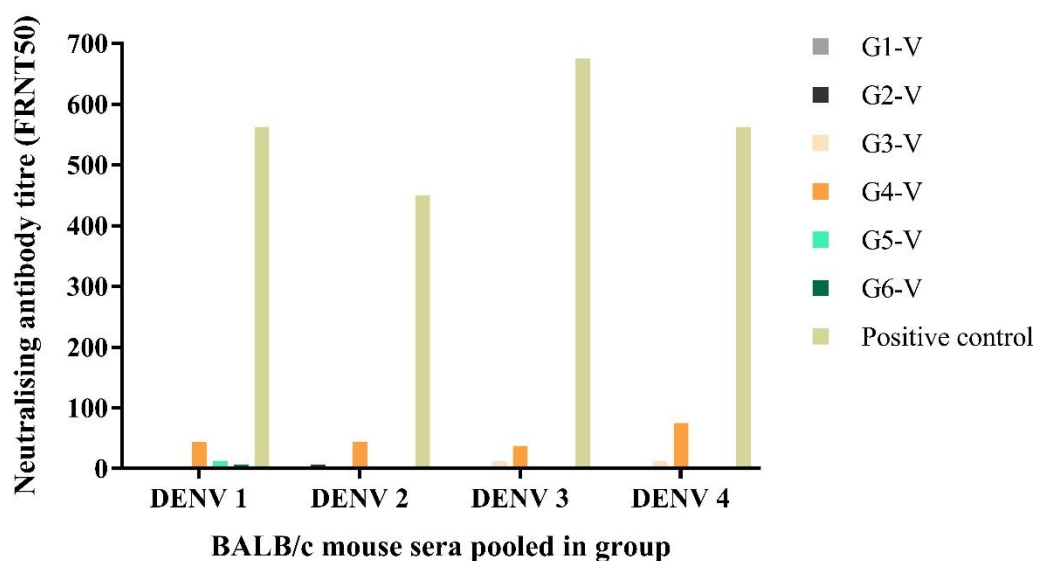


Figure 6.10: Virus neutralising antibody responses of chimeric mHBcAg VLPs-displaying cEDIII against four serotypes of DENV (VLPs (a) experiment). Mouse sera from day 42 were pooled in each group and serially-diluted in three-fold magnitude starting from 1:25 dilution. Neutralising antibody titre (FRNT50) was determined based on the reciprocal of the highest serum dilution that neutralised $\geq 50\%$ of the DENV as compared to virus-only control. The results ($n = 4$) are

expressed as the mean FRNT50 of two independent FRNT experiments. No significant neutralising activities were detected from all the immunisation groups. The positive control represents a DENV-infected patient serum which can neutralise all four serotypes and hence is used to validate the assay.

(ii) VLPs (b) experiment

Meanwhile, **Figure 6.11** presents the neutralising ability of the antiserum raised against the chimeric mHBcAg VLPs in VLPs (b) experiment. Although cEDIII-specific IgG production could be detected following the change of antigen dose for G5-V to G8-V (**Figure 6.5**), however no neutralising activities against DENV 1-4 were noted except for the positive control. In fact, the serum sample of DENV-infected patient had demonstrated strong neutralising responses at dilution up to 1:675. Since the antiserum failed to interact with native dengue viruses (**Figure 6.8**), it made sense that no reduction in virus FFU was obtained.

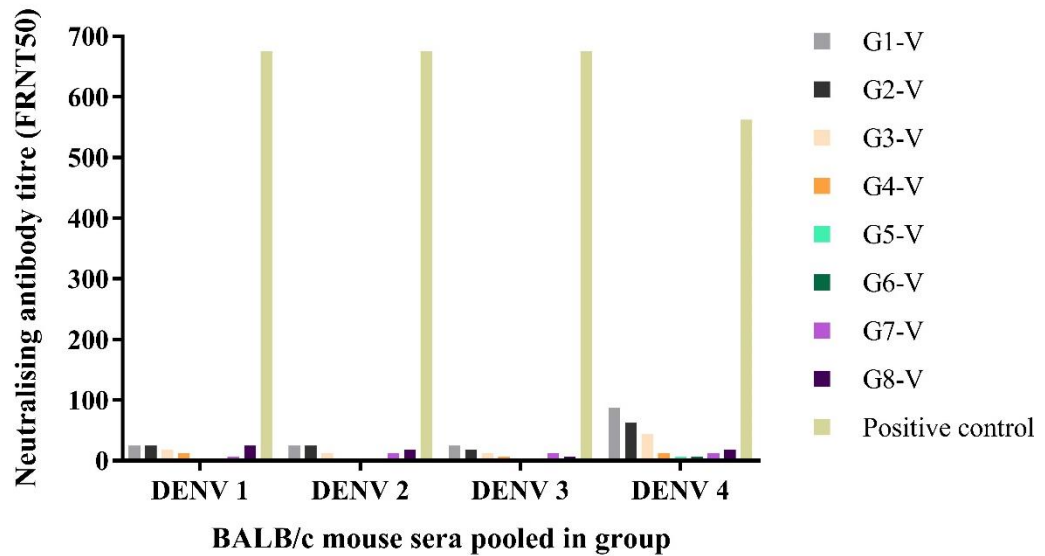


Figure 6.11: Virus neutralising antibody responses of chimeric mHBcAg VLPs-displaying cEDIII against DENV 1-4 serotypes (VLPs (b) experiment). Mouse sera from day 42 were pooled in each group and serially-diluted in three-fold magnitude starting from 1:25 dilution. The neutralising antibody titre (FRNT50) was calculated as the reciprocal of highest dilution that yielded 50% reduction of FFU as compared to the virus-only control. Results (n = 4) are expressed as the mean FRNT50 of two independent FRNT experiments. Apart from the positive control, neutralising antibody activities were not observed from mice immunised with the vaccine groups.

6.3.4 Assessing lymphocytes proliferation following antigen stimulation

6.3.4.1 Recombinant cEDIII proteins

Cell-mediated immune responses were assessed based on the ability of mouse splenocytes to proliferate upon antigen stimulation. **Figure 6.12** shows the cEDIII-specific lymphoproliferative response of BALB/c mice immunised with recombinant cEDIII proteins. A cut-off line was drawn at $SI = 1$, and only value above 1 was perceived as positive cell proliferation. ConA was used as a non-specific stimulus, in which splenocytes from all the groups had responded non-specifically to this mitogen. Although no significant differences were obtained among the antigen-stimulated G1-R to G6-R, however a relative comparison could be made to gauge the efficacy of different vaccine groups. In comparison to G3-R, the splenocytes of G4-R, G5-R and G6-R had showed higher cell proliferation. The SI of G3-R splenocytes however were somewhat comparable to the G1-R and G2-R control groups. The results are expressed as an average of two independent experiments.

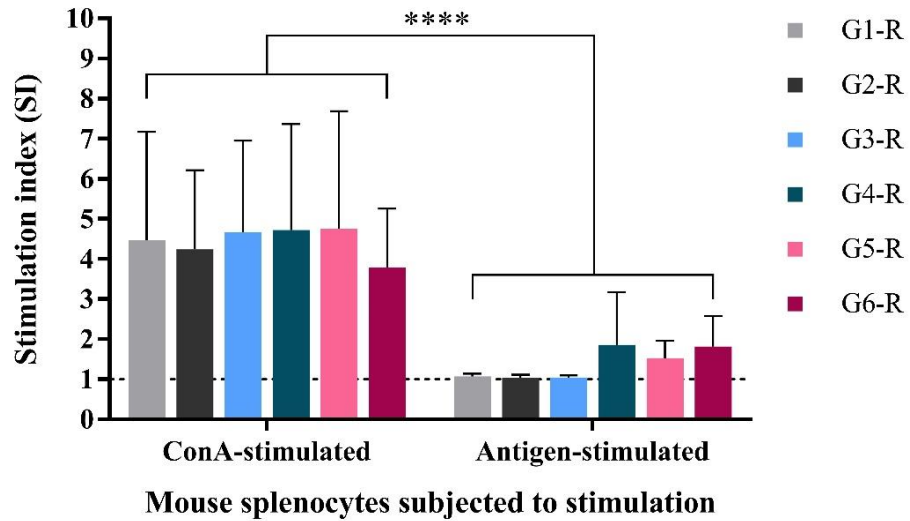


Figure 6.12: Lymphoproliferative responses of the splenocytes of BALB/c mice vaccinated with recombinant cEDIII proteins. Mouse spleens were pooled in group for splenocytes culture, and co-treated with ConA mitogen at 5 $\mu\text{g/ml}$ and CTB-cEDIII-KDEL (xTH) antigen at 5 $\mu\text{g/ml}$. The SI was calculated as the triplicate A_{370} readings of stimulated splenocytes over unstimulated splenocytes. Value of 1 (dashed line) indicates that there is no difference in proliferation between stimulated and unstimulated. The graph was plotted as the mean of $SI \pm SD$ from two independent mouse experiments. Two-way ANOVA indicates that a degree of significance of **** $P \leq 0.0001$ is obtained between ConA-stimulated and antigen-stimulated splenocytes.

6.3.4.2 Chimeric mHBcAg VLPs-displaying cEDIII

(i) VLPs (a) experiment

To study the lymphoproliferative responses of BALB/c mice vaccinated with chimeric mHBcAg VLPs from VLPs (a) experiment, BrdU assay was performed as shown in **Figure 6.13**. A cut-off line at SI = 1 was used to differentiate those with positive cell proliferation at value above 1. As expected, all the splenocytes groups had responded non-specifically to ConA stimulus. However, no sign of cell proliferation was detected from G5-V and G6-V, which were comparable to the G1-V to G4-V control groups. Taken together, these results have demonstrated that the mouse splenocytes are not responsive to cEDIII antigen and would not be used for further analyses.

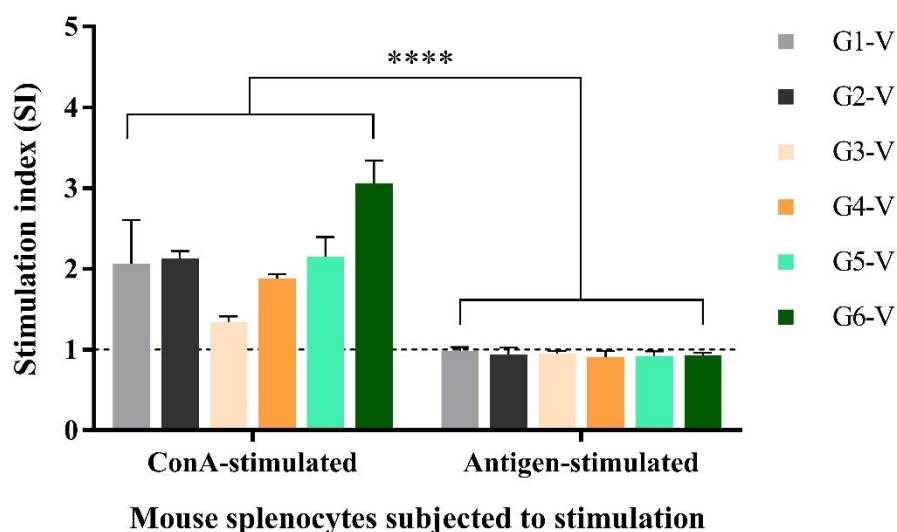


Figure 6.13: Lymphocyte proliferation activities of splenocytes of mice immunised with chimeric mHBcAg VLPs-displaying cEDIII (VLPs (a) experiment). The mouse spleens were pooled in group for splenocytes culture, and treated with 5 µg/ml of CTB-cEDIII-KDEL (xTH) antigen and 5 µg/ml of ConA mitogen for 72 hours. The SI was calculated based on the

triplicate A_{370} readings of stimulated splenocytes over unstimulated splenocytes. Value at 1 (dashed line) indicates that there is no discernible proliferation between stimulated and unstimulated splenocytes. The graph was expressed as the mean of $SI \pm SD$ of triplicate wells. Two-way ANOVA shows a degree of significance of **** $P \leq 0.0001$ between ConA-stimulated and antigen-stimulated splenocytes. The splenocytes of mice immunised with G5-V and G6-V did not respond to cEDIII antigen.

(ii) VLPs (b) experiment

Meanwhile, **Figure 6.14** presents the proliferation of splenocytes of mice immunised with chimeric mHBcAg VLPs of VLPs (b) experiment. As anticipated, the optimisation approach with VLPs (b) experiment had yielded positive outcome as cell proliferation could now be detected. The cut-off line at $SI = 1$ was used to identify positive cell proliferation activity. ConA mitogen generally had induced high proliferative response across all the splenocytes groups. Although the responses between antigen-stimulated groups were not statistically significant, but modest cell proliferation could be detected from G6-V and G8-V. In comparison to G2-V control group, the magnitude of lymphoproliferative response was determined as 1.5 folds higher for G6-V and 1.2 folds higher for G8-V.

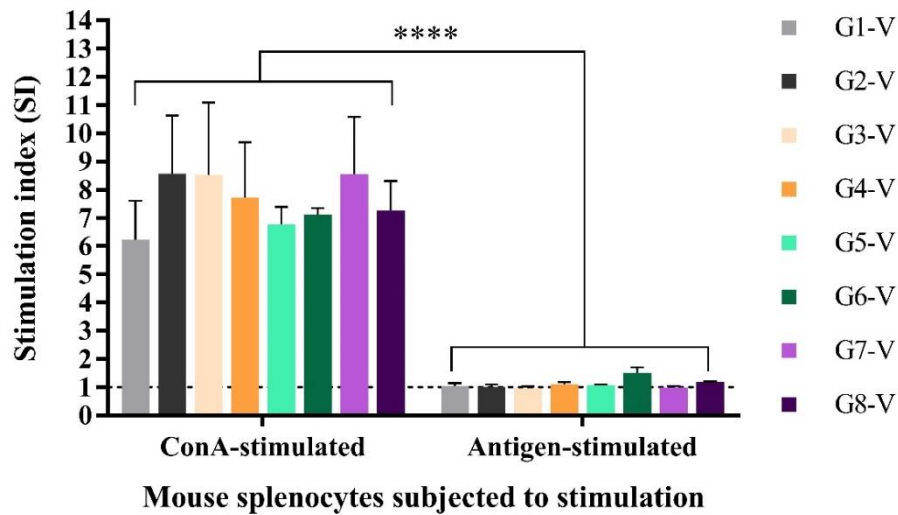


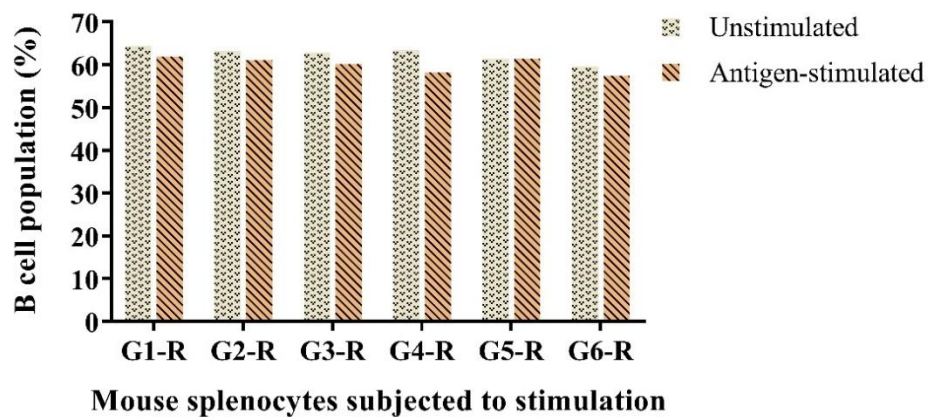
Figure 6.14: Lymphoproliferative responses of splenocytes of mice injected with chimeric mHBcAg VLPs-displaying cEDIII (VLPs (b) experiment). Mouse spleens were pooled in group for splenocytes culture, and cultured with CTB-cEDIII-KDEL (xTH) antigen as well as ConA mitogen at the same concentration of 5 $\mu\text{g/ml}$ for 72 hours. The SI was then determined based on the ratio of A_{370} readings of stimulated splenocytes over unstimulated splenocytes. The graph was expressed as the mean of $\text{SI} \pm \text{SD}$ of triplicate wells. The degree of significance between ConA-stimulated and antigen-stimulated splenocytes was determined by two-way ANOVA, and **** indicates $P \leq 0.0001$. Proliferative responses were detected from G6-V and G8-V.

6.3.5 Flow cytometric immunophenotyping

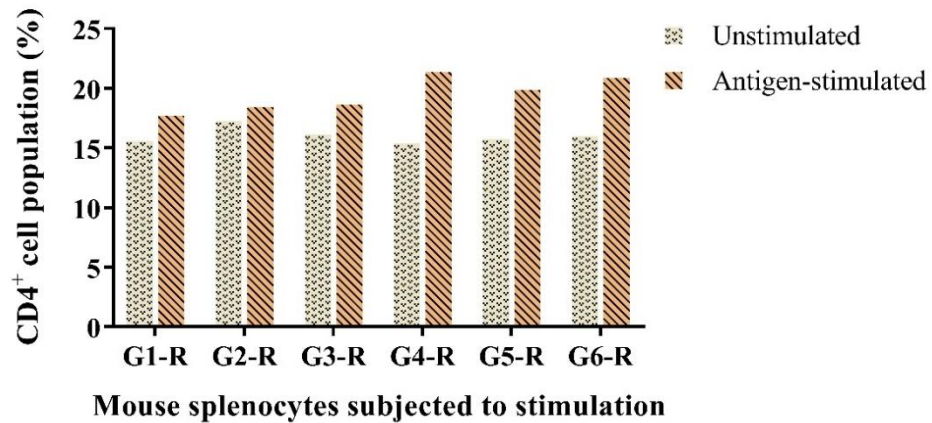
6.3.5.1 Recombinant cEDIII proteins

Following antigen stimulation, immunophenotyping was used to identify the lymphocyte populations based on the markers expressed on cell surface. A summary of the FACS analyses on splenocytes of mice immunised with recombinant cEDIII proteins is provided in **Figure 6.15**. Panel A shows that no obvious change in the B cell population was observed between unstimulated and antigen-stimulated splenocytes. Meanwhile, changes in the memory T cell populations could be reflected from the CD4⁺ T cells profile (Panel B) and CD8⁺ T cells profile (Panel C). In specific, G4-R, G5-R and G6-R were observed with notable increment of CD4⁺ and CD8⁺ T cells as compared to the G1-R and G2-R control groups.

Panel A Immunophenotyping of B cells



Panel B Immunophenotyping of CD4⁺ T Cells



Panel C Immunophenotyping of CD8⁺ T Cells

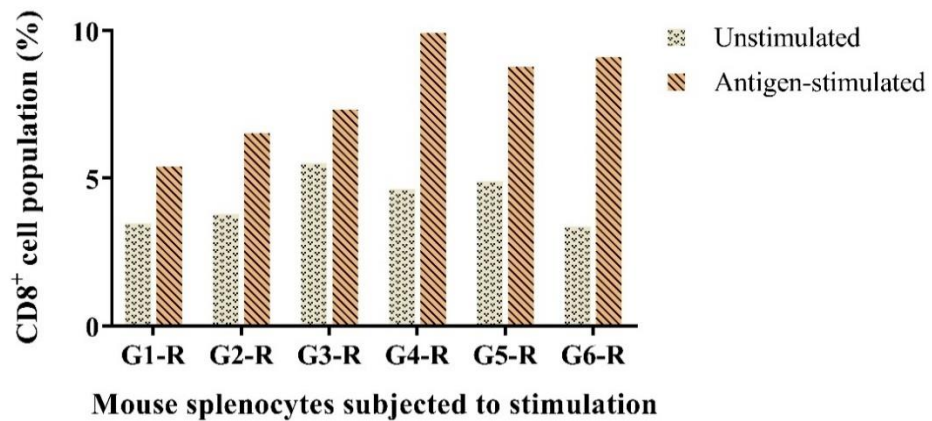
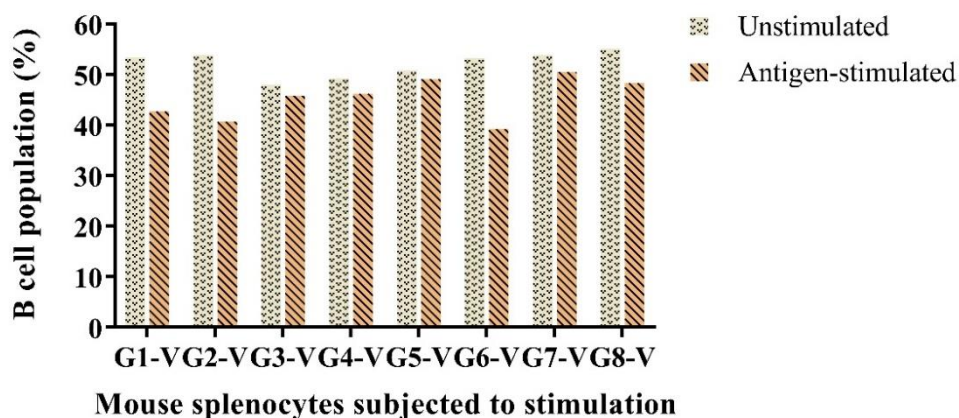


Figure 6.15: Immunophenotyping of lymphocyte populations in splenocytes of mice vaccinated with recombinant cEDIII proteins. Changes in B lymphocytes (Panel A), CD4⁺ T lymphocytes (Panel B) and CD8⁺ T lymphocytes (Panel C) populations were measured via flow cytometry following stimulation with CTB-cEDIII-KDEL (xTH) antigen. The results were expressed as the average of percentage of cells (%) from two independent experiments.

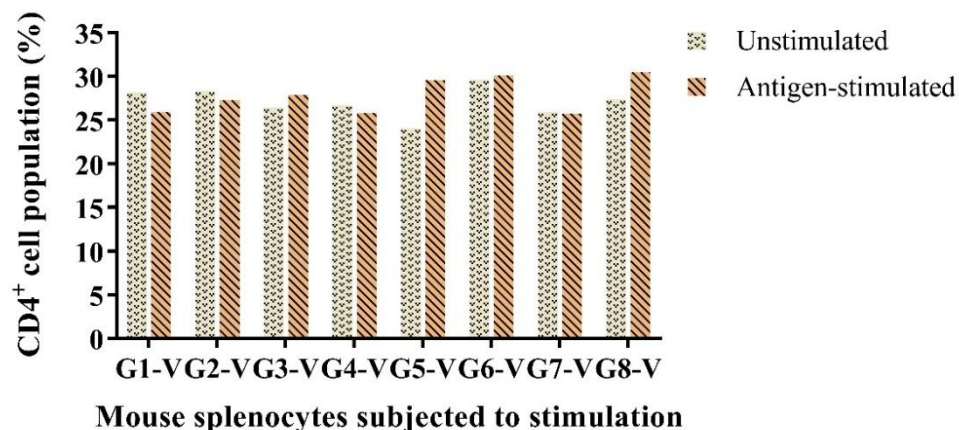
6.3.5.2 Chimeric mHBcAg VLPs-displaying cEDIII

Immunophenotyping of the lymphocyte populations in mice immunised with chimeric mHBcAg VLPs from VLPs (b) experiment is presented in **Figure 6.16**. Panel A suggests that no stimulatory effect on B cell population was observed following antigen stimulation. Analyses on the T cell responses indicate that the percentage of CD4⁺ T cells (Panel B) in G5-V and G8-V had shown discernible increment after stimulation. Peculiarly, the percentage of CD4⁺ T cells in G3-V was seen to rise as well. Meanwhile, the changes of CD8⁺ T cell population was apparent among the groups of G3-V, G4-V, G5-V, G6-V, G7-V and G8-V.

Panel A Immunophenotyping of B Cells



Panel B Immunophenotyping of CD4⁺ Cells



Panel C Immunophenotyping of CD8⁺ Cells

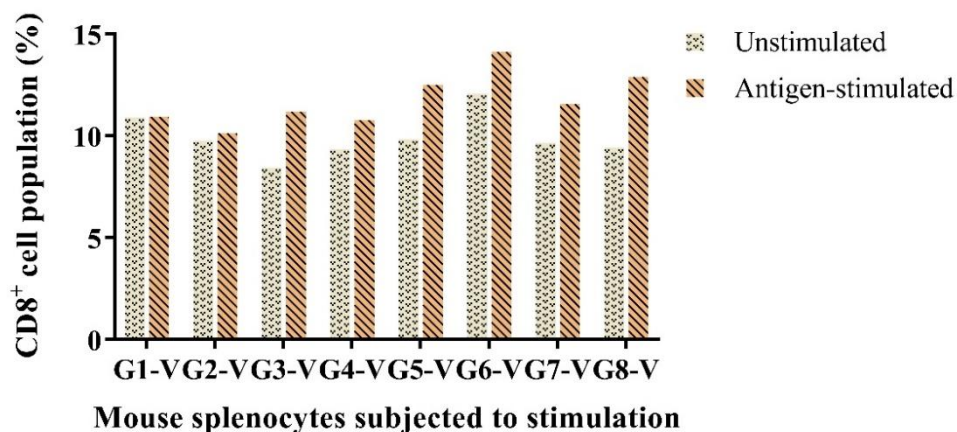
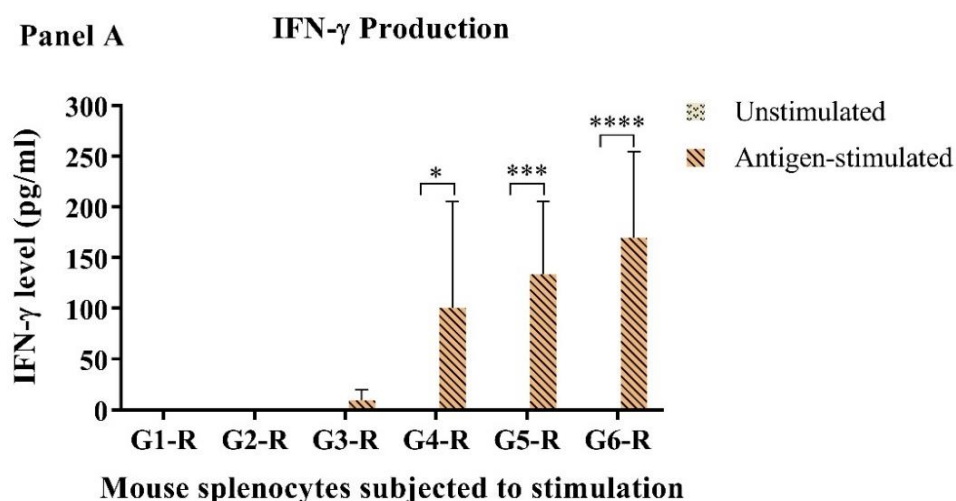


Figure 6.16: Immunophenotyping of cell populations in splenocytes of mice immunised with chimeric mHBcAg VLPs-displaying cEDIII. The changes in B lymphocytes (Panel A), CD4⁺ T lymphocytes (Panel B) and CD8⁺ T lymphocytes (Panel C) populations were measured via flow cytometry after stimulated with CTB-cEDIII-KDEL (xTH) antigen. Results were presented as the percentage of cells (%) from VLPs (b) experiment.

6.3.6 Measurement of secretory cytokines levels

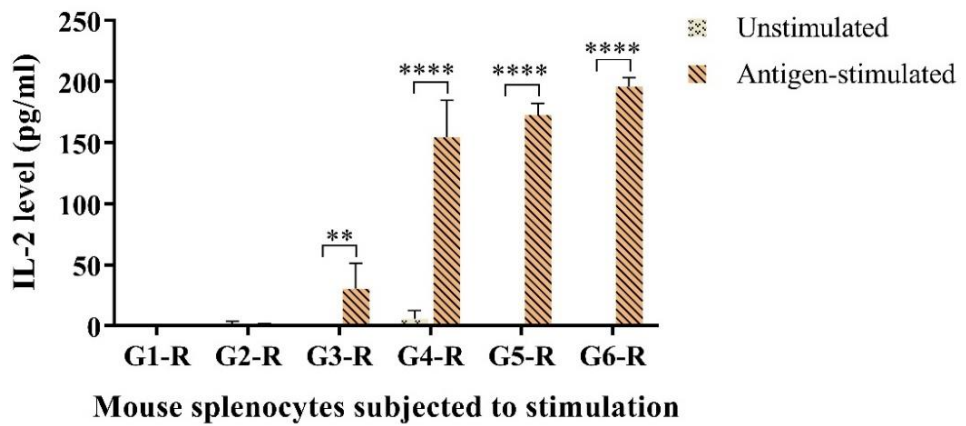
6.3.6.1 Recombinant cEDIII proteins

Following the observed changes in CD4⁺ and CD8⁺ T cell populations, cytokines profiling was used to differentiate the cell-mediated response into Th1 and Th2 subtypes. In specific, IFN- γ , IL-2 and IL-12 are signatures of Th1 response whereas IL-4 and IL-10 are representatives of Th2 response. The cytokines secretion profiles of splenocytes of BALB/c mice immunised with recombinant cEDIII proteins are summarised in **Figure 6.17**. Mouse splenocytes of G4-R, G5-R and G6-R were observed with significant secretion of IFN- γ and IL-2 following antigen stimulation (Panels A and B). Increased level of IL-4 was only significant in G6-R (Panel C) while production of IL-10 could be seen from both G5-R and G6-R (Panel D). Meanwhile, not much changes were noted for IL-12 levels after antigen stimulation (Panel E). These results suggest that cEDIII is potent in mediating the secretion of Th1 cytokines, and production of Th2 cytokines is only prominent when cEDIII was fused with CTB partner.



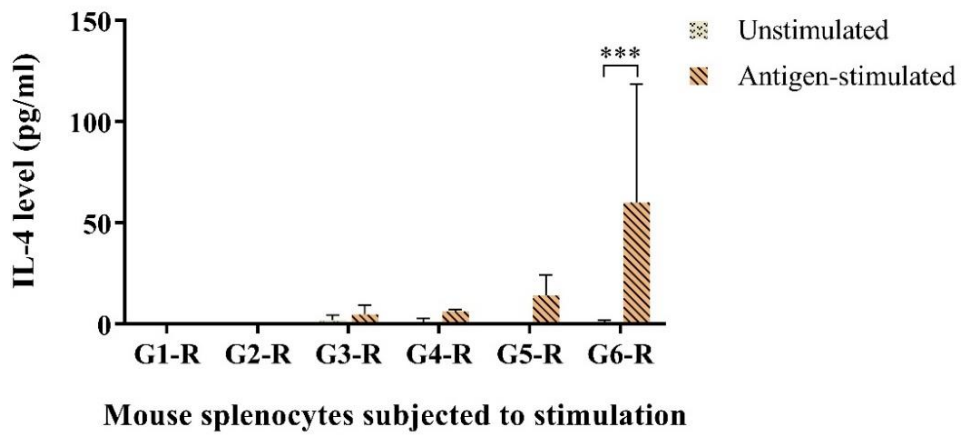
Panel B

IL-2 Production



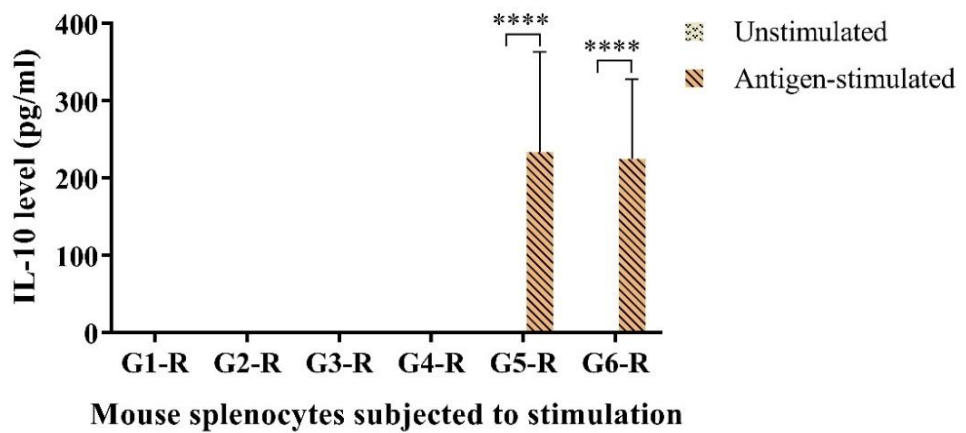
Panel C

IL-4 Production



Panel D

IL-10 Production



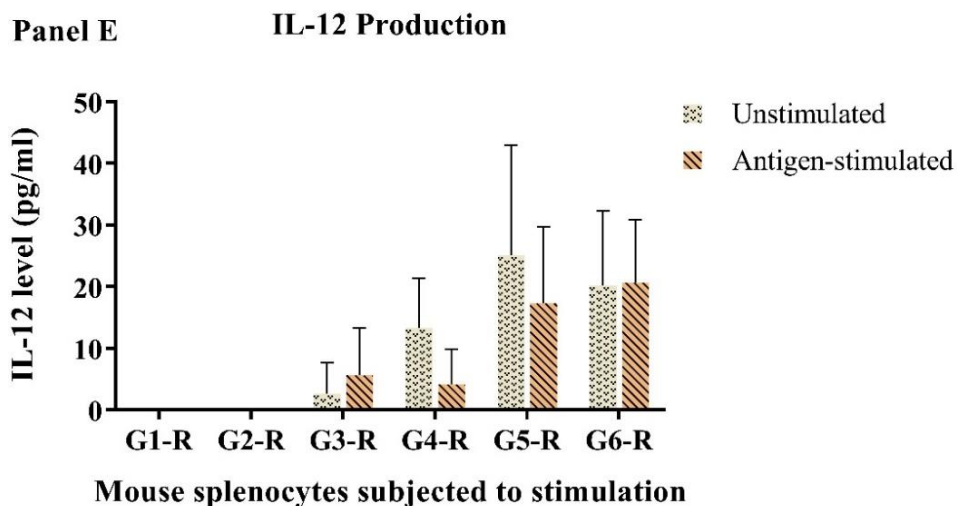
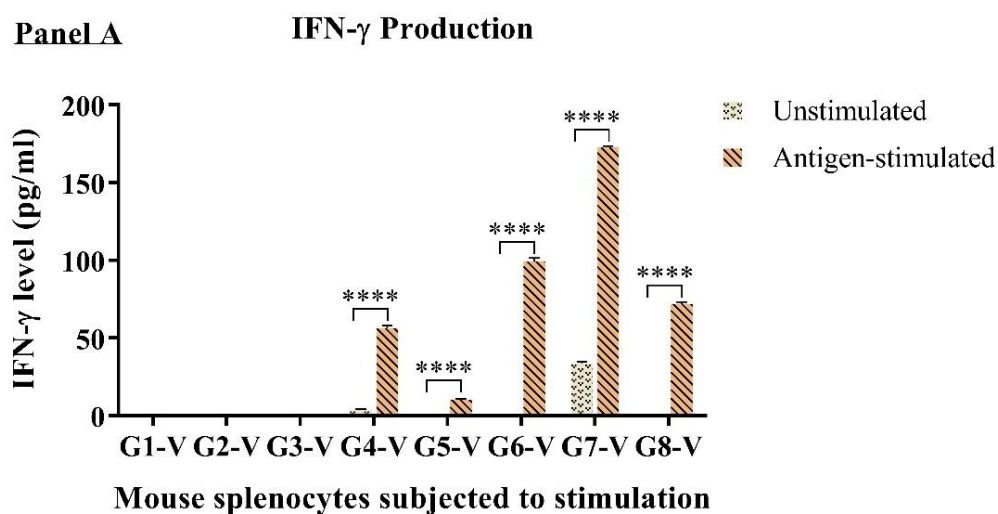


Figure 6.17: Cytokines secretion profiles of mice vaccinated with recombinant cEDIII proteins. Five panels were used to determine the concentrations of IFN- γ (Panel A), IL-2 (Panel B), IL-4 (Panel C), IL-10 (Panel D) and IL-12 (Panel E), correspondingly. The graphs showed mean of two independent experiments and were expressed as cytokine concentration (pg/ml) \pm SD. Sidak multiple comparisons test was used to calculate the degree of significance as compared to unstimulated controls where; *P \leq 0.05, **P \leq 0.01, ***P \leq 0.001 and ****P \leq 0.0001.

6.3.6.2 Chimeric mHBcAg VLPs-displaying cEDIII

Cytokines profiling of BALB/c mice immunised with vaccine constructs of VLPs (b) experiment is presented in **Figure 6.18**. Significant production of IFN- γ was noted among G4-V, G5-V G6-V, G7-V and G8-V (Panel A) while secretion of IL-2 was detected from G3-V, G4-V, G5-V, G6-V, G7-V and G8-V (Panel B). On top of that, increased production of IL-4 was seen among G4-V, G6-V, G7-V and G8-V (Panel C). Despite of the repeated analyses on IL-10 and IL-12, however no measurable level was obtained for all the splenocytes groups. Overall, the results suggest that the chimeric mHBcAg VLPs-displaying cEDIII could mediate a mixed Th1/Th2 cytokine response. However, the cytokine production in G3-V and G4-V is not expected since they do not carry the cEDIII antigen.



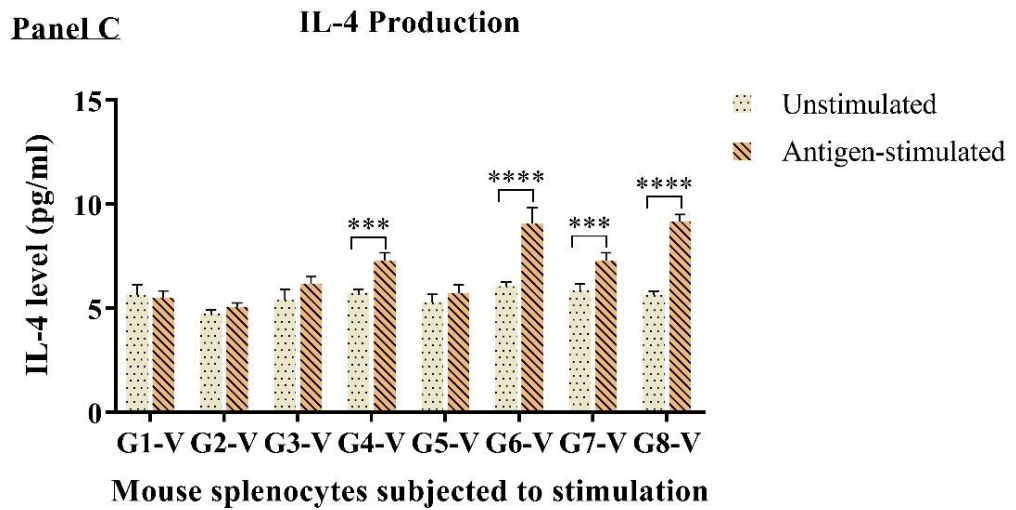
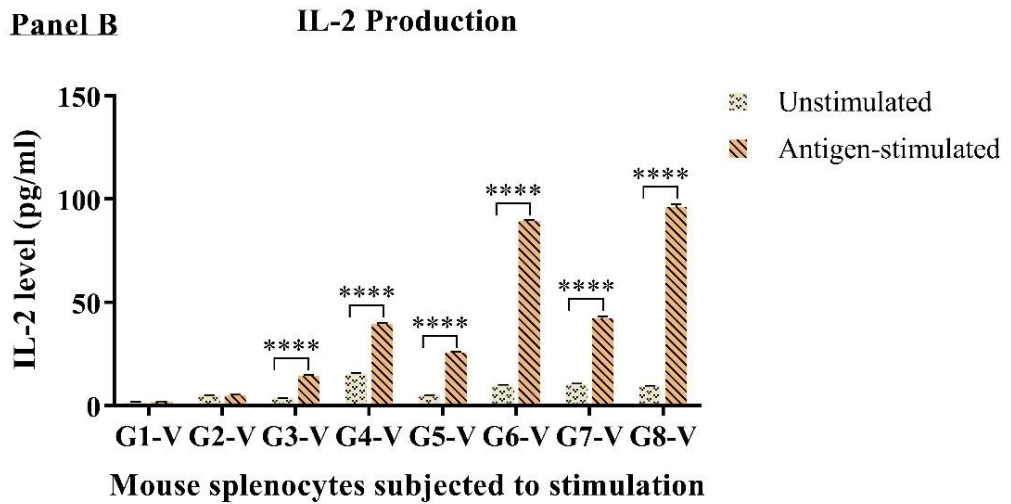


Figure 6.18: Cytokines profiling of mice immunised with chimeric mHBcAg VLPs displaying cEDIII. Three profiles were presented, namely IFN- γ (Panel A), IL-2 (Panel B) and IL-4 (Panel C). Graphs were plotted as the average cytokine levels (pg/ml) \pm SD of triplicate wells. The graph represents data from VLPs (b) experimental design and similar trend was acquired from two repeats. Sidak multiple comparisons test was used to calculate the degree of significance as compared to unstimulated controls where; ***P \leq 0.001 and ****P \leq 0.0001.

6.3.7 Comparative evaluation of the immunogenicity of different vaccine constructs

The capacity of plant-based recombinant cEDIII proteins to elicit humoral and cell-mediated immune responses is summarised in **Table 6.5**. cEDIII as the antigen of interest (vaccine group: G3-R), has demonstrated its ability to induce antigen-specific IgG production that can cross-neutralise all four DENV serotypes, along with the stimulatory production of Th1 cytokines. In comparison, stronger response was acquired when cEDIII was formulated with alum (vaccine group: G4-R), including: (i) 77.4-fold increment of cEDIII-specific antibodies production (**Figure 6.3**); (ii) significantly stronger virus binding (**Figure 6.6**) and neutralisation activities (**Figure 6.9**); (iii) 1.8 folds higher lymphoproliferative response to cEDIII antigen re-call (**Figure 6.12**); and (iv) higher levels of Th1 secretory cytokines production (**Figure 6.17**). Meanwhile, CTB-cEDIII-KDEL (xTH) protein (vaccine group: G5-R) has also demonstrated strong humoral and cell mediated immune responses than cEDIII alone where: (i) 63.3-fold increase in anti-cEDIII antibodies production (**Figure 6.3**); (ii) robust virus recognition with the capacity to neutralise all four DENV serotypes (**Figure 6.9**); (iii) 1.5-fold increment in the splenocytes proliferative response to cEDIII antigen (**Figure 6.12**); and (iv) the ability to mediate a balanced Th1/Th2 cytokines production (**Figure 6.17**). Nonetheless, the co-delivery of CTB-cEDIII-KDEL (xTH) with alum adjuvant had provided even stronger immune responses.

On the other hand, a summary of the immunogenicity test of chimeric mHBcAg VLPs-displaying cEDIII is provided in **Table 6.6**. It is useful to clarify that G5-V and G6-V were the vaccine candidates tested in VLPs (a) experiment, of which no cEDIII-specific humoral or cell-mediated response was detected. Therefore, a second experiment with VLPs (b) was attempted with an increased dosage of G5-V and G6-V, along with addition of G7-V and G8-V vaccine groups (see **Table 6.2b**). In general, the results shown that the alum-adjuvanted mHBcAg-cEDIII VLPs (vaccine construct: G8-

V) has stimulated slightly higher cEDIII-specific antibody response (**Figure 6.5**) with notable lymphocytes proliferation (**Figure 6.14**) and Th1 cytokines production (**Figure 6.18**) after antigen stimulation. Nonetheless, not much difference was noted between the immunogenicity of mHBcAg-cEDIII (L) VLPs (vaccine group: G6-V) and mHBcAg-cEDIII VLPs (vaccine group: G8-V); and both require co-delivery with alum in order to achieve a satisfactory immune stimulation.

Table 6.5: A comparison of the immunogenicity mediated by recombinant cEDIII proteins.

Immuno-assay	G3-R	G4-R	G5-R	G6-R
Antigen-specific IgG production	Yes (++)	Yes (++++)	Yes (+++)	Yes (+++++)
Recognition of native DENV	No	Yes, against DENV 1-4	Yes, against DENV 1-4	Yes, against DENV 1-4
Neutralisation of DENV serotypes	No neutralisation	Yes, against DENV 1-4	Yes, against DENV 1-4	Yes, against DENV 1-4
Lymphocytes proliferation	No	Yes	Yes	Yes
Secretory cytokines production	IL-2	IFN- γ , IL-2	IFN- γ , IL-2, IL-10	IFN- γ , IL-2, IL-4, IL-10

Table 6.6: A comparison of the immunogenicity mediated by chimeric mHBcAg VLPs-displaying cEDIII (VLPs (b) experiment).

Immuno-assay	G5-V	G6-V	G7-V	G8-V
Antigen-specific IgG production	No	Yes (+)	No	Yes (++)
Recognition of native DENV	No	No	No	No
Neutralisation of DENV serotypes	No neutralisation	No neutralisation	No neutralisation	No neutralisation
Lymphocytes proliferation	No	Yes	No	Yes
Secretory cytokines production	IFN- γ , IL-2	IFN- γ , IL-2, IL-4	IFN- γ , IL-2, IL-4	IFN- γ , IL-2, IL-4

6.4 Discussion

Development of a dengue vaccine has been a challenging goal due to the need to provide solid and durable protection against four DENV serotypes. Thereby, this chapter aimed to evaluate the immunogenicity of purified cEDIII antigens and most importantly, the ability of raised antibodies to neutralise DENV 1-4 simultaneously. Since cEDIII is claimed to be a poorly immunogenic small molecule (Chen *et al.*, 2013a; Chiang *et al.*, 2011) alum adjuvant is incorporated as a stimulus to potentiate an effective immune response. Alum specifically refers to aluminium potassium sulphate, an insoluble salt particle which has been used in human vaccines since it is inexpensive and has a long-standing safety record (Paneque-Quevedo, 2013). Though oil emulsions like Freund's adjuvant and Montanide have been routinely used in animal testing, but these are clinically less useful as most are too toxic for human prophylactic vaccine use (Aguilar and Rodríguez, 2007).

In this study, BALB/c mouse was used as this albino, inbred strain is known to be a good responder to immunisation (Potter and Boyce, 1962). Female BALB/c mouse was chosen considering the calmer behaviour that would allow easier handling. The male however, tends to fight aggressively which causes physiological stress that may lead to discrepancy of results. Moreover, a study found that young adult female BALB/c exhibited better B and T cells-mediated immune responsiveness than the male (Belisle and Strausser, 1981). For a more accurate representation of data, mice of the same sex were used to minimise variation too. Worthwhile to mention, barbering of furs were intermittently observed throughout the animal experiment (**Appendix A6.2**). Ironically, such behavioural pattern is not commonly seen among BALB/c mice (Canavello *et al.*, 2013), and female is in fact less aggressive. According to Garner *et al.* (2004), barbering is not a dominance behaviour, but rather an abnormal repetitive action affected by husbandry and social factors. If this reflects an underlying distress experienced by the

mice, it is therefore prudent to respond with pre-emptive improvements such as cage enrichment in future (Burkholder *et al.*, 2012).

Based on **Figure 6.3**, BALB/c mice were seropositive after receiving three doses of recombinant cEDIII proteins, namely G3-R, G4-R, G5-R and G6-R. In fact, anti-cEDIII IgG could be detected two weeks after primary immunisation with G5-R and G6-R. This thereby suggests that CTB-cEDIII-KDEL (xTH) may have the advantage to be developed as a vaccine that can accommodate shorter immunisation schedule. On top of that, the successful antiserum binding of G4-R, G5-R and G6-R to DENV 1-4 (**Figure 6.6**) implies the recombinant cEDIII proteins harboured epitopes that resembled native viruses. The failed interaction between G3-R sera and DENV was coherent to the neutralisation result (**Figure 6.9**) as no inhibition of virus infection was detected. In terms of the neutralising efficacy, G6-R seemed to confer almost equivalent potency as G4-R. The reason for lower neutralisation response against DENV 1 may be related to the accessibility of epitope, as the physical properties of virus particles could be affected by (i) the state of virion maturity, (ii) conformation flexibility of E proteins, and (iii) the structural heterogeneity resulted from 37°C incubation as seen from the expanded “bumpy” conformation of DENV 2 virion (Diamond and Pierson, 2015). Another plausible reason of lower neutralisation could be due to genotypic variation of DENV strains that were used to align the cEDIII sequence (**Appendix A3.10**) as this may lead to differences in antibody affinity (Wahala *et al.*, 2010). Nonetheless, successful neutralisation of four DENV serotypes was achieved in this study and future study may consider a more in-depth design of a global consensus sequence with a better understanding of the antibodies binding to the dynamic populations of DENV virions. As an emphasis, the serum samples used for virology test in this study had been heat-inactivated at 56°C for 30 minutes in order to eliminate potential complement interference in cell lysis assays. Hence, this would not lead to false positive

interpretations and the results obtained in this study are true representatives of the antiserum interactions with native dengue viruses.

The immunogenicity results for cEDIII conformed to Leng *et al.* (2009) findings, where no significant neutralising antibody titre could be detected when cEDIII was administered alone. The poor inhibition of viral infection might be attributed to the low antibody production, since virus neutralisation could be seen when cEDIII was adjuvanted. Pierson and Diamond (2009) explained that the neutralisation of flavivirus followed a ‘multiple-hit’ model, whereby the number of antibodies bound to a virion must surpass a required stoichiometric threshold in order to inhibit virus infection. For instance, a study with West Nile virus indicated that ~ 30 antibody molecules were needed to bind to the EDIII site for effective neutralisation (Pierson *et al.*, 2009). In general, it can be perceived that cEDIII is poorly immunogenic and thereby rationalises the objective of this study in terms of improving the immunogenicity of cEDIII via genetic fusion with CTB or being displayed as epitopes on VLPs carrier.

The VLPs (a) experiment for chimeric mHBcAg VLPs-displaying cEDIII did not work as anticipated, as the cEDIII-specific humoral and cell-mediated responses were not obtained. From a troubleshooting attempt however, IgG production against the mHBcAg carrier could be detected via ELISA (**Figure 6.4**). Therefore, it was hypothesised that the chimeric mHBcAg VLPs-displaying cEDIII were indeed presented to the mouse immune system, but the actual amount of cEDIII presented may be significantly lower than the recombinant proteins. It is obvious that the protein sequence of mHBcAg-cEDIII (L) composes mainly of mHBcAg carrier. Out of the 324 amino acids in mHBcAg-cEDIII (L) protein sequence, cEDIII only contributes to 103 amino acids. Hence, it is of no surprise that the mEL control (vaccine groups: G3-V and G4-V) would yield higher E.U. since an injection dosage of 20 µg does not correspond to an equal number of particles. In specific, mEL was short of 136 amino acids that were inserted into the c/e1 loop of mHBcAg-cEDIII (L). To verify the hypothesis, a second

experiment with VLPs (b) was repeated with an increased dosage of mHBcAg-cEDIII (L) to account for the 56.9% molecular size difference. An arbitrary calculation was made as shown below. In addition, mHBcAg-cEDIII VLPs were also included to see if the linker-less variant can induce better immune response. The mHBcAg-cEDIII did not have extra 29 amino acids from (GGG)_n linkers that flanked the cEDIII (see **Table 3.2**).

$$\begin{aligned}
 \text{Molecular size difference} &= \frac{\text{Size of mHBcAg-cEDIII (L)} - \text{Size of mEL}}{\text{Size of mEL}} \times 100 \% \\
 &= \frac{35.3 \text{ kDa} - 22.5 \text{ kDa}}{22.5 \text{ kDa}} \times 100 \% \\
 &= \sim 56.9 \%
 \end{aligned}$$

During VLPs (b) immunisation test, the dosage for the chimeric mHBcAg VLPs displaying cEDIII (vaccine groups: G5-V to G8-V) was raised to 30 µg, based on the estimated size difference from mEL (vaccine groups: G3-V and G4-V). As anticipated, induction of cEDIII-specific IgG could be detected after the adjustment (**Figure 6.5**). In fact, the linker-less mHBcAg-cEDIII (vaccine groups: G8-V) developed higher antibody titres than the mHBcAg-cEDIII (L) variant (vaccine groups: G6-V). This therefore conforms to the hypothesis of molecular size difference, and this should be considered when calculating the amount of inserted cEDIII sequence in relevant to the entire chimeric particle (Whitacre *et al.*, 2016). Despite that, further analyses indicate that no virus binding or neutralisation activities were observed. Such outcome mostly likely corroborates to the low antibody level as previously discussed. Hence, future study may take the molecular size into consideration, in order to gauge the optimal dose needed. For instance, Chua *et al.* (2013) did an explicit calculation to determine the specific number of EDIII copies available on the VLP per injection dose.

In relation to cell-mediated immune response, a cell is expected to undergo clonal expansion to mediate effector function upon recognition of the cEDIII antigen. CTB-

cEDIII-KDEL (xTH) was used for antigenic stimulation as this fusion protein was highly stable, expressed at higher yield and most importantly, it also harboured the cEDIII antigen. Since CTB is not a mitogen, it is presumed not to mediate any direct proliferative effect. In fact, a previous study showed that antigen-primed splenocytes that were incubated with CTB did not undergo cell proliferation (Wang *et al.*, 2003). In this study, bromodeoxyuridine (BrdU) labelling was used to identify dividing cells as BrdU could be incorporated into replicating DNA as an analogue of thymine. Following antigen stimulation, subsets of B and T lymphocytes were sorted based on the markers on cell surface known as cluster of differentiation (CD). This FACS results were complemented with secretory cytokines profiling in order to differentiate the cell-mediated immunity into Th1 or Th2 subtypes. For Th1 response, IL-2 is required for T cells proliferation while IL-12 induces differentiation of Th1 cells and produces IFN- γ that has direct killing effect on intracellular pathogens; whereas IL-4 and IL-10 represent Th2 response that induces B cell activation (Lydyard *et al.*, 2011). A general overview on the cellular responses mediated by T cells and their cytokines is illustrated in **Figure 6.19**.

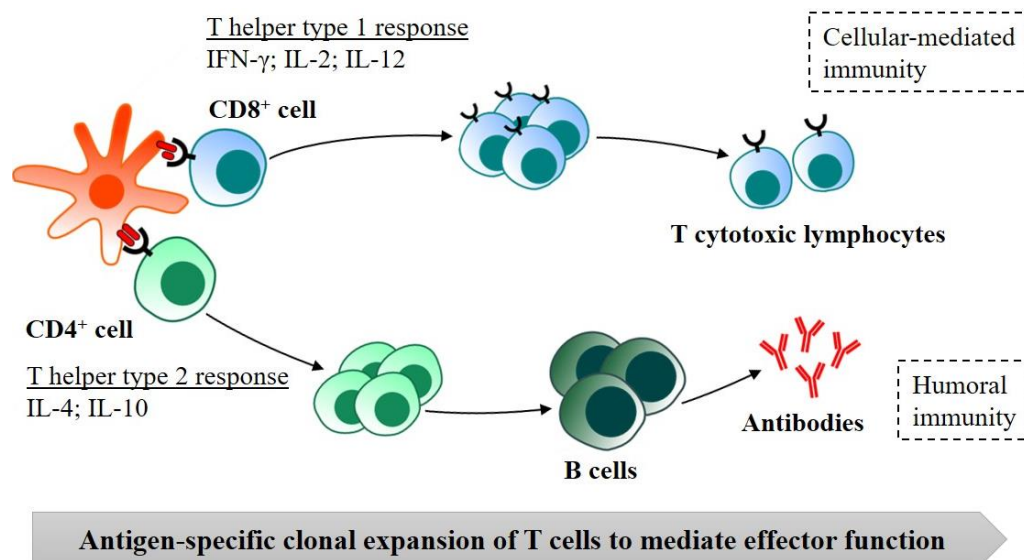


Figure 6.19: A schematic diagram of the aspects of cellular-mediated immune responses studied in this context. Note that Th1 and Th2 subtypes activate different arms of the immune system.

For mice immunised with recombinant cEDIII proteins, splenocytes of G4-R, G5-R and G6-R were seen to exhibit cEDIII-stimulated proliferation (**Figure 6.12**). In specific, the second mouse experiment in general had observed a lower stimulation index (SI) which could explain for the high error bar. The discrepancy might be attributed to the formation of proliferative clusters upon antigen stimulation, which thereby could affect anti-BrdU recognition and led to underestimated values. This can be prevented in future by thorough resuspension of cells after BrdU labelling to ensure optimal accessibility of antibodies. FACS analyses showed that increase of CD8⁺ T cells was substantial in G4-R, G5-R and G6-R (**Figure 6.15**), and in line with the robust stimulation of IFN- γ and IL-2 (**Figure 6.17**) to indicate a Th1 type immunity. The fact that G3-R also showed secretion of IL-2 suggests that the dengue envelope glycoprotein domain III (EDIII) may harbour a T cell epitope that stimulates a predominant Th1 type response (Li *et al.*, 2011). Moreover, significant levels of IL-4 and IL-10 in splenocytes of G6-R, and in G5-R to lesser extent, indicate the CTB partner had skewed the immune

response towards a mixed of Th1/Th2 type. It is hence believed that cEDIII fusion with CTB could impart a Th2 immune response, as agreed by Eriksson *et al.* (2003).

Meanwhile, the BrdU assay with mice immunised with the chimeric mHBcAg VLPs-displaying cEDIII also showed that dosage adjustment was effective as cell proliferation could now be seen from splenocytes of G6-V and G8-V (**Figure 6.14**). Next, FACS analyses showed that increment of CD8⁺ cells was noted for the six groups, from G3-V to G8-V (**Figure 6.16**), and in line with the production of IL-2 (**Figure 6.18**) to suggest a Th1-biased response. Besides, cEDIII-primed IFN- γ secretion was also prominent in G4-V, G5-V, G6-V, G7-V and G8-V. The rise of IL-4, a Th2 cytokine, however was significant in G4-V, G6-V, G7-V and G8-V. In fact, increased IFN- γ , IL-2 and IL-4 levels were observed from G3-V and G4-V that served as experimental controls without cEDIII epitopes presentation. Hence, the protein Basic Local Alignment Search Tool (BLAST) analysis was used to check the sequence similarity between the mHBcAg and CTB-cEDIII-KDEL (xTH) used for splenocytes stimulation. Peculiarly, a 35% sequence similarity was mapped at the N-terminus of mHBcAg 3' core segment (**Appendix A6.3**). One possible explanation could be that this region harboured one of the T cell peptide determinants that had been identified by Ferrari *et al.* (1991). Using G3-V and G4-V as the benchmarks, the extent of elevated cytokines production was still higher in G6-V, G7-V and G8-V. The results imply that though cEDIII and mHBcAg are serologically distinct but they may be cross-reactive at the T cell level. This may in part, due to the nature of T cells that can only recognise linear peptide while antibodies recognise the three-dimensional shape of VLPs (Lydyard *et al.*, 2011). From a different perspective, this may be beneficial in terms of priming for robust T-cell activation. This could be an interesting subject for future study as no information is available on the cross-reactivity. It could be that most studies have been focusing on the efficacy of chimeric VLPs-displaying desired epitope and may have overlooked other effects driven by the carrier molecule itself.

With the efforts to improve the immunogenicity of cEDIII, the vaccine constructs have been designed to harbour intrinsic adjuvants. As shown in **Table 6.5**, the adjuvant efficacy of CTB was well-demonstrated based on the superior performance of the cEDIII-fused CTB as compared to cEDIII alone. This is mediated by the capacity of CTB to bind with monosialotetrahexosylganglioside (GM1) on antigen-presenting cells (APCs) to promote antigen uptake that leads to more abundant peptides presentation on major histocompatibility complex (MHC) II, together with the increased levels of CD40 and CD86 costimulatory molecules on APCs and upregulated IL-12 and IFN- γ secretions to augment the T-cell activating potential of APCs (George-Chandy *et al.*, 2001). Besides, the assembly of pentameric CTB-cEDIII-KDEL (xTH) molecules may have served as a stabiliser for defined organisation of cEDIII and promotes antigen presentation to the dendritic cells. Studies had proven that conjugation with CTB could elicit > 10 folds stronger antibody response (Miyata, *et al.*, 2012; Miyata *et al.*, 2010). In this study, > 65 folds higher IgG titre was obtained when comparing cEDIII to CTB-cEDIII-KDEL (xTH). G3-R had an average IgG titre at 3590 E.U. in comparison to G5-R with an average 236090 E.U. by the end of immunisation. This signifies that a lower dosage is required to achieve immune stimulation if CTB-cEDIII-KDEL (xTH) fusion protein is harnessed for vaccine design. Immunisation with CTB alone was not attempted due to limited number of BALB/c mice permitted for use in this study and findings already showed that the response of CTB control would be similar to PBS (Lee *et al.*, 2015b).

Meanwhile, VLPs-based vaccine is known to prime immune response in a Th1-biased fashion (Guillén *et al.*, 2010). In this study, the uptake of HBcAg VLPs carrier is expected to deliver 180 – 240 copies of the cEDIII antigens from each particle to the APCs, following disruption in the lysosomal compartment (Cooper and Shaul, 2006). Such high-density of antigen presentation is hence greatly valued for the robust immune stimulation. In line with Milich *et al.* (1997b) findings, immunisation with chimeric

mHBcAg VLPs-displaying cEDIII (**Table 6.6**) induced high productions of IL-2 and IFN- γ , and lower of IL-4 levels, which preferentially primed for Th1 type response. Besides, the chimeric mHBcAg VLPs-displaying cEDIII still retained the C-terminal nucleic acid binding domain (see **Table 3.2**). Thus, it is speculated that the trace amount of encapsidated plant RNA in the VLPs might be responsible for the strong Th1 response (Riedl *et al.*, 2002), thereby reproducing the same effect as a CpG oligodeoxynucleotides (ODNs) adjuvant. Albeit the production of antigen-specific antibodies has been testified in this study, the dosage might still be sub-optimum. For instance, Yang *et al.* (2017) administrated at least 50 μ g of HBcAg-zDIII VLPs to ensure that 15 μ g of the Zika virus (ZIKV) EDIII was presented for immune activation. As ZIKV EDIII shares similar size as the cEDIII, future study may consider optimising the dose to 50 – 60 μ g of chimeric mHBcAg VLPs-displaying cEDIII. Besides, since the efficacy of mHBcAg-cEDIII VLPs and mHBcAg-cEDIII (L) VLPs was comparable, further study may focus on either one of the constructs. In favour of the molecular weight theory, the linker-less mHBcAg-cEDIII may be a better option. Theoretically, a preceding hepatitis B infection might seem to limit the use of HBcAg as an antigenic carrier. However, it should not be a concern as evidences showed that pre-existing immunity will not interfere with antigen presentation (Ruedl *et al.*, 2005; Schödel *et al.*, 1994), and most importantly, the major B cell epitope of HBcAg lies on the c/e1 loop where cEDIII antigen is inserted.

Worthwhile to mention, a preliminary study on the immunogenicity of tandem core HBcAg (tHBcAg) particles displaying cEDIII had been conducted in collaboration with iQur Ltd. (UK) (see **Appendix A6.4**). The results showed that successful production of cEDIII-specific IgG antibody is achieved following injection with tHBcAg-cEDIII VLPs; which thereby confirms that the cEDIII epitopes have been displayed in immunogenic context on the tandem core particles. Besides, immunisation with tHBcAg-cEDIII VLPs leads to higher CD8⁺ degranulation response and this is

favoured for the release of perforin and granzyme from CD8⁺ T cells lysosome that can mediate killing of DENV-infected cells (Yauch *et al.*, 2009). Although the tandem core approach is still relatively new, a recent publication had shown the feasibility of this technology whereby the mice immunised with a tandem core based influenza A vaccine had obtained 100% protection in a lethal challenge study (Ramirez *et al.*, 2018). This signifies that the tHBcAg-cEDIII VLPs also has the potential to be translated into an improved protective dengue vaccine, which warrants for further investigation.

Taken together, the co-delivery of vaccine construct with alum has boosted the immunogenicity of recombinant cEDIII, recombinant CTB-cEDIII-KDEL (xTH) fusion protein, mHBcAg-cEDIII VLPs and mHBcAg-cEDIII (L) VLPs. Albeit it is conventionally accepted that alum can mediate sustained release of antigen from the depot formed at inoculation site, but current findings prefer the theory of alum's abilities to activate the APCs and inflammasome (Wen and Shi, 2016). Although alum is known to generate strong Th2 response, but this effect is not discernibly reflected from the secretory cytokine profiles in this study. According to Marrack *et al.* (2009), it could be that alum had modulated the Th2 responses indirectly via Th1 suppression. Comparing the adjuvant efficacy, alum has seemed to perform better than CTB in terms of boosting the immunogenicity of cEDIII in this study. Although a marginal 1.2-fold difference in the anti-cEDIII antibodies production was observed between G4-R and G5-R (**Figure 6.3**), discernible neutralisation potencies were obtained from FRNT (**Figure 6.9**). This may correlate to the action of CTB that tends to skew the immune response towards B cell activation instead of mediating the intracellular killing activity via Tc lymphocytes. Nonetheless, the production of Th2 cytokines has the benefit of inducing sterilising immunity which can completely prevent virus invasion into host. In fact, the lack of this immune status would allow wild-type pathogens to circulate within vaccinated host, probe for the weakness of vaccine-induced immunity, and eventually evolve to revert to virulence. A significant example was shown from the abandoned vaccine used for

Marek's disease due to the 'leaky' infection resulted from virus mutation (Read *et al.*, 2015). In this context, the CTB-cEDIII-KDEL (xTH) vaccine candidate might have the added benefit to induce sterilising immunity and clear DENV-infected cells.

Momentously, this study represents the first in the field of plant-based dengue vaccine research (reviewed in **Section 2.5**) to demonstrate the abilities to neutralise four DENV serotypes simultaneously. So far, only two studies had tested the immunogenicity of non-adjuvanted, plant-produced cEDIII, by which both failed to show induction of antigen-specific antibodies production (Huy and Kim, 2017; Kim *et al.*, 2016a). In contrast to Kim *et al.* (2016a), the disparity may have come from the transgenic rice system used to produce the cEDIII. But when compared to Huy and Kim (2017), it is interesting to know that the cEDIII produced via pEAQ-*HT* vector in this study has outperformed the cEDIII derived from a tobacco mosaic virus (TMV)-based pro-vector of Icon Genetics. This has most likely corroborated to the benefit of using the non-replicative pEAQ-*HT* system to omit mutation issue. On top of that, Kim *et al.* (2017) had tried to boost the immunogenicity of cEDIII by fusing it to polymeric immunoglobulin G scaffold (PIGS). Although the delivery of cEDIII-PIGS with alum did induce high IgG titre at 1:1,000,000, but the vaccine construct only produced weak neutralisation titre against DENV 2, by which was not more than 1:100 dilution. Although the authors argued that this could be due to the lack of neutralising epitopes in cEDIII, but this study has solidly proven that cEDIII is capable of neutralising DENV 1-4 at satisfactory levels.

6.5 Conclusion

In summary, the immunogenicity of cEDIII in the form of recombinant proteins (vaccine candidates: recombinant cEDIII and recombinant CTB-cEDIII-KDEL (xTH) fusion protein) and as epitope display on chimeric mHBcAg VLPs (vaccine candidates: mHBcAg-cEDIII VLPs and mHBcAg-cEDIII (L) VLPs) had been studied.

Recombinant cEDIII protein has shown neutralising potencies against four DENV serotypes, with a predominant Th1 immune response. On the other hand, recombinant CTB-cEDIII-KDEL (xTH) fusion protein also has the capability to elicit cEDIII-specific antibodies production that inhibit DENV 1-4. Apart from Th1 immunity, fusion with CTB seems to skew the response towards a mixed of Th1 and Th2 that may be superior in terms of providing sterilising immunity while clearing virus-infected cells.

During the testing of chimeric mHBcAg VLPs-displaying cEDIII vaccine candidates, the adjustment of dosage based on molecular size has shed lights on the importance of sufficient presentation of cEDIII epitopes. Albeit successful production of cEDIII-specific antibodies had been achieved, further optimisation may be useful for better utilisation of these VLPs-based vaccines that were shown to confer a predominant Th1 immune response.

Based on Malaysian context, this study represents a significant step forward in realising the potential of developing an affordable local vaccine that can benefit all communities. To the best of my knowledge, this study is the first to demonstrate that a plant-based dengue vaccine candidate has the potency to neutralise all four DENV serotypes.

7 General discussion

The primary aim of this research was to explore the feasibility of using plant system to produce a viable dengue vaccine candidate to address the alarming rise of dengue epidemics. With close to 400 million global cases per annum, dengue is now regarded as a mosquito-borne disease of global importance (Bhatt *et al.*, 2013). Over the past 50 years, transmission of the disease has massively expanded by 30 folds (World Health Organization (WHO), 2014), which reflects that vector control programmes have been futile. Besides, the lack of anti-viral medications has driven sole reliance on fluid therapy. As experts believe that dengue cases will continue to escalate (Murray *et al.*, 2013), the development of a dengue vaccine is foreseen as a more sustainable approach to achieve disease control. Hitherto, Dengvaxia[®] has only been used in 11 out of 130 countries that are affected by dengue. Low adoption is held back by concerns like low efficacy, high cost, limited use for flavivirus-naïve population and risk of adverse events (see **Section 2.2.5.1**). In fact, Philippines has recently suspended its use after the dengue vaccine is found to cause severe illness and death (Antiporda, 2018). Such scenario signifies a typical problem of live-attenuated vaccine where it is hard to balance immunogenicity with safety. Hence, the development of subunit vaccine would be a better option based on its safe and precise immune targeting.

The domain III of dengue envelope glycoprotein (EDIII) has been primarily used for vaccine development as EDIII is characterised with potent serotype-specific neutralising determinants (Guzman *et al.*, 2010). Notably, this specificity is crucial to evade pathological effects from antibody-dependent enhancement (ADE). Several approaches have been used to generate a tetravalent vaccine based on EDIII, such as stoichiometrically mixing four monovalent EDIII (Block *et al.*, 2010), recombinant fusion of four EDIII in a single protein (Etemad *et al.*, 2008) or the use of a consensus EDIII (cEDIII) (Leng *et al.*, 2009). In this study, the expression of cEDIII was favoured because: (i) it obviates the need to produce and adjust doses of four individual

monovalent proteins; (ii) cEDIII is proven to be highly stable than individual EDIII; (iii) it comprises a single domain and hence is not subjected to structural hindrance as in linked EDIII domains; (iv) the consensus sequence would still be useful despite with evolution of new virus strain; and lastly (v) the small insert has allowed easier manipulation to be tagged with fusion partner or displayed on virus-like particles (VLPs) (**Chapter 3**).

As stated previously, EDIII possesses a single disulphide bond which is critical for its antigenic integrity. The structural antigenicity is so crucial that a single mutation in this region can alter the neutralisation outcome (Zhou *et al.*, 2013). Hence, expression in plant would be ideal due to its capability of post-translational modifications. In this study, the immunogenicity of plant-derived cEDIII in this study clearly outweighs bacteria-derived cEDIII (Chiang *et al.*, 2011; Leng *et al.*, 2009) in terms of higher neutralisation titres. To clarify, this study calculated the neutralising titres based on 50% reduction of DENV (FRNT50) while Chiang *et al.* (2011) and Leng *et al.* (2009) determined the titres at 40% reduction (FRNT40). So comparatively, stronger response was obtained in this study with FRNT50 at 1:119 – 1:356 while the bacterial studies reported FRNT40 at 1:8 – 128. Apart from the benefits of eukaryotic system, plant offers added safety advantage and is easy to scale-up which can revolutionise the accessibility of dengue vaccines to provide rapid yet affordable medical relief to affected regions. Making use of current advances in transient expression technology, speedy production of vaccine is now achievable via agroinfiltration. As applied in this study, syringe infiltration has facilitated rapid screening of different dengue vaccine constructs (**Chapters 4 and 5**) before proceeding with immunogenicity test to select the best candidate (**Chapter 6**). Only then, it would be useful to switch to vacuum infiltration for automated delivery of uniform products at industrial scale. *N. benthamiana* plant, as a non-food and non-feed crop, has been widely used for transient expression due to its

amenability to *Agrobacterium* infection and the large amount of leaf biomass that can be harvested (Goodin *et al.*, 2008).

To increase the chance of developing a strong vaccine, cEDIII as the antigenic determinant was designed to express in several forms: (i) recombinant protein; (ii) recombinant fusion to cholera toxin B subunit (CTB) and (iii) epitope display on hepatitis B core antigen (HBcAg) VLPs (**Chapter 3**). Worthwhile to mention, cEDIII was only obtained after tobacco etch virus (TEV) protease cleavage of recombinant cEDIII fused with green fluorescent protein (sGFP). Fusion to sGFP mainly served to facilitate better monitoring of the spatial and temporal expression of cEDIII recombinant protein. Meanwhile, fusion with CTB is rationalised based on its immunostimulatory properties that could be imparted to bystander cEDIII antigen. Besides, new information was elucidated from size exclusion chromatography (SEC) as CTB-cEDIII-KDEL (xTH) fusion protein was prone to fold into pentamer and to interact with neighbouring pentamers to strengthen overall lattice. The outstanding stability of CTB-cEDIII fusion further suggests that the protein may have the potential to be developed as a diagnostic agent other than vaccine. For VLPs production, HBcAg was chosen as the vaccine carrier for the high-density presentation of foreign epitopes on surface and direct activation of B and T cells. In fact, it is long known that strong immunogenicity of HBcAg is conferred by its dual functions as T cell-dependent and T cell-independent antigen (Francis *et al.*, 1990). Although the expression of chimeric VLPs with cEDIII epitopes had been achieved for monomeric core HBcAg (mHBcAg) and tandem core HBcAg (tHBcAg) constructs, it is speculated that insertion of cEDIII may have altered the surface properties and led to aggregation. But, aggregation could have been exacerbated by extrinsic factors such as heat-shock or hyperosmotic damage. This implies that the VLPs derived from either mHBcAg or tHBcAg construct are very fragile and require deliberate downstream processing to maximise sample recovery.

Practically speaking, expression of a heterologous protein is unlikely to be as straightforward as in its native milieu. For that reason, several improvement strategies had been applied in this study to boost the expression yield (**Chapter 3**). At the transcriptional and translation levels, codon usage, design of Kozak sequence and co-expression of gene silencing suppressor were considered. Firstly, all the expression cassettes containing cEDIII were synthesised with optimised *N. benthamiana* codons. Fine tuning the codon adaptation index (CAI) to ≥ 0.85 was likely to promote optimal and accurate translation by adapting to the codon usage of *N. benthamiana* host. Removal of mRNA secondary structure also helped in getting rid of elements that could inhibit expression. A Kozak context, on the other hand, was presumed to mediate efficient protein translation by promoting ribosomal recognition of the start codon. The use of tombusvirus P19 RNA silencing suppressor was favoured for the capacity to block activation of gene silencing complexes while boosting transgene expression (Zheng *et al.*, 2009). A significant advantage with pEAQ-*HT* vector is the ability to express P19 in *cis*; and hence eliminates the need to co-infiltrate another *Agrobacterium* clone that could have negative impact on plant due to the increased density of inoculated bacteria.

Besides, two strategies were used to modulate protein stability at the post-translational level, including subcellular localisation and design of protein linker. For the sequestration of heterologous protein in endoplasmic reticulum (ER), a proper design of targeting signals is imperative to ascertain precise targeting. Firstly, the ER retention signal (KDEL) should be positioned at the C-terminal tail to render efficient recognition for retrograde transport. Then, a combinatory use with the signal peptide of tobacco pathogenesis-related 1a protein (PR1a) was needed to ensure passage across the endomembrane system. This was verified via confocal imaging (**Chapter 4**), as the recombinant protein expressed by pEAQ-*HT*::PR1a-cEDIII-H-KDEL was stably retained at higher level in the ER, in contrast to the protein expressed by pEAQ-

HT::cEDIII-sGFP-KDEL-H which accumulated in the cytosol. Besides, kinetic studies unveiled rapid leaf necrosis after a progressive accumulation of cytosol-localised recombinant protein. Corresponding to the ER stress induced by transient overexpression, it is likely that proteolytic activities in cytoplasm had resulted in high amount of degraded products that no longer could be rescued by unfolded protein response (UPR). Thus, retention in ER is beneficial in the sense it prolongs the residence time of recombinant protein to achieve proper folding, as monitored by chaperones and molecular enzymes. Besides, the controversial disparity of plant and mammalian N-linked glycosylation could be avoided via ER localisation. On other hand, protein linker plays a key role to provide flexibility to connecting domains. The glycine-proline-glycine-proline (GPGP) linker between CTB and cEDIII proved to be useful as majority of the fusion proteins could fold into the pentameric form (**Chapter 5**). Lee *et al.* (2014) had attempted a linker-less fusion of antigen with CTB and found that majority of the proteins existed in an unstable oligomeric state. Meanwhile, the addition of glycine-rich (GGS) linker did not seem to yield discernible difference between the expression yield and particles assembly of mHBcAg-cEDIII and mHBcAg-cEDIII (L) constructs. This may be contributed by the intrinsic property of cEDIII which was claimed to have a defined fold relative to serotype-specific EDIII (Zidane *et al.*, 2013).

Preceding protein purification, it is noteworthy to emphasise that the PR1a signal peptide could be recognised by host signal peptidase for post-translational removal. Albeit the knowledge on KDEL signal processing is still obscure, but arguably it should not cause any deleterious effect since a vast majority of endogenous proteins in animal cells also harbour the KDEL motif, such as the binding immunoglobulin protein (BiP), protein disulphide isomerase and calreticulin (Pelham, 1989). Different purification procedures were designed to tailor for different forms of cEDIII antigens, namely recombinant fusion proteins and VLPs (**Chapter 5**). The recovery of cEDIII recombinant fusion proteins was primarily achieved via immobilised metal affinity

chromatography (IMAC), based on the binding affinity of C-terminal 6X histidine (His) tag for nickel ions (Ni^{2+}). Subsequent TEV cleavage of 6X His tag was attempted to minimise non-native sequence that may affect protein folding or activity. Though pure cEDIII could be harvested after digesting cEDIII-sGFP-H-KDEL protein, but the yield was relatively low at 13 – 14 mg/kg. Since the cleavage was not as effective as expected, future investment on immuno-affinity chromatography may be opted. Meanwhile, the cleavage of His tag from CTB-cEDIII-H-KDEL did not yield expected product separation, in which was found to be attributed to peculiarity of CTB pentamer to bind with metal-affinity resin (Dertzbaugh and Cox, 1998). Such distinguished property, was later utilised as means to achieve single step isolation of its variant, CTB-cEDIII-KDEL (xTH) fusion protein. On top of that, the purified CTB-cEDIII-KDEL (xTH) was proven to preserve the conformation of biological-active pentamers via binding with its native receptor known as monosialotetrahexosylganglioside (GM1).

Purification of VLPs, on the other hand, relies on the density gradient sedimentation to separate assembled VLPs from host proteins. Sucrose cushion was meant to concentrate all the VLPs in the clarified extract and relayed them to further purification by density gradient. Electron microscopy revealed that production of cEDIII in the form of mHBcAg and tHBcAg VLPs were successful. In comparison, nycodenz gradient was found to perform better owing to the clear fractionation from plant endogenous proteins. This suggests that a combinatory use of rate-zonal and isopycnic sedimentation may be more optimal for VLPs purification. Notably, immunogold labelling provided the first evidence that the cEDIII epitopes were correctly displayed on mHBcAg-cEDIII and mHBcAg-cEDIII (L) VLPs, as evident from the successful attachment of DENV 1-4 antibody to the surface of chimeric VLPs.

The immunogenicity results of cEDIII recombinant proteins revealed that both cEDIII and CTB-cEDIII-KDEL (xTH) elicited potent anti-cEDIII humoral response (**Chapter 6**). Conformed to Leng *et al.* (2009) findings, the immunisation with cEDIII

alone also induced low anti-cEDIII IgG titres without significant neutralising activities. This agrees to the notion that cEDIII is poorly immunogenic and hence requires co-delivery with alum adjuvant to potentiate the immune responses. Current study on the cellular-mediated immunity (CMI) revealed that cEDIII is likely to induce a predominant T helper (Th) type 1 response based on interferon-gamma (IFN- γ) and interleukin-2 (IL-2) secretions. In fact, a cohort study in Thailand found that the pre-existing IFN- γ -producing memory T cells was associated with lower risk of secondary infection (Hatch *et al.*, 2011). This thereby rationalises the use of cEDIII for vaccine development owing to the protective role of Th1-mediated virus clearance. On the other hand, the potency of CTB adjuvant was evident from the 63.3-fold increase in anti-cEDIII immunoglobulin G (IgG) titre, and that recombinant CTB-cEDIII-KDEL (xTH) itself was able to evoke neutralising protection against DENV 1-4 without alum. Complementary to the GM1-ELISA data, the active binding of CTB-cEDIII-KDEL (xTH) to GM1 gangliosides on antigen-presenting (ACPs) has potentially led to enhanced antigen uptake that stimulates robust CD4⁺ and CD8⁺ responses. In specific, cEDIII fusion with CTB has skewed the response towards a mixed Th1/Th2. This is in part mediated by the CTB partner that generates a default Th2 response, as shown from the productions of IL-4 and IL-10. This would be ideal for a virus vaccine development in terms of the ability to provide sterilising immunity while clearing DENV-infected cells in the host. In fact, immunisation with Dengvaxia[®] does not generate Th2 response (Guy, 2009); and this maybe one of the reasons that correlates with increased risk of ADE due to the lack of memory B cells to produce neutralising antibodies. Instead of eradicating virus-infected cells, sterilising immunity is able to block virus infection into the host and thereby prevent the evolution of virulence strain from ‘leaky’ infection (Read *et al.*, 2015).

For the immunogenicity studies of chimeric mHBcAg VLPs-displaying cEDIII, the first VLPs (a) experiment had failed to induce immune responses. Hence, VLPs (b)

experiment was designed as an improvement to VLPs (a), whereby the antigen dosage was increased to account for the molecular size difference as discussed in **Chapter 6**. This approach was also justified from the successful immunogold experiment, by which presentation of cEDIII epitopes in immunogenic context was convincingly shown. As anticipated, successful proof-of-concept was attained as cEDIII-specific humoral and cell-mediated responses could be detected by the end of VLPs (b) experiment. A predominant Th1 response was acquired after vaccination with mHBcAg-cEDIII VLPs and mHBcAg-cEDIII (L) VLPs, based on the high levels of IFN- γ and IL-2. Overall, it is noted that most of these chimeric VLPs require co-delivery with adjuvant to increase the stimulation of immune system. This is likely to correlate with the concept of molecular size difference, where adequate presentation of cEDIII epitopes may correspond to more efficient immune stimulation. Besides, it may be possible that aggregation of the VLPs has hindered effective display of cEDIII epitopes. However, this may be rather subjective as some researches claimed that aggregated VLPs can mediate stronger cytotoxic T cell responses with significant level of protection in mice, as compared to the non-aggregated form (Valdés *et al.*, 2009). Although the cross-presentation of aggregated species may be more effective, production of non-aggregated VLPs is still preferred considering the factor of product consistency.

Worthwhile to mention, this is the first study that reports on the successful production of chimeric HBcAg VLPs with dengue protein epitopes in plant system. In fact, the production of the monomeric core particles is proven to be feasible and is able to induce cEDIII-specific response (vaccine candidates: mHBcAg-cEDIII and mHBcAg-cEDIII (L)). This contradicts the perception made by previous studies (Peyret *et al.*, 2015; Walker *et al.*, 2011a), which claim that the chance of successful VLPs production can be perilously low and hence requires the use of new technology such as SplitCore and ‘Tandem Core’. However, this does not defy the usefulness of the tandem core approach, as preliminary evidence (**Appendix A6.4**) shown that the tHBcAg-cEDIII

particles could induce cEDIII-specific response with strong cytolytic activity. Thus, it seems promising to further explore the potential of tHBcAg-cEDIII VLPs as a dengue vaccine candidate, which may also address the low immunogenicity of the monomeric core particles.

Thus far, it is safe to say that cEDIII fusion with CTB performs better than chimeric VLPs with cEDIII display, at least at the equivalent dosage of 20 µg. Although the cEDIII formulated with alum seems to generate slightly stronger humoral response than the cEDIII fused with CTB, but latter is preferred due to the following reasons: (i) CTB has high T cell activating potential (ii) the built-in CTB enables easier vaccine preparation and reduces associated cost; and (iii) the potential use as multivalent vaccine against dengue and cholera diseases. In addition, it is believed that the pentamerisation of CTB-cEDIII-KDEL (xTH) fusion protein would impart added benefit for the development a highly stable vaccine with defined presentation of cEDIII on the oligomeric structure. Not to forget, CTB is a well-known mucosal adjuvant. Future prospect may consider developing the CTB-cEDIII-KDEL (xTH) fusion protein into an oral vaccine. For that, an *in vitro* antigen uptake assay can be performed using Peyer's patches to assess the binding ability to mucosal lymphoid tissues. Considering dengue often thrives in tropical developing nations, oral vaccination may be more amenable to mass immunisation without requiring specialised medical settings and assistance (Pang and Loh, 2017).

Comparing to other plant-based dengue vaccine researches (**Table 2.3**), one of the primary aspects in this study is the use of cEDIII antigen that simplifies the vaccine design that can offer tetravalent neutralisation with a considerably lower production cost. In fact, this is the first report which shows that non-adjuvanted, plant-produced cEDIII can elicit antigen-specific IgG production. It is greatly believed that the strategised ER localisation has preserved the correct folding of neutralising epitopes on EDIII. To enhance the immunogenicity of cEDIII, CTB-cEDIII-KDEL (xTH) protein was

developed in this study. The robustness of the fusion protein to be delivered in a self-adjuvanting manner is evidently shown, which can minimise the reliance on exogenous adjuvant. Likewise, Kim *et al.* (2017) had also attempted to engineer a self-adjuvanting molecule that features cEDIII fusion to polymeric immunoglobulin G scaffold (PIGS). However, its final yield at 17 mg/kg fresh weight tissue (FWT) was nearly 20 folds lower than CTB-cEDIII-KDEL (xTH). This may be explained from the use of *N. tabacum* optimised gene for expression in *N. benthamiana* system and the lack of subcellular localisation to improve protein stability. Although immunisation with adjuvanted cEDIII-PIGS yielded a remarkably high IgG titre at 1:1,000,000, but the poor neutralisation response against DENV 2 could be a demerit for the vaccine candidate. Following that, it is noteworthy to mention that this study is the first in the field of plant-based dengue vaccine research to demonstrate the ability of vaccine candidates to neutralise four DENV serotypes simultaneously. Besides, this study utilised the non-replicative system of pEAQ-*HT* vector by which there is no issue of sequence mutation as compared to the use of infectious RNA transcripts by Saejung *et al.* (2007).

Based on Malaysian context, local vaccine development would have a momentous impact as up to date, there are (i) no universal dengue vaccine is available yet; (ii) no effective containment of disease-carrying *Aedes* mosquitoes; and (iii) no specific anti-viral treatment to alleviate the potentially fatal illness. Particularly for nations with emerging economics, cost is the major determinant that affect the vaccine uptake and utilisation. A survey among policy-makers in South East Asia indicated that governments could afford to pay a price of \$0.50 – \$1.00 per dose of dengue vaccine given to the urgent need (DeRoeck *et al.*, 2003). However, this was not the case for Dengvaxia[®] as the price had been marked to approximately \$80 per shot for a national vaccination programme in Philippines (Afinidad-Bernardo, 2017). In fact, a survey indicated that only 17% of the Brazilian population would be willing to pay for this

vaccine (Godói *et al.*, 2017). Besides, an annual manufacturing capacity of 100 million doses of Dengvaxia® is insufficient to meet the demand of 3 billion people who are living in dengue-endemic areas (Dow and Mora, 2012). Following these reasons, it seems sensible to establish a local production system to deliver timely medical support. In addition, the production of dengue vaccine may bring added value to the nation's economy as the market is projected to capture an astounding value of USD \$4 billion – 21 billion (Kanagaraj *et al.*, 2011). Based on all the perspectives above, this study is viable and has shown the potential to make a significant impact in battling dengue disease which can benefit the global communities.

Limitations of current study and suggestions for improvements

Although the general objectives of the study had been achieved, some limitations were unavoidable and could be addressed in future for improvement. The first aspect is discussed in terms of the cassette designs of chimeric VLPs-displaying cEDIII (expressed by pEAQ-*HT*::mHBcAg-cEDIII, pEAQ-*HT*::mHBcAg-cEDIII (L) and pEAQ-*HT*::tHBcAg-cEDIII). Based on **Chapter 4**, the high expression of fusion proteins has spurred an interest of targeting the VLPs to cellular compartment to boost expression. Initially, there was a concern that the distinct pH conditions in different plant organelle can abolish VLPs assembly as shown by van Zyl *et al.* (2016). Nevertheless, there is exception as the hepatitis B virus surface antigen (HBsAg) VLPs could still assemble despite localisation to ER (Richter *et al.*, 2000; Sojikul *et al.*, 2003). Hence, it may be worthwhile to attempt subcellular localisation as a strategy to improve the expression yield of chimeric VLPs.

Apart from gene targeting, optimisation of coding sequence of HBcAg VLPs carrier could be considered as an improvement of cassette designs. To clarify, the *cEDIII* genes inserted into the c/el loop of the mHBcAg and tHBcAg VLPs carriers

were optimised with *N. benthamiana* codons (**Section 3.2.3**). But, the cloning vectors used for construction, namely pEAQ-*HT*::mEL for mHBcAg VLPs and pEAQ-*HT*::tHBcAg-VHH2 for tHBcAg VLPs, were previously codon-optimised for *E. coli* expression. Knowing that there might be a risk of low expression, codon optimisation of the VLPs carriers was not attempted as it was thought to be safer to continue working with the *E. coli*-optimised construct. This was because codon optimisation may not be always beneficial as some studies had observed a failed particle production when the plant codon-optimised gene was used (Maclean *et al.*, 2007; Šmídková *et al.*, 2010). Likewise, this strategy could be considered in future to explore the feasibility of improving the VLPs expression using *N. benthamiana* codon-optimised mHBcAg and tHBcAg sequences.

The second aspect is related to the improvement of agroinfiltration. In this study, only the agrobacterial strain LBA4404 was used for transgene delivery as this was the preferred strain. Future work may consider the employment of strain GV3101, as Shah *et al.* (2013) claimed that higher GFP expression could be obtained following the delivery of pEAQ-*HT* vector using GV3101. Other improvements may include optimisation of the bacterial inoculation density and adding additives in the infiltration medium to enhance transformation efficiency. Zhao *et al.* (2017) found that a combinative supplement of 0.56 mM ascorbate acid, 20 µM 5-azacytidine and 0.03% (v/v) Tween-20 could boost the transgene expression by up to 6 folds.

Thirdly, the purification procedures for cEDIII recombinant proteins could be improved with polishing step via ion exchange chromatography or SEC. This part was not focused in this study as the main objective was to recover satisfactory amount of recombinant proteins for immunogenicity test, which was primarily achieved via IMAC. Immuno-affinity chromatography may be used as a substitute of IMAC since low yield of cEDIII was obtained following TEV cleavage. Besides, future X-ray crystallographic study of cEDIII protein could be considered as this has not been studied yet, and this

information would help in understanding the protein structure and function for better utilisation of cEDIII in vaccine development. Meanwhile, the purification procedures for VLPs sample are rather well-established and future work may focus on standardising the use of nycodenz density gradient for isolation of chimeric VLPs.

The last aspect is considered in relevant to the immunogenicity analyses. For the immunisation with chimeric mHBcAg VLPs displaying cEDIII, it is now understood that the formulation of antigen dose should account for the molecular size of chimeric VLPs so that sufficient cEDIII epitopes could be presented to the mouse immune system. Although the VLPs (b) experiment is proven to be a successful modification, further optimisation of the injection dosage may serve valuable to determine the threshold needed to achieve a strong immune stimulation.

Conclusions and future perspectives

The work presented in this study provides a significant step in paving way towards plant-based dengue vaccine development. This is particularly important to address the alarming burden of dengue disease that has yet to meet a promising resolution. Establishment of the plant production system can solve a vast of the intriguing concerns of vaccine cost and accessibility faced by the poorer people in dengue-endemic areas. It is of no doubt that cEDIII is able to confer neutralising protection against four DENV serotypes along with stimulation of Th1 response. The antigen fusion with CTB, namely CTB-cEDIII-KDEL (xTH) has not only preserved its biologically-active pentameric structure, but also potentiates the immune responses with high neutralising antibody titres and robust activation of balanced Th1/Th2 responses. Meanwhile, the presentation of cEDIII epitopes on VLPs carrier is proven to be feasible, which also has been displayed in immunogenic context in mHBcAg-cEDIII VLPs, mHBcAg-cEDIII (L) VLPs and tHBcAg-cEDIII VLPs. In fact, the preliminary study on tHBcAg-cEDIII VLPs shows that it can elicit robust immunogenicity with high cytolytic activity that warrants for future investigation as a better VLPs-based vaccine.

Prevention is always better than cure. Considering that dengue outbreaks predominantly occur in developing nations including Malaysia, the development of an affordable and effective vaccine that can benefit all communities is highly desired. This also complements to the government's efforts in combating disease transmission and makes a significant impact in dengue control. It is believed that the findings reported in this study would deliver a substantial impact to the field of plant-based dengue vaccine development and make a leap to clinical trials in the nearest future.

8 References

- Abdalla, M., Eltayb, W. A., Samad, A., Elshareef, S., and Dafaalla, T. (2016). Important factors influencing protein crystallization. *Global Journal of Biotechnology and Biomaterial Science*, 2(1), 25–28.
- Abubakar, S., and Shafee, N. (2002). Outlook of dengue in Malaysia: a century later. *The Malaysian Journal of Pathology*, 24(1), 23–27.
- Afinidad-Bernardo, D. R. M. (2017). Dengue vaccine now available over the counter. Retrieved January 18, 2018, from <http://www.philstar.com/health-and-family/2017/03/31/1686369/dengue-vaccine-now-available-over-counter>
- Aguilar, J. C., and Rodríguez, E. G. (2007). Vaccine adjuvants revisited. *Vaccine*, 25, 3752–3762.
- Allison, S. L., Schalich, J., Stiasny, K., Mandl, C. W., Kunz, C., and Heinz, F. X. (1995). Oligomeric rearrangement of tick-borne encephalitis virus envelope proteins induced by an acidic pH. *Journal of Virology*, 69(2), 695–700.
- Alvarez, D. E., Lodeiro, M. F., Ludueña, S. J., Pietrasanta, L. I., and Gamarnik, A. V. (2005). Long-range RNA-RNA interactions circularize the dengue virus genome. *Journal of Virology*, 79(11), 6631–6643.
- Amor-Mahjoub, M., Suppini, J. P., Gomez-Vrielyunck, N., and Ladjimi, M. (2006). The effect of the hexahistidine-tag in the oligomerization of HSC70 constructs. *Journal of Chromatography B: Analytical Technologies in the Biomedical and Life Sciences*, 844, 328–334.
- Anfasa, F., Nainggolan, L., and Martina, B. E. E. (2015). Dengue virus infection in humans: epidemiology, biology, pathogenesis, and clinical aspects. In S. K. Singh (Ed.), *Human Emerging and Re-emerging Infections: Viral and Parasitic Infections, Volume I* (pp. 125–144). Hoboken: John Wiley & Sons, Inc.

Angov, E. (2011). Codon usage: Nature's roadmap to expression and folding of proteins. *Biotechnology Journal*, 6, 650–659.

Angov, E., Hillier, C. J., Kincaid, R. L., and Lyon, J. A. (2008). Heterologous protein expression is enhanced by harmonizing the codon usage frequencies of the target gene with those of the expression host. *PLoS ONE*, 3(5), e1289. doi: 10.1371/journal.pone.0002189.

Antiporda, J. (2018). Child dies after “Dengvaxia” shot. Retrieved January 16, 2018, from <http://www.manilatimes.net/child-dies-dengvaxia-shot/374380/>

Bäck, A. T., and Lundkvist, A. (2013). Dengue viruses - an overview. *Infection Ecology & Epidemiology*, 3, 19839. doi: 10.3402/iee.v3i0.19839.

Barta, A., Sommergruber, K., Thompson, D., Hartmuth, K., Matzke, M. A., and Matzke, A. J. M. (1986). The expression of a nopaline synthase - human growth hormone chimaeric gene in transformed tobacco and sunflower callus tissue. *Plant Molecular Biology*, 6, 347–357.

Bauer, K., Esquilin, I. O., Cornier, A. S., Thomas, S. J., del Rio, A. I. Q., Bertran-Pasarell, J., ... Innis, B. L. (2015). A phase II, randomized, safety and immunogenicity trial of a re-derived, live-attenuated dengue virus vaccine in healthy children and adults living in Puerto Rico. *American Journal of Tropical Medicine and Hygiene*, 93(3), 441–453.

Beckett, C. G., Jeffrey, T., Burgess, T., Danko, J. R., Tamminga, C., Simmons, M., ... Porter, K. R. (2011). Evaluation of a prototype dengue-1 DNA vaccine in a phase 1 clinical trial. *Vaccine*, 29(5), 960–968.

Belisle, E. H., and Strausser, H. R. (1981). Sex-related immunocompetence of BALB/c mice: II. Study of immunologic responsiveness of young, adult and aged mice. *Developmental and Comparative Immunology*, 5, 661–670.

Benchabane, M., Goulet, C., Rivard, D., Faye, L., Gomord, V., and Michaud, D. (2008). Preventing unintended proteolysis in plant protein biofactories. *Plant Biotechnology Journal*, 6, 633–648.

Benedict, M. Q., and Robinson, A. S. (2003). The first releases of transgenic mosquitoes: an argument for the sterile insect technique. *Trends in Parasitology*, 19(8), 349–355.

Bernama. (2017). Health Ministry releases *Wolbachia*-infected mosquitoes in Keramat. Retrieved April 16, 2018, from <https://www.nst.com.my/news/2017/03/225454/health-ministry-releases-wolbachia-infected-mosquitoes-keramat>

Bevan, M. W., Flavell, R. B., and Chilton, M. D. (1983). A chimaeric antibiotic resistance gene as a selectable marker for plant cell transformation. *Nature*, 304, 184–187.

Bhatt, S., Gething, P. W., Brady, O. J., Messina, J. P., Farlow, A. W., Moyes, C. L., ... Hay, S. I. (2013). The global distribution and burden of dengue. *Nature*, 496(7446), 504–507.

Block, H., Maertens, B., Priestersbach, A., Brinker, N., Kubicek, J., Fabis, R., ... Schäfer, F. (2009). Immobilized-metal affinity chromatography (IMAC). a review. In B. R. Richard and M. P. Deutscher (Eds.), *Guide to Protein Purification* (Second, Vol. 463, pp. 439–473). San Diego: Academic Press.

Block, O. K. T., Rodrigo, W. W. S. I., Quinn, M., Jin, X., Rose, R. C., and Schlesinger, J. J. (2010). A tetravalent recombinant dengue domain III protein vaccine stimulates neutralizing and enhancing antibodies in mice. *Vaccine*, 28(51), 8085–8094.

Bornhorst, J. A., and Falke, J. J. (2000). Purification of proteins using polyhistidine affinity tags. In J. Thorner, S. Emr, and J. Abelson (Eds.), *Methods in Enzymology* (Vol. 326, pp. 245–254). San Diego: Academic Press.

Bottcher, B., Wynne, S. A., and Crowther, R. A. (1997). Determination of the fold of

the core protein of hepatitis B virus by electron cryomicroscopy. *Nature*, 386, 88–91.

Brady, O. J., Gething, P. W., Bhatt, S., Messina, J. P., Brownstein, J. S., Hoen, A. G., ... Hay, S. I. (2012). Refining the global spatial limits of dengue virus transmission by evidence-based consensus. *PLoS Neglected Tropical Diseases*, 6(8), e1760. doi: 10.1371/journal.pntd.0001760.

Brown, A. L., Francis, M. J., Hastings, G. Z., Parry, N. R., Barnett, P. V, Rowlands, D. J., and Clarke, B. E. (1991). Foreign epitopes in immunodominant regions of hepatitis B core particles are highly immunogenic and conformationally restricted. *Vaccine*, 9, 595–601.

Bull, J. J., and Turelli, M. (2013). *Wolbachia* versus dengue: evolutionary forecasts. *Evolution, Medicine, and Public Health*, 2013(1), 197–201.

Burguán, J., and Havelda, Z. (2011). Viral suppressors of RNA silencing. *Trends in Plant Science*, 16(5), 265–272.

Burkholder, T., Foltz, C., Karlsson, E., Linton, C. G., and Smith, J. M. (2012). Health evaluation of experimental laboratory mice. *Current Protocols in Mouse Biology*, 2, 145–165.

Canavello, P. R., Cachat, J. M., Hart, P. C., Murphy, D. L., and Kalueff, A. V. (2013). Behavioral phenotyping of mouse grooming and barbering. In W. E. Crusio, F. Sluyter, R. T. Gerlai, and S. Pietropaolo (Eds.), *Behavioral Genetics of the Mouse Volume I: Genetics of Behavioral Phenotypes* (pp. 195–204). New York: Cambridge University Press.

Cañizares, M. C., Liu, L., Perrin, Y., Tsakiris, E., and Lomonosoff, G. P. (2006). A bipartite system for the constitutive and inducible expression of high levels of foreign proteins in plants. *Plant Biotechnology Journal*, 4, 183–193.

Capeding, M. R., Tran, N. H., Hadinegoro, S. R. S., Muhammad Ismail, H. I. H.,

Chotpitayasunondh, T., Chua, M. N., ... Bouckennooghe, A. (2014). Clinical efficacy and safety of a novel tetravalent dengue vaccine in healthy children in Asia: a phase 3, randomised, observer-masked, placebo-controlled trial. *The Lancet*, 384(9951), 1358–1365.

Centers for Disease Control and Prevention (CDC). (2013). Detection of cholera toxin. In *Laboratory Methods for the Diagnosis of Vibrio Cholerae*. Retrieved from August 10, 2016, from <https://www.cdc.gov/cholera/pdf/laboratory-methods-for-the-diagnosis-of-vibrio-cholerae-chapter-7.pdf>

Chambers, T. J., Nestorowicz, A., Mason, P. W., and Rice, C. M. (1999). Yellow fever/Japanese encephalitis chimeric viruses: construction and biological properties. *Journal of Virology*, 73(4), 3095–3101.

Chant, A., Kraemer-Pecore, C. M., Watkin, R., and Kneale, G. G. (2005). Attachment of a histidine tag to the minimal zinc finger protein of the *Aspergillus nidulans* gene regulatory protein AreA causes a conformational change at the DNA-binding site. *Protein Expression and Purification*, 39, 152–159.

Chaturvedi, U. C., Agarwal, R., Elbishbishi, E. A., and Mustafa, A. S. (2000). Cytokine cascade in dengue hemorrhagic fever: implications for pathogenesis. *FEMS Immunology & Medical Microbiology*, 28, 183–188.

Chaudhry, S., Swaminathan, S., and Khanna, N. (2006). Viral genetics as a basis of dengue pathogenesis. *Dengue Bulletin*, 30, 121–132.

Chávez, J. H., Silva, J. R., Amarilla, A. A., and Figueiredo, L. T. M. (2010). Domain III peptides from flavivirus envelope protein are useful antigens for serologic diagnosis and targets for immunization. *Biologicals*, 38, 613–618.

Cheah, W. K., Ng, K. S., Marzilawati, A. R., and Lum, L. C. S. (2014). A review of dengue research in Malaysia. *Medical Journal of Malaysia*, 69, 59–67.

Chen, H. W., Liu, S. J., Li, Y. S., Liu, H. H., Tsai, J. P., Chiang, C. Y., ... Pan, C. H. (2013a). A consensus envelope protein domain III can induce neutralizing antibody responses against serotype 2 of dengue virus in non-human primates. *Archives of Virology*, *158*, 1523–1531.

Chen, Q., and Lai, H. (2014). Plant-derived monoclonal antibodies as human biologics for infectious disease and cancer. In K. L. Hefferon (Ed.), *Plant-derived Pharmaceuticals: Principles and Applications for Developing Countries* (pp. 42–75). Wallingford: CAB International.

Chen, Q., Lai, H., Hurtado, J., Stahnke, J., Leuzinger, K., and Dent, M. (2013b). Agroinfiltration as an effective and scalable strategy of gene delivery for production of pharmaceutical proteins. *Advanced Techniques in Biology & Medicine*, *1*(1), 1–9.

Chiang, C. Y., Liu, S. J., Tsai, J. P., Li, Y. S., Chen, M. Y., Liu, H. H., ... Chen, H. W. (2011). A novel single-dose dengue subunit vaccine induces memory immune responses. *PLoS ONE*, *6*(8). doi: 10.1371/journal.pone.0023319.

Chua, A. J. S., Vituret, C., Tan, M. L. C., Gonzalez, G., Boulanger, P., Ng, M. L., and Hong, S. S. (2013). A novel platform for virus-like particle-display of flaviviral envelope domain III: induction of dengue and West Nile virus neutralizing antibodies. *Virology Journal*, *10*, 129. doi: 10.1186/1743-422X-10-129.

Clarke, B. E., Newton, S. E., Carroll, A. R., Francis, M. J., Appleyard, G., Syred, A. D., ... Brown, F. (1987). Improved immunogenicity of a peptide epitope after fusion to hepatitis B core protein. *Nature*, *330*, 381–384.

Clements, D. E., Collier, B. A. G., Lieberman, M. M., Ogata, S., Wang, G., Harada, K. E., ... Humphreys, T. (2010). Development of a recombinant tetravalent dengue virus vaccine: Immunogenicity and efficacy studies in mice and monkeys. *Vaccine*, *28*, 2705–2715.

- Coffman, R. L., Sher, A., and Seder, R. A. (2010). Vaccine adjuvants: putting innate immunity to work. *Immunity*, 33, 492–503.
- Coller, B. A. G., Clements, D. E., Bett, A. J., Sagar, S. L., and ter Meulen, J. H. (2011). The development of recombinant subunit envelope-based vaccines to protect against dengue virus induced disease. *Vaccine*, 29(42), 7267–7275.
- Cologna, R., and Rico-Hesse, R. (2003). American genotype structures decrease dengue virus output from human monocytes and dendritic cells. *Journal of Virology*, 77(7), 3929–3938.
- Connell, T. D. (2010). Cholera toxin, LT-I, LT-IIa, and LT-IIb: the critical role of ganglioside-binding in immunomodulation by type I and type II heat-labile enterotoxins. *Expert Review of Vaccines*, 6(5), 821–834.
- Cooper, A., and Shaul, Y. (2006). Clathrin-mediated endocytosis and lysosomal cleavage of hepatitis B virus capsid-like core particles. *Journal of Biological Chemistry*, 281(24), 16563–16569.
- Cornelissen, B. J. C., Horowitz, J., van Kan, J. A. L., Goldberg, R. B., and Bol, J. F. (1987). Structure of tobacco genes encoding pathogenesis-related proteins from the PR-1 group. *Nucleic Acids Research*, 15(17), 6799–6811.
- Crill, W. D., and Roehrig, J. T. (2001). Monoclonal antibodies that bind to domain III of dengue virus E glycoprotein are the most efficient blockers of virus adsorption to Vero cells. *Journal of Virology*, 75(16), 7769–7773.
- Crowther, R. A., Kiselev, N. A., Bottcher, B., Berriman, J. A., Borisova, G. P., Ose, V., and Pumpens, P. (1994). Three-dimensional structure of hepatitis B virus core particles determined by electron cryomicroscopy. *Cell*, 77, 943–950.
- Cruz-Oliveira, C., Freire, J. M., Conceição, T. M., Higa, L. M., Castanho, M. A. R. B., and Da Poian, A. T. (2015). Receptors and routes of dengue virus entry into the host

cells. *FEMS Microbiology Reviews*, 39, 155–170.

D'Aoust, M. A., Couture, M. M. J., Charland, N., Trepanier, S., Landry, N., Ors, F., and Vezina, L. P. (2010). The production of hemagglutinin-based virus-like particles in plants: a rapid, efficient and safe response to pandemic influenza. *Plant Biotechnology Journal*, 8, 607–619.

Dallas, W. S., and Falkow, S. (1980). Amino acid sequence homology between cholera toxin and *Escherichia coli* heat-labile toxin. *Nature*, 288, 499–501.

Davidson, E., Bryan, C., Fong, R. H., Barnes, T., Pfaff, J. M., Mabila, M., ... Doranz, B. J. (2015). Mechanism of binding to Ebola virus glycoprotein by the ZMapp, ZMAb, and MB-003 cocktail antibodies. *Journal of Virology*, 89(21), 10982–10992.

Demain, A. L., and Vaishnav, P. (2009). Production of recombinant proteins by microbes and higher organisms. *Biotechnology Advances*, 27, 297–306.

Dennis, S. J., Meyers, A. E., Guthrie, A. J., Hitzeroth, I. I., and Rybicki, E. P. (2018). Immunogenicity of plant-produced African horse sickness virus-like particles: implications for a novel vaccine. *Plant Biotechnology Journal*, 16(2), 442-450.

DeRoeck, D., Deen, J., and Clemens, J. D. (2003). Policymakers' views on dengue fever/dengue haemorrhagic fever and the need for dengue vaccines in four Southeast Asian countries. *Vaccine*, 22, 121–129.

Dertzbaugh, M. T., and Cox, L. M. (1998). The affinity of cholera toxin for Ni²⁺ ion. *Protein Engineering*, 11(7), 577–581.

Diamond, M. S., and Pierson, T. C. (2015). Molecular insight into dengue virus pathogenesis and its implications for disease control. *Cell*, 162(3), 488–492.

Dijkstra, J., and de Jager, C. P. (1998). *Practical plant virology: protocols and exercises*. Berlin, Heidelberg: Springer-Verlag Berlin Heidelberg.

Domingo, E. (1997). Rapid evolution of viral RNA genomes. *The Journal of Nutrition*,

127, 958S–961S.

Dopping-Hepenstal, P. J. C., and Beesley, J. E. (1993). Gold labelling in negative stain immune electron microscopy. In A. D. Hyatt and B. T. Eaton (Eds.), *Immuno-Gold Electron Microscopy in Virus Diagnosis and Research* (pp. 71–88). Florida: CRC Press, Inc.

Dow, G., and Mora, E. (2012). The maximum potential market for dengue drugs V 1.0. *Antiviral Research*, 96, 203–212.

Dowd, K. A., and Pierson, T. C. (2011). Antibody-mediated neutralization of flaviviruses: A reductionist view. *Virology*, 411(2), 306–315.

Duong-Ly, K. C., and Gabelli, S. B. (2014a). Gel filtration chromatography (size exclusion chromatography) of proteins. In J. Lorsch (Ed.), *Methods in Enzymology* (Vol. 541, pp. 105–114). San Diego: Elsevier Inc.

Duong-Ly, K. C., and Gabelli, S. B. (2014b). Using ion exchange chromatography to purify a recombinantly expressed protein. In J. Lorsch (Ed.), *Methods in Enzymology* (Vol. 541, pp. 95–103). San Diego: Elsevier Inc.

Durbin, A. P., Kirkpatrick, B. D., Pierce, K. K., Elwood, D., Larsson, C. J., Lindow, J. C., ... Whitehead, S. S. (2013). A single dose of any of four different live attenuated tetravalent dengue vaccines is safe and immunogenic in flavivirus-naive adults: A randomized, double-blind clinical trial. *Journal of Infectious Diseases*, 207, 957–965.

Durbin, A. P., Kirkpatrick, B. D., Pierce, K. K., Schmidt, A. C., and Whitehead, S. S. (2011). Development and clinical evaluation of multiple investigational monovalent DENV vaccines to identify components for inclusion in a live attenuated tetravalent DENV vaccine. *Vaccine*, 29, 7242–7250.

Ebi, K. L., and Nealon, J. (2016). Dengue in a changing climate. *Environmental Research*, 151, 115–123.

Eckels, K. H., Dubois, D. R., Putnak, R., Vaughn, D. W., Innis, B. L., Henchal, E. A., and Hoke, C. H. (2003). Modification of dengue virus strains by passage in primary dog kidney cells: preparation of candidate vaccines and immunization of monkeys. *American Journal of Tropical Medicine and Hygiene*, 69(Suppl 6), 12–16.

Ellgaard, L. (2004). Catalysis of disulphide bond formation in the endoplasmic reticulum. *Biochemical Society Transactions*, 32(5), 663–667.

Eriksson, K., Fredriksson, M., Nordström, I., and Holmgren, J. (2003). Cholera toxin and its B subunit promote dendritic cell vaccination with different influences on Th1 and Th2 development. *Infection and Immunity*, 71(4), 1740–1747.

Etemad, B., Batra, G., Raut, R., Dahiya, S., Khanam, S., Swaminathan, S., and Khanna, N. (2008). An envelope domain III-based chimeric antigen produced in *Pichia pastoris* elicits neutralizing antibodies against all four dengue virus serotypes. *American Journal of Tropical Medicine and Hygiene*, 79(3), 353–363.

Faheem, M., Raheel, U., Riaz, M. N., Kanwal, N., Javed, F., us Sahar Sadaf Zaidi, N., and Qadri, I. (2011). A molecular evaluation of dengue virus pathogenesis and its latest vaccine strategies. *Molecular Biology Reports*, 38(6), 3731–3740.

Fanata, W. I. D., Lee, S. Y., and Lee, K. O. (2013). The unfolded protein response in plants: a fundamental adaptive cellular response to internal and external stresses. *Journal of Proteomics*, 93, 356–368.

Faye, L., Boulaflous, A., Benchabane, M., Gomord, V., and Michaud, D. (2005). Protein modifications in the plant secretory pathway: current status and practical implications in molecular pharming. *Vaccine*, 23, 1770–1778.

Fernandez-Garcia, M. D., Mazzon, M., Jacobs, M., and Amara, A. (2009). Pathogenesis of flavivirus infections: using and abusing the host cell. *Cell Host and Microbe*, 5(4), 318–328.

- Ferrari, C., Bertoletti, A., Penna, A., Cavalli, A., Valli, A., Missale, G., ... Fiaccadori, F. (1991). Identification of immunodominant T cell epitopes of the hepatitis B virus nucleocapsid antigen. *Journal of Clinical Investigation*, 88(1), 214–222.
- Fraley, R. T., Rogers, S. G., Horsch, R. B., Sanders, P. R., Flick, J. S., Adams, S. P., ... Woo, S. C. (1983). Expression of bacterial genes in plant cells. *Genetics*, 80, 4803–4807.
- Francis, M. J., Hastings, G. Z., Brown, A. L., Grace, K. G., Rowlands, D. J., Brown, F., and Clarke, B. E. (1990). Immunological properties of hepatitis B core antigen fusion proteins. *Proceedings of the National Academy of Sciences of the United States of America*, 87, 2545–2549.
- Freytag, L. C., and Clements, J. D. (2015). Mucosal adjuvants: new developments and challenges. In J. Mestecky, W. Strober, M. W. Russell, H. Cheroutre, B. N. Lambrecht, and B. L. Kelsall (Eds.), *Mucosal Immunology* (4th ed., Vol. 1, pp. 1183–1199). Oxford: Academic Press.
- Fried, J. R., Gibbons, R. V, Kalayanarooj, S., Thomas, S. J., Srikiatkachorn, A., Yoon, I. K., ... Cummings, D. A. T. (2010). Serotype-specific differences in the risk of dengue hemorrhagic fever: An analysis of data collected in Bangkok, Thailand from 1994 to 2006. *PLoS Neglected Tropical Diseases*, 4(3), e617. doi: 10.1371/journal.pntd.0000617.
- Fuscaldo, A. A., Aaslestad, H. G., and Hoffman, E. J. (1971). Biological, physical, and chemical properties of Eastern equine encephalitis virus. I. Purification and physical properties. *Journal of Virology*, 7(2), 233–240.
- Gaik, S. K., Pujar, N. S., and Titchener-Hooker, N. J. (2008). Study of detergent-mediated liberation of hepatitis B virus-like particles from *S. cerevisiae* homogenate: identifying a framework for the design of future-generation lipoprotein vaccine processes. *Biotechnology Progress*, 24, 623–631.

- Gallina, A., Bonelli, F., Zentilin, L., Rindi, G., Muttini, M., and Milanese, G. (1989). A recombinant hepatitis B core antigen polypeptide with the protamine-like domain deleted self-assembles into capsid particles but fails to bind nucleic acids. *Journal of Virology*, *63*, 4645–4652.
- Garner, J. P., Dufour, B., Gregg, L. E., Weisker, S. M., and Mench, J. A. (2004). Social and husbandry factors affecting the prevalence and severity of barbering (“whisker trimming”) by laboratory mice. *Applied Animal Behaviour Science*, *89*, 263–282.
- Gebhard, L. G., Filomatori, C. V., and Gamarnik, A. V. (2011). Functional RNA elements in the dengue virus genome. *Viruses*, *3*, 1739–1756.
- Gecchele, E., Merlin, M., Brozzetti, A., Falorni, A., Pezzotti, M., and Avesani, L. (2015). A comparative analysis of recombinant protein expression in different biofactories: bacteria, insect cells and plant systems. *Journal of Visualized Experiments*, *97*, e52459. doi: 10.3791/52459.
- Gehin, A., Gilbert, R., Stuart, D., and Rowlands, D. (2004). *U.S. Patent No. US 2001/0223965 A1*. Washington, DC: U.S. Patent and Trademark Office.
- George, R. A., and Heringa, J. (2003). An analysis of protein domain linkers: their classification and role in protein folding. *Protein Engineering*, *15*(11), 871–879.
- George-Chandy, A., Eriksson, K., Lebens, M., Nordström, I., Schön, E., and Holmgren, J. (2001). Cholera toxin B subunit as a carrier molecule promotes antigen presentation and increases CD40 and CD86 expression on antigen-presenting cells. *Infection and Immunity*, *69*(9), 5716–5725.
- Gerds, V., Mutwiri, G., Richards, J., van Drunen Littel-van den Hurk, S., and Potter, A. A. (2013). Carrier molecules for use in veterinary vaccines. *Vaccine*, *31*(4), 596–602.
- Gias, E., Nielsen, S. U., Morgan, L. A. F., and Toms, G. L. (2008). Purification of human respiratory syncytial virus by ultracentrifugation in iodixanol density gradient.

Journal of Virological Methods, 147, 328–332.

Gill, D. M. (1976). The arrangement of subunits in cholera toxin. *Biochemistry*, 15(6), 1242–1248.

Gleba, Y., Klimyuk, V., and Marillonnet, S. (2007). Viral vectors for the expression of proteins in plants. *Current Opinion in Biotechnology*, 18, 134–141.

Godói, I. P., Santos, A. S., Reis, E. A., Lemos, L. L. P., Brandão, C. M. R., Alvares, J., ... Júnior, A. A. G. (2017). Consumer willingness to pay for dengue vaccine (CYD-TDV, Dengvaxia®) in Brazil; implications for future pricing considerations. *Frontiers in Pharmacology*, 8, 41. doi: 10.3389/fphar.2017.00041.

Goodin, M. M., Zaitlin, D., Naidu, R. A., and Lommel, S. A. (2008). *Nicotiana benthamiana*: its history and future as a model for plant-pathogen interactions. *Molecular Plant-Microbe Interactions*, 21(8), 1015–1026.

Gottschamel, J., Lössl, A., Ruf, S., Wang, Y., Skaugen, M., Bock, R., and Clarke, J. L. (2016). Production of dengue virus envelope protein domain III-based antigens in tobacco chloroplasts using inducible and constitutive expression systems. *Plant Molecular Biology*, 91, 497–512.

Govindarajan, D., Meschino, S., Guan, L., Clements, D. E., ter Meulen, J. H., Casimiro, D. R., ... Bett, A. J. (2015). Preclinical development of a dengue tetravalent recombinant subunit vaccine: Immunogenicity and protective efficacy in nonhuman primates. *Vaccine*, 33, 4105–4116.

Green, A. M., Beatty, P. R., Hadjilaou, A., and Harris, E. (2014). Innate immunity to dengue virus infection and subversion of antiviral responses. *Journal of Molecular Biology*, 426(6), 1148–1160.

Griffiths, A. (2000). Centrifugation techniques. In K. Wilson and J. Walker (Eds.), *Principles and Techniques of Practical Biochemistry* (5th ed., pp. 263–311). Cambridge:

Cambridge University Press.

Grimsley, N., Hohn, T., Davies, J. W., and Hohn, B. (1987). *Agrobacterium*-mediated delivery of infectious maize streak virus into maize plants. *Nature*, 325, 177–179.

Gubler, D. J. (1998a). Dengue and dengue hemorrhagic fever. *Clinical Microbiology Reviews*, 11, 480–496.

Gubler, D. J. (1998b). Resurgent vector-borne diseases as a global health problem. *Emerging Infectious Diseases*, 4(3), 442–450.

Gubler, D. J. (2011). Dengue, urbanization and globalization: the unholy trinity of the 21st Century. *Tropical Medicine and Health*, 39(4), 3–11.

Gubler, D. J. (2014). Dengue viruses: their evolution, history and emergence as a global public health problem. In D. J. Gubler, E. E. Ooi, S. Vasudevan, and J. Farrar (Eds.), *Dengue and dengue hemorrhagic fever* (pp. 1–29). Oxfordshire: CAB International.

Gugerli, P. (1984). Isopycnic centrifugation of plant viruses in Nycodenz[®] density gradients. *Journal of Virological Methods*, 9(3), 249–258.

Guillén, G., Aguilar, J. C., Dueñas, S., Hermida, L., Guzmán, M. G., Penton, E., ... Herrera, L. (2010). Virus-like particles as vaccine antigens and adjuvants: application to chronic disease, cancer immunotherapy and infectious disease preventive strategies. *Procedia in Vaccinology*, 2(2), 128–133.

Guirakhoo, F., Arroyo, J., Pugachev, K. V, Miller, C., Zhang, Z. X., Weltzin, R., ... Monath, T. P. (2001). Construction, safety, and immunogenicity in nonhuman primates of a chimeric yellow fever-dengue virus tetravalent vaccine. *Journal of Virology*, 75(16), 7290–7304.

Guirakhoo, F., Pugachev, K., Arroyo, J., Miller, C., Zhang, Z. X., Weltzin, R., ... Monath, T. P. (2002). Viremia and immunogenicity in nonhuman primates of a tetravalent yellow fever-dengue chimeric vaccine: genetic reconstructions, dose

adjustment, and antibody responses against wild-type dengue virus isolates. *Virology*, 298, 146–159.

Guirakhoo, F., Pugachev, K., Zhang, Z., Myers, G., Levenbook, I., Draper, K., ... Monath, T. (2004). Safety and efficacy of chimeric yellow fever-dengue virus tetravalent vaccine formulations in nonhuman primates. *Journal of Virology*, 78(9), 4761–4775.

Guirakhoo, F., Weltzin, R., Chambers, T. J., Zhang, Z. X., Soike, K., Ratterree, M., ... Monath, T. P. (2000). Recombinant chimeric yellow fever-dengue type 2 virus is immunogenic and protective in nonhuman primates. *Journal of Virology*, 74(12), 5477–5485.

Guirakhoo, F., Zhang, Z. X., Chambers, T. J., Delagrave, S., Arroyo, J., Barrett, A. D. T., and Monath, T. P. (1999). Immunogenicity, genetic stability, and protective efficacy of a recombinant, chimeric yellow fever-Japanese encephalitis virus (ChimeriVax-JE) as a live, attenuated vaccine candidate against Japanese encephalitis. *Virology*, 257(2), 363–72.

Guy, B., Barban, V., Mantel, N., Aguirre, M., Gulia, S., Pontvianne, J., ... Lang, J. (2009). Evaluation of interferences between dengue vaccine serotypes in a monkey model. *American Journal of Tropical Medicine and Hygiene*, 80(2), 302–311.

Guzman, M. G., Halstead, S. B., Artsob, H., Buchy, P., Farrar, J., Gubler, D. J., ... Peeling, R. W. (2010). Dengue: a continuing global threat. *Nature Reviews Microbiology*, 8, S7–S16.

Hadinegoro, S. R., Arredondo-García, J. L., Capeding, M. R., Deseda, C., Chotpitayasunondh, T., Dietze, R., ... Saviile, M. (2015). Efficacy and long-term safety of a dengue vaccine in regions of endemic disease. *New England Journal of Medicine*, 373(13), 1195–1206.

Halstead, S. B. (2013). Identifying protective dengue vaccines: guide to mastering an empirical process. *Vaccine*, *31*, 4504–4507.

Halstead, S. B. (2015). Pathogenesis of dengue: dawn of a new era [version 1; referees: 3 approved]. *F1000Research*, *4*(F1000 Faculty Rev), 1353. doi: 10.12688/f1000research.7024.1

Hamorsky, K. T., Kouokam, J. C., Jurkiewicz, J. M., Nelson, B., Moore, L. J., Husk, A. S., ... Matoba, N. (2015). N-glycosylation of cholera toxin B subunit in *Nicotiana benthamiana*: impacts on host stress response, production yield and vaccine potential. *Scientific Reports*, *5*, 8003. doi: 10.1038/srep08003.

Harakuni, T., Sugawa, H., Komesu, A., Tadano, M., and Arakawa, T. (2005). Heteropentameric cholera toxin B subunit chimeric molecules genetically fused to a vaccine antigen induce systemic and mucosal immune responses: A potential new strategy to target recombinant vaccine antigens to mucosal immune systems. *Infection and Immunity*, *73*(9), 5654–5665.

Hatch, S., Endy, T. P., Thomas, S., Mathew, A., Potts, J., Pazoles, P., ... Rothman, A. L. (2011). Intracellular cytokine production by dengue virus-specific T cells correlates with subclinical secondary infection. *Journal of Infectious Diseases*, *203*(9), 1282–1291.

He, J., Peng, L., Lai, H., Hurtado, J., Stahnke, J., and Chen, Q. (2014). A plant-produced antigen elicits potent immune responses against West Nile Virus in mice. *BioMed Research International*, *2014*, 952865. doi: 10.1155/2014/952865.

Henchal, E. A., and Putnak, J. R. (1990). The dengue viruses. *Clinical Microbiology Reviews*, *3*(4), 376–396.

Heo, Y., Pyo, M. J., Bae, S. K., Lee, H., Kwon, Y. C., Kim, J. H., ... Kim, E. (2015). Evaluation of phototoxic and skin sensitization potentials of PLA₂-free bee venom. *Evidence-Based Complementary and Alternative Medicine*, *2015*, 157367. doi:

10.1155/2015/157367.

Herrera-Estrella, L., Depicker, A., and van Montagu, M. (1983). Expression of chimaeric genes transferred into plant cells using a Ti-plasmid-derived vector. *Nature*, 303, 209–213.

Ho, M. M., Bolgiano, B., Martino, A., Kairo, S. K., and Corbel, M. J. (2006). Preclinical laboratory evaluation of a bivalent *Staphylococcus aureus* saccharide-exotoxin A protein conjugate vaccine. *Human Vaccines*, 2(3), 89–98.

Hoffmann, A. A., Iturbe-Ormaetxe, I., Callahan, A. G., Phillips, B. L., Billington, K., Axford, J. K., ... O'Neill, S. L. (2014). Stability of the wMel *Wolbachia* infection following invasion into *Aedes aegypti* populations. *PLoS Neglected Tropical Diseases*, 8(9), e3115. doi: 10.1371/journal.pntd.0003115.

Hoffmann, A. A., Ross, P. A., and Rašić, G. (2015). *Wolbachia* strains for disease control: ecological and evolutionary considerations. *Evolutionary Applications*, 8(8), 751–768.

Hofgen, R., and Willmitzer, L. (1988). Storage of competent cells for *Agrobacterium* transformation. *Nucleic Acids Research*, 16(20), 9877.

Holland, J., Spindler, K., Horodyski, F., Grabau, E., Nichol, S., and VandePol, S. (1982). Rapid evolution of RNA genomes. *Science*, 215(4540), 1577–1585.

Holmes, E. C., and Twiddy, S. S. (2003). The origin, emergence and evolutionary genetics of dengue virus. *Infection, Genetics and Evolution*, 3(1), 19-28.

Holmgren, J. (1981). Actions of cholera toxin and the prevention and treatment of cholera. *Nature*, 292, 413–417.

Holmgren, J., Lonnroth, I., and Svennerholm, L. (1973). Tissue receptor for cholera exotoxin: postulated structure from studies with GM1 ganglioside and related glycolipids. *Infection and Immunity*, 8(2), 208–214.

- Horchani, H., Ouertani, S., Gargouri, Y., and Sayari, A. (2009). The N-terminal His-tag and the recombination process affect the biochemical properties of *Staphylococcus aureus* lipase produced in *Escherichia coli*. *Journal of Molecular Catalysis B: Enzymatic*, *61*, 194–201.
- Huang, K. C., Lee, M. C., Wu, C. W., Huang, K. J., Lei, H. Y., and Cheng, J. W. (2007). Solution structure and neutralizing antibody binding studies of domain III of the dengue-2 virus envelope protein. *Proteins: Structure, Function, and Bioinformatics*, *70*(3), 1116–1119.
- Huy, N. X., and Kim, M. Y. (2017). Overexpression and oral immunogenicity of a dengue antigen transiently expressed in *Nicotiana benthamiana*. *Plant Cell, Tissue and Organ Culture*, *131*, 567–577.
- Ikemura, T. (1985). Codon usage and tRNA content in unicellular and multicellular organisms. *Molecular Biology and Evolution*, *2*(1), 13–34.
- Imoto, J., and Konishi, E. (2007). Dengue tetravalent DNA vaccine increases its immunogenicity in mice when mixed with a dengue type 2 subunit vaccine or an inactivated Japanese encephalitis vaccine. *Vaccine*, *25*, 1076–1084.
- Innis, B. L., and Eckels, K. H. (2003). Progress in development of a live-attenuated, tetravalent dengue virus vaccine by the United States Army Medical Research and Materiel Command. *American Journal of Tropical Medicine and Hygiene*, *69*(Suppl 6), 1–4.
- Ishak, I. H., Jaal, Z., Ranson, H., and Wondji, C. S. (2015). Contrasting patterns of insecticide resistance and knockdown resistance (*kdr*) in the dengue vectors *Aedes aegypti* and *Aedes albopictus* from Malaysia. *Parasites and Vectors*, *8*(181). doi: 10.1186/s13071-015-0797-2.
- Jain, B., Chaturvedi, U. C., and Jain, A. (2014). Role of intracellular events in the

pathogenesis of dengue: an overview. *Microbial Pathogenesis*, 69–70, 45–52.

Janssen, B. J., and Gardner, R. C. (1989). Localized transient expression of GUS in leaf discs following cocultivation with *Agrobacterium*. *Plant Molecular Biology*, 14(1), 61–72.

Janssens, M. E., Geysen, D., Broos, K., de Goeyse, I., Robbens, J., van Petegem, F., ... Guisez, Y. (2010). Folding properties of the hepatitis B core as a carrier protein for vaccination research. *Amino Acids*, 38, 1617–1626.

Jin, T., Wang, J., Zhu, X., Xu, Y., Zhou, X., and Yang, L. (2015). A new transient expression system for large-scale production of recombinant proteins in plants based on air-brushing an *Agrobacterium* suspension. *Biotechnology Reports*, 6, 36–40.

Joensuu, J. J., Conley, A. J., Lienemann, M., Brandle, J. E., Linder, M. B., and Menassa, R. (2010). Hydrophobin fusions for high-level transient protein expression and purification in *Nicotiana benthamiana*. *Plant Physiology*, 152(2), 622–633.

Jones, J. D. G., Dean, C., Gidoni, D., Gilbert, D., Bond-Nutter, D., Lee, R., ... Dunsmuir, P. (1988). Expression of bacterial chitinase protein in tobacco leaves using two photosynthetic gene promoters. *Molecular and General Genetics*, 212, 536–542.

Kanagaraj, A. P., Verma, D., and Daniell, H. (2011). Expression of dengue-3 premembrane and envelope polyprotein in lettuce chloroplasts. *Plant Molecular Biology*, 76, 323–333.

Kanagarajan, S., Tolf, C., Lundgren, A., Waldenström, J., and Brodelius, P. E. (2012). Transient expression of hemagglutinin antigen from low pathogenic avian influenza A (H7N7) in *Nicotiana benthamiana*. *PLoS ONE*, 7(3), e33010. doi: 10.1371/journal.pone.0033010.

Kanekiyo, M., and Buck, C. B. (2017). Virus-like particle and nanoparticle vaccines. In K. Modjarrad and W. C. Koff (Eds.), *Human Vaccines: Emerging Technologies in*

Design and Development (pp. 87–98). London: Academic Press.

Kanasa-Thanan, N., Edelman, R., Tacket, C. O., Wasserman, S. S., Vaughn, D. W., Coster, T. S., ... Hoke, C. H. (2003). Phase 1 studies of Walter Reed Army Institute of Research candidate attenuated dengue vaccines: selection of safe and immunogenic monovalent vaccines. *American Journal of Tropical Medicine.*, 69(Suppl 6), 17–23.

Kapila, J., de Rycke, R., van Montagu, M., and Angenon, G. (1997). An *Agrobacterium*-mediated transient gene expression system for intact leaves. *Plant Science*, 122, 101–108.

Karpenko, L. I., Ivanisenko, V. A., Pika, I. A., Chikaev, N. A., Eroshkin, A. M., Veremeiko, T. A., and Ilyichev, A. A. (2000). Insertion of foreign epitopes in HBcAg: how to make the chimeric particle assemble. *Amino Acids*, 18, 329–337.

Kaslow, D. C., and Biernaux, S. (2015). RTS, S: Toward a first landmark on the Malaria Vaccine Technology Roadmap. *Vaccine*, 33, 7425–7432.

Kim, H. A., Kwon, S. Y., Yang, M. S., and Choi, P. S. (2014a). Expression of dengue virus EIII domain-coding gene in maize as an edible vaccine candidate. *Journal of Plant Biotechnology*, 41, 50–55.

Kim, M. Y., Chung, N. D., Yang, M. S., and Kim, T. G. (2013a). Expression of a cholera toxin B subunit and consensus dengue virus envelope protein domain III fusion gene in transgenic rice callus. *Plant Cell, Tissue and Organ Culture*, 112, 311–320.

Kim, M. Y., Jang, Y. S., Yang, M. S., and Kim, T. G. (2015). High expression of consensus dengue virus envelope glycoprotein domain III using a viral expression system in tobacco. *Plant Cell, Tissue and Organ Culture*, 122, 445–451.

Kim, M. Y., Kim, B. Y., Oh, S. M., Reljic, R., Jang, Y. S., and Yang, M. S. (2016a). Oral immunisation of mice with transgenic rice calli expressing cholera toxin B subunit fused to consensus dengue cEDIII antigen induces antibodies to all four dengue

serotypes. *Plant Molecular Biology*, 92, 347–356.

Kim, M. Y., Li, J. Y., Tien, N. Q. D., and Yang, M. S. (2016b). Expression and assembly of cholera toxin B subunit and domain III of dengue virus 2 envelope fusion protein in transgenic potatoes. *Protein Expression and Purification*, 139, 57-62.

Kim, M. Y., van Dolleweerd, C., Copland, A., Paul, M. J., Hofmann, S., Webster, G. R., ... Ma, J. K. (2017). Molecular engineering and plant expression of an immunoglobulin heavy chain scaffold for delivery of a dengue vaccine candidate. *Plant Biotechnology Journal*, 15, 1590-1601.

Kim, M. Y., Yang, M. S., and Kim, T. G. (2009). Expression of dengue virus E glycoprotein domain III in non-nicotine transgenic tobacco plants. *Biotechnology and Bioprocess Engineering*, 14, 725–730.

Kim, M. Y., Yang, M. S., and Kim, T. G. (2012). Expression of a consensus dengue virus envelope protein domain III in transgenic callus of rice. *Plant Cell, Tissue and Organ Culture*, 109, 509–515.

Kim, T. G., Kim, M. Y., and Yang, M. S. (2010). Cholera toxin B subunit-domain III of dengue virus envelope glycoprotein E fusion protein production in transgenic plants. *Protein Expression and Purification*, 74(2), 236–241.

Kim, T. G., Kim, M. Y., Huy, N. X., Kim, S. H., and Yang, M. S. (2013b). M cell-targeting ligand and consensus dengue virus envelope protein domain III fusion protein production in transgenic rice calli. *Molecular Biotechnology*, 54, 880–887.

Kim, T. G., Kim, M. Y., Tien, N. Q. D., Huy, N. X., and Yang, M. S. (2014b). Dengue virus E glycoprotein production in transgenic rice callus. *Molecular Biotechnology*, 56, 1069–1078.

Kirkpatrick, B. D., Durbin, A. P., Pierce, K. K., Carmolli, M. P., Tibery, C. M., Grier, P. L., ... Whitehead, S. S. (2015). Robust and balanced immune responses to all 4

dengue virus serotypes following administration of a single dose of a live attenuated tetravalent dengue vaccine to healthy, flavivirus-naive adults. *Journal of Infectious Diseases*, 212, 702–710.

Kirkpatrick, B. D., Whitehead, S. S., Pierce, K. K., Tibery, C. M., Grier, P. L., Hynes, N. A., ... Durbin, A. P. (2016). The live attenuated dengue vaccine TV003 elicits complete protection against dengue in a human challenge model. *Science Translational Medicine*, 8(330), 3–4.

Kliks, S. C., Nisalak, A., Brandt, W. E., Wahl, L., and Burke, D. S. (1989). Antibody-dependent enhancement of dengue virus growth in human monocytes as a risk factor for dengue hemorrhagic fever. *American Journal of Tropical Medicine and Hygiene*, 40(4), 444–451.

Klimyuk, V., Pogue, G., Herz, S., Butler, J., and Haydon, H. (2014). Production of recombinant antigens and antibodies in *Nicotiana benthamiana* using “magniffection” technology: GMP-compliant facilities for small- and large-scale manufacturing. In K. Palmer and Y. Gleba (Eds.), *Current Topics in Microbiology and Immunology* (Vol. 375, pp. 127–154). Heidelberg: Springer.

Kozak, M. (1999). Initiation of translation in prokaryotes and eukaryotes. *Gene*, 234(2), 187–208.

Kratz, P. A., Bottcher, B., and Nassal, M. (1999). Native display of complete foreign protein domains on the surface of hepatitis B virus capsids. *Proceedings of the National Academy of Sciences*, 96, 1915–1920.

Kuhn, R. J., Zhang, W., Rossmann, M. G., Pletnev, S. V., Corver, J., Lenches, E., ... Baker, T. S. (2002). Structure of dengue virus: implications for flavivirus organization, maturation, and fusion. *Cell*, 108, 717–725.

Kuno, G., Chang, G. J. J., Tsuchiya, K. R., Karabatsos, N., and Cropp, C. B. (1998).

Phylogeny of the genus *Flavivirus*. *Journal of Virology*, 72(1), 73–83.

Kwan, Y. P., Darah, I., Chen, Y., and Sasidharan, S. (2013). Cytotoxicity and genotoxicity assessment of *Euphorbia hirta* in MCF-7 cell line model using comet assay. *Asian Pacific Journal of Tropical Biomedicine*, 3(9), 692–696.

Kwon, K. C., Nityanandam, R., New, J. S., and Daniell, H. (2013). Oral delivery of bioencapsulated exendin-4 expressed in chloroplasts lowers blood glucose level in mice and stimulates insulin secretion in beta-TC6 cells. *Plant Biotechnology Journal*, 11(1), 77–86.

Kyle, J. L., and Harris, E. (2008). Global spread and persistence of dengue. *Annual Review of Microbiology*, 62, 71–92.

Lacroix, R., McKemey, A. R., Raduan, N., Kwee Wee, L., Hong Ming, W., Guat Ney, T., ... Murad, S. (2012). Open field release of genetically engineered sterile male *Aedes aegypti* in Malaysia. *PLoS ONE*, 7(8), e42771. doi: 10.1371/journal.pone.0042771.

Laing, W., and Christeller, J. (2004). Extraction of proteins from plant tissues. *Current Protocols in Protein Science*, 38, 4.7.1-4.7.7.

Lam, S. K. (1993). Two decades of dengue in Malaysia. *Tropical Medicine*, 35(4), 195–200.

Lee, H. H., Cherni, I., Yu, H., Fromme, R., Doran, J. D., Grotjohann, I., ... Mor, T. S. (2014). Expression, purification and crystallization of CTB-MPR, a candidate mucosal vaccine component against HIV-1. *International Union of Crystallography Journal*, 1, 305–317.

Lee, H. L., Rohani, A., Khadri, M. S., Nazni, W. A., Rozilawati, H., Nurulhusna, A. H., ... Teh, C. H. (2015a). Dengue vector control in Malaysia – challenges and recent advances. *The International Medical Journal Malaysia*, 14(1), 11–16.

Lee, H. L., Vasan, S., Ahmad, N. W., Idris, I., Hanum, N., Selvi, S., ... Murad, S. (2013).

Mating compatibility and competitiveness of transgenic and wild type *Aedes aegypti* (L.) under contained semi-field conditions. *Transgenic Research*, 22(1), 47–57.

Lee, J., Yoo, J. K., Sohn, H. J., Kang, H. K., Kim, D., Shin, H. J., and Kim, J. H. (2015b). Protective immunity against *Naegleria fowleri* infection on mice immunized with the rNfa1 protein using mucosal adjuvants. *Parasitology Research*, 114, 1377–1385.

Leitmeyer, K. C., Vaughn, D. W., Watts, D. M., Salas, R., de Chacon, I. V., Ramos, C., and Rico-Hesse, R. (1999). Dengue virus structural differences that correlate with pathogenesis. *Journal of Virology*, 73(6), 4738–4747.

Lencer, W. I., Hirst, T. R., and Holmes, R. K. (1999). Membrane traffic and the cellular uptake of cholera toxin. *Biochimica et Biophysica Acta*, 1450, 177–190.

Leng, C. H., Liu, S. J., Tsai, J. P., Li, Y. S., Chen, M. Y., Liu, H. H., ... Chen, H. W. (2009). A novel dengue vaccine candidate that induces cross-neutralizing antibodies and memory immunity. *Microbes and Infection*, 11(2), 288–295.

Lesieur, C., Cliff, M. J., Carter, R., James, R. F. L., Clarke, A. R., and Hirst, T. R. (2002). A kinetic model of intermediate formation during assembly of cholera toxin B-subunit pentamers. *Journal of Biological Chemistry*, 277(19), 16697–16704.

Leuzinger, K., Dent, M., Hurtado, J., Stahnke, J., Lai, H., Zhou, X., and Chen, Q. (2013). Efficient agroinfiltration of plants for high-level transient expression of recombinant proteins. *Journal of Visualized Experiments*, 77, e50521. doi: 10.3791/50521.

Levine, M. M., Kaper, J. B., Black, R. E., and Clements, M. L. (1983). New knowledge on pathogenesis of bacterial enteric infections as applied to vaccine development. *Microbiological Reviews*, 47(4), 510–550.

Li, S., Peng, L., Zhao, W., Zhong, H., Zhang, F., Yan, Z., and Cao, H. (2011). Synthetic peptides containing B- and T-cell epitope of dengue virus-2 E domain III provoked B- and T-cell responses. *Vaccine*, 29(20), 3695–3702.

- Li, X. (2011). Infiltration of *Nicotiana benthamiana* protocol for transient expression via *Agrobacterium*. *Bio-Protocol*, 1(14), e95. doi: 10.21769/BioProtoc.95.
- Libsittikul, S., Khongwichit, S., Smith, D. R., and Yap, Y. K. (2015). Evaluation of papaya ringspot virus as a vector for expression of dengue E protein domain III in *Cucurbita pepo* (zucchini) plants. *Journal of Animal and Plant Sciences*, 25(3), 809–815.
- Lico, C., Chen, Q., and Santi, L. (2008). Viral vectors for production of recombinant proteins in plants. *Journal of Cellular Physiology*, 216(2), 366–377.
- Liljeqvist, S., Ståhl, S., Andréoni, C., Binz, H., Uhlén, M., and Murby, M. (1997). Fusions to the cholera toxin B subunit: Influence on pentamerization and GM1 binding. *Journal of Immunological Methods*, 210, 125–135.
- Lim, S. K., Lee, Y. S., Namkung, S., Lim, J. K., and Yoon, I. K. (2016). Prospects for dengue vaccines for travelers. *Clinical and Experimental Vaccine Research*, 5(2), 89–100.
- Lisowska, E. (2002). The role of glycosylation in protein antigenic properties. *Cellular and Molecular Life Sciences*, 59, 445–455.
- Liu, W., Jiang, H., Zhou, J., Yang, X., Tang, Y., Fang, D., and Jiang, L. (2010). Recombinant dengue virus-like particles from *Pichia pastoris*: Efficient production and immunological properties. *Virus Genes*, 40, 53–59.
- Loh, F. F. (2015). GM mosquito project shelved. Retrieved January 12, 2018, from <https://www.thestar.com.my/news/nation/2015/03/06/gm-mosquito-project-shelved-plan-not-cost-effective-for-implementation-says-health-dg/>
- Loh, H. S., and Baranzan W, S. (2014). Optimizations of laboratory-scale vacuum-assisted agroinfiltration for delivery of a transgene in *Nicotiana benthamiana*. *Asian Journal of Biotechnology*, 6(1), 1-14.

Loh, H. S., Green, B. J., and Yusibov, V. (2017). Using transgenic plants and modified plant viruses for the development of treatments for human diseases. *Current Opinion in Virology*, 26, 81–89.

Lütcke, H. A., Chow, K. C., Mickel, F. S., Moss, K. A., Kern, H. F., and Scheele, G. A. (1987). Selection of AUG initiation codons differs in plants and animals. *The EMBO Journal*, 6(1), 43–48.

Luttmann, W., Bratke, K., Kupper, M., and Myrtex, D. (2006). *Immunology*. Burlington: Academic Press.

Lydyard, P., Whelan, A., and Fanger, M. (2011). *Immunology*. New York: Garland Science, Taylor & Francis Group, LLC.

Ma, J. K. C., Christou, P., Chikwamba, R., Haydon, H., Paul, M., Ferrer, M. P., ... Thangaraj, H. (2013). Realising the value of plant molecular pharming to benefit the poor in developing countries and emerging economies. *Plant Biotechnology Journal*, 11, 1029–1033.

Ma, J. K. C., Drake, P. M. W., and Christou, P. (2003). The production of recombinant pharmaceutical proteins in plants. *Nature Reviews Genetics*, 4, 794–805.

Maclean, J., Koekemoer, M., Olivier, A. J., Stewart, D., Hitzeroth, I. I., Rademacher, T., ... Rybicki, E. P. (2007). Optimization of human papillomavirus type 16 (HPV-16) L1 expression in plants: comparison of the suitability of different HPV-16 L1 gene variants and different cell-compartment localization. *Journal of General Virology*, 88(5), 1460–1469.

Main, G. D., Reynolds, S., and Gartland, J. S. (1995). Electroporation protocols for *Agrobacterium*. In K. M. A. Gartland and M. R. Davey (Eds.), *Agrobacterium Protocols* (pp. 405–412). Totowa, NJ: Springer New York.

Malaysian Remote Sensing Agency (ARSM), and Ministry of Science Technology and

Innovation (MOSTI). (2018). iDengue. Retrieved January 15, 2018, from <http://idengue.remotesensing.gov.my/idengue/>

Mani, S., Tripathi, L., Raut, R., Tyagi, P., Arora, U., Barman, T., ... Khanna, N. (2013). *Pichia pastoris*-expressed dengue 2 envelope forms virus-like particles without pre-membrane protein and induces high titer neutralizing antibodies. *PLoS ONE*, 8(5), e64595. doi: 10.1371/journal.pone.0064595.

Mansoor, O. D., Kristensen, D., Meek, A., Zipursky, S., Popovaa, O., Sharma, I., ... Lasher, H. (2013). Vaccine presentation and packaging advisory group: a forum for reaching consensus on vaccine product attributes. *Bulletin of the World Health Organization*, 91, 75–78.

Mardanov, E. S., Kotlyarov, R. Y., Kuprianov, V. V., Stepanova, L. A., Tsybalova, L. M., Lomonosoff, G. P., and Ravin, N. V. (2015). Rapid high-yield expression of a candidate influenza vaccine based on the ectodomain of M2 protein linked to flagellin in plants using viral vectors. *BMC Biotechnology*, 15(42). doi: 10.1186/s12896-015-0164-6.

Markoff, L. (2003). 5'- and 3'-noncoding regions in flavivirus RNA. *Advances in Virus Research*, 59, 177–228.

Marovich, M., Grouard-Vogel, G., Louder, M., Eller, M., Sun, W., Wu, S. J., ... Mascola, J. (2001). Human dendritic cells as targets of dengue virus infection. *Journal of Investigative Dermatology Symposium Proceedings*, 6(3), 219–224.

Marrack, P., McKee, A. S., and Munks, M. W. (2009). Towards an understanding of the adjuvant action of aluminium. *Nature Reviews Immunology*, 9(4), 287–293.

Marsian, J., Fox, H., Bahar, M. W., Kotecha, A., Fry, E. E., Stuart, D. I., ... Lomonosoff, G. P. (2017). Plant-made polio type 3 stabilized VLPs – a candidate synthetic polio vaccine. *Nature Communications*, 8, 245. doi: 10.1038/s41467-017-

00090-w.

Martin, K., and Nashar, T. O. (2013). *E. coli* heat-labile enterotoxin B subunit as a platform for the delivery of HIV Gag p24 Antigen. *Journal of Clinical and Cellular Immunology*, 4(2). doi:10.4172/2155-9899.1000140.

Martina, B. E. E., Koraka, P., and Osterhaus, A. D. M. E. (2009). Dengue virus pathogenesis: an integrated view. *Clinical Microbiology Reviews*, 22(4), 564–581.

Martinez, C. A., Topal, E., Giuliatti, A. M., Talou, J. R., and Mason, H. (2010). Exploring different strategies to express dengue virus envelope protein in a plant system. *Biotechnology Letters*, 32(6), 867–875.

Mason, H. S., Lam, D. M., and Arntzen, C. J. (1992). Expression of hepatitis B surface antigen in transgenic plants. *Proceedings of the National Academy of Sciences of the United States of America*, 89, 11745–11749.

Massonnet-Bruneel, B., Corre-Catelin, N., Lacroix, R., Lees, R. S., Hoang, K. P., Nimmo, D., ... Reiter, P. (2013). Fitness of transgenic mosquito *Aedes aegypti* males carrying a dominant lethal genetic system. *PLoS ONE*, 8(5), e62711. doi: 10.1371/journal.pone.0062711.

Mathew, L. G., Herbst-Kralovetz, M. M., and Mason, H. S. (2014). Norovirus Narita 104 virus-like particles expressed in *Nicotiana benthamiana* induce serum and mucosal immune responses. *BioMed Research International*, 2014, 807539. doi: 10.1155/2014/807539.

Mattsson, J., Schön, K., Ekman, L., Fahlén-Yrlid, L., Yrlid, U., and Lycke, N. Y. (2015). Cholera toxin adjuvant promotes a balanced Th1/Th2/Th17 response independently of IL-12 and IL-17 by acting on G α in CD11b⁺ DCs. *Mucosal Immunology*, 8(4), 815–827.

McArthur, M. A., Sztein, M. B., and Edelman, R. (2013). Dengue vaccines: recent

developments, ongoing challenges and current candidates. *Expert Review of Vaccines*, 12(8), 933–953.

McCue, J. T. (2014). Use and application of hydrophobic interaction chromatography for protein purification. In J. Lorsch (Ed.), *Methods in Enzymology* (Vol. 541, pp. 51–65). San Diego: Elsevier Inc.

Menassa, R., Ahmad, A., and Joensuu, J. J. (2012). Transient expression using agroinfiltration and its applications in molecular farming. In A. Wang and S. Ma (Eds.), *Molecular Farming in Plants: Recent Advances and Future Prospects* (pp. 183–198). Dordrecht: Springer Netherlands.

Merritt, E. A., Sarfaty, S., Akker, F. V. D., L’Hoir, C., Martial, J. A., and Hol, W. G. J. (1994). Crystal structure of cholera toxin B-pentamer bound to receptor GM1 pentasaccharide. *Protein Science*, 3, 166–175.

Merritt, E. A., Sarfaty, S., Chang, T. T., Palmer, L. M., Jobling, M. G., Holmes, R. K., and Hol, W. G. (1995). Surprising leads for a cholera toxin receptor-binding antagonist: crystallographic studies of CTB mutants. *Structure*, 3(6), 561–570.

Messina, J. P., Brady, O. J., Scott, T. W., Zou, C., Pigott, D. M., Duda, K. A., ... Hay, S. I. (2014). Global spread of dengue virus types: Mapping the 70 year history. *Trends in Microbiology*, 22(3), 138–146.

Mia, M. S., Begum, R. A., Er, A. C., Abidin, R. D. Z. R. Z., and Pereira, J. J. (2013). Trends of dengue infections in Malaysia, 2000-2010. *Asian Pacific Journal of Tropical Medicine*, 6(6), 462–466.

Micoli, F., Rondini, S., Pisoni, I., Proietti, D., Berti, F., Costantino, P., ... Martin, L. B. (2011). Vi-CRM₁₉₇ as a new conjugate vaccine against *Salmonella typhi*. *Vaccine*, 29(4), 712–720.

Miesenbock, G., and Rothman, J. E. (1995). The capacity to retrieve escaped ER

proteins extends to the trans-most cisterna of the Golgi stack. *Journal of Cell Biology*, 129(2), 309–319.

Milich, D. R., Chen, M., Schödel, F., Peterson, D. L., Jones, J. E., and Hughes, J. L. (1997a). Role of B cells in antigen presentation of the hepatitis B core. *Proceedings of the National Academy of Sciences of the United States of America*, 94, 14648–14653.

Milich, D. R., Schödel, F., Hughes, J. L., Jones, J. E., and Peterson, D. L. (1997b). The hepatitis B virus core and e antigens elicit different Th cell subsets: antigen structure can affect Th cell phenotype. *Journal of Virology*, 71, 2192–2201.

Min, K. T., and Benzer, S. (1997). *Wolbachia*, normally a symbiont of *Drosophila*, can be virulent, causing degeneration and early death. *Proceedings of the National Academy of Sciences of the United States of America*, 94(20), 10792–10796.

Miyata, T., Harakuni, T., Taira, T., Matsuzaki, G., and Arakawa, T. (2012). Merozoite surface protein-1 of *Plasmodium yoelii* fused via an oligosaccharide moiety of cholera toxin B subunit glycoprotein expressed in yeast induced protective immunity against lethal malaria infection in mice. *Vaccine*, 30(5), 948–958.

Miyata, T., Harakuni, T., Tsuboi, T., Sattabongkot, J., Kohama, H., Tachibana, M., ... Arakawa, T. (2010). *Plasmodium vivax* ookinete surface protein Pvs25 linked to cholera toxin B subunit induces potent transmission-blocking immunity by intranasal as well as subcutaneous immunization. *Infection and Immunity*, 78(9), 3773–3782.

Modis, Y., Ogata, S., Clements, D., and Harrison, S. C. (2003). A ligand-binding pocket in the dengue virus envelope glycoprotein. *Proceedings of the National Academy of Sciences of the United States of America*, 100(12), 6986–6991.

Modis, Y., Ogata, S., Clements, D., and Harrison, S. C. (2004). Structure of the dengue virus envelope protein after membrane fusion. *Nature*, 427, 313–319.

Modis, Y., Ogata, S., Clements, D., and Harrison, S. C. (2005). Variable surface

epitopes in the crystal structure of dengue virus type 3 envelope glycoprotein variable surface epitopes in the crystal structure of dengue virus type 3 envelope glycoprotein. *Journal of Virology*, 79(2), 1223–1231.

Mohd-Zaki, A. H., Brett, J., Ismail, E., and L'Azou, M. (2014). Epidemiology of dengue disease in Malaysia (2000– 2012): a systematic literature review. *PLoS Neglected Tropical Diseases*, 8(11), e3159. doi: 10.1371/journal.pntd.0003159.

Mohd Shahr, F. (2016). Health Ministry: UTM's Anti D'ngue must undergo pre-clinical and clinical studies. *New Straits Times Online*. Retrieved July 2, 2017, from <http://www.nst.com.my/news/2016/02/128571/health-ministry-utms-anti-dngue-must-undergo-pre-clinical-and-clinical-studies>

Morrison, A. C., Zielinski-Gutierrez, E., Scott, T. W., and Rosenberg, R. (2008). Defining challenges and proposing solutions for control of the virus vector *Aedes aegypti*. *PLoS Medicine*, 5(3), e68. doi:10.1371/ journal.pmed.0050068.

Morrison, D., Legg, T. J., Billings, C. W., Forrat, R., Yoksan, S., and Lang, J. (2010). A novel tetravalent dengue vaccine is well tolerated and immunogenic against all 4 serotypes in flavivirus-naive adults. *The Journal of Infectious Diseases*, 201, 370–377.

Mudin, R. N. (2015). Dengue incidence and the prevention and control program in Malaysia. *The International Medical Journal Malaysia*, 14(1), 5-9.

Muhammad Azami, N. A., Salleh, S. A., Neoh, H. M., Syed Zakaria, S. Z., and Jamal, R. (2011). Dengue epidemic in Malaysia: Not a predominantly urban disease anymore. *BMC Research Notes*, 4, 216. doi: 10.1186/1756-0500-4-216.

Munro, S., and Pelham, H. R. B. (1987). A C-terminal signal prevents secretion of luminal ER proteins. *Cell*, 48(5), 899–907.

Murray, N. E. A., Quam, M. B., and Wilder-Smith, A. (2013). Epidemiology of dengue: past, present and future prospects. *Clinical Epidemiology*, 5, 299–309.

Musa, Z. (2016). UTM's anti-dengue supplement also fights Zika virus. *The Star Online*. Retrieved July 2, 2017, from <http://www.thestar.com.my/news/nation/2016/02/18/anti-dengue-supplement-fights-zika/>

Nassal, M., Skamel, C., Vogel, M., Kratz, P. A., Stehle, T., Wallich, R., and Simon, M. M. (2008). Development of hepatitis B virus capsids into a whole-chain protein antigen display platform: new particulate Lyme disease vaccines. *International Journal of Medical Microbiology*, 298, 135–142.

Nausch, H., Mischofsky, H., Koslowski, R., Meyer, U., Broer, I., and Huckauf, J. (2012). Expression and subcellular targeting of human complement factor C5a in *Nicotiana* species. *PLoS ONE*, 7(12), e53023. doi: 10.1371/journal.pone.0053023.

Nemésio, H., Palomares-Jerez, F., and Villalaín, J. (2011). The membrane-active regions of the dengue virus proteins C and E. *Biochimica et Biophysica Acta*, 1808(10), 2390–2402.

Nisalak, A., Endy, T. P., Nimmannitya, S., Kalayanarooj, S., Thisyakorn, U., Scott, R. M., ... Vaughn, D. W. (2003). Serotype-specific dengue virus circulation and dengue disease in Bangkok, Thailand from 1973 to 1999. *American Journal of Tropical Medicine and Hygiene*, 68(2), 191–202.

Nishimura, A., Morita, M., Nishimura, Y., and Sugino, Y. (1990). A rapid and highly efficient method for preparation of competent *Escherichia coli* cells. *Nucleic Acids Research*, 18(20), 6169.

Noad, R., and Roy, P. (2003). Virus-like particles as immunogens. *Trends in Microbiology*, 11(9), 438–444.

Ooi, E. E., Goh, K. T., and Gubler, D. J. (2006). Dengue prevention and 35 years of vector control in Singapore. *Emerging Infectious Diseases*, 12(6), 887–893.

Op De Beeck, A., Rouillé, Y., Caron, M., Duvet, S., and Dubuisson, J. (2004). The

transmembrane domains of the prM and E proteins of yellow fever virus are endoplasmic reticulum localization signals. *Journal of Virology*, 78, 12591–12602.

Osorio, J. E., Huang, C. Y. H., Kinney, R. M., and Stinchcomb, D. T. (2011). Development of DENVax: A chimeric dengue-2 PDK-53-based tetravalent vaccine for protection against dengue fever. *Vaccine*, 29, 7251–7260.

Osorio, J. E., Partidos, C. D., Wallace, D., and Stinchcomb, D. T. (2015). Development of a recombinant, chimeric tetravalent dengue vaccine candidate. *Vaccine*, 33, 7112–7120.

Packierisamy, P. R., Ng, C. W., Dahlui, M., Inbaraj, J., Balan, V. K., Halasa, Y. A., and Shepard, D. S. (2015). Cost of dengue vector control activities in Malaysia. *American Journal of Tropical Medicine and Hygiene*, 93(5), 1020–1027.

Paneque-Quevedo, A. A. (2013). Inorganic compounds as vaccine adjuvants. *Biotechnología Aplicada*, 30(4), 250–256.

Pang, E. L., and Loh, H. S. (2016). Current perspectives on dengue episode in Malaysia. *Asian Pacific Journal of Tropical Medicine*, 9(4), 395–401.

Pang, E. L., and Loh, H. S. (2017). Towards development of a universal dengue vaccine – How close are we? *Asian Pacific Journal of Tropical Medicine*, 10(3), 220–228.

Pelham, H. R. B. (1989). Control of protein exit from the endoplasmic reticulum. *Annual Review of Cell Biology*, 5, 1–23.

Pelham, H. R. B. (1996). The dynamic organisation of the secretory pathway. *Cell Structure and Function*, 21, 413–419.

Pennsylvania Institutional Animal Care and Use Committee (IACUC). (2016). IACUC Guideline: Mouse and Rat Injections for Delivery of Experimental Agents. Retrieved January 31, 2017, from <http://www.upenn.edu/regulatoryaffairs/Documents/iacuc/guidelines/IACUCGuidelin>

Peyret, H. (2015). A protocol for the gentle purification of virus-like particles produced in plants. *Journal of Virological Methods*, 225, 59–63.

Peyret, H., and Lomonossoff, G. P. (2013). The pEAQ vector series: The easy and quick way to produce recombinant proteins in plants. *Plant Molecular Biology*, 83, 51–58.

Peyret, H., and Lomonossoff, G. P. (2015). When plant virology met *Agrobacterium*: The rise of the deconstructed clones. *Plant Biotechnology Journal*, 13, 1121–1135.

Peyret, H., Gehin, A., Thuenemann, E. C., Blond, D., El Turabi, A., Beales, L., ... Rowlands, D. J. (2015). Tandem fusion of hepatitis B core antigen allows assembly of virus-like particles in bacteria and plants with enhanced capacity to accommodate foreign proteins. *PLoS ONE*, 10(4), 1–20. doi: 10.1371/journal.pone.0120751.

Phuc, H. K., Andreasen, M. H., Burton, R. S., Vass, C., Epton, M. J., Pape, G., ... Alphey, L. (2007). Late-acting dominant lethal genetic systems and mosquito control. *BMC Biology*, 5(11). doi: 10.1186/1741-7007-5-11.

Pier, G. B. (2007). Is *Pseudomonas aeruginosa* exotoxin A a good carrier protein for conjugate vaccines? *Human Vaccines*, 3(2), 39–40.

Pierson, T. C., and Diamond, M. S. (2009). Molecular mechanisms of antibody-mediated neutralisation of flavivirus infection. *Expert Reviews in Molecular Medicine*, 10, e12. doi: 10.1017/S1462399408000665.

Pierson, T. C., Xu, Q., Nelson, S., Oliphant, T., Grant, E., Fremont, D. H., and Diamond, M. S. (2009). The stoichiometry of antibody-mediated neutralization and enhancement of West Nile virus infection. *Cell*, 1(2), 135–145.

Pillet, S., Aubin, É., Trépanier, S., Bussière, D., Dargis, M., Poulin, J. F., ... Landry, N. (2016). A plant-derived quadrivalent virus like particle influenza vaccine induces cross-reactive antibody and T cell response in healthy adults. *Clinical Immunology*, 168, 72–

Pitzschke, A. (2013). *Agrobacterium* infection and plant defense — transformation success hangs by a thread. *Frontiers in Plant Science*, 4, 519. doi: 10.3389/fpls.2013.00519.

Porath, J., Carlson, J., Olsson, I., and Belfrage, G. (1975). Metal chelate affinity chromatography, a new approach to protein fractionation. *Nature*, 258(5536), 598–599.

Porter, K. R., Ewing, D., Chen, L., Wu, S. J., Hayes, C. G., Ferrari, M., ... Raviprakash, K. (2012). Immunogenicity and protective efficacy of a vaxfectin-adjuvanted tetravalent dengue DNA vaccine. *Vaccine*, 30, 336–341.

Potter, M., and Boyce, C. R. (1962). Induction of plasma-cell neoplasms in strain BALB/c mice with mineral oil and mineral oil adjuvants. *Nature*, 193(4820), 1086–1087.

Pumpens, P., and Grens, E. (1999). Hepatitis B core particles as a universal display model: A structure-function basis for development. *FEBS Letters*, 442(1), 1-6.

Pumpens, P., and Grens, E. (2001). HBV core particles as a carrier for B cell / T cell epitopes. *Intervirology*, 1067, 98–114.

Pushko, P., Pumpens, P., and Grens, E. (2013). Development of virus-like particle technology from small highly symmetric to large complex virus-like particle structures. *Intervirology*, 56(3), 141–165.

Quax, T. E. F., Claassens, N. J., Söll, D., and van der Oost, J. (2015). Codon bias as a means to fine tune gene expression. *Molecular and Cellular Biology*, 59(2), 149–161.

Rajapakse, S., Rodrigo, C., and Rajapakse, A. (2012). Treatment of dengue fever. *Infection and Drug Resistance*, 5, 103–112.

Rajeh, M. A. B., Kwan, Y. P., Zakaria, Z., Latha, L. Y., Jothy, S. L., and Sasidharan, S. (2012). Acute toxicity impacts of *Euphorbia hirta* L extract on behavior, organs body

weight index and histopathology of organs of the mice and *Artemia salina*. *Pharmacognosy Research*, 4(3), 170–7.

Ramessar, K., Capell, T., and Christou, P. (2008). Molecular pharming in cereal crops. *Phytochemistry Reviews*, 7, 579–592.

Ramirez, A., Morris, S., Maucourant, S., D’Ascanio, I., Crescente, V., Lu, I. N., ...

Rosenberg, W. (2018). A virus-like particle vaccine candidate for influenza A virus based on multiple conserved antigens presented on hepatitis B tandem core particles. *Vaccine*, *In Press*. doi: 10.1016/j.vaccine.2017.12.053.

Ratcliff, F., Harrison, B. D., and Baulcombe, D. C. (1997). A similarity between viral defense and gene silencing in plants. *Science*, 276(5318), 1558–1560.

Raviprakash, K., Kochel, T. J., Ewing, D., Simmons, M., Phillips, I., Hayes, C. G., and Porter, K. R. (2000). Immunogenicity of dengue virus type 1 DNA vaccines expressing truncated and full length envelope protein. *Vaccine*, 18, 2426–2434.

Raviprakash, K., Luke, T., Doukas, J., Danko, J., Porter, K., Burgess, T., and Kochel, T. (2012). A dengue DNA vaccine formulated with Vaxfectin® is well tolerated, and elicits strong neutralizing antibody responses to all four dengue serotypes in New Zealand white rabbits. *Human Vaccines and Immunotherapeutics*, 8(12), 1764–1768.

Raviprakash, K., Porter, K. R., Kochel, T. J., Ewing, D., Simmons, M., Phillips, I., ... Hayes, C. G. (2000). Dengue virus type 1 DNA vaccine induces protective immune responses in rhesus macaques. *Journal of General Virology*, 81, 1659–1667.

Read, A. F., Baigent, S. J., Powers, C., Kgosana, L. B., Blackwell, L., Smith, L. P., ... Nair, V. K. (2015). Imperfect vaccination can enhance the transmission of highly virulent pathogens. *PLoS Biology*, 13(7), e1002198. doi: 10.1371/journal.pbio.1002198.

Richter, L. J., Thanavala, Y., Arntzen, C. J., and Mason, H. S. (2000). Production of hepatitis B surface antigen in transgenic plants for oral immunization. *Nature*

Biotechnology, 18(11), 1167–1171.

Rico-Hesse, R. (1990). Molecular evolution and distribution of dengue viruses type 1 and 2 in nature. *Virology*, 174(2), 479–493.

Rico-Hesse, R., Harrison, L. M., Salas, R. A., Tovar, D., Nisalak, A., Ramos, C., ... da Rosa, A. T. (1997). Origins of dengue type 2 viruses associated with increased pathogenicity in the Americas. *Virology*, 230(2), 244–51.

Riedl, P., Stober, D., Oehninger, C., Melber, K., Reimann, J., and Schirmbeck, R. (2002). Priming Th1 immunity to viral core particles is facilitated by trace amounts of RNA bound to its arginine-rich domain. *The Journal of Immunology*, 168(10), 4951–4959.

Rigau-Pérez, J. G. (1998). The early use of break-bone fever (Quebranta huesos, 1771) and dengue (1801) in Spanish. *American Journal of Tropical Medicine and Hygiene*, 59(2), 272–274.

Roehrig, J. T., Bolin, R. A, and Kelly, R. G. (1998). Monoclonal antibody mapping of the envelope glycoprotein of the dengue 2 virus, Jamaica. *Virology*, 246, 317–328.

Roehrig, J. T., Volpe, K. E., Squires, J., Hunt, A. R., Davis, B. S., and Chang, G. J. J. (2004). Contribution of disulfide bridging to epitope expression of the dengue type 2 virus envelope glycoprotein. *Journal of Virology*, 78(5), 2648–2652.

Roose, K., de Baets, S., Schepens, B., and Saelens, X. (2013). Hepatitis B core-based virus-like particles to present heterologous epitopes. *Expert Review of Vaccines*, 12(2), 183–198.

Ross, P. A., Wiwatanaratnabutr, I., Axford, J. K., White, V. L., Endersby-Harshman, N. M., and Hoffmann, A. A. (2017). *Wolbachia* infections in *Aedes aegypti* differ markedly in their response to cyclical heat stress. *PLoS Pathogens*, 13(1), e1006006. doi: 10.1371/journal.ppat.1006006.

- Ruedl, C., Schwarz, K., Jegerlehner, A., Storni, T., Manolova, V., and Bachmann, M. F. (2005). Virus-like particles as carriers for T-cell epitopes: limited inhibition of T-cell priming by carrier-specific antibodies. *Journal of Virology*, 79(2), 717–724.
- Rupp, R., Luckasen, G. J., Kirstein, J. L., Osorio, J. E., Santangelo, J. D., Raanan, M., ... Stinchcomb, D. T. (2015). Safety and immunogenicity of different doses and schedules of a live attenuated tetravalent dengue vaccine (TDV) in healthy adults: a phase 1b randomized study. *Vaccine*, 33, 6351–6359.
- Rush, B. (1951). An account of the bilious remitting fever, as it appeared in philadelphia, in the summer and autumn of the year 1780. *The American Journal of Medicine*, 11(5), 546–550.
- Rybicki, E. P. (2009). Plant-produced vaccines: promise and reality. *Drug Discovery Today*, 14, 16–24.
- Rybicki, E. P. (2010). Plant-made vaccines for humans and animals. *Plant Biotechnology Journal*, 8(5), 620–637.
- Sabchareon, A., Wallace, D., Sirivichayakul, C., Limkittikul, K., Chanthavanich, P., Suvannadabba, S., ... Lang, J. (2012). Protective efficacy of the recombinant, live-attenuated, CYD tetravalent dengue vaccine in Thai schoolchildren: a randomised, controlled phase 2b trial. *The Lancet*, 380(9853), 1559–1567.
- Sabin, A. B., and Schlesinger, R. W. (1945). Production of immunity to dengue with virus modified by propagation in mice. *Science*, 101(2634), 640–642.
- Sack, M., Hofbauer, A., Fischer, R., and Stoger, E. (2015). The increasing value of plant-made proteins. *Current Opinion in Biotechnology*, 32, 163–170.
- Saejung, W., Fujiyama, K., Takasaki, T., Ito, M., Hori, K., Malasit, P., ... Seki, T. (2007). Production of dengue 2 envelope domain III in plant using TMV-based vector system. *Vaccine*, 25, 6646–6654.

Sáez-Llorens, X., Tricou, V., Yu, D., Rivera, L., Jimeno, J., Villarreal, A. C., ... Wallace, D. (2017). Immunogenicity and safety of one versus two doses of tetravalent dengue vaccine in healthy children aged 2-17 years in Asia and Latin America: 18-month interim data from a phase 2, randomised, placebo-controlled study. *The Lancet Infectious Diseases*, *In Press*. doi: 10.1016/S1473-3099(17)30632-1.

Sainsbury, F., and Lomonosoff, G. P. (2008). Extremely high-level and rapid transient protein production in plants without the use of viral replication. *Plant Physiology*, *148*, 1212–1218.

Sainsbury, F., Lavoie, P. O., D'Aoust, M. A., Vezina, L. P., and Lomonosoff, G. P. (2008). Expression of multiple proteins using full-length and deleted versions of cowpea mosaic virus RNA-2. *Plant Biotechnology Journal*, *6*, 82–92.

Sainsbury, F., Saxena, P., Geisler, K., Osbourn, A., and Lomonosoff, G. P. (2012). Using a virus-derived system to manipulate plant natural product biosynthetic pathways. In D. A. Hopwood (Ed.), *Methods in Enzymology* (Vol. 517, pp. 185–202). Elsevier Inc.

Sainsbury, F., Thuenemann, E. C., and Lomonosoff, G. P. (2009). pEAQ: versatile expression vectors for easy and quick transient expression of heterologous proteins in plants. *Plant Biotechnology Journal*, *7*, 682–693.

Sam, S. S., Faridah, S., Omar, S., Teoh, B. T., Abd-Jamil, J., Abubakar, S., and Farrar, J. (2013). Review of dengue hemorrhagic fever fatal cases seen among adults: a retrospective study. *PLoS Negl Trop Dis*, *7*(5). doi: 10.1371/journal.pntd.0002194.

Sanchez, J., and Holmgren, J. (2011). Cholera toxin – a foe & a friend. *Indian Journal of Medical Research*, *133*, 153–163.

Sanofi. (2017). Sanofi updates information on dengue vaccine. Retrieved January 16, 2018, from <http://mediaroom.sanofi.com/sanofi-updates-information-on-dengue-vaccine/>

- Sathananthan, B., Rødahl, E., Flatmark, T., Langeland, N., and Haarr, L. (1997). Purification of herpes simplex virus type 1 by density gradient centrifugation and estimation of the sedimentation coefficient of the virion. *APMIS*, *105*, 238–246.
- Schnitzler, A. C., Burke, J. M., and Wetzler, L. M. (2007). Induction of cell signaling events by the cholera toxin B subunit in antigen-presenting cells. *Infection and Immunity*, *75*(6), 3150–3159.
- Schöb, H., Kunz, C., and Meins Jr, F. (1997). Silencing of transgenes introduced into leaves by agroinfiltration: a simple, rapid method for investigating sequence requirements for gene silencing. *Molecular Genetics and Genomics*, *256*, 581–585.
- Schödel, F., Moriarty, A. M., Peterson, D. L., Zheng, J., Hughes, J. L., Will, H., ... Milich, D. R. (1992). The position of heterologous epitopes inserted in hepatitis B virus core particles determines their immunogenicity. *Journal of Virology*, *66*, 106–114.
- Schödel, F., Wirtz, R., Peterson, D., Hughes, J., Warren, R., Sadoff, J., and Milich, D. (1994). Immunity to malaria elicited by hybrid hepatitis B virus core particles carrying circumsporozoite protein epitopes. *The Journal of Experimental Medicine*, *180*(3), 1037–46.
- Schröder, M., and Kaufman, R. J. (2005). ER stress and the unfolded protein response. *Mutation Research*, *569*, 29–63.
- Seifer, M., and Standring, D. N. (1995). Assembly and antigenicity of hepatitis B virus core particles. *Intervirology*, *38*(1–2), 47–62.
- Shafie, F. A., Mohd Tahir, M. P., and Sabri, N. M. (2012). *Aedes* mosquitoes resistance in urban community setting. *Procedia - Social and Behavioral Sciences*, *36*, 70–76.
- Shah, K. H., Almaghrabi, B., and Bohlmann, H. (2013). Comparison of expression vectors for transient expression of recombinant proteins in plants. *Plant Molecular Biology Reporter*, *31*(6), 1529–1538.

Shamloul, M., Trusa, J., Mett, V., and Yusibov, V. (2014). Optimization and utilization of *Agrobacterium*-mediated transient protein production in *Nicotiana*. *Journal of Visualized Experiments*, (86), e51204. doi: 10.3791/51204.

Sharp, P. M., and Li, W. (1987). The codon adaptation index – a measure of directional synonymous codon usage bias, and its potential applications. *Nucleic Acids Research*, 15(3), 1281–1295.

Shi, L., Sanyal, G., Ni, A., Luo, Z., Doshna, S., Wang, B., ... Volkin, D. B. (2005). Stabilization of human papillomavirus virus-like particles by non-ionic surfactants. *Journal of Pharmaceutical Sciences*, 94(7), 1538–1551.

Shoji, Y., Prokhnevsky, A., Leffert, B., Vetter, N., Tottey, S., Satinover, S., ... Yusibov, V. (2015). Immunogenicity of H1N1 influenza virus-like particles produced in *Nicotiana benthamiana*. *Human Vaccines and Immunotherapeutics*, 11(1), 118–123.

Silhavy, D., Molnar, A., Lucioli, A., Szittyá, G., Hornyik, C., Tavazza, M., and Burgyan, J. (2002). A viral protein suppresses RNA silencing and binds silencing-generated, 21- to 25-nucleotide double-stranded RNAs. *The EMBO Journal*, 21(12), 3070–3080.

Simasathien, S., Thomas, S. J., Watanaveeradej, V., Nisalak, A., Barberousse, C., Innis, B. L., ... Biologicals, G. (2008). Safety and immunogenicity of a tetravalent live-attenuated dengue vaccine in flavivirus naïve children. *American Journal of Tropical Medicine and Hygiene*, 78(3), 426–433.

Simmonds, P., Becher, P., Bukh, J., Gould, E. A., Meyers, G., Monath, T., ... ICTV Report Consortium. (2017). ICTV virus taxonomy profile: *Flaviviridae*. *Journal of General Virology*, 98, 2–3.

Skae, F. M. T. (1902). Dengue fever in Penang. *The British Medical Journal*, 1581–1582.

Slater, A., Scott, N., and Fowler, M. (2003). *Plant Biotechnology: The genetic*

manipulation of plants. New York: Oxford University Press Inc.

Šmídková, M., Müller, M., Thönes, N., Piuko, K., Angelisová, P., Velemínský, J., and Angelis, K. J. (2010). Transient expression of human papillomavirus type 16 virus-like particles in tobacco and tomato using a tobacco rattle virus expression vector. *Biologia Plantarum*, 54(3), 451–460.

Soares, R. O. S., and Caliri, A. (2013). Stereochemical features of the envelope protein domain III of dengue virus reveals putative antigenic site in the five-fold symmetry axis. *Biochimica et Biophysica Acta - Proteins and Proteomics*, 1834, 221–230.

Sojikul, P., Buehner, N., and Mason, H. S. (2003). A plant signal peptide-hepatitis B surface antigen fusion protein with enhanced stability and immunogenicity expressed in plant cells. *Proceedings of the National Academy of Sciences of the United States of America*, 100(5), 2209–2214.

Stahl, S. J., and Murray, K. (1989). Immunogenicity of peptide fusions to hepatitis B virus core antigen. *Proceedings of the National Academy of Sciences of the United States of America*, 86, 6283–6287.

Stephens, H. A. F., Klaythong, R., Sirikong, M., Vaughn, D. W., Green, S., Kalayanarooj, S., ... Chandanayingyong, D. (2002). HLA-A and -B allele associations with secondary dengue virus infections correlate with disease severity and the infecting viral serotype in ethnic Thais. *Tissue Antigens*, 60(4), 309–318.

Stephenson, J. R. (2005). Understanding dengue pathogenesis: implications for vaccine design. *Bulletin of the World Health Organization*, 83(4), 308–314.

Stratmann, T. (2015). Cholera toxin subunit B as adjuvant - an accelerator in protective immunity and a break in autoimmunity. *Vaccines*, 3, 579–596.

Sugrue, R. J., Fu, J., Howe, J., and Chan, Y. C. (1997). Expression of the dengue virus structural proteins in. *Journal of General Virology*, 78, 1861–1866.

- Sun, W., Cunningham, D., Wasserman, S. S., Perry, J., Putnak, J. R., Eckels, K. H., ... Edelman, R. (2009). Phase 2 clinical trial of three formulations of tetravalent live-attenuated dengue vaccine in flavivirus-naïve adults. *Human Vaccines*, 5(1), 33–40.
- Sun, W., Edelman, R., Kanesa-Thasan, N., Eckels, K. H., Putnak, J. R., King, A. D., ... Innis, B. L. (2003). Vaccination of human volunteers with monovalent and tetravalent live-attenuated dengue vaccine candidates. *American Journal of Tropical Medicine and Hygiene*, 69(Suppl 6), 24–31.
- Suzarte, E., Marcos, E., Gil, L., Valdés, I., Lazo, L., Ramos, Y., ... Hermida, L. (2014). Generation and characterization of potential dengue vaccine candidates based on domain III of the envelope protein and the capsid protein of the four serotypes of dengue virus. *Archives of Virology*, 159(7), 1629–1640.
- Tagliamonte, M., Tornesello, M. L., Buonaguro, F. M., and Buonaguro, L. (2017). Virus-like particles. In M. Skwarczynski and I. Toth (Eds.), *Micro- and Nanotechnology in Vaccine Development* (pp. 205–219). Oxford: Matthew Deans.
- Teng, A. K., and Singh, S. (2001). Epidemiology and new initiatives in the prevention and control of dengue in Malaysia. *Dengue Bulletin*, 25, 7-14.
- Teoh, B. T., Sam, S. S., Tan, K. K., Johari, J., Shu, M. H., Danlami, M. B., ... AbuBakar, S. (2013). Dengue virus type 1 clade replacement in recurring homotypic outbreaks. *BMC Evolutionary Biology*, 13, 213. doi: 10.1186/1471-2148-13-213.
- Teoh, P. G., Ooi, A. S., Abubakar, S., Othman, R. Y., and Plopper, G. E. (2009). Virus-specific read-through codon preference affects infectivity of chimeric cucumber green mottle mosaic viruses displaying a dengue virus epitope. *Journal of Biomedicine and Biotechnology*, 2009, 781712. doi:10.1155/2009/781712.
- Thomas, S. J., Eckels, K. H., Carletti, I., de la Barrera, R., Dessy, F., Fernandez, S., ... Innis, B. L. (2013). A phase II, randomized, safety and immunogenicity study of a re-

derived, live-attenuated dengue virus vaccine in healthy adults. *American Journal of Tropical Medicine and Hygiene*, 88(1), 73–88.

Thuenemann, E. C., Lenzi, P., Love, A. J., Taliansky, M., Becares, M., Zuniga, S., ... Lomonosoff, G. P. (2013). The use of transient expression systems for the rapid production of virus-like particles in plants. *Current Pharmaceutical Design*, 19, 5564–5573.

Tissot, A. C., Renhofs, R., Schmitz, N., Cielens, I., Meijerink, E., Ose, V., ... Bachmann, M. F. (2010). Versatile virus-like particle carrier for epitope based vaccines. *PLoS ONE*, 5(3), e9809. doi: 10.1371/journal.pone.0009809.

Tschofen, M., Knopp, D., Hood, E., and Stöger, E. (2016). Plant molecular farming: much more than medicines. *Annual Review of Analytical Chemistry*, 9(1), 271–294.

Twiddy, S. S., Woelk, C. H., and Holmes, E. C. (2002). Phylogenetic evidence for adaptive evolution of dengue viruses in nature. *Journal of General Virology*, 83, 1679–1689.

Twyman, R. M. (2004). Host plants, systems and expression strategies for molecular farming. In R. Fischer and S. Schillberg (Eds.), *Molecular Farming: Plant-made Pharmaceuticals and Technical Proteins* (pp. 191–216). Weinheim: Wiley-VCH Verlag GmbH & Co.

Valdés, I., Bernardo, L., Gil, L., Pavón, A., Lazo, L., López, C., ... Hermida, L. (2009). A novel fusion protein domain III-capsid from dengue-2, in a highly aggregated form, induces a functional immune response and protection in mice. *Virology*, 394(2), 249–258.

van der Schaar, H. M., Rust, M. J., Chen, van der Ende-Metselaar, H., Wilschut, J., Zhuang, X., and Smit, J. M. (2008). Dissecting the cell entry pathway of dengue virus by single-particle tracking in living cells. *PLoS Pathogens*, 4(12), e1000244. doi:

10.1371/journal.ppat.1000244.

van Heyningen, S. (1976). Activation by cholera toxin of adenylate cyclase solubilized from rat liver. *Biochemical Journal*, *157*, 785–787.

van Zyl, A. R., Meyers, A. E., and Rybicki, E. P. (2016). Transient Bluetongue virus serotype 8 capsid protein expression in *Nicotiana benthamiana*. *Biotechnology Reports*, *9*, 15–24.

Vaughn, D. W., Green, S., Kalayanarooj, S., Innis, B. L., Nimmannitya, S., Suntayakorn, S., ... Nisalak, A. (2000). Dengue viremia titer, antibody response pattern, and virus serotype correlate with disease severity. *The Journal of Infectious Diseases*, *181*(1), 2–9.

Villar, L., Dayan, G. H., Arredondo-García, L., Rivera, D. M., Cunha, R., Deseda, C., ... Noriega, F. (2015). Efficacy of a tetravalent dengue vaccine in children in Latin America. *The New England Journal of Medicine*, *372*(2), 113–123.

Villordo, S. M., and Gamarnik, A. V. (2009). Genome cyclization as strategy for flavivirus RNA replication. *Virus Research*, *139*, 230–239.

Vogel, M., Diez, M., Einfeld, J., and Nassal, M. (2005). *In vitro* assembly of mosaic hepatitis B virus capsid-like particles (CLPs): rescue into CLPs of assembly-deficient core protein fusions and FRET-suited CLPs. *FEBS Letters*, *579*(23), 5211–5216.

Vogel, M., Vorreiter, J., and Nassal, M. (2005). Quaternary structure is critical for protein display on capsid-like particles (CLPs): efficient generation of hepatitis B virus CLPs presenting monomeric but not dimeric and tetrameric fluorescent proteins. *Proteins: Structure, Function and Genetics*, *58*, 478–488.

Voinnet, O., Rivas, S., Mestre, P., and Baulcombe, D. (2003). An enhanced transient expression system in plants based on suppression of gene silencing by the p19 protein of tomato bushy stunt virus. *The Plant Journal*, *33*, 949–956.

- Volk, D. E., Lee, Y. C., Li, X., Thiviyanathan, V., Gromowski, G. D., Li, L., ... Gorenstein, D. G. (2007). Solution structure of the envelope protein domain III of dengue-4 virus. *Virology*, *364*(1), 147–154.
- von Heijne, G. (1983). Patterns of amino acids near signal-sequence cleavage sites. *European Journal of Biochemistry*, *133*, 17–21.
- Wahala, W. M. P. B., Donaldson, E. F., de Alwis, R., Accavitti-Loper, M. A., Baric, R. S., and de Silva, A. M. (2010). Natural strain variation and antibody neutralization of dengue serotype 3 viruses. *PLoS Pathogens*, *6*(3), e1000821. doi: 10.1371/journal.ppat.1000821.
- Walker, A., Skamel, C., and Nassal, M. (2011a). SplitCore: An exceptionally versatile viral nanoparticle for native whole protein display regardless of 3D structure. *Scientific Reports*, *1*, 5. doi: 10.1038/srep00005.
- Walker, T., Johnson, P. H., Moreira, L. A., Iturbe-Ormaetxe, I., Frentiu, F. D., McMeniman, C. J., ... Hoffmann, A. A. (2011b). The wMel *Wolbachia* strain blocks dengue and invades caged *Aedes aegypti* populations. *Nature*, *476*, 450–453.
- Wallace, H. G., Lim, T. W., Rudnick, A., Knudsen, A. B., Cheong, W. H., and Chew, V. (1980). Dengue hemorrhagic fever in Malaysia: the 1973 epidemic. *The Southeast Asian Journal of Tropical Medicine and Public Health*, *11*(1), 1–13.
- Wang, E., Ni, H., Xu, R., Barrett, A. D. T., Watowich, S. J., Gubler, D. J., and Weaver, S. C. (2000). Evolutionary relationships of endemic/epidemic and sylvatic dengue viruses. *Journal of Virology*, *74*(7), 3227–3234.
- Wang, M., Bregenholt, S., and Petersen, J. S. (2003). The cholera toxin B subunit directly costimulates antigen-primed CD4⁺ T cells *ex vivo*. *Scandinavian Journal of Immunology*, *58*(3), 342–349.
- Wang, X., Huang, X., and Wang, S. (2009). Study on immunity of dengue virus and

dengue vaccine development. *Frontiers of Biology in China*, 4(2), 125–128.

Wan-Norafikah, O., Nazni, W. A., Lee, H. L., Zainol-Arifin, P., and Sofian-Azirun, M. (2010). Permethrin resistance in *Aedes aegypti* (Linnaeus) collected from Kuala Lumpur, Malaysia. *Journal of Asia-Pacific Entomology*, 13(3), 175–182.

Watanaveeradej, V., Simasathien, S., Nisalak, A., Endy, T. P., Jarman, R. G., Innis, B. L., ... Mammen, M. P. (2011). Safety and immunogenicity of a tetravalent live-attenuated dengue vaccine in flavivirus-naïve infants. *American Journal of Tropical Medicine and Hygiene*, 85(2), 341–351.

Welsch, S., Miller, S., Romero-Brey, I., Merz, A., Bleck, C. K. E., Walther, P., ... Bartenschlager, R. (2009). Composition and three-dimensional architecture of the dengue virus replication and assembly sites. *Cell Host and Microbe*, 5(4), 365–375.

Wen, Y., and Shi, Y. (2016). Alum: an old dog with new tricks. *Emerging Microbes & Infections*, 5(3), e25. doi: 10.1038/emi.2016.40.

Whitacre, D., Espinosa, D., Peterson, D., Zavala, F., and Milich, D. (2016). Use of VLPs in the design of malaria vaccines. In Y. Khudyakov and P. Pumpens (Eds.), *Viral Nanotechnology* (pp. 209–232). Boca Raton: CRC Press.

Whitehead, S. S. (2016). Development of TV003/TV005, a single dose, highly immunogenic live attenuated dengue vaccine; what makes this vaccine different from the Sanofi-Pasteur CYD™ vaccine? *Expert Review of Vaccines*, 15(4), 509–517.

Whitehead, S. S., Blaney, J. E., Durbin, A. P., and Murphy, B. R. (2007). Prospects for a dengue virus vaccine. *Nature Reviews Microbiology*, 5, 518–528.

Whitehead, S. S., Durbin, A. P., Pierce, K. K., Elwood, D., McElvany, B. D., Fraser, E. A., ... Kirkpatrick, B. D. (2017). In a randomized trial, the live attenuated tetravalent dengue vaccine TV003 is well-tolerated and highly immunogenic in subjects with flavivirus exposure prior to vaccination. *PLoS Neglected Tropical Diseases*, 11(5),

e0005584. doi: 10.1371/journal.pntd.0005584.

Whitehorn, J., and Simmons, C. P. (2011). The pathogenesis of dengue. *Vaccine*, 29, 7221–7228.

Wilder-Smith, A., and Massad, E. (2016). Age specific differences in efficacy and safety for the CYD-tetravalent dengue vaccine. *Expert Review of Vaccines*, 15(4), 437–441.

World Health Organization (WHO). (1980). *Guide for diagnosis, treatment and control of dengue haemorrhagic fever (second edition)*. Retrieved August 16, 2016, from http://iris.wpro.who.int/bitstream/handle/10665.1/10508/Guide_for_diagnosis_2nd_ed_eng.pdf

World Health Organization (WHO). (2009). *Dengue: guidelines for diagnosis, treatment, prevention, and control – new edition*. Retrieved August 9, 2016, from <http://www.who.int/tdr/publications/documents/dengue-diagnosis.pdf>

World Health Organization (WHO). (2012). *Global strategy for dengue prevention and control 2012-2020*. Retrieved September 3, 2016, from http://apps.who.int/iris/bitstream/10665/75303/1/9789241504034_eng.pdf

World Health Organization (WHO). (2014). *A global brief on vector-borne diseases*. Retrieved July 27, 2016, from http://apps.who.int/iris/bitstream/10665/111008/1/WHO_DCO_WHD_2014.1_eng.pdf

World Health Organization (WHO). (2017). Dengue and severe dengue. Retrieved January 10, 2018, from <http://www.who.int/mediacentre/factsheets/fs117/en/>

World Health Organization Western Pacific Region (WPRO). (2018). Dengue situation update number 533. Retrieved January 17, 2018, from http://www.wpro.who.int/emerging_diseases/dengue_biweekly_report_20180102.pdf?

ua=1

Wong, L. P., and AbuBakar, S. (2013). Health beliefs and practices related to dengue fever: a focus group study. *PLoS Neglected Tropical Diseases*, 7(7), e2310. doi: 10.1371/journal.pntd.0002310.

Wroblewski, T., Tomczak, A., and Michelmore, R. (2005). Optimization of *Agrobacterium*-mediated transient assays of gene expression in lettuce, tomato and *Arabidopsis*. *Plant Biotechnology Journal*, 3(2), 259–273.

Wu, S. J. L., Grouard-Vogel, G., Sun, W., Mascola, J. R., Brachtel, E., Putvatana, R., ... Frankel, S. S. (2000). Human skin Langerhans cells are targets of dengue virus infection. *Nature Medicine*, 6(7), 816–820.

Wynne, S. A., Crowther, R. A., and Leslie, A. G. W. (1999). The crystal structure of the human hepatitis B virus capsid. *Molecular Cell*, 3, 771–780.

Xu, H., Montoya, F. U., Wang, Z., Lee, J. M., Reeves, R., Linthicum, D. S., and Magnuson, N. S. (2002). Combined use of regulatory elements within the cDNA to increase the production of a soluble mouse single-chain antibody, scFv, from tobacco cell suspension cultures. *Protein Expression and Purification*, 24, 384-394.

Xue, M., Yu, L., Jia, L., Li, Y., Zeng, Y., Li, T., ... Xia, N. (2016). Immunogenicity and protective efficacy of rotavirus VP8* fused to cholera toxin B subunit in a mouse model. *Human Vaccines and Immunotherapeutics*, 12(11), 2959–2968.

Yang, M., Lai, H., Sun, H., and Chen, Q. (2017). Virus-like particles that display Zika virus envelope protein domain III induce potent neutralizing immune responses in mice. *Scientific Reports*, 7, 7679. doi: 10.1038/s41598-017-08247-9.

Yao, J., Weng, Y., Dickey, A., and Wang, K. Y. (2015). Plants as factories for human pharmaceuticals: Applications and challenges. *International Journal of Molecular Sciences*, 16, 28549–28565.

- Yauch, L. E., Zellweger, R. M., Kotturi, M. F., Qutubuddin, A., Sidney, J., Peters, B., ... Shresta, S. (2009). A protective role for dengue virus-specific CD8⁺ T cells. *Journal of Immunology*, 182(8), 4865–4873.
- Yeap, H. L., Mee, P., Walker, T., Weeks, A. R., O'Neill, S. L., Johnson, P., ... Hoffmann, A. A. (2011). Dynamics of the “popcorn” *Wolbachia* infection in outbred *Aedes aegypti* informs prospects for mosquito vector control. *Genetics*, 187, 583–595.
- Yong, Y. K., Thayan, R., Chong, H. T., Tan, C. T., and Sekaran, S. D. (2007). Rapid detection and serotyping of dengue virus by multiplex RT-PCR and real-time SYBR green RT-PCR. *Singapore Medical Journal*, 48(7), 662–668.
- Yusibov, V., Streatfield, S. J., and Kushnir, N. (2011). Clinical development of plant-produced recombinant pharmaceuticals: vaccines, antibodies and beyond. *Human Vaccines*, 7(3), 313–321.
- Zabel, F., Kündig, T. M., and Bachmann, M. F. (2013). Virus-induced humoral immunity: on how B cell responses are initiated. *Current Opinion in Virology*, 3(3), 357–362.
- Zahin, M., Joh, J., Khanal, S., Husk, A., Mason, H., Warzecha, H., ... Jenson, A. B. (2016). Scalable production of HPV16 L1 protein and VLPs from tobacco leaves. *PLoS ONE*, 11(8), e0160995. doi: 10.1371/journal.pone.0160995.
- Zahmanova, G. G., Naimov, S. I., Mazalovska, M., Valkova, R. P., Minkov, I. N., and Zahmanova, G. (2014). Transient expression of modified hepatitis B capsid protein in *Nicotiana benthamiana* plants for viral nanoparticles production. *Journal of Bioscience and Biotechnology, SE/ONLINE*, 11–16.
- Zeddani, J. L., Orbe, K., Léry, X., Dangles, O., Dupas, S., and Silvain, J. F. (2008). An isometric virus of the potato tuber moth *Tecia solanivora* (Povolny) (Lepidoptera: Gelechiidae) has a tri-segmented RNA genome. *Journal of Invertebrate Pathology*,

99(2), 204–211.

Zhang, S., Liang, M., Gu, W., Li, C., Miao, F., Wang, X., ... Li, D. (2011). Vaccination with dengue virus-like particles induces humoral and cellular immune responses in mice. *Virology Journal*, 8, 333. doi: 10.1186/1743-422X-8-333.

Zhao, H., Tan, Z., Wen, X., and Wang, Y. (2017). An improved syringe agroinfiltration protocol to enhance transformation efficiency by combinative use of 5-azacytidine, ascorbate acid and Tween-20. *Plants*, 6, 9. doi: 10.3390/plants6010009.

Zhao, H. L., Yao, X. Q., Xue, C., Wang, Y., Xiong, X. H., and Liu, Z. M. (2008). Increasing the homogeneity, stability and activity of human serum albumin and interferon- α 2b fusion protein by linker engineering. *Protein Expression and Purification*, 61(1), 73–77.

Zhao, X., Li, G., Liang, S., Zhao, X., Li, G., and Liang, S. (2013). Several affinity tags commonly used in chromatographic purification. *Journal of Analytical Methods in Chemistry*, 2013, 581093. doi: 10.1155/2013/581093.

Zheng, J., Schödel, F., and Peterson, D. L. (1992). The structure of hepadnaviral core antigens. *Biochemistry*, 267(13), 9422–9429.

Zheng, N., Xia, R., Yang, C., Yin, B., Li, Y., Duan, C., ... Xie, Q. (2009). Boosted expression of the SARS-CoV nucleocapsid protein in tobacco and its immunogenicity in mice. *Vaccine*, 27, 5001–5007.

Zhou, Y., Austin, S. K., Fremont, D. H., Yount, B. L., Huynh, J. P., de Silva, A. M., ... Messer, W. B. (2013). The mechanism of differential neutralization of dengue serotype 3 strains by monoclonal antibody 8A1. *Virology*, 439(1), 57–64.

Zidane, N., Dussart, P., Bremand, L., Villani, M. E., and Bedouelle, H. (2013). Thermodynamic stability of domain III from the envelope protein of flaviviruses and its improvement by molecular design. *Protein Engineering, Design & Selection*, 26(6),

389-399.

9 Appendices

Appendices for Chapter 3

A3.1 Nucleotide and amino acid sequences of the mEL expression cassette in pEAQ-*HT*::mEL vector

Nucleotide sequence

ATG GAT ATC GAC CCA TAT AAA GAA TTT GGC GCG ACG GTT GAG CTG
CTG AGC TTT CTG CCA AGC GAT TTC TTT CCG AGC GTC CGC GAC CTG
CTG GAT ACC GCC AGC GCA CTG TAT CGT GAA GCC CTG GAG AGC CCG
GAA CAT TGC AGC CCG CAT CAT ACG GCC CTG CGT CAG GCA ATC CTG
TGC TGG GGC GAA CTG ATG ACC CTG GCA ACC TGG GTC GGC AAT AAT
CTG GTC GAC GCT GGT GGA GGT CCT AGG GGT GGG TCT GGT ATT AAT
GAC CCA GCA AGC CGT GAT CTG GTT GTT AAT TAC GTG AAC ACC AAC
ATG GGC CTG AAG ATC CGC CAA CTG CTG TGG TTT CAT ATC AGC TGT
CTG ACG TTT GGC CGC GAG ACG GTG CTG GAA TAC CTG GTT AGC TTT
GGC GTT TGG ATT CGT ACG CCA CCG GCC TAC CGC CCA CCA AAC GCA
CCG ATT CTG AGC ACG CTG CCG GAA ACG ACG GTT GTT CGT CGC CGT
GAT CGC GGC CGT AGC CCG CGC CGC CGT ACG CCG AGC CCA CGT CGT
CGC CGC AGC CAG AGC CCG CGC CGC CGT CGC AGC CAG AGC CGT GAA
AGC CAA TGT TAG

Amino acid sequence

MDIDPYKEFGATVELLSFLPSDFFPVSRDLLDTASALYR
EALSPHCSPHHTALRQAILCWGELMTLATWVGNNLV
DAGGGPRGSGINDPASRDLVVNYVNTNMGLKIRQLLW

FHISCLTFGRETVLEYLVSFGVWIRTPPAYRPPNAPILST
LPETTVVRRRDRGRSPRRRTSPRRRRRSQSPRRRRRSQSR
ESQC*

Feature

5' core I	: Nucleotide (1...228)	: Amino acid (1...76)
SalI RE site	: Nucleotide (229...234)	: Amino acid (77...78)
c/e1 loop	: Nucleotide (235...264)	: Amino acid (79...88)
AseI RE site	: Nucleotide (265...270)	: Amino acid (89...90)
3' core	: Nucleotide (271...597)	: Amino acid (91...199)

A3.2 Nucleotide and amino acid sequences of the tHBcAg-VHH2 expression cassette in pEAQ-HT::tHBcAg-VHH2 vector

Nucleotide acid sequence

ATG GAC ATT GAT CCG TAC AAA GAA TTT GGC GCG ACC GTC GAG CTG
CTG AGC TTC CTG CCG AGC GAT TTT TTC CCA AGC GTG CGT GAC CTG
CTG GAC ACC GCG AGC GCA CTG TAT CGT GAA GCA CTG GAA AGC CCA
GAG CAC TGT AGC CCG CAC CAC ACC GCC CTG CGC CAG GCG ATT CTG
TGC TGG GGT GAA CTG ATG ACC CTG GCC ACC TGG GTG GGT AAT AAT
CTG GAA CCC GGG GCT GGT GGA AGT TCT GGT CAA TTG GAC CCG GCG
AGC CGT GAT CTG GTC GTC AAC TAT GTG AAT ACC AAC ATG GGT CTG
AAA ATT CGT CAG CTG CTG TGG TTT CAT ATT AGC TGC CTG ACC TTC
GGT CGT GAA ACC GTG CTG GAG TAT CTG GTG AGC TTC GGT GTG TGG
ATT CGC ACC CCG CCA GCG TAT CGT CCG CCG AAC GCG CCA ATT CTG
AGC ACG CTG CCG GAG ACC ACC GTG GTT GGT GGA AGT TCT GGT GGT
AGT GGA GGA AGT GGT GGT TCT GGT GGA AGC GGT GGT AGT GGT GGG
ACT GGT ACA ATG GAT ATC GAC CCA TAT AAA GAA TTT GGC GCG ACG
GTT GAG CTG CTG AGC TTT CTG CCA AGC GAT TTC TTT CCG AGC GTC
CGC GAC CTG CTG GAT ACC GCC AGC GCA CTG TAT CGT GAA GCC CTG
GAG AGC CCG GAA CAT TGC AGC CCG CAT CAT ACG GCC CTG CGT CAG
GCA ATC CTG TGC TGG GGC GAA CTG ATG ACC CTG GCA ACC TGG GTC
GGC AAT AAT CTG GTC GAC GGT GGT GGT GGA AGC GGA GGT GGT GGT
TCT GGT GGT GGT GGT TCA CCT AGG ATG GCT GTT CAG CTT CAA GAA
AGC GGT GGT GGA CTT GTT CAA GCT GGT GGA TCT CTT AGG CTT AGC
TGC ACT GCT AGC GGT AGG ATC TCC AGC TCT TAT GAT ATG GGA TGG
TTC AGG CAG GCT CCT GGT AAA GAG AGA GAG TTC GTT GCT GCT ATC
AGC TGG TCT GGT GGT ACT ACC GAT TAC GCT GAT TCT GTG AAG GGA

AGG TTC GCT ATC AGC AAG GAT AAC GCT AAG AAC GCT GTG TAC CTG
CAG ATG AAC TCT CTG AAG CCT GAG GAT ACC GCA GTT TAC TAC TGT
GCT GCT AAG TGG AGG CCT CTG AGG TAC TCT GAT TAC CCT AGC AAC
AGC GAT TAC TAC GAT TGG GGT CAG GGT ACT CAG GTG ACC GTT TCA
TCT CCT GCA GGT GGT GGT GGT AGT GGT GGT GGT GGA TCA GGT GGT
GGT GGA TCT ATT AAT GAC CCA GCA AGC CGT GAT CTG GTT GTT AAT
TAC GTG AAC ACC AAC ATG GGC CTG AAG ATC CGC CAA CTG CTG TGG
TTT CAT ATC AGC TGT CTG ACG TTT GGC CGC GAG ACG GTG CTG GAA
TAC CTG GTT AGC TTT GGC GTT TGG ATT CGT ACG CCA CCG GCC TAC
CGC CCA CCA AAC GCA CCG ATT CTG AGC ACG CTG CCG GAA ACG ACG
GTT GTT CGT CGC CGT GAT CGC GGC CGT AGC CCG CGC CGC CGT ACG
CCG AGC CCA CGT CGT CGC CGC AGC CAG AGC CCG CGC CGC CGT CGC
AGC CAG AGC CGT GAA AGC CAA TGT TAG

Amino acid sequence

MDIDPYKEFGATVELLSFLPSDFFPVSRDLLDTASALYR
EALESPEHCSPHHTALRQAILCWGELMTLATWVGNNLE
PGAGGSSGQLDPASRDLVVNYVNTNMGLKIRQLLWFHI
SCLTFGRETVLEYLVSFGVWIRTPPAYRPPNAPILSTLPE
TTVVGGSSGGSSGGSSGGSSGGSSGGTGTMDIDPYKEFG
ATVELLSFLPSDFFPVSRDLLDTASALYREALESPEHCSP
HHTALRQAILCWGELMTLATWVGNNLVDGGGGSSGGG
SGGGSPRMAVQLQESGGGLVQAGGSLRLSCTASGRISS
SYDMGWFRQAPGKEREFVAAISWSSGGTTDYADSVKGRF
AISKDNAKNAVYLYQMNSLKPEDTAVYYCAAKWRPLRY
SDYPSNSDYDYGQGTQVTVSSPAGGGSSGGGGSSGGG
GSINDPASRDLVVNYVNTNMGLKIRQLLWFHISCLTFGR

ETVLEYLVSFVWIRTPPAYRPPNAPILSTLPETTVVRRR
 DRGRSPRRRTPSPRRRRSQSPRRRRS QSRESQC*

Feature

5' Core I	: Nucleotide (1...231)	: Amino acid (1...77)
XmaI RE site	: Nucleotide (232...237)	: Amino acid (78...79)
Core I c/e1 loop	: Nucleotide (238...255)	: Amino acid (80...85)
MfeI RE site	: Nucleotide (256...261)	: Amino acid (86...87)
3' Core I	: Nucleotide (262...477)	: Amino acid (88...159)
(GGS)n linker	: Nucleotide (478...549)	: Amino acid (160...183)
5' Core II	: Nucleotide (550...777)	: Amino acid (184...259)
SalI RE site	: Nucleotide (778...783)	: Amino acid (260...261)
(GGS)n linker	: Nucleotide (784...828)	: Amino acid (262...276)
AvrII RE site	: Nucleotide (829...834)	: Amino acid (277...278)
VHH2	: Nucleotide (835...1218)	: Amino acid (279...406)
SbfI RE site	: Nucleotide (1219...1226 [#])	: Amino acid (407...409 [#])
(GGS)n linker	: Nucleotide (1225 [#] ...1269)	: Amino acid (409 [#] ...423)
AseI RE site	: Nucleotide (1270...1275)	: Amino acid (424...425)
3' Core II	: Nucleotide (1276...1602)	: Amino acid (410...534)

Annotation: # Indicates that part of the (GGS)n linker overlaps with SbfI RE site.

A3.3 Nucleotide and amino acid sequences of synthesised cEDIII-sGFP-KDEL

Nucleotide sequence

AAG GGA ATG TCA TAC GCT ATG TGT ACT GGA AAG TTC AAG TTG GAG
AAG GAG GTG GCA GAG ACT CAG CAC GGA ACC ATC TTA ATC AAA GTT
AAA TAT GAA GGT GAT GGT GCT CCT TGT AAG ATT CCT TTC GAA ATC
CAA GAT GTT GAG AAG AAA CAT GTG AAT GGA AGG TTG ATT ACC GCT
AAC CCA ATC GTT ACT GAT AAG GAG TCA CCT GTG AAT ATT GAA GCA
GAG CCT CCA TTT GGT GAT AGT TAT ATT GTT ATC GGT GTG GGA GAT
AAG GCA CTT AAA TTG AAC TGG TTC AAG AAG GGA TCT TCA GAA AAC
CTT TAC TTC CAG GGA ATG GTT TCA AAA GGT GAA GAG CTT TTT ACT
GGT GTT GTG CCA ATT CTT GTT GAG TTG GAT GGA GAT GTG AAT GGT
CAC AAG TTC AGT GTT TCT GGT GAA GGA GAG GGT GAT GCT ACA TAC
GGA AAG TTA ACC CTC AAA TTT ATC TGT ACT ACT GGA AAG TTG CCT
GTT CCT TGG CCT ACA TTG GTG ACC ACT TTT ACC TAT GGA GTG CAA
TGC TTT TCT AGG TAT CCT GAT CAC ATG AAG CAG CAC GAT TTC TTT
AAA TCA GCT ATG CCT GAA GGA TAC GTT CAA GAG AGA ACA ATT TTC
TTT AAG GAT GAT GGT AAC TAC AAA ACT AGG GCA GAG GTT AAG TTT
GAG GGA GAT ACA CTT GTG AAC AGA ATC GAA TTG AAG GGT ATC GAT
TTC AAA GAG GAT GGA AAC ATC CTC GGT CAT AAG CTC GAA TAC AAC
TAC AAC AGT CAC AAC GTT TAC ATC ATG GCT GAT AAG CAA AAG AAT
GGA ATC AAG GTG AAC TTC AAA ATT AGG CAT AAC ATC GAG GAT GGT
TCT GTT CAG CTT GCA GAT CAC TAT CAA CAG AAT ACC CCA ATT GGA
GAT GGT CCA GTT CTT TTG CCT GAT AAC CAT TAC TTA TCA ACA CAG
AGT GCT CTC TCT AAA GAT CCT AAC GAA AAG AGA GAT CAC ATG GTT
CTT CTT GAA TTT GTG ACT GCT GCT GGT ATT ACA CAC GGT ATG GAT
GAA TTA TAC AAG CCT AAA GAT GAG TTG

Amino acid sequence

KGMSYAMCTGKFKLEKEVAETQHGTILIKVKYEGDGAP
CKIPFEIQDVEKKHVNGRLITANPIVTDKESPVNIEAEP
FGDSYIVIGVGDKALKLNWFKKGSSENLYFQGMVSKGE
ELFTGVVPILVELDGDVNGHKFSVSGEGEGDATYGKLT
LKFICTTGKLPVPWPTLVTTFTYGVQCFSRYPDHMKQH
DFFKSAMPEGYVQERTIFFKDDGNYKTRAEVKFEGDTL
VNRIELKGIDFKEDGNILGHKLEYNYNSHNVYIMADKQ
KNGIKVNFKIRHNIEDGSVQLADHYQQNTPIGDGPVLLP
DNHYLSTQSALS KDPNEKRDHMLLEFVTAAGITHGMD
ELYKPKDEL

Feature

cEDIII	: Nucleotide (1...309)	: Amino acid (1...103)
TEV cleavage site	: Nucleotide (310...330)	: Amino acid (104...110)
sGFP	: Nucleotide (331...1050)	: Amino acid (111...350)
KDEL signal	: Nucleotide (1051...1062)	: Amino acid (351...354)

A3.4 Nucleotide and amino acid sequences of synthesised PR1a-cEDIII-sGFP-H-KDEL

Nucleotide sequence

AAC AAT GGG ATT CGT TTT ATT CTC TCA ACT TCC TTC ATT TCT CCT TGT
GTC AAC TCT TTT GCT CTT CCT CGT TAT TAG TCA TTC TTG TAG AGC TAA
AGG AAT GTC TTA TGC TAT GTG TAC TGG AAA GTT CAA ATT GGA AAA
GGA GGT TGC TGA AAC ACA ACA TGG AAC CAT TCT TAT CAA GGT GAA
ATA CGA GGG TGA TGG AGC ACC ATG CAA AAT TCC TTT TGA AAT CCA
GGA TGT TGA GAA GAA ACA TGT GAA TGG AAG GCT TAT TAC AGC TAA
CCC AAT CGT TAC CGA TAA GGA ATC ACC TGT GAA TAT TGA AGC AGA
GCC TCC ATT TGG TGA TAG TTA TAT TGT TAT CGG TGT GGG AGA TAA
GGC TCT TAA ATT GAA CTG GTT CAA GAA GGG ATC TTC AGA AAA CCT
CTA CTT CCA AGG AAT GGT TTC TAA AGG TGA AGA GTT GTT TAC TGG
TGT TGT GCC AAT TCT TGT TGA GTT GGA TGG AGA TGT GAA TGG TCA
TAA GTT CAG TGT TTC TGG TGA AGG AGA GGG TGA TGC AAC TTA TGG
AAA GTT AAC ACT CAA GTT TAT CTG TAC TAC TGG AAA GTT GCC TGT
TCC TTG GCC TAC TTT GGT GAC CAC TTT TAC TTA TGG TGT TCA ATG CTT
TTC TAG GTA TCC TGA TCA CAT GAA GCA GCA CGA TTT CTT TAA ATC
AGC TAT GCC TGA AGG ATA CGT TCA GGA GAG AAC AAT TTT CTT TAA
GGA TGA TGG TAA CTA CAA AAC CAG GGC AGA GGT TAA GTT TGA GGG
AGA TAC ACT TGT GAA CAG AAT CGA ATT GAA GGG TAT CGA TTT CAA
AGA GGA TGG AAA CAT CCT CGG TCA TAA GCT CGA ATA CAA CTA CAA
CAG TCA CAA CGT TTA CAT CAT GGC TGA TAA GCA AAA GAA TGG AAT
CAA GGT GAA CTT CAA AAT TAG GCA TAA CAT CGA GGA TGG TTC TGT
TCA GTT GGC AGA TCA CTA TCA ACA GAA TAC TCC AAT TGG AGA TGG
TCC AGT TCT TTT GCC TGA TAA CCA TTA CTT ATC AAC ACA AAG TGC

TCT CTC TAA AGA TCC TAA CGA AAA GAG AGA TCA CAT GGT TCT TCT
TGA ATT TGT GAC TGC TGC TGG TAT TAC TCA CGG TAT GGA TGA ACT
TTA CAA ACA TCA CCA TCA CCA TCA CAA GGA TGA GCT TTG A

Amino acid sequence

MGFVLFSQLPSFLLVSTLLLFLVISHSCRAKGM SYAMCT
GKFKLEKEVAETQHGTILIKVKYEGDGAPCKIPFEIQDV
EKKHVNGRLITANPIVTDKESPVNIEAEPFPGDSYIVIGV
GDKALKLNWFKKGSENLYFQGMVSKGEELFTGVVPIL
VELDGDVNGHKFSVSGEGEGDATYGKLTCLKFICTTGKL
PVPWPTLVTTFTYGVQCFSRYPDHMKQHDFFKSAMPEG
YVQERTIFFKDDGNYKTRAEVKFEGDTLVNRIELKGIDF
KEDGNILGHKLEYNYNSHNVYIMADKQKNGIKVNFKIR
HNIEDGSVQLADHYQQNTPIGDGPVLLPDNHYLSTQSAL
SKDPNEKRDHMVLLFVTAAGITHGMDELYKHHHHHH
KDEL *

Feature

Kozak sequence	: Nucleotide (1...4)	
PR1a signal	: Nucleotide (5...94)	: Amino acid (1...30)
cEDIII	: Nucleotide (95...403)	: Amino acid (31...133)
TEV cleavage site	: Nucleotide (404...424)	: Amino acid (134...140)
sGFP	: Nucleotide (425...1144)	: Amino acid (141...380)
6X His tag	: Nucleotide (1145...1162)	: Amino acid (381...386)
KDEL signal	: Nucleotide (1163...1174)	: Amino acid (387...390)

A3.5 Nucleotide and amino acid sequences of synthesised CTB-cEDIII-KDEL

Nucleotide sequence

ATG ATT AAG CTC AAG TTT GGT GTT TTC TTT ACC GTG TTA CTC TCT TCA
GCA TAC GCA CAT GGA ACC CCT CAG AAT ATT ACA GAT TTG TGT GCT
GAA TAC CAT AAC ACT CAA ATC CAC ACA CTC AAC GAT AAG ATT TTC
TCT TAC ACT GAA TCT CTC GCT GGA AAG AGA GAG ATG GCA ATC ATC
ACA TTC AAG AAC GGT GCT ACC TTC CAG GTT GAA GTG CCT GGA TCA
CAA CAT ATT GAT AGT CAG AAG AAA GCA ATT GAG AGA ATG AAG GAT
ACC TTA AGG ATT GCT TAT CTC ACT GAA GCA AAG GTT GAG AAG TTG
TGT GTG TGG AAT AAC AAA ACA CCA CAC GCT ATT GCT GCA ATC TCT
ATG GCA AAC GGT CCT GGA CCA AAG GGA ATG TCT TAT GCT ATG TGC
ACC GGA AAG TTT AAA CTT GAA AAA GAG GTT GCA GAA ACC CAA CAT
GGA ACT ATC TTG ATC AAG GTT AAG TAC GAG GGT GAT GGT GCT CCT
TGC AAG ATT CCA TTC GAA ATC CAG GAT GTT GAG AAG AAA CAC GTG
AAT GGT AGG CTT ATT ACT GCT AAC CCT ATC GTT ACA GAT AAA GAG
AGT CCA GTG AAT ATT GAA GCA GAG CCT CCA TTC GGA GAT TCA TAT
ATT GTT ATC GGT GTG GGA GAT AAG GCA CTT AAA TTG AAC TGG TTC
AAG AAG GGT TCT TCA GAA AAC CTT TAC TTC CAA GGA AAG GAT GAG
TTG

Amino acid sequence

MIK L K F G V F F T V L L S S A Y A H G T P Q N I T D L C A E Y H N T Q I H
T L N D K I F S Y T E S L A G K R E M A I I T F K N G A T F Q V E V P G S Q H
I D S Q K K A I E R M K D T L R I A Y L T E A K V E K L C V W N N K T P H A
I A A I S M A N G P G P K G M S Y A M C T G K F K L E K E V A E T Q H G T I

LIKVKYEGDGAPCKIPFEIQDVEKKHVNGRLITANPIVT
DKESPVNIEAEPFGDSYIVIGVGDKALKLNWFKKGSSE
NLYFQ GKDEL

Feature

CTB	: Nucleotide (1...372)	: Amino acid (1...124)
GPGP linker	: Nucleotide (373...384)	: Amino acid (125...128)
cEDIII	: Nucleotide (385...693)	: Amino acid (129...231)
TEV cleavage site	: Nucleotide (694...714)	: Amino acid (232...238)
KDEL signal	: Nucleotide (715...726)	: Amino acid (239...242)

A3.6 Nucleotide and amino acid sequences of synthesised PR1a-CTB-cEDIII-H-KDEL

Nucleotide sequence

AAC AAT GGG ATT CGT GCT CTT CAG TCA ACT TCC TTC ATT CTT GCT
CGT TTC AAC TTT GCT CTT ATT CCT CGT GAT TTC TCA TTC TTG TAG GGC
TAT GAT CAA GTT GAA GTT CGG TGT TTT CTT TAC TGT GCT TTT GTC TTC
AGC TTA TGC ACA TGG AAC ACC TCA AAA TAT TAC CGA TTT GTG TGC
AGA ATA CCA TAA CAC TCA GAT CCA CAC ACT CAA CGA TAA GAT TTT
CTC TTA CAC AGA AAG TCT CGC TGG AAA GAG AGA GAT GGC AAT CAT
CAC TTT CAA GAA CGG TGC TAC ATT CCA AGT TGA AGT GCC TGG ATC
TCA ACA TAT TGA TTC ACA GAA GAA AGC AAT TGA GAG AAT GAA GGA
TAC ACT TAG GAT TGC TTA CTT GAC CGA AGC AAA GGT TGA GAA ACT
TTG TGT GTG GAA TAA CAA AAC TCC ACA CGC TAT TGC TGC AAT CAG
TAT GGC AAA TGG TCC TGG ACC AAA GGG AAT GTC TTA CGC TAT GTG
CAC TGG AAA GTT TAA ACT TGA AAA AGA GGT TGC AGA AAC CCA ACA
TGG AAC TAT CTT GAT CAA GGT TAA GTA TGA GGG TGA TGG TGC TCC
TTG CAA GAT TCC ATT CGA AAT CCA GGA TGT TGA GAA GAA ACA CGT
GAA TGG TAG GCT TAT TAC CGC TAA CCC TAT CGT TAC TGA TAA AGA
GTC ACC AGT GAA TAT TGA AGC AGA GCC TCC ATT TGG AGA TTC TTA
CAT TGT TAT CGG TGT GGG AGA TAA GGC TTT AAA ACT CAA CTG GTT
CAA GAA GGG TAG TTC TGA AAA CCT CTA CTT CCA GGG ACA TCA CCA
TCA CCA TCA CAA GGA TGA GCT TTG A

Amino acid sequence

MGFVLFSQLPSFLLVSTLLLFLVISHSCRAMIKLKFGVFF
TVLLSSAYAHGTPQNITDLCAEYHNTQIHTLNDKIFSYT
ESLAGKREMAIITFKNGATFQVEVPGSQHIDSQKKAIER
MKDTLRIAYLTEAKVEKLCVWNNKTPHAIAAISMANGP
GPKGMSYAMCTGKFKLEKEVAETQHGTILIKVKYEGDG
APCKIPFEIQDVEKKHVNGRLITANPIVTDKESPVNIEAE
PPFGDSYIVIGVGDKALKLNWFKKGSSENLYFQGHHHH
HHKDEL*

Feature

Kozak	: Nucleotide (1...4)	
PR1a signal	: Nucleotide (5...94)	: Amino acid (1...30)
CTB	: Nucleotide (95...466)	: Amino acid (31...154)
GPGP linker	: Nucleotide (467...478)	: Amino acid (155...158)
cEDIII	: Nucleotide (479...787)	: Amino acid (159...261)
TEV cleavage site	: Nucleotide (788...808)	: Amino acid (262...268)
6X His tag	: Nucleotide (809...826)	: Amino acid (269...274)
KDEL signal	: Nucleotide (827...838)	: Amino acid (275...278)

A3.7 Nucleotide and amino acid sequences of synthesised cEDIII (L)

Nucleotide sequence

GGT GGT GGA AGC GGA GGT GGT GGT TCT GGT GGT GGT GGT TCA ACG
CGT AAG GGA ATG TCA TAC GCT ATG TGT ACT GGA AAG TTC AAG TTG
GAG AAG GAG GTG GCA GAG ACT CAG CAC GGA ACC ATC TTA ATC AAA
GTT AAA TAT GAA GGT GAT GGT GCT CCT TGT AAG ATT CCT TTC GAA
ATC CAA GAT GTT GAG AAG AAA CAT GTG AAT GGA AGG TTG ATT ACC
GCT AAC CCA ATC GTT ACT GAT AAG GAG TCA CCT GTG AAT ATT GAA
GCA GAG CCT CCA TTT GGT GAT AGT TAT ATT GTT ATC GGT GTG GGA
GAT AAG GCA CTT AAA TTG AAC TGG TTC AAG AAG GGA TCT TCA TCC
GGA GGT GGT GGT GGT AGT GGT GGT GGT GGA TCA GGT GGT GGT GGA
TCT

Amino acid sequence

GGGSGGGGSGGGGSTRKGM SYAMCTGKFKLEKEVAET
QHGTILIKVKYEGDGAPCKIPFEIQDVEKKHVNGRLITA
NPIVTDKESPVNIEAEPFPGDSYIVIGVGDKALKLNWFK
KGSSSGGGGSGGGGSGGGGS

Feature

(GGS)n linker	: Nucleotide (1...42)	: Amino acid (1...14)
MluI RE site	: Nucleotide (43...48)	: Amino acid (15...16)
cEDIII	: Nucleotide (49...357)	: Amino acid (17...119)
BspEI RE site	: Nucleotide (358...363)	: Amino acid (120...121)
(GGS)n linker	: Nucleotide (364...408)	: Amino acid (122...136)

A3.8 List of primers used in this study

Primer	Sequence
PFGS (sGFP)	GTG ATC GCG ACC GGT AAG G
PFGS (CTB)	GTG ATC GCG ACC GGT ATG ATT AAG C
PRGS	AGA AGA CCC GGG CAA CTC ATC
CTBcED3F	CAA GGA CCG GTA ACA ATG GGA TTC GTG CT
CTBcED3R (1 st)	AGA ACT ACC CTT CTT GAA CCA GTT GAG TTT TAA AGC C
CTBcED3R (2 nd)	GCT GAC TCG AGT TAC AAT TCG TCT TTA GAA CTA CCC TTC TTG
cED3F (mono)	CAT TAG TCG ACA AGG GAA TGT CAT ACG CTA TG
cED3R (mono)	CGC AGC ATT AAT TGA AGA TCC CTT
cED3F (monoL)	CAT AGT CGA CGG TGG TGG AAG CGG A
cED3R (monoL)	CGC TAC GCA TTA ATA GAT CCA CCA CCA
cED3F	GAA TAC CTA GGA AGG GAA TGT CAT ACG CTA TGT GTA CTG GAA AG
cED3R	CAT TGC CTG CAG GTG AAG ATC CCT TCT TGA AC
C1	AAC GTT GTC AGA TCG TGC TTC GGC ACC
C3	CTG AAG GGA CGA CCT GCT AAA CAG GAG
5' MCS	GTT TTC CCG TGG TTT TCG AAC TTG
3' MCS	CTT TAG TTT GAA TTT ACT GTT ATT CGG TGT GC
5' core c/e1	GAA CTG ATG ACC CTG GCA ACC TG
3' core c/e1	GTG ATC TGG TTG TTA ATT ACG TGA ACA CC

A3.9 An example of the alignment of sequencing results with expected DNA sequence

Panel A: First alignment of PR1a-cEDIII-sGFP-H-KDEL sequence to the DNA sequenced by C1 primer

5501	GTGAGCGATC CACTCGCTAG	TTCAACGTTG AAGTTGCAAC	TCAGATCGTG AGTCTAGCAC	CTTCGGCACC GAAGCCGTGG	AGTACAACGT TCATGTTGCA	TTTCTTTCAC AAAGAAAAGTG	TGAAGCGAAA ACTTCGCTTT	TCAAAGATCT AGTTTCTAGA	CTTTGTGGAC GAAACACCTG	ACGTAGTGCG TGCATCACGC	Sequenced region with C1 primer
5601	GCGCCATTAA CGCGGTAATT	ATAACGTGTA TATTGCACAT	CTTGTCTTAT GAACAGGATA	TCTTGTGGGT AGAACAGCCA	GTGGTCTTGG CACCAGAACC	GAAAAGAAAG CTTTTCTTTC	CTTGTGGAG GAACGACCTC	GCTGCTGTTT CGACGACAAG	AGCCCCATAC TCGGGGTATG	ATTACTTGTG TAATGAACAA	
5701	ACGATTCTGC TGCTAAGACG	TGACTTTGGG ACTGAAAGCC	CGGGTGCAAT GCCCACGTTA	ATCTCTACTT TAGAGATGAA	CTGCTTGACG GACGAACCTG	AGGTATTGTT TCCATAACAA	GCCTGTACTT CGGACATGAA	CTTCTTCTT GAAAGAGAA	CTTCTGTGCTG GAAGAACGAC	ATTGGTCTTA TAACCAAGAT	
5801	TAAGAAATCT ATTCTTAGA	AGTATTTTCT TCATAAAGA	TTGAAACAGA AACTTTGTCT	GTTTTCCCGT CAAAAGGGCA	GGTTTTCGAA CCAAAAGCTT	CTTGGAGAAA GAACCTCTTT	GATTGTTAAG CTAACAAATC	CTTCTGTATA GAAGACATAT	TTCTGCCCAA AAGACGGGTT	ATTCGCGACC TAAGCGCTGG	
5901	GGTAAACAATG CCATTGTTAC	GGATTCTGTTT CCTAAGCAAA	TATTCTCTCA ATAAGAGAGT	ACTTCCTTCA TGAAGGAAGT	TTTCTCCTTG AAAAGGAAAC	TGTCAACTCT ACAGTTGAGA	TTTGTCTTTC AAACGAGAAG	CTCGTTATTA GAGCAATAAT	GTCATTCTTG CAGTAAGAAC	TAGAGCTAAA ATCTCGATTT	
6001	GGAAATGCTTT CCTTACAGAA	ATGCTATGTG TAGGATACAC	TACTGGAAAG ATGACCTTTC	TTCAAATTTG AAGTTAACC	AAAAGGAGGT TTTTCTCCA	TGCTGAAACA ACGACTTTGT	CAACATGGAA GTTGTACCTT	CCATTCTTAT GGTAAGAATA	CAAGGTGAAA GTTCCACTTT	TACGAGGGTG ATGCCTCCAC	
6101	ATGGAGCACC TACCTCGTGG	ATGCAAAATT TACGTTTAA	CCTTTTAAA GGAAAACCTT	TCCAGGATGT AGGTCTTACA	TGAGAAGAAA ACTCTTCTT	CATGTGAATG GTACACTTAC	GAAGGCTTAT CTTCCGAATA	TACAGCTAAC ATGTCGATTG	CCAATCGTTA GGTTAGCAAT	CCGATAAGGA GGCTATTCCCT	
6201	ATCACCTGTG TAGTGGACAC	AATATTGAAG TTATAACTTC	CAGAGCCTCC GTCTCGGAGG	ATTTGGTGAT TAAACCACTA	AGTTATATTG TCAATATAAC	TTATCGGTGT AATAGCCACA	GGGAGATAAG CCCTTATTC	GCTCTTAAAT CGAGAATTTA	TGAAGTGGTT ACTTGACCAA	CAAGAAGGGA GTTCTTCCCT	
6301	TCCTCAGAAA AGAAGTCTTT	ACCTCTACTT TGGAGATGAA	CCAAGGAATG GGTTCCTTAC	GTTTCTRAAG CAAAGATTTT	GTGAAGAGTT CACTTCTCAA	GTTTACTGGT CAAATGACCA	GTTGTGCCAA CAACACGGTT	TTCTTGTGTA AAGAACAAC	GTTGGATGGA CAACCTACCT	GATGTGAATG CTACACTTAC	
6401	GTCCATAAGTT CAGTATTCAA	CAGTGTTTCT GTCACAAAGA	GGTGAAGGAG CCACTTCCCT	AGGGTGATGC TCCCCTACG	AACCTATGGA TTGAATACCT	AAGTTAACAC TTCAAATTTG	TCAAGTTTAT AGTTCAAATA	CTGTACTACT GACATGATGA	GGAAAGTTGC CCTTCAACG	CTGTTCCCTG GACAAGGAAC	
6501	GCCTACTTTG CGGATGAAC	GTGACCACTT CACTGGTGAA	TTACTTATGG AATGAATACC	TGTTCAATGC ACAAGTTACG	TTTTCTAGGT AAAAGATCCA	ATCCTGATCA TAGGACTAGT	CATGAAGCAG GTACTTCGTC	CACGATTCTT GTGCTAAAGA	TTAAATCAGC AATTTAGTCG	TATGCCTGAA ATACGGACTT	
6601	GGATACGTTT CCTATGCAAG	AGGAGAGAAT TCCTCTCTTG	AATTTCTTTT TTAAAAGAAA	AAGGATGATG TTCTTACTAC	GTAECTACAA CATTTGATGT	AACCAGGGCA TTGGTCCCGT	GAGGTTAAGT CTCCAATTCA	TTGAGGGAGA AACTCCCTCT	TACACTTGTG ATGTGAACAC	AACAGAATCG TTGTCTTAGC	
6701	AATTGAAGGG TTAACTTCCC	TATCGAATTC ATAGCTAAAG	AAAGAGGATG TTTCTCCTAC	GAACACTCCT CTTTGTAGGA	CGGTCAATAAG GCCAGTATTC	CTCGAATACA GAGCTTATGT	ACTACAACAG TGATGTTGTC	TCACAACGTT AGTGTGCAA	TACATCATGG ATGTAGTACC	CTGATAAGCA GACTATTCTG	
6801	AAAGAATGGA TTTCTTACCT	ATCAAGGTGA TAGTTCCTACT	ACTTCAAAT TGAAAGTTTA	TAGGCATAAC ATCCGATTTG	ATCGAGGATG TAGTCTCTAC	GTTCTGTCCA CAACGCAAGT	GTTCGCAGAT CAACCCGCTA	CACATATCAAC GTGATAGTTG	AGAATACTCC TCTTATGAGG	AATTGGAGAT TTAACCCTTA	
6901	GGTCCAGTTC CCAGGTCAAG	TTTTGCCTGA AAACGGACT	TAACCATTAC ATTGTAATG	TTATCAACAC AATAGTTGTG	AAAGTGCTCT TTTACAGAGA	CTCTAAAGAT GAGATTTCTA	CCTAACGAAA GGATTGCTTT	AGAGAGATCA TCTCTTAGT	CATGGTCTT GTACCAAGAA	CTTGAATTTG GAACTTAAAC	
7001	TGACTGCTGC ACTGACGACG	TGATATTACT ACCATAATGA	CACGGTATGG GTGCCATACC	ATGAACCTTA TACTTGAAT	CAAACATCAC GTTTGTAGTG	CATCACCATC GTAGTGGTAG	ACAAGGATGA TGTTCTTACT	GCTTTGACTC CGAAACTGAG	GAGGCCTTTA CTCCGGAAT	ACTCTGGTTT TGAGACCAA	
7101	CATTAATTTT GTAATTTAAA	TCTTTAGTTT AGAAATCAAA	GAATTTACTG CTTAAATGAC	TTATTCGGTG AATAAGCCAC	TGCATTTCTA ACGTAAAGAT	TGTTTGGTGA ACAAACCAC	GCGGTTTTCT CGCAAAGA	GTGCTCAGAG CACGAGTCTC	TGTGTTTATT ACACAAATA	TTATGTAATT AATACATTA	

PR1a-cEDIII-
sGFP-H-KDEL
expression cassette
(in red text)

Panel B: Second alignment of PR1a-cEDIII-sGFP-H-KDEL sequence to the DNA sequenced by C1 and C3 primers

PR1a-cEDIII-
sGFP-H-KDEL
expression cassette
(in red text)

5501	GTGAGCGATC CACTCGCTAG	TTCAACGTTG AAGTTGCAAC	TCAGATCGTG AGTCTAGCAC	CTTCGGCACC GAAGCCGTGG	AGTACAACGT TCATGTTGCA	TTTCTTTCAC AAAGAAAGTG	TGAAGCGAAA ACTTCGCTTT	TCAAAGATCT AGTTTCTAGA	CTTTGTGGAC GAAACACCTG	ACGTAGTGCC TGCATCACCG	
5601	GCGCCATTAA CGCGGTAATT	ATAACGTGTA TATTGCACAT	CTTGTCCTAT GAACAGGATA	TCTTGTGCGT AGAACAGCCA	GTGGTCTTGG CACCAGAACC	GAAAAGAAAG CTTTCTTTC	CTTGCTGGAG GAACGACCTC	GCTGCTGTT CGACGACAAG	AGCCCCATAC TCGGGGTATG	ATTACTTGTT TAATGAACAA	
5701	ACGATTCTGC TGCTAAGACG	TGACTTTCGG ACTGAAAGCC	CGGGTGAAT GCCACGTTA	ATCTCTACTT TAGAGATGAA	CTGCTTGACG GACGAACTGC	AGGTATTGTT TCCATAACAA	GCCTGTACTT CGGACATGAA	CTTTCTTCTT GAAAGAAGAA	CTTCTTGCTG GAAGAACGAC	ATTGGTTCTA TAACCAAGAT	
5801	TAAGAAATCT ATTCTTTAGA	AGTATTTTCT TCATAAAGA	TTGAAACAGA AACTTTGTCT	GTTTTCCCGT CAAAAGGGCA	GGTTTTCGAA CCAAAAGCTT	CTTGGAGAAA GAACCTCTTT	GATTGTTAAG CTAACAAATC	CTTCTGTATA SAAGACATAT	TCTTGCCCAA AAGACGGGTT	ATTGCGGACC TAAGCGCTGG	AgeI _{...} (5899)
5901	GGTAACAATG CCATTGTAC	GGATTCGTTT CCTAAGCAAA	TATTCTCTCA ATAAGAGAGT	ACTTCCTTCA TGAAGGAAGT	TTTCTCCTTG AAAGAGGAAC	TGCAACTCT ACAGTTGAGA	TTTGCTCTTC AAACGAGAAG	CTCGTTATTA GAGCAATAAT	GTCATTCCTG CAGTAAGAAC	TAGAGCTAAA ATCTCGATTT	
6001	GGAAATGCTT CCTTACAGAA	ATGCTATGTG TACGATACAC	TACTGGAAG ATGACCTTTC	TTCAAATTGG AAGTTAACC	AAAAGGAGGT TTTTCCCTCA	TGCTGAAACA ACGACTTTGT	CAACATGGA GTTGTACCTT	CCATCTTAT GGTAAGAATA	CAAGGTGAAA GTTCCACTTT	TACGAGGGTG ATGCTCCAC	
6101	ATGGAGCACC TACCTCGTGG	ATGCAAAATT TACGTTTTAA	CCTTTTGAAA GGAAACTTTT	TCCAGGATGT AGGTCTTACA	TTGAGAAGAA ACTCTTCTTT	CATGTGAATG GTACACTTAC	GAAGGCTTAT CTTCCGAATA	TACAGCTAAC ATGTCGATTG	CCAATCGTTA GGTTAGCAAT	CCGATAAGGA GGCTATTCC	
6201	ATCACCTGTG TAGTGGACAC	AATATTGAAG TTATAACTTC	CAGAGCCTCC GTCTCGGAGG	ATTTGGTGAT TAAACCACTA	AGTTATATTG TCAATATAAC	TTATCGGTGT AATAGCCACA	GGGAGATAAG CCCTCTATTC	GCTCTTAAAT CGAGAATTTA	TGAAGTGGTT ACTTGACCAA	CAAGAAGGGA GTTCTTCCT	
6301	TCTTCAGAAA AGAAGTCTTT	ACCTCTACTT TGGAGATGAA	CCAAGGAATG GGTTCCTTAC	GTTTCTAAAG CAAAGATTTT	GTGAAGAGTT CACTTCTCAA	GTTTACTGTT CAAATGACCA	GTTGTGCCAA CAACACGGTT	TTCTTGTGGA AAGAACAATC	GTTGGATGGA CAACCTACCT	GATGTGAATG CTACACTTAC	
6401	GTCATAAGTT CAGTATTCAA	CAGTGTCTCT GTCACAAAGA	GGTGAAGGAG CCACTTCCCTC	AGGGTGATGC TCCCCTACTG	AACCTATGGA TTGAATACCT	AAGTTAACAC TTCAAATTGT	TCAAGTTTAT AGTTCAAATA	CTGTACTACT GACATGATGA	GGAAAGTTGC CCTTTCACAG	CTGTTCCCTG GACAAGGAAC	
6501	GCCTACTTTG CGGATGAAAC	GTGACCACCT CACTGGTGAA	TTACTTATGG AATGAATACC	TGTTCAATGC ACAAGTTACG	TTTTCTAGGT AAAAGATCCA	ATCCTGATCA TAGGACTAGT	CATGAAGCAG GTACTTCGTC	CACGATTTCT GTGCTAAAAG	TTAAATCAGC AATTTAGTCG	TATGCCTGAA ATACGGACTT	
6601	GGATACGTTT CCTATGCAAG	AGGAGAGAAC TCCTCTCTTG	AATTTTCTTT TTAAAAGAAA	AAGGATGATG TTCCTACTAC	GTAACACAA CATTGATGTT	AACCAGGGCA TTGGTCCCGT	GAGGTTAAGT CTCCAATTC	TTGAGGGAGA AACTCCCTCT	TACACTTGTG ATGTGAACAC	AACAGAATCG TTGCTTAGC	
6701	AATTGAAGGG TTAACTTCCC	TATCGATTTT ATAGCTAAAG	AAAGAGGATG TTTCTCCCTAC	GAAACATCCT CTTTGTAGGA	CGGTCAATAAG GCCAGTATTC	CTCGAATACA GAGCTTATGT	ACTACAACAG TGATGTTGTC	TCACAACGTT AGTGTGCAA	TACATCATGG ATGTAGTACC	CTGATAAGCA GACTATTCCG	
6801	AAAGAATGGA TTTTCTTACC	ATCAAGGTGA TAGTCCACT	ACTTCAAAT TGAAGTTTTA	TAGGCATAAC ATCCGTATTG	ATCGAGGATG TAGCTCCTAC	GTTCTGTTCA CAAGACAAGT	GTTGGCAGAT CAACCGTCTA	CACTATCAAC GTGATAGTTG	AGAATACTCC TCTTATGAGG	AATTGGAGAT TTAACCTCTA	
6901	GGTCCAGTTC CCAGGTCAAG	TTTTGCCTGA AAACGGACT	TAACCATTAC ATTGGTAATG	TTATCAACAC AATAGTTGTG	AAAGTGCTCT TTTCACGAGA	CTCTAAAGAT GAGATTTCTA	CCTAACGAAA GGATTGCTTT	AGAGAGATCA TCTCTTAGT	CATGGTTCTT GTACCAAGAA	CTTGAATTTG GAACTTAAAC	
7001	TGACTGCTGC ACTGACGACG	TGGTATTACT ACCATAATGA	CACGGTATGG GTGCCATACC	ATGAACTTTA TACTTGAAAT	CAAACATCAC TACTTGTAGT	CATCACCATC TGTTCTACT	ACAAGGATGA TGTTCTACT	GCTTTGACTC CGAAACTGAG	GAGGCCTTTA CTCCGGAAAT	ACTCTGGTTT TGAGACCAA	XhoI _{...} (7079)
7101	CATTAAATTT GTAATTTAAA	TCITTAGTTT AGAAATCAAA	GAATTTACTG CTTAAATGAC	TTATTCCGGT AATAAGCCAC	TGCATTTCTA ACGTAAAGAT	TGTTTGGTGA ACAAACCACT	CGGGTTTCT CGCAAAAGA	GTGCTCAGAG CAGGAGTCTC	TGTGTTTATT ACACAATAA	TTATGTAATT AATACATTA	

Sequenced
region with
C1 primer

Sequenced
region with
C3 primer

Panel C: Third alignment of PR1a-cEDIII-sGFP-H-KDEL sequence to the DNA sequenced by C1, C3 and cED3F primers

PR1a-cEDIII-sGFP-H-KDEL expression cassette (in red text)	5501	GTGAGCGATC CACTCGCTAG	TTCAACGTTG AAGTTGCAAC	TCAGATCGTG AGTCTAGCAC	CTTCGGCACC GAAGCCGTGG	AGTACAACGT TCATGTTGCA	TTTCTTTCAC AAAGAAAGTG	TGAAGCGAAA ACTTCGCTTT	TCAAAGATCT AGTTTCTAGA	CTTTGTGGAC GAAACACCTG	ACGTAGTGGC TGCATCACGC	Sequenced region with C1 primer	
	5601	GCGCCATTA CGCGGTAAT	ATAACGTGTA TATTGCACAT	CTTGTCTTAT GAACAGGATA	TCTTGTGGT AGAACAGCCA	GTGGTCTTGG CACCAGAACC	GAAAAGAAAG CTTTTCTTTC	CTTGCTGGAG GAACGACCTC	GCTGCTGTTC CGACGACAAG	AGCCCCATAC TCGGGGTATG	ATTACTTGT TAATGAACAA		
	5701	ACGATTCTGC TGCTAAGACG	TGACTTTCGG ACTGAAAGCC	CGGGTGAAT GCCACGTTA	ATCTCTACTT TAGAGATGAA	CTGCTTGACG GACGAACTGC	AGGTATTGTT TCCATAACAA	GCCTGTACTT CGGACATGAA	CTTCTTCTT GAAAGAAGAA	CTTCTTGCTG GAAGAACGAC	ATTGTTTCTA TAACCAAGAT		
	5801	TAAGAAATCT ATTCTTTAGA	AGTATTTTCT TCATAAAAGA	TTGAAACAGA AACTTTGICT	GTTTTCCCGT CAAAAGGGCA	GGTTTTCGAA CCAAAAGCTT	CTTGGAGAAA GAACCTCTTT	GATTGTTAAG CTAACAAATC	CTTCTGTATA GAAGACATAT	TTCTGCCCAA AAGACGGGTT	ATTCGCGACC TAACGCGTGG		
	5901	GGTAAACAATG CCATTGTTAC	GGATTCTGTT CCTAAGCAAA	TATTCTCTCA ATAAGAGAGT	ACTTCTCTCA TGAAGGAAGT	TTTCTCCTTG AAAGAGGAAC	TGTCAACTCT ACAGTTGAGA	TTTGCTCTTC AAACGAGAAG	CTCGTTATTA GAGCAATAAT	GTCATCTTG CAGTAAGAAC	TAGAGCTAAA ATCTCGATT		Sequenced region with cED3F primer
	6001	GGAATGTCTT CCTTACAGAA	ATGCTATGTG TACGATACAC	TACTGGAAA ATGACCTTTC	TTCAAATTGG AAGTTAACC	AAAAGGAGGT TTTTCTCCA	TGCTGAAACA ACGACTTGT	CAACATGGAA GTTGTACCTT	CCATCTTAT GGTAAGAATA	CAAGGTGAAA GTFCCACTTT	TACGAGGGTG ATGCTCCAC		
	6101	ATGGAGCACC TACCTCGTGG	ATGCAAAATT TACGTTTTAA	CCTTTTGAAA GGAAAACCTT	TCCAGGATGT AGGTCCTACA	CTGAGGAAA ACTCTCTTT	CATGTGAATG GTACACTTAC	GAAGGCTTAT CTTCCGAATA	TACAGCTAAC ATGTCGATTG	CCAATCGTTA GGTTAGCAAT	CCGATAAGGA GGCTATTCCT		
	6201	ATCACCTGTG TAGTGGACAC	AATATTGAAG TTATAACTTC	CAGAGCCTCC GTCTCGGAGG	ATTTGGTGAT TAAACCACTA	AGTTATATTG TCAATATAAC	TTATCGGTGT AATAGCCACA	GGGAGATAAG CCCTCTATT	GCTCTTAAAT CGAGAATTTA	TGAAGTGGT ACTTGACCAA	CAAGAAGGGA GTTCTCCCT		
	6301	TCCTCAGAAA AGAAGTCTTT	ACCTCTACTT TGGAGATGAA	CCAAGGAATG GGTCCCTTAC	GTTTCTAAG CAAAGATTTC	GTGAAGGATT CACTTCTCAA	GTTTACTGGT CAAATGACCA	GTTGTGCCAA CAACACGGTT	TTCTTGTGA AAGAACAAC	GTTGGATGGA CAACCTACCT	GATGTGAATG CTACACTTAC		
	6401	GTCATAAGTT CAGTATTCAA	CAGTGTCTT GTCACAAAGA	GGTGAAGGAG CCACTTCCCT	AGGGTGATGC TCCCCTACTG	AACTTATGGA TTGAATACCT	AAGTTAACAC TTCAAATTGTG	TCAAGTTTAT AGTTCAAATA	CTGTACTACT GACATGATGA	GGAAAGTTGC CCTTTCACG	CTGTTCCCTG GACAAGGAAC		
	6501	GCCTACTTTG CGGATGAAAC	GTGACCACCT CACTGGTGAA	TTACTTATGG AATGAATACC	TGTTCAATGC ACAAGTTACG	TTTTCTAGGT AAAAGATCCA	ATCCTGATCA TAGGACTAGT	CATGAAGCAG GTACTTCGTC	CACGATTTCT GTGCTAAAGA	TTAAATCAGC AATTTAGTCG	TATGCCTGAA ATACGGACTT		
	6601	GGATACGTTT CCTATGCAAG	AGGAGAGAAC TCCTCTCTTG	AATTTCTTTT TTAAAAGAAA	AAGGATGATG TTCCTACTAC	GTAECTACAA CATTGATGTT	AACCAGGGCA TTGGTCCCGT	GAGGTTAAGT CTCCAATTCA	TTGAGGGAGA AACTCCCTCT	TACACTTGTG ATGTGAACAC	AACAGAATCG TTGCTTTAGC		
	6701	AATTGAAGGG TTAACTTCCC	TATCGATTTT ATAGCTAAAG	AAAGAGGATG TTTCTCCTAC	GAAACATCCT CTTTGTAGGA	CGGTCATAAG GCCAGTATTC	CTCGAATACA GAGCTTATGT	ACTACAACAG TGATGTTGTC	TCACAACGTT AGTGTGCAA	TACATCATGG ATGTAGTACC	CTGATAAGCA GACTATTCTG		
	6801	AAAGAATGGA TTTCTTACCT	ATCAAGGTGA TAGTCCACT	ACTTCAAAT TGAAGTTTTA	TAGGCATAAC ATCCGATTG	ATCAGGATG TAGCTCTAC	GTTCTGTTCA CAAGACAAGT	GTTGGCAGAT CAACCCCTA	CACTATCAAC GTGATAGTTG	AGAATACTCC TCTTATGAGG	AATTGGAGAT TTAACCCTA		
	6901	GGTCCAGTTC CCAGGTCAA	TTTTGCCTGA AAAACGGACT	TAACCATTAC ATTGGTAATG	TTATCAACAC AATAGTTGTG	AAAGTGCTCT TTTCCAGAGA	CTCTAAAGAT GAGATTCTA	CCTAACGAAA GGATTGCTTT	AGAGAGATCA TCTCTCTAGT	CATGGTTCTT GTACCAAGAA	CTTGAATTTG GAACTTAAAC		
	7001	TGACTGCTGC ACTGACGAGC	TGGTATTACT ACCATAATGA	CACGGTATGG GTGCCATACC	ATGAACTTTA TACTTGAAT	CAAACATCAC GTTTGTAGT	CATCACCATT GTAGTGGTAG	ACAAGGATGA TGTTCTACT	GCTTTGACTC CGAACTGAG	GAGGCCTTTA CTCCGGAAT	ACTCTGGTTT TGAGACCAA		
	7101	CATTAAATTT GTAATTTAAA	TCCTTAGTTT AGAAATCAAA	GAATTTACTG CTTAAATGAC	TTATTCGGTG AATAAGCCAC	TGATTTTCTA ACGTAAAGAT	TGTTTGGTGA ACAAACCACT	CGGTTTCTC CGCCAAAAGA	GTGCTCAGAG CAGGATCTC	TGTGTTTATT ACACAAATAA	TTATGTAATT AATACATTAA		

Panel D: Fourth alignment of PR1a-cEDIII-sGFP-H-KDEL sequence to the DNA sequenced by C1, C3, cED3F and cED3R primers

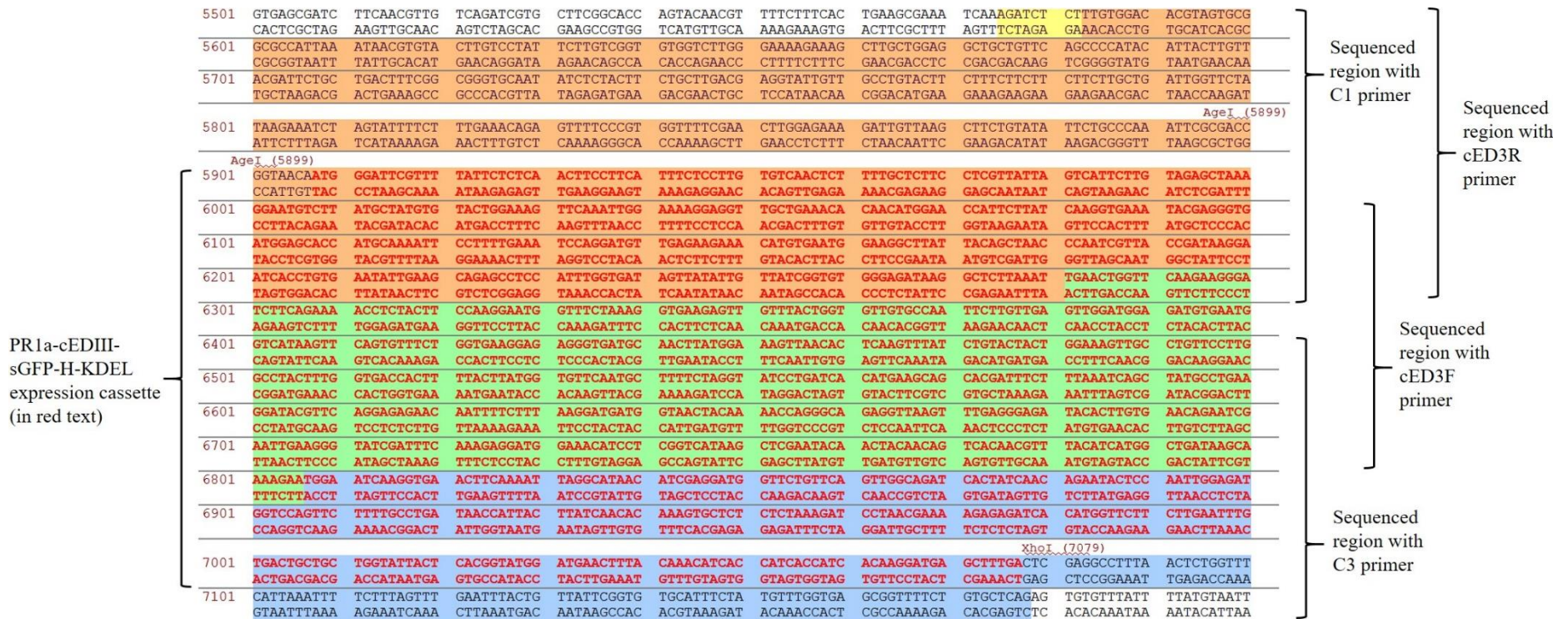


Figure A3.9: A step-wise alignment of the DNA sequencing results for PR1a-cEDIII-sGFP-H-KDEL expression cassette. A total of four sequencing primers were used, namely C1 (Panel A), C3 (Panel B), cED3F (Panel C) and cED3R (Panel D).

A3.10 Sequence alignment of cEDIII from isolates of four dengue serotypes (DENV 1-4)

The consensus sequence of each dengue virus serotype, namely DENV 1-consensus, DENV 2-consensus, DENV 3-consensus and DENV 4-consensus, was first obtained before aligning the four consensus sequences to generate an ultimate cEDIII sequence.

<u>DENV 1 consensus</u>	KGMSYVMCTGSFKLEKEVAETQHGTVLVQVKYEGTDAPCKIPFSSQDEKGVTONGRLITANPIVTDKEKPVNIEAEPFPGESYIVVGAGEKALKLSWFKKGSS
Nauru/West Pac/1974	-----
Brazil/97-11/1997	--T-----T-----T-----
Singapore/S275/1990	-----T-----QC-----
Thailand/AHF 82-80/1980	--V-----I-----
Jamaica/CV1636/1977	-----I-----S-----
<u>DENV 2 consensus</u>	KGMSYSMCTGKFKVVKIEAETQHGTVIRVQYEGDGS PCKIPFEIMDLKRRHVLGRLITVNP I VTEKDSPVNIEAEPFPGDSY I I IGV EPGQLKLNWFKKGSS
Jamaica/1409/1983	-----I-----
Malaysia M3	--I-----I-F-----I-----C---Y-----D-----I-----H-L-----
China/D2-04	-----QI-----L-----H-----
Tonga/EKB194/1974	-----I-----D-----
Peru/IQT2913/1996	-----I-----A-----D-----
Puerto Rico/PR159-S1/1969	-----T-----T-----D-----
Malaysia M2	-----E-----L---DN-----V---L-----
Thailand/0168/1979	-----
Thailand/NGS-C/1944	-----
Thailand/PUO-218/1980	-----
Thailand/TH-36/1958	-----E-----
Thailand/16681/84	-----
16681-PDK53	-----

DENV 3 consensus	KGMSYAMCLNTFVLKKEVSETQHGTILIKVEYKGEDAPCKIPFSTEDGQKAHNGRLITANPVVTKKEE PVNIEAEPFPGESNIVIGIGDKALKINWYKKGSS
Philippines/H87/1956	-----R-----
Singapore/8120/1995	-----
Martinique/1243/1999	-----T-----N-----
Sri Lanka/1266/2000	-----T-----N-----
China/80-2/1980	-----R-----
DENV 4 consensus	KGMSYTMCSGKFSIDKEMAETQHGTTVVKVYEGAGAPCKVPIEIRDVNKEKVVGRIISSTPFAENTNSVTNIELEPPFGDSYIVIGVGD SALT LHWFRKGS S
Dominica/814669/1981	-----L-----N-----
Singapore/8976/1995	-----V-----L-----N-----
Thailand/0348/1991	-----T-----
Thailand/0476/1997	-----R-----T-----
Philippines/H241/1956	-----Y-----

DENV 1-4 consensus	KGMSYAMCTGKFKLEKEVAETQHGTILIKVKYEGDGAPCKIPFEIQDVEKKHVNGRLITANPIVTDKESPVNIEAEPFPGDSYIVIGVGD KALKLNWFKKGSS
DENV1 consensus	---V---S-----V-VQ---TD-----SS--EKGVTQ-----K-----E---V-A-E---S-----
DENV2 consensus	---S---VV--I-----V-R-Q---S-----M-L-R--L---V---E-D-----I---EPGQ-----
DENV3 consensus	---LNT-V-K--S-----E-K-ED-----STE-GQG-AH-----V-K-E-----E-N---I---I-Y-----
DENV4 consensus	---T--S---SID--M-----TVV-----A---V-I--R--N-EK-V--I-SST-FAENTN-VT---L-----S--T-H--R---

Figure A3.10: The alignment of cEDIII sequence, which is representative of the EDIII sequence of DENV serotypes 1 to 4. Source: Leng *et al.* (2009).

Appendices for Chapter 4

A4.1 List of buffers and consumables used in Chapter 4

(i) Buffers used for protein extraction (**Section 4.2.7**)

Buffer	Recipe
Tris extraction buffer	50 mM Tris base, pH 7.25; 300 mM sodium chloride; 0.1% (v/v) Triton X-100; Complete Protease Inhibitor Cocktail tablet (Roche, Switzerland)
Sodium phosphate extraction buffer	100 mM Sodium phosphate, pH 7.5; Complete Protease Inhibitor Cocktail tablet (Roche, Switzerland)
VLPs extraction buffer A	100 mM Sodium phosphate, pH 6.8; 150 mM sodium chloride; 0.1% (v/v) Triton X-100; Complete Protease Inhibitor Cocktail tablet (Roche, Switzerland)
VLPs extraction buffer B	100 mM Sodium phosphate, pH 8.0; 150 mM sodium chloride; 0.1% Triton (v/v) X-100; Halt Protease Inhibitor Cocktail (Thermo Scientific, USA)

(ii) Buffers used for SDS-PAGE (**Section 4.2.8**)

Buffer	Recipe
Laemmli running buffer	25 mM Tris base, pH 8.3; 192 mM glycine; 0.1% (w/v) sodium dodecyl sulphate
Lithium dodecyl sulphate sample buffer containing β -mercaptoethanol (LDS- β ME)	4X LDS sample buffer (Invitrogen, USA) and β -mercaptoethanol in 3:1 ratio

(iii) Buffers used for Western blotting (**Section 4.2.10**)

Buffer	Recipe
Phosphate-buffered saline (PBS)	137 mM Sodium chloride; 3.7 mM potassium chloride; 10 mM disodium phosphate; 1.8 mM monopotassium phosphate, pH 7.4
Western blot transfer buffer	25 mM Tris base, pH 8.3; 192 mM glycine; 0.1% (w/v) sodium dodecyl sulphate; 20% (v/v) methanol
Enhanced chemiluminescence (ECL) solution	1.25 mM luminol; 200 mM paracoumaric acid; 27 mM hydrogen peroxide; 100 mM Tris-hydrochloride, pH 8.5

(iv) SeeBlue Plus2 Pre-Stained Standard (Invitrogen, USA) was used as the protein marker in this study. Distinct separation range is obtained when different running buffer is used for SDS-PAGE (**Figure A4.1**).

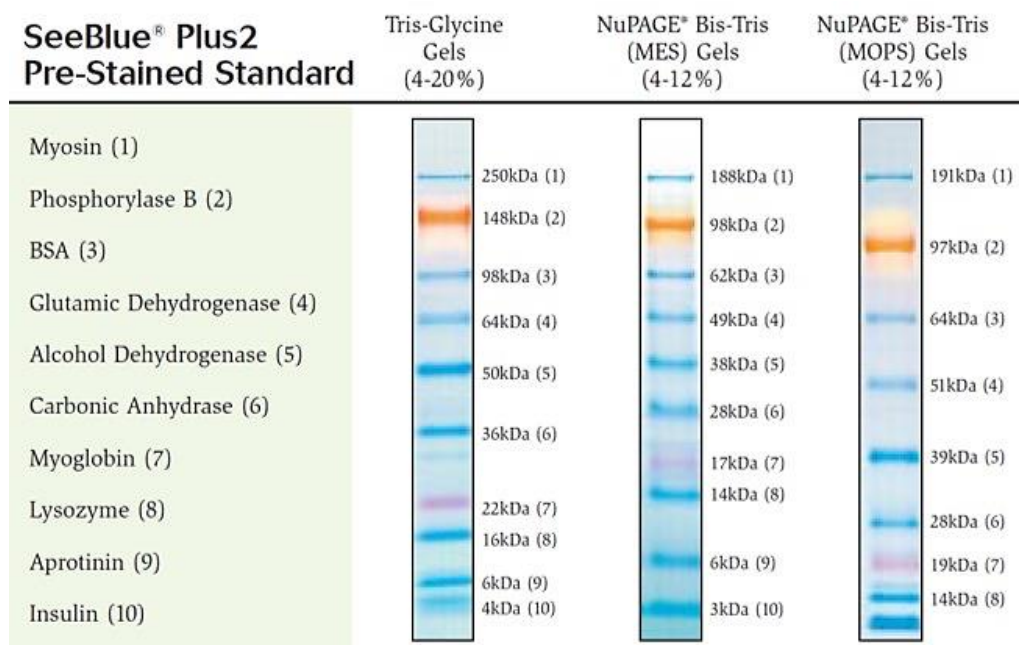
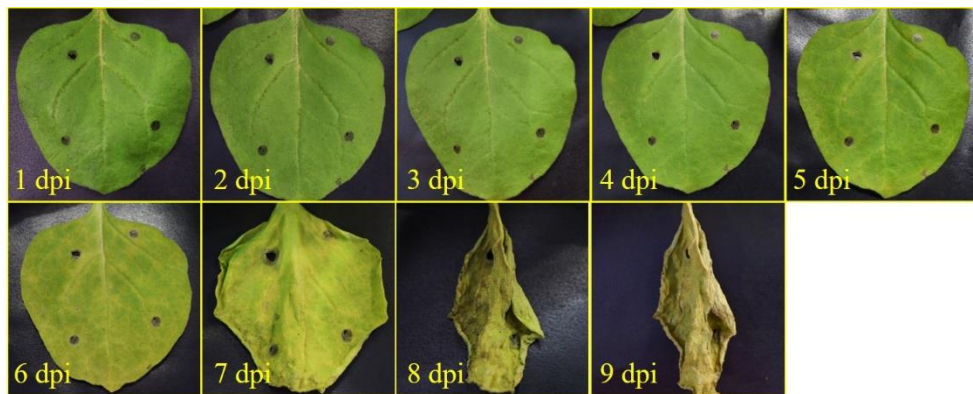


Figure A4.1: The separation range of SeeBlue Plus2 Pre-Stained Standard in different types of buffer systems.

A4.2 Illustrations of the early necrosis suffered by *Nicotiana benthamiana* leaves infiltrated with pEAQ-*HT*::cEDIII-sGFP-KDEL-H and pEAQ-*HT*::CTB-cEDIII-KDEL-H vectors

Panel A: Physical appearance of *N. benthamiana* leaf infiltrated with pEAQ-*HT*::cEDIII-sGFP-KDEL-H

Following agroinfiltration with pEAQ-*HT*::cEDIII-sGFP-KDEL-H vector, the leaf was monitored daily from 1st – 9th dpi for sign of morphological distortions. Leaf chlorosis was detected around 7th dpi, which rapidly led to cell death on 8th dpi.



**Panel B: Physical appearance of *N. benthamiana* leaf infiltrated with pEAQ-
HT::CTB-cEDIII-KDEL-H**

Infiltrated leaf was monitored daily from 1st – 9th dpi for sign of morphological distortions. Following the use of pEAQ-*HT*::CTB-cEDIII-KDEL-H vector, leaf chlorosis started to appear on 6th dpi and modest necrosis was observed by the end of the time course study.

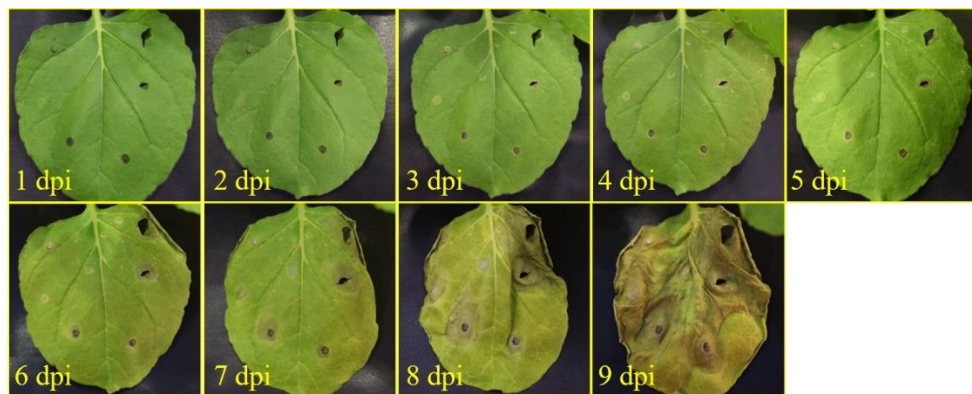


Figure A4.2: Daily observations of the infiltrated *N. benthamiana* leaf. Panel A: Leaf infiltrated with pEAQ-*HT*::cEDIII-sGFP-KDEL-H; Panel B: Leaf infiltrated with pEAQ-*HT*::CTB-cEDIII-KDEL-H. These leaves were found to suffer from severe necrotic symptoms during the kinetic assays.

A4.3 Post translational removal of PR1a signal peptide was predicted using Signal-BLAST

The protein sequence of PR1a signal peptide was analysed with Signal-BLAST and the result indicated that a cleavage site was found at the end of the PR1a sequence, specifically after residue 30 (**Figure A4.3**). Hence, PR1a was not included in the estimation of expressed protein size (expression vectors: pEAQ-*HT*::PR1a-cEDIII-sGFP-H-KDEL, pEAQ-*HT*::PR1a-CTB-cEDIII-H-KDEL and pEAQ-*HT*::PR1a-CTB-cEDIII-KDEL (xTH)).

Signal-BLAST

```
Query Sequence:
M G F V L F S Q L P S F L L V S T L L L F L V I S H S C R A...
-----
Significant Alignments:
Name                               Bitscore      SValue
-----
PR1A_TOBAC (Signal Peptide)        60.8          100.0
PR1B_TOBAC (Signal Peptide)        50.4          0.0
PR1C_TOBAC (Signal Peptide)        50.1          0.0
VKT22_LYCMC (Signal Peptide - Potential.) 22.3          0.0
VKT21_LYCMC (Signal Peptide - Potential.) 22.3          0.0
CAH5_CAEEL (Signal Peptide - Potential.) 22.3          0.0
CALC_MOUSE (Signal Peptide - Potential.) 21.9          0.0
CALCA_MOUSE (Signal Peptide - Potential.) 21.9          0.0
CVNH_CERRI (Signal Peptide - Potential.) 21.6          0.0
AGRE4_MOUSE (Signal Peptide - Potential.) 21.6          0.0
-----
Insignificant Alignments:
-----
Most Significant SValue:
>PR1A_TOBAC (Cleavage Site after AA 30)
    Length = 60

Score = 60.8 bits (146), Expect = 1e-10
Identities = 30/30 (100%), Positives = 30/30 (100%)
```

Figure A4.3: A Signal-BLAST profile that shows the predicted cleavage site of PR1a signal peptide.

Appendices for Chapter 5

A5.1 Details of buffers used in Chapter 5

(i) Buffers used for IMAC purification (**Section 5.2.4.1**)

Buffer	Recipe
Tris extraction buffer	50 mM Tris base, pH 7.25; 300 mM sodium chloride; 0.1% (v/v) Triton X-100, Complete Protease Inhibitor Cocktail tablet (Roche, Switzerland)
IMAC washing buffer with 5 mM imidazole	Tris extraction buffer supplemented with 5 mM imidazole
IMAC washing buffer with 10 mM imidazole	Tris extraction buffer supplemented with 10 mM imidazole
IMAC washing buffer with 20 mM imidazole	Tris extraction buffer supplemented with 20 mM imidazole
IMAC elution buffer	50 mM Tris base, pH 7.25; 300 mM sodium chloride; 250 mM imidazole

(ii) Buffers used for GM1-ELISA (**Section 5.2.5.1**)

Buffer	Recipe
Sodium bicarbonate buffer	15 mM Sodium carbonate; 35 mM sodium bicarbonate, pH 9.6
Phosphate-buffered saline (PBS)	137 mM Sodium chloride; 2.7 mM potassium chloride; 80 μ M disodium phosphate; 1.5 mM monopotassium phosphate, pH 7.0

(iii) Buffers used for immunogold labelling (**Section 5.2.7.2**)

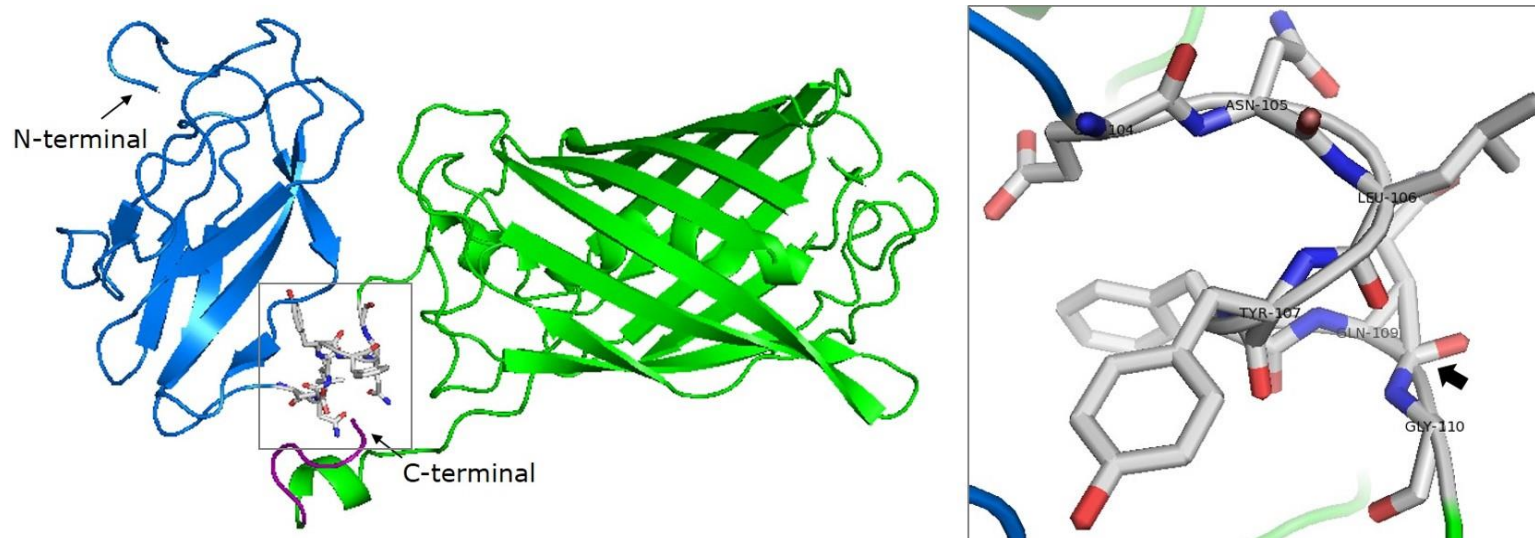
Buffer	Recipe
Tris-buffered saline (TBS)	20 mM Tris base, pH 8.0; 500 mM sodium chloride

A5.2 SWISS modelling used to predict the tobacco etch virus (TEV) protease cleavage site in recombinant cEDIII fusion proteins

Panel A: A predictive modelling of cEDIII-sGFP-H-KDEL fusion protein

The blue colour ribbon represents cEDIII protein that is fused to its sGFP partner in green. A closed-up view of the TEV cleavage site is shown in the grey box.

The cleavage site (ENLYFQG) should be accessible for protease digestion.



Panel B: A predictive modelling of CTB-cEDIII-H-KDEL fusion protein

The blue colour ribbon represents cEDIII protein that is fused to its CTB partner in red. A closed-up view of the TEV cleavage site is shown in the grey box.

The cleavage site (ENLYFQG) should be accessible for protease digestion.

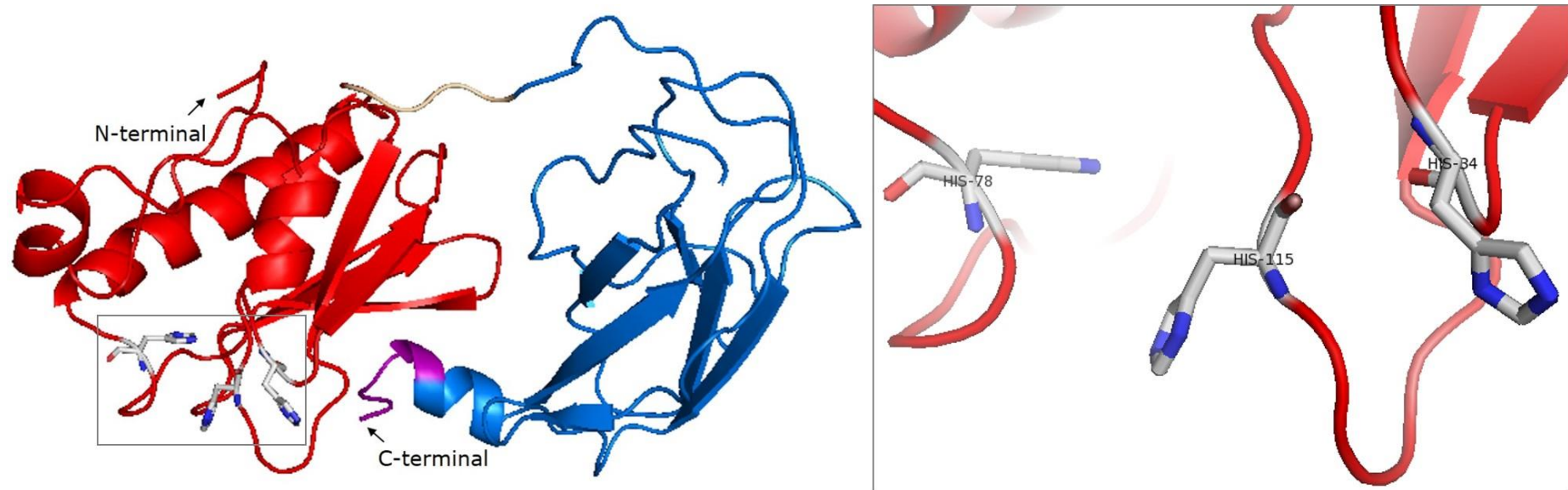


Figure A5.2: Predictive models of recombinant cEDIII fusion proteins. Panel A: cEDIII-sGFP-H-KDEL fusion protein; Panel B: CTB-cEDIII-H-KDEL fusion protein.

A5.3 Chromatograms of protein standard used to analyse the different fractions of CTB-cEDIII-KDEL (xTH) protein separated via size exclusion chromatography (SEC)

Ribonuclease A, ovalbumin and conalbumin were used to estimate the range of molecular mass (Mr) between 10,000 to 80,000.

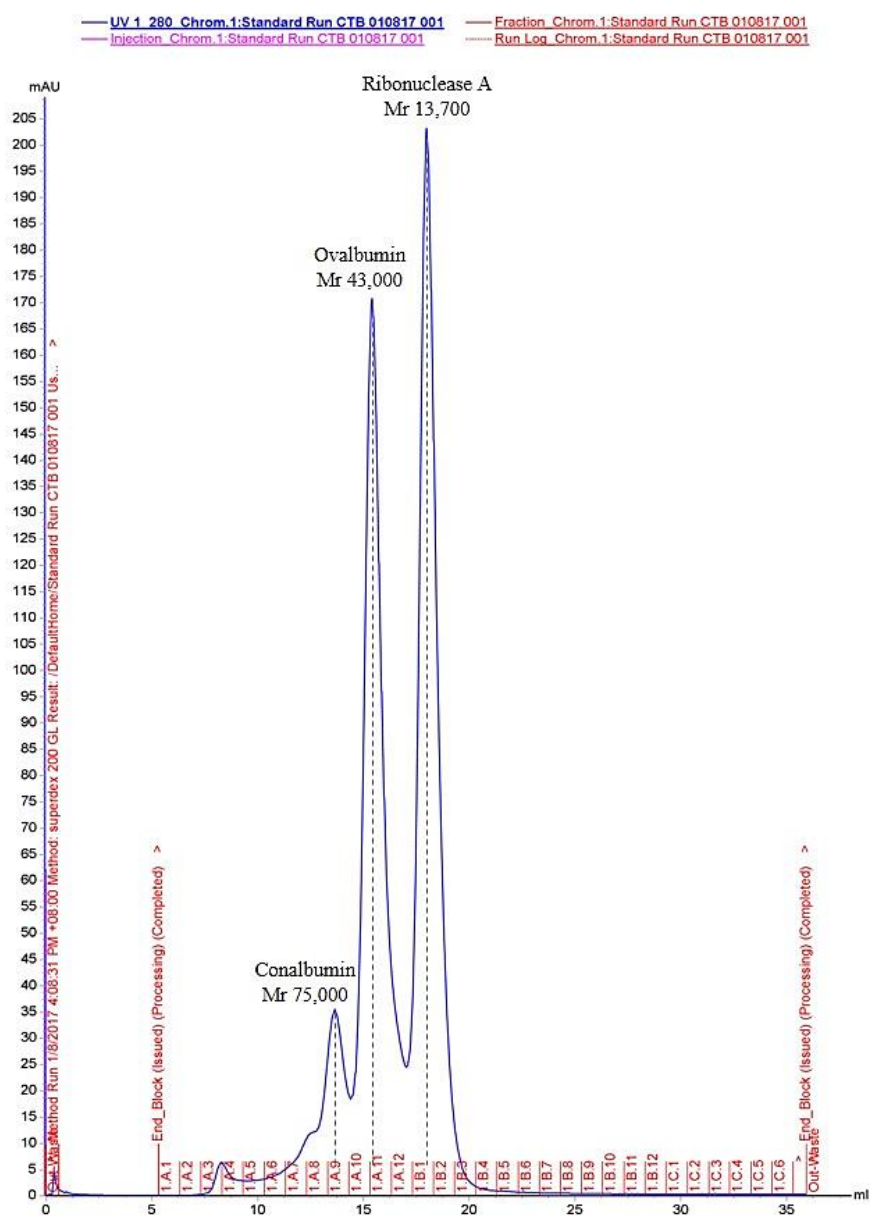


Figure A5.3: SEC chromatogram of protein standards separated under the same conditions as CTB-cEDIII-KDEL (xTH) protein.

A5.4 Relative comparison of the purification efficiency achieved by different density gradient media

As shown in **Figure A5.4**, the use of sucrose and nycodenz as density gradient media had observed a discernible separation outcome. The sedimentation point of the chimeric VLPs was matched based on the corresponding Western blot profiles of fractionated samples. When sucrose gradient was used, the VLPs were found to co-sediment with some green contaminants around the 45% – 55% sucrose fraction. Meanwhile, nycodenz gradient offered a cleaner separation with the VLPs deposited below the plant debris.

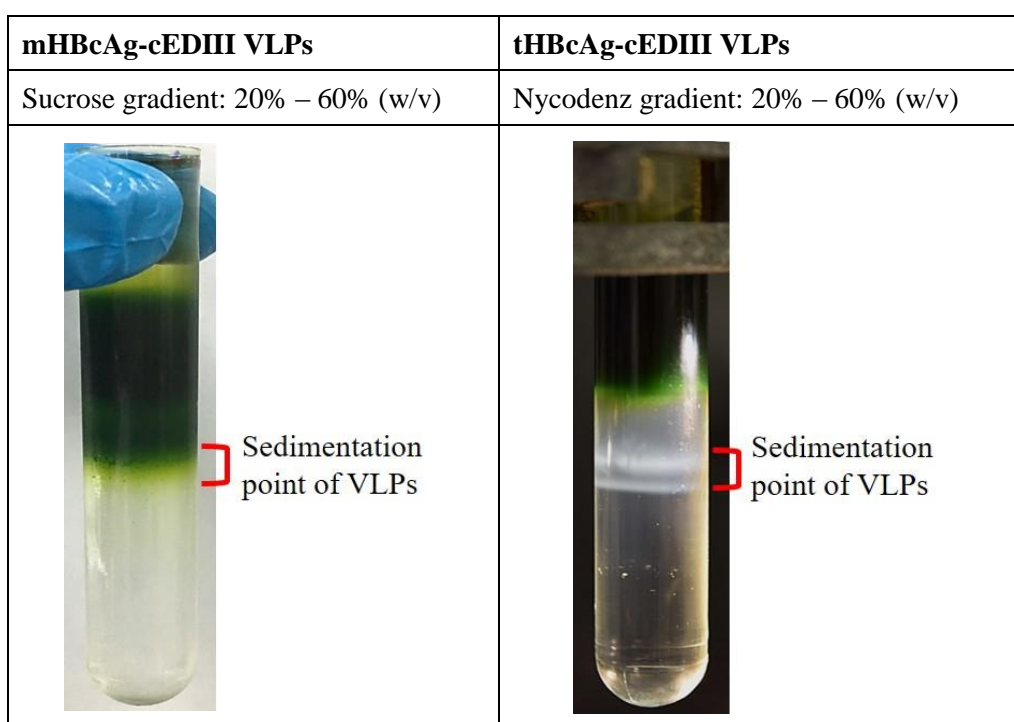


Figure A5.4: A comparison of different density gradient media used in VLPs purification process. VLPs could be more effectively separated from the green impurities when nycodenz gradient was used.

Appendices for Chapter 6

A6.1 Details of buffers used in Chapter 6

- (i) Buffers used for cell culture work (**Section 6.2.6; Section 6.2.7; Section 6.2.8.2; Section 6.2.8.3; Section 6.2.10.1**)

Buffer	Recipe
MEM-10 medium	Minimum essential media (MEM) (Thermo Scientific, USA); 10% (v/v) fetal bovine serum (FBS) (Thermo Scientific, USA); 1% (v/v) HEPES buffer (Thermo Scientific, USA); 1% (v/v) penicillin-streptomycin (Thermo Scientific, USA)
MEM-2 medium	MEM (Thermo Scientific, USA); 2% FBS (Thermo Scientific, USA); 1% (v/v) HEPES buffer (Thermo Scientific, USA); 1% (v/v) penicillin-streptomycin (Thermo Scientific, USA)
2X Plaque medium	MEM (Thermo Scientific, USA); 4% FBS (Thermo Scientific, USA); 2% (v/v) HEPES buffer (Thermo Scientific, USA); 2% (v/v) penicillin-streptomycin (Thermo Scientific, USA)
RPMI-10 medium	RPMI 1640 medium (Corning, USA); 10% FBS (Thermo Scientific, USA); 1% (v/v) penicillin-streptomycin (Thermo Scientific, USA)
ACK lysing buffer	150 mM Ammonium chloride; 10 mM potassium bicarbonate; 0.1 mM disodium ethylenediaminetetraacetate dehydrate, pH 7.4

- (ii) Buffers used for ELISA work (**Sections 6.2.8.1; Section 6.2.10.4**)

Buffer	Recipe
Sodium bicarbonate buffer	15 mM Sodium carbonate; 35 mM sodium bicarbonate, pH 9.6
Sodium phosphate buffer	130 mM Monosodium phosphate; 88 mM disodium phosphate, pH 6.5
Phosphate-buffered saline (PBS)	137 mM Sodium chloride; 3.7 mM potassium chloride; 10 mM disodium phosphate; 1.8 mM monopotassium phosphate, pH 7.4

Assay diluent	PBS supplemented with 10% (v/v) FBS
---------------	-------------------------------------

(iii) Buffers used for FFA work (**Sections 6.2.7; Section 6.2.8.3**)

Buffer	Recipe
Tris-buffered saline (TBS)	50 mM Tris base, pH 7.5; 150 mM sodium chloride
Alkaline phosphatase (AP)-based substrate	66 μ l Nitro-blue tetrazolium (50 mg/ml) and 33 μ l 5-bromo-4-chloro-3'-indolyphosphate (50 mg/ml) in 10 ml AP substrate buffer (100 mM Tris base, pH 9.5; 100 mM sodium chloride; 5 mM magnesium chloride)

(iv) Buffers used for FACS work (**Section 6.2.10.3**)

Buffer	Recipe
Staining buffer	0.5% (v/v) Bovine serum albumin (BSA) and 2 mM ethylenediaminetetraacetic acid dissolved in 1X Dulbecco's phosphate-buffered saline (DPBS) (Nacalai Tesque, Japan)

A6.2 Mouse barbering behaviour was intermittently observed throughout the animal experiment

Barbering behaviour was intermittently observed among the female BALB/c mice that led to significant hair loss (**Figure A6.2**). It is speculated that the physiological stress induced by husbandry factors may have caused the abnormal behaviour.

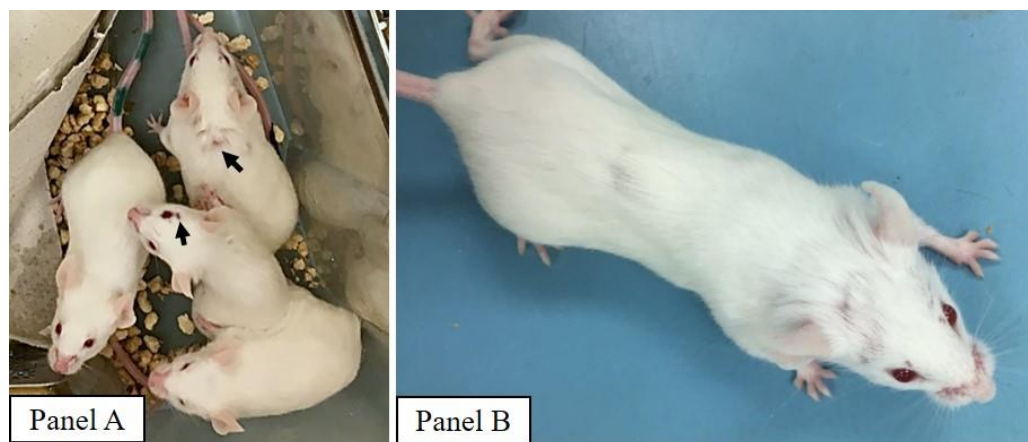


Figure A6.2: An illustration of the barbering behaviour among female BALB/c mice used in this study. Panel A: BALB/c mice housed within the same individual ventilation cage (IVC); Panel B: A closed-up view of a single mouse.

A6.3 Protein Basic Local Alignment Search Tool (BLAST) analysis

A protein BLAST analysis was used to identify region of local similarity between two protein sequences, namely mEL VLPs and the CTB-cEDIII-KDEL (xTH) protein used for antigenic stimulation. This was due to the non-specific stimulatory responses observed from splenocytes of mice immunised with G3-V and G4-V (see **Figure 6.19**). As a result, a 35% sequence similarity was found at the N-terminal region of mHBcAg 3' core sequence (**Figure A6.3**). Note that this similarity region only came from 8% of the CTB-cEDIII-KDEL (xTH) sequence, which comprised of 235 amino acids in length.

	Description	Max score	Total score	Query cover	E value	Ident	Accession
<input checked="" type="checkbox"/>	CTB-cEDIII-KDEL (xTH) Antigen	16.9	16.9	8%	0.25	35%	Query_128899

CTB-cEDIII-KDEL (xTH) Antigen

Sequence ID: Query_128899 Length: 235 Number of Matches: 1

Range 1: 210 to 226 [Graphics](#)

Score	Expect	Method	Identities	Positives	Gaps
16.9 bits(32)	0.25	Compositional matrix adjust.	6/17(35%)	10/17(58%)	0/17(0%)

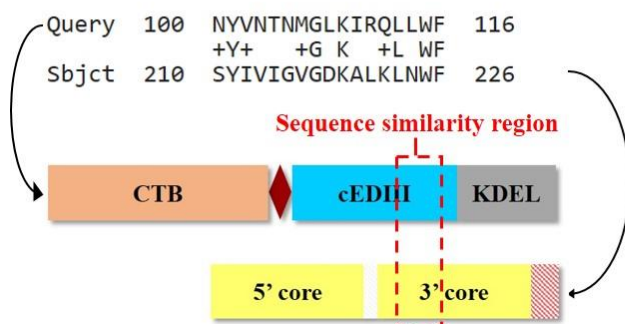


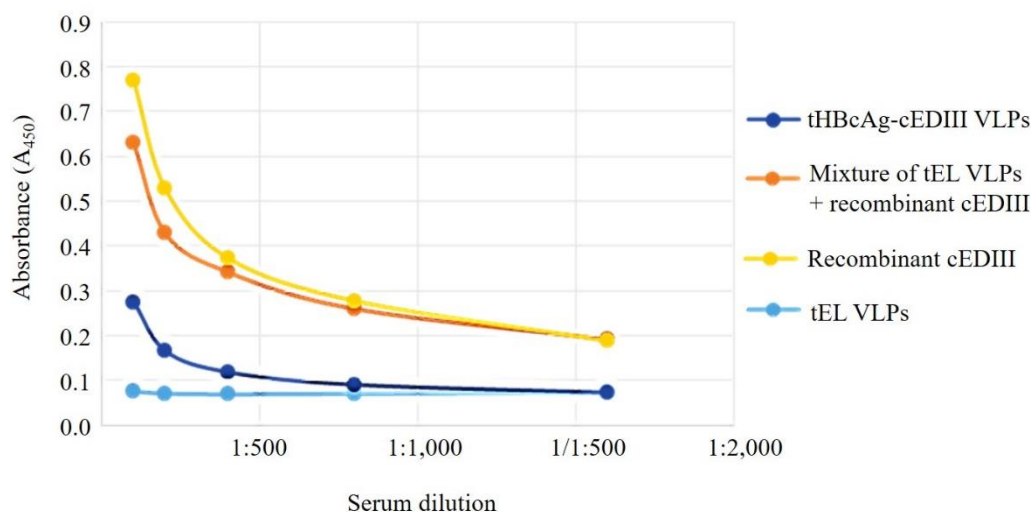
Figure A6.3: A protein sequence alignment results of mEL and CTB-cEDIII-KDEL (xTH), as generated from protein BLAST analysis.

A6.4 A case study on the immunogenicity evaluation of tandem core virus-like particles (VLPs)-displaying cEDIII

A preliminary study of the immunogenicity of tHBcAg-cEDIII VLPs was conducted by iQur Ltd. (UK) as part of collaboration. Immunisation was performed using 8 – 10 weeks old female BALB/c mice. The mice (n = 5) were intraperitoneally injected with 10 µg of the purified VLPs for three times at one-week intervals.

Two findings had been summarised from the preliminary study (**Figure A6.4**), including: (i) successful production of cEDIII-specific IgG antibody (Panel A); and (ii) positive CD8⁺ T cell-mediated killing activity in response to cEDIII antigen (Panel B). Based on the results obtained, it was confirmed that the cEDIII antigen inserted into the c/e1 loop of tandem core particles was displayed in an immunogenic context. Nevertheless, the IgG titre elicited by the recombinant cEDIII alone seemed to be stronger than tHBcAg-cEDIII VLPs; by which has most likely conformed to the molecular size difference as discussed in **Chapter 6**. However, a key aspect was discovered whereby vaccination with tHBcAg-cEDIII VLPs led to higher CD8⁺ degranulation response in comparison to recombinant cEDIII protein. As the high degranulation activity is correlated to efficient Tc cells killing activity, it is foreseen that the tHBcAg-cEDIII VLPs has the potential to be developed into a protective dengue vaccine.

Panel A: Analyses of mouse sera anti-cEDIII humoral response



Panel B: Detection of T cell degranulation activity

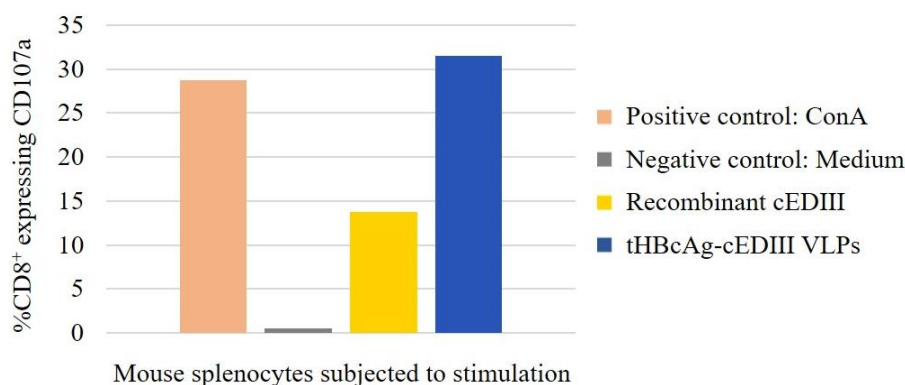


Figure A6.4: A summary of the immunogenicity assessment of tHBcAg-cEDIII VLPs. Panel A: cEDIII-specific IgG responses in mice. Mouse sera (n = 5) were pooled and assayed in duplicate. The results are expressed as an average of A₄₅₀ readings for respective group. Panel B: Degranulation activity of activated CD8⁺ T cell in immunised mice. Mouse spleens were pooled in group (n = 5) and subjected to cEDIII antigenic stimulation. The bars were expressed as an average of triplicate staining.